NASA Conference Publication 2219

Helicopter Handling Qualities

Proceedings of a Specialists Meeting on Helicopter Handling Qualities held at NASA Ames Research Center Moffett Field, California April 14-15, 1982

NASA

NASA Conference Publication 2219

Helicopter Handling Qualities

Proceedings of a Specialists Meeting on
Helicopter Handling Qualities sponsored by
the NASA Ames Research Center and the
American Helicopter Society and held at
NASA Ames Research Center
Moffett Field, California
April 14-15, 1982

NASA
National Aeronautics
and Space Administration

**Scientific and Technical
Information Branch**

1982

PREFACE

This conference publication contains the formal papers of a specialists' meeting on helicopter handling qualities. The conference was co-sponsored by the American Helicopter Society - San Francisco Bay Area Chapter, and the NASA Ames Research Center, and was held April 14 and 15, 1982 at the NASA Ames Research Center, Moffett Field, California.

Helicopters are being called upon by the military and civilian communities to perform more and more tasks, and extend operations into poor weather and at night. Accompanying this increased use is a significant increase in pilot workload and a need for better handling qualities. The ability to define handling qualities required to perform such missions has not kept pace with the actual uses. The objective of this specialists' meeting was therefore to develop an overview of the status and problems in the development and specification of helicopter handling-qualities criteria, and highlight topics for future research efforts by government and industry.

The conference was divided into five sessions and a round-table discussion:

Overview of Current Criteria - an overview of problems and needs for criteria, specification standards of helicopters and high-speed rotorcraft.

Agility and Maneuverability - the subject of agility and maneuverability and how to define maneuvers that can aid mission performance and survivability.

All Weather and Night - minimum requirements for stability, control, and displays in IFR landing approach and distinction that must be made for one- or two-pilot operation.

Integrated Cockpit - techniques and criteria for improving the pilot-helicopter interface and integration of control display devices with flight-control tasks automation.

Handling-Qualities Technology - generic handling-qualities research techniques and facilities.

Round-Table Discussion - an exchange of views on current handling-qualities criteria and techniques, particularly, the problem areas and future needs.

Special appreciation is due to the Session Chairmen, Mr. Dale E. Hutchins, Mr. Tommie L. Wood, Mr. Bruce B. Blake, Mr. Dean E. Cooper, and Dr. James A. Franklin, for their efforts in developing the technical program. Also to the General Chairman, Mr. C. Thomas Snyder for his guidance and support to the conference objectives, to the Arrangements Chairman, Mr. George E. Tucker, for handling all the local arrangements for the conference activities, and to the Technical Information Division for preparing and publishing the proceedings of the meeting.

David L. Key
Conference Technical Chairman

CONTENTS

VTOL AND VSTOL HANDLING QUALITIES SPECIFICATIONS
AN OVERVIEW OF THE CURRENT STATUS

Kevin W. Goldstein
Aerospace Engineer
Naval Air Development Center
Warminster, PA

The highlights of a comparative analysis between the current helicopter and VSTOL handling qualities specifications and four representative state of the art rotary wing aircraft are presented. Longitudinal, lateral, and directional control power and dynamic stability characteristics were analyzed for hovering conditions. Forward flight static and dynamic stability were analyzed for the longitudinal and lateral-directional axes. Results of the analyses in terms of the applicability/utility of the MIL-H-8501A criteria are presented for each of the above areas. The review of the MIL-H-8501A criteria against those in MIL-F-83300 and AGARD 577 indicated many areas in which MIL-H-8501A does not give adequate design guidance.

Notation

M_q	Pitch Rate Damping (second^{-1})
M_{δ_B}	Pitch Control Sensitivity (rad/second^2/inch)
N_r	Yaw Rate Damping (second^{-1})
N_{δ_A}	Yaw Control Sensitivity (rad/second^2/inch)
n	Normal Acceleration (feet/second^2)
α	Angle of Attack (radians)
δ_A	Lateral Control Deflection (inch)
ω_n	Undamped Natural Period (rad/second)
ζ	Damping Ratio
ϕ_1	Roll Angle Attained within One Second (degrees)
CTOL	Conventional Take-off and Landing
VSTOL	Vertical/Short Take-off and Landing

Introduction

With the development of a new generation of rotary wing aircraft for military operations, it has become apparent that the present helicopter handling qualities specification, MIL-H-8501A[1], cannot accurately assess the characteristics of these aircraft. The fact that MIL-H-8501A was last updated 20 years ago only tends to amplify this point. The Navy Light Airborne Multi-Purpose System (LAMPS) SH-60B, the Army Utility Tactical Transport Aircraft System (UTTAS) UH-60A, and the Advanced Attack Helicopter (AAH) all use advanced flight control systems for stability and control augmentation. The need to adequately address the flying qualities of these state of the art vehicle/control systems has necessitated the use of "type specifications" or "prime item development specifications" uniquely devised for each new aircraft/control system. Many papers have been written describing the numerous shortcomings of MIL-H-8501A in realistically regulating handling qualities of present and future helicopters[2-6], indicating a very real need for an updated version of MIL-H-8501A. A summary of the major problem areas described by the above papers is presented as a background and overview of the current status.

To facilitate the development of revised criteria it is necessary first to compile a data base of past and present helicopter stability and control characteristics. This paper presents the beginning of such a compilation. Six degree of freedom math models of the SH-60B and the CH-53D single rotor helicopters were analyzed against the fundamental stability and control aspects addressed by MIL-H-8501A. Vertical control response and autorotation criteria were not included at this time. Flight test data for the XH-59A Advancing Blade Concept (ABC), the XV-15 tilt-rotor, and the CH-46A tandem rotor were also included and discussed.

In the development of the present day VSTOL handling qualities specifications, MIL-F-83300[7] and AGARD 577[8] extensive rotary wing pilot rating data were analyzed to substantiate the finalized hover/low speed criteria. Although AGARD 577 is not intended to be a helicopter specification and MIL-F-83300 has not been used by the Navy or Army for a helicopter development program, these specifications do supply alternative methods of addressing VTOL handling qualities characteristics. The alternative criteria from MIL-F-83300 and AGARD 577 were directly compared with the criteria from MIL-H-8501A to highlight helicopter specification deficiences and vehicle anomalies.

MIL-H-8501A Deficiencies

As described above, the major military helicopter development programs since 1965 have used type specifications designed exclusively for the flying qualities characteristics of a particular vehicle mission and rotor configuration. Although the type specifications were at first basically MIL-H-8501A with slight revisions, recent development of the SH-60B and the AAH was based on type specifications very different from MIL-H-8501A. This is due to the need to address the increased mission requirements of these helicopters. The launch and recovery of the SH-60B from a seaborne platform in up to Sea State 5 conditions is an example of these requirements. Recent work with the HXM type specification highlighted new problem areas, including the need to address characteristics that may be unique to a tilt-rotor configuration. Through the past decade many papers have been written describing specific areas in which MIL-H-8501A is deficient. Three of these areas are discussed in the following paragraphs.

MIL-H-8501A presently addresses helicopter flying qualities in terms of the longitudinal, lateral, directional, and vertical axes. There is no systematic delineation between hover/low speed characteristics and forward flight characteristics. In hover a helicopter pilot tends to use longitudinal, lateral and directional controls independently. For example, in a station keeping task, translation along the longitudinal and lateral axes is implemented by the respective cyclic input, while heading angle is controlled by pedal inputs. Forward flight characteristics of a helicopter tend to resemble those of an airplane, thus the pilot needs to use lateral and directional controls in a coupled manner. Also many single rotor helicopters show a coupled pitch-roll dynamic oscillation in hover, whereas in forward flight a dutch-roll type response is often found. A breakdown of the helicopter specification into hover/low speed criteria and forward flight criteria (similar to MIL-F-83300) would be a means to address the different axis couplings between hover and forward flight.

A suggestion by Key[4] is that a restructuring of MIL-H-8501A in line with MIL-F-83300 and MIL-F-8785C would allow for a more thorough treatment of degraded flying qualities. MIL-H-8501A presently has qualitative criteria for failures of power boosted controls, automatic stabilization systems and engine failures. Table 1 presents one section of the criterion addressing failure of an automatic stabilization system. There is little quantitative guidance available defining sufficient levels of control or stability. With the complex augmentation systems being employed on the SH-60B and the CH-53E there is a need to set minimum quantitative levels of degraded flying qualities for partial AFCS failures and single or dual engine failures. The three levels of flying qualities (see Table 2) used in the VSTOL and CTOL specifications could be incorporated in MIL-H-8501A to specify quantitative levels of degraded flying qualities for control response, static stability, and dynamic stability in any flight mode.

Table 1. Example of MIL-H-8501A criteria for stabilization system failures

3.5.9(d)	Helicopters employing automatic stabilization and control or stability augmentation equipment or both shall possess a sufficient degree of stability and control with all the equipment disengaged to allow continuation of normal level flight and the maneuvering necessary to permit a safe landing under visual flight conditions.

Table 2. Flying qualities levels

Pilot Rating	FQ Level	FQ Description
1.0-3.5	1	Flying qualities clearly adequate for the mission Flight Phase
3.5-6.5	2	Flying Qualities adequate to accomplish the mission Flight Phase but some increase in pilot workload or degradation in mission effectiveness or both, exists.
6.5-9.0	3	Flying qualities such that the airplane can be controlled safely, but pilot workload is excessive or mission effectiveness is inadequate, or both.

A third area that could benefit from a restructuring of MIL-H-8501A is in defining criteria that are mission oriented. The helicopter specification currently uses a weight parameter for hover control power considerations that is the result of scaling laws and not meant to represent the variations in control response which may be required for vehicle mission differences. Both the VSTOL and CTOL specifications define four classes of vehicles according to overall

mission requirements, although in MIL-F-83300 the class distinctions are only used for control force limits and roll control effectiveness in forward flight. Table 3 shows a general breakdown of mission as used in MIL-F-83300. Shipboard recovery and nap-of-the-earth (NCE) flight mission categories could be incorporated into these type of class divisions.

Table 3. MIL-F-83300 classification of aircraft

CLASS	DESCRIPTION
I	Small, light aircraft such as - light utility - light observation
II	Medium weight, low-to-medium maneuverability aircraft such as - utility - search and rescue - anti-submarine - assault transport
III	Large, heavy, low-to-medium maneuverability aircraft such as - heavy transport - heavy bomber
IV	High maneuverability aircraft such as - fighter - attack

The Navy has begun a program assessing the basic flying qualities criteria in MIL-H-8501A against the VSTOL specifications (MIL-F-83300 and AGARD 577) and representative present and future rotary wing aircraft. The significant results from the assessment of hover control power criteria and dynamic response criteria are presented in the following sections.

Hover Control Power

Helicopter control power requirements are usually determined by the hover mission control requirements. As described above, MIL-H-8501A uses a weight parameter to specify attitude response within one second or less. In an extensive review of MIL-H-8501A, Walton and Ashkenas [2] suggest that the MIL-H-8501A weight dependency is too simplified to give adequate guidance for various vehicle missions. In comparison to MIL-H-8501A the two VSTOL specifications define a constant limit of attitude response. The boundaries for roll attitude per inch of lateral control displacement as a function of the vehicle gross weight for all three specifications are shown in Fig. 1. The lower boundaries of all three specifications are substantiated by the level 2 rating given to the XV-15 with augmentation off. There are two other major points to be raised from Fig. 1. First the CH-53D AFCS on response has been described as quite adequate for the assault mission, yet the vehicle does not satisfy the VSTOL boundary. This then substantiates the need for some type of weight dependency as used by MIL-H-8501A. It is questionable though whether or not pilots will accept a lower response for extremely large vehicles. For example, a vehicle in the heavy lift helicopter (HLH) gross weight category (gw≈130000 lb) would only need to attain a bank angle of 2.1 degrees within one second for a one inch lateral stick displacement to satisfy the MIL-H-8501A requirement.

The second point from Fig. 1 is the large difference in roll response between the similar weight SH-60B and CH-46A (ten degrees per inch versus four degrees per inch). The CH-46A has been described as having very satisfactory response characteristics for its assault and vertical replenishment missions. The SH-60B has been qualitatively described as having just adequate response characteristics for a turbulent, high sea state condition, indicative of the LAMPS mission. Yet the SH-60B shows a response well above the visual flight rules (VFR) or instrument flight rules (IFR) MIL-H-8501A boundaries. The difference between these two vehicles then raises the point of having attitude response criteria dependent on the vehicle mission and weight. In particular the small landing platforms and dynamic atmospheric conditions Navy helicopters will be expected to launch and recover from are an example of a mission that may not be adequately designed for by the still wind, out-of-ground effect control power criteria presently in MIL-H-8501A.

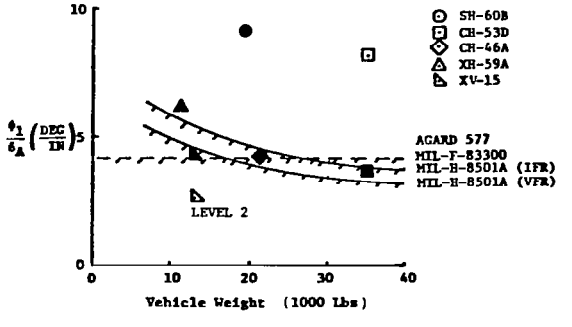

Fig. 1. Hover roll response comparisons

To insure that the helicopter response is not initially too sensitive MIL-H-8501A also has minimum angular rate damping criteria for the longitudinal, lateral, and directional axes. Using these damping boundaries with the above attitude response criteria, rate damping versus sensitivity boundaries can be developed. Fig. 2 shows the ABC and tilt-rotor compared to the MIL-H-8501A requirements for the yaw axis. The interesting point here is that neither aircraft satisfied the requirement yet the ABC has been described in a recent Navy flight test program [9] as having "crisp, predictable" yaw control and that the "high yaw rates (in excess of 45 degrees per second) that resulted from one inch pedal step inputs were well-damped and easily arrested, allowing large, rapid heading changes." The XV-15 in comparison was described as sluggish and not adequate. The point here is not that the ABC is good and the XV-15 bad, but the differences in the two rotor configurations. The ABC develops yaw control through differential collective of the two rotor systems while the tilt-rotor develops yaw control via differential cyclic inputs. The results presented in Fig. 2 show an apparent anomaly between MIL-H-8501A and the different rotor configurations of the ABC and tilt-rotor. Fig. 3 shows the pitch response characteristics of the SH-60B, CH-53D and the XV-15. Similar to the directional axis MIL-H-8501A adequately predicts the single rotor vehicle ratings (the SH-60B and the CH-53D) but again the tilt-rotor shows a discrepancy.

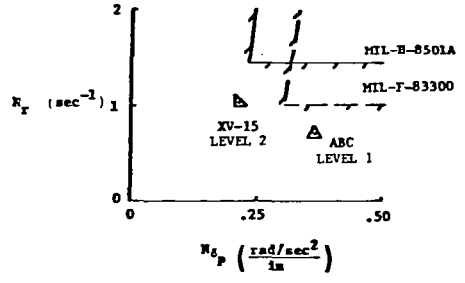

Fig. 2. Yaw rate vs. sensitivity comparisons

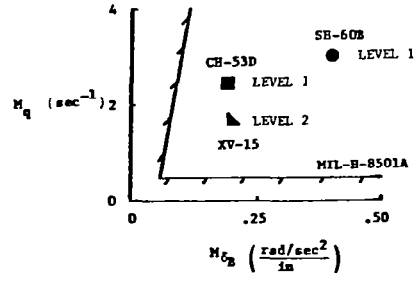

Fig. 3. Pitch rate vs. sensitivity comparisons

Overall it was found that the MIL-H-8501A attitude response and angular rate damping criteria gave minimal design guidance in comparison to the vehicles analyzed. Further analysis and data are needed to determine the effect of vehicle mission and varied rotor configurations.

Dynamic Stability

Following a disturbance (control or atmospheric) to a helicopter in hover the rate damping criteria discussed above should ensure an initial satisfactory response. After this initial response the aircraft may still have an unacceptable dynamic response. In a precision hover task it is mandatory that the pilot be able to correct easily for unwanted oscillatory responses. Uncommanded pitch or roll responses can cause tracking or station keeping errors, plus any short period dynamic responses must be well-damped so as not to impede precise control of the helicopter.

Satisfactory boundaries for dynamic stability characteristics are defined by each of the specifications reviewed through the use of second-order response parameters. The general trend is similar for all the specifications such that short period oscillations require a damped response while for longer periods, neutral stability to slight instability is acceptable. Fig. 4 shows a plot of nondimensional damping ratio versus damped natural period with a comparison of the three specifications for pitch or roll hover dynamic responses. Note that only MIL-H-8501A has a separate boundary for VFR conditions.

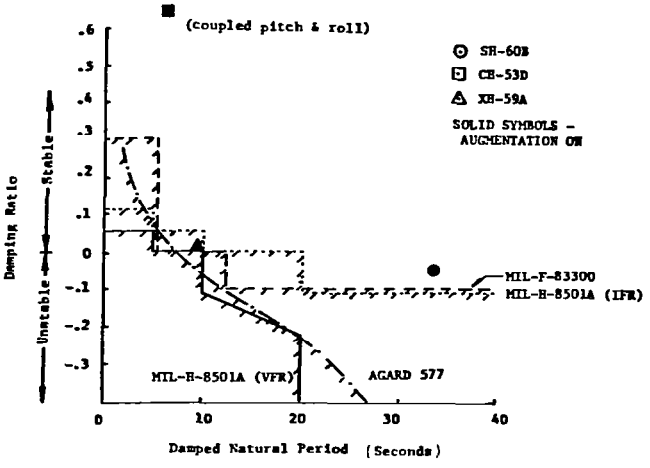

Fig. 4. Hover longitudinal dynamic stability requirements

It should be noted that it is assumed within MIL-F-83300 that "IFR capability is inherent in all military aircraft operational missions." For the limited data available very few conclusions can be drawn about the adequacy of the specifications boundaries. Of the three aircraft shown only the SH-60B shows a "conventional" phugoid mode. Within reference 3 the point is presented that for modern helicopters the MIL-F-83300 boundary shown in Fig. 4 is generally undemanding. This is questionable considering the SH-60B response that Navy pilots described as adequate for the LAMPS mission. Both the CH-53D and the XH-59A have also been qualitatively described as having level 1 characteristics. In particular the CH-53D has essentially dead-beat dynamic responses in hover. From the data analyzed it appears that MIL-H-8501A gives adequate guidance for hover dynamic responses.

Just as in hovering conditions, it is necessary that a helicopter have satisfactory dynamic response characteristics in forward flight. For example, in contour flying or mine sweeping missions, a slowly divergent phugoid response with a gradual altitude loss would be objectionable. MIL-H-8501A specifies VFR and IFR dynamic response criteria for the longitudinal axis (the same as the above hover requirements), while only stipulating IFR criteria for the lateral-directional axes.

Looking first at the longitudinal criteria, Fig. 5 shows a comparison between the VSTOL and helicopter specification boundaries. The helicopter specification is by far the most lenient in specifying stability requirements, in particular for long period responses (>20 seconds) under VFR conditions. In contrast, the VSTOL specifications do not allow divergent long period dynamic responses. With augmentation on, the three vehicles shown on Fig. 5 easily satisfied all the specifications.

Each aircraft has also been given level 1 ratings, in particular the SH-60B is described as having excellent phugoid damping. It should be noted that both VSTOL specifications have additional requirements for short period oscillations such that the damping ratio must be at least 0.3. AGARD 577 defines a short period response such that the damped period is less than 3 to 6 seconds. MIL-F-83300 specifies short period requirements according to Fig. 6. Note that the frequency boundary is a function of the vehicle n/α ratio. The CH-53D was the only vehicle analyzed that showed a short period type response, and it compared favorably with the Fig. 6 boundaries (e.g. $\zeta > 0.3$). For the vehicles compared against MIL-H-8501A, the specification gives lenient but adequate guidance for normal flight conditions.

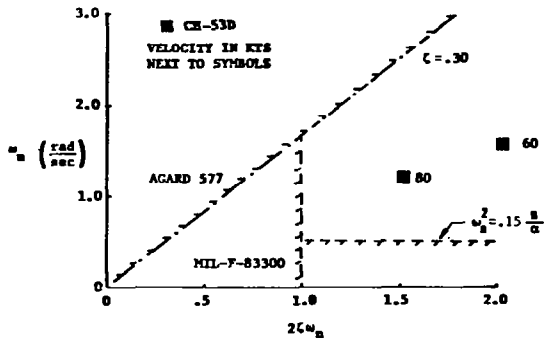

Fig. 6. VSTOL specification short period requirements

The lateral-directional dynamic stability requirements as specified by the VSTOL and helicopter specifications are shown on Fig. 7. The same general trend is followed by each criterion. Note that MIL-H-8501A has no requirement for VFR lateral-directional dynamic stability.

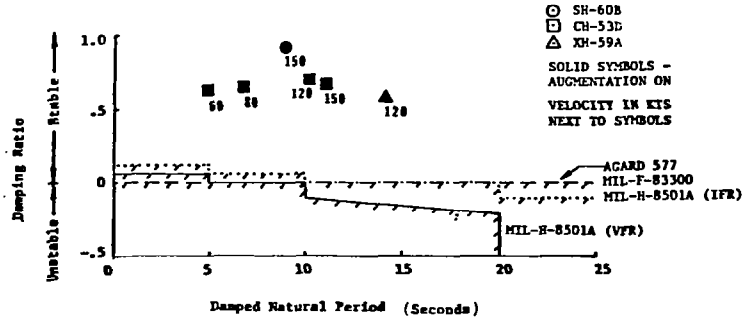

Fig. 5. Forward flight longitudinal dynamic stability requirements

The cluster of open symbols shows a common damped dutch roll response for the single rotor helicopters (SH-60B, CH-53D, SH-3A) analyzed. This type of yaw-roll coupled dynamic response has been given unsatisfactory ratings for single rotor helicopters. Thus there should at least be a baseline criteria limiting allowable divergent responses for VFR conditions. For augmentation on the responses are all well-damped over a wide range of frequencies. An interesting comparison between varied rotor configurations is shown on Fig. 7 as the ABC has a dutch roll response that falls right on the MIL-F-83300 level 1 boundary. Pilots described the ABC as having very satisfactory lateral-directional forward flight characteristics that were very similar to a fixed wing aircraft. A Sikorsky report (reference 10) on the ABC compared this response to MIL-F-8785, the fixed wing flying qualities specification. The ABC again appears as an anomaly in comparison to the helicopter specification boundary. For the vehicles analyzed MIL-H-8501A gives adequate guidance for IFR lateral-directional dynamic responses but has no guidance for VFR conditions.

guidance to address the differences in handling qualities characteristics between hovering and forward flight conditions.

MIL-H-8501A has very limited guidance for degraded flying qualities, especially towards defining minimum characteristics for AFCS failures.

The hover control power criteria (attitude response and rate damping criteria) inadequately address varied mission characteristics or rotor configuration differences.

Dynamic response criteria are in general adequate but very lenient, in particular for VFR mission requirements where no guidance is given for lateral-directional responses.

Analyses in the areas of height control response, aerodynamic and gyroscopic cross-coupling characteristics, and autorotation criteria are underway.

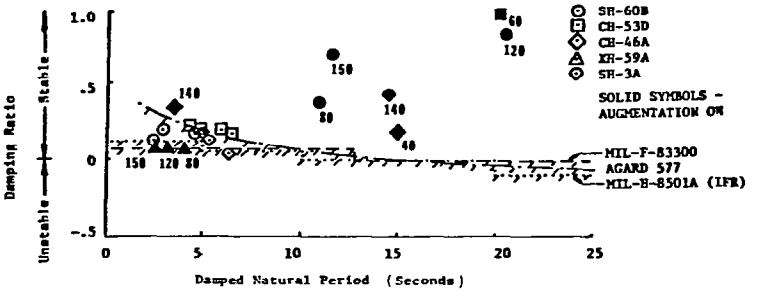

Fig. 7. Forward flight lateral-directional dynamic stability requirements

Conclusions

Although the need to update MIL-H-8501A has been known for many years, very little systematic work has been directed towards developing modern criteria. A step towards this goal is the future Army-Navy program designed to develop an updated rotary-wing handling qualities specification. This paper has presented the major deficiences in MIL-H-8501A as cited by many previous papers as well as the significant results of a preliminary Navy assessment of MIL-H-8501A. In particular:

MIL-H-8501A does not give adequate

References

1. Anonymous, "Helicopter Flying and Ground Handling Qualities; General Requirements for," MIL-H-8501A, 7 Sep 1961.

2. Walton, R. P. and Ashkenas, I. L., "Analytical Review of Military Helicopter Flying Qualities," Systems Technology, Inc., Technical Report No 143-1, Aug 1967.

3. Green, D. L. and Richards, R. B. Jr., "Review of MIL-F-83300 'Flying Qualities of Piloted VSTOL Aircraft' to Assess the Applicability to Helicopters," Pacer Systems, Inc., Technical Report No PWR-054-72, Mar 1972.

4. Key, D. L., "A Critique of Handling Qualities Specifications for US Military Helicopters," AIAA Paper 80-1592, Aug 1980.

5. Dooley, L. W., "Handling Qualities Considerations for NOE Flight," American Helicopter Society Journal, 22, (4), Oct 1977.

6. Pitt,D. M. and Heacock, F. E., "Advanced Scout Helicopter Flying Qualities Requirements, How Realistic Are They?" AHS Report 79-28, May 1979.

7. Anonymous, "Flying Qualities of Piloted VSTOL Aircraft," MIL-F-83300, Dec 1970.

8. Anonymous, "VSTOL Handling Qualities Criteria, Part I - Criteria and Discussion Dec 1970; Part II - Documentation," NATO AGARD Report 577, Jun 1973.

9. MacDonald, LCDR T. L., USN, and Kolwey, S., "Advanced Helicopter Rotor Systems Second NAVY Evaluation of the XH-59A Advancing Blade Concept (ABC) Demonstrator Aircraft," NATC Report RW-39R-80, 24 Dec 1980.

10. Ruddell, A. J., et al, "Advancing Blade Concept (ABC) Technology Demonstrator," USAAVRADCOM-TR-81-D-5, Apr 1981.

CIVIL (FRENCH/U.S.) CERTIFICATION OF THE COAST GUARD'S HH-65A DAUPHIN

J. C. Hart
Manager of Flight Test and Certification, SRR
Aerospatiale Helicopter Corporation
Grand Prairie, Texas

J. M. Besse
Director of Flight Test Department
Helicopter Division,
Societe National Industrielle, Aerospatiale
Marignane, France

K. W. McElreath
Manager Systems Design and Verification
Flight Control Systems Department
Rockwell Collins Government Avionics Division
Cedar Rapids, Iowa

ABSTRACT

One of the requirements imposed by the Coast Guard for the new Short Range Recovery helicopter is that it be FAA certified. The Aerospatiale HH-65A Dauphin is in the certification process, both in France and in the United States. The basic aircraft/engine combination is being certified in France for VFR daytime operation with FAA compliance under FAA Brussells. The night Category II IFR certification is being conducted at Grand Prairie, Texas under cognizance of FAA Southwest Region.

This paper will describe both certification programs with particular emphasis on handling qualities requirements for each. Completion of the VFR Type Certification is scheduled to be completed late this year and the IFR certification in the United States in August 1982. The authors will attempt to identify differences, if any, in the certification requirements of the two countries. This program is unique in that the Automatic Flight Control System is a four-axis system including stabilization through the collective control. Thus, stabilized flight in the low speed regime will be an integral part of the development flight test program.

In this program a dynamic simulator was designed and constructed by Rockwell Collins Government Avionics Division to support and verify the dynamic aspects of the avionics system, particularly the Automatic Flight Control System (AFCS). The role of the Dynamic Simulator in this program will be discussed.

INTRODUCTION

In June 1979 the U.S. Coast Guard signed a contract with Aerospatiale Helicopter Corporation (AHC) of Grand Prairie, Texas, for 90 HH-65A helicopters. These aircraft are intended to be used as Short Range Recovery helicopters, replacing the current HH-52's. Derived from the Aerospatiale SA 365N civil helicopter, the HH-65A is required to be FAA certified before the first delivery to the Coast Guard in late 1982. This certification includes both the aircraft and its avionic systems and will encompass VFR, dual-pilot IFR, and Category II ILS requirements. Furthermore, the nature of the rescue mission demands that the aircraft and its systems be designed to perform extended low-speed and hover operations, thus causing the certification effort to address capabilities heretofore not available.

The FAA certification criteria for Transport Category Rotorcraft, FAR part 29, and FAA Southwest Region's Airworthiness Criteria for Helicopter Instrument Flight are the primary governing documents for the certification of the HH-65A. In addition, all of the aircraft and avionic systems will be certified to perform their intended functions, whether or not regulatory criteria exist.

Unique Aircraft/Avionics System Capabilities to Support the Night, Over-Water, Adverse-Weather Rescue Mission

The avionics system allows the crew and helicopter to confidently perform operations which would be difficult or impossible otherwise. Although only the Automatic Flight Control System, or AFCS, directly impacts the aircraft handling qualities and stability, the total impact of sensors, displays and guidance computations on the pilot workload and performance is equally great. In particular, the integration of all of these elements to automatically perform given tasks, such as an approach to hover at a rescue site, contribute significantly to crew effectiveness, safety and mission success. Singularly important system features are the following:

Four-Axis AFCS (Pitch, Roll, Yaw, Collective)

The four-axis AFCS provides full-time stability and command augmentation over the entire flight envelope for all maneuvers in pitch, roll and yaw. It also provides automatic trim, hands-off attitude and heading hold, and coupled following of the flight director commands. It is fail-passive and allows the pilot to make manual control inputs at any time. The design goal of the AFCS was to enhance the natural handling qualities of the aircraft, making them more consistent, but not substantially altering them.

Helicopter Coupled Flight Director System (FDS)

The FDS complements the pilot by providing automatic path following or maneuvering through the AFCS. The pilot selects the desired FD mode to perform the desired maneuver automatically. He then may modify that mode by using beep/sync switches on the control stick or by making manual control stick inputs. The five modes designed especially for low speed helicopter operations are the Approach mode (APPR), the Transition-to-Hover mode (T-HOV), the Airspeed and Vertical Speed/Altitude hold mode (IAS-VS), the Hover Augmentation mode (HOV AUG) and the Takeoff/Go-Around mode (GA). As a reversionary feature, the pilot may fly the pitch, roll and collective FDS steering commands on the Attitude Director Indicator to continue a task in case a partial failure of the AFCS occurs.

Mission Navigation Computer

The Mission Navigation Computer acts as a full-time navigator on board the helicopter, automatically fixing the aircraft position, managing the navigation radios and sensors, computing flight plan courses and even generating precise search patterns to be automatically followed by the FDS through the AFCS. In addition, the computer provides synthetic three-dimensional approach to hover guidance at any point where the pilot desires to hover. The pilot indicates his desired final hover position by pressing a button when overflying the point. The computer then generates a lateral course and 5 degree descending approach path to a point just downwind of the target, similar to ILS guidance. Using the flight director's APPR and T-HOV modes, the pilot may accomplish an automatic approach and transition to a stabilized hover.

Horizonal Situation Video Display (HSVD) System

To complement the guidance and the pilot's task of monitoring the flight and aircraft situation, the HSVD system displays various modes associated with a given mission phase or task. Besides conventional HSI, MAP and RADAR or FLIR video presentations, the HSVD also has a hover display mode for low-speed operations. Significant data displayed in this mode are computed wind speed and direction, the current omnidirectional airspeed vector and the flight director commanded longitudinal and lateral speed reference for automatic hovering. Such information apprises the pilot continually of the aircraft flight condition and allows him to make decisions based on known hover data. Both sideward and forward/rearward flight can be carefully controlled and used to the best advantage during low speed or hover operations. This display mode then complements the automatic hover capability of the FDS and AFCS for safe, confident maneuvering.

Although all of the above avionic capabilities normally operate in a coordinated fashion, they independently provide reversionary capability in case of any single failure. Thus, the pilot can still safely continue the flight or task if any single element fails.

Verification and Certification Program

The VFR, daytime, Type Certificate for the HH-65A is being issued by the French civil aviation authority, or DGAC, to Aerospatiale Division Helicopters of France, with FAA compliance via FAA Brussels. Then AHC of Grand Prairie is requesting Supplemental Type Certification (STC) of the night, IFR, and Category II operations, including all avionics and mission equipment, through the FAA's Southwest Region in Fort Worth, Texas.

Dynamic Simulator Testing

Because of the innovative nature and advanced capability of the avionics system for IFR flight and low-speed, remote area operation, along with the attendant impact upon crew workload and performance, AHC and Rockwell-Collins planned to reduce the development and certification schedule risk by initially evaluating the avionics system on a fixed-base "dynamic simulator." This engineering development simulator combined actual avionics flight hardware, displays and computers with a simulated cockpit and aircraft response model. The aircraft model was programmed to cover the entire flight envelope, from 20 knots rearward to 140 knots forward flight and up to ±1500 feet per minute vertical speed. The cockpit incorporated the aircraft and avionics controls and displays to perform a total mission profile with realistic scenarios. In addition, the actual aircraft control system with properly emplaced AFCS servos and feel/trim units duplicated the proper feel and pilot-AFCS interaction. Thus, the avionic equipment interfaced and performed exactly as it later would in flight. Two objectives were addressed and met using the dynamic simulator: (1) The system operation was verified and refined to reduce the flight test schedule and schedule risk. That this goal was successfully achieved was manifested when the AFCS successfully stabilized and controlled the aircraft the first time it was engaged in flight. (2) The test pilots and U.S. Coast Guard personnel could evaluate the suitability of the avionics system and the integrated system operation for the intended missions, especially for search and rescue. The early use of the simulator enabled many aspects of the system to be refined and modified while the program schedule impact was still minimal.

STC Flight Testing

The HH-65A flight testing of the avionics and mission equipment commenced in July 1981. The AFCS, flight director system, HSVD multifunction display system, com/nav system and omnidirectional

airspeed system have completed the engineering development testing. The testing of the mission computer functions and the combined mission suitability of the various systems is in progress. The lower end of this IFR speed envelope is limited primarily by the static stability characteristics of the aircraft. The HH-65A, as is typical of most helicopters, exhibits deteriorating static stability characteristics on the backside of the power curve. During the handling qualities survey, a reversal in the cyclic stick position versus airspeed curve was noted below 40 knots. This, of course, is contrary to FAA standards.

Low-speed IFR flight potential is further limited by the lack of displayed OADS information. This data is processed by the flight director computer for the generation of steering commands during T-HOV and GA maneuvers. Demonstrably safe IMC approaches to and departures from hovering flight are possible either in coupled or manual flight. This capability should lead, at least in theory, to landing minimums significantly lower than those currently available. This, unfortunately is not the case at the present time.

Expansion of the low-speed IFR flight envelope will require, first of all, a means of either satisfying FAA static stability standards or modifying those requirements. Secondly, inclusion of an airspeed indicating system, such as the recently developed Collins ASI-800, is necessary. This system displays both lateral and longitudinal OADS information and speeds from rearward flight to the forward flight limit of the aircraft. This indicator utilizes OADS data at speeds less than 40 knots, a blend of OADS and pitot from 40 to 60 knots, and pitot information only above 60 knots. Hopefully, further technical advances and experience gained, as a result of this and future certification programs, will make IFR certification to zero speed possible in the near future.

PROGRAM STATUS

The currently projected date for delivery of the first aircraft to the Coast Guard is September 1982. The FAA certification process began in February with submission of system functional, interface and fault analysis data to the Southwest Region, along with meetings and presentations. Three critical safety items were of particular interest to the FAA: 1) the fail-passive design of the AFCS, which is intended for use in hands-off automatic hovering; 2) the survivability of those system functions which are redundant; and 3) the qualification of digital software for the multiple data bus, the HSVD system and the mission computer functions.

The major remaining milestones prior to FAA certification are the production conformity inspection, the Type Inspection Authorization approval, and the FAA certification flight testing. From the standpoint of handling qualities and crew workload, the IFR evaluation will examine all normal and degraded modes of operation for IFR suitability.

CONCLUSION

The requirement for FAA certification has meshed well with the originally stated Coast Guard mission and system performance requirements. Several special configuration changes have occurred due to the FAA involvement; namely, the routing of the wiring cables and the independence of certain displayed information. However, the overall process and outcome reflects how similar the Coast Guard's mission and aircraft requirements are to the typical sophisticated offshore or corporate helicopter operators.

As a result of the HH-65A program, the groundwork has been laid for the application of many

advances in helicopter avionics and integrated systems technology to the civil helicopters of the 1980's. Notable achievements are the four-axis AFCS, the low-speed coupled flight director system, multifunction CRT displays, omnidirectional airspeed system, computerized automatic navigation and other mission aids and a multiplex data bus interconnect system. With the groundwork of FAA certification once accomplished, the rapid introduction of these and other similarly advanced concepts is greatly facilitated.

BOEING 234 FLIGHT CONTROL DEVELOPMENT

James J. Morris
Technology Manager, Commercial Chinook
Boeing Vertol Company
Philadelphia, Pennsylvania

Abstract

The Boeing 234 is the commercially certified derivative of the CH-47 Chinook. The automatic flight control system and flight director with coupler have been designed to reduce pilot workload for missions of approximately six hour duration during VFR, IFR, day and night conditions. The AFCS system for the 234 is essentially the same system as developed for the CH-47D, which has airspeed hold, attitude hold, and maneuver enhancement in all three axes. The system also has the capability to couple to the Sperry Helcis flight director system which provides for enroute navigation and landing approaches. Certification testing has been completed, by both the FAA and CAA, to FAR Part 29 for Transport Category Rotorcraft and BCAR Section G: Rotorcraft. The aircraft was certified for civil operation in June 1981.

Introduction

The Boeing 234 is the commercial derivative of the CH-47 Chinook tandem rotor helicopter which has accumulated over one and half million hours of flight. The aircraft (as shown in Figure 1) is designed to carry 44 passengers for a distance of 574 nautical miles with IFR fuel reserves at its maximum internal load gross weight of 48,500 pounds. FAA and CAA certification was received in June of 1981. Revenue service with the initial customer, British Airways Helicopters (BAH), began on July 1, 1981.

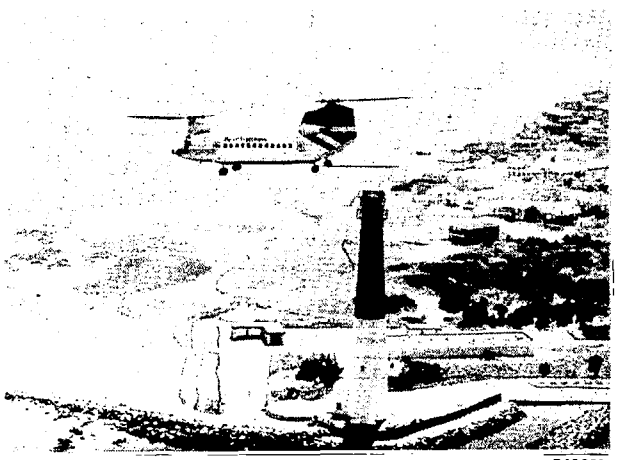

Figure 1. Boeing 234 Helicopter

Figure 2 shows a typical offshore oil mission for the 234 in which advantage is taken of its range capability to go directly from Aberdeen, Scotland to the Dunlin oil platform. This replaces the previous practice of flying fixed wing from Aberdeen to Sumburgh in Shetland Islands, and then flying by helicopter from Sumburgh to the Dunlin platform. The 234 handling qualities and flight control systems have been designed to accommodate this type of mission under IFR, VFR, day, and night conditions. This paper will describe the 234 flight control system, the criteria which led to this system, and the results of testing the aircraft.

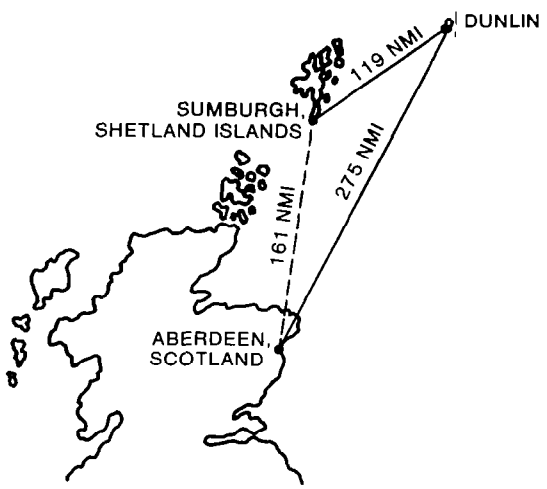

Figure 2. Typical Offshore Oil Mission

Flight Control System Development Criteria

Development of the 234 flight control system encompassed three considerations which had to be satisfied in order to achieve a satisfactory system for civil operation.

The first consideration was that the applicable civil regulations had to be satisfied since it was a program requirement to be certified by FAA and CAA. The relevant FAA documents were FAR Part 29 and the interim IFR standards dated December 15, 1978. The applicable CAA documents were BCAR Section G: Rotorcraft, and for IFR working papers, number 612 (Instrument Flight) and number 615 (Automatic Flight Control and Stability Augmentation Systems). These defined a minimum level of flight characteristics during normal and degraded mode operations, the criteria used to judge the system during certification flight testing, and a minimum level of reliability for system operation. Table I summarizes the pertinent criteria (in a general sense) to which the 234 was certified and shows that, for the basic stability and controllability criteria, the FAA and CAA requirements are very similar. For AFCS failures, the CAA requirement is significantly more stringent with a maximum time delay of five seconds compared to the FAA maximum of three seconds. With regard to what failures are to be evaluated, the FAA is more stringent with their 10^{-9} probability of occurrence compared to the CAA requirement of 10^{-7}.

TABLE I. HANDLING QUALITIES CERTIFICATION CRITERIA FOR VFR AND IFR FLIGHT

ITEM	FAA	CAA
Controllability and Maneuverability	The rotorcraft must be safely controllable and maneuverable	The rotorcraft shall be safely controllable and maneuverable
Trim Control	Must be able to trim out steady forces No undesirable discontinuities in control force gradients	Must be able to trim out steady forces No undesirable discontinuities
Static Longitudinal Stability	Must demonstrate static longitudinal stability from hover through V_{NE}	Must demonstrate static longitudinal stability from hover through V_{NE}
Static Lateral Directional Stability	Must demonstrate static lateral directional stability throughout IFR envelope	Must demonstrate lateral directional stability throughout IFR envelope
Dynamic Stability	Must demonstrate dynamic stability characteristics Stability level varies with frequency of oscillation	Must demonstrate dynamic stability characteristics Stability level varies with frequency of oscillation
AFCS Failures	Must demonstrate failures with time delays varying from normal pilot reaction to 3 seconds, depending on flight condition	Must demonstrate failures with time delays varying from 1.5 seconds to 5 seconds, depending on flight condition
Probability of Failure which would Prevent Continued Safe Flight	Extremely improbable (10^{-9})	Extremely remote (10^{-7})

The second consideration was that two specific operational requirements had to be satisfied. The first requirement was to provide for an approximate six hour flight over water during IFR and VFR, day, and night conditions. The second was to be able to operate in adverse atmospheric conditions — specifically cross winds of up to 50 knots. This criteria is especially necessary for operation in the North Sea, where in winter months it is not unusual to have winds up to 50 knots.

The final consideration was the systems had to be acceptable by pilot qualitative evaluation. Included in these pilot evaluations were handling qualities evaluation during VFR, IFR, and flight in turbulence for normal AFCS operation and degraded mode operation. During these evaluations trimability, stability, control cross coupling, and dynamic stability were evaluated. The criteria of acceptability by pilot qualitative evaluation determined the signal paths and the gain levels and shaping in each of the signal paths for the basic AFCS.
Evaluation of these requirements resulted in the definition of an AFCS system which provides full time attitude and airspeed hold, maneuver enhancement, and vernier trim capability, and includes the incorporation of a flight director and coupler which has navigation capture and tracking, approach guidance capture and tracking, altitude hold, vertical speed hold, heading hold and course select.

Chinook Flight Control History

The Boeing 234 configuration is a result of over 20 years of development of the flight control system as well as the evaluation of requirements. The history of the development of the Chinook flight control system is interesting in that it parallels the development of the state of the art of flight control systems.

Table II summarizes the features of the automatic flight control system for the CH-47A, B, C, and D. On the CH-47A the SAS was essentially a rate damping system which improved the stability characteristics and provided a short term hands-off capability through a pseudo pitch attitude hold (lagged pitch rate). A scheduled airspeed input into a differential collective pitch actuator was provided to obtain a positive longitudinal stick gradient with airspeed. The CH-47B maintained the same basic configuration of the SAS but modified the signal shaping in the pitch axis and the yaw axis. On the CH-47C a Pitch Stability Augmentation System (PSAS) was incorporated which added the features of airspeed and pitch attitude feedback for improved pitch stability. The CH-47D and 234 are the current step in the automatic flight control system (AFCS) development. As shown on Table II, continuous airspeed and pitch attitude hold and stability has been added; bank angle hold logic has been changed from a wings level hold to a capability to hold any bank angle; heading and altitude hold and maneuver enhancement in the pitch, roll, and yaw axes has been added. Cross coupled feedbacks have been added to the pitch, roll, and yaw extensible links for improved failure characteristics. With this generation of the Chinook automatic flight control system a hands off capability has been obtained.

TABLE II. CHINOOK AUTOMATED FLIGHT CONTROL SYSTEM CAPABILITY

HANDLING QUALITIES FUNCTION	CH-47A (SAS)	CH-47B (SAS)	CH-47C (PSAS)	CH-47D (AFCS)	234
Rate Damping	All Axes	All Axes	All Axes	All Axes	All Axes
Pitch Attitude	Pseudo Attitude	Pseudo Attitude	About Trim	Continuous	Continuous
Hold and Stability	Hold	Hold			
Roll Attitude Hold	No	No	Wings Level	Any Bank Angle	Any Bank Angle
Heading Hold	No	No	No	Yes	Yes
Airspeed Hold	No	No	About Trim	Continuous	Continuous
Altitude Hold	No	No	No	Yes	Yes
Maneuver Enhancement	Yaw (Turn Entry Only)	Yaw (Turn Entry Only)	Yaw (Turn Entry Only)	Pitch, Roll, and Yaw	Pitch, Roll, and Yaw
Cross Coupled Feedback for Improved Failure Characteristics	No	No	No	Pitch, Roll, and Yaw	Pitch, Roll, and Yaw
Flight Director	No	No	No	No	Yes

Automatic Flight Control System (AFCS) Configuration

The control system configuration is shown schematically in Figures 3 through 7. The AFCS is in general dualized; i.e., input signals, signal conditioning, and differential actuation. The collective parallel actuator has not been dualized. Philosophy of the system mechanization has been to dualize differential actuation paths which influence basic handling qualities and maintain a single system for parallel paths which do not affect basic aircraft handling qualities. Mechanization of the system is such that the handling characteristics of the aircraft are essentially unchanged on single or dual AFCS.

The pitch axis of the AFCS (Figures 3 and 4) is comprised of two parts — dualized high rate, low authority, hydraulically powered, extensible links for pitch damping; and dualized low rate, high authority, electromechanical Differential Airspeed Hold (DASH) actuators for pitch attitude and airspeed hold. Dual system authority for the extensible links is ± 25 percent of cockpit control and for the DASH is 50 percent of cockpit control. Also included in the control laws for the DASH system is a longitudinal stick pick off for maneuver enhancement. Data signals used by the AFCS for the pitch axis are pitch attitude (from which pitch rate is derived), airspeed, and longitudinal stick position.

The roll axis of the AFCS is shown on Figure 5. It consists of signal paths for roll rate damping, roll attitude hold with synchronization logic so that any commanded bank angle can be held, lateral stick position feedback for maneuver enhancement,

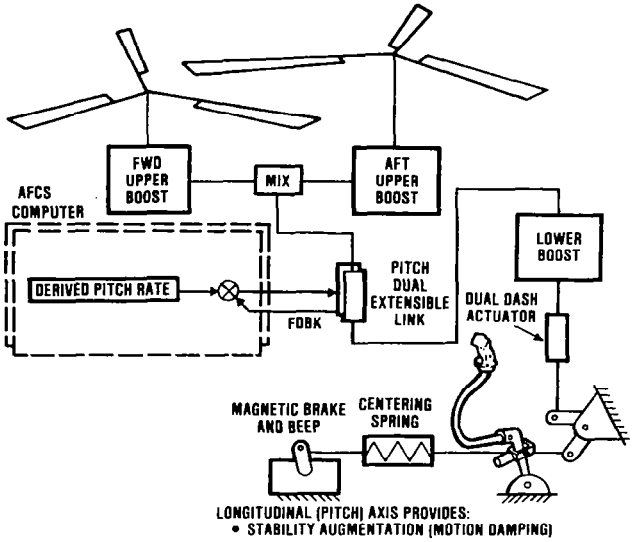

Figure 3. Pitch AFCS Mechanization

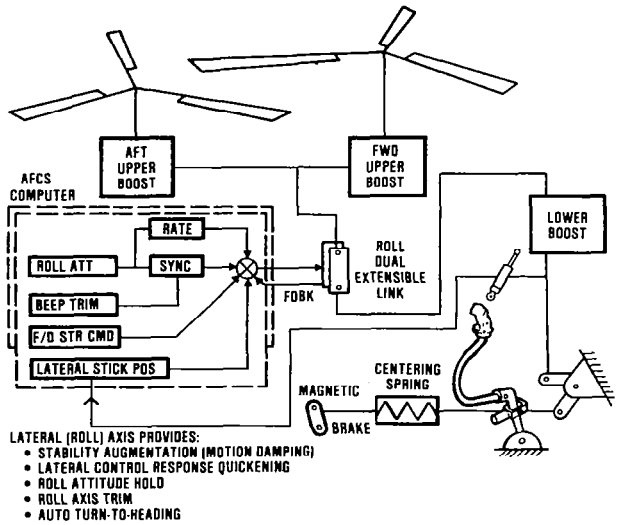

Figure 5. Roll AFCS Mechanization

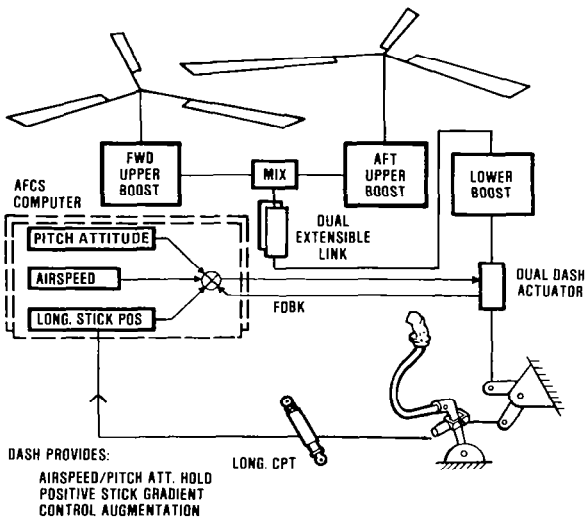

Figure 4. Pitch AFCS (Dash) Mechanization

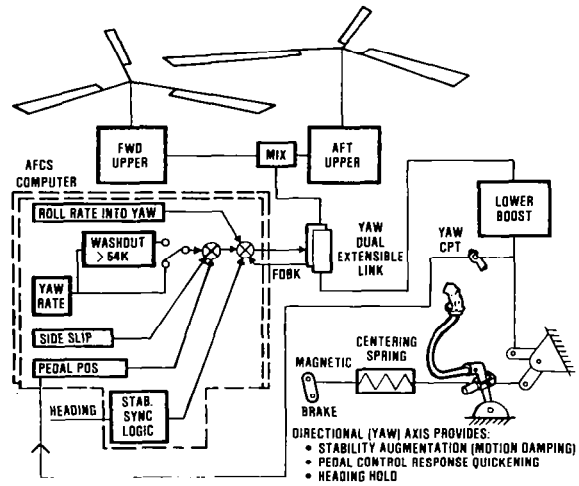

Figure 6. Yaw Axis Mechanization

roll attitude beep for vernier attitude control, and flight director steering commands. Actuation for the roll axis AFCS is provided by dualized hydraulically powered extensible links. Dual system authority for the extensible links is ± 26 percent of cockpit control authority. Data signals used by the roll AFCS are roll attitude (from which roll rate is derived), lateral stick position, flight director steering command, and beep trim command.

The yaw axis of the AFCS is shown on Figure 6. It consists of signal paths for yaw damping, heading hold, sideslip stability, pedal position for maneuver enhancement, and roll rate into yaw for turn entry coordination. Actuation for the yaw axis is provided by dualized hydraulically powered extensible links. Dual system authority for the extensible links is ± 30 percent of cockpit control. Data signals used by the yaw axis are heading, sideslip angle from sideslip transducers on the nose of the aircraft, yaw rate from rate gyros, roll rate derived from roll attitude, and pedal position. Logic for the operation of the yaw damping and holding hold signal paths varies in the yaw axis depending upon flight condition. For yaw damping at low speed there is full time rate damping. At high speed (above 54 knots) the rate damping is washed out with a four second time constant so that the yaw AFCS is not saturated during turns. For heading hold at low speed, the heading hold function is synchronized with pedals out of detent so that the aircraft may be turned with pedals and relatches when the pedals are returned to detent and the yaw rate is less than one and a half degrees per second. At higher speed (above 54 knots) the heading hold circuit synchronizes for lateral stick or pedals out of detent so that the aircraft can be turned with the stick or sideslipped with pedals. Heading hold relatches when the stick

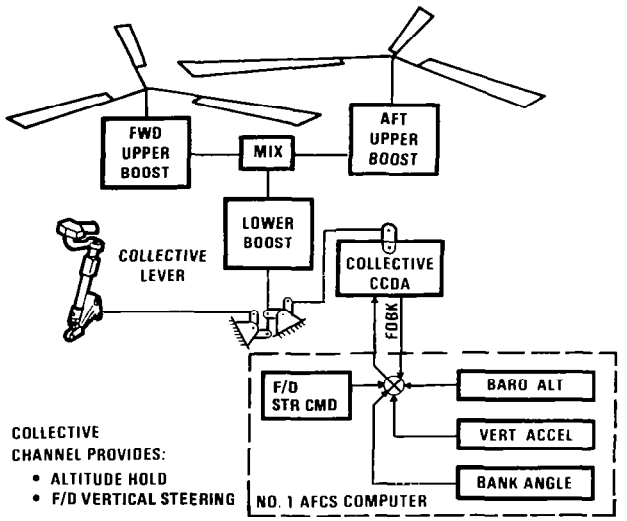

Figure 7. Collective Axis Mechanization

and/or pedals are back in detent, roll rate is less than one and a half degrees per second, yaw rate is less than one and a half degrees per second, and roll attitude is less than one and a half degrees.

The collective axis of the AFCS is shown on Figure 7. It consists of a parallel actuator with signal paths for flight director commands and for altitude hold. The collective axis is not redundant and operates through the Number 1 AFCS unit.

The flight director with its interfaces is shown on Figure 8. The flight director is the Sperry Helcis system which provides for enroute navigation and landing approach with the capability for coupling into the automatic flight control system for lateral steering commands through the aircraft roll control and vertical steering command through the collective parallel actuator. *The system can be used in the coupled or uncoupled mode.*

The flight director system consists of a mode selector panel (Figure 9) and a computer with sensor inputs provided from radio navigation, attitude, acceleration, and air data devices. The flight director mode selector panel provides the controls for engaging/disengaging and displaying the status of any available flight director mode. The modes provided are as shown in Table III.

TABLE III. FLIGHT DIRECTOR SELECTOR PANEL MODES

	Lateral Axis	Collective Axis
Heading Select Mode (HDG)	X	
Navigation Mode (NAV)	X	
Instrument Landing System Mode (ILS)	X	X
Back Course Mode (BC)	X	
Go-Around (GA)	X	X
VOR Approach Mode (VOR APR)	X	
Altitude Hold Mode (ALT)		X
Vertical Speed Hold Mode (VS)		X
Standby Mode (SBY)	–	–

Heading Select Mode (HDG)

The Heading Select Mode is selected by pressing the HDG *button on the mode selector. In the HDG mode, the flight* director computer provides inputs to the roll steering pointer to command a turn to the heading indicated by the heading bug on the HSI. When HDG is selected, it overrides the NAV, BC,

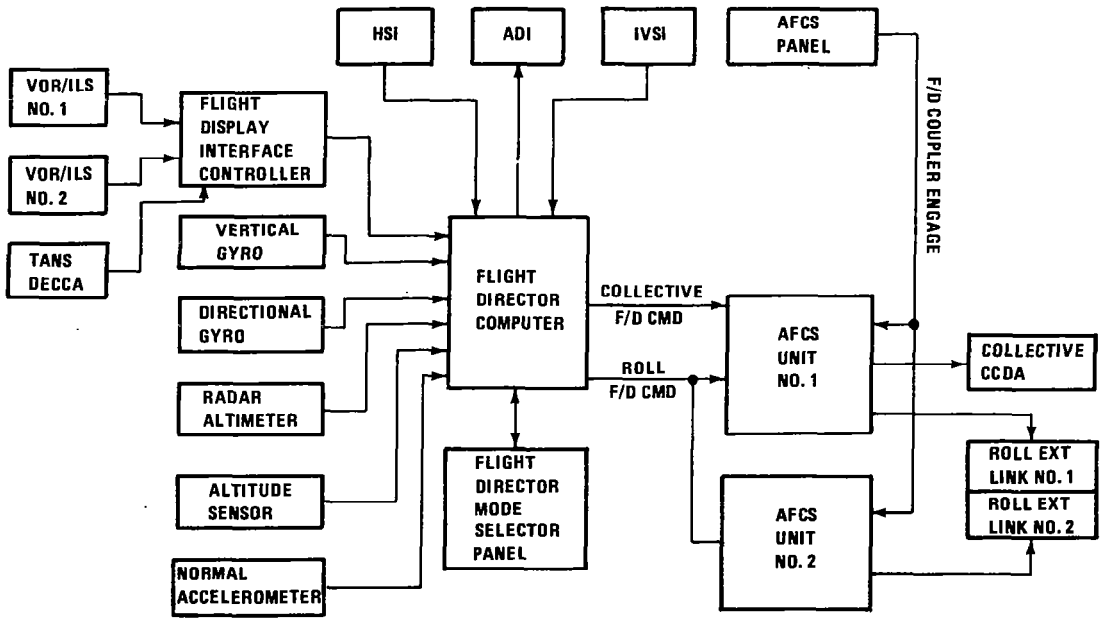

Figure 8. Flight Director/AFCS Interface

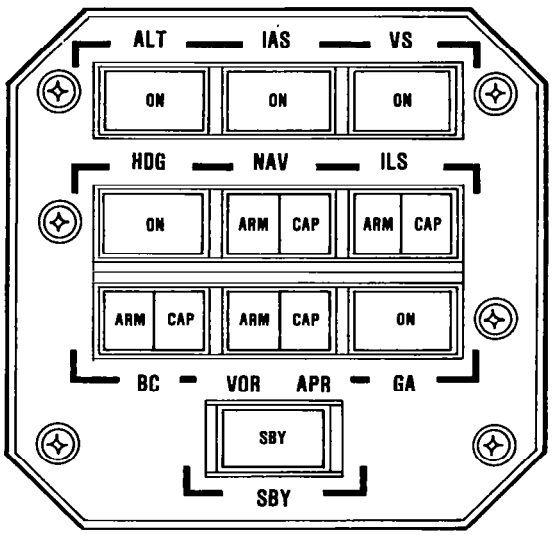

Figure 9. Flight Director Mode Select Panel

and ILS modes. In the event of a loss of valid signal from either the vertical or directional gyros, the roll steering pointer is biased out of view.

Navigation Mode (NAV)

The NAV Mode provides steering commands for both VOR and localizer navigation.

VOR Mode

Pressing the NAV button on the F/D MSP with the navigation receiver tuned to a VOR frequency engages the VOR mode. When outside the lateral bracket sensor trip point, the roll steering pointer receives a heading select command as described above, and both the NAV ARM and HDG mode annunciators are illuminated. Upon reaching the lateral bracket sensor trip point, the system automatically switches to the VOR mode – HDG and NAV ARM annunciators extinguish and the NAV capture NAV CAP annunciator illuminates. At capture, a command is generated to capture and track the selected VOR course. When passing over the station, an over-station sensor detects station passage, removing the VOR deviation signal from the command until it is no longer erratic. While over the station, course changes are made by selecting a new course on the HSI.

If the NAV receiver is not valid prior to the capture point, the lateral beam sensor will not trip and the system will remain in the HDG mode. After capture, if the NAV receiver, compass data, or vertical gyro go invalid, the roll steering pointer will be biased out of view.

Localizer Mode

The Localizer Mode is selected by depressing the NAV button on the MSP and being tuned to a loc frequency. Mode selection and annunciation in the LOC mode is the same as the VOR mode.

Instrument Landing System Mode (ILS)

The ILS Mode is used to make an ILS approach. Pressing the ILS button with a LOC frequency tuned, arms both the localizer and glideslope modes. In the ILS mode, both the NAV and ILS modes are armed to capture the localizer and glideslope, respectively. The initial localizer capture angle is set using the heading bug similar to the VOR mode.

With ILS mode armed, the collective axis can be in any one of the other collective modes, except Go-Around. When reaching the vertical beam sensor trip point, the system automatically switches to the glideslope mode. The collective mode and ILS ARM annunciators extinguish and ILS GS annunciator illuminates. At capture, a command is generated to intercept the glideslope beam. Capture can be made from above or below the beam.

Glideslope mode is interlocked so the localizer must be captured prior to glideslope capture. If the glideslope receiver is not valid prior to capture, the vertical beam sensor will not trip and the system will remain in the existing collective mode. After capture, if the glideslope receiver or vertical gyro become invalid, the collective steering pointer will bias out of view.

Back Course Mode (BC)

The Back Course Mode is selected by pressing the BC button on the Mode Selector. Back Course operates the same as the LOC mode with the deviation and course signals locked out when in the BC mode. When BC is selected outside the lateral beam sensor trip point, BC ARM and HDG will be annunciated. At the capture point, BC CAP will be annunciated with BC ARM and HDG extinguished.

Go-Around (GA)

The Go-Around Mode may be engaged by pressing either the GA button on the mode selector or the remote GA button located on the pilot's collective pitch lever. When selected, all other modes are reset and the GA annunciator is illuminated. The roll steering cue receives a roll zero command while the collective cue commands a positive rate of climb of 500 fpm.

VOR Approach Mode (VOR APR)

Pressing the VOR APR button on the mode selector with the navigation receiver tuned to a VOR frequency engages the VOR Approach Mode. The mode operates identically to the VOR mode with the gains optimized for a VOR approach.

Altitude Hold Mode (ALT)

The Altitude Hold Mode is selected by pressing the ALT button on the mode selector. When ALT is selected, it overrides the ILS GS, GA, or VS modes and the altitude at time of selection will be maintained. In the ALT mode, the collective command is proportional to altitude error relative to the engage reference. Once engaged in the altitude hold mode, the collective steering pointer will bias out of view if either the VG or altitude sensor goes invalid, and the collective AFCS will revert to manual control.

Vertical Speed Hold Mode (VS)

The vertical speed hold mode is engaged by pressing the VS button on the mode selector. When VS is selected, it overrides the ILS, GA, and ALT modes. A vertical speed reference is set by the bug on the pilot's vertical speed indicator. Once engaged, if either the vertical gyro or altitude sensor go invalid, the collective steering pointer will be biased out of view.

Standby Mode (SBY)

Pressing the SBY button on the Mode Selector resets all the other flight director modes and biases both flight director command bars from view. While depressed, SBY acts as a lamp test, causing all mode annunciator lights to be lit and the flight director warning flag on the ADI to come in view. When the button is released, all the other mode annunciator lights extinguish and the flight director warning flag retracts from view.

Handling Qualities Characteristics

The handling qualities of an aircraft are quantitatively evaluated by its static and dynamic stability characteristics. Because of the tandem rotor design and the configuration of the AFCS the handling characteristics of the 234 are essentially independent of variations in gross weight, center of gravity, and density altitude. Representative static longitudinal stability characteristics are shown in Figure 10. There are several characteristics which should be noted. First the longitudinal stick gradient is essentially independent of flight condition with cruise being slightly more stable. Second, varying airspeed is a longitudinal axis task only — there is no significant cross-coupling with the lateral or directional axis. Third, the true stability level of the aircraft to external disturbances is masked due to the longitudinal stick pickoff which cancels part of the airspeed feedback. The stability level to external disturbances is approximately four times that shown. Representative lateral directional static stability characteristics are shown in Figure 11. Note that the stability level is essentially independent of flight condition and that there is no cross coupling with the longitudinal axis. Dynamic stability characteristics in cruise are shown in Figure 12. The response to pitch, roll, and yaw control pulses are well damped. Note that in the pitch axis the system is designed for a return to trim capability, but the logic in the roll and yaw axis is such that when the stick is returned to detent a new attitude is held.

AFCS failures from dual system operation are mild due to the cross coupled feedback scheme on the extensible links (Figure 13). The effect of this mechanization is to obtain immediate relief from a number 1 or number 2 system actuator hardover. Figures 14 and 15 show typical failure characteristics in cruise in the pitch, roll, and yaw axes. Failures from single system operation are more abrupt and are characterized by delay times of one to two seconds and maximum pitch, roll, or yaw rates in the axis of failure of 10 to 15 degrees per second.

Crosswind trim characteristics are shown in Figure 16. The tandem rotor configuration is especially suited for this type of operation because of its insensitivity to wind direction. Note from the figure that low speed control is a one axis control task — lateral stick. There is essentially no cross coupling with longitudinal or directional control.

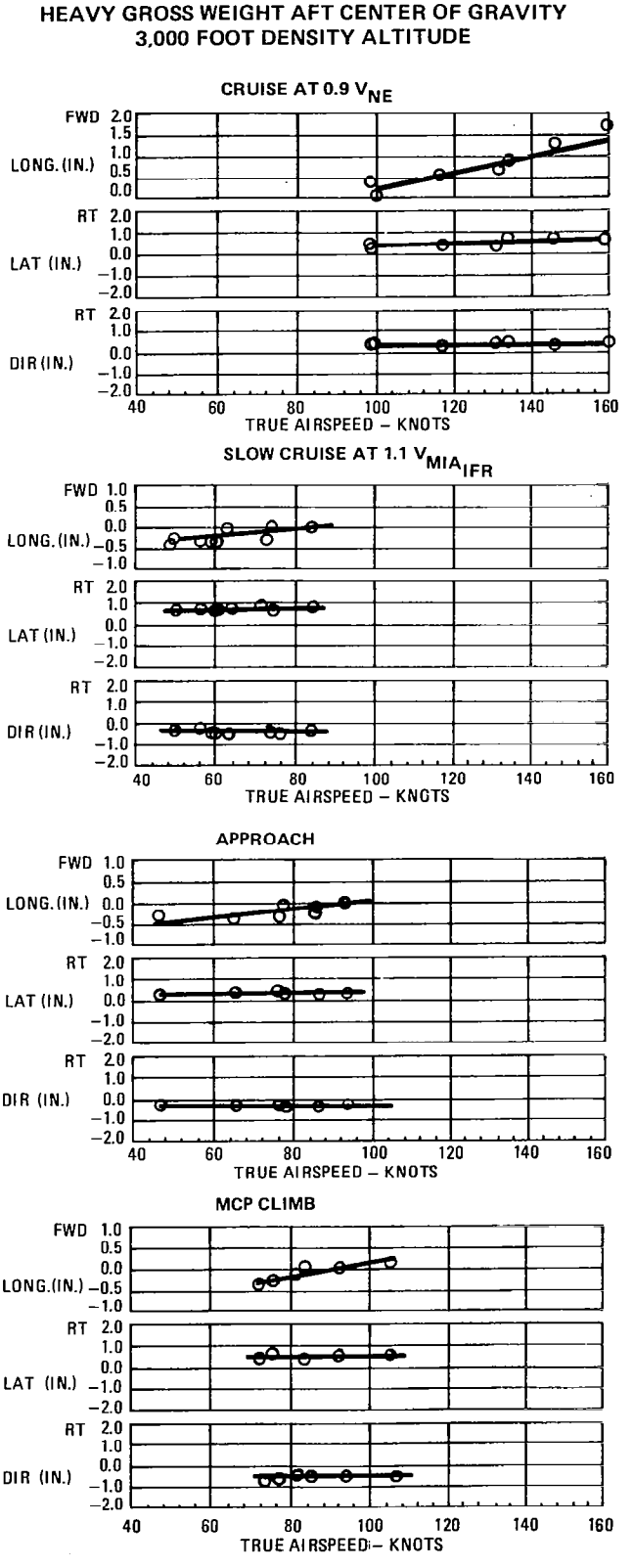

Figure 10. Static Longitudinal Stability

HEAVY GROSS WEIGHT AFT CENTER OF GRAVITY
3,000 FEET DENSITY ALTITUDE

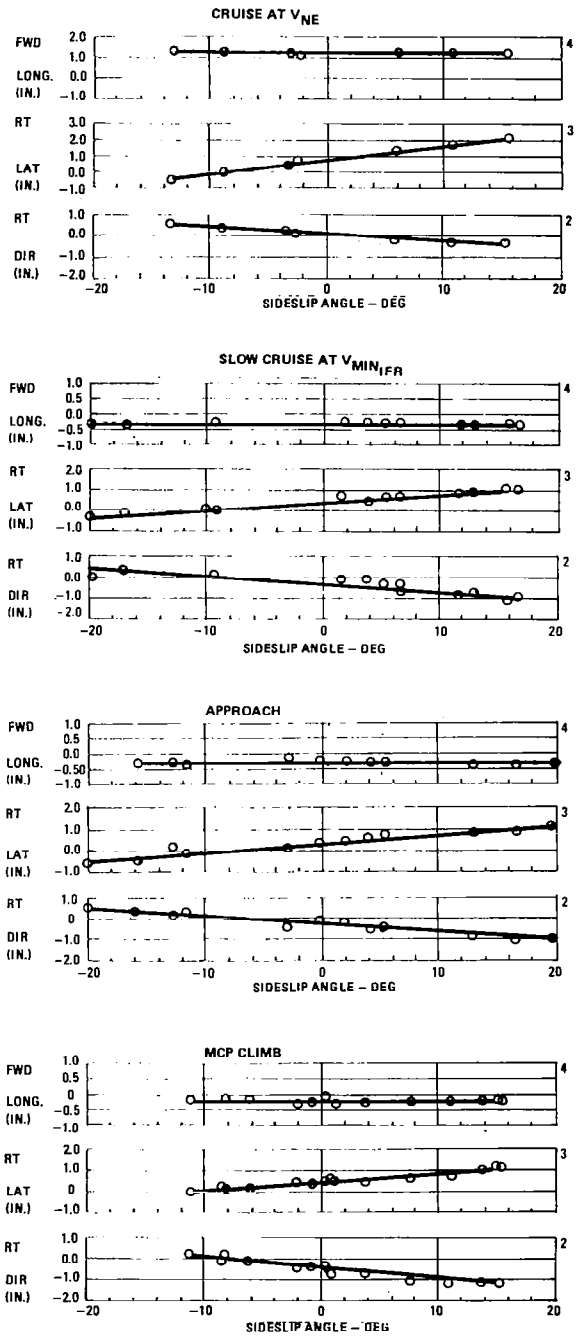

Figure 11. Static Lateral Directional Stability

HEAVY GROSS WEIGHT AFT CENTER OF GRAVITY

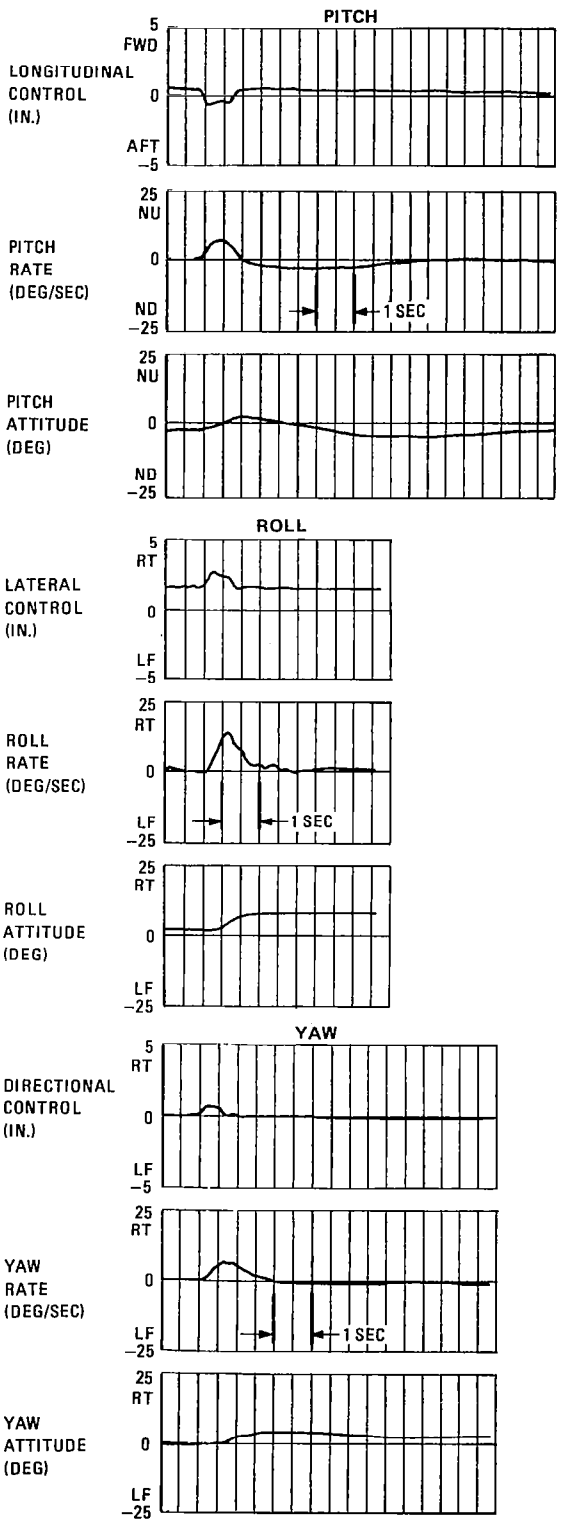

Figure 12. Cruise Dynamic Stability

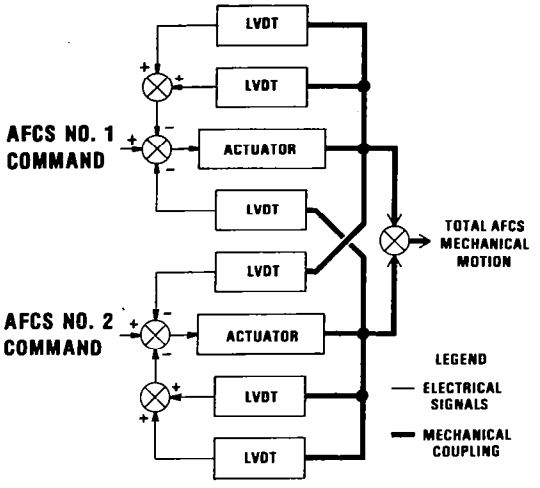

Figure 13. Extensible Link — Cross Coupled Feedback

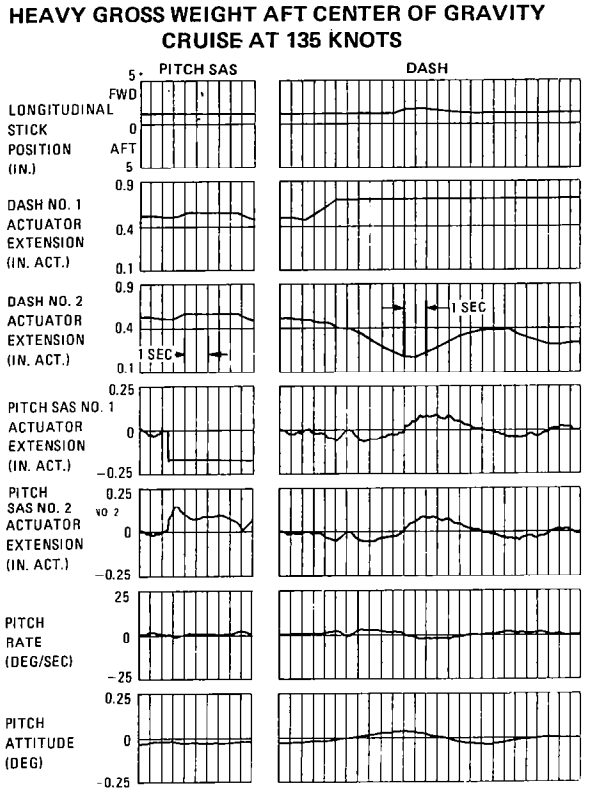

Figure 14. AFCS Failure Characteristics — Pitch Axis

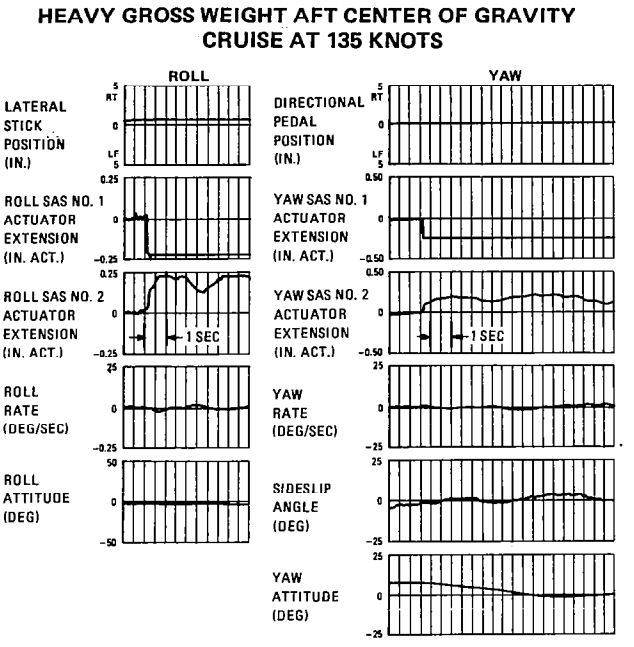

Figure 15. AFCS Failure Characteristics — Roll and Yaw Axis

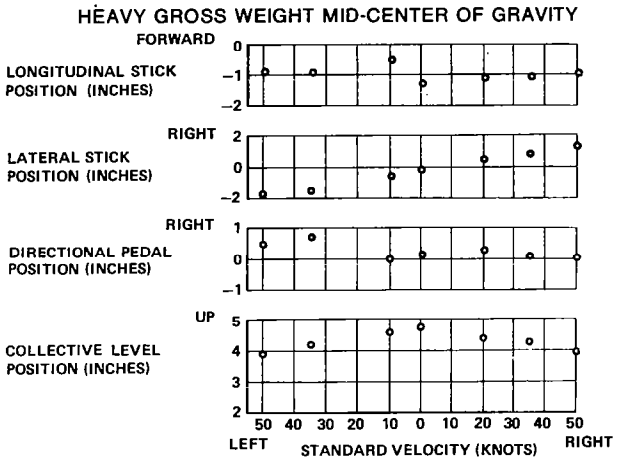

Figure 16. Slow Speed Controllability

Conclusions

Development of a flight control system for today's helicopters must consider the certification criteria for the countries in which it is to be operated; diverse operational criteria which include IFR, VFR, long duration missions, and high wind conditions; and addition of pilot aids such as a flight director and coupler to minimize the overall mission workload. For the Boeing 234 these criteria and needs have resulted in an AFCS with airspeed and attitude hold and maneuver enhancement and a flight director with a coupling capability.

INFLUENCE OF MANEUVERABILITY ON HELICOPTER COMBAT EFFECTIVENESS

Michael Falco

Senior Staff Scientist

Grumman Aerospace Corporation

Bethpage, New York

Dr. Roger Smith

Aerospace Engineer

U.S. Army Aviation Research

and Development Command

St. Louis, Missouri

Abstract

An investigation was conducted to quantify the impact of maneuver capability on the combat effectiveness of current and advanced design helicopters in one-on-one engagements against specific threats. A newly developed computational procedure employing a stochastic learning method in conjunction with dynamic simulation of helicopter flight and weapon system operation was used to derive helicopter maneuvering strategies. The derived strategies maximize either survival or kill probability and are in the form of a feedback control based upon threat visual or warning system cues. Maneuverability parameters implicit in the strategy development included maximum longitudinal acceleration and deceleration, maximum sustained and transient load factor turn rate at forward speed, and maximum pedal turn rate and lateral acceleration at hover. Results are presented in terms of probability of kill for all combat initial conditions for two threat categories. In the first category the use of maneuverability is examined in a defensive role against an anti-tank guided missile (ATGM) launched by a threat helicopter. The second category is concerned with the impact of maneuverability in both defensive and offensive roles against a gun armed helicopter threat.

Introduction

In the early stages of military helicopter conceptual design, there is a need for methodology to better quantify combat effectiveness in terms of the major aircraft/weapon system attributes such as design maneuver capability and maximum speed, weapon capability, passive/active survivability equipments performance, detectability, and threat warning. To analyze the maneuver capability contribution to combat effectiveness against various threats, the associated models are required to be of high fidelity in terms of the dynamical simulation of helicopter flight and yet permit the maneuver contribution to be assessed either singly or in concert with the other system attributes in an equally detailed way. It is necessary for the methodology to develop an optimal probability of kill or survival solution for all relative geometries for which combat can be initiated. Solution optimality is important for consistent effectiveness comparisons between aircraft/weapon concepts and serves to minimize the effect of maneuver strategy prejudgments and other preliminary bias factors introduced by the analyst.

Application of modern optimal control and differential game theory methods seems well suited to these problems at first sight. However, the pioneering effort of Isaacs (Ref. 1), followed by those of Breakwell and Merz (Ref. 2), indicate that there does not appear to be a general systematic method for solution of even some simply structured pursuit-evasion games. This difficulty has led applications-oriented investigators (Ref. 3, 4, 5) toward consideration of discrete game approximations which circumvent the analytical problems of the continuous theory, and still offer some form of suboptimal solution in more realistic combat models.

This paper presents a partial summary of recent computational experience gained in military helicopter design applications using variations of a stochastic learning method first reported in Ref. 4. Representative computational results are presented for two important categories of one-on-one helicopter air combat: the first, a study of maneuver capability in defending against an anti-tank guided missile (ATGM) launched by a threat helicopter; the second, maneuverability employed defensively and offensively against a gun-armed threat helicopter. An explanation of the maneuver strategy development and effectiveness assessment methodology is given in both case studies. The representative results reported here limit helicopter maneuvering to constant altitude flight paths; solutions using variable altitude maneuvering with terrain constraints in the

air-to-air gun study were not available in time for inclusion in this publication. Geographical terrain features have not been considered in these studies; the ground is modeled as a plane.

The same approach has been extended to problems of land warfare, particularly armored vehicle maneuver effectiveness and survivability against anti-tank missile threats. Corroboration of the computer derived solutions for specific threat cases has been obtained in independent field trials with the actual systems. Additional effort must be dedicated to flight trial verification of the model approximations and computed solutions. Continued research is warranted in the application of optimal control, differential game, and the stochastic processes branches of applied mathematics to provide effective numerical procedures for helicopter combat analyses.

Maneuverability in Air-to-Air Missile Avoidance

Missile Threat

The threat is an optically tracked, wire guided missile employing a semi-automatic command to line of sight guidance system. This threat was primarily designed as an anti-tank guided missile (ATGM), but has air-to-air application as well. It is assumed to have a 245 m/s sustainer velocity, maximum range of 4 km, and maximum flight time of 16.3 s. In addition, it is assumed to have a 4 g maximum lateral maneuver capability, and that the launch aircraft is at co-altitude with the target. The low combat flight altitude of the target (dictated by detection and masking considerations) allows the survivability results to be safely extrapolated to ground launched cases as well. This threat is normally equipped with a shaped-charge contact fuze warhead for armor penetration. However, proximity fuze warheads employing expanding rod or fragment kill mechanisms are also indicated to be adaptable to this missile airframe, and two of these types were considered in this investigation. The contact fuze warhead lethality model utilizes a probability of kill, P_K = 1.0 for missile contact anywhere on the helicopter fuselage envelope. Two proximity fuze warhead models are described in Fig. 1. Warhead A denotes an expanding rod warhead as used in short range air-to-air missiles. Warhead B is the largest blast/fragment warhead that can be accommodated by the missile airframe and propulsion configuration. The kill effectiveness, P_K, of these two warheads is given as a function of detonation distance R_{DET} (from the target cg). The data shown represent an average of all warhead/target detonation aspects; however, functional dependence upon aspect is considered in the studies.

Threat Warning and Maneuver Strategy

Earlier investigations have postulated the need for evading aircraft to be equipped with a threat warning system in order to achieve a reasonable measure of survivability against missile threats. The aircraft in these investigations are assumed to employ an active radar warning system supplying relative range and azimuth information regarding the incoming threat. The baseline configuration for this warning receiver model employs 12 azimuth gates and 7 range gates from 0.25 km out to a maximum detection range of 5 km, as shown in Fig. 2. This configuration is indicative of the warning receiver performance levels that are projected for operational systems in the near future.

At each threat warning contingency (represented by one of the 7 x 12 = 84 range/azimuth cells), the aircraft is allowed a choice from a finite number of elemental maneuvers. Five elemental maneuver choices are shown in Fig. 2. The choices may be comprised of maximum performance turns, longitudinal acceleration, deceleration, and a straight ahead constant speed policy. In vertical plane maneuvering studies climb and pushover maneuver choices would be added. An aircraft evasive maneuvering strategy is the selection of an elemental maneuver for each threat warning cell. An optimal strategy is a strategy which maximizes aircraft survivability for all launch initial conditions.

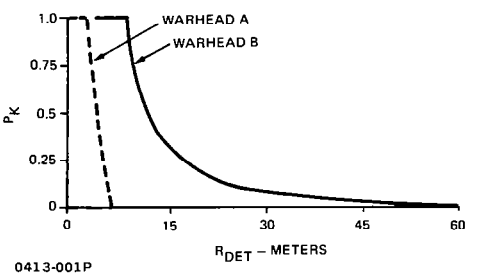

Figure 1. Warhead Lethality

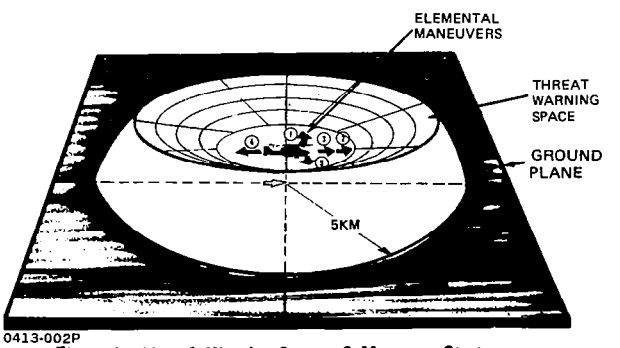

Figure 2. Aircraft Warning System & Maneuver Strategy

Stochastic Learning Method

The stochastic learning method is comprised of two phases: a reinforcement learning phase, in which the optimized evasive strategy is ultimately derived, and a statistics phase. The learning phase involves the development of a

decision table that consists of a probability distribution used in the selection of an elemental maneuver for each warning contingency. That table is shown in its initial form at the upper right of Fig. 3. The column indices 1, ... 5 under the control caption are the five elemental maneuver choices. The row indices, labled R, ranging from 1, ... 84 represent the threat warning contingencies. Initially, the choice of maneuver for each contingency is governed by sampling from the equally likely discrete distribution, as shown.

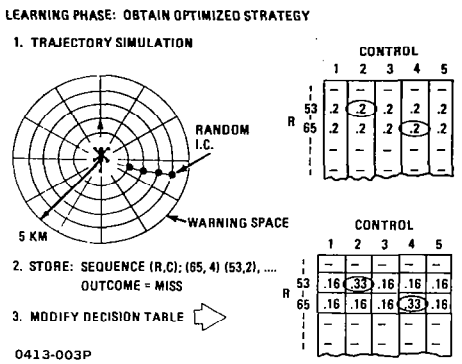

Figure 3. Stochastic Learning Method

A random initial condition for the combat is selected and both aircraft and threat trajectories dynamically simulated. The aircraft employs a selected maneuver within the initial contingency cell until a second cell is entered and another maneuver choice is made. Threats may be launched outside the range of the warning space. In this case, the aircraft maintains its current speed and heading until the threat first enters the warning space at which time the control selection process begins. This simulation process is continued until warhead detonation or flyby, and a kill or survival event is calculated using the probability of kill distribution derived from the warhead lethality function. In the process of simulating the trajectories, the sequential contingency/control pairs employed by the aircraft are temporarily stored. Based upon the kill/survival event, the probability associated with those control choices made for each contingency are modified by a reinforcement rule. For the survival event, the probabilty of employing the same elemental maneuver for each stored contingency is increased, and is decreased for the kill event. The trajectory simulation and table modification process is repeated over all possible threat launch range and azimuth initial conditions using a random selection method. Approximately 100 launches per warning cell or 8400 total trajectories are numerically simulated to produce a converged decision table. The 8400 trajectories require approximately 20 minutes CPU time on IBM 370/168 systems.

In the statistics phase the converged decision table is fixed. Random starting conditions are then selected and trajectories dynamically simulated. In a manner typical of Monte Carlo approaches, the averaged probability of kill and missile warhead detonation distance statistics are computed for each warning (or launch) cell.

Elemental Maneuvers

In this paper, the helicopter maneuver choices are restricted to those which maintain a low constant altitude. The maneuver vectorgram, labeled control set I in Fig. 4, is aimed at quantifying the impact of longitudinal and turn maneuver capability in constructing an effective evasive maneuvering strategy throughout the whole speed range from hover to maximum level of flight speed. At forward speed, the helicopter can command maximum transient (or sustained) load factor turns, labeled (1) and (5); maximum longitudinal acceleration, (2); or maximum longitudinal deceleration, (4); as well as maintaining the current speed and heading, (3). At very low forward speeds including hover, the load factor turns are replaced with maximum rate pedal turns.

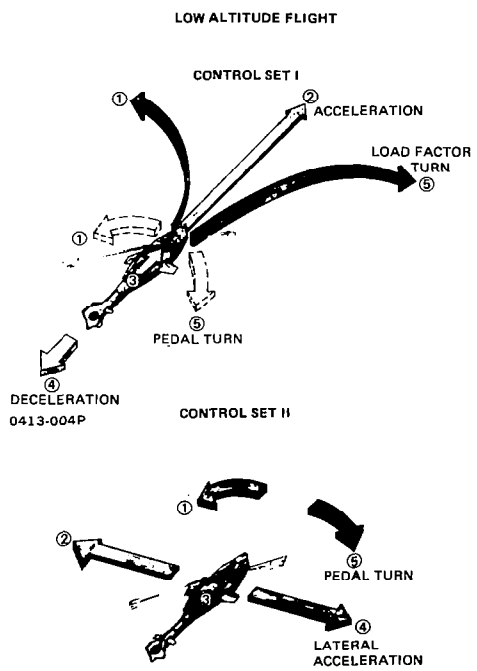

Figure 4. Elemental Maneuvers

The maneuver vectorgram at the right in Fig. 4, captioned control set II, is aimed at quantifying the impact of lateral acceleration (sideward flight) and pedal turn capability in constructing a maneuver strategy at or near hover speeds only. Choices (1) and (5) represent

maximum performance pedal turns; choices (2) and (4), maximum performance lateral accelerations; and choice (3) maintains current lateral speed at the current aircraft heading. Similarly, vertical or composite vertical/horizontal maneuver models can be constructed and investigated without change in the basic methodology.

Helicopter Maximum Maneuver Capability

Figure 5 graphically summarizes the sea level maximum maneuver capability data associated with the elemental maneuver models of Fig. 4, for a conceptual enhanced performance version of a current helicopter design. The maximum commanded turn capabilities shown at upper left are employed for choices (1) and (5) in control sets I and II. For the case of maximum transient turn, the associated longitudinal transient deceleration is shown at the upper right. The maximum longitudinal acceleration and deceleration capabilities utilized for choices (2) and (4) in control set I, are given in the two lower diagrams. The lateral acceleration required for choices (2) and (4) of control set II is given in the diagram at lower left. These studies employ first order models for the aircraft transient response to the maximum acceleration and rate commands.

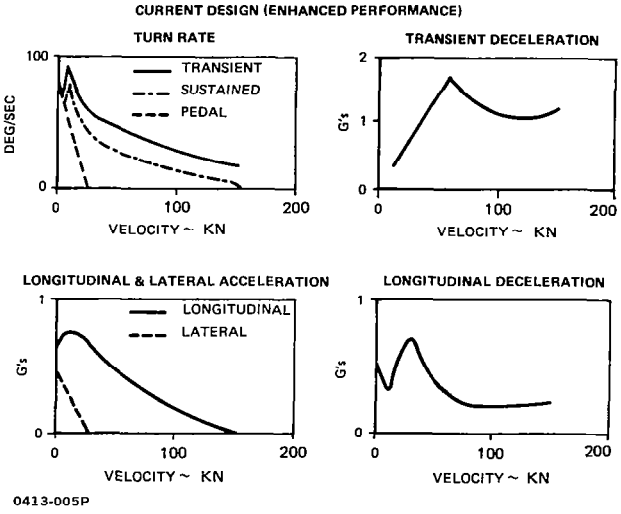

Figure 5. Maximum Maneuver Capability

Effectiveness of Maneuverability

The aircraft survivability or equivalently the missile kill effectiveness results (P_K) for the ATGM threat for all launch conditions are calculated and presented in the helicopter warning space coordinate system for convenience. In this case the maximum effective launch range of the threat (4 km) was less than the maximum detectable range of the warning system (5 km). (The results could also be presented in a space relative to the launch aircraft and would represent the effective launch envelope for that missile against an optimally maneuvered evader.) Threat launches were initiated from 72 of the 84 range/azimuth cells within the 5 km maximum range in both learning and statistics phases. No launches were simulated from the 12 cells making up the inner range ring (range less than 0.25 km) due to severe missile guidance transients at very short target ranges. It should be noted that in all results presented, the attacking aircraft is assumed to maintain a speed equal to the initial speed of the target, and fly a pure pursuit navigation course toward the target during missile flyout.

Figure 6 shows the kill effectiveness of the ATGM equipped with the expanding rod type warhead. Because of left-right symmetry considerations, only half of the warning space need be shown. Four levels of kill effectiveness (P_K) are given to simplify the presentation. The legend at lower center is employed throughout this section. The origin of each semicircular plot corresponds to the helicopter position at missile launch, and the aircraft initial heading (0°) is shown by the helicopter symbol. Head-on launches correspond to 0° to 30° aximuth sectors, and tail aspects launches 150° to 180°, respectively. The kill results are presented for four helicopter initial speed condition groups, beginning with hover at upper left, and progressing clockwise to maximum speed at the lower left. Within each of the four speed groups, the left semicircle, labeled nonmaneuver, represents missile kill effectiveness when the aircraft maintains its current speed and heading. This case is important for quantifying target speed effects without maneuver, and is useful for establishing baseline survivability measures without use of threat warning and optimal maneuver. Clearly, a scan of the nonmaneuver cases for the four initial speeds indicates improving survivability in longer range rear aspect launches with increasing speed, but at the expense of reduced survivability in the corresponding forward launch cases. In addition, a small window of improving survivability for short range beam launch cases can be seen developing with increased speed; this is due to guidance transients associated with high line of sight rate targets. The nonmaneuver cases show that speed alone (equivalent to no threat warning) does not provide sufficient survivability against the ATGM with Warhead A. The semicircles labeled OPT I in each of the four speed groups quantifies the survivability improvements that can be achieved with the 84 cell warning system, together with an optimal maneuvering strategy derived from control set I. In the four results labeled OPT I, the helicopter employed its maximum transient load factor turn performance for choices (1) and (5). One can see that survivability is still poor with combat initiated at hover, although small improvements exist for tail launches at the 4 km range. This is due to helicopter acceleration away from the oncoming missile and the missile maximum range limitation. However, at higher initial speeds,

optimal maneuvering, employing transient load factor performance can provide high survivability. The lack of effectiveness of control set II (lateral acceleration and pedal turns) in constructing an optimal maneuver strategy from hover is shown by the shaded semi-circle labeled OPT II. This result, together with that for OPT I to the immediate left, indicate the low survivability afforded by maneuver against the ATGM with Warhead A at hover flight speeds.

The sensitivity of survivability of the enhanced performance helicopter to variations in ATGM warhead type and lethality is shown in Fig. 7. The three warhead types: contact, proximity Warhead A, and proximity Warhead B, have been examined at the helicopter minimum power required initial speed. The helicopter employs control set I with maximum transient turns for elemental maneuvers (1) and (5) in the optimal strategy development. The nonmaneuver and optimal survivability results for Warhead A are repeated at lower left. Corresponding survivability results for the contact fuzed warhead are shown upper center; those for Warhead B are shown at the lower right. The nonmaneuver results are statistically equivalent in all cases and typify the small miss distances achievable by the missile guidance system against constant velocity targets. The helicopter can be made completely survivable against the contact fuzed ATGM using optimal maneuvering at this initial aircraft speed. However, the corresponding result for Warhead B indicates that optimal maneuver would be completely ineffective. These results indicate the strong interplay between missile warhead lethality and guidance, and the need for carefully timed deployment of the aircraft's maximum maneuver capability to generate adequate miss distances against this threat.

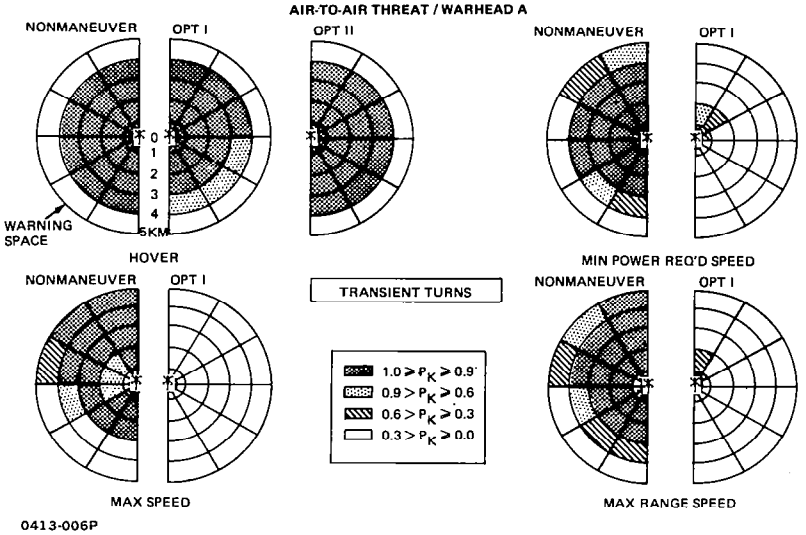

Figure 6. Helicopter Survivability

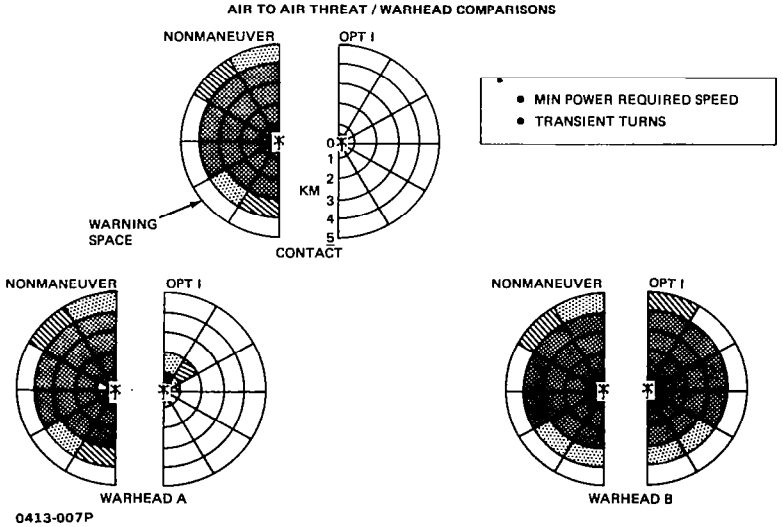

Figure 7. Helicopter Survivability

Three optimal evasive trajectories from hover using maneuver set I against the contact fuzed warhead are shown in Fig. 8. The survivability results for nonmaneuver and optimal maneuver are presented at the upper left of the figure. For each case illustrated, only the terminal portion of the missile path and the entire helicopter path are shown because of scale effects. The head-on case at upper right and beam aspect case at lower right illustrate pedal turns immediately following launch, followed by straight accelerated flight and finally, a maximum performance load factor turn near termination. The tail aspect launch at lower left employs only the acceleration segment followed by the load factor turn at termination. In all cases shown, the aircraft maneuvers to achieve a tail aspect to present its minimal fuselage envelope dimension at missile flyby. Launches within 2 km cannot be made highly survivable because the missile flight time termination is too short to permit adequate forward acceleration and load factor turn maneuvers to avoid fuselage hits.

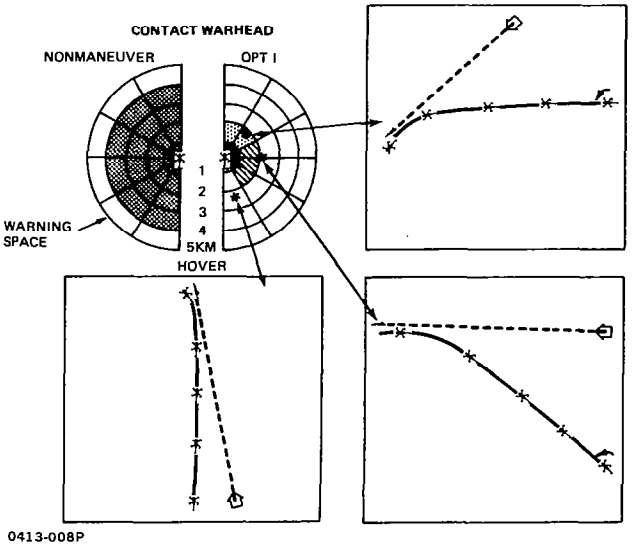

Figure 8. Evasive Maneuvers (From Hover)

Maneuverability in Air-to-Air Gun Combat

This section concerns quantifying the impact of aircraft maneuverability, gun capability and ballistic hardening in air-to-air visual range gun combat effectiveness. Three blue (friendly) helicopter design concepts are separately evaluated against the same red (threat) helicopter. The first blue aircraft, called the baseline, is representative of a current operational attack helicopter design, and the second, an advanced light helicopter concept (LHX) having greater maximum maneuver capability and level flight speed. The third concept aircraft is a variant of the second; employing equivalent maneuverability but with improved ballistic hardening.

Visual Model

The visual model employed in the gun combat studies is displayed in Fig. 9. Each combatant is assumed to have a visual contact volume extending to a maximum range of visual detectability. Within this volume each combatant is permitted to select a maximum performance tactical maneuvering strategy for flight path control of the aircraft. For these studies the maximum range has been arbitrarily set at 3 km for both combatants. This is consistent with line of sight visual capabilities at low altitudes in typical rolling terrains. Aircraft size, paint/camouflage, and background contrast factors have been neglected. A helmet mounted sight operational tracking volume associated with a turreted gun fire control system is also considered as illustrated. Gun firing opportunities exist only when the target is within the tracking volume limits.

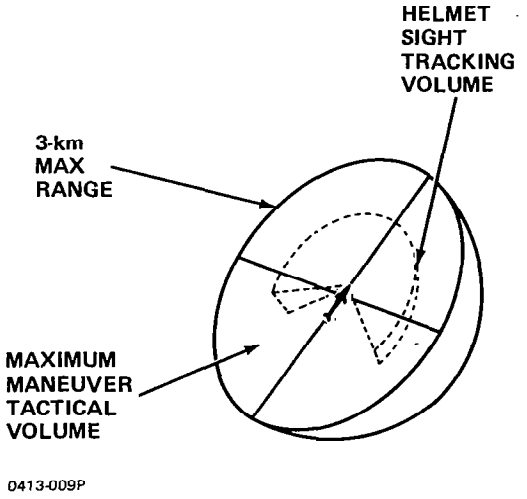

Figure 9. Visual Model

The maximum maneuver volume of each combatant is decomposed into a finite set of tactical contigencies by an assignment of thresholds involving the relative positions, velocities, and other observables during the combat. For the constant altitude maneuvering model, each combatant is assumed to measure relative range, angle off and relative heading as depicted in Fig. 10. Relative range has been divided into 5 cells from zero to 3 km; angle-off into eight 45° sectors from 0° around the compass to 360°; and relative heading divided into the four quadrants as shown in Fig. 10. These thresholds divide the maximum maneuver volume into 160 contingencies for the constant altitude combat case.

Gun Model

Both blue and red aircraft are assumed to be equipped with a turreted gun with target tracking accomplished by a helmet mounted sight. Fire control lead prediction employing target range, range rate, angular rate in flight data together with specific projectile ballistics is

considered in the armament simulation. Depending upon the gun and projectile, a firing opportunity requires satisfaction of the following: target entry into the tracking volume; a "pipper" settle time delay associated with entry; and target range within a prespecified maximum firing range.

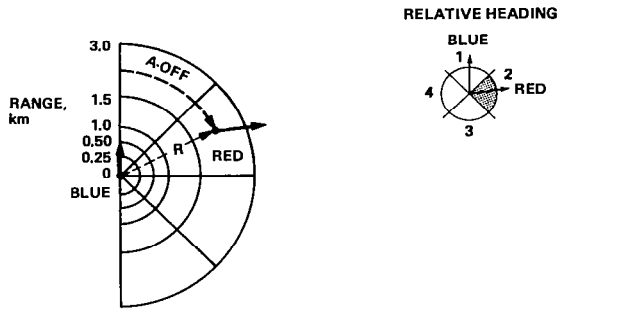

OBSERVABLES	# THRESHOLDS
• RELATIVE RANGE	(5)
• ANGLE OFF	(8)
• RELATIVE HEADING	(4)
• RELATIVE SPEED	(3)
• RELATIVE ALTITUDE	(3)

} CONSTANT ALTITUDE CASE 160 CONTINGENCIES

0413-010P

Figure 10. Maximum Maneuver Volume Thresholds

The probability of kill associated with an N-shot gun burst is developed from single shot considerations as follows:

SINGLE SHOT

$$P_{K_{SS}} = \frac{A_V}{2\pi\,(TERMX \cdot TERMY)^{1/2}} \cdot \exp\left\{-\frac{1}{2}\left[\frac{dx^2}{TERMX} + \frac{dy^2}{TERMY}\right]\right\}$$

- $TERMX = \sigma_D^2 + \sigma_{TX}^2 + \frac{A_V}{2\pi}$
- $TERMY = \sigma_D^2 + \sigma_{TY}^2 + \frac{A_V}{2\pi}$
- A_V GIVEN FOR SPECIFIC VIEWS

N-SHOT BURST

$$P_{K_N} = 1 - (1-P_{K_{SS}})^N$$

In the above σ_D is the dispersion error of projectile; σ_{TX}, σ_{TY} the composite target tracking errors in x, y coordinates; and A_V the ballistic vulnerability of the aircraft to the threat projectile (measured in terms of vulnerable area). Other N-shot vulnerability models (such as the salvo fire model) can easily have been employed in these studies without alteration of the basic methodology but are not reported here. In the computational results to follow both blue and red aircraft were assumed equipped with a 25 mm gun. The respective vulnerabilities of the aircraft are given in Table I for that threat projectile. The areas have been normalized by the numerical value of the vulnerable area in the side aspect for the baseline aircraft. The N-shot burst probability of kill for each combatant is employed at each step in the trajectory numerical integration process to determine the termination event; kill by red, kill by blue, mutual kill, and no kill by either.

Table 1. Aircraft Relative Vulnerability

ATTACK ASPECT / A/C	FRONT	SIDE	REAR	BOTTOM	TOP
BASELINE	.18	1.0	.22	.64	.59
LHX	.25	.76	.27	.71	.72
LHX/VR	.088	.27	.096	.26	.26
RED	.24	.75	.17	.47	.77

Maneuver Strategy Development

The constant altitude maneuver strategy for both combatants employs the elemental maneuver set labled "control set 1" in Fig. 4. The associated maximum maneuver capabilities of the blue and red aircraft are summarized in Fig. 11. The transient response of all combatants to maximum commanded rates or accelerations is represented by a family of first order models as shown at the lower right of Fig. 11. The time constant associated with longitudinal commands is given by TAUPIT; load factor turn commands by TAUROL; and pedal turn commands by TAUYAW.

Each combatant's maneuvering strategy is represented by a choice of an elemental maneuver for each contingency cell of the maximum maneuver volume shown in Fig. 10. The stochastic learning methodology is easily extended to the two combatant case as depicted in Fig. 12. In contrast to the single decision table learning phase described in the missile avoidance application of Fig. 3, a blue and red decision table are now sequentially modified to produce optimal maneuver strategies for both combatants.

Helicopter/Armament System Combat Effectiveness

The one-on-one gun combat problem requires that one determine the domains of combat initial conditions (positions, velocities) for which each of the combatants has a unilateral capability in deciding the outcome of the combat. The comparative size of these domains furnishes a quantitative measure of superiority of one aircraft/armament system over the other. To determine these domains, the computational method is first employed with each side maximizing his kill probability, and secondly, with one combatant maximizing kill probability with the other maximizing survivability. These separate solutions determine domains where each vehicle

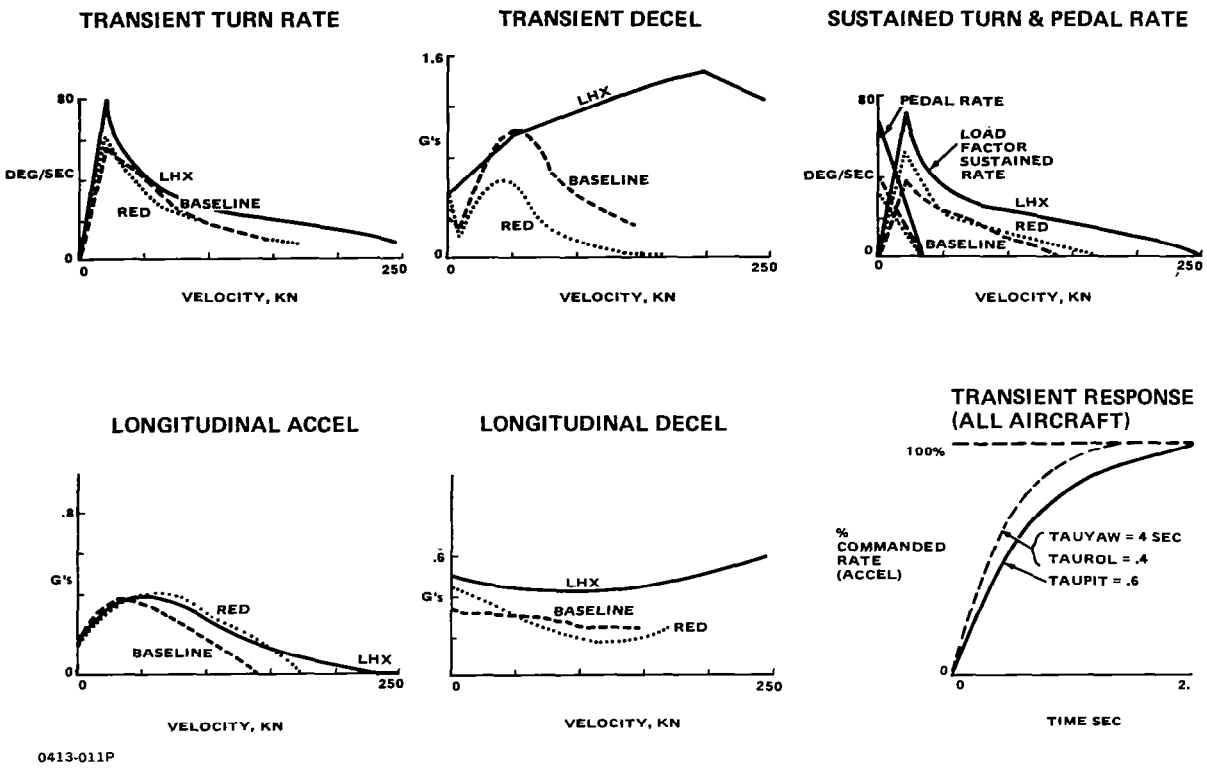

Figure 11. Sea Level Maximum Maneuver Performance

is best operated offensively, and where each should operate defensively with survivability as the main goal.

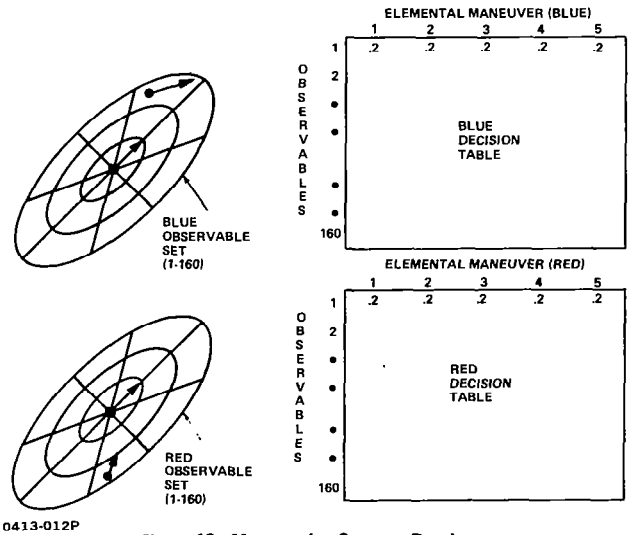

Figure 12. Maneuvering Strategy Development

Each of the offensive/defensive computational results emerging from the stochastic learning solution methodology is presented in terms of a discretized initial condition space centered on the blue combatant as shown in Fig. 13. The probabilities of kill for each combatant and other important terminal statistics are computed for each discretized initial condition region as shown.

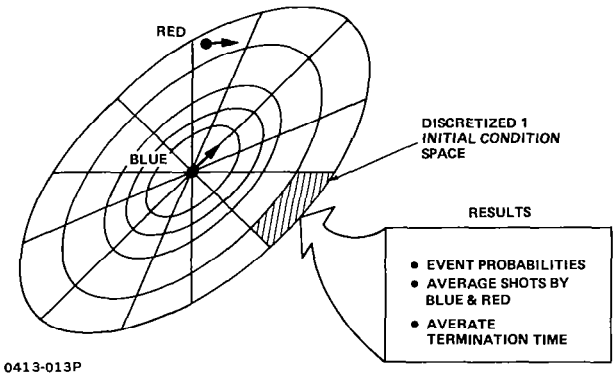

Figure 13. Format for the Computational Results

Two representative computational solutions employing the initial condition polar format of Fig. 13 are given in Figs. 14 and 15. The optimal solution in Fig. 14 considers the case of the blue LHX aircraft in an unarmed defensive role against an offensive red adversary equipped with a 25 mm, 1500 spm turreted gun. This solu-

tion considers combat initial speeds of 87 kn for both combatants with both helicopters employing sustained turn for their load factor turn elemental maneuver choices. The four half-polar charts (due to initial condition symmetry) give the probability of kill for red in terms of relative range, angle-off, and relative heading. The result at upper right corresponds to the coincident heading case, as schematically represented by the B and R vectors in small auxiliary diagram. The remaining three heading cases are interpreted with the aid of the rotated R vector in the auxiliary diagrams. The cells of high kill probability for Red (P_{K_R}) are shaded according to the accompanying legend. The solution in Fig. 15 considers the LHX in the offensive role against an offensive red adversary for the same initial speed case of 87 kn. The LHX is equipped with identical turreted gun armament and fire control as the red helicopter. The initial condition cells of high kill effectiveness are shown for each combatant using the P_{K_B}, P_{K_R} legend as indicated.

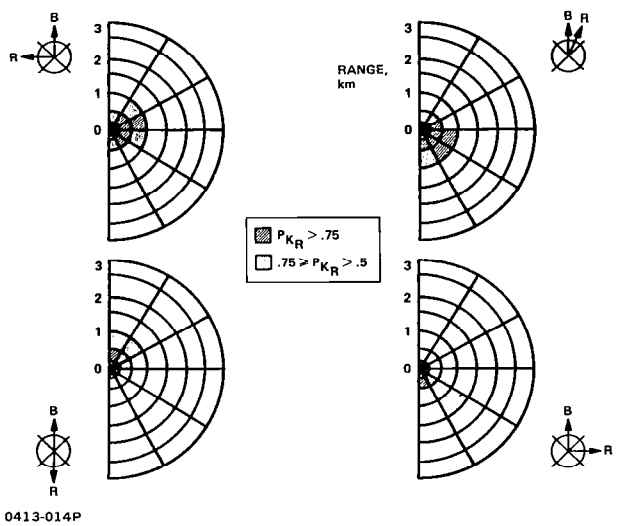

Figure 14. LHX Defensive Solution, 87 kn

A more compact bar summary format enabling convenient combat effectiveness comparisons between helicopter/armament systems is shown in Fig. 16. The total of high kill and mutual kill area for both combatants as a percent of total area within a fixed radius of initial conditions for Fig. 15 is now plotted on the vertical scale at the right. The fixed radius is taken as 1.5 km representative of ranges associated with change encounter initiation of helicopter engagements. The data shown in the circles at top and bottom of the bar graph indicate the average shots/kill achieved by each combatant in the high kill and mutual kill areas. The percent of total initial area dominated by each combatant is a quantitative measure of his combat effectiveness or air superiority.

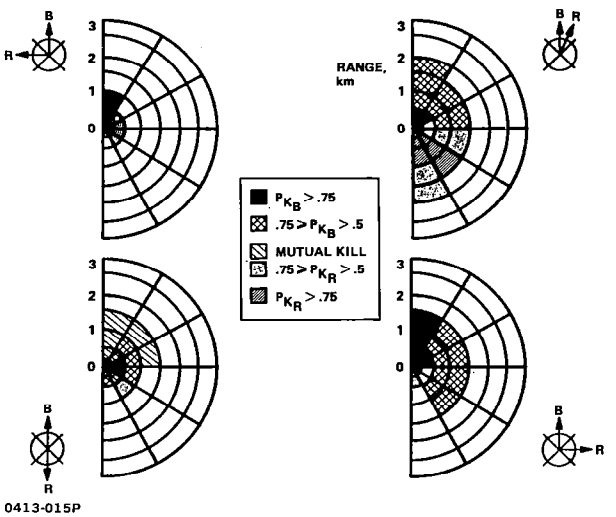

Figure 15. LHX Offensive Solution, 87 kn

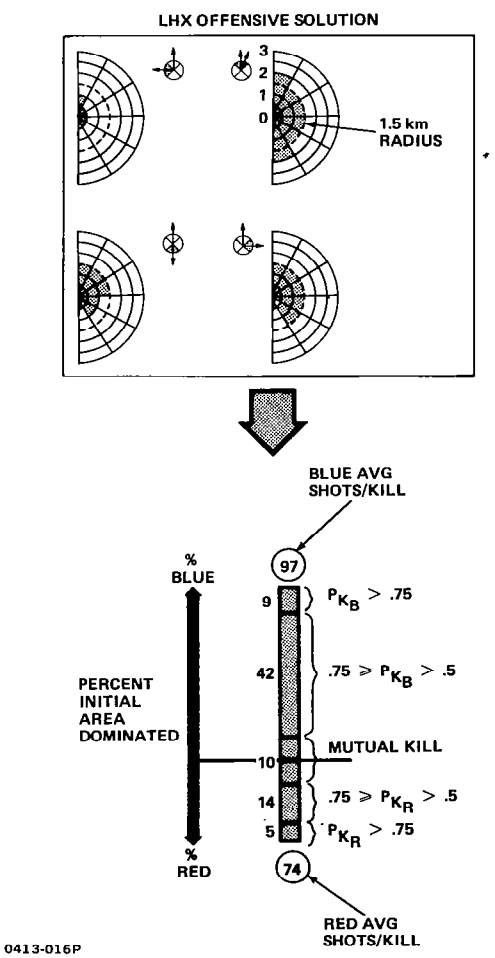

Figure 16. Bar Summary Format

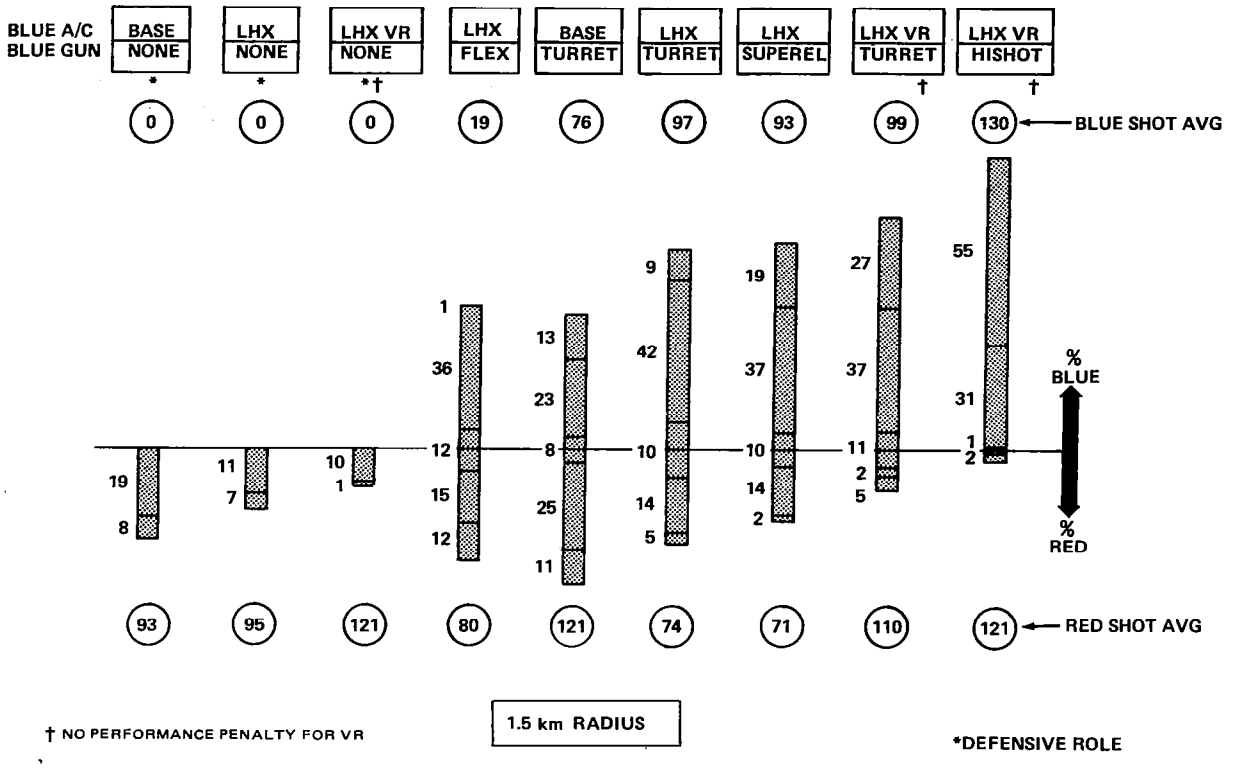

Figure 17. Helicopter/Armament Combat Effectiveness Comparisons

A comparison of combat effectiveness of the baseline and LHX aircraft including variations in ballistic hardening, gun mount, and shot rate characteristics is shown in Fig. 17. All solutions shown are for combat initiated at 87 kn for both combatants with maximum sustained turn capability employed as the load factor turn elemental maneuver choice. The first three bar graphs (from the left) correspond to defensive solutions for various blue helicopters against the offensive red adversary. The red threat employs a 25 mm, 1500 spm, turreted gun with ±90 degree azimuth capability, and +21° and -50 elevation capability. The reduction in red kill effectiveness achieved by the more maneuverable LHX and LHX with ballistic hardening can be compared with the baseline aircraft.

Bar graphs four through nine consider various blue aircraft/armament configurations in an offensive role against the offensive red threat previously described. In the fourth case, labeled (LHX/FLEX) the LHX aircraft was equipped with a limited sweep (±6° elevation and azimuth) gun mount. The composite tracking error in this case was assumed to be σ_{TX} = 6 mil and the projectile dispersion σ_D = 5 mil. The gun caliber and shot rate were assumed equivalent to that employed by the threat. (Note: for all 25 mm turreted gun applications, both blue and red, the composite tracking error was assumed to be σ_{TX} = 20 mil. and the dispersion σ_D = 5 mil). The low shots/kill by blue reflects the smaller ammunition expenditure obtained by the assumed 6 mil error fire control tracking error performance of a limited sweep HUD system.

The fifth column corresponds to the baseline helicopter equipped with the same turreted gun as the red adversary. The % area ratio for measuring dominance is nearly 1:1 against red. The sixth column shows the LHX capability with the same turreted gun against the red threat. The gain in combat effectiveness of the higher maneuverability LHX compared to the baseline is appreciable, but is somewhat offset by the higher ballistic vulnerability of the LHX. Column seven quantifies the gains achievable by the LHX if superelevation of the turreted gun to +50° were permissible (rather than +21° because of rotor clearance). Bar graph eight illustrates the impact of ballistic hardening improvements to the turreted gun LHX. Comparison with the standard LHX results in column six indicates an applicable reduction in the kill effectiveness area of red while improving the % area of highest kill probability (9% improved to 27%). The last column on the right illustrates the high combat effectiveness achieved with a 3000 spm turret gun equipped LHX design incorporating ballistic hardening. These results illustrate the significant interdependence of maneuverability, armament, and ballistic hardening factors for friendly and threat helicopters that enter the combat effectiveness evaluation.

LHX Maneuver Effectiveness

In the design concept phase, it is often important to quantify the sensitivity of combat effectiveness to maneuver parameter variations on a one at a time basis while holding other aircraft and armament parameters fixed. As an example of this, the original sea level maximum longitudinal acceleration parameter of the LHX (labeled LHA A in Fig. 18) was enhanced to that given by the function labeled LHX B. All other maneuver, ballistic hardening, and armament parameters were held fixed. The corresponding improvement in combat effectiveness for the blue offensive/red offensive case for the 87 kn initial speed is shown in Fig. 19. The bar graph on the left is the result originally obtained for the LHX turret case first illustrated in Fig. 17.

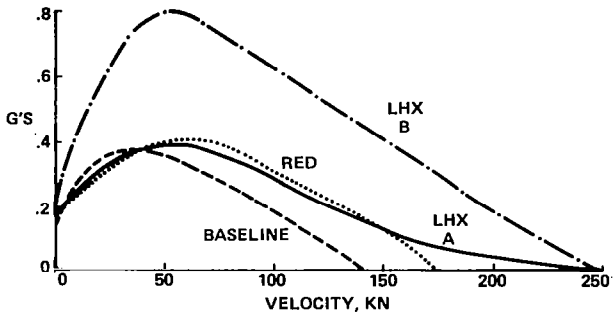

Figure 18. Sea Level Maximum Longitudinal Acceleration Variation

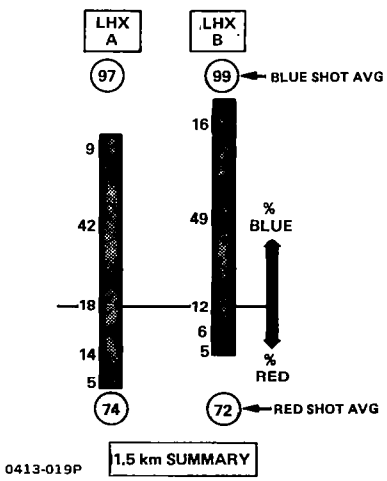

Figure 19. Sensitivity of Combat Effectiveness

Conclusions

This paper has sketched the development and application of a digital simulation technique incorporating optimization and game theory concepts for assessment of combat helicopter maneuver effectiveness in the one-on-one setting. The numerical experience to date suggests that a respectable amount of detail regarding the integrated use of maneuver, threat warning, ballistic hardening, and armament capability can be considered in design studies and that combat effectiveness assessments can be accomplished with reasonable computer time budgets.

Although the results show that combat effectiveness is strongly dependent upon the integrated use of the above factors, a maneuver capability advantage can provide sizable gains in survivability in the defensive role and kill effectiveness in the offensive role. The results presented here have combat maneuvers limited to constant altitude, however, similar computational models which include vertical plane maneuvering are currently under investigation with results available in the near future.

Acknowledgments

The authors would like to thank the following personnel and their organizations for their technical contributions in the development of the helicopter/armament system computer models utilized in these studies:

Mr. J. Means and Dr. L. Feaster; U.S. Army AVRADCOM, St. Louis, MO

Mr. E. V. Merritt and Mr. J. Anderson; U.S. Army AVRADCOM, Ft. Eustis, VA

Mr. P. Townsend and Mr. T. Hung; U.S. Army ARRADCOM, Dover, N.J.

Mr. R. Bruce and J. Wagner; General Electric Co., Burlington, VT

Mr. F. Sobierajski and Mr. H. Hinz; Grumman Aerospace Corp., Bethpage, N.Y.

REFERENCES

1. Issacs, R., Differential Games, John Wiley, New York, 1965

2. Breakwell, J.V. and Merz, A.W., "Toward a Complete Solution of the Homicidal Chauffeur Game", Proceedings of the First International Conference on Theory and Applications of Differential Games, Amherst, Mass., October 1969

3. Baron, S., Kleinman, D., Serben, S., "A Study of the Markov Game Approach to Tactical Maneuvering Problems", NASA Report CR-1979, February 1972

4. Falco, M., Cohen, V., "Strategy Synthesis in Aerial Dogfight Game Models", AIAA 11th Aerospace Sciences Meeting, Washington, D.C., AIAA Paper 73-233, January 1973

5. Falco, M., and Carpenter, G., "Survivability Analysis of Air and Land Vehicles to Missile Threats", 4th Symposium on Vulnerability and Survivability, American Defense Preparedness Association, Tyndall AFB, Florida, March 1979, (and Grumman Research Department Memorandum).

FLIGHT TESTS FOR THE ASSESSMENT OF TASK PERFORMANCE AND CONTROL ACTIVITY

Heinz-Jürgen Pausder and Dieter Hummes
Deutsche Forschungs- und Versuchsanstalt
für Luft- und Raumfahrt e.V. (DFVLR)
Institut für Flugmechanik, Braunschweig, FRG

Abstract

Helicopter flight tests were conducted to look at the influences of pilot and helicopter system on the performance in NOE-flying. A visual dolphin course was built up. The tests were performed with the helicopters BO 105 and UH-1D. Closely connected with tactical demands the six test pilots' task was to minimize the time and the altitude over the obstacles. The data reduction yields statistical evaluation parameters describing the control activity of the pilots and the achieved task performance. The results are shown in form of evaluation diagrams. Additionally dolphin tests with varied control strategy were performed to get more insight into the influence of control techniques. From these test results recommendations can be derived to emphasize the direct force control and to reduce the collective to pitch cross-coupling for the dolphin.

Introduction

The military or civil user of a helicopter primarily emphasizes the demand for a successful completion of his special mission. This requirement is an unsufficiently defined basis for the design efforts of a helicopter system. Therefore the need exists to transform tactical demands in standards of technical terminology. With such diagnostic tool the contractor is thus enabled to check the achieved adaptation of the overall requirement of adequate mission performance during the design phase. Once the helicopter has been built, the question about the qualities of the flying characteristics is also asked. If it doesn't meet the mission demands, the question is: Why not? Consequently flying quality specifications should contain technical scales for a quantitative evaluation and they should set the standards for 1) checking the tactical missions demands, 2) transforming these demands in measurable data, 3) proving the efforts during the design phase, and 4) a quantitative evaluation during the certification phase.

Nevertheless, the specification MIL-H-8501 A[1] is valid still nowadays. The basis of these requirements was constituted of simulation and flight test results performed in the Fifties. The development in the field of helicopter design which happened during the last two decades has not been taken into consideration. Implementing rotors with non-hinged blades and divergent flying characteristics of the helicopter pointed out that the application of the specifications can yield wrong conclusions. Although the requirements could not be met, acceptable flying qualities have been inferred from pilot evaluations.[2]

As a consequence of these discrepancies several attempts have been made to revise the specifications. The specification MIL-F-83300[3] was published for V/STOL-systems. Closely following the structure and format of the specification for conventional aircraft, the different demands of maneuvers are considered by coordinating requirements to three categories of flight phases. MIL-F-83300 attempted to include the helicopter systems, but the essential criticism of its application for helicopters implies that the specific problems of helicopter flying qualities and helicopter missions are not taken into account sufficiently.

The application of helicopters are greatly extended. This includes the expansion of mission types, and the specific demands of mission phases. In Fig. 1 typical mission parts are skeletonized as they are presently being discussed in the F.R.G.:

1) Anti tank.
2) Combat rescue.
3) Air to air.

The mission phases can be characterized by the required low altitude above ground and by the flight speed. Demanding of the pilot/helicopter system to use the terrain as cover against exposure and to obtain superiority in direct contact with the enemy high agility is required of helicopter system. Current specifications for flying qualities regarding the demands of such specific missions phases don't exist. Alternatively an assessment of adequate flying characteristics can be performed due to pilot evaluations given in flight or simulation tests. But this approach doesn't get rid of the urgent problem of formulating requirements for flying qualities in parameters. Those can be registered by measurements and can be applied to a certification as evaluation scales.

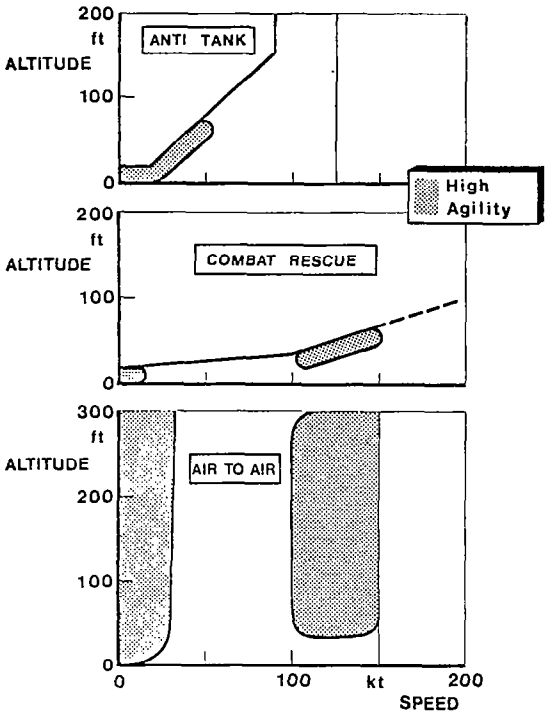

Fig. 1 Helicopter missions

Primarily, the objective of flight mechanical investigations is to constitute a data base for deriving recommendations for flying quality criteria. The different tactical mission demands of today require a mission- and task-oriented adaptation of the evaluation. In several institutions activities exist with this objective.[4],[5] At the Institute for Flight Mechanics of the DFVLR a technical approach was also developed with the overall objectives as follows: 1) to investigate task-oriented flying qualities; 2) to constitute a flying qualities data base for the assessment of quantitative requirements for helicopter systems.

DFVLR Evaluation Method

In this paper a brief review of the DFVLR evaluation method shall be given. More details are presented in Ref. 6. The ulterior motive is the correlation of pilot ratings from flight tests with parameters obtained by a statistical analysis of measured data. The statistical parameters, which include a good correlation with the ratings, are collected in the data base.

Fig. 2 shows the general approach. Starting from a given mission, elements are selected which are representative for this mission and which include the demands which are critical for a flight mechanical

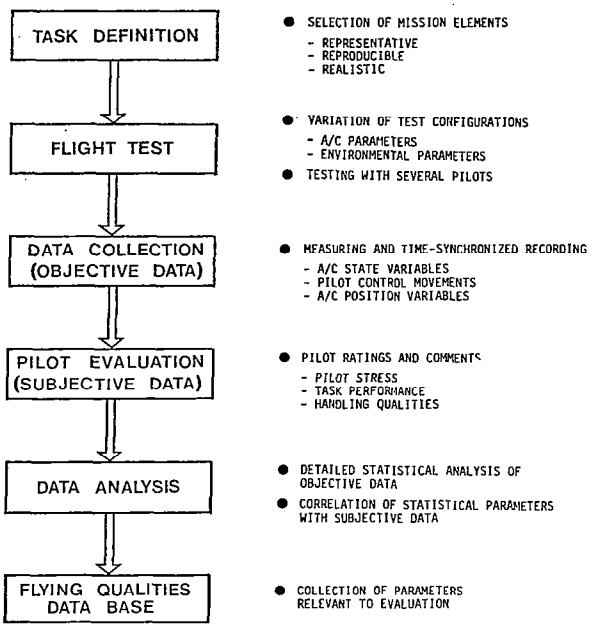

Fig. 2 Evaluation approach

evaluation. The statistical analysis of the test data calls for a definition of the flight test task that allows a reproducable test performance. This includes clear instructions of task conditions and test objectives for the test pilot. On the other hand, the test conditions should as much as possible correspond to the realistic conditions of the selected mission element. In order to obtain a broad data base, the test configurations are varied. This can be achieved by variation of:

1) Helicopter characteristics.
2) Environmental conditions.

In order to register and eliminate the individuality of the pilots, several pilots should be engaged in the tests.

The following data are measured and recorded: 1) state variables of the helicopter, 2) control inputs of the pilot, and 3) position variables of the helicopter. One test is composed of a number of runs with equal conditions. Additionally the pilot ratings and comments are collected of each test. The applied rating scale corresponds to the Cooper-Harper scale[7], but it is slightly modified by dividing them into three groups of questions referring to the workload of the pilot, the task performance and the handling qualities of the helicopter. This yields a redundancy of the ratings. By adding the pilot comments the interpretation of the ratings is facilitated more.

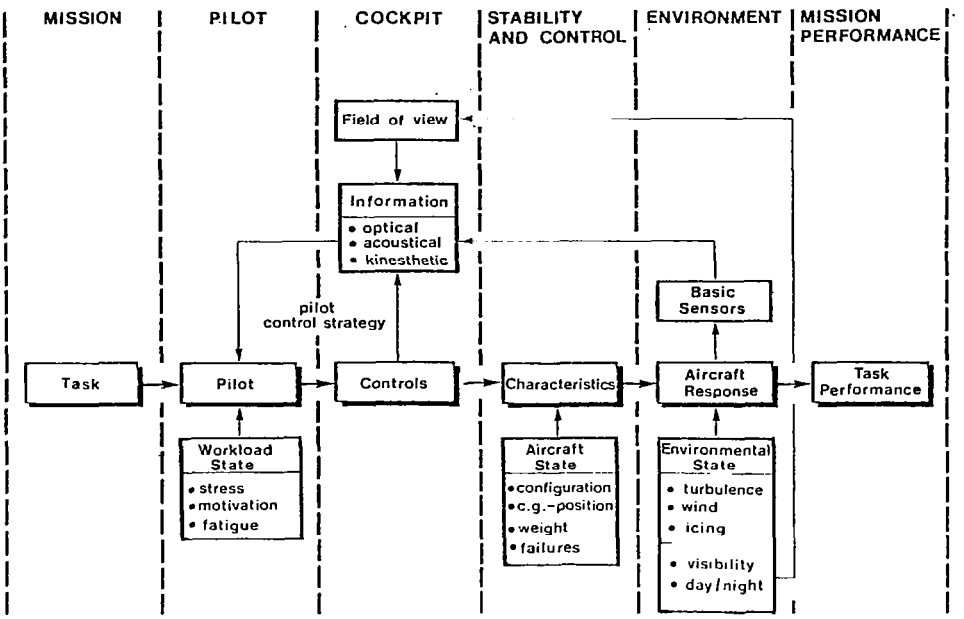

Fig. 3

Factors influencing pilot/helicopter system performance

In a detailed statistical analysis the measured data are then reduced to parameters characterizing the dynamic behaviour of the closed-loop system. By correlating the pilot ratings and comments with the statistical parameters the relevance to the evaluation is being checked. Parameters with high correlation to the ratings are collected in the flying qualities data base.

Influence Factors

The task performance and the control activity depends on various influences, described in the pilot-in-the-loop diagram of Fig. 3. Proceeding from the defined flight task, the elements of the loop with partly time dependent characteristics are passed through to get the task performance as the result. The main influence factors result form the pilot and the helicopter system.

The pilot transfers the task instructions in a conception of an adequate task performance as reference for the system performance achieved in the test. The human pilot adapts to the task, the characteristics of the helicopter and the subsystems, and the environmental state by means of a control strategy appearing optimal to him. In doing so, he profits his high capability of adaptation. The handling qualities of the helicopter system represent the limitations for the pilots adaptation. The feedback to the pilot with different types of information includes influences intensifying with extreme environmental states and technically displayed information.

To define the conditions of flight testing and to interpret the test results, those many influence factors have to be taken into consideration. This involves 1) a well defined test task, 2) clear pilot instructions, 3) a qualified selection of test pilots, 4) well defined environmental conditions, and 5) a definition of helicopter state and pilot information.

Description of Experiments

Evaluation Task

The starting point for the DFVLR studies was the German anti tank mission. This mission includes phases with high portions of precise hovering, quick stop maneuvers and flying near the ground making use of the terrain as a cover. With close reference to the tactical demands, the DFVLR evaluation tasks were defined (Fig. 4). First studies were conducted with a hovering tracking task.[8,9]

For the dolphin task a course was built with two obstacles, as shown in Fig. 5. The distance between the obstacles was 350 m. The run started 200 m before the first obstacle and ended 200 m behind the second obstacle. The obstacles had an altitude of 15 m. They were built up as to put the pilot into a - as much as possible - realistic situation which he has to deal with. For safety aspects the last 3 m are consist of bushes. The centerline of the course is marked on the ground to fa-

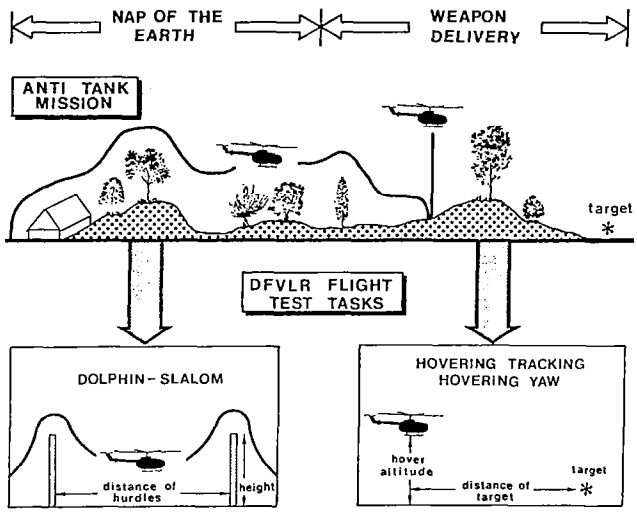

Fig. 4 Definition of evaluation tasks

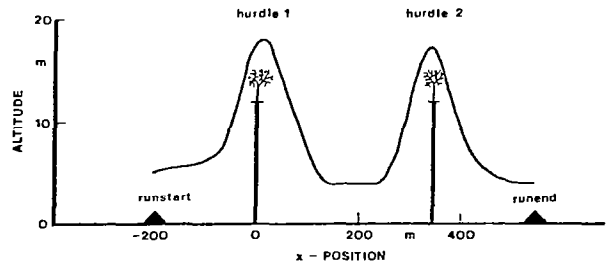

Fig. 5 Dolphin course

cilitate the heading for the pilots. In the dolphin tests, the pilots are instructed to traverse the course while minimizing the time and the altitude over the obstacles. The altitude of entering and finishing the course is 15 ft over ground and the pilots have to align the helicopter on the 15 ft altitude between the obstacles if possible. The speed was defined in the test conditions and had to be flown in the beginning, between the obstacles and at the end of the course. Deviations of heading, lateral position, and bank attitude was to be avoided.

To study the influence of control strategy the task is slightly varied. The pilots have to perform the course at first with a control combination of the pilot's concept, secondly with using only stick inputs and thirdly using primarily collective inputs and the longitudinal cyclic for minimizing the pitch attitudes due to coupling.

Flight Tests

The flight tests were conducted with the helicopters BO 105 of the DFVLR and UH-1D of the German Forces Flight Test Center (Fig. 6). Different test configurations were achieved by varying the test parameters speed and gross weight. Table 1 shows the test matrix for the dolphin test with the BO 105.

Table 1. Test configurations dolphin

	Gross weight	
Speed	G_{min}	G_{max}
40 kt	X	X
60 kt	X	X
80 kt	X	X
100 kt	X	X

In order to obtain a broad spectrum of pilot's behaviour, six test pilots were involved (3 of the Flight Test Center, 1 of the DFVLR and 2 tactical test pilots of the Army). The control strategy tests were performed with both helicopters and three test pilots. Table 2 reviews the configurations.

Table 2. Test configurations control strategy

	BO 105/UH-1D (G_{min})		
Speed	Comb. control	Cyclic control	Collect. control
40 kt	X	X	X
60 kt	X	X	X
80 kt	X	X	X
100 kt	X	X	X

The testing procedure was always the same to guarantee reproducable test results. After explaining the objectives the task instructions were given to the pilot. Although all pilots were experienced in NOE-flying, sufficient time was given to them to train the course. Subsequently, each test was conducted by flying seven isolated runs of the same kind. A quicklook was installed in the ground station to control the training and the test.

Data Acquisition

After each test, the pilot had to answer a questionnaire relating only to the test performed. The questions concerned the

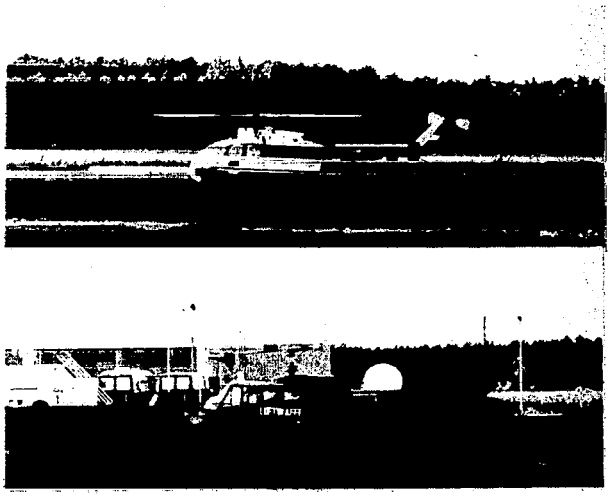

Fig. 6 Test helicopters

pilot workload, the quality of task performance and the handling qualities. In addition to that the pilots commented on the reasons for their ratings. The data acquisition was provided by an analog magnetic tape recording in the ground station. Recorded variables included control inputs, attitudes, rates, accelerations, air speed, altitude, torque and rotor speed. The helicopter position data relativ to the obstacles was measured by a laser position tracking system and was recorded time synchronized with the helicopter state and control data. To register these data in the helicopter and to transmit them to the ground a programmable multipurpose instrumentation system was used.[10] The concept made it possible to reach a quick adaptation to the test technique (helicopter type, direction of flight). The data were digitized online in the ground station and were available for data analyzing, sampled with a frequency of 20 Hz.

Discussion of Dolphin Results

The pilot ratings of the task performance and handling qualities are compared with the ratings of workload as shown in Fig. 7. There are clear differences of up to three points between the ratings evaluating the handling qualities and the workload with the tendency to give the handling qualities a better rating. Applying the original Cooper-Harper scale a close relation is suggested between the demand on the pilot and the aircraft characteristics. Indeed, the precondition for this assumption is observing exactly a tentatively defined task performance. In more complicated flight tasks as the dolphin, the pilots yield a variation of performing the task. In this way, the ratings for the handling qualities are influenced too. This behaviour also accounts for the good

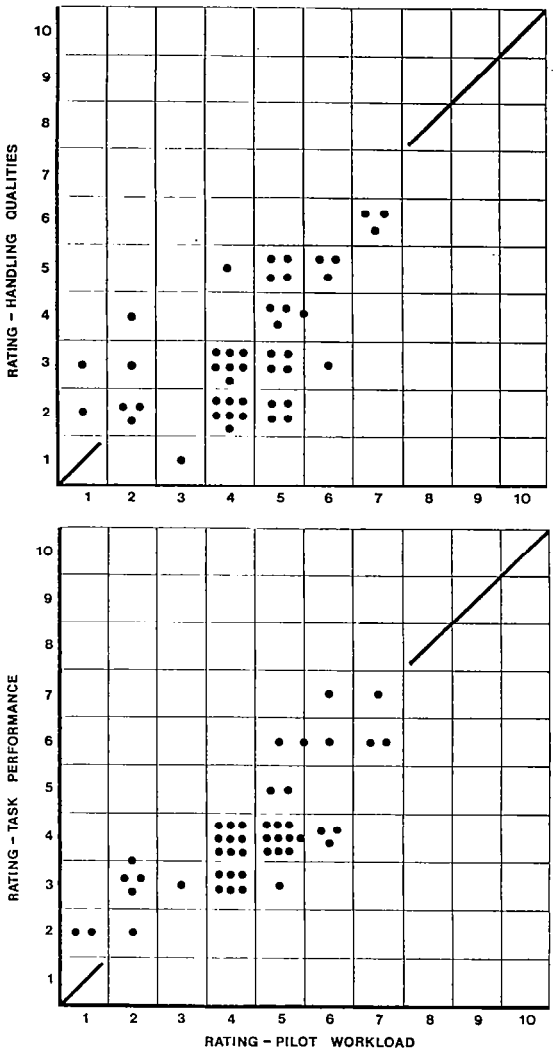

Fig. 7 Pilot ratings of dolphin tests

correlation between the ratings for the workload and the task performance. The pilot will give high ratings, if he doesn't come up to the wanted system performance in spite of high effort.

The information content of the signal data are summarized for each run by the statistical analysis. The run parameters are checked with a confidential test and averaged for each flight test. By correlating the statistical parameters with the ratings of the pilot's workload, the evaluation parameters are determined. They are as follows for the dolphin tests:

1) Sum of the standard deviations of longitudinal and collective control inputs (control activity).

2) Time integral of altitude over the obstacles (evaluation area).

3) Peak-to-peak value of pitch attitude.

4) Peak-to-peak value of acceleration in z-direction.

Table 3. Correlation of parameters with pilot ratings for workload

Evaluation parameter	Pilot 1	2	3	4	5	6
Evaluation area	.72	.11	.60	.56	.79	.63
Peak to peak pitch attit.	.62	.89	.22	.20	.87	.20
Peak to peak z-acceler.	.57	.78	.74	.86	.96	.84
Control activity	.51	.48	.10	.67	.85	.03

Table 3 shows the correlation coefficients. Divergences exist between the pilots. The reasons for low correlation values are the pilot hasn't altered the parameter with speed and gross weight and/or the relationship between parameter and rating isn't linear.

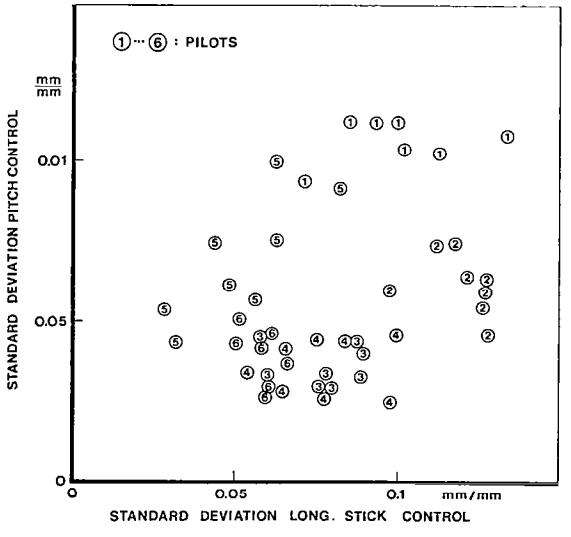

Fig. 8 Control strategies of pilots

Adapting the dolphin instructions, the pilots choose a control strategy characterized by a combination of the main controls longitudinal cyclic and collective. Deviations in state and position due to coupling are compensated with the other controls. Fig. 8 shows the control strategy depending on the pilot. Pilot 1 tends to a relative high activity in the collective, while pilot 2 flies the dolphin with high longitudinal control inputs for example. Fig. 9 points out the tendencies of standard deviations of controls with speed. The pilot's behaviour in the control strategy illustrates the broad spectrum of pilot adaptation.

The influence of the pilots also affects the resulting system performance. The levels of accelerations obtained in the tests have a linear dependency on the speed. The peak-to-peak of pitch attitude and the evaluation area parameter includes the divergent weighting of the pilots for flying the dolphin. While some pilots keep the evaluation area constant this parameter increases with speed for the others. The pilots influence upon the pitch attitude values seems to be still higher. Depending on the pilot the attitude level increases, decreases or keeps constant.

The test results of all pilots can be summarized in the evaluation diagrams. The relation between the control activity and the evaluation area as the main task performance parameter is shown in Fig. 10. The pilot ratings describe clear tendencies for the defined evaluation scales. Accordingly evaluation boundaries are inserted in the diagrams. The ratings deteriorates with increasing evaluation area and the pilots have experienced a higher workload. With area values over the additionally drawn boundary the pilots have substantiated their workload with minimizing the time and altitude over the obstacles. Relative to the control activity there exists an evaluation optimum. A relation between evaluation and the separated activity in the controls can't be constituted. The causes for the disorientation of some test results in Fig. 10 are due to the values of other parameters (see Fig. 11 and 12). With higher levels of pitch attitude the workload of the pilots increases, because high attitudes render more difficult the orientation of the pilots in the course. The reasons for the relative good ratings of pitch levels higher than 40 deg are high accelerations. Moreover the pilots mentioned acceleration levels over 1.6g as a reason of their workload in the comments. But also lower accelerations influence the pilot ratings workload.

Summarizing the evaluation diagrams characteristics of the helicopter systems

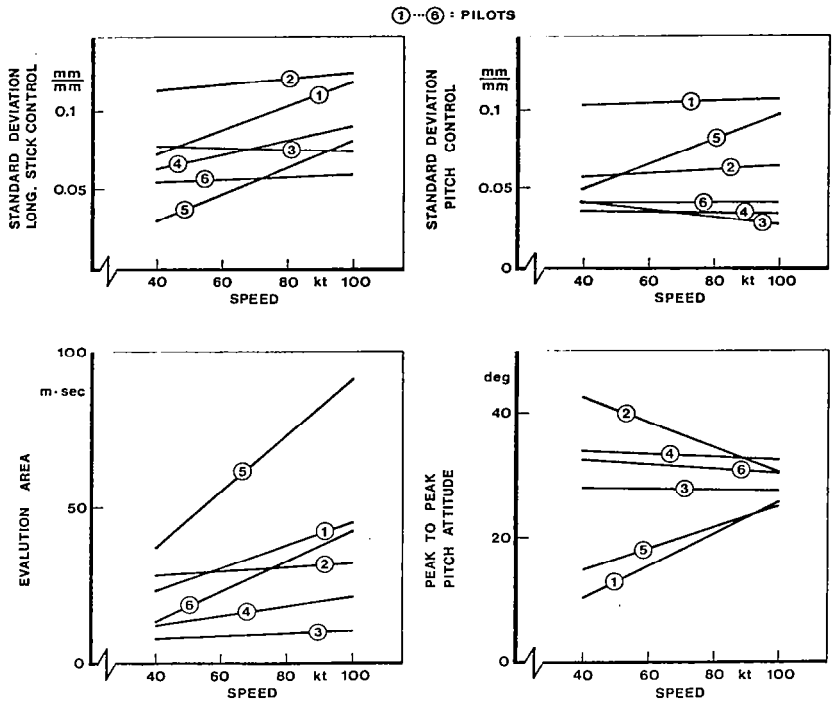

Fig. 9

Tendencies of evaluation parameters

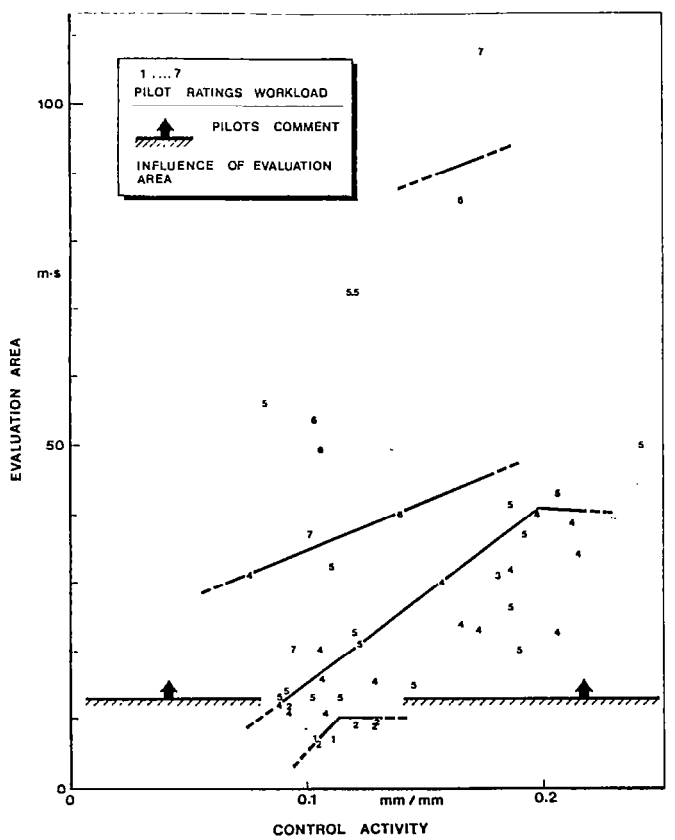

Fig. 10

Pilot rating trends with control activity and evaluation area

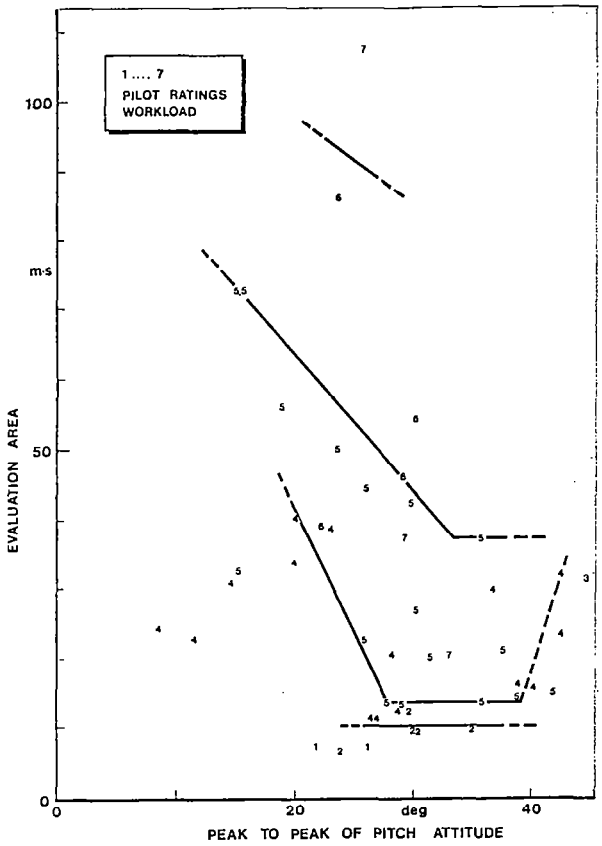

Fig. 11 Pilot rating trends with pitch attitude and evaluation area

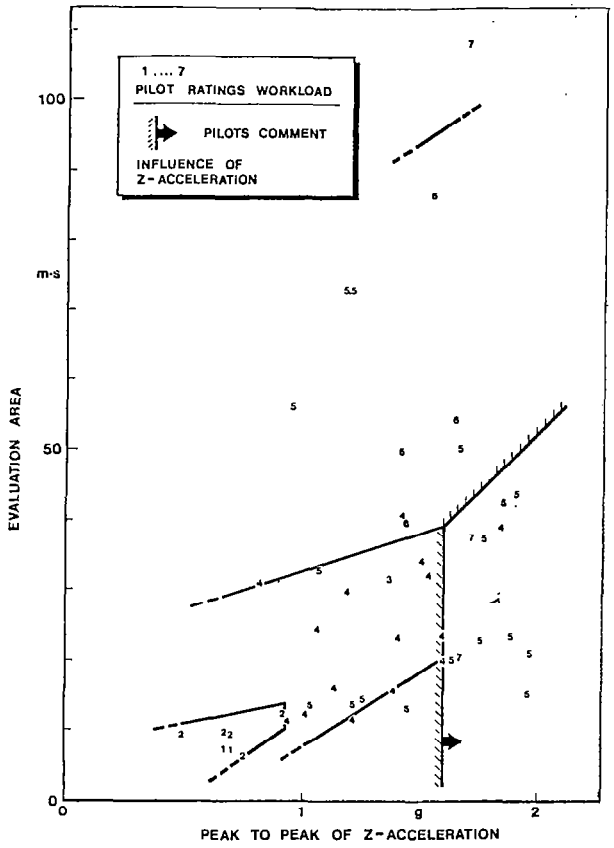

Fig. 12 Pilot rating trends with z-acceleration and evaluation area

can be recommended related to the flown task. Independent of the helicopter state, the fulfillment of the dolphin task should be possible for a satisfactory evaluation: 1) with low altitudes and short times above the obstacles (evaluation area lower than 3 m·sec), 2) with a maximum level of z-acceleration of $\pm$ 0.45 g, and 3) with a low level of pitch attitude. For the necessary control activity an optimum exists, but a separated influence of longitudinal cyclic and collective controls can't be achieved by the test results.

Discussion of Control Strategy Results

The objective of the additionally conducted control strategy tests is to assess the influence of different control combinations on the task performance in the dolphin. More than that the NOE-flying must give an answer to the question whether a moment control or a force control of helicopter offers the better technique to fly closely over obstacles. As mentioned above the task includes three control strategies:

1) Combination of longitudinal stick and pitch control.
2) Stick control.
3) Primarily pitch control.

As an example Fig. 13 shows test data of the BO 105. The curves give an impression of the signal contents in amplitude and dynamics. The cross correlation of control and a/c state signals is evident.

The realization of the defined strategies by the pilots is skeletonized in Fig. 14 and 15. All test configurations were feasible for the pilots and were accepted after sufficient time of exercise with the exception of the 40 kt stick configuration of the UH-1D. When comparing the helicopters it was noted that in the UH-1D tests the pilots used higher collective inputs, especially for the stick configuration. The UH-1D requires a lower stick activity on account of the lower collective to pitch cross-coupling. For the BO 105 the coupling

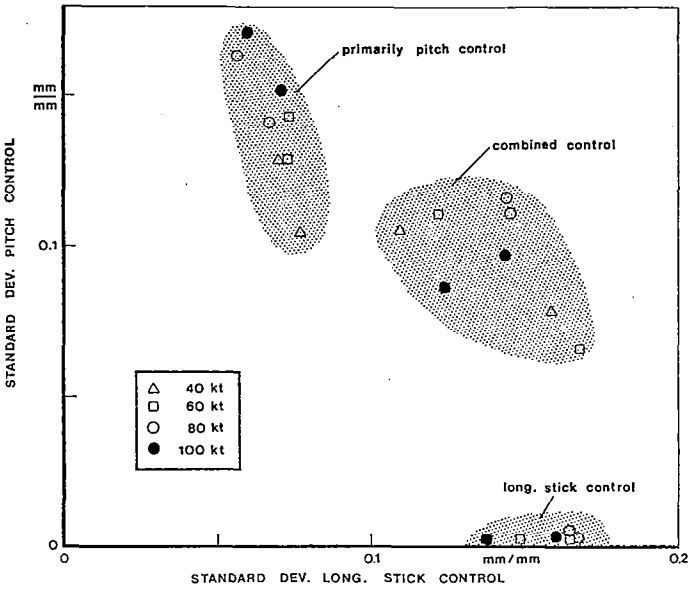

Fig. 15

Control strategy verification (UH-1D)

is nearly doubled with the speed from 40 to 100 kt. Two pilots tried to compensate this behaviour with appropiate longitudinal cyclic inputs.

To evaluate the achieved task performance the resulting parameters are drawn versus the ratio of the standard deviations for collective and longitudinal cyclic. Fig. 16 and 17 summarize the test results. All parameters show quite the same tendencies with increasing of control ratio except the deteriorating values of pitch attitude and evaluation area for extreme high pitch to stick control ratio for the BO 105 due to coupling.

To derive recommendations from these results for the helicopter system the dolphin task can be performed in a better way with emphasis on collective control that means direct force control consequently. Naturally a decrease of the collective to pitch cross-coupling is assumed. This can be mainly achieved by the design compromise of the rotor system or by additional feedback systems. Carrying out the dolphin task with high control moment capacity is not adequate, but produces relative higher values of attitude, acceleration, and evaluation area. For the application and adaptation of a direct force control additional studies including engine dynamics have to be performed.

Conclusions

A test and analysis technique has been developed at DFVLR and has been proven as a valuable tool for the evaluation of closed loop flying qualities with regard to the mission. This technique has been applied to a dolphin task that is derived from the German Anti Tank Helicopter mission. From the test results the following general tendencies and conclusions are noted:

1) The described method leads to an acceptable assessment of task performance and control activity.

2) The combinations of the parameters yield flying qualities recommendations for helicopters related to the dolphin task.

3) The parameters for a quantitative evaluation are the evaluation area, the level of pitch attitude, the level of vertical acceleration, and the activity in longitudinal and collective control.

4) With emphasis on collective control (direct force control) the dolphin task can be performed in a better way. Therefore a low collective to pitch cross-coupling is necessary.

References

1. "Helicopter Flying and Ground Handling Qualities; General Requirements for Military Specification", MIL-H-8501 A, Sept. 1961.

2. Reichert, G., and Delker, P., "Handling Qualities with the Bolkow Rigid Rotor System", Paper No. 218, American Helicopter Society 24th Annual Forum, Washington, D.C., May 1968.

3. "Flying Qualities of Piloted V/STOL Aircraft; Military Specification", MIL-F-83300, Dec. 1970.

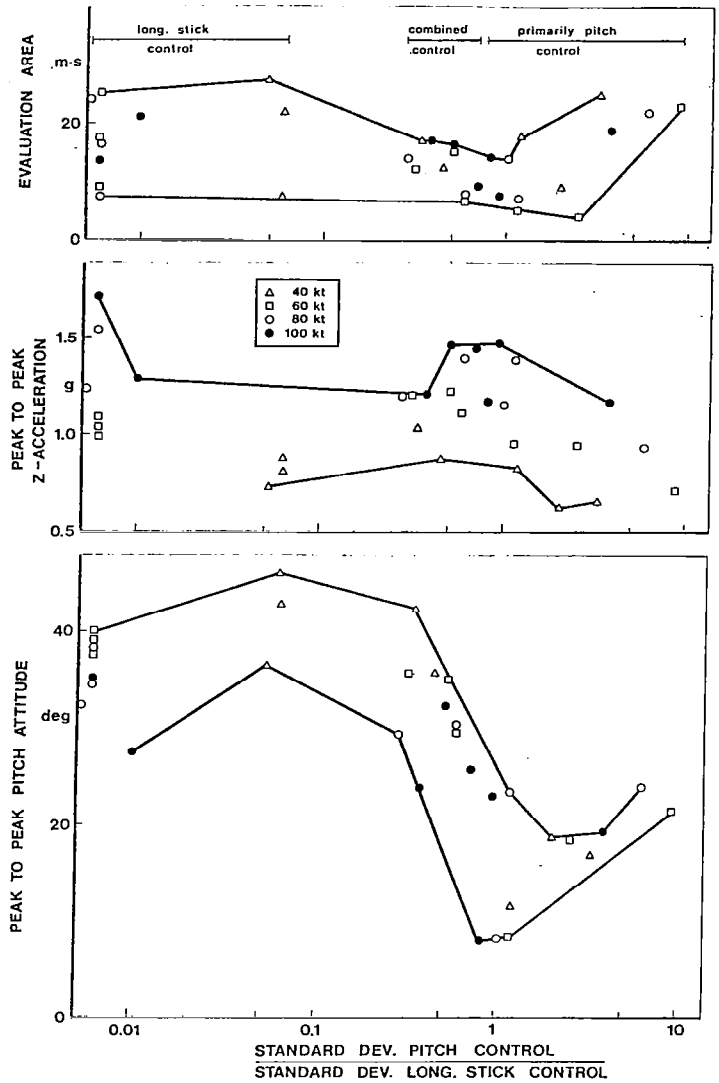

Fig. 16 Effect of control ratio on evaluation parameters (BO 105)

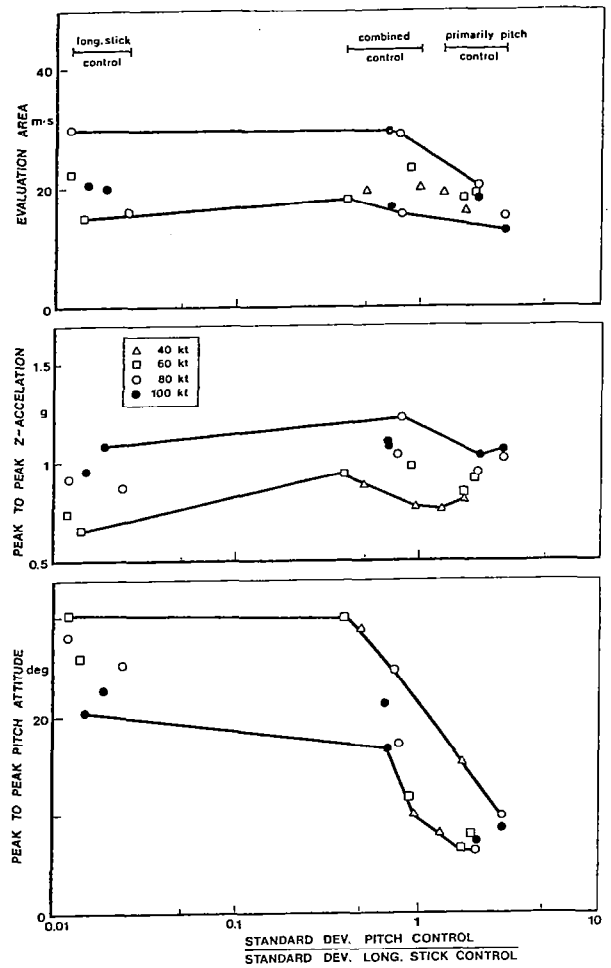

Fig. 17 Effect of control ratio on evaluation parameters (UH-1D)

4. Corliss, L.D., and Carico, G.D., "A Preliminary Flight Investigation of Cross-Coupling and Lateral Damping for Nap-of-the-Earth Helicopter Operations", Paper No.81-28, American Helicopter Society 37th Annual Forum, New Orleans, La, May 1981.

5. Tomlinson, B.N., and Padfield, G.D., "Piloted Simulation Studies on Helicopter Agility", Paper No. 30, 5th European Rotorcraft and Powered Lift Aircraft Forum, Amsterdam, The Netherlands, Sept. 1979.

6. Pausder, H.-J., and Gmelin, B.L., "Flight Test Results for Task Oriented Flying Qualities Evaluation", Paper No. 80-29, American Helicopter Society 36th Annual Forum, Washington, D.C., May 1980.

7. Cooper, G.E., and Harper, R.P., "The Use of Pilot Rating in the Evaluation of Aircraft Handling Qualities", AGARD Report No. 567, April 1969.

8. Sanders, K., Pausder, H.-J., and Hummes, D., "Flight Tests and Statistical Data Analysis for Flying Qualities Investigations", Paper No. 56, 6th European Rotorcraft and Powered Lift Aircraft Forum, Bristol, England, Sept. 1980.

9. Gmelin, B.L., and Pausder, H.-J., "The Impact of Helicopter Flight Mechanics on Mission Performance", AGARD-CP-313, Paris, France, April 1981, pp. 15-1-15-14.

10. Karmann, R., "Programmable Multipurpose Flight Test Instrumentation System", AGARD-CP-299, Geilo, Norway, Oct. 1980, pp. 22-1-2213.

A HELICOPTER HANDLING-QUALITIES STUDY OF THE EFFECTS OF ENGINE RESPONSE CHARACTERISTICS, HEIGHT-CONTROL DYNAMICS, AND EXCESS POWER ON NAP-OF-THE-EARTH OPERATIONS

Lloyd D. Corliss
U.S. Army Aeromechanics Laboratory
U.S. Army Research and Technology Laboratories (AVRADCOM)
NASA Ames Research Center
Moffett Field, California

Abstract

A ground-based simulation study was conducted on a large-scale motion simulator to study the effects in the vertical axis of engine response characteristics on handling qualities for a nap-of-the-earth (NOE) operating environment. This study concentrated specifically on the helicopter configuration with an rpm-governed gas-turbine engine and expands previous work by focusing on aspects peculiar to rotary-wing and NOE operations. A wide range of engine response time, vehicle damping and sensitivity, and excess power levels was studied. The data are compared with the existing handling-qualities specifications, MIL-F-83300 and AGARD 577, and in general show a need for higher minimums when performing such NOE maneuvers as a dolphin and bob-up task.

Nomenclature

K_n, K_u, K_e, K_1, K_2 $K_{PT}, K_P, K_R, K_T, K_q, \tau_e, \tau_p$	engine parameters (see Fig. 3)
N_1	engine gas generator speed, rpm
N_{11}	engine power turbine speed, rpm
NOE	nap-of-the-earth
PR	Cooper-Harper pilot rating
Q_{lim}	maximum torque, ft-lb
Q_{PT}	power turbine torque, ft-lb
Q_{ra}	torque required, ft-lb
T_{main}	thrust, main rotor, lb
T/W	thrust-to-weight ratio
Z_w	vertical damping, sec^{-1}
$\bar{Z}_w$	equivalent vertical damping, sec^{-1}
Z_{w_a}	aerodynamic vertical damping, sec^{-1}
$Z_{w_{fus}}$	fuselage vertical damping, sec^{-1}
$Z_{w_{inflow}}$	inflow vertical damping, sec^{-1}
Z_{w_s}	stability augmentation vertical damping, sec^{-1}
Z_{δ_c}	collective sensitivity g/in
ΔT	pure time delay, sec
ζ	damping ratio
τ_{eng}	equivalent first-order engine time-constant, (engine response time), sec^{-1}
τ_T	thrust time constant, sec^{-1}
Ω	rotor speed, rad/sec
ω_F	fuel flow, lb/hr
ω_n	second-order engine frequency, rad/sec

Introduction

The potential for improving helicopter flying qualities through the use of electronic fuel-control devices on helicopter gas turbine engines has led to a renewed interest in the study of coupling effects due to engine dynamics on the vehicle height and yaw responses. An understanding and quantification of these engine coupling effects is essential for the successful exploitation of the use of such controls. It is equally important to determine excess power requirements for specific tasks such as those pertaining to nap-of-the-earth (NOE) operations.

Early studies in the area of VTOL flying qualities[1-3] have provided a foundation for understanding fundamental effects such as the thrust response time-constant and excess power requirements. These studies involved ground-based simulation experiments that considered the near-hover tasks of station-keeping and rapid ascent and descent. Later studies[4,5] expanded this work to consider the coupling effects of thrust response

time with vertical velocity damping. These studies — together with the results of Ref. 6, which considers vertical damping only — form the basis for the vertical-axis handling-qualities specifications found in MIL-F-83300 and AGARD 577.

Reference 7 provides a good summary of the above studies and criteria; however, it is important to preface that those engine coupling studies considered a fixed wing VTOL (aircraft) for which the engine response time (τ_{eng}) and thrust response time (τ_T) were the same as depicted in Fig. 1. Such is not, in general, the situation for a rotary-wing aircraft with an rpm-governed rotor response, as shown in Fig. 2. This thrust response is influenced by a combination of the energy stored in the rotor, engine governor response, and the $\dot{h}$ damping resulting from rotor inflow. Thus, while the engine response of Fig. 2 may be simplified to a first-order time constant, the thrust response, as a rule, cannot be. Reference 8 does, in a limited sense, address this problem; however, what is needed is a review of the existing criteria and of the appropriateness of these requirements for rotary-wing vehicles. It is also essential that specific mission tasks be addressed (e.g., NOE operation) so that the criteria may be more directly applied to the design of modern military helicopters.

This paper describes a ground-simulation experiment that considered a wide range of engine response times and a wide range of vehicle vertical damping and collective control sensitivities for a helicopter model powered by an rpm-governed gas turbine engine. Several levels of available engine torque were also evaluated. The tasks performed were the NOE tasks of dolphin, quick-stop, and bob-up, and the study was performed on the Ames five-degree-of-freedom Vertical Motion Simulator (VMS) that used a model terrain-board visual system. An aural cueing system was used which provided the pilot with the sound of rotor overspeed and underspeed, blade slap, and transmission noise, and was based on an approach used in Ref. 9. The real-time simulation mathematical model consisted of a nine-degree-of-freedom helicopter model coupled to a simplified engine model, which included the first-order dynamics of the governor, gas generator, power turbine, and rotor/transmission inertias. The data obtained for this experiment are compared with previous studies and, where possible, with the existing criteria.

Description of Experiment

A requirement for this study was the development of a real-time engine model and the establishment of a meaningful task. The test matrix consisted of variations in the vehicle z-axis dynamics (Z_w, $Z_{\delta c}$), the engine response dynamics (ζ, ω_n), and available torque or excess power (T/W max); the remaining vehicle characteristics were unchanged. The vehicle simulated was an 8000-lb, two-bladed teetering-rotor helicopter, sufficiently augmented to yield a pilot rating of 2.5-3.0 for the tasks considered in this experiment. The stability derivative matrices for the baseline augmented configuration at 40 knots and hover are shown in Table 1.

Engine Model

The basis for the gas turbine engine model comes from a model developed for real-time simulation by Bell Helicopter[10] and represents an XT-53 engine with the inertias for a UH-1C rotor and transmission system. A block diagram of the adaptation of that model for this study is shown in Fig. 3. Provisions are included for a pure time delay Δt and torque limiting Q_{lim} at the power turbine stage. By ignoring the nonlinearities in ΔT and Q_{lim}, a transfer function with a second-order denominator can be generated (Fig. 3). As indicated in Ref. 10, most of the terms of that expression vary as a function of the gas generator speed N_1; for example, a range of 60-95% on N_1 for the XT-53 engine results in a range of frequencies of ω_n = 4-8 rad/sec and a range of damping ζ = 0.6-1.1. In this experiment, the engine terms were held constant for a given configuration and the configurations studied varied over a range of ω_n = 2-10 rad/sec and ζ = 0.3-1.0. In addition to frequency and damping, Q_{lim} was varied to provide a steady state (T/W) max. in hover ranging from 1.025 to 1.25. Bear in mind that actual transient thrust can exceed these limits via the stored energy in the rotor system.

Task and Simulation Set-Up

The determination of an appropriate task required the selection of one that would be minimally affected by such simulation limitations as limited field of view and limited motion cues and yet one that would place large demands on the engine and vertical axis. Both requirements were sufficiently satisfied by flying the course outlined in Fig. 4. The task consists of a constant-speed (40 knots) berm-hopping maneuver (called a "dolphin") followed by a deceleration to hover and then a bob-up maneuver. The pilot was requested to change altitude during the dolphin maneuver, primarily through collective control inputs. He was instructed to maximize his masking by crossing the four berms with minimal clearance and staying low between the berms. Because of a protective probe on the terrain board camera, a minimum scaled clearance of 17 ft was necessary. The pilot was provided with a software-generated radar altimeter reading to assist him in determining his altitude. After the fourth berm, the pilot performed a deceleration of his choosing in preparation for the bob-up maneuver. The hover bob-up required the sighting of three objects through 45° directional turns while maintaining maximum masking by the trees. The course was completed after the bob-down and reestablishment of a steady hover.

The pilot provided two Cooper-Harper pilot ratings for each run, one for the dolphin portion of the course and one for the bob-up portion. Evaluation of the deceleration segment was combined with the bob-up maneuver during the experiment when

changes were being made to the engine dynamics only and was evaluated separately during the time when changes were being made to the vehicle dynamics. The latter was necessary since Z_w varies as a function of speed and could only be specified at 40 knots and hover.

The cockpit instrument panel is shown in Fig. 5. The primary instruments the pilot included in his scan were radio altimeter, torque, rpm, and airspeed; an rpm warning light was added. The pilot also had an rpm "beep" trim switch, for his used on the collective grip.

Five pilots — two NASA test pilots, two Army test pilots, and an Army tactical pilot — participated in this experiment. Most configurations were evaluated by at least three of the pilots and were often repeated; there was a total of about 200 data runs.

Discussion of Results

The discussion that follows is based primarily on averaged pilot ratings and is presented in three subsections. Variations in the engine dynamics only, with the vehicle characteristics held at those described in Table 1, are discussed first. Data for variations in vehicle height damping Z_w and collective control sensitivity Z_{δ_c}, with the engine dynamics held constant, are discussed second, and trade-offs between engine response time and height damping for the bob-up maneuver are discussed last. Excess power requirements for specific tasks are also discussed in each subsection.

Effects of Engine Dynamics

As was shown in Fig. 3, the engine model in this study can be represented by an expression with a second-order denominator. It was through this representation that the engine response time and damping (i.e., ω, and ζ) were controlled. Alterations in ω_n and ζ in this model can be thought of as changes in the power train inertias, gas generator dynamics, and speed governor or power turbine gains. No attempt was made to isolate these terms specifically; instead the engine parameters were varied to provide an overall governed response in terms of the desired ω_n and ζ.

Figures 6 and 7 present the average pilot ratings for the engine configurations as a function of ω_n and ζ for unlimited T/W. Figure 6 presents data for the constant-speed dolphin maneuver, and Fig. 7 shows the results for the deceleration and hover bob-up maneuver. Also shown on these figures are the pilot ratings for the ideal governor (i.e., Ω held constant); this case resulted in pilot ratings of 2.5 for the dolphin and 3.0 for the bob-up.

Time histories of the thrust and torque responses to a 0.5-in. collective step for several engine models are shown in Fig. 8. The rpm and rate of climb responses are also shown; as can be seen, the slower governors have an effect of increasing the $\dot{h}$ rise time. The thrust responses all exhibit an immediate maximum thrust because of stored energy in the rotor followed by the transient behavior of the engine response and the $\dot{h}$ damping owing to the rotor inflow and augmentation. Note that since the maximum thrust is achieved almost immediately, all the thrust responses satisfy the 0.3-sec level 1 Vertical Flight Characteristics (par. 3.2.5.2) criteria of MIL-F-83300 and the 0.5-sec rise time criteria of AGARD 577. However, the resulting pilot ratings for these governors in the bob-up varied from 3.0 for the ideal governor to 6.5 for engine configuration E27 (i.e., $\omega_n = 2.0$ rad/sec, $\zeta = 0.7$). Based on pilot commentary, these ratings reflected not only the changes to the vehicle response resulting from the engine dynamics but also reflected the attention required for undesirable governor droop and overspeed.

It should be noted that the data for the MIL-F-83300 thrust-response criteria were extracted from experiments based on configurations similar to the one shown in Fig. 1; therefore, they do not account for effects of rotor-speed control, stored energy, or inflow damping. Hence, since helicopter thrust responses, as described by Fig. 2, are quite different in nature, it is reasonable to expect that additional criteria to cover these responses are necessary. Perhaps a criterion based on vertical acceleration or on a frequency-domain approach would be more appropriate.

Several engine configurations (i.e., $\omega_n = 2$, 4, 6, and 10 rad/sec) were studied at various levels of excess power, ranging from a steady state T/W = 1.025 to 1.25. Figure 9 shows how pilot ratings varied with changes in engine dynamics and T/W for the hover bob-up. The vertical damping was held at a fixed augmented level of $Z_w \approx -0.65$ sec^{-1} and $Z_{\delta_c} \approx 0.38$ g/in. for hover. The engine response is depicted in terms of both frequency ω_n (at $\zeta = 0.7$) and the equivalent first-order time-constant τ_{eng}. Also shown in Fig. 9 is a line below which it was found that the engine power or torque limiting would likely occur sometime during the run. These data indicate that a satisfactory flying-qualities boundary is formed by T/W > 1.1 and an engine response of $\tau_{eng} < 0.2$ sec (i.e., $\omega_n \geq 7.0$ rad/sec). Based on time histories and pilot commentary, the lower bound on T/W was influenced by excessive power limiting, and the bound on engine response time τ_{eng} was dictated by excessive engine overspeed and underspeed, as well as sluggish response.

Effect of Vehicle Characteristics

In this segment of the experiment, variations in the vertical damping Z_w and collective control sensitivity Z_{δ_c} were studied. During this phase a highly responsive engine governor ($\omega_n = 10$ rad/sec) was used, thus keeping the effects of the engine response minimal and yet realistic. Vertical damping Z_w was varied through stability augmentation of the basic speed-dependent aerodynamic damping which was -0.25 sec^{-1} in hover. A range of $Z_w = 0$ to -4 sec^{-1} in hover was studied.

Figures 10 and 11 show how pilot ratings varied with Z_w and Z_{δ_c}. The results for the 40-knot dolphin task are shown in Fig. 10 along with an approximate pilot rating (PR) = 3.5 fit to the data. Also shown are the characteristics of the basic simulation model and several current generation helicopters.[11] As can be seen, all of these basic configurations lie outside of the PR = 3.5 region determined by this experiment. These data indicate a need with this task for a higher damping and sensitivity than currently provided.

The results for the hover bob-up maneuver are shown on Fig. 11. The PR = 3.5 contours for these data along with those of several previous near-hover studies are also given. The current results describe a subset of the previous results, favoring, in general, higher sensitivities. The current results and the low-speed handling-qualities criteria given in MIL-F-83300 and AGARD 577 are compared in Fig. 12. Also shown are the characteristics of several helicopters including the unaugmented model used in this experiment. The results from this study do fall within the MIL-F-83300 Level 1 boundaries; however, for the hover bob-up task, they indicate a need for a higher minimum for both damping and sensitivity.

The effects of vertical damping (Z_w) on excess power requirements (T/W) has been addressed in Refs. 1, 3, and 4, and form the basis for the criteria given in MIL-F-83300. Figure 13 shows the data from this experiment for the hover bob-up maneuver. The solid lines on that figure are the criteria as given by MIL-F-83300. These criteria are for a vehicle whose vertical damping is composed of an aerodynamic contribution only (i.e., $Z_w = Z_{w_a}$). The damping of the vehicle in this experiment is represented by both an aerodynamic and stability augmentation contribution (i.e., $Z_w = Z_{w_a} + Z_{\delta_c}(K_{\delta_c/w})$). In the case of a helicopter model, however, the aerodynamic damping can be further broken down into at least the inflow and fuselage contributions (i.e., $Z_{w_a} = Z_{w_{fus}} + Z_{w_{inflow}}$) where in hover the inflow damping is predominant (i.e., $Z_{w_a} \approx Z_{w_{inflow}}$). For the model used in this experiment the aerodynamic damping in hover is -0.25 sec^{-1} and hence $Z_{w_a} \approx Z_{w_{inflow}} = -0.25$ sec^{-1}. From the time histories shown in Fig. 8 and from the diagram shown in Fig. 2, it can be seen that the inflow damping and stability augmentation damping cause the thrust response to decay, and since the steady-state value of thrust returns to its original level, it can be concluded that $Z_{fus} \approx 0$ (i.e., $Z_w \approx Z_{w_s} + Z_{w_{inflow}}$). Since the criteria of MIL-F-83300 is intended for comparison with the portion of damping which does not cause thrust decay (e.g., $Z_{w_{fus}}$), one is led to conclude that the data from this experiment should be compared with boundaries based on an inherent damping equal to zero. These MIL-F-83300 boundaries are shown in Fig. 8. However, a further look at the time histories in Fig. 8 indicates that while the thrust response returns to the original level, the torque response (i.e., engine output) does not. This peculiarity, along with the stored energy in the rotor, makes a comparison of helicopter data with the MIL-F-83300 boundaries questionable. However, what can be said of the data shown is that the required level of T/W does depend on Z_w and is minimized at a total damping of Z_w = -0.8 to -1.0 sec^{-1} in hover.

Trade-Offs between Vertical Damping Z_w and Engine Response τ_{eng}

A final segment of this experiment studied the trade-off between engine response (τ_{eng}) and damping (Z_w) on the overall height response of the vehicle. First consider the representation given in Fig. 1. This configuration consists of two cascaded first-order systems, which can be approximated by a single first-order time-constant and is shown by $\overline{Z_w}$, in Table 2. Several lines of constant $\overline{Z_w}$ resulting from that table are plotted in Fig. 14. Also shown in Fig. 14 are the results of Ref. 5, which show a satisfactory boundary (i.e., PR $\leq$ 3.5) for a trade-off between τ_{eng} and Z_w. Although that study did not address the idea of an equivalent $\overline{Z_w}$, it can be seen that the boundary lies along a constant $\overline{Z_w}$ of -1.0 sec^{-1}. This treatment implies that by maintaining an equivalent damping of greater than -1.0 sec^{-1}, satisfactory flying qualities can be obtained. Such a trade-off of Z_w for τ_{eng} represents a considerable departure from the MIL-F-83300 Level 1 criteria shown in that figure.

Now consider the representation given in Fig. 2. Exploring the possible trade-off between engine response and vertical damping for a helicopter is not as straightforward because of the complex nature of the thrust response, which, in general, cannot be characterized by a first-order time-constant τ_T. A closer look at the time histories in Fig. 8, however, shows that the engine governor does have an effect on the $\dot{h}$ response and hence on the effective damping Z_w. Specifically, the engine configuration E67 ($\tau_{eng} \approx 0.23$ sec) causes an increase in $\dot{h}$ rise time (i.e., time to 63%) of from 1.5 sec, for the ideal case, to 1.8 sec. This results in a decrease in effective damping of from -0.65 sec^{-1} to -0.56 sec^{-1}. A further decrease in effective damping can be noted in the distorted $\dot{h}$ response for the engine configuration E27 ($\tau_{eng} \approx 0.7$ sec^{-1}). Thus a trend in equivalent or effective damping exists for Fig. 2 which is similar in nature to that shown for Fig. 1. However, the results for this case, which are shown in Fig. 15, indicate a far more restrictive trade-off between τ_{eng} and Z_w than is shown in Fig. 14. As was indicated earlier, an upper limit on τ_{eng} exists which is determined more by tolerable levels of engine overspeed and underspeed than by resulting $\dot{h}$ response.

Conclusions

The effects of vertical axis response on the handling qualities of an rpm-governed helicopter operating in an NOE environment were studied. The results from this motion-based simulation show several areas where present handling-qualities criteria need extension or modification. The following trends or conclusions are summarized:

1) An engine governor response of 0.2 sec or faster is required for satisfactory flying qualities and rpm control for the tasks performed in this experiment.

2) In addition to engine response time an excess power level of $T/W > 1.1$ is required during the bob-up. This excess power level is a function of Z_w and is minimized at a Z_w of between -0.8 and -1.0 sec^{-1}.

3) For satisfactory flying qualities there is a restricted trade-off between engine response time and vehicle damping; however, increases in engine time-constant are limited by poor rpm overspeed and underspeed control.

4) The results from this experiment indicate that higher minimums for both Z_w and Z_{δ_c} are required for these NOE tasks than are specified by MIL-F-83300 and AGARD 577.

5) The thrust response for an rpm-governed helicopter cannot be compared directly with the thrust response time-constant criteria of MIL-F-83300. The helicopter thrust response is composed of a combination of stored energy, governed response, and inflow damping, and hence cannot be characterized as a first order; thus a new criterion is needed.

References

1. Gerdes, R. M., and Weick, R. F., "A Preliminary Piloted Simulator and Flight Study of Height Control Requirements for VTOL Aircraft," NASA TN D-1201, 1962.

2. Garren, J. F., Jr., and Assadourian, A., "A VTOL Height-Control Requirement in Hover as Determined from Motion Simulator Study," NASA TN D-1488, 1962.

3. Gerdes, R. M., "A Piloted Motion Simulator Investigation of V/STOL Height-Control Requirements," NASA TN D-2451, 1964.

4. Kelly, J. R., and Garren, J. F., Jr., "Flight Investigation of V/STOL Height-Control Requirements for Hovering and Low-Speed Flight under Visual Conditions," NASA TN D-3977, 1967.

5. Vinje, E. W., and Miller, D. P., "Analytical and Flight Simulation Studies to Develop Design Criteria for VTOL Aircraft Control Systems," AFFDL-TR-68-165, Apr. 1969.

6. A'Harrah, R. C., and Kwiatkowski, S. F., "A New Look at V/STOL Flying Qualities," Aerospace Engineering, 20 (7), July 1961, pp. 22-23, 86-92.

7. Hoh, R. H., and Ashkenas, I. L., "Development of VTOL Flying Qualities Criteria for Low Speed and Hover," NADC-77052-30, Dec. 1979.

8. Vinje, E. W., and Miller, D. P., "Flight Simulator Experiments and Analyses in Support of Further Development of MIL-F-83300 — V/STOL Flying Qualities Specification," AFFDL-TR-73-34, June 1973.

9. Parrish, R. V., et al., "Empirical Comparison of a Fixed-Base and a Moving-Base Simulation of a Helicopter Engaged in Visually Conducted Slalom Runs," NASA TN D-8424, 1977.

10. Sonneborn, W., and Torres, I., "UH-1C Data for Hybrid Computer Simulation," Report 204-099-892, Bell Helicopter Company, undated.

11. Heffley, R. K., et al., "A Compilation and Analysis of Helicopter Handling Qualities Data," Vol. I, NASA CR-3144, 1979.

Table 1. Baseline Augmented Configuration

F matrix is: 40 Knots

U	W	Q	THETA	V	P	PHI	R
-.67094E-01	.63303E-02	.12532E 02	-.19605E 02	-.93550E-03	-.94208E 00	.54309E-01	.18724E 01
-.16087E 00	-.10555E 01	.92916E 02	.20898E 02	-.26210E-01	-.28947E 01	-.97003E 00	.55438E 00
.11542E-01	.28087E-02	-.29061E 01	-.22198E 01	.14908E-03	.14730E 00	-.44039E 02	.37028E-02
.00000E 00	.00000E 00	.10000E 01	.00000E 00	.00000E 00	.00000E 00	.00000E 00	.00000E 00
-.14550E-01	-.37659E-02	-.23983E 00	.61808E 00	-.15947E 00	-.43990E 01	.22246E 02	-.63077E 02
-.56975E-02	-.10780E-02	-.25133E 00	.50135E 00	-.92668E-02	-.49574E 01	-.62792E 01	.69372E 00
.00000E 00	.00000E 00	.00000E 00	.00000E 00	.00000E 00	.10000E 01	.00000E 00	.48996E-01
.52419E-02	.16625E-02	-.25227E 00	.31119E 00	.23276E-01	-.87597E 00	-.86469E 00	-.40001E 01

G matrix is:

DELTA E	DELTA C	DELTA A	DELTA P
-.19903E 01	.67605E 00	-.39219E-02	.22316E-01
-.38370E 01	-.12363E 02	-.11006E-01	-.33018E-02
.35294E 00	-.58116E-02	-.69883D-03	-.48941E-03
.00000E 00	.00000E 00	.00000E 00	.00000E 00
-.13503E 00	-.77366E-01	.18137E 01	-.99206E 00
.90781E-02	-.57286E-01	.10868E 01	-.25149E 00
.00000E 00	.00000E 00	.00000E 00	.00000E 00
.18877E 00	-.34315E-02	.24901E-01	.72604E 00

$\dot{X} = FX + GU$

F matrix is: Hover

U	W	Q	THETA	V	P	PHI	R
-.73200E-01	-.17236E-01	.16619E 02	-.18397E 02	.76353E-03	-.99232E 00	.17848E-01	-.67649E-01
.37640E-01	-.65021E 00	.14357E 00	-.13880E 01	-.39558E-01	.67401E-01	-.32754E 00	-.25043E-01
.11312E-01	.64809E-02	-.27200E 01	-.22171E 01	.19824E-03	.15302E-00	-.82793E-03	-.38976E-01
.00000E 00	.00000E 00	.10000E 01	.00000E 00	.00000E 00	.00000E 00	.00000E 00	.24197E-02
-.65185E-02	-.56082E-02	-.96860E 00	.52645E-02	-.13565E 00	-.69056E 01	.22318E 02	.37598E 01
-.55066E-03	.28817E-02	-.81417E 00	.11131E-02	-.14528E-01	-.45552E 01	-.62638E 01	.62447E 00
.00000E 00	.00000E 00	-.10730E-03	.00000E 00	.00000E 00	.10000E 01	.00000E 00	.44342E 01
.71576E-02	.14523E-01	-.55445E 00	.77832E-04	.13836E-01	-.10268E 01	-.92055E 00	-.36767E 01

G matrix is:

DELTA E	DELTA C	DELTA A	DELTA P
-.22040E 01	.53581E 00	.00000E 00	.88440E-04
-.95908E-02	-.12090E 02	-.31445E 03	.00000E 00
.35720E 00	-.31973E-02	-.12692E-02	.78661E-02
.00000E 00	.00000E 00	.00000E 00	.00000E 00
-.34403E-01	-.16805E 00	.18064E 01	-.10006E 01
.93418E-01	-.97817E-01	.10870E 01	-.25364E 00
.00000E 00	.00000E 00	.00000E 00	.00000E 00
.24561E 00	.37786E-01	.35604E-01	.73235E 00

Table 2. Equivalent damping for configuration in Fig. 1.

Engine Response Time τ_{eng} (sec)	ω_n at $\zeta = 0.7$ (rad/sec)	Damping $- Z_{w_a}$ (sec^{-1}) 0	-0.5	-1.0	-1.5	-2.0	-3.0	-4.0
1.4	1	0	-0.3	-0.42	-0.52	-0.6	-0.71	-0.71
0.71	2	0	-0.42	-0.59	-0.73	-0.84	-1.03	-1.4
0.5	3	0	-0.5	-0.71	-0.87	-1.0	-1.22	-1.73
0.35	4	0	-0.5	-0.84	-1.04	-1.2	-1.46	-2.07
0.23	6	0	-0.5	-1.0	-1.3	-1.47	-1.81	-2.55
0.18	8	0	-0.5	-1.0	-1.45	-1.67	-2.04	-2.89
0.14	10	0	-0.5	-1.0	-1.48	-1.9	-2.31	-3.27

$\bar{Z}_w$

	Case I	Case II	Case III
	$\frac{1}{\tau_{eng}} \geq 5\, Z_{w_a}$	$\frac{1}{\tau_{eng}} \simeq Z_{w_a}$	$Z_{w_a} \geq 5\, \frac{1}{\tau_{eng}}$
$\bar{Z}_w \simeq$	Z_{w_a}	$\sqrt{\frac{Z_{w_a}}{4\,\tau_{eng}}}$	$\frac{1}{\tau_{eng}}$

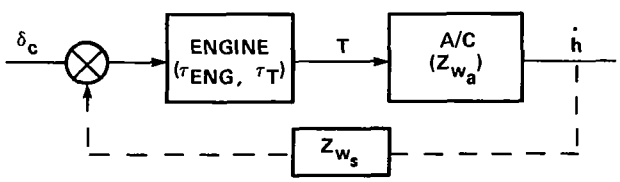

Fig. 1. VTOL (jet lift) vertical control.

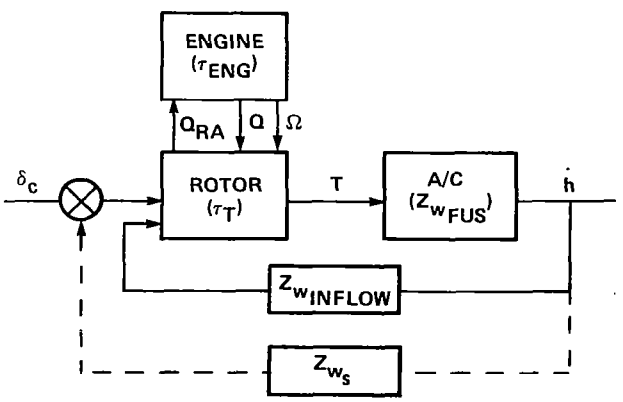

Fig. 2. Helicopter vertical control.

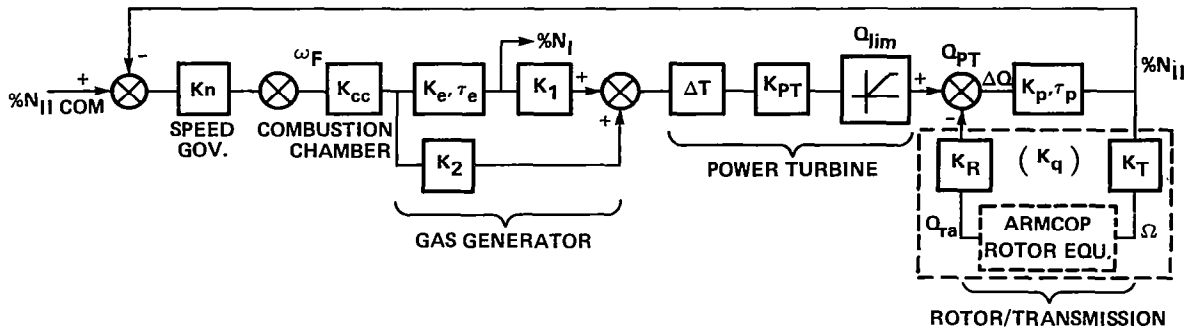

$$\bullet\ \frac{\%N_{II}}{\Delta Q} \alpha \frac{S + 1/\tau_e}{S^2 + \underbrace{(1/K_p + 1/\tau_e + K_{PT} K_n K_{cc} K_2 + K_q)}_{2\zeta\omega_n} S + \underbrace{\frac{1}{\tau_e K_p} + \frac{K_{PT} K_n K_{cc} K_1 K_e}{\tau_e} + \frac{K_p K_n K_{cc} K_2}{\tau_e} + \frac{K_q}{\tau_e}}_{\omega_n^2}}$$

- T-53 ENGINE WITH UH-1C

$\zeta \Rightarrow 0.6 - 1.1$ $\qquad$ $\omega_n \Rightarrow 4 - 8$ rad/sec

Fig. 3. Engine model.

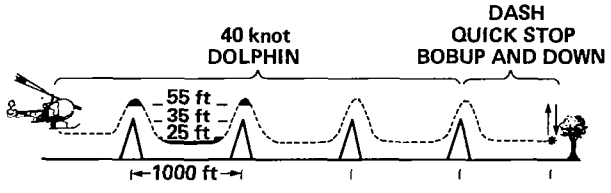

Fig. 4. Simulation task.

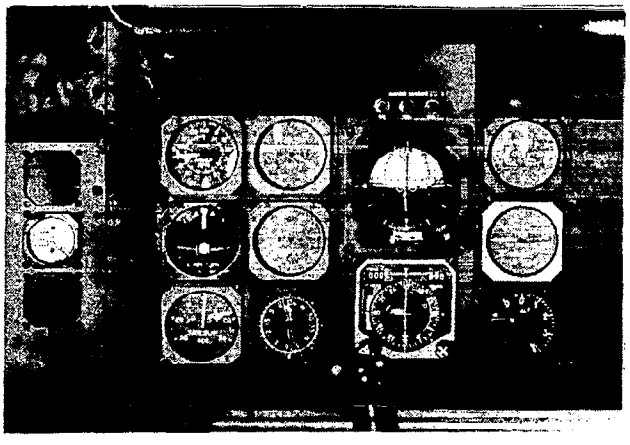

Fig. 5. Cockpit instrumentation.

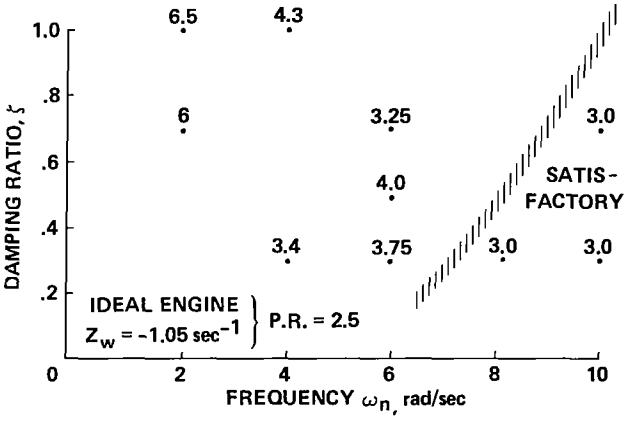

Fig. 6. Effects of engine frequency and damping — dolphin.

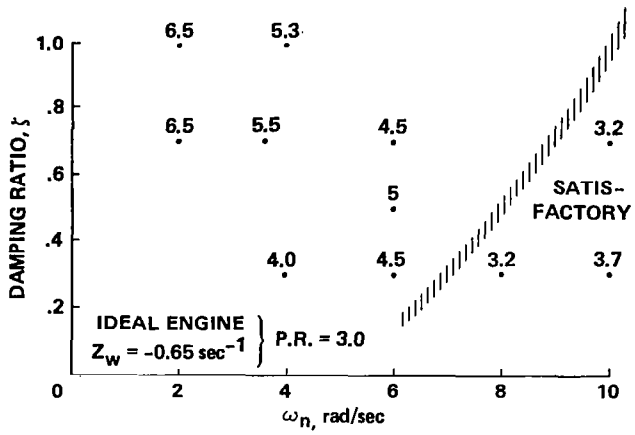

Fig. 7. Effects of engine frequency and damping — quick stop/bob-up.

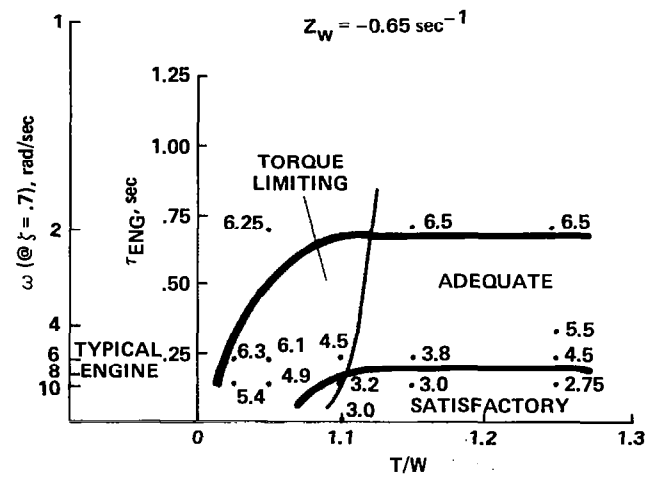

Fig. 9. Engine response time versus T/W — bob-up maneuver.

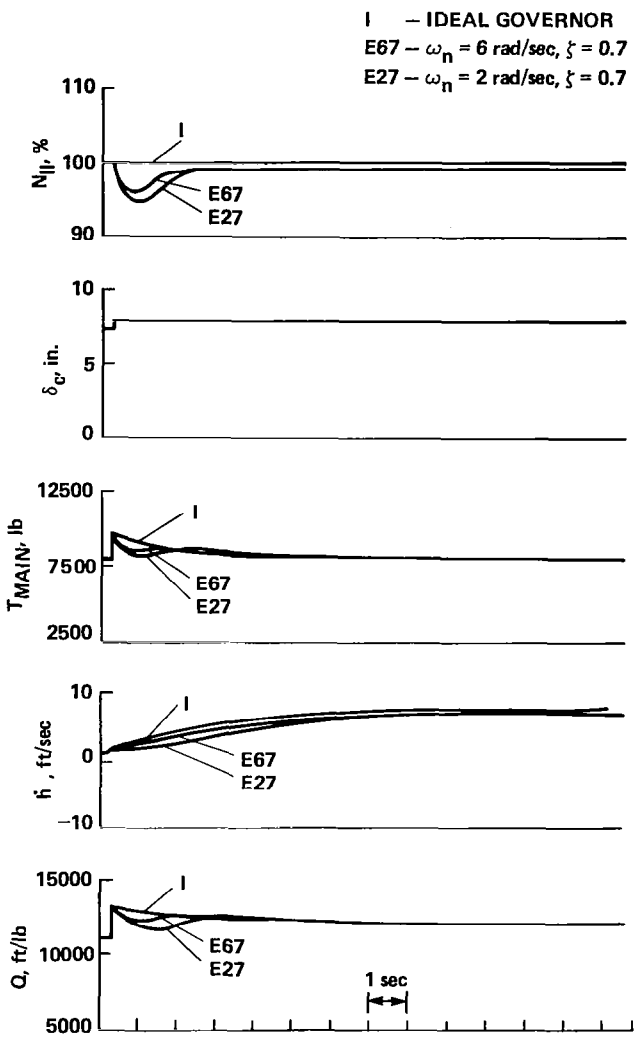

Fig. 8. Engine response time histories; collective steps (Z_w = -.65 sec^{-1}).

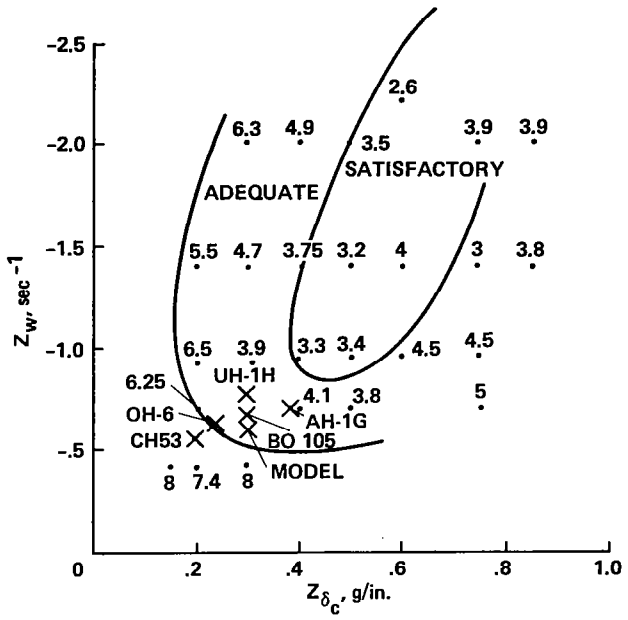

Fig. 10. Vertical damping and collective sensitivity — dolphin maneuver.

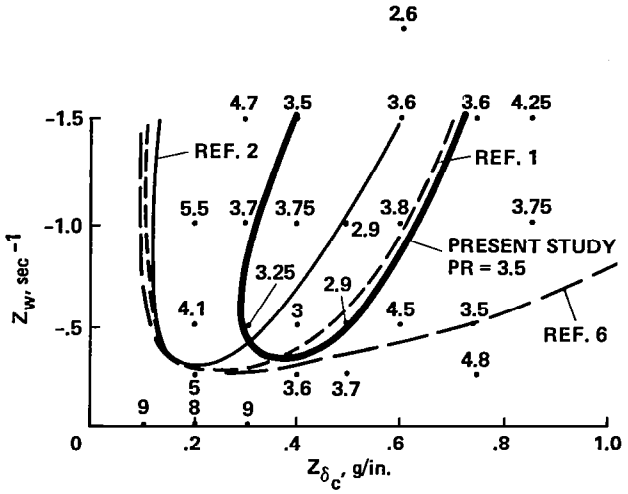

Fig. 11. Vertical damping and collective sensitivity — bob-up maneuver.

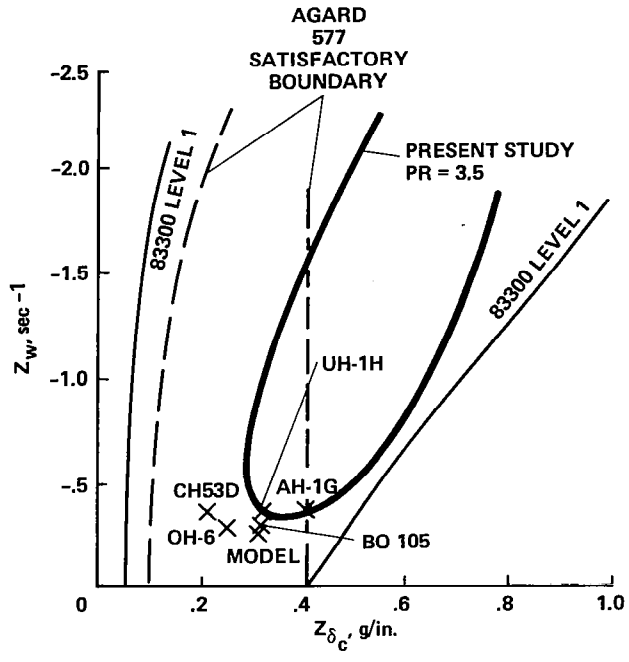

Fig. 12. Comparison of bob-up data with existing criteria.

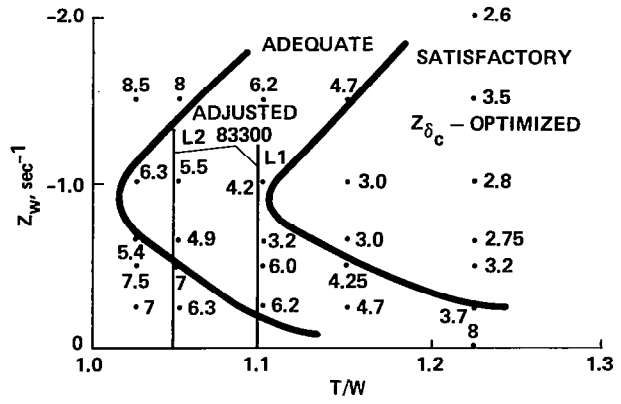

Fig. 13. Vertical damping and T/W — bob-up maneuver.

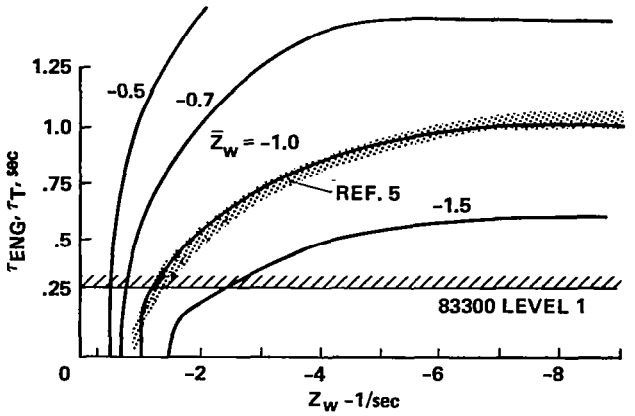

Fig. 14. Trade-off between Z_w and τ_T for configurations of Fig. 1.

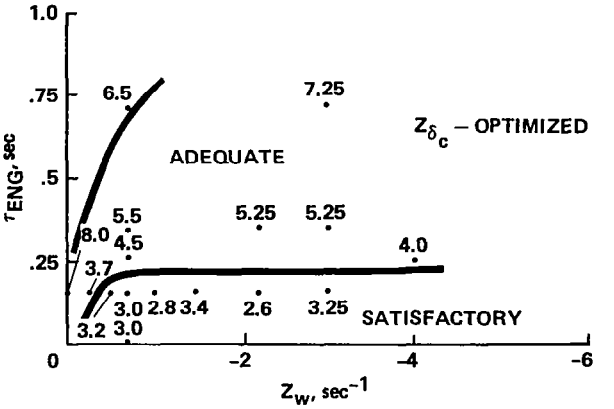

Fig. 15. Trade-off between Z_w and τ_{eng} for the hover bob-up.

UNIFIED RESULTS OF SEVERAL ANALYTICAL AND EXPERIMENTAL STUDIES OF HELICOPTER HANDLING QUALITIES IN VISUAL TERRAIN FLIGHT

Robert T. N. Chen
NASA Ames Research Center,
Moffett Field, California

Abstract

A series of helicopter handling-qualities studies--analyses, piloted ground-based simulations, and a flight experiment--is described. The studies, conducted at Ames Research Center, were undertaken to investigate the effects of rotor design parameters, interaxis coupling, and various levels of stability and control augmentation on the flying qualities of helicopters performing low-level, terrain-flying tasks in visual meteorological conditions. Some unified results are presented, and the validity and limitations of the flying-qualities data obtained are interpreted. Selected results, related to various design parameters, provide guidelines for the preliminary design of rotor systems and aircraft augmentation systems.

Introduction

In recent years, the Army helicopter mission has placed considerable emphasis on terrain-flying tactics for purposes of survival and effectiveness in modern combat environments.[1] The terrain-flying tasks in these missions place strong demands on the agility and precision control capabilities of the helicopter and have raised questions concerning the flying qualities needed for such tasks and the means of achieving them. The existing flying-qualities specification for military helicopters, MIL-H-8501A, is a 1961 update of a 1951 document; it does not address specifically such present-day requirements of terrain flying.

To answer these flying-qualities questions, a joint NASA/Army research program was established at Ames Research Center. A series of analyses, piloted ground-based simulations, and flight experiments involving terrain-flying tasks and low-altitude tactical missions has been and is still being conducted. Studies and experiments designed to examine the effect of aircraft design parameters, interaxis coupling, and levels of stability and control augmentation on the flying qualities and man-machine performance of the low-level flying tasks in visual meteorological conditions were performed.[2-10] The influence of engine dynamics and excess power on these tasks was also examined.[11] In addition, research is in progress to investigate the effect of flight directors, vision aids, and side-stick controllers on performance of these terrain-flying missions in instrument meteorological or night conditions.[12,13]

The first visual terrain-flight experiment[2] was conducted on a fixed-based simulator to explore the effects on the handling characteristics of basic single-rotor helicopters of large variations in rotor design parameters, such as flapping-hinge offset, flapping-hinge restraint, blade inertia (or Lock number), and pitch-flap coupling. In the second ground-based simulation experiment, representative configurations from the first experiment were evaluated on a moving-base simulator [the Flight Simulator for Advanced Aircraft (FSAA)] to examine the effect of motion cues[3] and the effects of various levels of stability and control augmentation.[4] A more sophisticated stability and control augmentation system (SCAS) was also synthesized, using linear optimal control theory to meet a set of comprehensive performance criteria.[5] This system, designed expressly for a hingeless-rotor helicopter, was subsequently evaluated in the third piloted ground-simulator experiment on the FSAA.[6] A flight experiment[7] was conducted on the variable stability UH-1H/VSTOLAND helicopter[14] to verify some selected configurations from the first two ground experiments, to explore additional configuration variations, and to investigate the effect of field of view on helicopter flying qualities for nap-of-the-Earth (NOE) operations. To relate directly some of the results of these flying-qualities experiments to the design parameters of the helicopter, an analytical study[9,10] was conducted to develop a design rule for the selection of some primary rotor parameters to decouple the longitudinal and lateral motions of the helicopter.

The purposes of this paper are to consider this set of flying-qualities data for visual terrain-flying tasks in a unified framework, to interpret the validity and limitations of these data, and to relate the results directly, where possible, to design parameters, thus making them

available as guidelines for use in the preliminary design of basic helicopters and their stability and control augmentation systems.

In what follows, we discuss the flying-qualities factors considered in designing the experiments, describe the conduct of the experiments, and discuss the main results and their design implications.

Factors Influencing Pilot-Vehicle Performance and Pilot Workload in Visual Terrain Flight

In terrain flight, especially in NOE flight, the pilot is often called upon to fly complicated and rapidly changing flight-path trajectories. These trajectories are generated, for example, from the need to avoid obstacles vertically or horizontally and to unmask and rapidly remask by accelerating and decelerating the aircraft vertically, longitudinally, or laterally. The quickness, ease, and precision with which the pilot is able to fly these trajectories are essential if mission performance is to be enhanced with a concomitant increase in endurance. Training, particularly in navigation skills, is of critical importance in NOE flight; however, the characteristics or qualities of the helicopter that permit the pilot to fly these complicated trajectories easily, precisely, and quickly are the key to safe and successful operation. These qualities or characteristics may be defined as "agility."

To fly these NOE trajectories quickly, the helicopter must be able to change rapidly the magnitude and direction of its velocity vector in space. It must, therefore, be able to rotate quickly the thrust vector of the main rotor and to change its magnitude to overcome drag and gravitational forces. Adequate control powers in pitch, roll, and yaw are therefore required to make possible the rapid rotation of thrust vector necessary to achieve the desired direction of the aircraft velocity vector; adequate thrust capability, installed power, and responsiveness of the engine/governor system are needed to meet the demand for rapid change in thrust magnitude.

To fly these complex NOE trajectories easily and precisely, the helicopter must possess satisfactory flying qualities. Thus, adequate damping in consonance with appropriate control sensitivity is needed in pitch, roll, yaw, and heave; interaxis cross-coupling must be minimized so that unnatural or complicated control coordination is not required; and adequate stability must be provided to damp out upsets owing to external wind/turbulence disturbances or to uncommanded control inputs from the pilot.

As a result of these requirements, there are many factors that influence helicopter agility: the basic performance capabilities of the aircraft and the engine/governor dynamic characteristics, as well as the flying qualities discussed above. The sequence of experiments described in the next section was designed to examine only the flying qualities while holding the performance factors and propulsion system characteristics constant. However, the effects of the latter two factors on the pilot-vehicle performance and pilot workload have also been examined recently at Ames.[11]

Design and Conduct of Experiments

The simulation models and experimental variables, the flight simulation facilities, the evaluation tasks, and the acquisition of the experimental data for this series of experiments (outlined in Table 1) are described in this section.

Helicopter Mathematical Model

The generic real-time helicopter simulation model (ARMCOP) developed at Ames for this series of piloted ground-simulation experiments[2-6] consists of five modules describing aerodynamic force and moment contributions of the main rotor, tail rotor, fuselage, vertical tail, and horizontal stabilizer. The main-rotor and tail-rotor modules are discussed in Ref. 15. The rotor model was derived from a linearly twisted rigid blade with an offset flapping hinge, a spring restraint about the flapping hinge, and pitch-flap coupling. For the first two experiments,[2-4] a common fuselate, tail rotor, and empennage with characteristics similar to those of an AH-1G helicopter were used; the main-rotor characteristics were varied. For the third experiment,[6] the generic mathematical model was configured to simulate a hingeless rotor helicopter with characteristics similar to those of a BO-105.

The ARMCOP model also includes a general form of SCAS (Fig. 1). The augmentation system employs a complete state feedback and a control mixing structure that facilitates implementation of control cross-feed[4,5] and control-quickening from each of the four cockpit control inputs. Also, the augmentation system gains may be programmed as functions of flight parameters such as airspeed. A limited attempt was made to validate the generic model, as discussed in Refs. 2 and 3.

Experiment Variables

The general objective of experiment I (Ref. 2) was to explore the effects on terrain-flight flying qualities of large variations in four primary rotor design parameters: flapping-hinge offset, flapping-hinge restraint, blade Lock number, and pitch-flap coupling. Forty-four combinations of the four parameters, which cover the teetering, articulated, and hinged rotor system families, were configured in the generic mathematical model ARMCOP, using a common fuselage, tail rotor, and empennage. To investigate systematically both the major and interactive effects, these configurations were designed and related to three sets of flying qualities parameters: damping and control sensitivity in pitch and roll axes; pitch-roll cross-coupling owing to aircraft angular rate; and longitudinal static stability.

In experiment II (Ref. 4), the objective was to investigate the use of various levels of SCAS to improve the flying qualities in terrain flight. Five basic single-rotor helicopters – one teetering, two articulated, and two hingeless – which were found to have major deficiencies in experiment I were selected as baseline configurations. The major handling-qualities deficiencies included inadequate damping and sensitivity in pitch and roll; excess pitch-roll coupling; and excess pitch and yaw coupling resulting from collective input. The SCAS that were designed and evlauated included simple control augmentation systems (CAS) to decouple pitch and yaw responses caused by collective input and to quicken the pitch and roll control responses; rate-command-type SCAS, designed to optimize the sensitivity and damping and to decouple the pitch-roll caused by aircraft angular rate; and attitude-command-type SCAS. The general form of the augmentation system in the ARMCOP was used to configure the above types of SCAS.

The objective of experiment III (Ref. 6) was simply to conduct a comparative evaluation to determine the extent to which the handling qualities of a basic hingeless-rotor helicopter can be improved by incorporating a sophisticated SCAS designed on the basis of linear optimal control theory.[5] Again, the basic aircraft and the SCAS system were implemented on the ARMCOP model. The mechanization was done in such a way that two levels of augmentation could be evaluated: stability augmentation only, and complete stability and control augmentation.

Experiment IV, the in-flight simulation experiment, was conducted to investigate the effects of variations in roll damping, roll sensitivity, and pitch-roll cross-coupling on the helicopter flying qualities for NOE operations and to correlate the results with the ground-based experiments, I and II.

Flight Simulation Facility

A fixed-base simulator, in conjunction with a Redifon closed-circuit television system, was used in experiment I. The simulator consisted of a Bell UH-1A cabin section facing a shrouded screen and TV projector. The UH-1A control system was used with working hydraulics, bungee cords, and magnetic brake. A 1:400 scale terrain model was used in this simulation. The Ames Flight Simulator for Advanced Aircraft (FSAA), a six-degree-of-freedom moving-base simulator (Fig. 2), was used in experiments II and III. The pilot was again provided with conventional pedals, cyclic stick, and collective controls, and a basic set of flight instruments, as shown in Fig. 3. The visual scene was generated from the same terrain model used in experiment I; the scene was presented through the cab window on a color TV monitor with a collimating lens.

Experiment IV, the flight experiment,[7] was conducted on the NASA/Army variable-stability UH-1H helicopter, which incorporates a V/STOLAND avionics system. The V/STOLAND system, equipped with two digital flight computers, was designed for flight control, display, navigation, and guidance research. The flight control portion of the V/STOLAND system was used in this experiment. Each control channel uses a combination of a limited-authority (20% to 30%) series servo and a full-authority parallel servo. In the research mode, the left cyclic stick, controlled by the evaluation pilot, is mechanically disconnected from the right stick and operated in a fly-by-wire status. The safety pilot on the right retains control of the aircraft through the standard UH-1H cyclic and cockpit instruments. The fixed-based simulator facility used for experiment I can be tied directly to the V/STOLAND hardware and was used in software development and checkout for this flight experiment.

Evaluation Tasks

Experiment I comprised three tasks: the longitudinal dolphin task – flying over a sequence of barriers (hurdles) placed at irregular intervals; a lateral task – flying a slalom course of trees spaced similar to the barriers in a straight line; and a combined longitudinal and lateral-directional task – flying a course of barriers combined with trees

placed down the centerline of the barriers. Only the combination course (Fig. 4) was used in experiments II and III. A slightly different scaling was used in experiment I; it resulted in somewhat larger trees (75 ft instead of 50 ft), larger barriers (50 ft instead of 33 ft), and a correspondingly longer spacing between barriers (700 to 1400 ft). The pilots were given instructions to fly as low as possible and as fast as possible through the courses, banking alternately left and right around the trees and dropping down between the barriers. The tasks started at a trimmed, level-flight initial conditions of 40 knots at about 100 ft AGL for experiment I (60 knots for Exp. II, and 100 knots at 500 ft AGL for Exp. III). Minimum vertical obstacle clearance was limited to about 17 ft by a device designed to protect the television camera optics from inadvertent impact with the model terrain. Generally, each pilot was allowed a limited number of runs with a standard configuration at the beginning of his simulation test period in order to allow him to become reaccustomed to the simulator and task. Wind and turbulence were not introduced in these tasks.

For the flight experiment (Exp. IV), the task was to fly through a prescribed slalom course over a runway at the NASA Flight System Research Facility at Crows Landing, California (Fig. 5). The pilots were asked to fly through the course while maintaining speed and altitude constant at 60 knots and 100 ft AGL, respectively. Most of the evaluations were conducted in calm-air conditions or with winds below 10 knots at directions of no more than 40° to the centerline of the course runway.

Data Acquisition

Data collected from these experiments were of two types: 1) Cooper-Harper Pilot Ratings[16] and verbal comments recorded at the conclusion of each evaluation; and 2) time histories of helicopter trajectories, motion variables, and control usage for real-time monitoring and for postflight analysis. Two pilots participated in experiment I and completed a total of 172 evaluations. A total of 127 evaluations were achieved in experiment II by three participating pilots. In experiment III, two pilots completed a total of 21 NOE evaluations in addition to evaluations for tasks other than terrain flight. A total of 150 evaluations were achieved by four participating pilots in experiment IV.

Results and Discussions

The results of this series of experiments are combined and grouped in terms of major factors influencing the flying qualities of the helicopter in visual terrain flight. For this paper, only the Cooper-Harper Pilot Rating (CHPR) data will be used to quantify the flying-qualities results; other experimental data pertaining to the pilot comments and the task performance will not be discussed. The latter have been discussed elsewhere[2-10] in the results of each individual experiment.

Sensitivity and Damping in Pitch and Roll

The combined effects of control sensitivity and damping were expected to have a significant influence on NOE flying qualities, since they determine the short-term characteristics of the pitch and roll responses to cockpit cyclic controls. However, taking together all the pilot ratings for this series of experiments, the results indicate that the relationship of the sensitivity and damping in pitch and roll alone is not a predominant factor for the tasks evaluated. Other factors, such as yaw damping, pitch-roll coupling caused by aircraft angular rate, and collective input couplings to pitch and yaw also were found to be important.

Figure 6 shows the results of the pilot rating data for configurations with low yaw damping ($N_r = -1.2$ sec^{-1}) and a low level of pitch-roll coupling caused by aircraft angular rate ($|Lq/L\rho| < 0.3$). Most of the configurations covering a wide range of sensitivity and damping combinations in roll received ratings of acceptable (CHPR < 6.5) for the lateral task. In terms of the change in roll attitude at the end of 1 sec in response to an inch-step input in the lateral stick, $\Delta\phi_1$, these configurations extend from about 4° to 30°. It is noted, however, that the extreme low sensitivity and low damping combinations were found to be unacceptable. These configurations were brought into the region of "clearly acceptable" ratings in experiment II by increasing the damping and sensitivity to a level of $L_p = -5$ sec^{-1} and $L_{\delta a} = 1.4$ rad/sec^2/in, respectively (and with slight augmentation in yaw damping from $N_r = -1.2$ to -1.6 sec^{-1}).

Increasing the yaw damping to a high value ($N_r = -3.5$ sec^{-1}) while reducing the pitch-roll coupling owing to angular rate to near zero improved the pilot rating considerably, as shown in Fig. 7. Nevertheless, the improvement for the low sensitivity and low damping combinations was insufficient to achieve a rating better than marginally acceptable. Limitations of in-flight simulation capabilities hindered the exploration of a wider range of sensitivity and damping combinations in experiment IV. Based on

this set of data, as well as on the pilot commentary, it appears that there is a level of sensitivity and damping combination below which a precise roll control may not be achieved without a tendency to overcontrol or to develop pilot-induced oscillations. The data also suggest that a minimum roll damping of about $-3\ sec^{-1}$ with $\Delta\phi_1$ from 4° to 30°/in in 1 sec results in clearly acceptable flying qualities.

The flight experiment (Exp. IV) did not examine the effect of sensitivity-damping combinations in pitch. However, based on the result of experiments I and II, a minimum pitch damping (M_q) of about $-1.5\ sec^{-1}$ with $\Delta\theta_1$ (which is the change in pitch attitude, at the end of 1 sec, in response to an inch-step input in longitudinal stick) in the range of 4°-25° may be appropriate for acceptable flying qualities for the longitudinal task.

Pitch-Roll Cross-Coupling Resulting from Aircraft Angular Rate

Unlike fixed-wing aircraft, for which pitch-roll coupling is rare except in high-angle-of-attack operations, helicopters generally exhibit undesirable pitch-roll coupling because of aircraft angular motion. For example, in response to a roll rate to the right, the tip-path plane (TPP) tilts to the left with respect to the rotor hub to provide desirable roll damping; however, the TPP response can also include tilt in the fore-aft direction which produces an undesirable pitching moment. This coupling characteristic, for a general configuration, is a result of combined effects of gyroscopic and aerodynamic moments acting on the rotor system.

The ratio of the roll moment resulting from pitch rate to the roll moment resulting from roll rate, L_q/L_p, for example, plays an important role in determining the roll-rate-to-pitch-rate ratio in the short-term aircraft response to a step input in the longitudinal stick; similarly, the ratio M_p/M_q determines the ratio of pitch rate to roll rate in the short-term response to a step input in the lateral stick. Figure 8 shows the variation of the pilot rating with L_q/L_p from experiments I, II, and III. For comparison purposes, the boundaries discussed in Ref. 17 are also shown in the figure. The boundaries indicate that if the value of the coupling parameter exceeds 0.3, ratings better than acceptable cannot be achieved. (Values greater than 0.5 imply unacceptable flying qualities.) In experiment I, adverse comments on this kind of coupling were made by the pilots when $|L_q/L_p|$ exceeded 0.25. In experiment II, improvement in the pilot rating from unacceptable or marginally acceptable to at least acceptable was achieved when the coupling was reduced or the damping was increased or both.

The results from experiment IV (Ref. 7) pertaining to the effect on pilot rating of the pitch-roll cross-coupling are shown in Fig. 9 for three levels of roll damping with sensitivity held constant. With pitch and roll sensitivities fixed, the pilot commented that the aircraft was a little oscillatory with low damping and sluggish with high damping. Increasing the cross-coupling ratio degraded significantly the pilot rating for the highest damping, but only slightly for the low- and medium-damping cases. In particular, when the most favorable combination of sensitivity and damping ($L_p = -4$, $L_{\delta a} = -0.55$, $\Delta\phi_1 = 6$) the degradation of flying qualities with cross-coupling was not as severe as observed in the simulation experiments.

Collective Input Coupling

The effects of collective input coupling to pitch and yaw were expressly examined in experiment II. Data pertaining to these effects can also be extracted from the results of experiment III. The benefit of reducing the collective input to yaw coupling was found to be dependent on the level of yaw damping. For a moderate yaw damping ($N_r = -1.6\ sec^{-1}$), an improvement of about one rating point was achieved in experiment II (see Fig. 10) by decoupling yaw to collective response. When the yaw damping was high ($N_r = -3.5\ sec^{-1}$) such as in some configurations examined in experiments III and IV, the results suggest that only a slight improvement is realized by this decoupling.

In the speed range flown for the evaluation tasks (40 to 80 knots), the coupling to pitch from the collective input became substantial for hingeless rotor or stiffened hinged-rotor configurations. Experiments I, II, and III indicate that this sort of coupling has a significant effect on the flying qualities. Figure 11 shows the effect on pilot rating of doubling and eliminating the collective input coupling to pitch ($M_{\delta c}$), and a combined effect of eliminating both pitch and yaw coupling for a hingeless-rotor helicopter examined in experiment II.

Type of Flight Control System

As shown in Table 1, two types of flight control systems in the pitch and roll axes were examined in this sequence of experiments: 1) a rate type (including the basic aircraft, considered in experiments I, II, and IV, and 2) an attitude type, examined in experiments II and III. Taking

all the experiments together, the results do not indicate a clear preference by the pilots for either of the two types of control system for the tasks flown. This was reported previously in the results of experiment II and was further substantiated in experiments III and IV. Figure 12 shows the results for a pilot (pilot A) who participated in all four experiments.

It should be emphasized that the result is valid only for the tasks evaluated. The tasks were flown at an airspeed in the range of 40 to 80 knots. In this flight regime, the pilot can perform the precision flight-path control task equally well and with ease with either a properly designed rate-type or attitude-command-type control system in pitch and roll. This result should not be extrapolated, however, to include other NOE tasks such as precision hover over the ground in turbulence. For these other precision position control tasks near hover an attitude system or another type of control system, such as a velocity-command type, may be preferred to the angular rate-type system.[12]

Effect of Longitudinal Static Stability

Limited consideration was given in experiment I to investigating the effect of variations in longitudinal static stability with respect to angle of attack (M_w) using a δ_3 hinge. The effect of variations in longitudinal static stability with speed (M_u) was not investigated in this series of experiments, because the tasks evaluated in the ground simulations did not call for precise speed control. The result obtained from experiment I suggests that, for the demanding tasks evaluated, some longitudinal static instability with angle of attack, such as is the case for some hingeless-rotor helicopters in forward flight, appears acceptable. However, this result must be qualified somewhat because the tasks were flown in calm air. In turbulence, degraded flying qualities caused by static instability may be expected.

Design Guidelines

The experimental results clearly indicate that the interaxis coupling, such as pitch-roll cross-coupling and collective input coupling to pitch and yaw, and levels of sensitivity and damping are major factors influencing the flying qualities of the helicopter in terrain flight. Analytical studies were performed to relate some of the experimental results to the design parameters of the rotor system and aircraft augmentation systems; this was done to develop means of improving the flying qualities. Some results and lessons learned are discussed in the following paragraphs.

Elimination of Interaxis Coupling

Pitch-Roll Decoupling

A design rule[9,10] has been developed for the selection of the design parameters of the rotor systems to reduce the undesirable pitch-roll coupling caused by aircraft angular rate in pitch and roll. The basic idea of the design rule is to cancel perfectly in hover the inertia and aerodynamic factors that contribute to the steady-state coupling in rotor tip-path-plane (TPP) response to the aircraft angular rate in pitch and roll. In essence, the method is to "tune" the flapping frequency ratio, P

$$P = \left[1 + \frac{K_\beta}{I_\beta \Omega^2} + \frac{eM_\beta}{I_\beta} + \frac{\gamma K_1}{8}\left(1 - \frac{4}{3}\varepsilon\right)\right]^{\frac{1}{2}} \quad (1)$$

to the decoupling flapping frequency ratio P_D given by

$$P_D = \left[1 + \frac{\frac{\gamma^2}{4}\left(\frac{1}{4} - \frac{\varepsilon}{3}\right)\left(\frac{1}{4} - \frac{2}{3}\varepsilon + \frac{\varepsilon^2}{2}\right)}{2\left(1 + \frac{eM_\beta}{I_\beta}\right)}\right]^{\frac{1}{2}} \quad (2)$$

through use of a pitch-flap coupling δ_3 ($K_1 = \tan\delta_3$) or a flapping restraint K_β or both for a given hinge offset e. In Eqs. (1) and (2) above, γ is the Lock number of the rotor blade; ε is the ratio of e to rotor radius; Ω is the angular velocity of the rotor system; and M_β and I_β are, respectively, the blade mass moment and moment of inertia of the blade about the flapping hinge.

The values of pitch-flap coupling required to achieve pitch-roll decoupling are generally moderate, as shown in Fig. 13, even for extreme combinations of ε and K_β. They are effective in reducing the the coupling ratio L_q/L_p (and M_p/M_q) in hover and in forward flight (as shown in Fig. 14) and they result in well-behaved TPP transient response. Figure 15 shows an example of the TPP transient response to a unit change in roll rate (and pitch rate) at hover and at an advance ratio of 0.3 for a rotor with $\varepsilon = 0.05$, $\gamma = 12$, with and without the use of decoupling δ_3.

Decoupling pitch and roll caused by aircraft angular rate may also be achieved using feedback control, as was done in experiment II by feeding the pitch rate to lateral cyclic and roll rate to longitudinal cyclic control.

Decouplihg Collective to Yaw and Pitch

The yawing moment resulting from collective input, N_{δ_C}, which exists in all conventional single-rotor helicopters, should be eliminated, particularly when the yaw damping of the aircraft is low. The yaw coupling can be eliminated simply by cross-feeding collective to the pedals. The gain is a nonlinear function of airspeed, the shape of which is similar to the familiar power required curve.[4] Care must be exercised, however, in deriving the cross-feed gain, especially when small-perturbation derivatives are used. Control derivatives such as N_{δ_C} can be a strong function of the magnitude as well as direction of perturbations, as shown in Fib. 16. Modifications to the initial design were required in experiments II and III to accommodate this kind of nonlinearity.

Increased control power obtained through hinge offset or a stiffened flapping hinge produces a coupling in pitching moment caused by collective input, which increases with airspeed. This pitching moment can be eliminated simply by cross-feeding the collective to the longitudinal cyclic and scheduling the gain with airspeed. Again, care must be exercised in mechanizing the system so as not to introduce the undesirable effect of reducing the longitudinal static stability with speed.[17]

Selection of Sensitivity and Damping in Pitch, Roll, and Yaw

The wide range of acceptable sensitivity in pitch and roll axes, as exemplified in Figs. 6 and 7, makes it somewhat difficult to select this parameter in the preliminary design stage. However, a proper selection may be accomplished by judiciously relating the sensitivity requirement to the task demands: lower sensitivity for demands with smaller attitude excursions, higher for tasks demanding larger attitude excursions. For example, to clear the obstacles in a slalom course, the radius for banked turns must be smaller than one half of the spacing between two obstacles. The turn radius is a function of the speed of flight and the bank angle, as shown in Fig. 17. For a spacing of 1000 ft, as used in experiment IV, bank angles of about 30° or more are required if a speed of 60 knots is maintained. Had the task been flown at 80 knots or with the spacing reduced to 500 ft, the bank angle required would have been about 50° or more; the lower roll sensitivity of $\Delta\phi_1 = 4.5°$, which received good pilot ratings (see Fig. 7), might have been down-rated for the more demanding task. In experiment II (Ref. 4), the design of the rate-type SCAS used $\Delta\theta_1 = 7.5°$, $\Delta\phi_1 = 10°$, and $\Delta\psi_1 = 7.5°$, approximately, and in experiment III (Ref. 5) the sensitivity criterion used for the SCAS design was $3 \leq \Delta\theta_1 \leq 20°$, $4 \leq \Delta\phi_1 \leq 20°$, and $6 \leq \Delta\psi_1 \leq 23°$ for pitch, roll, and yaw, respectively. The designs resulted in pilot ratings of satisfactory for the tasks flown.

The minimum acceptable damping required for the tasks considered in the experiments appears to be about $M_q = -1.5$ to -2 sec^{-1}, $L_p = -3$ to -4, and $N_r = -1.6$ to -2, respectively for pitch, roll and yaw. The pitch and roll damping may be obtained by appropriately choosing the design parameters of the rotor system such as flapping-hinge offset, flapping restraint, and Lock number.[2] A cursory survey indicates, however, that yaw damping may be inadequate for many production helicopters for terrain flight; an augmentation in yaw damping is thus desirable.

Attitude SCAS Design

A few combinations of the two major design parameters associated with the attitude command system in pitch and roll, namely the sensitivity in aircraft attitude, change per unit stick deflection, and the bandwidth, were examined in experiment II. As expected, these parameters had significant effect on the flying qualities for the tasks evaluated. The "optimized" sets of these two parameters for the pitch and roll axes, as shown in Table 2, provide a guide for future design of such SCAS systems.

Finally, it is of interest to note that for a hingeless-rotor helicopter, it has been found beneficial[5,6] to feed back pitch-rate and pitch-attitude signals to collective pitch in addition to the longitudinal cyclic pitch. Because the available pitching moment resulting from collective pitch increases with speed, the gains to collective pitch must be scheduled with airspeed accordingly; however, the gains to the cyclic pitch may be held constant, because of essentially constant control effectiveness with the cyclic pitch for the hingeless-rotor helicopter.

Conclusions

A series of analytical and experimental studies investigating the effect of rotor design parameters, interaxis coupling, and levels of stability and control augmentation on the flying qualities of the helicopter in visual terrain flight has been conducted. The evaluation tasks used in the experimental studies consisted of a longitudinal dolphin task, a lateral

slalom task, and a combined longitudinal and later-directional task; all tasks were flown in the airspeed range of 40 to 80 knots. The following conclusions were reached:

1) Minimum levels of damping and sensitivity in pitch and roll are required to achieve clearly acceptable or better flying qualities (CHPR < 5). For damping, a minimum of about $-3\ sec^{-1}$ for roll and -1.5^{-1} for pitch are appropriate; for sensitivity – in terms of the change in attitude at the end of 1 sec following an inch-step input in cyclic stick – a minimum of about 4° for both pitch and roll is suggested for the tasks at the flight conditions noted.

2) To achieve satisfactory flying qualities, the absolute value of the ratio of roll moment caused by pitch rate to roll damping must be less than 0.35. This coupling ratio can be reduced to nearly zero using a design rule developed in this series of studies.

3) In forward flight, the large pitching moment resulting from collective input associated with rotors having a large flapping-hinge offset and a stiff flapping hinge can be detrimental to flying qualities in terrain flight. Significant improvement in pilot ratings has been achieved by cross-feeding longitudinal cyclic from collective input.

4) The coupling to yaw caused by collective input can be objectionable, especially when damping in yaw is low. Augmenting the yaw damping or cross-feeding collective input to the pedals to decouple the yawing moment substantially improves the pilot rating.

5) Properly designed, both rate-command and attitude-command SCAS made substantial improvements in terrain-flight flying qualities in otherwise unacceptable helicopter configurations; no evidence was found for a clear-cut preference for either type of augmentation for the tasks flown.

6) The design of attitude-type SCAS for hingeless-rotor or stiff-hinged-rotor helicopters should include the feedback of pitch rate and pitch attitude to collective pitch, as well as their feedback to the longitudinal cyclic pitch.

References

1. U.S. Army Field Manual 1-1, Oct. 1, 1975.

2. Chen, R.T.N., and Talbot, P.D., "An Exploratory Investigation of the Effects of Large Variations in Rotor System Dynamics Design Parameters on Helicopter Handling Characteristics in Nap-of-the-Earth Flight," Preprint No. 77.34-41, 33rd Annual National Forum of the American Helicopter Society Washington, D.C., May 1977.

3. Talbot, P. D., Dugan, D. C., Chen, R.T.N., and Gerdes, R. M., "Effects of Rotor Parameter Variations on Handling Qualities of Unaugmented Helicopters in Simulated Terrain Flight," NASA TM-81890, 1980.

4. Chen, R.T.N., Talbot, P. D., Gerdes, R. M., and Dugan, D. C., "A Piloted Simulator Investigation of Augmentation Systems to Improve Helicopter Nap-of-the-Earth Handling Qualities," Preprint No. 78-29, 34th Annual National Forum of the American Helicopter Society, Washington, D.C., May 1978.

5. Miyajima, K., "Analytical Design of a High Performance Stability and Control Augmentation System for a Hingeless Rotor Helicopter," Preprint No. 78-27, 34th Annual National Forum of the American Helicopter Society, Washington, D.C., May 1978.

6. Miyajima, K. and Chen, R.T.N., "Analytical and Experimental Study of an ADvanced Stability and Control Augmentation System for a Hingeless Rotor Helicopter," NASA TM, in preparation.

7. Corliss, L. D. and Carico, G. D., "A Preliminary Flight Investigation of Cross-Coupling and Lateral Damping for Nap-of-the-Earth Helicopter Operations," Preprint No. 81-28, 37th Annual National Forum of the American Helicopter Society, New Orleans, LA, May 1981.

8. Gerdes, R. M., "A Pilot's Assessment of Helicopter Handling-Quality Factors Common to Both Agility and Instrument Flying Tasks," NASA TM-81217, 1980.

9. Chen, R.T.N., "Effects of Primary Rotor Parameters on Flapping Dynamics," NASA TP-1431, 1980.

10. Chen, R.T.N., "Selection of Some Rotor Parameters to Reduce Pitch Roll Coupling of Helicopter Flight Dynamics," Preprint No. I-6, National Specialists' Conference on Rotor Systems Design of the American Helicopter Society, Philadelphia, PA, Oct. 1980.

11. Corliss, L. D., "The Effect of Helicopter Engine Response Dynamics and Excess Power on NOE Handling Qualities," American Helicopter Society H.Q. Specialists' Conference, Ames Research Center, NASA, Moffett Field, Calif., Apr. 1982.

12. Aiken, E. W. and Merrill, R. K., "Results of a Simulator Investigation of Control System and Display Variations for an Attack Helicopter Mission," Paper No. 80-28, 36th Annual National Forum of the American Helicopter Society, Washington, D.C., May 1980.

13. Landis, K. H., and Aiken, E. W., "An Assessment of Various Side-Stick Controller/Stability and Control Augmentation Systems for NOE Flight Using Piloted Simulation," American Helicopter Society H.Q. Specialists' Conference, Ames Research Center, NASA, Moffett Field, Calif., Apr. 1982.

14. Baker, F. A., Jaynes, D. N., Corliss, L. D., Liden, S., Merrick, R. B., and Dugan, D. C., "V/STOLAND Avionics System Flight – Test Data on a UH-1H Helicopter," NASA TM-78591, 1980.

15. Chen, R.T.N., "A Simplified Rotor System Mathematical Model for Piloted Flight Dynamics Simulation," NASA TM-78575, 1979.

16. Cooper, G. E., and Harper, Jr., R. P., "The Use of Pilot Rating in the Evaluation of Aircraft Handling Qualities," NASA TND-5153, 1969.

17. Huston, R. J., and Ward, J. F., "Handling Qualities and Structural Characteristics of the Hingeless-Rotor Helicopter," Proceedings of the V/STOL Aircraft Conference, Apr. 1966.

18. Forrest, R. D., Chen, R.T.N., Gerdes, R. M., Alderete, T. S., and Gee, D. R., "Piloted Simulator Investigation of Helicopter Control Systems Effects on Handling Qualities during Instrument Flight," Paper No. 79-26, 35th Annual National Forum of the American Helicopter Society, Washington, D.C., May 1979.

Table 1. Summary of terrain flight experiments

Experiments	Objective	Tasks	Simulator	Rotor type	Control system type
I	To determine effect of large variations in rotor design parameters	Longitudinal vertical task Lateral slalom task Combined task	Fixed base (Ames S-19)	Teetering Articulated Hingeless	Basic helicopter (rate-type in pitch, roll, and yaw)
II	To assess effect of various levels of SCAS	Combined task	Moving base (Ames FSAA)	Teetering Articulated Hingeless	SCAS Input Decoupling Rate command Attitude command in pitch and roll
III	To evaluate a sophisticated SCAS for hingeless rotor helicopter	Combined task	Moving base (Ames FSAA)	Hingeless	SCAS Attitude and rate Stability augmentation Control augmentation
IV	To investigate roll damping, roll sensitivity, and pitch-roll cross-coupling and correlate results with Experiments I and II.	Prescribed lateral slalom course over a runway	In-flight (UH-1H/ VSTOLAND)	Teetering	Rate-type in pitch, roll, and yaw

Table 2. Partially optimized characteristics of attitude SCAS in pitch and roll.

	Pitch	Roll
Frequency and damping ratio		
ω_n , rad/sec	1.9 to 2.0	1.8 to 2.0
ζ	0.9 to 1.0	1 to 1.2
Attitude sensitivities		
$\Delta\theta/\delta_e$, deg/in	5 to 10	20 to 22
$\Delta\phi/\delta_a$, deg/in		

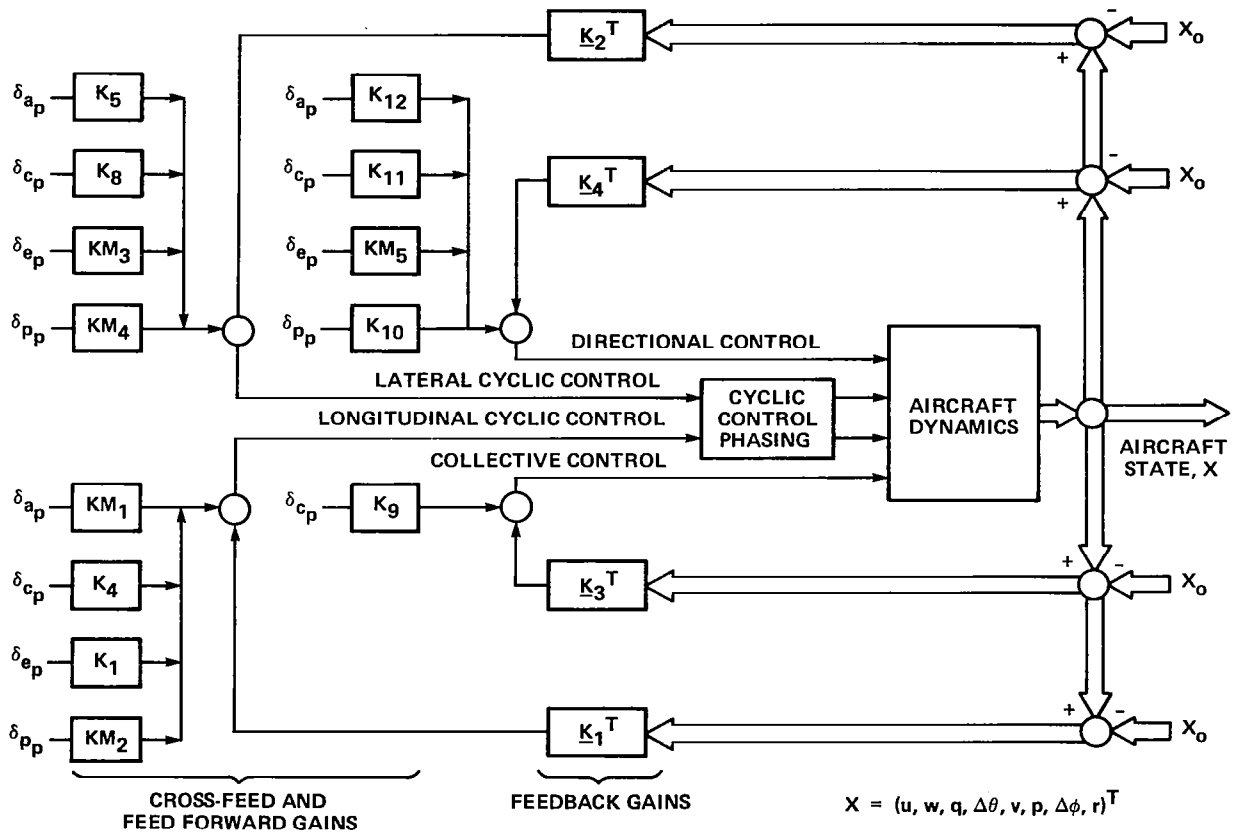

Fig. 1. General stability and control augmentation system structure of the ARMCOP model.

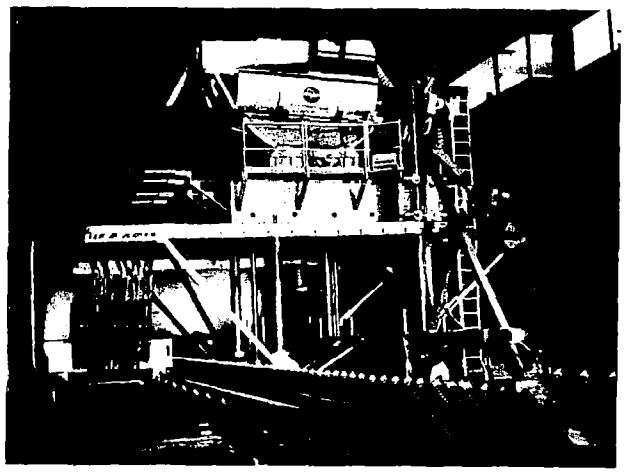

Fig. 2. The flight simulator for advanced aircraft.

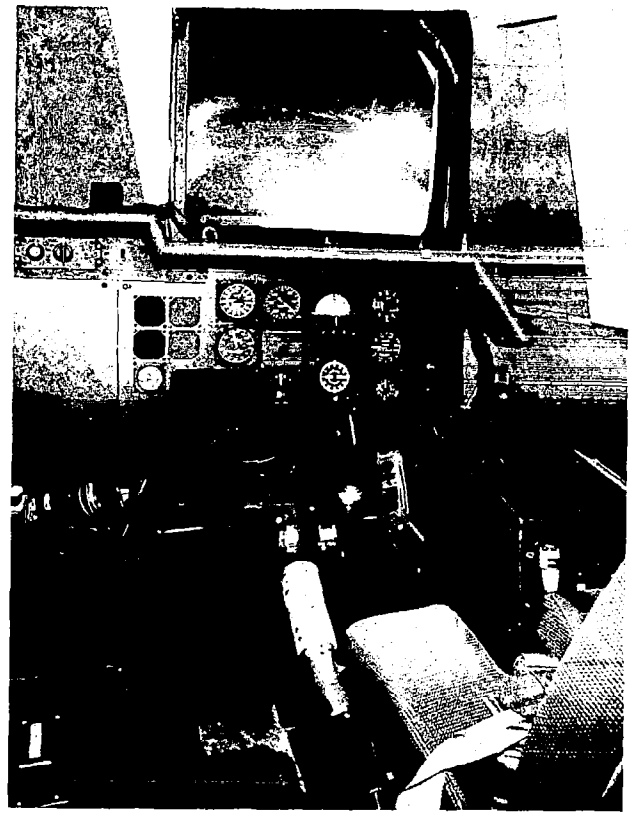

Fig. 3. Instrument configuration in simulator cab.

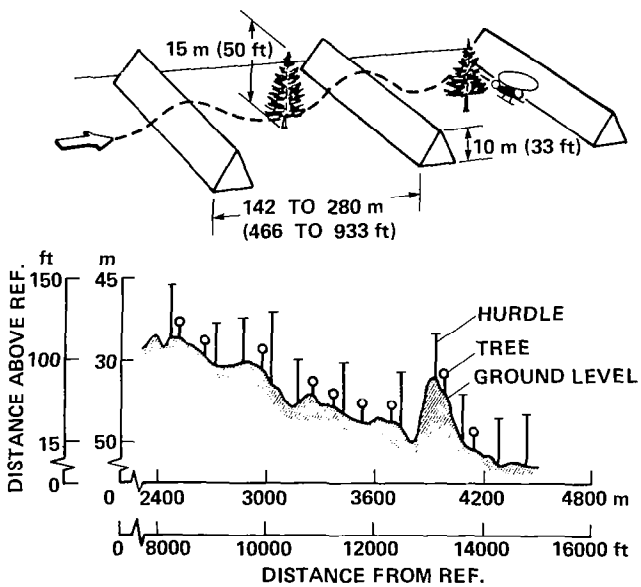

Fig. 4. Layout of nap-of-the-Earth terrain-avoidance obstacle course.

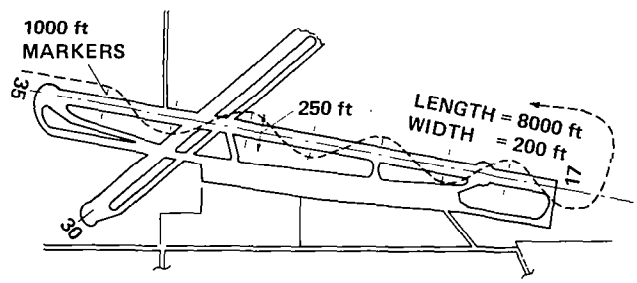

Fig. 5. Slalom-course task for the flight experiment (Crows Landing, Calif.).

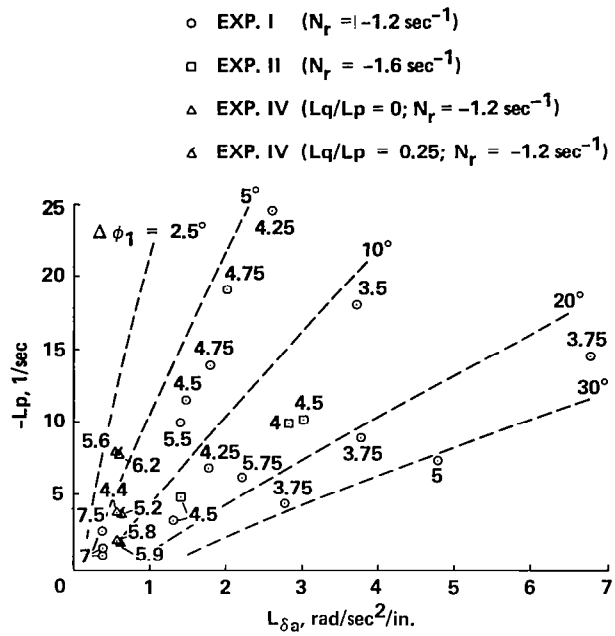

Fig. 6. Effect of roll damping and sensitivity on average pilot rating, $L_q/L_p < 0.3$; $N_r = -1.2$ sec^{-1}.

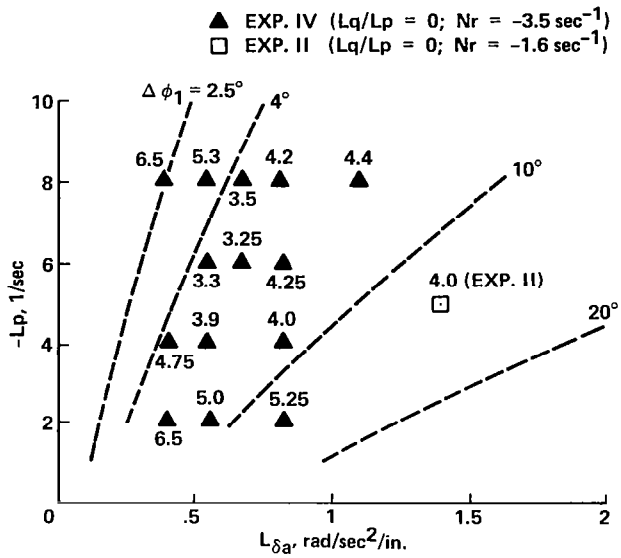

Fig. 7. Effect of roll damping and sensitivity on average pilot rating, $L_q/L_p = 0$; $N_r = -3.5$ sec^{-1}.

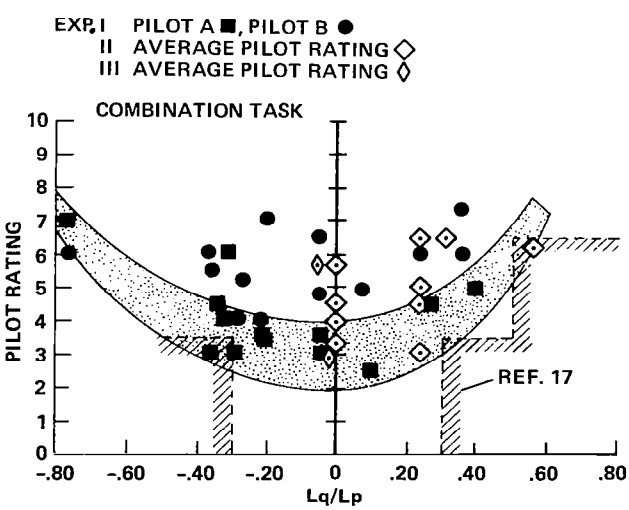

Fig 8. Pilot rating vs. L_q/L_p.

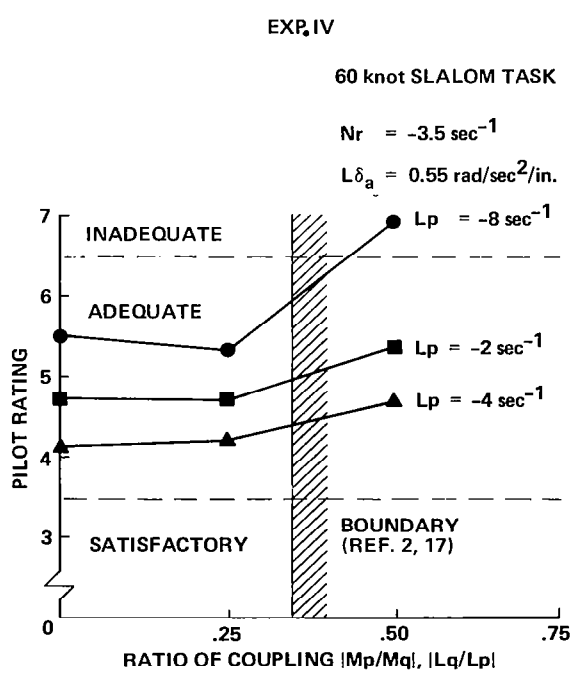

Fig. 9. Trends of pilot rating with ratio of coupling (from ref. 7).

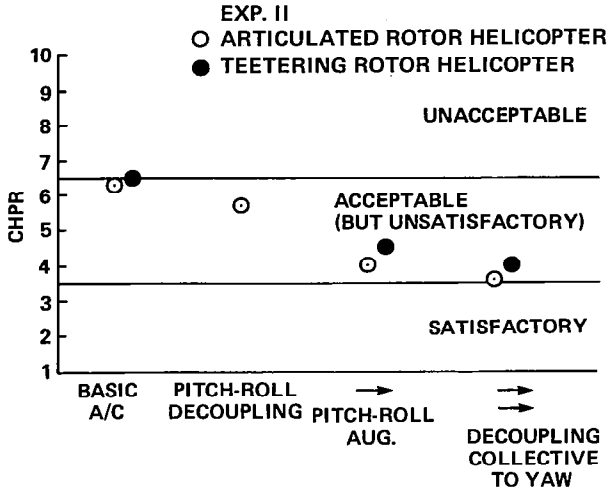

Fig. 10. Effect of pitch-roll coupling and yaw resulting from collective input on pilot rating.

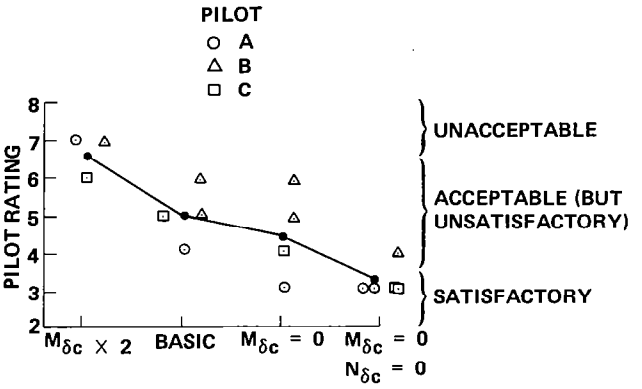

Fig. 11. Effect of pitch and yaw due to collective input on pilot rating, hingeless rotor, all pilots.

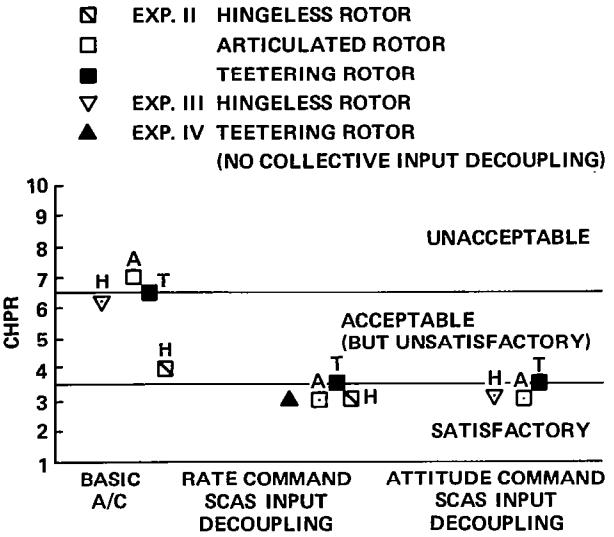

Fig. 12. Effect of SCAS mode on pilot rating, pilot A.

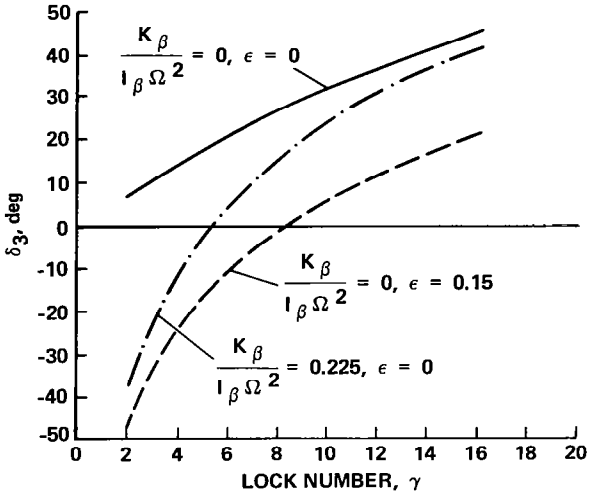

Fig. 13. Pitch-flap coupling required to decouple tip-path plane tilt for extreme values of flapping restraint and hinge offset.

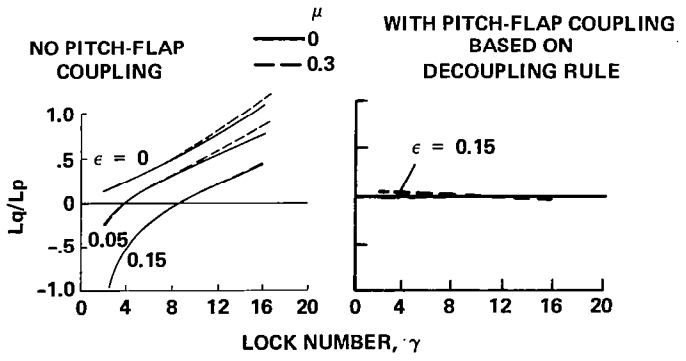

Fig. 14. Effect of decoupling rule on L_q/L_p.

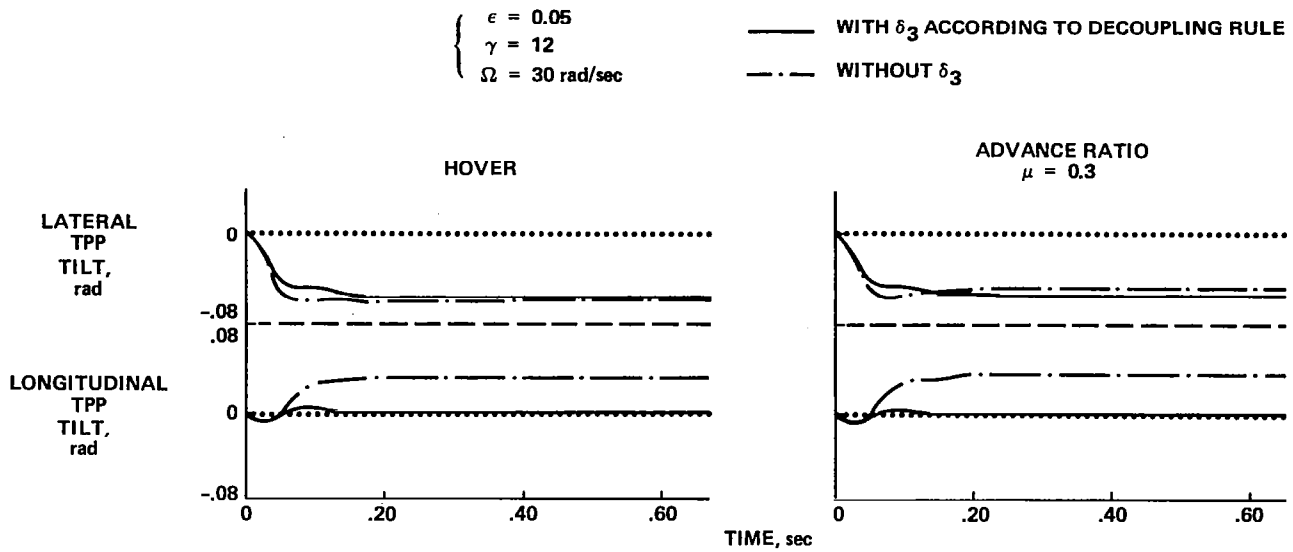

Fig. 15. Effect of decoupling rule on TPP transient response to 1 rad/sec step change in roll rate.

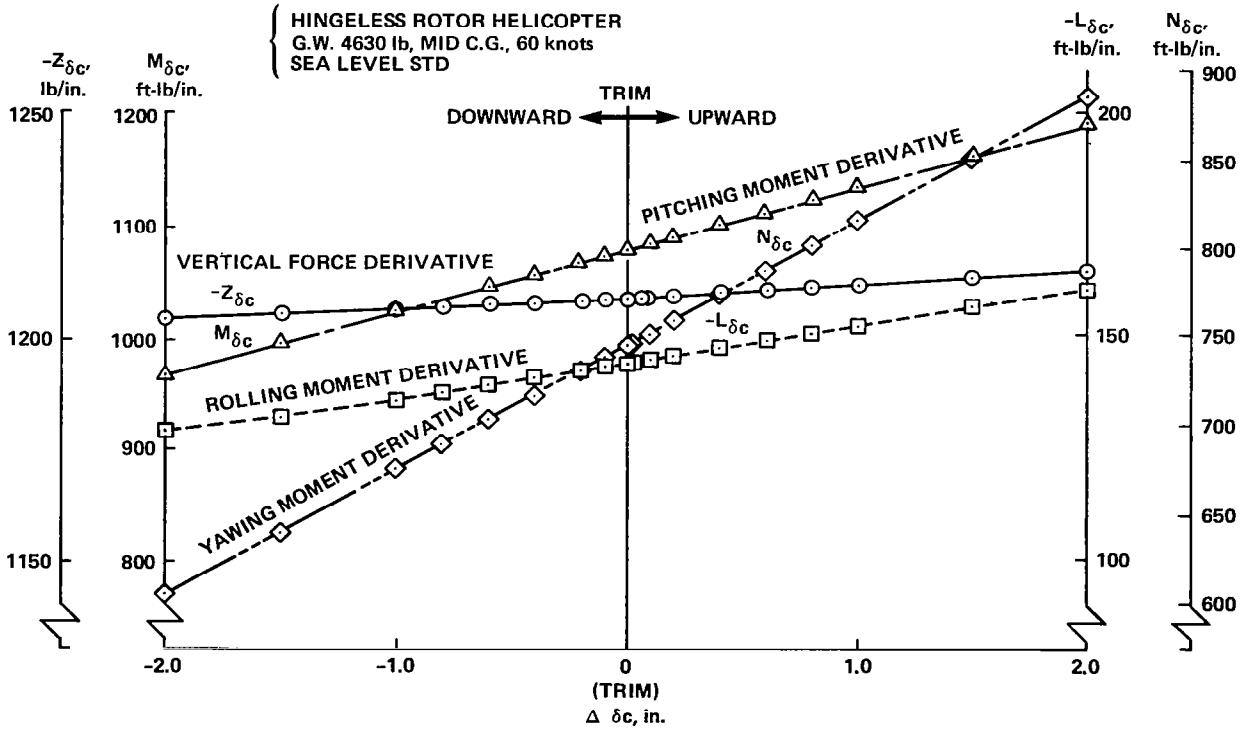

Fig. 16. Nonlinear effect of collective control derivatives.

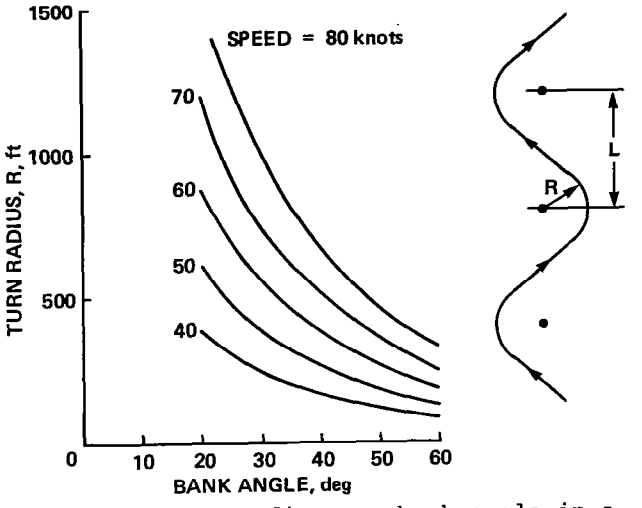

Fig. 17. Turn radius vs. bank angle in a slalom course.

An Assessment of Various Side-Stick Controller/Stability and Control Augmentation Systems for Night Nap-of-Earth Flight Using Piloted Simulation

Kenneth H. Landis
Engineering Specialist
Boeing Vertol Company
Philadelphia, Pennsylvania

Edwin W. Aiken
Aerospace Engineer
Aeromechanics Laboratory
U. S. Army Research and Technology Laboratories (AVRADCOM)
Ames Research Center
Moffett Field, California

ABSTRACT

A series of piloted simulator experiments was conducted to assess the interactive effects of side-stick controller characteristics and level of stability and control augmentation on attack helicopter handling qualities. Several night nap-of-the-earth mission tasks were evaluated using a helmet-mounted display which provided a limited field-of-view image with superimposed flight control symbology. A wide range of stability and control augmentation designs was investigated. Variations in controller force-deflection characteristics and the number of axes controlled through an integrated side-stick controller were studied. In general, a small displacement controller was preferred over a stiff-stick controller particularly for maneuvering flight. Higher levels of stability augmentation were required for IMC tasks to provide handling qualities comparable to those achieved for the same tasks conducted under simulated visual flight conditions.

NOTATION

AAH	Advanced Attack Helicopter
ACC/AFCS	Advanced Cockpit Controls/ Advanced Flight Control System
ADOCS	Advanced Digital/Optical Control System
BUCS	Back Up Control System
DOCS	Digital Optical Control System
FLIR	Forward-Looking Infrared
HLH	Heavy Lift Helicopter
IHADSS	Integrated Helmet and Display Sighting System
IMC	Instrument Meteorological Conditions
NOE	Nap-of-the-Earth
PFCS	Primary Flight Control System
PNVS	Pilot Night Vision System
SCAS	Stability and Control Augmentation System
SSC	Side-Stick Controller
VMC	Visual Meteorological Conditions

INTRODUCTION

The Army's Advanced Digital/Optical Control System (ADOCS) Program is aimed at developing a battlefield-compatible advanced flight control system which can substantially increase aircraft mission effectiveness in part through decreased pilot workload and improved handling qualities. The objectives of the program are: (1) the development of the technology required for a digital optical flight control system, (2) the integration of the new technology with advanced flight control concepts into a demonstrator aircraft, and (3) the demonstration of the advantages of the system in the areas of: mission effectiveness, handling qualities, flight safety, cost, weight/volume, survivability/vulnerability, and reliability/maintainability. The program is divided into two phases: the first involves the development of component technology for a digital optical flight control system while the second is devoted to the development of the ADOCS demonstrator system. The first flight of the demonstrator aircraft, a UH-60A Black Hawk, is scheduled for the fall of 1984.

This paper presents the results of a conceptual design and piloted simulation study of the cockpit controller configuration, flight control laws, and display logic required to achieve satisfactory handling qualities for the mission defined for the ADOCS demonstrator aircraft: an attack helicopter mission conducted under both day and night/adverse weather conditions. The simulation, as part of the Advanced Cockpit Controls/ Advanced Flight Control System (ACC/AFCS) element of the ADOCS program was conducted using the Boeing Vertol Flight Simulation Facility. Although both day VMC and night IMC missions were simulated, this paper emphasizes the low-speed night NOE segments of the ADOCS mission and assesses the interactive effects on

handling qualities of the integrated side-stick controller characteristics, flight control laws, and helmet-mounted display symbol dynamics.

EXPERIMENT DESIGN

Pilot workload and the level of performance achieved during a specific attack helicopter mission task are influenced by combined elements of the helicopter control/display system design. The primary elements considered during this simulation program were:

(1) Side-stick Controller (SSC) Configuration - Stiff or displacement type, and level of integration ranging from a fully-integrated four-axis side-stick controller to a 2+1+1 arrangement; i.e., a two-axis side-stick for pitch and roll control with small-displacement directional pedals and collective lever.

(2) Stability and Control Augmentation System (SCAS) Characteristics - Several generic types of feedback stabilization and feedforward command shaping in each of the four control axes (pitch, roll, yaw, and vertical).

(3) Visual Display - Either day VMC with the simulator four-window, wide angle field-of-view visual system, or night IMC using a simulated FLIR image and superimposed YAH-64 Pilot Night Vision System (PNVS)[1] symbology presented on a helmet-mounted display.

GENERAL APPROACH

The approach to the systematic investigation of these elements is illustrated in Figure 1. The overall investigation was directed toward defining those combinations of SSC, SCAS, and display that produce Level 1, 2, and 3 handling qualities ratings[2].

In applying this general approach to the specific problem, the blocks defined in Figure 1 were broken down further into more detailed configuration matrices. For example, each side-stick controller configuration block contains variations in force/displacement relationships as well as ergonomic characteristics. Generic control laws can be mechanized in several different ways with significantly different results. Display symbology involves a myriad of variations in parameters, format, scaling, and logic.

Degraded modes can also be visualized in Figure 1. Since the selected controller configuration will be part of the primary flight control system, all allowable degraded modes will lie in the control-law/display-law plane. For example, certain failures such as FLIR loss will affect the display axis only, while loss of a ground velocity signal may seriously affect the system control law and display symbology.

By considering the overall system design as a series of matrix levels of increasing detail, the interactive effect on handling qualities of each variation in an element of the system is kept in perspective. A discussion of important issues to be considered within each primary system element follows, including specific details about the controller/SCAS/display characteristics evaluated.

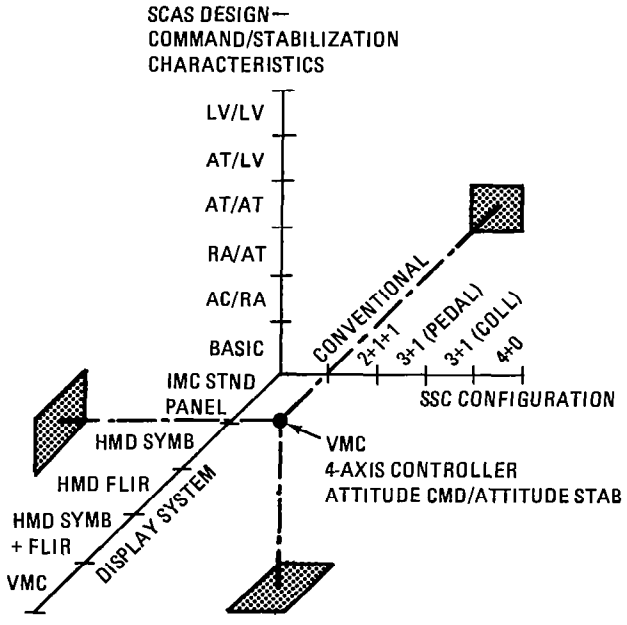

Figure 1 Three-Dimensional Flight Control System Description

INTEGRATED SIDE-STICK CONTROLLER

Fly-by-wire or fly-by-optics flight control systems allow flexibility not only in the synthesis of the control laws but also in the design of the pilot's controllers. The potential benefits of employing an integrated, multi-axis, side-stick controller include: improved visibility, enhanced crashworthiness, easier ingress and egress, a reduction in cockpit space requirements, and an increased potential for single-pilot operations.

Related Research and Development Programs

Handling qualities research examining the effects of the characteristics of a two-axis side-stick controller was conducted in support of the development of the F-16 aircraft. In a flight investigation of the effects of variations in force-deflection characteristics for certain fighter aircraft tasks[3], it was concluded that a small amount of side-stick motion provided improved flying qualities over those achieved with a fixed controller. The results of this and other similar flight experiments were incorporated in a design guide for two-axis side-stick controllers used in fighter aircraft[4]; included in the guide are recommendations for stick neutral position, breakout forces, and force-deflection characteristics in both the longitudinal and

lateral axes.

Research involving the use of side-stick controllers in Army helicopters began in 1968 with the Tactical Aircraft Guidance System (TAGS) program[5]. The system implemented in a CH-47B aircraft initially included an integrated four-axis large-displacement controller. Because of coupling problems between the longitudinal and vertical axes, a three-axis controller was eventually implemented with vertical control effected through a standard collective lever. On the Heavy Lift Helicopter (HLH)[6], a four-axis displacement controller was implemented at the load-controlling crewman's station in conjunction with a ground velocity command and stabilization system.

Side-stick control of single-rotor helicopters has been implemented in a production aircraft - side-stick cyclic control at the copilot's station of the AH-1 series of aircraft - and investigated using both ground- and in-flight simulation. In a three-degree-of-freedom moving-base simulation of the unaugmented Lynx helicopter at RAE Bedford, a two-axis displacement side-stick was compared to the conventional cyclic controller for eleven different flight tasks[7]. When a suitable control sensitivity was selected, the side-stick compared favorably with the conventional controller and, in fact, was preferred for certain of the tasks.

A feasibility study of a four-axis isometric side-stick controller was recently conducted in the Canadian National Aeronautical Establishment Airborne Simulator, a variable stability Bell Model 205A-1, for a wide range of flight tasks[8]. Two primary side-stick configurations, a four-axis controller and a three-axis controller with normal pedal control, were evaluated together with three SCAS variations: rate command/ attitude hold in roll and pitch with augmented yaw rate damping; augmented roll, pitch and yaw rate damping; and the basic 205 with stabilizer bar removed and horizontal stabilizer fixed. With appropriate gains, shaping, and prefiltering applied to the pilot's force input in each controlled axis, pilot ratings comparable to those obtained with conventional controllers were achieved by both primary side-stick configurations.

These investigations indicate that a comprehensive evaluation of multi-axis side-stick control for an attack helicopter mission must include variations in: 1) the number of axes controlled through the side-stick device, 2) the force-deflection characteristics of the controller, and 3) the attendant SCAS characteristics.

Level of Integration (Number of Axes)

Four variations in controller configuration representing different levels of controller integration were investigated. Figure 2 shows the controller configurations including:

(1) 4+0: All control axes (pitch, roll, yaw, and vertical) on the side-stick controller,

(2) 3+1 (Collective): Three-axis side-stick for pitch, roll and yaw control, and a separate collective lever for vertical control,

(3) 3+1 (Pedal): Three-axis side-stick for pitch, roll and vertical control, and pedals for directional control, and

(4) 2+1+1: Two-axis side-stick for pitch and roll control, with separate collective lever for vertical control, and pedals for directional control.

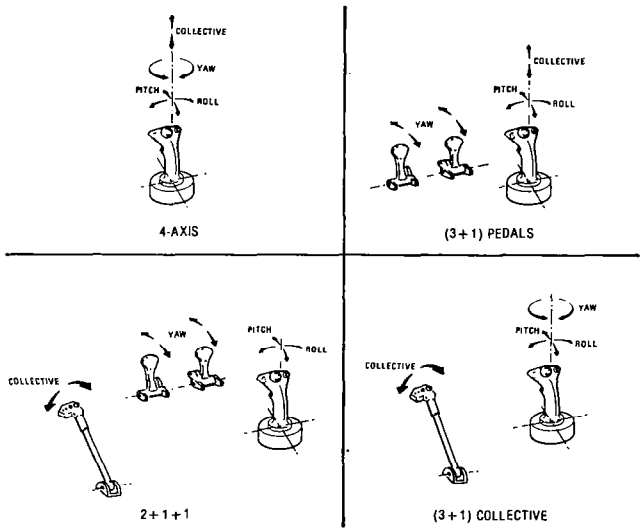

Figure 2 Controller Configurations

Force/Deflection Characteristics

A definition of acceptable/unacceptable ranges of force/deflection gradient for each controller configuration option (4+0, 3+1, or 2+1+1) was necessary. The determination of force-deflection characteristics was performed using three 4-axis side-stick controllers:

(1) A stiff-stick force controller,

(2) A small-deflection controller with two force/deflection gradient configurations, and

(3) A large-deflection controller with an assortment of springs which provided independent adjustment of force/deflection gradients and breakout forces in each axis. This controller is a modified load-controlling crewman's controller used during the HLH program.

All controllers are a base-pivot type for pitch and roll motion. Fore-aft force produces longi-

tudinal control input and right-left force a lateral control input. Yaw control is obtained by twisting about the grip centerline, and vertical control through application of pure up and down forces. Figure 3 shows the three controllers.

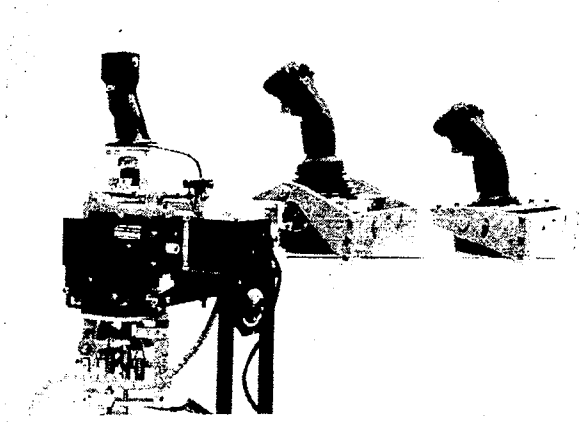

Figure 3 Four-Axis Side-Stick Controllers

The selection of pitch and roll force/deflection gradients was guided by a review of previously described published data. References 4 and 9 defined preferred regions of longitudinal and lateral force/deflection gradient developed from Air Force flight test evaluation of a two-axis variable force-deflection side-stick controller. Figure 4 shows the recommended force/deflection gradient range, in addition to five specific longitudinal controller force/deflection configurations evaluated during this study. The gradients were chosen to cover a range from a "stiff" force gradient with very small deflection to a "soft" force gradient with large deflection (±12 degrees). The F-16 side-stick controller design is also shown for comparison.

Complete force/deflection characteristics for the five 4-axis controller configurations utilized during this simulation are presented in Table 1. Operating force range, maximum deflection, and force/deflection gradient are given for the four control axes. Yaw and vertical controller compliance for both small-deflection configurations were relatively "stiff" compared to the pitch and roll axes. In contrast, the medium- and large-deflection configurations were evaluated with lighter yaw and vertical force/deflection gradients for harmony with pitch and roll.

Evaluation of the (3+1) collective, (3+1) pedal, and 2+1+1 controller configurations was performed using a conventional collective lever and directional pedal controls. The simulator variable force-feel collective lever was implemented as a "stiff" force controller with small deflection. A pedal force control system was configured using a mechanical spring capsule attached directly to the pedals. The directional pedal configuration selected had a force/deflection gradient of 40 lbs/inch with a force breakout of 6.0 lbs.

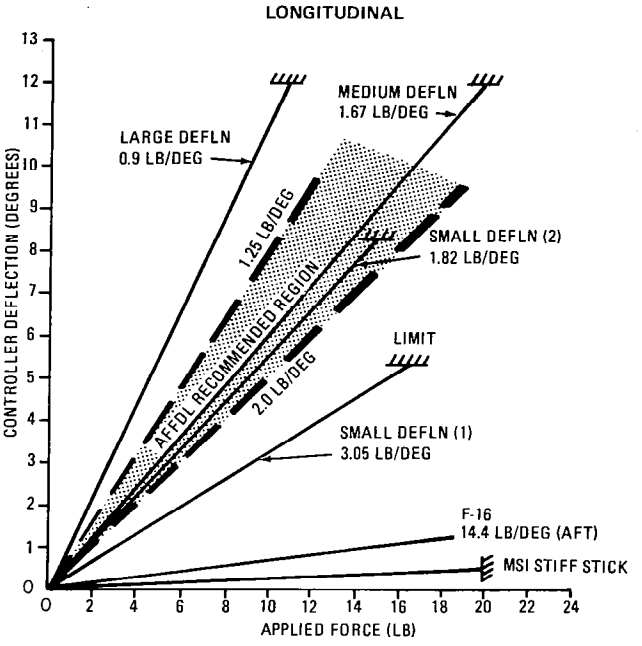

Figure 4 Longitudinal Axis Force-Deflection Characteristics

4-AXIS CONTROLLER CONFIGURATIONS	OPERATING FORCE LINEAR RANGE (±)				MAXIMUM DEFLECTION (±)				FORCE/DEFLECTION			
	X LONG LB/DEG	Y LAT LB	Z VERT LB	ψ YAW IN LB	X LONG DEG	Y LAT DEG	Z VERT IN.	ψ YAW DEG	X LONG LB	Y LAT LB/DEG	Z VERT LB/IN.	ψ YAW IN LB/DEG
(1) STIFF STICK – MEASUREMENT SYSTEMS, INC PHASES 1 AND 2	20	20	40	60	0.5	0.5	–	–	40	40	–	–
(2) SMALL DEFLECTION – CONFIG NO. 1 MEASUREMENT SYSTEMS, INC PHASE 1	16	12	40	60	5.3	5.3	0.1	4.0	3.05	2.25	400.0	15.0
(3) SMALL DEFLECTION – CONFIG NO. 2 MEASUREMENT SYSTEMS, INC. PHASE 2	15	12	40	60	8.3	8.3	0.15	6.0	1.82	1.45	267.0	10.0
(4) MEDIUM DEFLECTION – HLH PROTOTYPE PHASE 1	20	12.6	17.5	40	12.0	12.0	0.5	15.0	1.67	1.05	35.0	2.7
(5) LARGE DEFLECTION – HLH PROTOTYPE PHASE 1	10.8	7.2	7.5	22	12.0	12.0	0.5	15.0	0.9	0.6	15.0	0.7

Table 1 Four-Axis Controller Force-Deflection Characteristics

STABILITY AND CONTROL AUGMENTATION SYSTEM (SCAS) CHARACTERISTICS

The segments of the attack helicopter mission considered to be critical from a handling qualities point-of-view are those spent in nap-of-the-earth (NOE) flight; those inherently high workload tasks include low-speed point-to-point maneuvering using dash, quick stop, and sideward flight techniques, masked hover in ground effect, and unmasked hover out of ground effect including target search, acquisition, and weapon delivery. This simulation was designed to provide a preliminary definition of flight control laws and SCAS mode switching logic requirements for the various mission phases. In addition, the effects on both handling qualities and flight safety of degraded SCAS modes were to be determined. The effect of the side-stick controller configuration under degraded SCAS mode

conditions is important, since high levels of vehicle stability may mask undesirable characteristics of some controller options. SCAS redundancy requirements also need to be weighed in final selection of a controller configuration. For example, a 3+1 axis controller configuration requiring only rate stabilization may be more cost effective than a 4-axis side-stick controller requiring attitude stabilization to achieve Level 2 handling qualities.

Results presented herein are for the first of two scheduled simulation phases, which concentrated on the low speed portion of the NOE mission, that is, airspeeds below approximately 50 knots. High speed control laws and transition requirements will be evaluated during the second simulation phase.

Figure 5 presents a block diagram of the flight control system design concept developed for the ADOCS Demonstrator Program. The use of this system formulation allows for development of handling qualities requirements while still considering aspects of hardware design and redundancy management. Major advantages of this system design concept are:

- Satisfactory unaugmented flight is attained by providing feed-forward command augmentation and shaping as an integral part of the primary flight control system (PFCS). Control mixing and prefiltering are included in the PFCS to reduce pilot workload to an acceptable level for unaugmented flight.

- Stabilization feedback loops are optimized solely for maximum gust and upset rejection. This allows use of high full-time stabilization gains required for good attitude or velocity hold during NOE maneuvering or tight position hold for precision hover tasks. Also, aircraft attitude excursions are minimized for improved target acquisition and weapon delivery. No compromise for control response is necessary.

- Use of a control response model provides forward loop commands to tailor the short and long term responses to pilot control inputs as required to achieve satisfactory pilot ratings and performance. Any desired control response can be obtained by appropriate feed-forward shaping regardless of the level of stabilization.

- Pilot display symbology is driven by the same sensor set used for flight control. For some failure modes, redundant signals may be available in the AFCS as backup inputs to the symbology display.

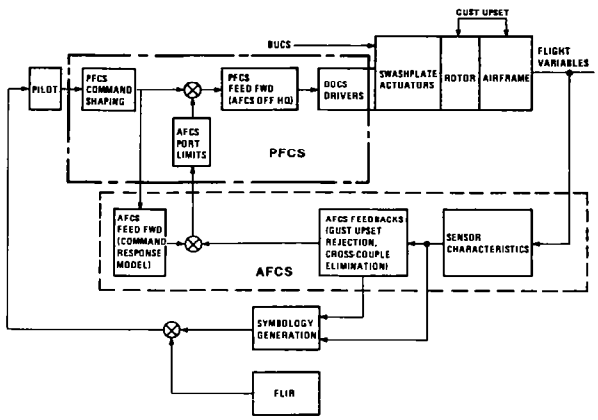

Figure 5 ADOCS Demonstrator-Flight Control System Concept

Various control system concepts were formulated to accomplish the attack helicopter low speed/hover maneuvers. The generic SCAS configurations chosen for evaluation are identified in Figure 6 in the form of a command response/stabilization matrix. A simple identification code (Figure 6) was established. For example, a system with angular rate command and attitude stabilization in pitch and roll was identified with

RESPONSE COMMAND MODEL	STABILIZATION LEVEL: LONGITUDINAL/LATERAL RA	AT	LV	LP	DIRECTIONAL RA	AT	VERTICAL LV	LP
AC	●				●	●		
RA	●	●	●			●	NA	
AT		●	●					
LA					NA		●	●
LV			●	●				●

IDENTIFICATION CODE

	PITCH/ROLL	YAW	VERTICAL
ANGULAR ACCELERATION	AC	$\dot{\psi}^{\bullet}$	–
ANGULAR RATE	RA	$\dot{\psi}$	–
ANGULAR ATTITUDE	AT	ψ_H	–
LINEAR ACCELERATION	LA	–	$\ddot{h}$
LINEAR VELOCITY	LV	–	$\dot{h}$
LINEAR POSITION	LP	–	h_H

EXAMPLE: RA/AT
ANGULAR RATE COMMAND/ATTITUDE STABILIZATION
$\dot{\psi}/\psi_H$
YAW RATE COMMAND/HEADING HOLD

Figure 6 Generic SCAS Configurations-Command Response/Stabilization Matrix

the letter code RA/AT. It should be noted that the longitudinal and lateral control axes were always evaluated with the same command response and stabilization system.

The method of SCAS implementation used for the simulation is illustrated in Figure 7 for the lateral axis. All control axes were implemented in a similar manner. The stabilization gains shown on the diagram were selected prior to the piloted evaluation phase using the helicopter/stability augmentation system model shown in Figure 8. Elements of the model include transfer functions to represent the dynamics of the basic helicopter, rotor and actuators as well as a computational time delay. Nichols chart techniques were used to select feedback gains. Multiple feedback paths, each increasing overall stability, were closed around the model based on a damping ratio design criteria ($\zeta = 0.7$). The stabilization loop gains derived by this method were similar to gains of previously developed aircraft systems (i.e., TAGS, HLH).

A six degree-of-freedom small-perturbation model of the helicopter was used to develop the command response model for each axis. The analytical study established control response model gains for cancellation of undesirable roots of the vehicle characteristic equation. Control response model feedforward parameters were defined for each of the response types previously described. For example, Figure 9 shows the lateral response to step force input for a rate, attitude, and velocity response type. For the angular rate command model, identical response characteristics were provided for both the attitude and velocity stabilized systems. Similarly, the attitude response model characteristics were the same regardless of the level of stabilization.

During this preliminary control response design process, information from available literature, as well as related experience, was used to develop design criteria and quantitative guidelines. Design guidance for SCAS intended for low speed and hovering flight is contained in Reference 10 which develops tentative VTOL aircraft flying qualities criteria from the existing experimental data base. Requirements for generic SCAS such as angular rate command, attitude command, and translational rate command are proposed together with suggested vertical augmentation system characteristics. In addition,

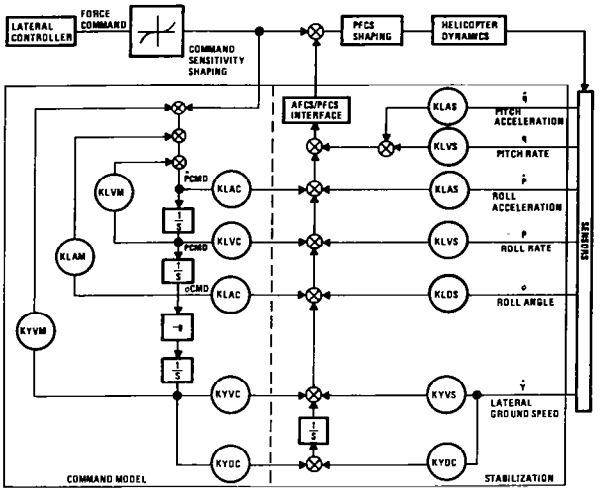

Figure 7 Lateral Axis Stability and Control Augmentation System

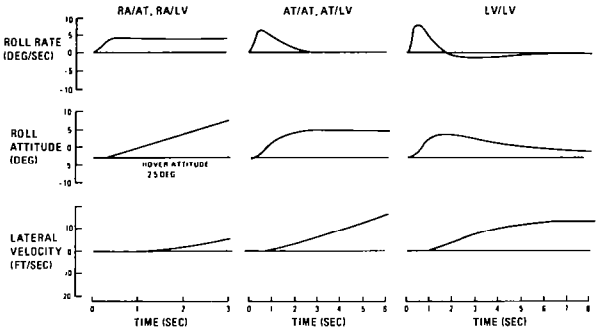

Figure 9 Lateral Response to Step Force Input

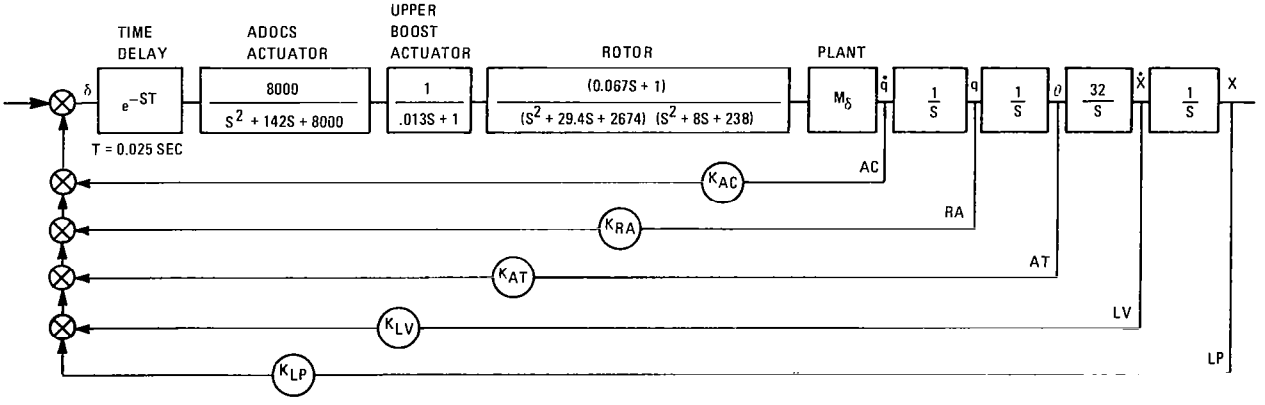

Figure 8 Helicopter/Stability Augmentation System Model-Longitudinal Axis

the use of velocity command system for the precision hover task was flight demonstrated on the HLH Program (References 11 and 12), and the desirability of this control concept was confirmed based on study results published in References 13 and 14.

The preliminary analytical study established baseline response characteristics to begin piloted evaluations. Final response characteristics developed during the initial phase of simulation are presented in the Experiment Results section.

IMC DISPLAY (IHADSS)

Since the ADOCS mission is to be flown in night/adverse weather conditions as well as in VMC, it is necessary to consider not only the effects of the controller and SCAS characteristics but also the impact on handling qualities of the pilot's night vision aids. For this program it is assumed that the pilot is provided with the AH-64 Pilot Night Vision System (PNVS) and associated avionics[1] which include a helmet-mounted display of flight control and fire control symbology superimposed upon a limited field-of-view monochromatic image of the outside world slaved to the pilot's head motions.

The display system selected for simulation of the IMC mission is the Honeywell Integrated Helmet Mounted Display/Sight System (IHADSS) developed for the Army's YAH-64 Advanced Attack Helicopter (AAH). The IHADSS permits NOE, low level, and contour flight under IMC. Since the Helmet Mounted Display (HMD) is coupled to the pilot's head, he is able to scan a wide field-of-view without being constrained to a head-down or look-forward position. The pilot's line of sight is tracked with a Helmet Mounted Sight (HMS) that provides closed-loop command signals to point the sensors.

The importance of superimposed flight control symbology to the enhancement of handling qualities with a limited field of view FLIR image of the outside world has been reported in Reference 15. Baseline display laws and information format used for this investigation were defined based on the AH-64 Pilot Night Vision System (PNVS)[1]. The selectable display modes, which are used to meet the operational requirements for various AAH mission tasks, are:

(1) Cruise: high-speed level flight enroute to the forward edge of the battle area;

(2) Transition: low-speed NOE maneuvers such as dash, quick stop, and sideward flight;

(3) Hover: stable hover with minimum drift; and

(4) Bob-up: unmask, target acquisition, and remask maneuvers over a selected ground position.

Figure 10 presents the display mode symbology divided into three categories - central, peripheral, and weapon delivery/fire control symbology. The characteristics of each symbol are described and the symbols which appear for the three low-speed mission modes used during this investigation are identified.

In a simulator investigation of a night-time attack helicopter mission which included a head-up display of the PNVS symbology[13], it was found that the dynamics of the symbology used to aid the pilot in achieving a precision hover at night had a significant effect on the handling qualities of the vehicle. As a result, because of the wide variation in candidate SCAS concepts to be investigated, it is necessary also to ensure compatibility of the symbol dynamics with the varying dynamic characteristics of the augmented helicopter.

Variations to the baseline AH-64 symbology were made based on Reference 13 as well as a review of reported display system characteristics implemented on the PNVS surrogate trainer flown at the U.S. Army Test Proving Ground, Yuma, Arizona. Changes were incorporated in the programmed symbology primarily to improve low speed maneuvering and hover hold task performance, as well as to reduce pilot workload. These changes, evaluated during the preliminary IHADSS check-out testing, were as follows:

(1) Velocity vector sensitivity was decreased by a factor of two for all modes - from 6 knots to 12 knots full scale in the hover and bob-up modes, and from 60 knots to 120 knots full scale in the transition and cruise modes.

(2) Hover position sensitivity was decreased for the bob-up mode from a full scale deflection of 44 feet to 88 feet.

(3) A horizon line was included in the symbology format for all modes. The AH-64 has the horizon line in the transition and cruise modes only.

(4) Lateral acceleration was used to drive the "ball" display instead of sideslip angle to augment the simulation turn coordination cues at low speed.

(5) The cyclic director, or longitudinal and lateral acceleration cue, approximated by washed-out pitch and roll attitudes, required different sensitivity and time constant values as a function of the command response system type, i.e., rate, attitude, or velocity. Values were established in the same manner discussed in Reference 13.

EXPERIMENT ACTIVITIES

To reduce the large number of possible SSC/SCAS combinations to a manageable set of configurations for evaluation, the experiment was designed with two major phases of simulation activity as shown in Figure 11. Phase I accomplished IHADSS familiarization and controller development. Phase 2 concentrated on evaluation of controller/SCAS configuration combinations.

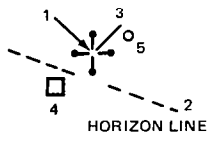

CENTRAL SYMBOL		INFORMATION	MODES		
			CRUISE/TRANS	HOVER	BOB-UP
1.	Aircraft reference	Fixed reference for horizon line velocity vector, hover position, cyclic director, and fire control symbols	X	X	X
2.	Horizon line	Pitch and roll attitude with respect to aircraft reference (indicating nose up pitch and left roll)	X	X	X
3.	Velocity vector	Horizontal Doppler velocity components (indicating forward and right drift velocities). Sensitivity varies with mode	X	X	X
4.	Hover position	Designated hover position with respect to aircraft reference symbol (indicating aircraft forward and to right of desired hover position)		X	X
5.	Cyclic director (Acceleration Cue)	Cyclic stick command with respect to hover position symbol (indicating left and aft cyclic stick required to return to designated hover position). Approximated by washed out pitch/roll attitude		X	X

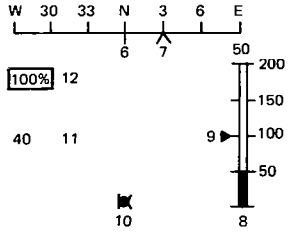

PERIPHERAL SYMBOL		INFORMATION	MODES		
			CRUISE/TRANS	HOVER	BOB-UP
6.	Aircraft heading	Moving tape indication of heading (indicating North)	X	X	X
7.	Heading error	Heading at time bob up mode selected (indicating 030)			X
8.	Radar altitude	Height above ground level in both analog and digital form (indicating 50 ft)	X	X	X
9.	Rate of Climb	Moving pointer with full scale deflection of ± 1,000 ft/min (indicating 0 ft min)	X	X	X
10.	Lateral acceleration	Inclinometer indication of side force	X	X	X
11.	Airspeed	Digital readout in knots	X	X	X
12.	Torque	Engine torque in percent	X	X	X

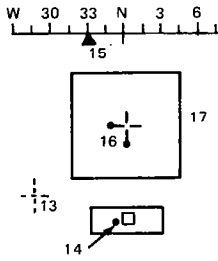

FIRE CONTROL SYMBOL		INFORMATION	MODES		
			CRUISE/TRANS	HOVER	BOB-UP
13.	Cued line of sight	Overlays designated target positon on background video when target is in display field of view			X
14.	Coarse target location	Designated target position with respect to display field of view (inner rectangle) and sensor limits (outer rectangle)			X
15.	Target bearing	Designated target bearing (indicating 330° or 30° to left of current heading)			X
16.	Target location dots	Illumination of two adjacent dots indicates display quadrant in which designated target is located			X
17.	Missile launch constraints	Limits with respect to aircraft reference for successful weapon lock-on to designated target			X

Figure 10 Display Mode Symbology

Specific steps followed for controller development were:

(1) Evaluation of the 4-axis stiff-stick controller to determine best individual axis response/force characteristics and desired non-linear response shaping requirements.

(2) Evaluation of the three 4-axis deflection controllers to define effect of force/deflection gradient on pilot task performance.

(3) Comparison of the stiff-stick and deflection controllers for various pitch and roll SCAS configurations.

(4) Definition of desired response/force characteristics for a conventional collective lever and pedals configured as force controllers.

A best 4-axis controller design was selected based on the above results. This design was used to evaluate the 4+0, (3+1) pedals, (3+1) collective, and 2+1+1 configurations for the primary and secondary controller/SCAS configuration matrices as follows:

(1) Primary configuration matrix - Variations to the pitch and roll SCAS with a fixed directional and vertical command/stabilization system (yaw rate command/heading hold and vertical rate command/altitude hold).

(2) Secondary configuration matrix - Variations to the vertical and directional SCAS for a limited portion of the primary configuration matrix with emphasis given to the less highly augmented pitch and roll systems, particularly the rate/attitude (RA/AT) and attitude/attitude (AT/AT) systems.

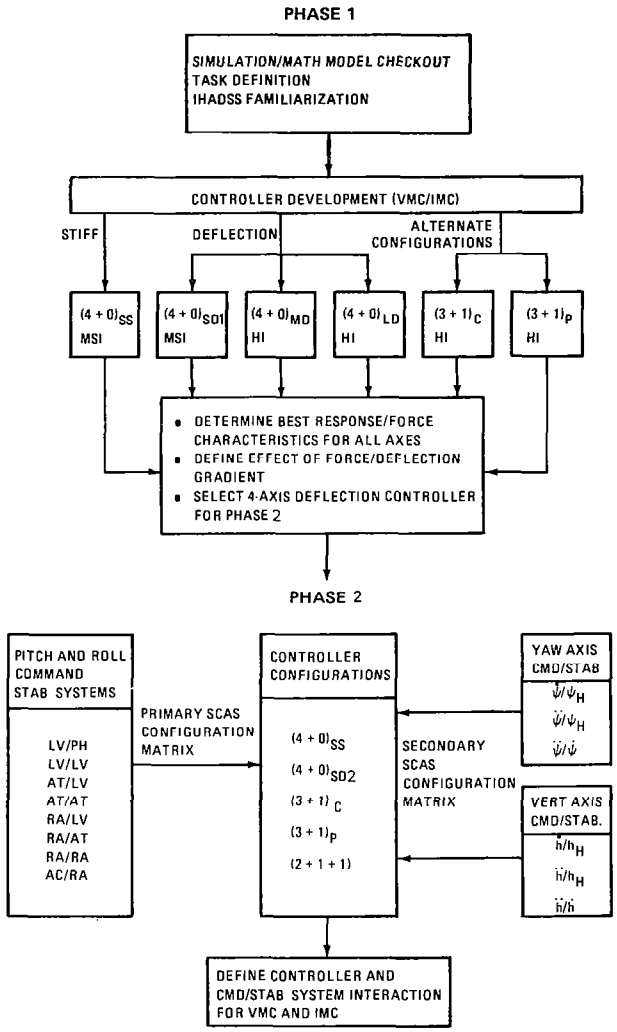

Figure 11 Simulation Experiment Flow Diagram

CONDUCT OF THE EXPERIMENT

EQUIPMENT

This experiment was conducted at the Boeing Vertol Flight Simulation Facility. Major elements of the facility shown in Figure 12 include:

- Single-seat cockpit cab mounted on a six-degree-of-freedom limited-motion base.
- Conventional helicopter flight and performance instruments, and a SCAS mode select panel.
- Conventional helicopter collective and directional pedals implemented as small-displacement force controllers, and three 4-axis side-stick controllers. An adjustable mounting bracket attached to the armrest allowed orientation of each 4-axis side-stick controller for comfort and to minimize inter-axis control inputs. A forward tilt of six degrees and a counter-clockwise rotation of five degrees relative to the armrest was selected.
- Xerox Sigma 9 digital computer to drive the entire simulation. The Sigma 9 was programmed with a UH-60 full-flight envelope math model and easily variable SCAS configurations for this study.
- Four-camera wide-angle television/terrain model visual display system for the simulation of terrain flight under either:

  VMC - Four-window cockpit visual display covering a field-of-view 125°x75°, or

  IMC - FLIR image with superimposed symbology presented by a Honeywell helmet mounted display and sight system (IHADSS) including head tracker.

The FLIR sensor signal was simulated using the center window video channel to provide a 40°x30° outside world field-of-view display. A Gaertner Symbology Generator was utilized to overlay computer generated symbols (Figure 10) on the video picture. The ability to compare directly VMC and IMC handling qualities with a specific controller/SCAS combination was a unique feature of this simulation.

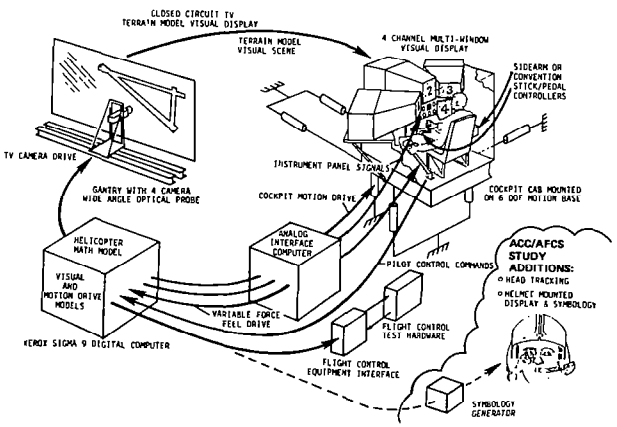

Figure 12 Boeing Vertol Flight Simulation Facility

EVALUATION TASK DESCRIPTION

Evaluation of total system (pilot, controllers, SCAS, displays) performance was accomplished using four specific low speed tasks - the slalom, acceleration/deceleration, nap-of-the-earth, and bob-up task. No secondary duties (e.g., armament, communication, or navigation system management) were required during the performance of each task. For this experiment a 200:1 scale model board (1-1/8 mile long by 3/5 mile wide) with an existing 3000 ft airport runway was modified as shown on Figure 13 to include terrain features and obstacles necessary to perform the planned maneuvers.

Slalom - Low-speed lateral avoidance maneuver requiring the pilot to fly around 50 ft. high obstacles placed 400 feet apart on the runway centerline. From a hover at 30 feet AGL, the pilot accelerates the helicopter to an airspeed of 30 knots. The pilot appropriately controls bank angle and heading to coordinate turns around the obstacles while maintaining a constant airspeed of 30 knots and an altitude of 30 feet throughout the maneuver.

Acceleration/Deceleration - Forward translation of the helicopter while holding a lateral ground track parallel to the runway. From an initial hover position offset from the runway, the pilot acclerates the helicopter to a forward speed of 50 knots, followed by a deceleration maneuver to arrive at a desired hover position near the last runway obstacle. The pilot attempts to hold lateral ground track and altitude, as well as complete the task in minimum time.

Nap-of-the-Earth (NOE) - A multi-axis control task requiring the pilot to fly through three legs of a narrow canyon (125 feet wide and 50 feet high), having two sharp turns (70° left and 80° right) and two obstacles (50 feet high), to reach a termination hover area. During the first leg of the course, an acceleration to 50 knots is performed before crossing a road, followed by a deceleration to 25 knots while maintaining a lateral ground track and an altitude of 30 feet. After executing a coordinated left turn to enter the second leg, the pilot must control altitude to fly over an obstacle and remask to 30 feet in as short a time as possible while attempting to maintain an airspeed of 25 knots. Following a sharp right turn, the pilot flies over a second obstacle, controls altitude back to 30 feet, and decelerates to a hover point in the termination area.

Bob-Up - A multi-axis task consisting of a vertical unmask maneuver from 25 feet to 100 feet, a heading turn to acquire a target, and a vertical remask to the original hover height. The pilot attempts to hold a fixed horizontal ground position throughout the vertical unmask/remask and heading turn maneuvers.

TEST PILOT BACKGROUND AND PARTICIPATION

Five experimental test pilots with extensive flight experience participated in this simulation study - one each from Boeing Vertol, NASA, and the National Aeronautical Establishment (NAE) of Canada, and two pilots from the U.S. Army assigned to NASA. Table 2 presents an

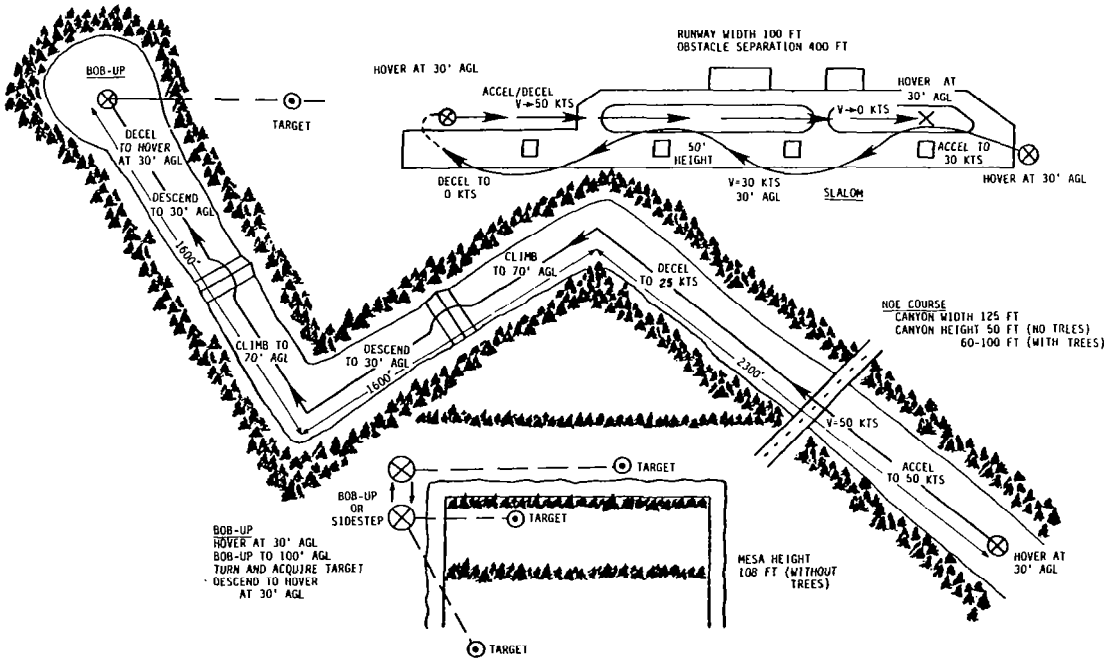

Figure 13 Terrain Model for Evaluation Tasks

experience summary for each evaluation pilot including total flight time broken down by helicopter and fixed wing time. After the initial phase of simulation development, two pilots (A and B) were given 3 hours of IHADSS flight training on the PNVS Surrogate Trainer at the U.S. Army Yuma Proving Ground.

		FLIGHT TIME (HOURS)		RELATED EXPERIENCE			
				SIDE-STICK CONTROLLER DEVELOPMENT		VISUAL DISPLAYS FOR IMC	
PILOT	AFFILIATION	HELICOPTER FIXED-WING	TOTAL	FLIGHT TEST	SIMULATION	FLIGHT TEST	SIMULATION
A	BOEING VERTOL	3,600 (H) 2,800 (F)	6,400	X	X	X*	
B	NASA	2,300 (H) 700 (F)	3,000		X	X*	X
C	NAE CANADA	450 (H) 5,600 (F)	6,050	X	X		
D	U.S. ARMY	1,000 (H) 2,200 (F)	3,200			X	
E	U.S. ARMY	2,500 (H) 700 (F)	3,200		X		X

* IHADSS TRAINING ON PNVS SURROGATE TRAINER INCLUDED FOR PILOT A AND B

Table 2 Summary of Pilot Experience

A total of 204 simulation flight hours was accumulated during this simulation experiment. Sixty-three percent of the total time was utilized for VMC evaluation, and thirty-seven percent for IMC evaluation. A breakdown of the total hours by controller configuration and pilot is given in Table 3. Pilots A, B, and C were the primary evaluators with Pilot A having the largest flight time (54%) since he participated during all eight weeks of the experiment. Pilot B participated for three weeks of the study, and pilot C participated for four weeks. Pilot D, who had significant IHADSS experience on the AH-64, participated for one week and assessed the realism of the simulated IMC system compared to real life hardware. Pilot E, who participated the first week, helped to define the specific tasks used for the remainder of the experiment.

CONTROLLER CONFIGURATION	VMC	IMC	TOTAL
• 4 AXIS STIFF STICK	33	11	44
• 4 AXIS SMALL DEFLN (1)	19	4	23
• 4 AXIS SMALL DEFLN (2)	11	16	27
• 4 AXIS MEDIUM DEFLN	5	4	9
• 4 AXIS LARGE DEFLN	12	1	13
• 3 AXIS + PEDALS	15	11	26
• 3 AXIS + COLLECTIVE	13	15	28
• (2+1+1) PEDALS + COLLECTIVE	14	9	23
• CONVENTIONAL	7	4	11
TOTAL HOURS	129	75	204

PILOT FLIGHT HOURS	VMC	IMC	TOTAL
A	68	42	110
B	21	13	34
C	28	12	40
D	8	5	13
E	4	3	7
TOTAL HOURS	129	75	204

Table 3 Summary of Simulation Flight Hours

DATA COLLECTION AND ANALYSIS

Experimental data collected for this investigation consist of both qualitative pilot evaluation data and quantitative system performance data. Pilot Cooper-Harper ratings and commentary were recorded for each controller/SCAS/display/task combination evaluated. At the end of each evaluation run, the pilot assigned a numerical Cooper-Harper rating to the task according to a structured decision making process defined by Reference 16. The pilot's comments were used to aid data analysis by identifying areas or parameters that most strongly influenced each rating.

Qualitative pilot rating data is emphasized in this paper. Quantitative measures of system performance and/or pilot workload are being calculated using statistical analysis programs. For instance, the mean and standard deviation of helicopter flight parameters relative to a reference position or desired flight path are being computed as a measure of system performance. As an indication of pilot workload, the mean and standard deviations of control command movements are being analyzed. Certain time indices are also being evaluated as an indication of helicopter/pilot performance. Where applicable, time to perform the entire task or portion of a task, i.e., unmask time, is used as a performance index.

OTHER EXPERIMENTAL CONSIDERATIONS

Certain factors which might affect the outcome of the evaluations were identified. An effort was made, where possible, to account for these factors. Specific examples are given below:

(1) The exact stabilization level selected for each evaluation run was not revealed to the pilot.

(2) The command response type (e.g., angular pitch/roll rate versus attitude) was revealed to eliminate surprises and to reduce effects on pilot rating and performance caused by re-learning a certain response characteristic.

(3) Established habit response patterns occasionally had a noticeable effect when changing to a different controller configuration. For instance, after many years of flying conventional pedals, an adjustment period to adapt to control of yaw from the side-stick was common for all pilots. Likewise, after flying side-stick twist to control yaw for several flight hours, converting back to the pedals was not always done with ease. A similar effect was noticed when switching vertical controller configurations, that is, changing from side-stick to conventional lever or

vice-versa. If any configuration change resulted in poor performance, the pilot repeated the run and the best one was used for valid data.

(4) Learning the IHADSS concept and symbology took a significant period of time. The rate of improvement of pilot ratings with IMC simulation flight time was much slower than for VMC flight time. IMC data presented in this paper were obtained during the second simulation phase when the pilots demonstrated a more consistent level of proficiency with IHADSS.

EXPERIMENT RESULTS

Experimental results are based on an analysis of pilot ratings and comments, and discussion of these results is organized according to the major activity phases - controller development and primary-secondary matrix evaluation. Results are summarized using average pilot ratings to indicate general trends; the statistical validity of this simplified approach is not implied and it is understood that care must be used in the interpretation of results, particularly when a large range of ratings is averaged.

CONTROL RESPONSE CHARACTERISTICS

Before different controller configurations were evaluated, a set of control response characteristics for the four control axes and the generic system types (Figure 6) were defined through a series of mini-experiments. Response time constants and sensitivities were varied within the command model and effects on controllability evaluated. A set of best response values was selected, initially for the stiff controller, and the same set of values was then evaluated using the three alternate 4-axis deflection controllers. Additional variations were made about the nominal response values to define the effects on pilot ratings and task performance.

This control response selection process is depicted by Figure 14. Roll attitude sensitivities were evaluated for the slalom maneuver with the various 4-axis controllers. Pilot comments indicated a range where the roll control sensitivity was too high producing a tendency to overcontrol. In contrast, low roll attitude sensitivities less than 4.0 degrees/lb. resulted in heavy control forces and sluggish response characteristics. The best pilot ratings were obtained when all controllers had a roll attitude sensitivity of approximately 6.0 degrees/lb. Figure 14 also shows that pilot ratings of the large-deflection controller were generally degraded compared with the other configurations, and demonstrated a rapid degradation as control response sensitivities were reduced and/or control forces became heavy. The same tendency to degrade quickly was evident with the stiff-stick. The small-deflection controller was much more tolerant to changes in sensitivity as indicated by the relatively shallow slope in the high sensitivity range. Best ratings were achieved with the small-deflection and medium-deflection controllers in the range from 5.5 to 7.5 degrees/lb.

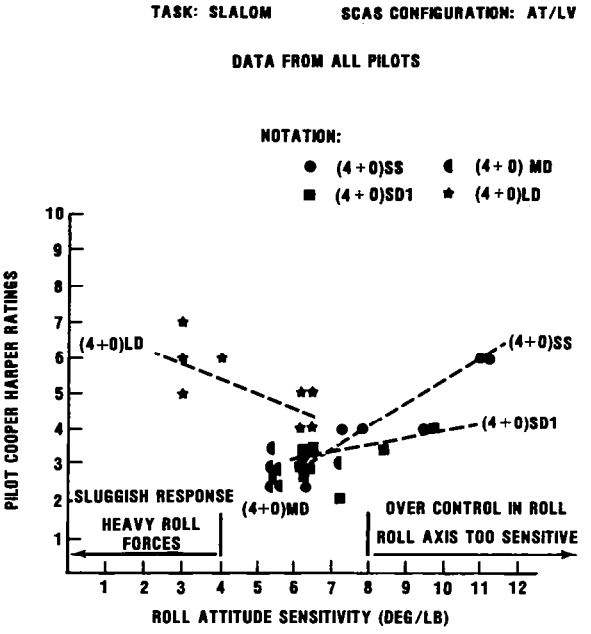

Figure 14 Control Response Selection Process

The same procedure was followed to select pitch/roll rate and longitudinal/lateral velocity response characteristics. Table 4 summarizes the final selected control response characteristics. Except for the acceleration command response, characteristics are approximated by an equivalent 1st order system response. The pitch and roll acceleration response system was designed to provide a short-term rate response, with a long-term acceleration response to automatically eliminate steady control forces required for helicopter trim. This trim function was accomplished with a low-gain integral feed-forward path. Higher integral feed-forward gains were used in the yaw and vertical axes to obtain purer acceleration command responses as indicated in Table 4 by the ratio of steady-state to initial response.

To provide acceptable response characteristics for small precision control tasks and large maneuvers, as well as to minimize the effect of inadvertent inter-axis control inputs, non-linear control response shaping (Figure 15) was used. Each force command signal was passed through a shaping function that allowed variation of deadzone, initial sensitivity gradient, breakpoint, and high sensitivity gradient. Pitch, roll, and yaw control response shaping was symmetrical, whereas the vertical control shaping was asymmetric with a smaller breakout and higher response sensitivity in the down direction.

SENSITIVITY/POUND (SENS) AND TIME CONSTANT (TC)

		ANGULAR RESPONSE						LINEAR RESPONSE			
		ACCEL (AC)		RATE (RA)		ATTITUDE (AT)		ACCEL (AC)		VELOCITY (LV)	
AXIS	CONTROLLER	INITIAL SENS (DEG/SEC^2)	STEADY STATE SENS (DEG/SEC^2)	SENS (DEG/SEC)	TC (SEC)	SENS (DEG)	TC (SEC)	INITIAL SENS (FT/SEC^2)	STEADY STATE SENS (FT/SEC^2)	SENS (FT/SEC)	TC (SEC)
LONGITUDINAL	SIDE-STICK	4.0	0.2	2.0	0.4	4.5	1.2	–	–	12.0	3.0
LATERAL	SIDE-STICK	10.0	1.0	3.5	0.25	6.0	1.2	–	–	16.0	4.0
DIRECTIONAL	SIDE-STICK	2.2	1.8	4.7	0.4	–	–	NA			
	PEDALS	0.6	0.44	1.4	0.60	–	–				
VERTICAL + UP – DOWN	SIDE-STICK	NA						+5.0 −7.7	4.0 −6.2	+6.5 −9.0	0.60
	COLLECTIVE LEVER							±1.6	±1.3	±2.0	0.50

Table 4 Selected Control Response Characteristics

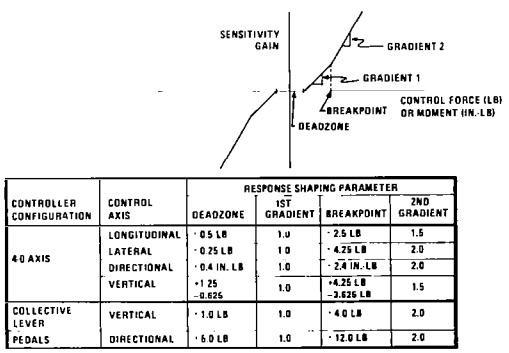

CONTROLLER CONFIGURATION	CONTROL AXIS	RESPONSE SHAPING PARAMETER DEADZONE	1ST GRADIENT	BREAKPOINT	2ND GRADIENT
4-0 AXIS	LONGITUDINAL	·0.5 LB	1.0	·2.5 LB	1.5
	LATERAL	·0.25 LB	1.0	·4.25 LB	2.0
	DIRECTIONAL	·0.4 IN.-LB	1.0	·2.4 IN.-LB	2.0
	VERTICAL	+1.25 −0.625	1.0	+4.25 LB −3.625 LB	1.5
COLLECTIVE LEVER	VERTICAL	·1.0 LB	1.0	·4.0 LB	2.0
PEDALS	DIRECTIONAL	·5.0 LB	1.0	·12.0 LB	2.0

Figure 15 Force Control Response Shaping

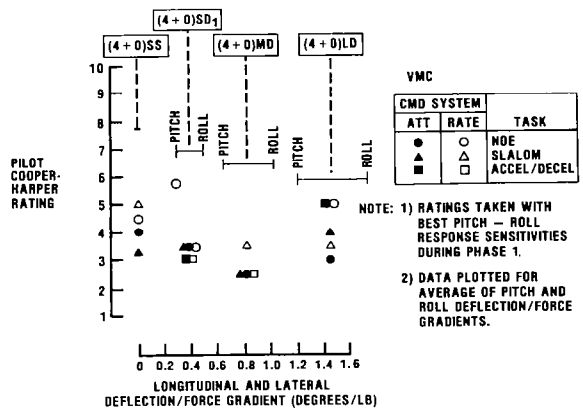

Figure 16 Effect of Side-Stick Controller Deflection/Force Gradient on Pilot Ratings

CONTROLLER DEFLECTION/FORCE GRADIENT

Various side-stick deflection/force gradients were evaluated using the 4-axis stiff controller and three 4-axis deflection controllers described earlier in Table 1. Task performance with each controller was rated for both rate and attitude command systems in pitch and roll. Figure 16 shows the best pilot ratings obtained as a function of controller average deflection/force gradient. The small-deflection and medium-deflection controllers achieved the best pilot ratings.

Commentary from three pilots who compared the stiff-stick and small-deflection controllers was very consistent. All agreed that task performance improved substantially with the introduction of deflection. Typical comments were as follows:

Stiff Controller:

- o "Defining best control sensitivities was more difficult and more critical with a stiff controller than deflection controller."
- o "Inter-axis force harmony/sensitivities appeared to be more critical, especially during larger amplitude maneuvering."
- o "Tendency to over-control, particularly during high frequency manipulative control tasks."
- o "Tendency to release forces abruptly and create inadvertent sharp acceleration response."

Small-deflection Controller:

- o "This controller has a softer feel of actuation than the stiff controller, and control inputs seem to be smoother in application."
- o "Very noticeable improvement over stiff-stick using the same sensitivities. Ability to shape control commands during large amplitude maneuvers and control reversals was a major improvement."
- o "This controller gave an immediate and very obvious improvement in handling qualities. Subjectively, I felt much more 'in the loop'. While tendencies to cross couple remained (compared to stiff controller), they were far depressed below the primary control task and were insignficant. Control inputs seemed much more natural and, although the response seemed to be more sensitive, this effect was quite tolerable."

Acceptance of the medium-deflection controller was mixed. One pilot gave the controller degraded ratings because height control was difficult due to a high force breakout in the vertical axis. A second pilot gave the same controller improved ratings compared to the small-deflection controller because he felt more in control during large maneuvers.

Two pilots evaluated the large-deflection controller and gave degraded ratings compared to the small-deflection controller. Comments indicated a more sluggish pitch control response and less precise control of attitude for high-frequency inputs.

Based on these results, a second 4-axis small-deflection controller design, (4+0)SD2, having a 50% higher deflection/force gradient, was selected for evaluation of the primary and secondary controller/SCAS configuration matrices.

PRIMARY/SECONDARY CONFIGURATION MATRIX

A basic primary matrix - consisting of five controller and five pitch/roll SCAS configurations - was evaluated for all four tasks under both IMC and VMC. The matrix for the bob-up task also included two velocity command systems - one with velocity stabilization and the other with position hold. For both IMC and VMC, a total of 220 possible task/controller/SCAS combinations was evaluated.

Figure 17 presents a matrix of data gathered for the NOE task and performed under IMC with the IHADSS. Each matrix element contains an average rating for each pilot who evaluated the particular configuration combination, as well as

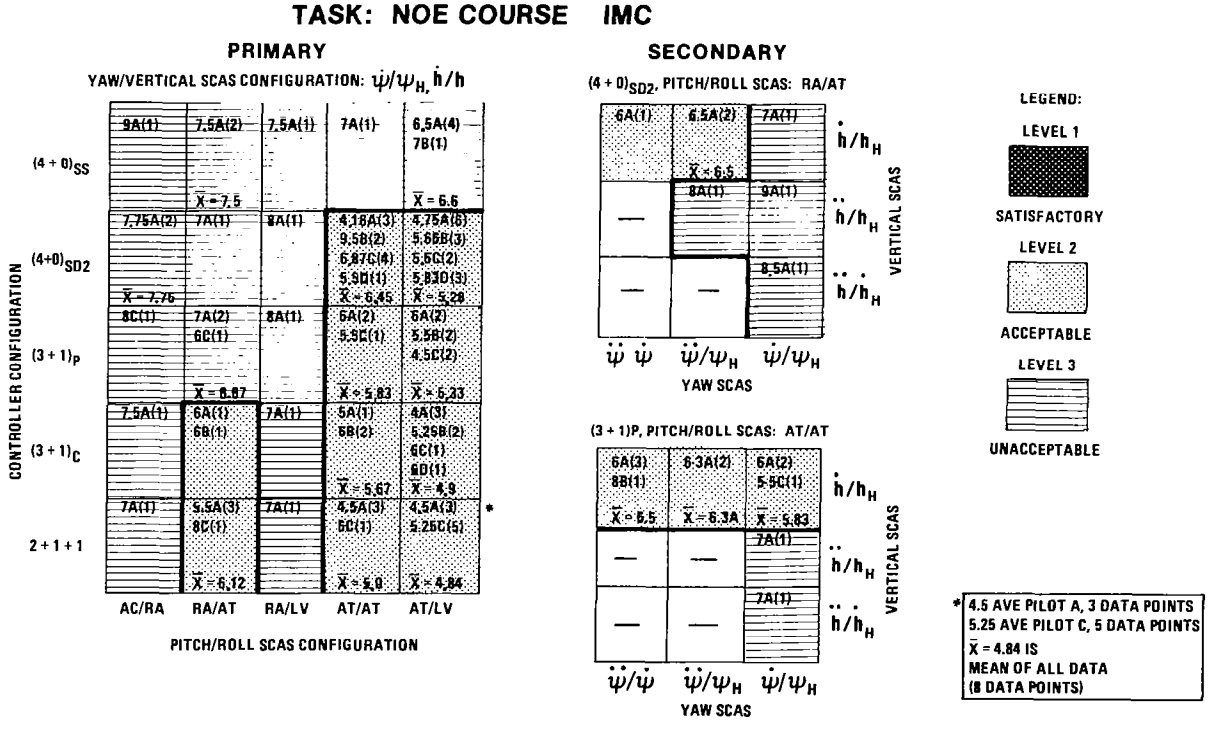

Figure 17 Controller/SCAS Configuration Matrices

the number of test data points included in the average rating. A mean of the individual average ratings in each block is also calculated. Various levels of the handling qualities rating scale are shaded on the matrix to emphasize where the major change from acceptable to unacceptable occurs. It can be seen that Level 1 flying qualities was not achieved for the NOE task under IMC for any controller configuration. The interaction of SCAS/controller configurations can be determined from the matrix. An attitude command system achieved Level 2 ratings regardless of the stabilization type for all controller configurations with the exception of the 4-axis stiff-stick. A RA/AT system exhibited marginal Level 2 flying qualities for the 2+1+1 and (3+1) collective configurations.

Secondary SCAS matrices are also shown on Figure 17. An improvement from Level 3 to Level 2 ratings occurred when a yaw acceleration command was implemented for directional control in place of yaw rate command for the (4+0)SD and RA/AT combination. In contrast, the (3+1) pedal and AT/AT combination degraded to a Level 3 rating when vertical acceleration command was used in place of vertical rate command.

Average pilot rating data contained in the primary SCAS/controller matrices are presented for the four tasks in Figures 18 and 19. Interactive effects of task, controller, and SCAS configurations are more easily seen by this method of presentation, and are described in the following discussion.

CONTROLLER/DISPLAY EFFECTS

The NOE task (Figure 18) was the most difficult of the low-speed maneuvering tasks. Primary factors causing higher workload and degraded flight path performance for the NOE task under IMC were: (1) inability to precisely control height, (2) tendency to couple side-stick vertical control imputs into pitch and/or roll, (3) difficult coordination of lateral-directional control in turns, and (4) tendency to over control roll in high workload situations.

The most serious deficiency reported was poor height and vertical speed resolution due to the small field-of-view, lack of peripheral cues, and/or lack of surface texture/picture detail. Weak motion cues as well as a lack of rotor/drive system noise may have contributed to a tendency for overcontrol of the vertical axis. The pilot had to rely almost totally on display information for vertical speed with no acceleration lead cues.

The 4+0 axis controller received poorer ratings for the NOE course where collective control inputs were required to clear the obstacles. Inadvertent inputs to pitch and roll increased the workload required to maintain airspeed and flight path control. Overcontrol in roll was occasionally experienced when corrective action was required to compensate for an inadvertent control input.

The IMC bob-up task (Figure 18) was essentially an instrument reference task with necessary information such as velocity vector, X-Y position, acceleration cue, and altitude provided by the display symbology. Marginal Level 2 ratings were obtained with an AT/LV system. Level 1 ratings were achievable with a velocity command system having either velocity or position stabilization.

In contrast to the ratings assigned for the other tasks under VMC, ratings for the bob-up task were more degraded. This degradation in VMC ratings was caused by lack of good visual space references at altitudes above 75 feet in the bob-up location. In fact, VMC performance measured by X-Y position hold during the bob-up was significantly degraded over the IMC task.

Because of inadvertent cross-coupled inputs, the 4-axis side-stick controller received poorer pilot ratings for the bob-up task. Separation of the controllers, particularly vertical, improved pilot ratings significantly. The best ratings were achieved using a (3+1) collective configuration combined with a velocity stabilized system.

The IMC acceleration/deceleration task (Figure 19), primarily a single-axis longitudinal maneuver with altitude hold and heading hold selected, was the easiest of the four IMC tasks. Level 2 ratings of approximately 4.0 were obtained with all controllers except for the (3+1) pedal configuration. Workload and task performance were influenced primarily by the following factors: (1) tendency to couple pitch control into side-stick vertical control, (2) vertical control coupling into lateral-directional requiring pilot compensation, (3) pilot disorientation during a nose-up maneuver, and (4) poor resolution of longitudinal/lateral positioning during deceleration to hover. Precise control of aircraft position during the deceleration to hover was difficult due to poor resolution of longitudinal speeds and rate of closure, thought to be caused by the small field-of-view and limited peripheral cues. Small lateral speeds were difficult to discern from small yaw rates especially at slow forward speeds.

Performance of the slalom task (Figure 19) under IMC with altitude and heading hold selected was primarily a two-axis lateral-directional control task. Pilot ratings were degraded by approximately one point compared to the acceleration/deceleration task. Task performance was judged principally on the ability to execute coordinated turns and achieve a desired curvilinear path around obstacles at constant speed. Primary factors which increased workload and degraded pilot ratings were: (1) tendency to couple side-stick yaw control inputs into roll and/or pitch, (2) difficult turn coordination due to lack of peripheral cues with the IMC visual display, and (3) tendency to become disoriented

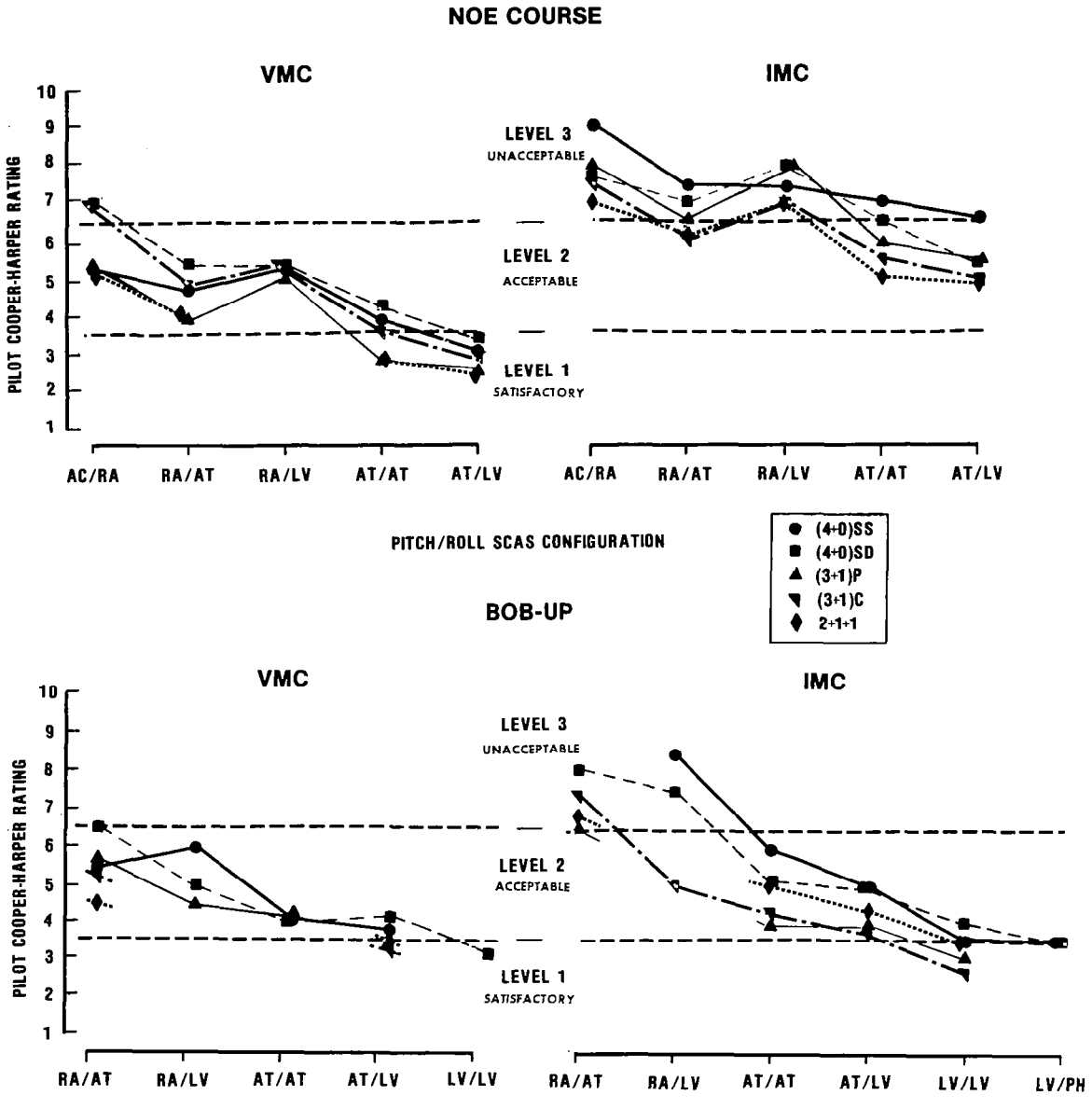

Figure 18 Effect of Primary SCAS/Controller Variations on Pilot Ratings - NOE and Bob-Up Tasks

with IHADSS when head movements were made to locate desired flight path projection. It was difficult to distinguish head response from aircraft response.

For the acceleration/deceleration and slalom tasks, the (3+1) pedal configuration received more degraded pilot ratings than all other configurations. If large errors were allowed to build up, precise corrective control inputs with the pedals were difficult to achieve, and overcontrol of yaw often resulted. Precision yaw control on the side-stick provided improved lateral-directional control for IMC.

PRIMARY SCAS EFFECTS - LONGITUDINAL/ LATERAL

For the most difficult IMC tasks (NOE and Slalom), the acceleration command/rate stabilization system (AC/RA) exhibited Level 3 handling qualities. With the addition of attitude stabilization, the RA/AT system received mar-

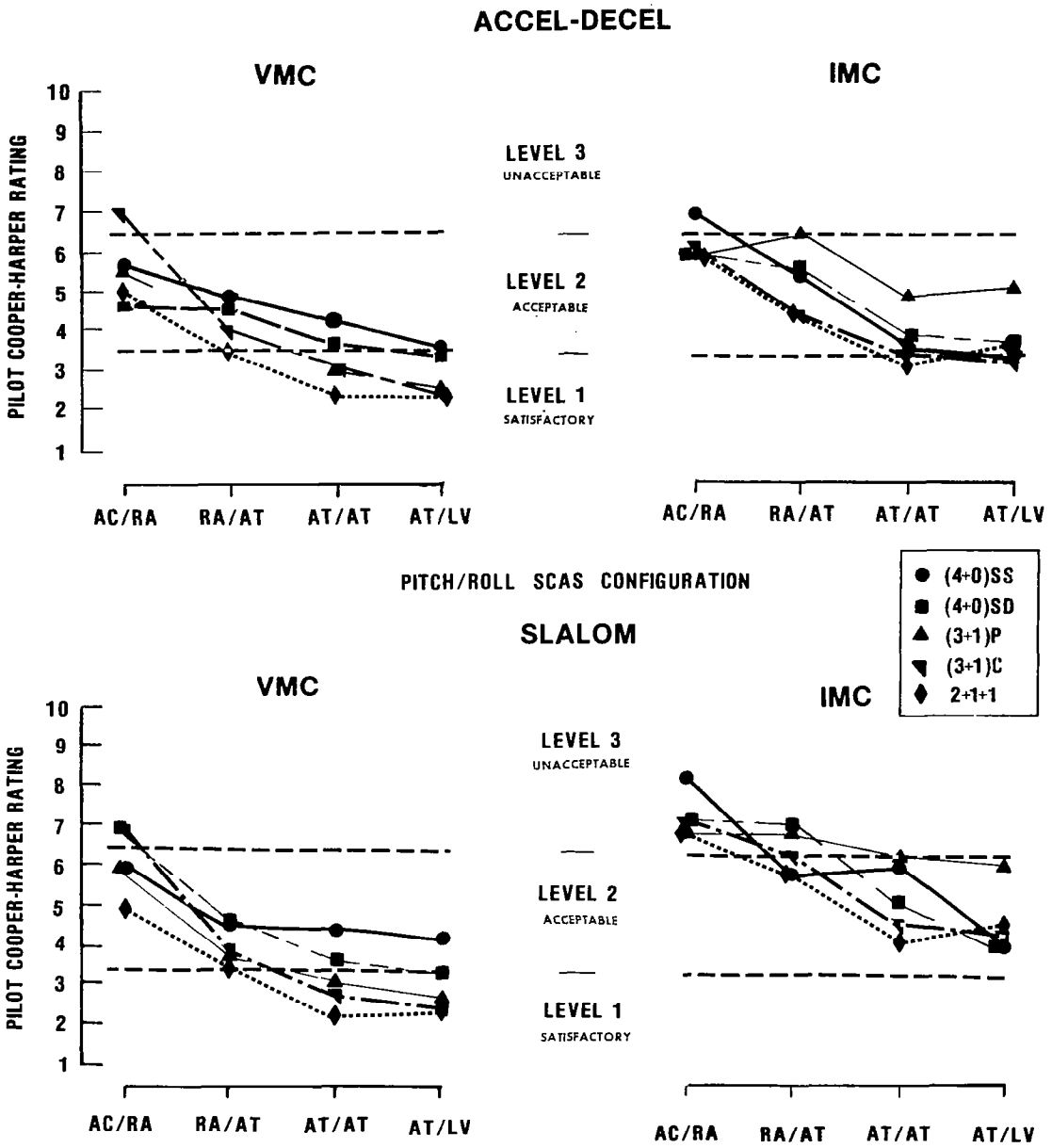

Figure 19 *Effect of Primary SCAS/Controller Variations on Pilot Ratings - Acceleration/Deceleration and Slalom Tasks*

ginal Level 2 ratings for IMC with high workload required to achieve adequate performance. It was extremely difficult to maintain precise flight control parameters (airspeed, lateral ground track, sideslip, etc.). Continuous pulse-type control inputs were required for best performance. When velocity stabilization was combined with a rate command system (RA/LV), for all low-speed maneuvering tasks there was a significant degradation in pilot ratings (Figure 18), particularly noticed in turn maneuvers. Pilot workload and compensation to achieve lateral-directional coordination were noticeably higher, possibly indicating an inherent conceptual design problem with this combination (i.e., having the stabilization type more than one integration away from the command type).

A large improvement in IMC ratings for all tasks was obtained with an attitude command system. With the same level of attitude stabilization, an attitude command system (AT/AT) improved pilot ratings an average of one rating point when compared to the rate command system (RA/AT). A similar improvement occurred in the VMC ratings. Pilot comments indicated that the attitude command system exhibited a noticeably stronger feel of "apparent" stability. The pilots felt more continuous in the control loop with a strong force/attitude (force/linear acceleration) relation. By having more precise control of attitude, maintenance of airspeed and ground track and execution of coordinated turns were performed with lower workload. There was also less tendency to overcontrol with an attitude command system particularly for large maneuvers and/or control reversals.

When combined with an attitude command system, velocity stabilization improved pilot ratings for maneuvering tasks by about half a rating point for both IMC and VMC. It was most noticed by the ease of maintaining airspeed and effecting turn coordination during slalom and NOE tasks, and by the ease of varying airspeed and maintaining lateral ground track during the acceleration/deceleration and NOE tasks.

The influence of SCAS configuration on pilot ratings for the bob-up task is shown in Figure 18. The attitude command system yielded pilot ratings in the low Level 2 region (CHPR $\approx$ 4.5). Use of a velocity command/velocity stabilization system reduced pilot workload, improved task performance, and achieved Level 1 pilot ratings for the bob-up task with all controllers except the 4-axis small-deflection configuration.

Velocity command response characteristics were reported to be more jerky than the attitude response system, however, small position changes could be made easily. The addition of position stabilization, evaluated only with 4-axis controllers, made the bob-up task a series of single-axis control maneuvers. Level 1 ratings were achieved and excellent position hold was generally achieved.

Figure 20 presents an example of bob-up task performance achieved as a function of SCAS configuration. Deviations in longitudinal and lateral position from the initial/desired hover location are used to calculate a mean radius, i.e. a circle containing one-half the total number of data points. Data are presented for Pilot A and five controller configurations as a function of pitch/roll SCAS configuration. Compared to the rate command system, a large improvement in performance and pilot rating can be seen for an attitude command system. Best performance was achieved with a velocity command system (mean radius $\leq$ 12 feet) for all controller configurations. Data for the 4-axis controllers show degraded performance and pilot ratings, particularly for the attitude command system.

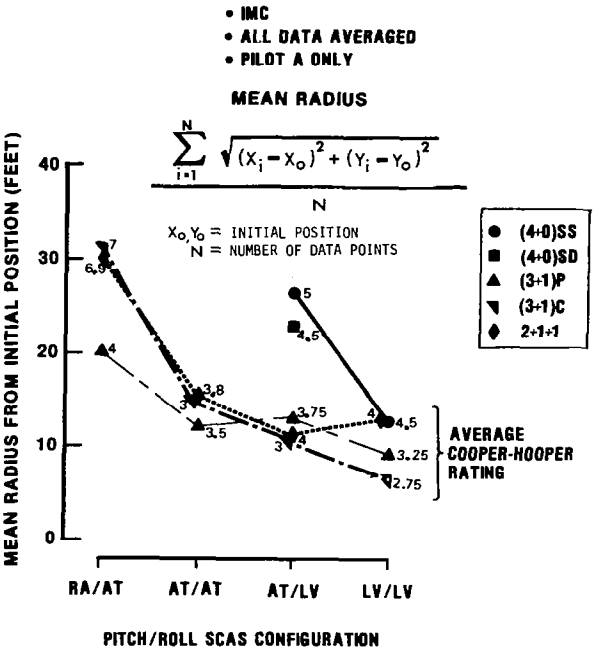

Figure 20 Bob-Up Task Performance

SECONDARY SCAS/CONTROLLER EFFECTS - DIRECTIONAL/VERTICAL

Directional and vertical SCAS configurations were varied for the RA/AT, AT/AT, and AT/LV systems of the primary SCAS matrix. All controller configurations were evaluated. In general, the yaw rate command/heading hold system provided the best pilot ratings with the pitch/roll attitude command systems for all controller configurations and tasks. Turn coordination and lateral ground track could be controlled easily, particularly for VMC. A yaw acceleration command system made it more difficult to execute precise heading changes or to establish a zero yaw rate at a desired heading. Low speed turn coordination and lateral ground track were also degraded due to this inability to modulate or vary yaw rate precisely, particularly with the pedals.

An important interactive directional SCAS/controller effect is shown in Figure 21 where yaw control on the 4-axis side-stick is compared to yaw control with the (3+1) pedal configuration for the slalom task. Yaw acceleration command from the (3+1) pedal or 2+1+1 configuration degraded pilot ratings with all pitch/roll SCAS configurations when compared to the yaw rate command system. When yaw acceleration command was implemented on the side-stick, either a (3+1) collective or 4+0 configuration, pilot ratings were degraded with the pitch/roll attitude command system, but improved with the rate command system. For the low speed coordinated turn maneuver, yaw acceleration com-

mand improved control capability by eliminating the requirement for steady forces to control yaw rate. It is difficult for the pilot to modulate forces in one or two axes (pitch/roll rate control) while holding a steady force in another axis (yaw rate command for turn coordination). The yaw acceleration command system provided improved control harmony for lateral-directional maneuvering when implemented with the pitch and roll rate command systems.

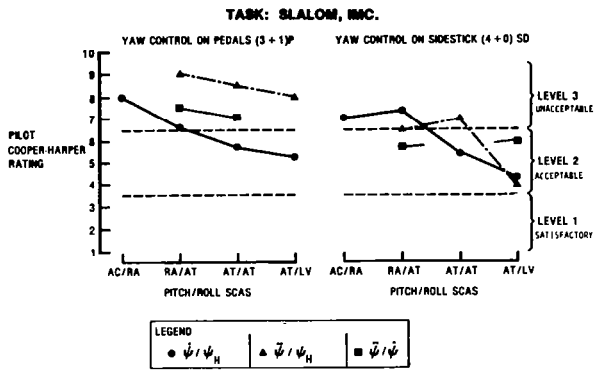

Figure 21 Effect of Yaw SCAS Variations on Pilot Ratings

Also shown on Figure 21, the yaw acceleration command/yaw rate stabilization system generally received better pilot ratings than the yaw acceleration command/heading hold system. As previously noted for the primary SCAS RA/LV system, a degradation of task performance was observed if the stabilization level was more than one integration away from the command type.

The vertical rate command/altitude hold system achieved the best pilot ratings for all pitch/roll SCAS systems and controller configurations. Vertical rate command provided good control of vertical speed and precise control of altitude, particularly for VMC. Acceleration command in the vertical control axis degraded control accuracy and necessitated pulse control inputs to achieve the best flight path performance.

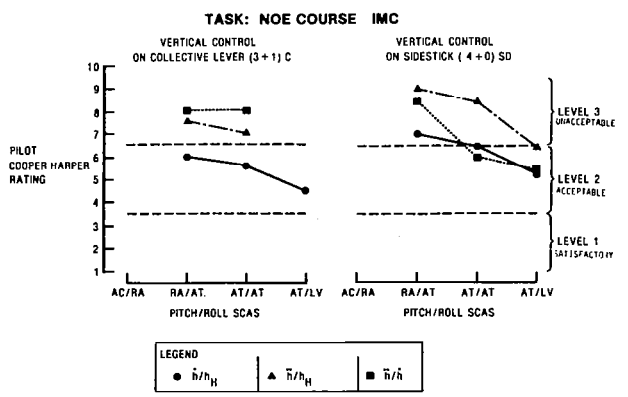

Figure 22 Effect of Vertical SCAS Variations on Pilot Ratings

Figure 22 compares vertical control on the side-stick and conventional collective lever. Vertical acceleration command on the collective lever degraded the IMC handling qualities to Level 3. As with yaw control on the side-stick, vertical acceleration command on the side-stick offers the benefit of eliminating the need to hold steady vertical control forces to achieve a steady vertical rate. However, based upon the results, the benefit of altitude hold and vertical rate command apparently offset the requirement to hold vertical control forces. These particular results may be biased by the lack of strong vertical motion and rotor/drive system noise cues in the simulator.

SUMMARY OF PILOT RATINGS

In order to summarize task and SCAS configuration effects on pilot workload and performance, all data were reorganized into a task/SCAS matrix. Pilot rating data for all controller configurations were averaged for each task/SCAS combination. Figure 23 presents the results of this analysis. In addition to the effect of SCAS configuration, there was a significant effect of task on pilot ratings for IMC. The IMC display effects showed an additive degradation of pilot workload/performance as task difficulty increased. In comparison, VMC pilot ratings were predominantly affected by SCAS configuration and, except for the bob-up task where visual cues become weak, task had little effect. When comparing IMC results to VMC, the mean increase in pilot rating points for each task was: NOE course 2.3, slalom 2.0, acceleration/deceleration 1.2, and bob-up 1.3.

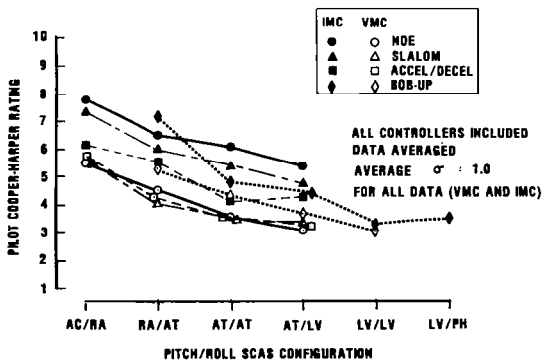

Figure 23 Summary of Task Effect on Pilot Ratings

The effect of primary SCAS configuration on pilot ratings for the slalom, acceleration/ deceleration, and NOE tasks is summarized in Figure 24. Pilot ratings from the three tasks were combined into a single primary SCAS/ controller matrix, thereby tending to average out the ef-

fect of task. A comparison of VMC with IMC is also shown. The average degradation of IMC ratings compared to VMC ratings for all SCAS configurations is 1.8 on the Cooper-Harper rating scale. For each SCAS configuration, the range of pilot ratings from the best to worse controller configuration was an average of one and one-half rating points for both IMC and VMC.

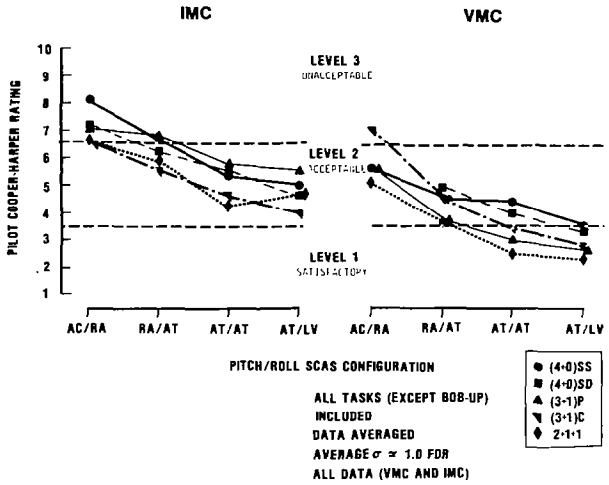

Figure 24 Summary of Primary SCAS/Controller Effects

Figure 24 shows that an acceleration command/rate stabilization system (AC/RA) exhibited Level 3 ratings for the IMC tasks, and the addition of attitude stabilization with a rate command response system (RA/AT) received marginal Level 2 ratings. With the same level of attitude stabilization, an attitude command system (AT/AT) improved both IMC and VMC pilot ratings by over one rating point. When velocity stabilization was combined with an attitude command system, pilot ratings for the maneuvering tasks improved an average of half a rating point for IMC and VMC.

Based on average pilot ratings, from Figures 18 and 19, a ranking of controller configurations was determined for each task as shown in Table 5. Each task was weighted equally to obtain an overall IMC and VMC ranking for each controller configuration.

The (3+1) collective controller configuration provided the best overall pilot ratings for all IMC tasks. A tendency to cross-couple directional control into roll was observed during coordinated lateral-directional turn maneuvers, particularly during initial evaluations. However, this cross-coupling tendency diminished quickly and pilot adjustment to yaw control on the side-stick was easily made.

Pilot ratings for the (3+1) pedal configuration were more degraded than other controller configurations for lateral-directional maneuvering tasks under IMC (Figure 24). However, for the VMC tasks, the (3+1) pedal ratings ranked in the middle and received improved ratings when compared to the 4-axis configuration.

The 2+1+1 controller configuration in general achieved good pilot ratings for all three IMC low-speed maneuvering tasks. For the IMC bob-up task (Figure 18), the 2+1+1 configuration ranked better than the 4+0 but worse than the 3 + 1 configurations. The 2+1+1 configuration achieved the best ratings for all the VMC maneuvering tasks.

DISPLAY	CONTROLLER CONFIGURATION	RANKING BY TASK				OVERALL RANKING (ALL TASKS)
		ACCEL/DECEL	SLALOM	NOE	BOB-UP	
IMC	(4 + 0) SS	3	4	5	4	5
	(4 + 0) SD	4	3	4	4	3
	(3 + 1) PEDAL	5	5	3	2	3
	(3 + 1) COLLECTIVE	1	1	1	1	1
	2 + 1 + 1	2	1	1	3	2
VMC	(4 + 0) SS	5	5	4	DATA NOT AVAILABLE FOR ALL CONTROLLER CONFIGURATIONS	5
	(4 + 0) SD	4	4	5		4
	(3 + 1) PEDAL	2	3	1		2
	(3 + 1) COLLECTIVE	2	2	3		3
	2 + 1 + 1	1	1	1		1

Table 5 Controller Configuration Ranking

CONCLUSIONS

Piloted simulation investigations of the effects on handling qualities of variations in side-stick controller configuration and stability and control augmentation system characteristics for both day VMC and night IMC terrain flight were conducted using the Boeing Vertol Flight Simulation Facility.

Conclusions from these investigations are organized according to the major elements of the simulation study: side-stick controller design, controller configuration, SCAS design, and IMC display effects.

SIDE-STICK CONTROLLER DESIGN

A small-deflection side-stick controller is preferred for low speed NOE maneuvering and precision hover tasks when compared to a stiff-stick controller for the following reasons:

(1) It is easier to modulate force control inputs, particularly during large maneuvers and control reversals. In high workload situations, there is less tendency to over-contol and/or cross-couple control inputs.

(2) Pilot ratings with a deflection controller are less sensitive to variations in control response/force gradient. As a result, it would be easier to design acceptable control response character-

istics for a wider range of pilot preferences if a small-deflection device were implemented.

CONTROLLER CONFIGURATION

The (3+1) collective configuration achieved the best overall pilot ratings for all IMC tasks, followed in rank order by the 2+1+1 and 4+0 or (3+1) pedal configurations. This particular controller configuration provides the following significant advantages for IMC terrain flight:

(1) A separate collective controller eliminates unintentional collective to pitch/roll coupling common to the 4-axis and (3+1) pedal configurations.

(2) Directional control on the side-stick provides more precise heading control than the pedals. There is a tendency to inadvertently couple yaw control to roll; however, all pilots adjusted easily to eliminate or minimize this characteristic. The (3+1) pedal configuration significantly degrades pilot ratings because of yaw controllability for the IMC tasks. The limited field-of-view helmet-mounted display had a strong effect on lateral-directional control.

In contrast, the 2+1+1 and (3+1) pedal configurations achieved the best pilot ratings for VMC. With good peripheral visual cues, directional control becomes a less demanding task.

SCAS DESIGN

A trend of handling qualities improvements attainable by various generic SCAS configurations was defined. Conclusions based upon these results are as follows:

(1) Level 1 handling qualities were not achieved for any of the controller/SCAS combinations investigated for the maneuvering tasks conducted in IMC.

(2) A longitudinal and lateral velocity command system provided Level 1 handling qualities for the bob-up task.

(3) A pitch and roll attitude command system with longitudinal and lateral velocity stabilization generally provided the best pilot ratings for the low-speed maneuvering tasks conducted in IMC.

(4) Altitude and heading stabilization were beneficial for all tasks and controller configurations.

(5) Yaw rate and vertical rate command systems are generally preferred for all tasks and controllers. However, with a pitch and roll rate command system, there exists a preference for side-stick yaw acceleration and vertical acceleration command systems to eliminate the requirement to hold steady forces during multi-axis maneuvers.

(6) For rigid or small-deflection force controllers, elimination of steady forces for steady-state helicopter trim must be automatic through design of the primary control system and/or AFCS control response laws. The build-up of long-term steady forces is unacceptable.

IMC DISPLAY EFFECTS

Pilot ratings for the most difficult IMC maneuvering task were degraded by approximately two points when compared to the same task under VMC; degradation in both longitudinal and lateral handling qualities was caused by the limited field-of-view available from the helmet-mounted display.

RECOMMENDATIONS

Continued simulation studies and design effort should be directed toward:

(1) Improvement of vertical axis control using a (3+1) collective or 4-axis configuration. Emphasis should be given to human factor aspects such as grip design, side-arm support, and controller orientation.

(2) Development of a (3+1) collective configuration using a left-hand side-stick vertical controller instead of a conventional collective lever. Consideration should be given to having both controllers available for vertical control. The 4-axis controller would be used for low workload situations, i.e., level flight and contour flying to free the left hand for cockpit adjustments and secondary functions. The separate left-hand controller would be available for high workload flight maneuvers, e.g., IMC/VMC nap-of-the-earth maneuvers, autorotational landings, emergency situations.

(3) Refinement of control laws to achieve Level 1 pilot ratings for IMC. Possible SCAS modifications include: Automatic low-speed turn coordination, inter-axis control paths to decouple responses, and alternate control response shaping characteristics.

(4) Assessment of the effect of large motion cues on vertical SCAS/controller design and overall pilot ratings using the Vertical Motion Simulator at NASA Ames.

(5) Investigation of the effects of turbulence on system performance and pilot workload.

(6) Comparison of alternate configurations for SCAS off or degraded mode conditions.

ACKNOWLEDGEMENTS

The experiment described in this paper was conducted by the Boeing Vertol Company for the Aeromechanics Laboratory, U. S. Army Research and Technology Laboratories (AVRADCOM) under NASA Ames Research Center Contract NAS2-10880 as part of the Army's Advanced Digital/ Optical Control System Program managed by the Applied Technology Laboratory, Fort Eustis, Va.

The authors gratefully acknowledge the contributions of P. Dunford and S. Glusman of Boeing Vertol for their able assistance in gathering and preparing the data presented herein and the services of participating test pilots:

L. Freisner	Boeing Vertol
R. Merrill	U. S. Army
M. Morgan	National Aeronautical Establishment, Canada
P. Morris	U. S. Army-Ames
G. Tucker	NASA Ames

REFERENCES

1. Troubanos, C. M. and Kelley M. B.: "Pilot Night Vision System (PNVS) for Advanced Attack Helicopter (AAH)". AHS Preprint No. 78-16, 34th Annual National Forum of the American Helicopter Society, Washington, D.C., May 1978.

2. "Military Specification - Flying Qualities of Piloted V/STOL Aircraft." MIL-F-83300.

3. Hall, G. W. and Smith, R. E.: "Flight Investigation of Fighter Side-Stick Force-Deflection Characteristics". AFFDL-TR-75-39, 1975.

4. Black, G. T. and Moorhouse, D. J.: "Flying Qualities Design Requirements for Sidestick Controllers". AFFDL-TR-79-3126, 1979.

5. Deardorff, J. C.; Freisner, A. L.; and Albion, N.: "Flight Test Development of the Tactical Aircraft Guidance System". AHS Preprint No. 761, 29th Annual National Forum of the American Helicopter Society, Washington, D.C., May 1973.

6. Hutto, A. J.: "Flight Test Report on the Heavy-Lift Helicopter Flight-Control System". AHS Preprint No. 961, 31st Annual National Forum of the American Helicopter Society, Washington, D.C., May 1975.

7. Padfield, G. D.; Tomlinson, B. N.; and Wells, P. M.: "Simulation Studies of Helicopter Agility and Other Topics". RAE Technical Memorandum, 1978.

8. Sinclair, M. and Morgan, M.: "An Investigation of Multi-Axis Isometric Side-Arm Controllers in a Variable Stability Helicopter". NRC, NAE LR-606, 1981.

9. Smith, Stephen B. and Miller, Charles M., Captain, USAF, "An Evaluation of Sidestick Force-Deflection Characteristics on Aircraft Handling Qualities", AFFDL-TR-78-171, pp. 395-413, December 1978.

10. Hoh, R. H. and Ashkenas, I. L.: "Development of VTOL Flying Qualities Criteria for Low Speed and Hover". NADC-77052-30, 1979.

11. "Heavy Lift Helicopter Flight Control System, Volume III-Automatic Flight Control System Development and Feasibility Demonstration", USAAMRDL-TR-77-40C, September 1977.

12. Davis, J. M.; and Landis, K. H.; Leet, J. R., "Development of Heavy Lift Handling Qualities for Precision Cargo Operations." AHS Preprint No. 940; 31st Annual National Forum of the American Helicopter Society, Washington, D.C , May 1975.

13. Aiken, E. W. and Merrill, R. K.: "Results of a Simulator Investigation of Control System and Display Variations for an Attack Helicopter Misson". AHS Preprint No. 80-28, 36th Annual Forum of the American Helicopter Society, Washington, D.C., May 1980.

14. Hoh, R. H. and Ashkenas, I. L., "Handling Quality and Display Requirements for Low Speed and Hover in Reduced Flight Visibility." AHS Preprint No. 79-29; 35th Annual National Forum of the American Helicopter Society, Washington, D.C., May 1979.

15. Keane, W. P., Shupe, N. K., Sun, P. B., Robbins, T., and Campagna, R. W., "A Versatile Display for NOE Operations." AHS Preprint No. 77.33-24; 33rd Annual National Forum of the American Helicopter Society, Washington, D.C., May 1977.

16. Cooper, G. W. and R. P. Harper, Jr., "The Use of Pilot Rating in the Evaluation of Aircraft Handling Qualities." NASA TND-5153, 1969.

DEFINITION OF DISPLAY/CONTROL REQUIREMENTS FOR ASSAULT TRANSPORT NIGHT/ADVERSE WEATHER CAPABILITY

R. Joseph Milelli and Gary W. Mowery
Program Engineers
Martin Marietta Corporation
Orlando, Florida

Carmen Pontelandolfo
HNVS Project Engineer
Naval Air Development Center
Warminster, Pennsylvania

Abstract

The U.S. Marine Corps is currently developing a Helicopter Night Vision System (HNVS) to improve low-altitude night and/or adverse weather assault transport capabilities. Martin Marietta Aerospace, under contract to the Naval Air Development Center, has performed a number of man-in-the-loop simulation experiments in its Simulation and Test Laboratory (STL) to define the minimum display and control requirements for the assault transport mission. These simulation studies have investigated forward looking infrared (FLIR) sensor requirements, along with alternative displays such as panel mounted displays (PMD), helmet mounted displays (HMD), and integrated control display units. Also explored were navigation requirements, pilot/copilot interaction, and overall cockpit arrangement. Based on pilot performance and opinion data, pilot use of an HMD and copilot use of a PMD appear as both the preferred and most effective night navigation combination.

Introduction

State-of-the-art forward looking infrared (FLIR) systems make it possible for transport helicopters to conduct missions under conditions that would normally preclude operations. The transport mission requires the transport helicopter to fly at extremely low altitudes at the highest speed possible. Pilots must also approach and land in unimproved landing zones. Personnel and equipment must be quickly offloaded because the aircraft must depart to permit landing of the remaining formation. This mission must be accomplished day and night and in adverse weather conditions.

The United States Marine Corps is presently developing and evaluating design requirements for a Helicopter Night Vision System (HNVS) that would improve transport helicopter low-level night and reduced visibility capabilities.

In support of this effort, tradeoff analyses and system alternative studies were conducted to determine which type of night vision system could provide pilots with precise visual cues required as an aid to navigation and for terrain avoidance. Several types of systems were examined, such as night vision goggles, pyroelectric vidicon, active gated TV, low light level TV, and forward looking infrared (FLIR) devices. Related Army and Navy studies have concluded that FLIR devices perform better than other electro-optical systems on a significantly greater number of occasions. Consequently, a FLIR system capable of being configured and integrated into the assault transport helicopter was selected as the night vision system with the best potential for satisfying HNVS mission requirements.

The HNVS concept, shown in Figure 1, is based on a FLIR system that is mounted on the forward section of the assault helicopter. FLIR imagery is provided on panel mounted displays (PMDs) or helmet mounted displays (HMDs) for the pilot and copilot. The FLIR permits the pilot to operate under conditions of total darkness, and flight symbology superimposed on the FLIR imagery minimizes the pilot's and copilot's scan patterns. In addition, support avionics (such as a self-contained navigation system, radar altimeter, aircraft transducer, central computer, and control panels) are also required. The entire system will be designed to enable the mission to be performed safely with a minimal workload for both pilot and copilot.

Prior simulation experiments conducted in Martin Marietta's man-in-the-loop facility using a six-degree-of-freedom motion base concentrated primarily on basic system design parameters and aircrew interaction using panel mounted displays during the enroute portion of the transport mission. The Navy continued the simulation studies to 1) further expand, verify, and refine the data base during the approach and landing portion of the transport mission; 2) to evaluate alternative displays; 3) to further refine the overall cockpit configuration, and 4) to evaluate incorporation of a control display unit to support the navigation requirements of the mission. Results of the these studies were compared with data obtained in actual flight tests of FLIR and helmet display technologies at Yuma Proving Grounds.

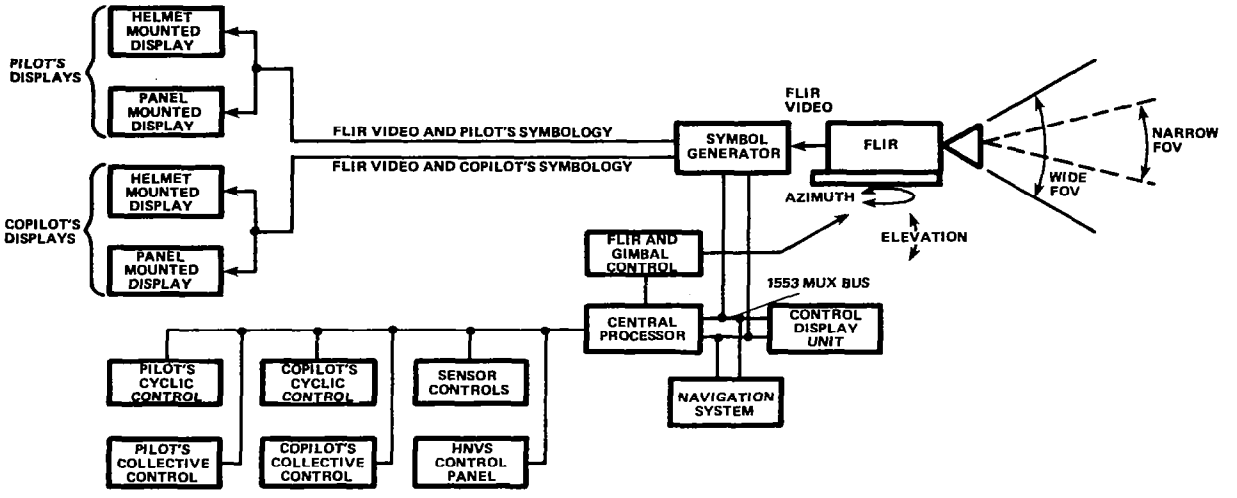

Figure 1. HNVS Block Diagram

Man/Machine Simulation Objective

The objective of the man/machine simulation experiment was to obtain human factors data for low-level assault transport operations using night vision sensors and ancillary hardware during the approach and landing portion of the mission. These data were collected and analyzed, then recommendations were developed that have been reviewed for incorporation into flight test evaluations and HNVS system specifications.

Approach

The HNVS simulation experiment used classical modeling, validation, and experimentation techniques. A highly realistic CH-53D cockpit developed for prior enroute simulations was used for these studies. Thirty-five operational fleet Marine pilots participated as subjects in the experiment and represented both CH-53 and CH-46 squadrons. These pilots had between 270 and 4000 helicopter flight hours, with an average of 695 hours. Experiments were conducted to investigate aircrew performance during approach and landing using different display combinations of panel mounted and helmet mounted displays, including the copilot's use of a Virtual Head Up Display (HUD). Additionally, pilot performance was investigated using a control display unit to assist in the visual navigation requirements. A variable landing zone size was used to increase workload as a a measure of system performance.

CH-53 Cockpit

The CH-53D cockpit is shown on a six-degree-of-freedom motion base in Figure 2. The interior of the cockpit (Figure 3) was precisely modeled to CH-53D dimensions using consoles and control panels from a stricken aircraft. A special-purpose rotorcraft simulator modeled the CH-53D aerodynamic characteristics. The Automatic Flight Control System (AFCS), the Stability Augmentation System (SAS), and the outerloop attitude and heading hold modes were modeled on analog computers. McFadden Systems three-axis force control loaders were used to duplicate the control system's mechanical characteristics.

Figure 2. Cockpit on Motion Base

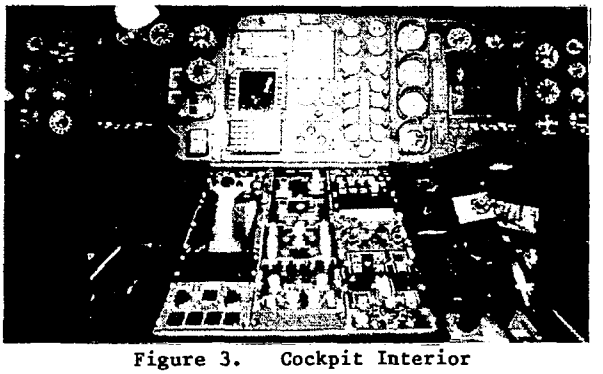

Figure 3. Cockpit Interior

HNVS Controls

The HNVS controls, readily accessible to both pilots, were arranged to provide rapid and accurate control selection and actuation. Sensor control was provided on both collectives and on the center console. Symbology select and field-of-view (FOV) select were provided on both cyclic controls and the center console.

Panel Mounted Displays (PMD)

The instrument panel (Figure 3) was modified with the installation of two nine-inch diagonal CRT displays for presentation of simulated terrain imagery to the pilot and copilot. The displays were located so that the pilot and copilot design eyepoints were at the outside edge of the display from a viewing distance of 34 inches. Brightness and contrast controls were located directly below each display. A red filter was installed over the display for simulated night operations. A 50-degree FOV provided on the nine-inch monitor, at the design eye distance of 34 inches, yielded a 0.30:1 minification of the real-world view.

Helmet Mounted Display (HMD)

The Integrated Helmet and Display Sight System (IHADSS), shown in Figure 4, was installed in the cockpit for both pilot and copilot. The sight determined the pointing directions of the pilot's line of sight (LOS), and the HMD provided both pilot and copilot with collimated video displays. The IHADSS was used to slave the HNVS sensor to the pilot's LOS and display HNVS imagery to both pilot and copilot HMDs. Since copilots might find it objectionable or become disoriented with the HMD continually presenting sensor imagery while they scanned instruments in the cockpit, a virtual HUD presentation was included for the copilot. As the copilot turned his helmet away from a 30- by 40-inch window located straight ahead, the terrain image moved off the HMD as if he were looking at a stationary HUD. The 50-degree FOV provided on the HMD yielded a 1:1 real-world view to the pilots.

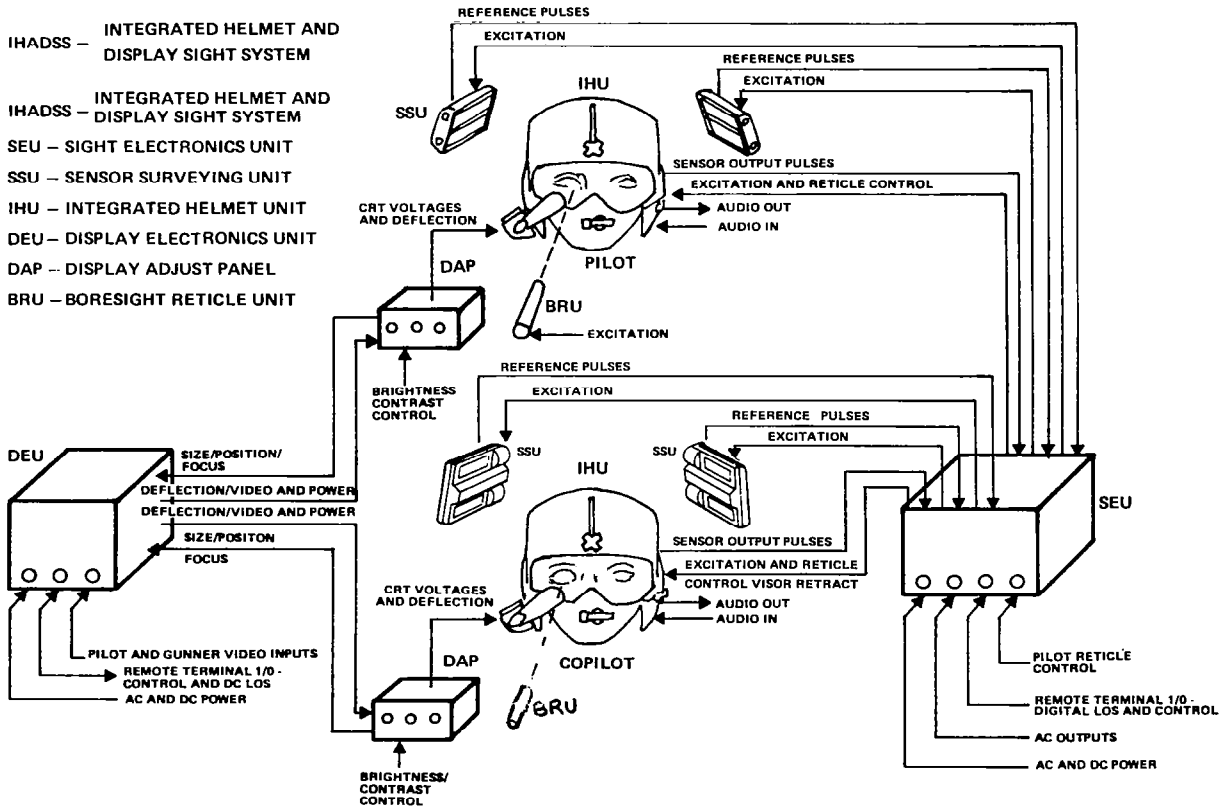

Figure 4. IHADSS System Diagram

Control Display Unit (CDU)

The CDU (Figure 5) was the primary man/machine interface for navigation initialization and mode control. It consists of a CRT display, master function switches, line key, and an alphanumeric key set that enables the copilot to view either the mission flight plan, or the navigation plot showing fly-to-point data, reference points, and aircraft position along a projected course.

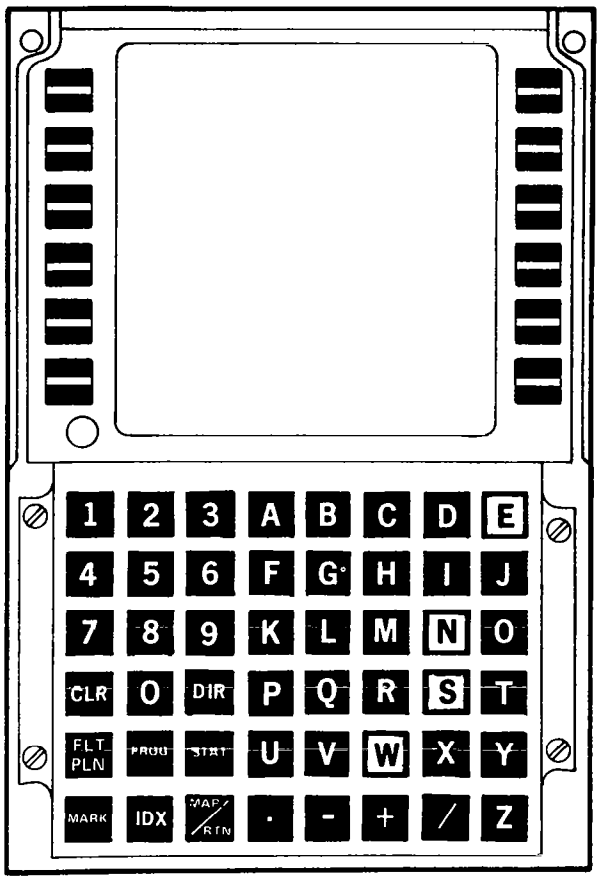

Figure 5. Control Display Unit

Symbology

Two symbology formats were provided. The Flight Symbology format (Figure 6) was developed as a piloting aid during enroute flight and commencement of approach to hover. The Hover/Transition Symbology format (Figure 7) was designed as an aid to transition the aircraft from forward flight to hover and as a precise hover aid. Numerous symbology formats were evaluated during the simulation. The Flight and Hover/Transition Symbology formats provided the best pilot performance for aircraft control during the entire enroute and hover portions of the mission.

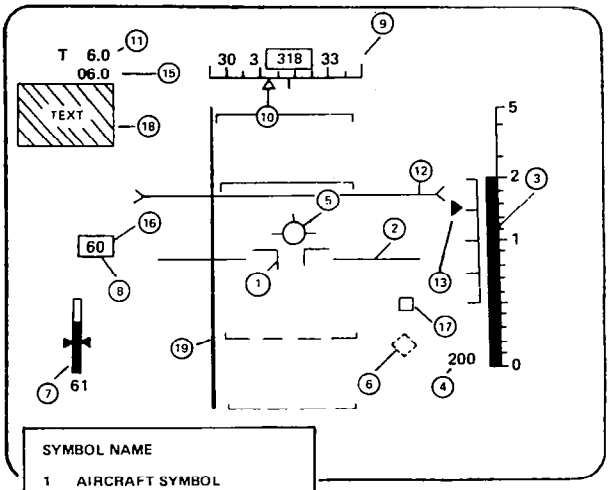

SYMBOL NAME	
1	AIRCRAFT SYMBOL
2	HORIZON/PITCH BARS
3	RADAR ALTITUDE (ANALOG)
4	RADAR ALTITUDE (DIGITAL)
5	VELOCITY VECTOR
6	IR SENSOR
7	TORQUE
8	GROUNDSPEED/AIRSPEED
9	AIRCRAFT HEADING
10	NAVIGATION STEERING
11	DISTANCE TO GO
12	ALTITUDE REFERENCE BAR
13	VERTICAL SPEED
15	TIME TO GO
16	AIRSPEED INDICATION
17	POINT OF INTEREST
18	FAILURE WARNING INDICATOR
19	CORRIDOR BAR

Figure 6. Flight Symbology Format

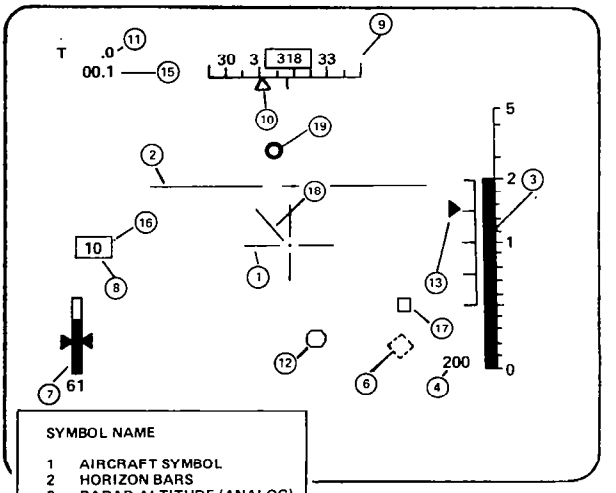

SYMBOL NAME	
1	AIRCRAFT SYMBOL
2	HORIZON BARS
3	RADAR ALTITUDE (ANALOG)
4	RADAR ALTITUDE (DIGITAL)
6	IR SENSOR
7	TORQUE
8	GROUNDSPEED/AIRSPEED
9	AIRCRAFT HEADING
10	NAVIGATION STEERING
11	DISTANCE TO GO
12	POSITION BOX
13	VERTICAL SPEED
15	TIME TO GO
16	AIRSPEED INDICATION
17	POINT OF INTEREST
18	HOVER VELOCITY
19	HOVER ACCELERATION

Figure 7. Hover/Transition Symbology Format

Hybrid Computing System

The simulation was controlled by a hybrid computing system consisting of two Sigma 5 digital computers, three EAI 231-RV analog computers, appropriate instrumentation, and interface and peripheral equipment. The computer arrangement controlled the aerodynamics, processed position commands to the terrain model (Figure 8) and TV, handled operational mode logic and switching functions, generated commands to position symbology on the cockpit displays, and stored performance data.

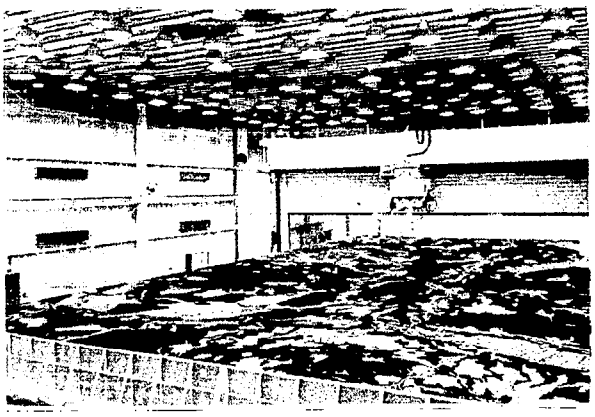

Figure 8. Terrain Model

Experimental Procedures

Pilots were given an orientation to Martin Marietta's Simulation and Test Laboratory (STL), a system briefing, and an experiment briefing. Ground school was conducted on HNVS cockpit controls and displays. The pilot groups then progressed through fixed and motion-base familiarization flights, and finally progressed to training configurations that mirrored the data acquisition procedures. When all pilots approached their learning asymptote, as evidenced by their performance, data collection commenced. Before each session of data runs, a briefing structured to resemble an air intelligence briefing was held. Pilots were given a map of the area, a flight card, and a simulated 8 by 10 inch black and white reconnaissance photos of checkpoints and the landing zone. Route legs and checkpoints were presented on the map. The pilots participated in informal debriefing sessions at the conclusion of data run sets, and they completed extensive debriefing questionnaires when they completed all data sessions. The informal debriefing sessions and questionnaires were designed to obtain subjective information from the participants on relevant HNVS issues.

Pilot Performance Data

A large number of pilot performance measures was gathered during the data runs, and several measurements of pilot performance were taken as part of each evaluation. Pilot performance data tends to support pilot opinion data, but it is not as pronounced, a result typical in simulation programs.

Display Combination Evaluation

To determine the effects of display combinations on crew performance during approach and landing, three treatment conditions were tested: 1) pilot and copilot using PMDs, 2) pilot using HMD and copilot using PMD, and 3) pilot and copilot using HMDs. Each combination was evaluated in landing zones with two difficulty levels. The large zone was 3.5 rotor diameters (difficulty level 2) or more, and the small landing zone was 3.4 rotor diameters or less (difficulty level 1).

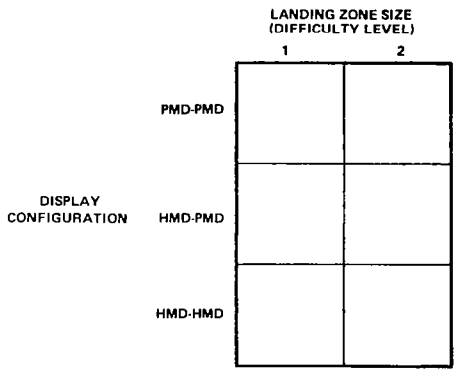

Figure 9. Experimental Matrix for Approach and Landing PMD/HMD/CDU Evaluation

The data matrix for this evaluation is shown in Figure 9. A Greco Latin Square design allowed order effects to be evenly distributed across all subjects and treatments.

Touchdown and Approach Data for Display Combination Evaluation

The touchdown performance data were analyzed on five dependent variables (landing time, radial landing error, X drift, Y drift, and Z drift) and three approach variables (percent under 100 feet, average altitude, and average groundspeed). The independent variables were three display configurations: PMD-PMD, PMD-HMD, and HMD-HMD. Table 1 shows the levels of significance resulting from this analysis. The significant difference in landing error was expected as a function of zone size. Although no display combinations resulted in significant performance differences, trends in favor of the HMD combinations do appear. The HMD-PMD combination had the greatest time under 100 feet, the lowest mean radar altitude, the only mean altitude under 100 feet, and the least amount of Z drift. Tables 2 through 5 show the touchdown and approach results, along with relative rankings of these results between display configurations. The HMD-HMD combination had the shortest landing time and the best overall ranking on

touchdown performance. These results indicate that the pilot's display affects performance most significantly, and performance is better with the HMD.

Table 1. Pilot Performance in HMD-PMD Evaluation: Touchdown and Approach

DEPENDENT VARIABLES	OVERALL MEAN	STANDARD DEVIATION	INDEPENDENT VARIABLES		
			DISPLAY CONFIGURATION	DIFFICULTY LEVEL	INTERACTION
TOUCHDOWN:					
LANDING TIME	234.52S	100.70	NS**	NS	NS
RADIAL LANDING ERROR	31.67 FT	34.41	NS	p = 0.046	NS
-X DRIFT	-1.61 FT/S	1.68	NS	NS	NS
+X DRIFT	2.41 FT/S	3.18	NS	NS	NS
-Y DRIFT	-1.88 FT/S	1.89	NS	NS	NS
+Y DRIFT	1.24 FT/S	1.29	NS	NS	NS
Z DRIFT	4.46 FT/S	2.88	NS	NS	NS
APPROACH:					
PERCENT UNDER 100 FEET	38.68 %	28.81	NS	LANDING ZONE DOES NOT AFFECT APPROACH VARIABLES	
AVERAGE GROUNDSPEED	59.57 KN	12.36	NS		
AVERAGE ALTITUDE	119.03 FT	56.79	NS		

Table 2. HMD-PMD Evaluation: Touchdown Performance Trends

DISPLAY CONFIGURATION	LANDING ZONE SIZE AND TOUCHDOWN VARIABLES													
	LANDING TIME (SECONDS)		LANDING ERROR (FEET)		-X DRIFT (FT/S)		+X DRIFT (FT/S)		-Y DRIFT (FT/S)		+Y DRIFT (FT/S)		Z DRIFT (FT/S)	
	LARGE	SMALL	LARGE	SMALL	LARGE	SMALL	LARGE	SMALL	LARGE	SMALL	LARGE	SMALL	LARGE	SMALL
PMD-PMD	233	277	36	21	0.89	1.89	3.66	1.23	1.39	2.15	1.24	1.32	4.69	4.57
HMD-PMD	234	220	44	27	1.85	1.23	3.03	4.59	0.98	2.58	1.26	1.28	4.16	3.74
HMD-HMD	224	210	40	19	3.35	1.82	1.92	1.55	2.62	0.08	0.95	1.30	4.52	4.93

Table 3. HMD-PMD Evaluation: Relative Rankings of Touchdown Trends

DISPLAY CONFIGURATION	LANDING ZONE SIZE AND TOUCHDOWN VARIABLES														OVERALL RANK
	LANDING TIME (SECONDS)		LANDING ERROR (FEET)		-X DRIFT (FT/S)		+X DRIFT (FT/S)		-Y DRIFT (FT/S)		+Y DRIFT (FT/S)		Z DRIFT (FT/S)		
	LARGE	SMALL	LARGE	SMALL	LARGE	SMALL	LARGE	SMALL	LARGE	SMALL	LARGE	SMALL	LARGE	SMALL	
PMD-PMD	2	3	1	2	1	3	3	1	2	2	2	3	3	2	3*
HMD-PMD	3	2	3	3	2	1	2	3	1	3	3	1	1	1	2
HMD-HMD	1	1	2	1	3	2	1	2	3	1	1	2	2	3	1

*1 = BEST RANKING

Table 4. HMD-PMD Evaluation: Approach Performance Trends

DISPLAY CONFIGURATION	APPROACH VARIABLES		
	PERCENT UNDER 100 FEET	AVERAGE GROUNDSPEED	AVERAGE ALTITUDE
PMD-PMD	35.91	59.63	131.75
HMD-PMD	44.27	58.70	107.10
HMD-HMD	38.51	59.78	113.24

Table 5. HMD-PMD Relative Rankings of Approach Trends

DISPLAY CONFIGURATION	APPROACH VARIABLES			OVERALL RANK
	PERCENT UNDER 100 FEET	AVERAGE GROUNDSPEED	AVERAGE ALTITUDE	
PMD-PMD	3	2	3	3*
HMD-PMD	1	3	1	1.5
HMD-HMD	2	1	2	1.5

*3 = WORST RANKING

Smoothness of Approach and Landing for Display Combination Evaluation

Regression analyses were run on the distributions. The radar altitude for the last nautical mile before touchdown was significantly ($p = 0.10$) smoother for the HMD-PMD configuration than for that of the PMD-PMD. Figure 10 shows the radar altitudes approaching the landing zone (LZ) as lower and smoother for the HMD-PMD configuration. Significant differences in distance distributions were also found in pitch angle. The pitch angle for the HMD-HMD configuration was significantly ($p = 0.0028$) smoother than the PMD-PMD configuration, and difficulty level 1 (small LZ) was significantly smoother than level 2 (large LZ). This difference is shown in Figures 11 and 12. Examining the time distribution indicated that the rate of descent was more consistent for the larger LZs. The display combination trends, although not statistically significant, show the PMD-PMD combination to be more erratic across all variables than both configurations in which the pilot uses the HMD.

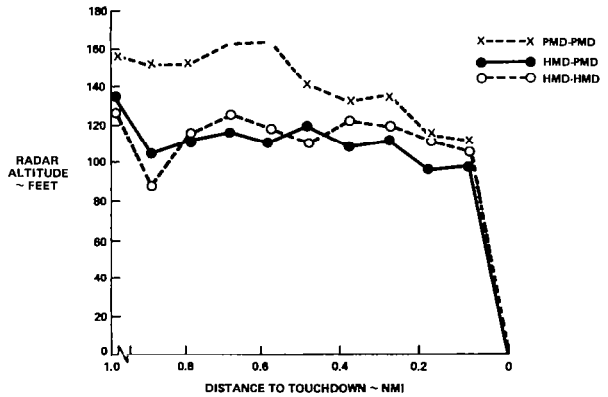

Figure 10. Radar Altitude during Landing Phase

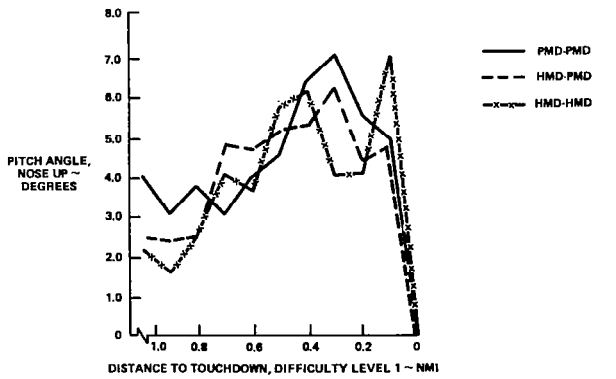

Figure 11. Pitch Angle during Landing Phase: Small LZ

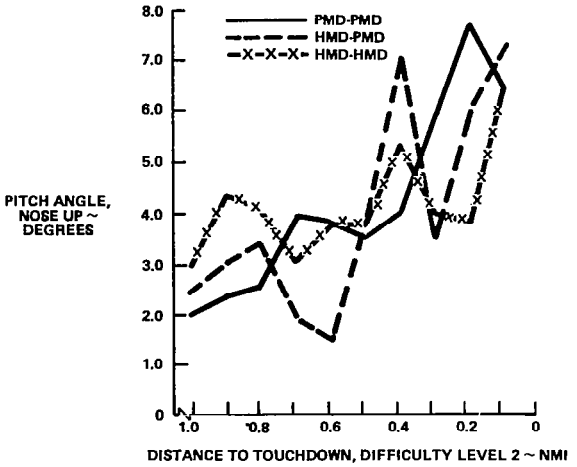

Figure 12. Aircraft Pitch Angle during Landing Phase: Large LZ

Crash Rates for Display Combination Evaluation

An examination (by chi-square analysis) of the frequency of noncrash landings per attempts showed no significant differences due to display configurations of LZ size. Any frequency differences appeared due to chance and not experimental conditions.

Virtual Head Up Display (HUD) Evaluation

The virtual HUD evaluation varied the copilot display combinations from PMD, HMD, and HMD virtual HUD while the pilot remained on the HMD. The ANOVA results shown in Table 6 indicate that route change as a variable has a significant effect on percentage of time under 100 feet and average groundspeed. Runs without route changes had a higher percentage under 100 feet with the virtual HUD configuration (73.5 percent), followed by common HMD video (57.5 percent) as shown in Table 7. In runs that contained a route change, the HMD-PMD configuration had the highest percentage of time under 100 feet (56 percent). Overall, the HMD configuration with the virtual HUD had the lowest average radar altitude. However, the variability between display combinations is small, i.e., only 11 feet. Runs with a route change had faster average groundspeeds than those without (Table 8). This increase in groundspeed was predictable, since the altitudes of changed routes tended to be higher. The virtual HUD has the fastest groundspeed in runs with changes and the lowest in runs without. Overall, the HMD-HMD combination video had the fastest average groundspeed.

Table 6. Pilot Performance in Virtual HUD Evaluation: Enroute*

DEPENDENT VARIABLES	OVERALL MEAN	STANDARD DEVIATION	INDEPENDENT VARIABLES			
			DISPLAY CONFIGURATION	ROUTE DIFFICULTY	ROUTE CHANGE	INTERACTION
PERCENT UNDER 100 FEET	55.34 %	14.42	NS**	NS	p = 0.01	NS
AVERAGE GROUNDSPEED	69.10 KN	16.01	NS	NS	p = 0.02	NS
AVERAGE ALTITUDE	104.99 FT	17.18	NS	NS	NS	NS

*SIGNIFICANCE LEVEL LIMITED TO $p \leq 0.10$
**DIFFERENCES NOT SIGNIFICANT

Table 7. Virtual HUD Evaluation: Average Altitude Enroute

DISPLAY COMBINATION	DIFFICULT ROUTE		EASY ROUTE		OVERALL MEAN
	NO ROUTE CHANGE	ROUTE CHANGE	NO ROUTE CHANGE	ROUTE CHANGE	
HMD-PMD	120.58 (42%)*	105.08 (56%)	95.04 (62%)	125.10 (37.5%)	111.45
HMD-HMD (COMMON VIDEO)	93.39 (62%)	118.18 (45%)	112.45 (57.5%)	106.02 (54%)	107.51
HMD-HMD (VIRTUAL HUD)	84.06 (73.5%)	113.00 (47%)	83.11 (73.5%)	122.86 (37.5%)	100.75

*PERCENT OF TIME UNDER 100 FEET

Table 8. Virtual HUD Evaluation: Average Altitude Enroute

DISPLAY COMBINATION	DIFFICULT ROUTE		EASY ROUTE		OVERALL MEAN	SURROGATE TRAINER*	
	NO ROUTE CHANGE	ROUTE CHANGE	NO ROUTE CHANGE	ROUTE CHANGE		DAYLIGHT NOE	NIGHT NOE
HMD-PMD	68.16	67.06	65.94	69.99	67.78	–	–
HMD-HMD (COMMON VIDEO)	71.58	64.97	73.01	85.76	73.83	27	16
HMD-HMD (VIRTUAL HUD)	62.48	80.84	65.14	65.98	68.61	–	–

For comparison, data collected for the Army's Surrogate Trainer is shown in Table 8. The Surrogate Trainer is a AH-1S helicopter equipped with a AN/AAQ-11 Pilot Night Vision Sensor (FLIR), IHADSS, symbol generator, and navigation system. The groundspeed data shown for both day (27kts) and night (16kts) flights highlights the differences between the Army's tactic of nap-of-the-earth (NOE) flight and the low-level flight concepts utilized by Marine pilots in the simulator. A typical altitude plot is presented in Figure 13, which indicates the pilot flew the helicopter below 15 feet. This altitude is significantly lower than the 107.51 mean altitude when the HMD-HMD configuration was used in the simulator.

These differences underscore the inverse relationship between clearance altitude and groundspeed and potentially reflect the difference in aircraft size.

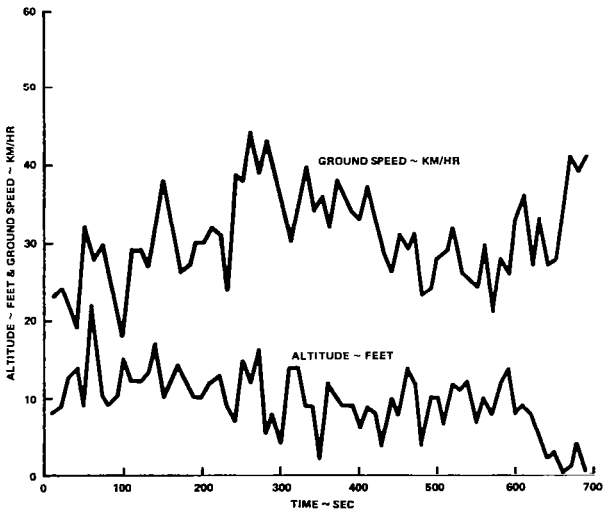

Figure 13. Typical Night NOE Flight Profiles for Surrogate Trainer

Control Display Unit (CDU) Evaluation

Copilot performance was evaluated as a function of display combination during low-level flights over longer routes that required a substantial navigation workload. An enroute course change was added as a variable so that the difficulty of the copilot inserting a route change into the CDU midway in a mission could be evaluated. Figure 14 contains the data matrix. Random route conditions were used so that pilots could not predict course changes. All enroute data runs required the copilot to manually capture the LZ.

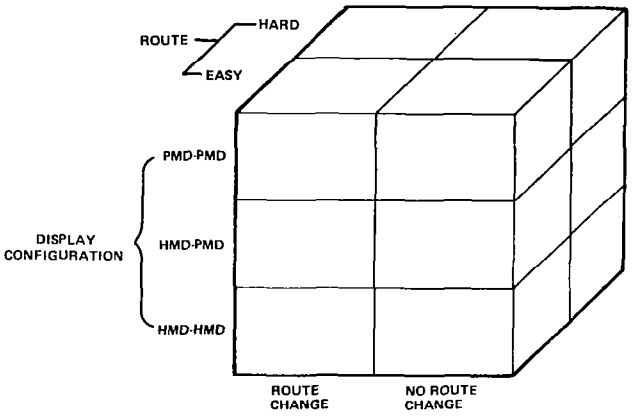

Figure 14. Experimental Matrix for Approach and Landing PMD-HMD-CDU Evaluation

Capturing the LZ required a specific three-key operation of the flight plan master function key (MFK) and line keys 9 and 6. Most runs had an addendum to this sequence, which was several scale changes (line keys 11 and 12). Discrete data was examined to determine actual sequences. There were 2 errors in 17 operations when this sequence was performed, and both involved parallax problems with line key 9.

The random enroute change also involved a specific sequence of events to properly execute the new route and capture checkpoints in the old. The PMD-PMD configuration had the fewest CDU errors (6), followed by the HMD-PMD configuration (7) and the HMD-PMD configuration (11). There were 11 line key errors and 13 total MFK errors encountered during route changes. Tables 9 and 10 display the type of errors that occurred. These tables show consistent problems with parallax and misunderstanding of key functions. The copilots depressed line keys several times in succession in trying to obtain a response or to correct an error. The copilots did not cue in on the CDU feedback (for example, the asterisk that appears with the capture function). These errors indicate that the display arrangement needs to be correctd and CDU feedback must be furnished when a function key is initialized.

Table 9. Line Key Errors during Route Changes

FREQUENCY	ERROR SEQUENCE
4	DEPRESSED LINE KEY 8 INSTEAD OF 9
1	DEPRESSED LINE KEY 4 INSTEAD OF 3
2	DEPRESSED LINE KEY 10 INSTEAD OF 9
1	DEPRESSED LINE KEY 2 INSTEAD OF 3
2	SEVERAL LINE KEY ENGAGES AFTER ONE MFK
1	SEVERAL PAGE CHANGES AFTER ONE DIR

Table 10. Master Function Key Errors during Route Changes

FREQUENCY	ERROR SEQUENCE
3	DEPRESSED FTL/PLN INSTEAD OF DIR
2	DEPRESSED MARK INSTEAD OF FTL/PLN
3	DEPRESSED STAT INSTEAD OF DIR
2	DEPRESSED PROG INSTEAD OF DIR
2	DEPRESSED MARK INSTEAD OF DIR
1	DEPRESSED MAP/RTN INSTEAD OF FLT/PLN

Pilot Performance Data Summary

The size of the landing zones affected pilot performance more consistently and predictably than any other factor. The smaller zones required more precise maneuvering, which resulted in longer landing times, higher radar altitudes during approach, smaller radial error, etc. To land in these zones, the pilot must have the helicopter under control. The pilots evaluating the HMD-PMD combination generally performed better using the HMD. Ease of slewing the sensor allowed pilots to examine terrain features and maintain low altitude with comparative ease. The pilots' landing approaches and touchdowns were also smoother when using the HMD.

During the enroute portion of the mission, crew performance in flatter terrain was slightly better while the pilot used the PMD, but performance in mountainous terrain was better when the pilot used the HMD. Copilot operation of the CDU indicated that it is a useful part of the navigation system that reduces the dead reckoning navigation workload task. However, the excessive number of copilot input errors during route changes indicates that changes need to be made in keyboard layout and in CDU feedback cues.

Pilot Opinion Data

After the data runs, the pilots were asked to rate the safety and ease of display configurations during an approach to the landing zone (Figures 15 and 16). While there was little variability in response, consistent trends were apparent. Pilots rated the HMD safer and easier than dual PMDs in all phases. The variability is small, but the pilot's HMD display is apparently the critical preferred feature.

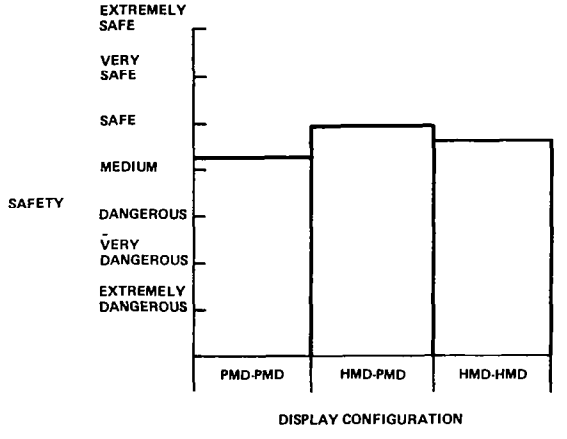

Figure 15. Safety of Approach to LZ

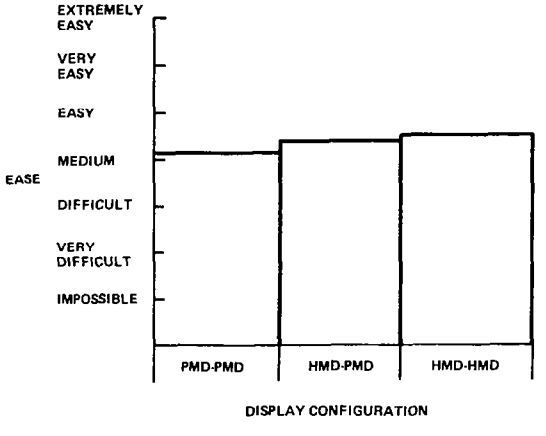

Figure 16. Ease of Approach to LZ

Participants were asked to indicate the minimum safe target altitude at 60 to 80 knots and the maximum safe target groundspeed at 50 to 100 feet above ground level (AGL) that was attainable on an actual night mission. Table 11 shows the pilot ratings of actual mission altitudes and speeds. They believe that lower altitudes and higher speeds are attainable when the pilot uses the HMD.

Table 11. Minimum Safe Altitude at 60 to 80 Knots and Maximum Safe Speed at 100 to 150 Feet AGL

TERRAIN	RADAR ALTITUDE (FT) AND SPEED (KN) BY DISPLAY CONFIGURATION					
	PMD-PMD		HMD-PMD		HMD-HMD	
	ALTITUDE	SPEED	ALTITUDE	SPEED	ALTITUDE	SPEED
FLAT	61.88	106.56	64.06	115.94	64.29	107.86
ROLLING HILLS	95.63	85.38	90.00	93.21	92.86	86.67
MOUNTAINOUS	143.44	62.86	129.38	66.43	122.14	63.33
OVERALL MEAN	100.32	84.93	94.48	91.86	93.10	85.95

Pilots showed a consistent preference for the HMD-PMD configuration across all aspects of mission ease and safety. The HMD-HMD virtual HUD was considered the most dangerous and difficult display configuration. However, pilots expressed a preference for the copilot to use the PMD for map reading and navigation. They felt that the virtual HUD made it difficult to turn their head and use the CDU, and that the time required to regain the display created a dangerous situation. All pilots felt the HMD-PMD configuration was the safest, most effective configuration; the HMD-HMD virtual HUD configuration was felt to be the least effective and safe.

Seventy-five percent of the pilots felt the CDU helped to maintain low altitude, and 50 percent felt it helped to increase groundspeed. These respondents felt the CDU simplified navigation duties and increased orientation, which allowed more time for concentration on flight tasks. Copilots felt the tactical map display was useful.

Pilot Opinion Data Summary

Evaluating the HMD-PMD combination resulted in a definite preference for the pilot to have a helmet display. The copilot preferred an HMD for mission ease and a PMD for mission safety. The enroute evaluation indicates a consistent preference for the HMD-PMD configuration.

Copilots felt that the virtual HUD configuration was more difficult and dangerous than the HMD-HMD or HMD-PMD configurations. They also preferred the HMD-PMD configuration.

The CDU was found to be an extremely useful navigation tool. It enables copilots to accurately assess present position, desired position, and overall mission. The HMD increased copilot task loading, but operation of the CDU was still possible.

Conclusions

The simulation experiments have demonstrated the ability of pilots and copilots to fly a night mission at low altitudes, ranging from 50 to 150 feet AGL, with the night visionics equipment package tested.

Although this experiment required no data to be generated on dead reckoning versus navigation system requirements, both pilot performance and opinion data reinforced that crew station workload was reduced with Doppler command steering information. Incorporating the CDU navigation capability was also instrumental in further reducing navigation workload.

Most pilots preferred flying the night transport mission with the HMD instead of the PMD, regardless of which display configuration the copilot was using. The precise slewing of the sensor with the HMD using a pilot's natural head movements allowed control over the sensor without changing hand position on the collective during critical flight maneuvers, which is required when operating the sensor manually.

By contrast, most copilots preferred using the PMD. They found constantly moving imagery somewhat distracting when performing the CDU line key and master function tasks.

The copilot group evaluating the virtual HUD mode of IHADSS did not find this mode useful. Of particular concern was losing symbolic aircraft attitude and altitude information and losing imagery while performing cockpit tasks using the virtual HUD.

The preferred cockpit display configuration was to have the pilot use the HMD and the copilot use the PMD. The HMD provides the pilot with precise slewing control over the sensor and more visual feedback information than available with the PMD. The PMD provides the copilot with sufficient aircraft position, attitude, and altitude information, yet simplifies cockpit workload tasks. The PMD does not introduce the visual interference characteristic of the HMD or the complete loss of aircraft information characteristic of the virtual HUD.

Copilots found the CDU to be a useful navigational aid in reducing the navigation workload task. The present keyboard inputs required for enroute changes, however, are somewhat cumbersome through nonalignment of CDU symbology with the appropriate line keys. The result was copilot confusion and numerous copilot input errors. Through lack of an indication for positive CDU line key actuation, numerous other copilot line key input errors resulted.

Further HNVS Efforts

As a result of these experiments, a baseline HNVS configuration has been established and is presently being evaluated in actual flight tests by the Naval Air Development Center and Naval Air Test Center. The cockpit configuration is identical to that utilized in the simulation studies. Addtionally, an HNVS System Specification has been developed by the Naval Air Development Center for procuring actual production prototype hardware for flight test. The HNVS System Specification was developed, in large part, from data generated during this and prior simulation experiments.

References

Martin Marietta Aerospace, Final Cockpit and Software Preparation Task Report, OR 15,647-1, May 1980.

Martin Marietta Aerospace, Helicopter Night Vision System Simulation Evaluation Phase I Final Report, OR 15,986, July 1980.

Martin Marietta Aerospace, Helicopter Night Vision System Simulation Evaluation Phase II Final Report, OR 16,015, July 1980.

Martin Marietta Aerospace, Helicopter Night Vision System Simulation Final Report, OR 16,026, July 1980.

Martin Marietta Aerospace, Helicopter Night Vision System Simulation Final Report, OR 16,551, December 1981.

SOME PILOTING EXPERIENCES WITH MULTI FUNCTION ISOMETRIC SIDE-ARM CONTROLLERS IN A HELICOPTER

J. Murray Morgan

Airborne Simulator Facility Manager

Flight Research Laboratory

National Research Council Canada

Ottawa, Ontario

Abstract

The installation of two side-arm mounted, isometric controllers in the NAE Airborne Simulator, a modified, variable stability Bell 205A is described, as is the development of various control systems for use with them. The results of two experiments are presented indicating both the feasibility and acceptability of such systems for a wide variety of tasks in a conventional single rotor helicopter, with a minimum of stability augmentation. Areas of future research are indicated.

Introduction

In the fall of 1979, the National Aeronautical Establishment (NAE), a division of the National Research Council Canada, was approached by the Sikorsky Aircraft division of United Technologies, with a proposal for a co-operative project to flight test a pair of isometric side-arm controllers in the NAE Airborne Simulator. This was of sufficient interest to the NAE, relating closely to an area of active research interest, that it was possible to agree to such a program, the results of which were reported in Reference 1. Sikorsky provided the two controllers installed in a seat with side-arm supports, NAE provided the interface between the electrical outputs of the units and the simulator computers and developed suitable control systems, while pilots from both organizations took part in the formal evaluations. This paper will describe the development process that led to the evaluated systems, some of the problems encountered and their solution. Data from the first co-operative experiment and a more recent NAE experiment employing similar controllers will be presented, and intentions for future work in this area will be indicated.

Experimental Hardware

The NAE Airborne Simulator

The NAE Airborne Simulator is an extensively modified Bell 205A-1 with the stabilizer bar removed, the standard hydraulically boosted actuators replaced with dual mode electro-hydraulic actuators (which provide full authority electrical or fly-by-wire control from the right seat or full authority hydraulically boosted mechanical control from the left, or safety-pilot's seat) and extensive hybrid real-time computational capability. The safety pilot, whose controls reflect all computer inputs to the actuator system, can assume control at any time, while a safety system, which monitors the status or condition of many elements of the fly-by-wire system can cause an automatic reversion to left seat control if a 'fault' or 'out-of-limits' condition is sensed.

The on-board hybrid computation system comprises three PDP-11 processors, in mutual communication and operating on a computational cycle of 1/64 second, supported by three fields of analog computation.

The Simulator is equipped with a wide range of motion sensing systems which provide high quality measurements of its velocity relative both to the earth and the ambient airmass. A nose boom carries vanes for angle-of-attack and sideslip measurement, together with a swivelling static pressure source while dynamic pressure is taken from two wide-angle pitot probes, nose-mounted. The usual range of inertial sensors is supported by a doppler radar for earth referenced velocity measurement, while a radio altimeter provides height data, when within some 750 metres of the surface.

Figure 1 shows a simplified block diagram of a typical simulation channel as used in this series of experiments.

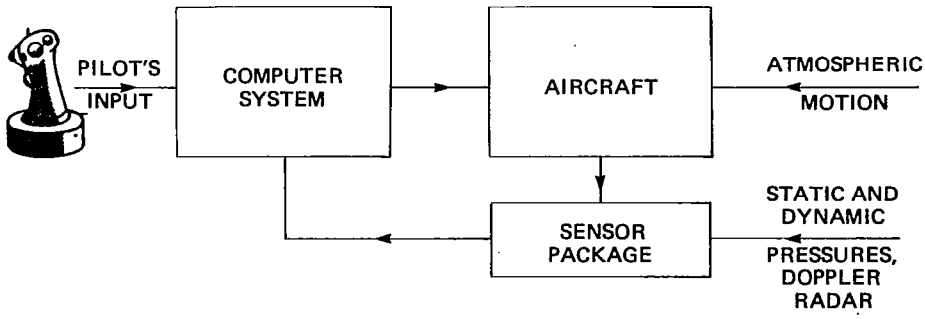

FIG. 1: A TYPICAL SIMULATION CHANNEL FOR THE ISOMETRIC SIDE – ARM CONTROLLER EXPERIMENTS

Side-Arm Controllers

The hand controllers (Fig. 2), standard, commercially available, '4-axis' units were mounted on a standard Bell seat as shown in Figure 3. Each had independant outputs in four control axes, X (fore/aft), Y (lateral), Z (vertical) and θ (torque about the Z axis) as shown in Figure 3, while their transducing characteristics were as listed in Table 1. The controller units themselves exhibited essentially zero compliance in response to forces and moments up to the rated maximum input, but when installed the system showed slight movement due to the compliance of the supporting structure. In addition to the primary force sensing transducers, each unit carried several discrete switches, namely, a trigger, a standard aircraft 'coolie hat' two axis thumb switch, and either side of the latter a simple contact closure push button. The outputs from these were read and interpreted by the on-board computers, while the functions allocated to them were 1) Trigger-communication 2) Coolie hat – progressive trim in X or Y as appropriate 3) Inboard push button – datum reset trim system activation.

Table 1. Controller transducing characteristics.

Axis	Max Input	Sensitivity	Max Output
X	20 lb. F	0.5 volt/lb.	10.0 volts
Y	20 lb. F	0.5 volt/lb.	10.0 volts
Z	40 lb. F	0.25 volt/lb.	10.0 volts
θ	60 in. lb.	0.167 v/in. lb.	10.0 volts

FIG. 2: AN ISOMETRIC CONTROL UNIT

FIG. 3: CONTROLLER/SEAT INSTALLATION

Experimental Software

Modelling

The initial proposal called for a simulation of the Blackhawk helicopter, however, since this would have required a complex, model following procedure and would have caused delays in the program and uncertainties in the validity of the model, it was not undertaken. As a compromise, the basic Bell 205 was used as the baseline model and two levels of SAS were provided, a simple rate-damping augmentation about all axes and a rate command/attitude hold mode in pitch and roll with both stiffness and damping augmentation in yaw and augmented heave damping. This approach had the advantage of being simple and certain in its implementation while presenting a 'real' helicopter, with all the cross-couplings and asymmetries inherent in this class of aircraft.

Control Modes

The experimental software was arranged so that, prior to engagement of the fly-by-wire system, the various outputs from the hand controllers could be assigned to drive different control actuators, enabling a variety of control modes to be investigated. In all, two primary and three secondary control modes were examined (Fig. 4). For the three modes which had duplicated control functions on the two controllers, both inputs were read at all times by the computers and summed, giving the pilot the option of using either hand for the primary control task.

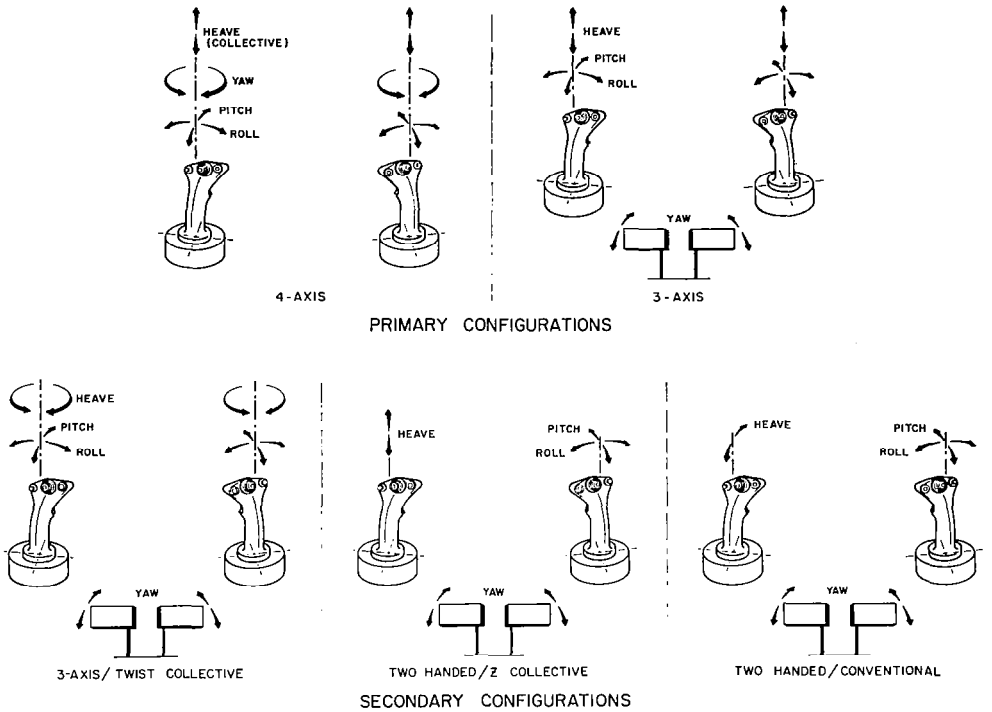

FIG. 4: ISOMETRIC CONTROL CONFIGURATIONS

System Development

Control Signal Shaping

Figure 5 shows three forms of signal shaping which represent the progression in the development process from the first flight to the point at which the system was offered for formal evaluation. The simple dead-band and linear slope of Figure 5a proved to be too sensitive for other than very limited hovering, and even that required a very high pilot workload. The dual slope arrangement in Figure 5b was quite acceptable at the hover, but still produced problems at other points in the manoeuvring flight envelope where the 'knee' became obvious to and created difficulties for the pilot. Therefore the approach shown in Figure 5c, a small linear range blending into a quadratic non-linear characteristic was finally evolved. This gave the pilot the lower sensitivity he desired around neutral, while still permitting large and rapid inputs to be made without any disturbing discontinuities in slope.

The extent of the dead band, and the extent and magnitude of the linear slope segment, which were adjustable *in flight with the fly-by-wire system disengaged, were optimized* for various control functions and flight conditions. For the formal evaluations a compromise set of characteristics, biased towards operating at and near the hover were used.

During the development flying it was noted that, due to arm/armrest/controller geometry, it was significantly easier to apply a Z force in the up rather than the down direction. Therefore, to provide the pilot with a more subjectively even response in this channel an overall asymmetry was applied to it, effectively magnifying inputs in the UP-Z sense.

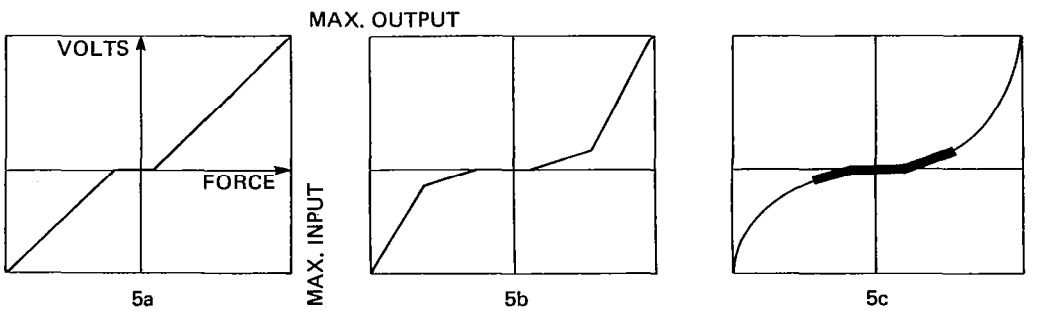

FIG. 5: CONTROL SIGNAL SHAPING

Trimming

Prior to first flight, two trim systems were installed, a progressive, constant rate trim, activated by the 'coolie hat' and applied to the X and Y function of the appropriate controller, and a datum reset system. This latter system was activated by pressing the inboard thumb button on either controller which action disengaged that unit from the drive system, while the inputs to the control channels were held constant by the computer. The pilot was then able to relax any held force and reconnect the controller by releasing the button. Both of these proved to be unsatisfactory. While the progressive system could be used, the force changes associated with repositioning the hand on the controller to make contact with the switch were sufficient to introduce unwanted inputs to the system, thereby making unacceptably large demands on the pilot in terms of the care and physical accuracy of his hand movements. The datum reset was somewhat easier to use, (except that again repositioning the hand and applying sufficient force to the button to overcome its spring generally caused inadvertent inputs), but suffered from a more fundamental problem. If, during the period when the controller was disconnected from the controlled system, the aircraft was externally disturbed, then on reconnection the pilot could find himself with an out of trim condition even greater than that which he had been in the process of relieving initially.

To overcome these difficulties, a selectable, continuous integral trim was devised, which provided an integral-plus-proportional command signal from the hand controller to the system, with the inboard thumb button being reassigned to the activation of this system. The final configuration is shown in Figure 6. As reported in Reference 1, the handling characteristics of this type of system depend on the ratio of integral to proportional gains (K_{ip}), and the optimum value need not remain constant over the entire flight envelope. However, for this experiment a set of constant values was used, and they are reproduced here in Table 2.

Table 2. Integral/proportional gain ratios.

Channel	K_{ip}
Roll	1.0
Pitch	0.5
Yaw	1.9
Heave	1.5

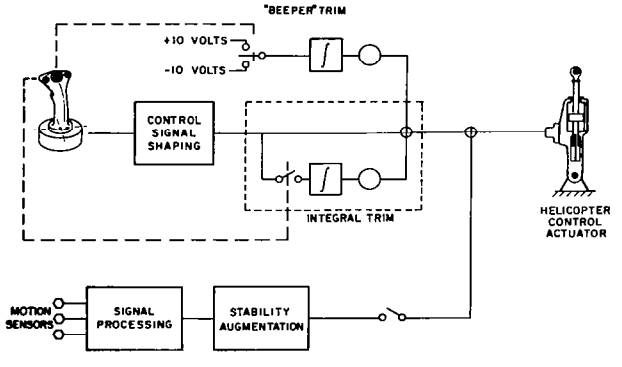

FIG. 6: TYPICAL SIMULATION CONTROL CHANNEL

Control Position Indicators

Late in the evaluation phase of the first experiment, when one of the subject pilots elected to attempt off-level landings and take-offs, a significant and anticipated operational disadvantage of isometric controllers was highlighted. In a conventional helicopter the pilot has a direct bio-mechanical indication of the tip-path-plane orientation; the cyclic position is a direct analog of the normal to that plane. This information is used by and is of great importance to the pilot during all take-offs, but especially when lifting off from a slope. A rigid controller inherently robs the pilot of this important piece of information and, under some circumstances, visual information may not suffice as a replacement. Operational limitations associated with the absence of another performance related cue, tail rotor collective pitch, sensed in a conventional helicopter from pedal displacement, also were evident in these experiments. This information is used by the pilot as an indication of yaw control authority remaining when operating with large yaw rates or in the presence of large sideslip velocities. Figure 7 shows a rudimentary Control Position Indicator (CPI) that was fitted above the instrument panel coaming to compensate for the loss of these cues and while far from ideal (the indicator was adapted from a fixed wing auto pilot trim indicator) it sufficed to expand the useable envelope in the areas indicated above.

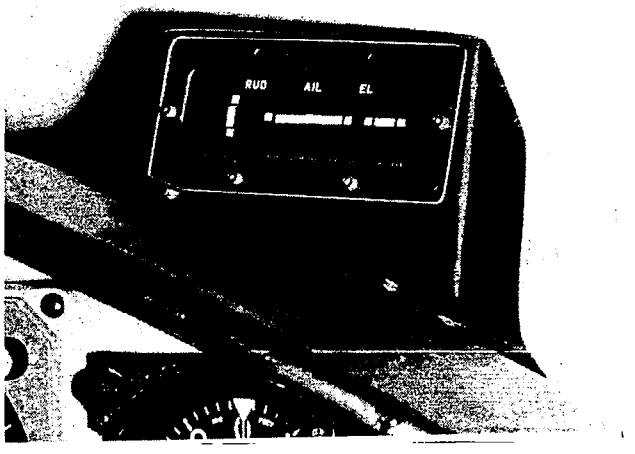

FIG. 7: CPI INSTALLATION

First Experimental Evaluation

Description of the Experiment

A series of tasks, shown in detail in Appendix A and intended to represent the greater part of the flight envelope of the 205, was selected for evaluation by a group of five pilots, two from Sikorsky and three from NAE. Cooper Harper ratings were required for each task and, subsequent to the completion of the experiment the subjects were asked to reply to a general questionnaire; their responses are reported in full in Reference 1.

The decision was made to introduce the subjects directly to the two primary control configurations rather than to train them via a force analog of a conventional displacement system. To provide an overall comparison, one of the NAE pilots, with some five years experience on the aircraft was asked to rate the tasks using the basic, unaugmented, aircraft and displacement controls. The experience levels of the evaluation pilots are shown in Table 3.

Table 3. Evaluation pilot experience levels.

Pilot	Total Hours	Helicopter/Fixed Wing
A	3500	3250/250
B	5700	400/5300
C	6900	900/6000
D	6500	4000/2500
E	5600	1550/4050

Results of the First Experiment

Cooper Harper Ratings

Figures 8 to 10 are plots of the Cooper Harper ratings obtained during the experiment. All data points have been used and they are coded by task rather than pilot so that any effect of task on opinion can be examined.

Summary of Pilots Comments

As a supplement to the numerical opinions obtained during the experiment, the following summary of the subjects' written and verbal comments for which there was reasonable commonality is produced below:

1) When using a three axis configuration, force rather than displacement pedals were preferred. the need to use leg and foot movement when applying only forces with the hand generally being judged less natural than applying forces to all controls.

2) The assignment of collective to a twist function was not liked since it tended to be prone to inputs in the incorrect sense, and the instinctive relationship between input and control response, present when collective was driven via the Z axis, was absent.

3) All subjects felt that the more fully supported and erect posture inherent in the side-arm controller installation reduced fatigue compared to the conventional helicopter seating position.

Pilot Adaptation

With one exception, discussed in more detail below, all subject pilots adapted easily to the multi-function configurations, to the extent that the majority of them elected to commence data runs before the allotted training period was complete.

Discussion of Results of First Experiment

Four Axis System

Consider Figure 8 and ignore, for now, the circled data points. While the degree of acceptability increased with increasing stability augmentation, as might be expected, the main point of interest is that even the most primitive form of augmentation brought the peak of the rating distribution to the acceptable side of the 3.5 boundary. Note too, that the data in the left hand column suggest that there is little difference between the basic, unaugmented, aircraft when flown with displacement and isometric, four function controllers. Also, the spread of points due to individual tasks suggests that no particular portion of the manoeuvring flight envelope examined produced opinions radically different from any other.

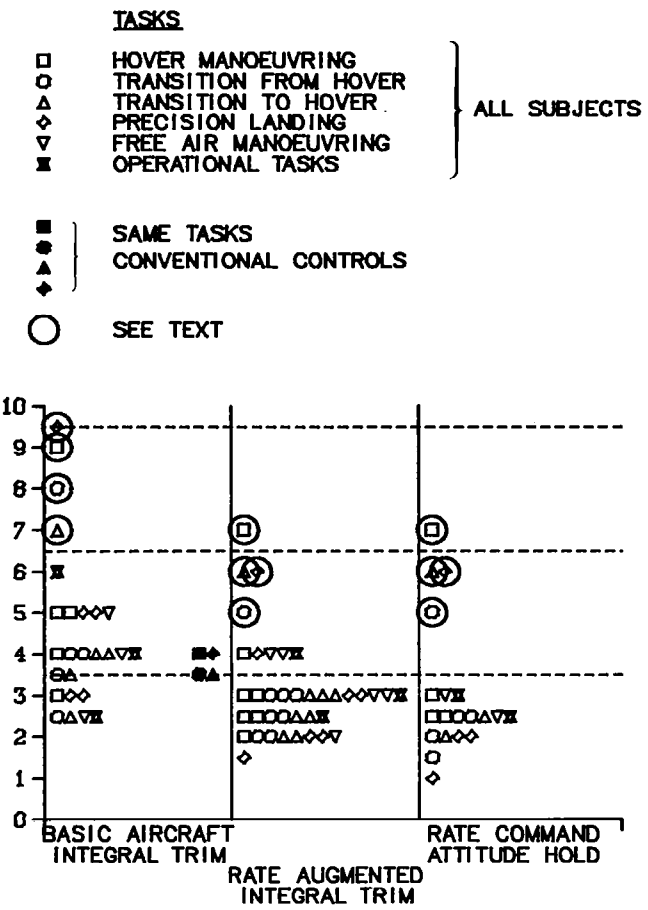

FIG. 8: 4 FUNCTION, RIGHT HAND, EVALUATIONS

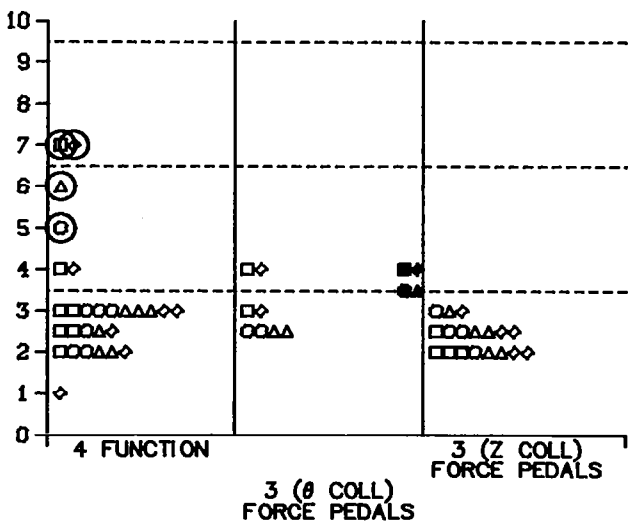

FIG. 9: RATE AUGMENTED, INTEGRAL TRIM

The circled data points are of special interest, and may have a particular significance. They were all contributed by a single subject, who was the exception to the general pattern of easy adaptation to the isometric, multi function system. It is possible that he may represent a sub-group in the piloting body who will adapt only with great difficulty to such systems, and if so, this could have significance in the areas of trainee selection or training washout.

Effect of Control Configurations

From the evidence of Figure 8, the rate damped model was selected to examine the effects of various control configurations on pilot opinion, the results being plotted in Figure 9. Of the two primary configurations there is a slight preference for the three-plus-pedals over the four-axis mode, with all data points for the former configuration being on the acceptable side of the 3.5 boundary.

The Effect of Increasing Stability

The final plot in this series shows the effect of increasing stability when using the preferred control configuration. It suggests that while the tendency for acceptability to increase with increasing stability augmentation is present, even the 'basic aircraft' is within the fully acceptable boundary with this control system.

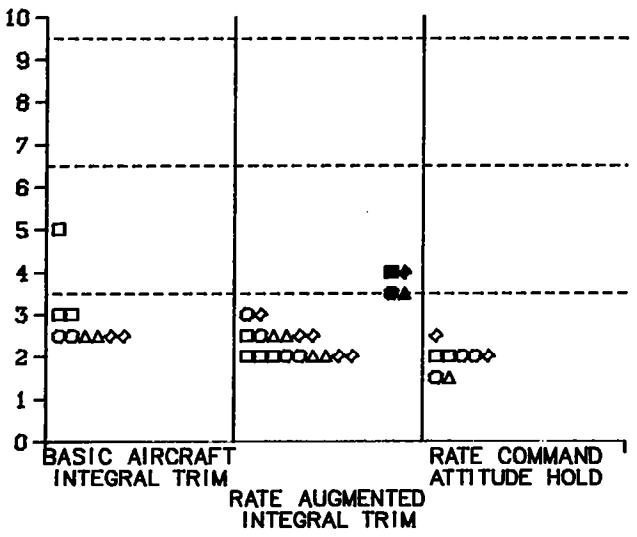

FIG. 10: 3 FUNCTION, Z COLLECTIVE, FORCE PEDALS

Biasing Factors

When interpreting the above data, two factors should be considered. The possible sense of euphoria experienced by the pilots on discovering that they could not only fly, but fly well, with such a radically new control system may have introduced a favourable bias in the ratings. On the other hand their very low experience level at the time of rating (no more than some 10 hours each by the end of the flight phase, with the exception of the development pilot, who had about 22 hours) might have been expected to produce the reverse effect. These effects are reasonably expected to diminish as work in this area proceeds.

The Interim Period

From the end of the initial experiment to the summer of 1981, no formal investigations were carried out, but the controllers were flown quite frequently, often riding 'piggy-back' on other experiments or for the purpose of demonstration to pilots from other organizations and countries. In this period too, they were flown in the IFR environment, where the ability to free one hand for ancilliary tasks, without having to abandon the control task met general approval. The pattern of relatively easy adaptation for the majority of pilots was maintained.

Development of an Alternate Hand Grip

Both during the initial experiment and subsequent flying, it had been noticed that, although the controller units themselves had little inherent cross-talk, in use there were several coupling tendencies, the dominant ones being a nose-up pitch with UP-Z commands and a roll into yaw. Both these effects appeared to be, if not due to, at least exacerbated by the hand grip design. Figure 11a shows the original hand grip supplied with the isometric controller. If a lightly cupped hand applies a force to this grip in the UP-Z direction, the pressure point on the handle is sufficiently displaced from the force sensing axis to result in an appreciable moment in the nose-up sense. Similarly roll inputs, generally applied with the inside edge of thumb or forefinger produce a moment about the Z axis, hence producing a yaw command.

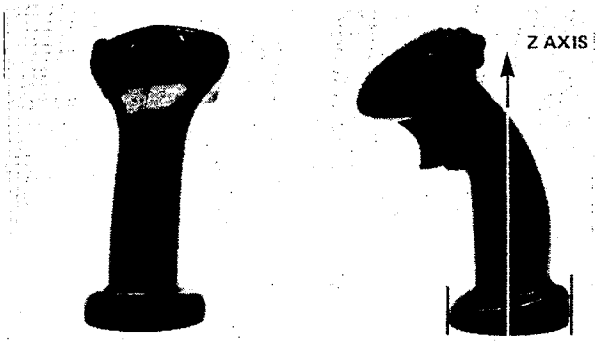

FIG. 11a

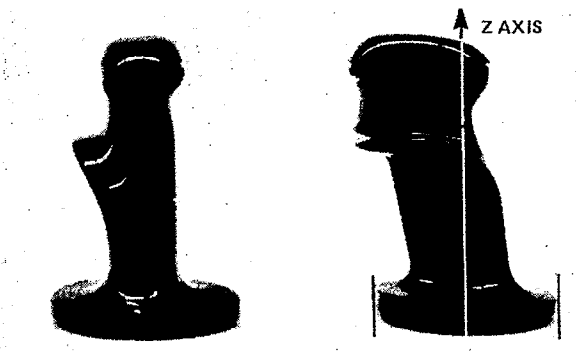

FIG. 11b

FIG. 11: HAND CONTROLLER CONFIGURATIONS

One other problem noted with the original grip was that the slimness and almost circular cross section of the lower portion of the design made the application of larger yaw inputs relatively more difficult than inputs in the other three axes. This was one action for which it was necessary to grip the handle firmly, a most undesirable technique which leads to both rapid hand fatigue and undesired inputs, both pilot and environment induced.

To eliminate, or at least reduce the effects of these undesirable characteristics, the handle shown in Figure 11b was designed and manufactured at the NAE. Its main features are the elimination of the curvature in the X-Z plane, a somewhat ovoid cross section and, to assist in the application of a 'clean' Z force, a much larger base flange and a good sized thumb/finger support table.

While no formal evaluations of this design have been made, it has found general acceptance among the project pilots and has been used in a recent series of tests.

The Second Experiment

Following the initial work with these controllers, it was felt important that a more direct comparison between the multi-axis, isometric systems and conventional controls should be made. To this end an experiment was designed and flown in the summer and fall of 1981.

Description of the Experiment

Using the marked ground course, shown in Appendix A, pilots were required to fly, in a single run, an accelerate/stop segment, rearward, lateral and quarter translations, two 'pedal' turns, a precision touch-down and a lift-off. The briefing to them included instructions to pay close attention to height-keeping and tracking, and to fly the course 'briskly'.

Qualitative and quantitative data were recorded using both the aircraft data acquisition system and ground observation. The pilots were also asked to provide a subjective assessment of the relative ease and precision of the task when using the multi-function controllers, compared to the conventional controls.

The subjects were required to fly the course alternating two runs with conventional controls and two runs with either the four-axis or the three-axis plus pedals configurations using the isometric side-arm controllers. Each flight consisted, generally, of one practice and eight data runs. Two complete sets of runs were flown with each isometric configuration and refamiliarization was permitted for each pilot between his evaluating with the different side-arm controller systems.

The data were analyzed for precision, control activity and time as a means of investigating the relative performance of a particular subject as he moved from one control system to another.

The subject pilots for this exercise were all from NAE and Table 4 summarizes their relevant experience to the end of this experiment.

Table 4. Pilot flying experience at the end of the second experiment

Pilot	Total	Helicopter/Side-Arm
C	7200	995/37
B	6054	432/70
G	905	313/13
H	4002	4002/9

Results

While most of the data from this experiment still awaits analysis, some preliminary results are presented in Figures 12 to 14, specifically, the pilots' subjective opinions, track deviations in the lateral translation segment, and touch-down scatter.

Pilot Opinions

As illustrated in Figure 12, the pilots generally considered isometric control to be more difficult and less precise, in this type of closely bounded task, than conventional control. There is also a suggestion that this judgement is less severe in the case of the three axis system than in that of the fully integrated, four axis configuration. However, the greater number of opinions fall between the 'same/more difficult' and 'same/less precise' responses, indicating no great difference from displacement controls. The relatively very short exposure of the subject pilots should also be considered when looking at these replies.

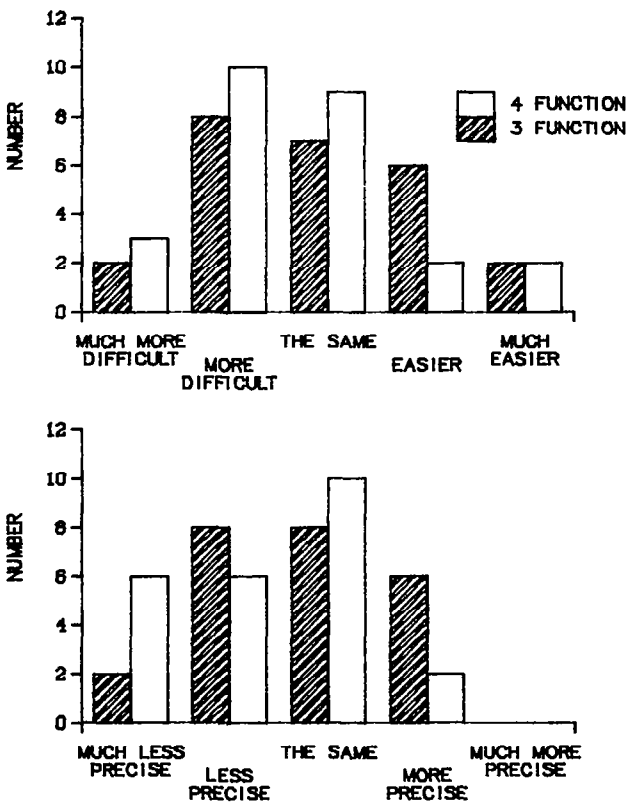

FIG. 12: PILOT'S SUBJECTIVE ASSESSMENTS

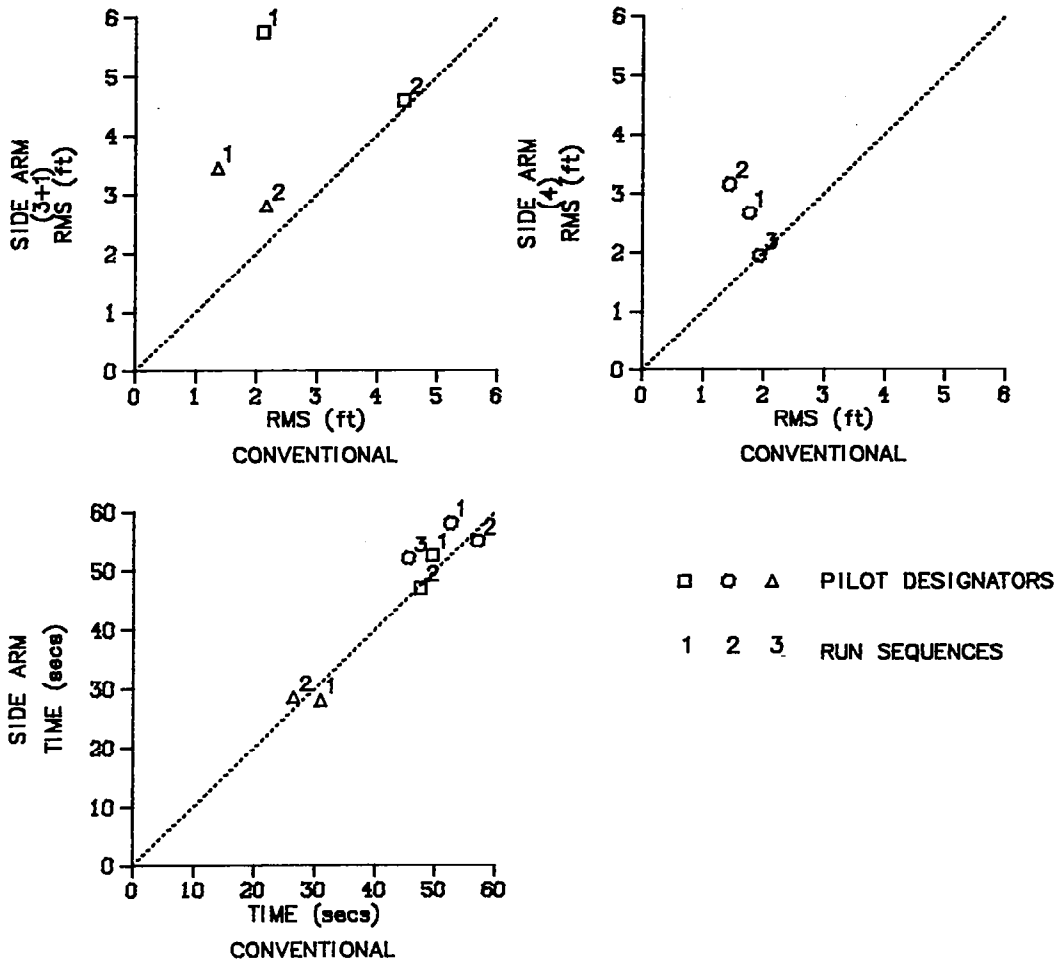

FIG. 13: PERFORMANCE COMPARISONS, CONVENTIONAL AND SIDE-ARM CONTROLLERS LATERAL TRANSLATION TRACKING

Lateral Tracking

To obtain the data plotted in Figure 13 time-adjacent pairs of runs were analysed for RMS deviations and plotted one against the other, thereby eliminating, as far as possible, any effects due to changing atmospheric conditions or pilot fatigue.

While the general tendency is towards a more unsteady tracking performance with the isometric controllers, it is possible that learning curve effects are still present, since there is a consistent tendency for the RMS values for the two control systems to approach one another the later into each flight the data are taken. It is noteworthy that there is no indication of any time penalty when using the force controllers, which may suggest that even though the subjects considered the tasks to be more difficult, and their performance to be less precise with the isometric than with the conventional system, the level of degradation was not such as to cause them to proceed with unusual caution.

Landing Accuracy

Figure 14 compares landing accuracy of systems, and a definite degradation in performance is noted for the isometric systems. (It should be emphasized that the control system being flown in these tests had not been specifically optimized for the landing task.) There is an interesting difference in the pattern of landing errors between the systems; using conventional controls the errors tend to lie along the lateral axis of the aircraft, while with the isometric systems, there is a definite slew towards the longitudinal. This may be due to a change in the type of visual cues required by a pilot when landing with isometric systems compared to those he habitually uses when operating with displacement controls. This may demand that more of his visual attention be directed towards the front of the aircraft than to the side and, considered in combination with a natural tendency to drift the aircraft along the line of sight, may have caused this dispersion pattern. (It is worthy of note that in the Simulator the evaluation pilot sits on the right, and that there are no errors either to the left or the rear with any control system.)

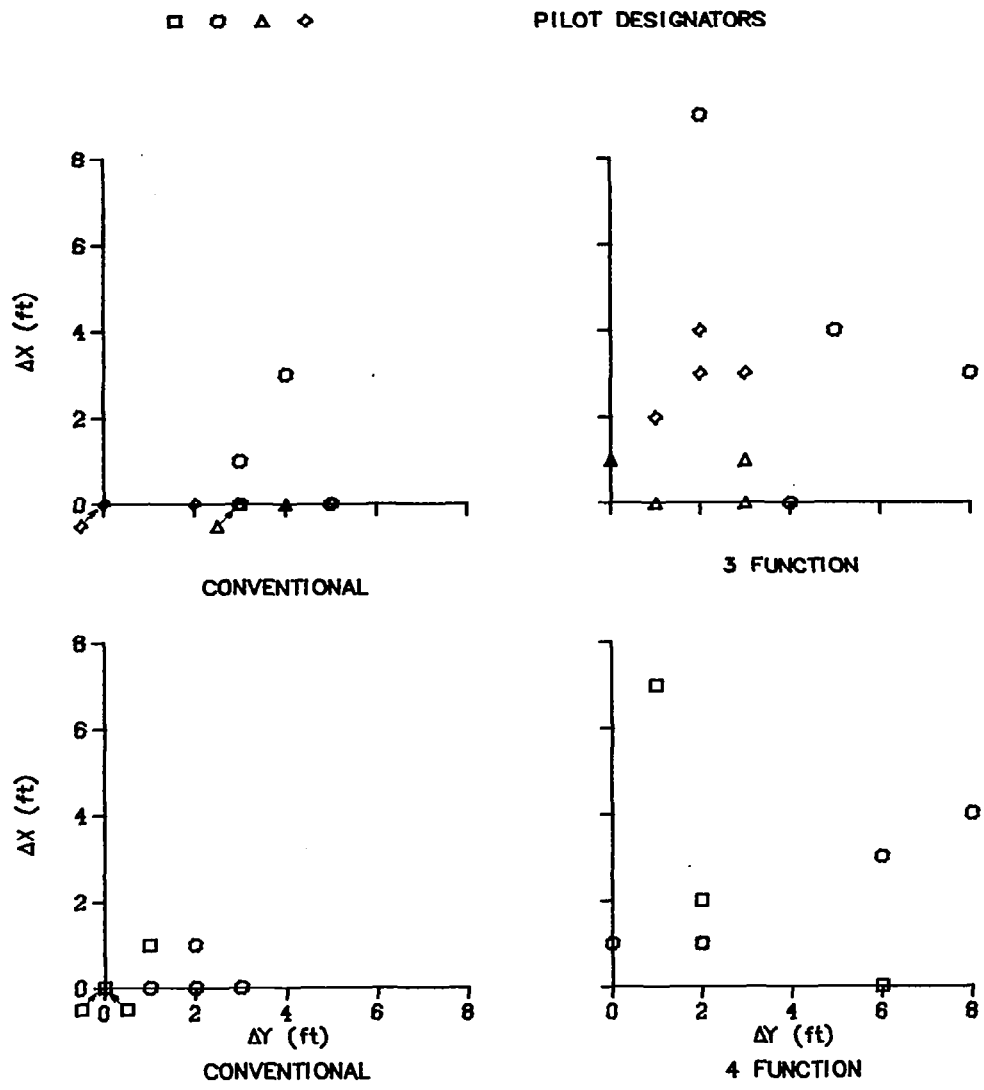

FIG. 14: TOUCHDOWN SCATTER COMPARISONS

Future Intentions

The National Aeronautical Establishment will continue its investigation of integrated, multi-axis control systems as part of the aircraft flight systems and flight mechanics research program. At the time of writing, for example, a controller, similar to the one described in this paper but with some compliance, is being prepared for installation in the Airborne Simulator. The potential merits of limited motion will be investigated.

It is expected that the main areas of interest for future study will be:

1) Evaluation of the limited motion controller.
2) An investigation into more sophisticated control systems, including mission and task level optimization, and adaptive or scheduled variations in control system characteristics.
3) Further direct comparisons between displacement, limited compliance and isometric controllers.
4) Investigations of integrated control/display systems using multi-axis controllers and advanced electronic displays.

Conclusion

The work at the NAE over the last two years has demonstrated both the feasibility and acceptability of using multi-function, isometric, side-arm controllers to perform a wide variety of tasks in a conventional helicopter, with the minimum of stability augmentation. While these two short test programs do not provide definitive answers to all of the questions which the designer must ask about such radically unconventional control systems, they do indicate that this will be a fruitful area for future research efforts.

Acknowledgement

The names of the subject pilots, in alphabetical order, with their affiliations are:

K. Davidson	NAE
S. Kereliuk	NAE
G. Kohler	Sikorsky Aircraft
M. Morgan	NAE
R. Murphy	Sikorsky Aircraft
D. Sattler	NAE
A.D. Wood	NAE

Reference

Report–Sinclair, M., and Morgan, M., "An Investigation of *Multi-Axis Isometric Side-Arm Controllers in a Variable* Stability Helicopter", National Research Council Canada, Aeronautical Report LR-606, August 1981.

APPENDIX

SOME PILOTING EXPERIENCES WITH MULTI FUNCTION ISOMETRIC SIDE-ARM CONTROLLERS IN A HELICOPTER

Task Details for the Two Experiments

First Experiment

Table 1 details the tasks required to be performed by the subject pilots in the first experiment. A single Cooper Harper rating was requested for each task, with the exception of Task 2A, where separate ratings for the transition to and from the hover were required.

Table 1. Task details for the first experiment.

Task #	Title	Content
1	Manoeuvring at Hover	1.1 Hover into and across wind 1.2 360° turn left and right 1.3 Lateral translation, *moderate rate* 1.4 Accelerate and rapid stop
2A	Circuit from and to Hover	2.1 *Transition from hover* 2.2 Transition to hover
2B	Landing	2.3 Zero speed landing from hover to terminate in marked zone
3	High Speed Flight	3.1 Summetrical pull-ups 3.2 Steep turns 3.3 Roll *reversals* 3.4 Partial power descents 3.5 Sideslips 3.6 High power climb
4	Operational *Manoeuvres*	4.1 Pop-up and point 4.2 NOE *course* 4.3 Downwind take-off and turn

Second Experiment

Figure 1 represents the ground course marked out for the second experiment. The boxes contain instructions to the subject, while the circled numbers indicate radio transmissions required for data correlation. Table 2 gives the dimensions of the various linear segments.

Table 2. Ground course dimensions.

From	To	Distance (ft.)
A	B	670
B	C	445
C	D	450
D	E	500

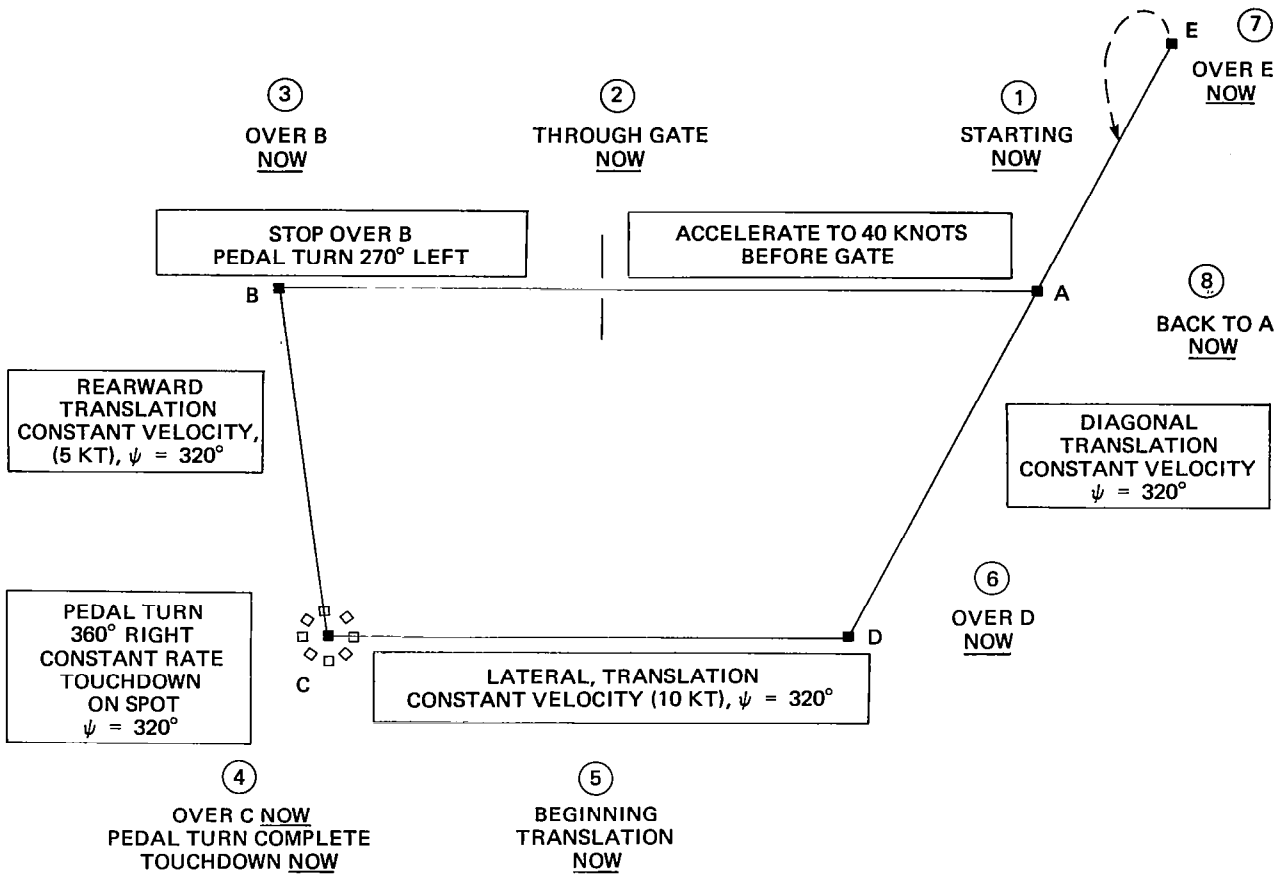

FIG. 1: COURSE FOR INTEGRATED SIDE ARM CONTROLLER EVALUATIONS

RESULTS OF NASA/FAA GROUND- AND FLIGHT-SIMULATION EXPERIMENTS CONCERNING HELICOPTER IFR AIRWORTHINESS CRITERIA

J. Victor Lebacqz, Robert T. N. Chen, Ronald M. Gerdes, and Jeanine M. Weber
NASA Ames Research Center
Moffett Field, California

Raymond D. Forrest
Federal Aviation Administration
NASA Ames Research Center
Moffett Field, California

Abstract

A sequence of ground- and flight-simulation experiments was conducted at the Ames Research Center as part of a joint NASA/FAA program to investigate helicopter instrument-flight-rules (IFR) airworthiness criteria. This paper describes the first six of these experiments and summarizes major results. Five of the experiments were conducted on large-amplitude motion base simulators at Ames Research Center; the NASA-Army V/STOLAND UH-1H variable-stability helicopter was used in the flight experiment. Taken together, the results of the experiments indicate, among other things, that 1) some level of artificial stability and control augmentation is generally required for adequate flying qualities during precision instrument flight; 2) neutral longitudinal or lateral control position gradients do not result in inadequate flying qualities, given good directional characteristics, but an unstable longitudinal gradient can prove to be inadequate for instrument operations in turbulence; 3) pitch and roll attitude augmentation in the stability and control augmentation system (SCAS) plus directional augmentation including at least yaw damping is required to achieve satisfactory precision instrument flying qualities irrespective of the type of rotor or level of display assistance; 4) flight directors provide some compensation for poor flying qualities in dual-pilot situations but are of minimal assistance in this regard for single-pilot operations; and 5) the SCAS level required for ratings of satisfactory is the same (pitch and roll attitude augmentation) for the range of approach types considered (nonprecision versus precision, constant speed versus deceleration to a low speed).

Introduction

Current and projected expansion of civil helicopter operations has led to increasing efforts to assess problem areas in civil helicopter design, certification, and operation. Of concern are the influences of the helicopter's inherent flight dynamics, flight-control system, and display complement on flying qualities for instrument flight rules (IFR) flight, both in terms of design parameters to ensure a good IFR capability, and with regard to the characteristics that should be required for certification.

As a part of their respective research programs, NASA and the FAA have instituted a joint program at Ames Research Center to investigate helicopter IFR certification criteria. This series of investigations has the following two general goals:

1) To provide analyses and experimental data to ascertain the validity of the Airworthiness Criteria for Helicopter Instrument Flight,[1] which have been proposed as an appendix to FAR Parts 27 and 29 (Refs. 2, 3).

2) To provide analyses and experimental data to determine the flying qualities, flight control, and display aspects required for a good helicopter IFR capability, and to relate these aspects to design parameters of the helicopter.

With respect to the first goal, the sections of the Ref. 1 criteria that deal with static and dynamic stability attempt to prescribe quantitative values of several helicopter flight characteristics that would be required for IFR certification. To the extent that these values are a carryover from fixed-wing practice or an amalgam of previous handling-qualities requirements for military aircraft (e.g., Ref. 4), it is necessary to ascertain their validity for civil helicopter certification. One aspect of interest has to do with the requirements for stable force or position control gradients longitudinally, laterally, or directionally. Another aspect of interest is the difference in criteria for normal category rotorcraft depending on whether the aircraft is to be certificated single or dual pilot, particularly since most of existing substantiating data pertain only to dual-pilot operation. Yet another area of concern is the influence of displays on the instrument meteorological conditions (IMC) flying qualities, which is not considered in Ref. 1 but has been shown in some cases to compensate for less-than-satisfactory inherent flying qualities (e.g., Ref. 5).

With respect to the second general goal, most helicopters currently certificated for single-pilot IFR operations use advanced stability and control augmentation systems (SCAS) or displays or both.[6] Of concern is the level of complexity of the SCAS required to achieve a good IMC capability because of the cost, control authority, and reliability factors the SCAS introduces. Of interest also is the expansion of helicopter IMC operations to exploit the helicopter's unique capability to fly at very low airspeeds; this expansion requires

additional definition of the required flight dynamics, flight controls, and displays.

The various experiments discussed in this paper were designed to investigate elements of interest in achieving both goals in a consistent fashion. Specifically, the objectives of each experiment, listed in chronological order, may be summarized as follows. 1) First experiment (ground simulation, 1978):[7] develop generic models of current helicopters having three different rotor types; explore SCAS concepts and influence of longitudinal static stability; and determine relative influence of IFR compared to VFR approaches. 2) Second experiment (ground simulation, 1979):[8,9] determine suitability of requirements on cockpit control position; examine efficacy of several SCAS concepts; and explore influence of turbulence. 3) Third experiment (ground simulation, 1980):[10] determine influence of crew-loading (single pilot versus dual pilot); determine influence of three-cue flight director displays; and examine suitability of additional SCAS concepts. 4) Fourth experiment (flight, 1980):[11] validate selected results of ground-simulation experiments in flight concerning static longitudinal stability, level of SCAS, and flight director displays. 5) Fifth experiment (ground simulation, 1980):[12] examine influences of unstable static control gradients, angle-of-attack stability, and pitch-speed coupling; and examine influence of failed SCAS. 6) Sixth experiment (ground simulation, 1981):[13] investigate SCAS requirements for decelerating instrument approach; explore influence of electronic display format; and examine influence of approach geometry and deceleration profile.

The remainder of this paper is organized as follows. The following section summarizes the designs of the experiments with an emphasis on variations that were carried across all of them, and the next section provides a review of their conduct, again emphasizing the similarities. Following these summaries, the results of all the experiments are compared with each other, followed by some general conclusions.

Experimental Design

Mathematical Models

In the ground-simulation experiments, the basic mathematical model used to simulate the flight dynamics of the helicopters was a nine-degree-of-freedom model developed for use in nap-of-the-earth (NOE) simulations.[14] The model explicitly includes the three-degree-of-freedom tip-path-plane dynamic equations for the main rotor[15] and the six-degree-of-freedom rigid-body equations. The main-rotor model includes several major rotor-system design parameters, such as flapping-hinge restraint, flapping-hinge offset, blade Lock number, and pitch-flap coupling. Simulation of different rotor systems (e.g., hingeless, articulated, and teetering) was accomplished by appropriate combinations of those design parameters.

The model is structured to permit full-state feedback to any of the four controllers (longitudinal and lateral cyclic, collective stick, and directional pedals) plus control interconnects and gearings. All feedback and control gains may be programmed as functions of flight parameters, such as airspeed. This structure permits the construction of typical SCAS networks; it may also be used as a response-feedback variable stability system to modify the basic characteristics of the simulated helicopter.

In the first experiment, the rotor design and helicopter geometric parameters of the mathematical model were selected and tuned to simulate stability and control characteristics similar to those of the UH-1H, OH-6A, and BO-105 aircraft, which use teetering-, articulated-, and hingeless-rotor systems, respectively.[7] These same three generic helicopters were used as the baseline configurations for the second experiment; only the teetering model was used in the successive experiments. Reference 9 lists several of the geometric and rotor design parameters for them. It is emphasized that the resulting static and dynamic characteristics are intended to be representative of the three types of rotor systems investigated for the three weight classes of helicopters that were simulated; they are not, in all respects, identical to the characteristics of the UH-1H, OH-6A, or BO-105.[7]

Static Stability

One type of configuration variation carried across most of these experiments was changes in longitudinal, lateral, or directional static stability as measured through cockpit control positions with speed or sideslip. For the purposes of this paper, the variations in longitudinal control position with velocity will be emphasized. Of the three baseline helicopter models developed in the first experiment, the models with articulated and hingeless rotors had stable control position gradients at 60 knots; the position gradient for the teetering rotor was unstable. One of the SCAS concepts considered (rate damping with input decoupling, longitudinal cyclic to collective gearing scheduled with speed) turned out to destabilize this gradient, yielding an almost neutral gradient for the hingeless rotor, an unstable gradient for the articulated rotor, and a more unstable gradient for the teetering rotor.[7] In addition, a preliminary investigation of the influences of this gradient was made in a controlled fashion for the hingeless-rotor model by using the variable-stability aspect of the model structure, with feedback of longitudinal velocity to longitudinal cyclic being used to vary the effective M_u. Table 1 summarizes the gradients and the times to either half or double amplitude of the prevalent low-frequency roots.

This variable-stability capability was used in succeeding experiments to control the longitudinal control position gradient with speed, including the influences of the SCAS gearings. In the second experiment, two levels of gradients were considered for the hingeless rotor (stable and neutral), and neutral values were designed for the teetering and articulated rotor models also.[8,9] In the third experiment, only the teetering-rotor model was used, with the gradient held at neutral (to

highlight influences of SCAS and displays, as will be described below).[10] The flight experiment considered three levels of gradient (basic airframe, increased value to roughly that of the ground experiments, decreased value to neutral), with the variable-stability capability of the aircraft being used in a fashion analogous to the ground simulation model to vary M_u, and the resulting control gradient being measured in flight.[11] In the fifth experiment, this gradient was systematically varied for the teetering-rotor model from quite stable to unstable values, yielding times-to-double-amplitude down to about 6 sec.[12] The values considered across all the experiments are summarized in Table 1 for SCAS implementations incorporating only rate feedbacks.

Other Baseline Characteristics

As was mentioned above, ground simulation models of helicopters having hingeless-, articulated-, or teetering-rotor systems were used in the first two experiments; in the remaining ground-simulation experiments (and of course in the flight experiment), emphasis was on only the teetering-rotor system. Reference 7 describes the wide range of response characteristics among the three unaugmented baseline models and the resulting flying-qualities deficiencies. For the hingeless and teetering models in particular, however, the addition of SCAS incorporating rate damping and input decoupling effectively minimized these differences, particularly when high-gain feedbacks were used with the teetering model in the second experiment.[9] For this reason, only baseline configuration changes to the teetering-rotor model will be discussed here.

Table 2 lists some of the stability derivatives at 60 knots of the baseline teetering-rotor ground-simulation model. These characteristics were held constant across all the experiments, but in the fifth experiment selected variations were also considered.[12] One of these variations was the steady-state attitude-to-speed gradient. For the baseline model, this gradient was very low (-0.03°/knot at 60 knots), which considerably aggravates the difficulty of controlling speed at low-control gradients; the variation considered was to increase artificially the drag damping (X_u) to produce an attitude-to-speed gradient of -0.33°/knot at 60 knots. Another variation was the angle-of-attack stability, which was nearly zero for the baseline configuration (Table 2). This derivative was made very stable (M_w = -0.025), using the variable-stability system; as is discussed in Ref. 12, this variation had a negligible influence on the longitudinal control position gradient (in contrast to its effect on a fixed-wing vehicle), but did modify short-term response to cyclic. Again, these variations were considered in only the fifth experiment.

Stability and Control Augmentation System (SCAS)

As was discussed in the introduction, one of the major aspects of concern in this sequence of experiments was the type of stability and control augmentation required for a good helicopter IMC capability. Variations in the type of augmentation, and to some extent the level of it, were carried out across all the experiments. In the first experiment, these variations for each of the three baseline aircraft consisted of 1) no augmentation; 2) pitch/roll/yaw rate damping; 3) input decoupling to reduce off-axes accelerations to control inputs added to (2); and 4) pitch and roll attitude augmentation added to (3).[7] The second experiment considered again the last two of these concepts, with the gains for the teetering-rotor configuration increased to provide response characteristic roots similar to the hingeless-rotor configuration; in addition, turn-following augmentation (increased directional stiffness and feedbacks to reduce the Dutch roll excitation) was considered, as was a rate-command-attitude-hold system in pitch and roll that was implemented by adding proportional-plus-integral prefilters to the pitch and roll command channels.[8]

These SCAS types were all considered again in the third experiment, with a selectable wing-leveler (roll-attitude feedback) also added to the rate-damping and rate-damping-input-decoupled SCAS mechanizations to study split-axis augmentation in a preliminary way. For this experiment, reduced levels of rate and attitude feedback were used for these SCAS types, to be more consistent with actual teetering-rotor capabilities. An additional velocity-hold SCAS was designed, which augmented the vertical velocity time-constant to roughly 0.5 sec and used longitudinal velocity feedbacks to increase the effective phugoid frequency and partially eliminate lift-change caused by speed (Z_u).[10]

The fourth (flight) experiment included only the two SCAS types of rate-damping-input-decoupling and pitch/roll attitude augmentation, with the levels designed to be consistent with the third experiment.[11] These same two SCAS types at the same level were also used in the longitudinal axis for the fifth experiment, with the lateral axis held fixed at a high-gain rate-command-attitude-hold type. In addition, a failed longitudinal pitch-rate damper was also simulated by eliminating the pitch-rate feedback in the rate-damping-input-decoupling SCAS.[12] Finally, the sixth experiment also included rate-damping-input-decoupling, rate-command-attitude-hold, and attitude-command SCAS types, with somewhat higher augmentation levels considered because of the decelerating task. Additional designs were a velocity command system and an acceleration-command-velocity-hold system, that incorporated high-gain feedback of longitudinal velocity to longitudinal cyclic (constant term of hovering cubic about 1.7).

Because of the consistency across most of the experiments of rate-damping-input-decoupled, rate-command-attitude-hold, and attitude-command SCAS types, these results will be emphasized in this paper.

Displays

Figure 1 shows the instrument panel layout used in all the ground simulation experiments, except the last. The instruments were arranged in

a standard "T," and were conventional, with the exception of the electromechanical attitude indicator (ADI), which was a 5-in. unit incorporating heading (through longitudinal lines on the ball) as well as pitch-roll information. Turn-rate-slip information was presented on a separate instrument, as is frequently done in helicopters, rather than with the attitude indicator. Figure 2 shows the primary flight instruments for the flight experiment. The horizontal situation indicator (HSI) is similar to the one used in the ground experiments, but the ADI incorporated integrated glide-slope and localizer deviation data plus turn-rate-slip information not included in the ground simulator unit. In the last ground simulation experiment, the ADI was replaced with a black-and-white cathode ray tube (CRT) unit to present electronic formats. Figures 3 and 4 illustrate the two electronic formats considered in this experiment. As can be seen, the first is a simplified analog of an electromechanical ADI such as the one used in the flight experiment; the second is one way of integrating a variety of information into one presentation, but will not be discussed in this paper.

Excluding the integrated electronic format, therefore, the primary display variable considered across the experiments was the extent of flight director information provided to the pilot in addition to the raw deviation data. Because the task considered for the first two experiments was a VOR approach, only course-deviation information was presented on the HSI, with the ADI flight director needles biased off scale. In the remaining ground-simulation experiments and in the flight experiment, a precision MLS approach task was considered; for these experiments, azimuth and elevation deviation plus DME (range to go) information was given on the HSI. In the third experiment, one-, two-, or three-cue flight directors were a display variable; in the flight experiment, either no directors or three-cue directors were the variable; in the sixth experiment, all configurations included a three-cue flight director; in the fifth experiment, no flight directors were considered. The general philosophy of the flight director design is discussed in Ref. 10.

Crew-Loading Situation

All but the third experiment were conducted as typical flying-qualities experiments; the pilot's sole task was to perform the desired control task, with no auxiliary tasks of communications or navigation. This scenario of full-attention-available-for-control is consistent with a dual-pilot crew-loading situation. In the third experiment, the configurations were evaluated assuming this situation but they were then also evaluated in as realistic a simulation of a single-pilot situation as possible. For the single-pilot simulations, the pilot always had to communicate with Approach Control and Tower, set a transponder frequency, and switch communication frequencies; for approaches including a missed approach, he also had to switch communication frequencies again, copy a clearance from Departure Control, switch navigation and transponder frequencies, and track a VORTAC. Radio "chatter" from two other helicopters in the area was simulated. To provide a lack of repetition, four different approach plates to four oil rigs were devised, with different frequencies and alternates for each plate; these four possibilities were mixed randomly among the control-display combinations. Finally, on the single-pilot approaches, the pilot did not know whether he would be able to continue the approach or be forced to do a missed approach; the simulated fog was made to start clearing at 100 ft above the decision height and then to either re-fog or continue clearing just below decision height. As a result, the pilot had to make the decision whether to continue.

Wind and Turbulence

An additional variable carried across the experiments was the level of winds and turbulence present. For the ground-simulation experiments, a simple model for atmospheric turbulence[16] was used; it included three independent Gaussian gusts plus a mean wind which could shear in direction or magnitude. In the first experiment, all evaluations were conducted in no turbulence. In the second experiment, the configurations were evaluated in both no turbulence and at a representative level of turbulence ($\sigma_u = \sigma_v = 3.0$ ft/sec, $\sigma_w = 1.5$ ft/sec) with no mean wind. The third experiment added a 10-knot mean wind that sheared rapidly in direction a total of 100° at a range of about 1 mile out; all the configurations were evaluated in this wind and turbulence combination, with no zero-turbulence evaluations. This same wind and turbulence model was again used in the fifth experiment, with evaluations conducted both with it and in no turbulence. The sixth experiment included a vertical shear of the mean wind (from 10 knots at altitude to 2 knots at ground level) in addition to the shear in direction, and considered 1.5 times more turbulence ($\sigma_u = \sigma_v = 4.5$ ft/sec, $\sigma_w = 2.25$ ft/sec); again evaluations were conducted in both calm air and with this turbulence model.

For the flight experiment, the level of wind and turbulence was not a controlled variable. As is discussed in Ref. 11, tower estimates of wind magnitude and direction plus the pilots' qualitative estimate of the turbulence level were used to separate the data into two groups: one in which headwinds with little or no turbulence were present, and one in which there was a tailwind component or moderate turbulence or both.

Conduct of the Experiments

Equipment

The first three ground-simulation experiments were conducted using the Flight Simulator for Advanced Aircraft (FSAA) ground-based simulation facility at Ames Research Center; the last two used the Vertical Motion Simulator (VMS) facility at Ames (Figs. 5 and 6). Both facilities include a complex movable structure to provide six-degree-of-freedom motion; in the case of the VMS, a large vertical travel (±30 ft) is available to enhance simulation fidelity of longitudinal motions, and the FSAA is characterized by a large lateral travel (±50 ft). In both facilities, a visual scene from

a terrain board is presented through the cab window on a color television monitor with a collimating lens. For the first two experiments, the approaches were conducted to a model of a STOL airport with helipads; the last three ground-simulation experiments considered approaches to a model of an off-shore oil rig.

Instrument conditions were simulated using an electronic fog generator which could obscure all or part of the visual scene as a function of range or altitude. In the first two experiments, the instrument runs were conducted entirely in the fog to a minimum descent altitude of 600 ft, with no breakout simulated. The third and fifth experiments did include a partial clearing of the fog starting at about 100 ft above the decision height, which could then refog at the decision height to force a missed approach; in the sixth experiment, the fog always disappeared at the decision height.

The flight experiment was conducted on a UH-1H helicopter which had been modified as an in-flight simulator by adding an avionics system called V/STOLAND (Fig. 7). The system provides integrated navigation, guidance, display, and control functions through two flight digital computers; it may be operated with or without flight-director commands, in the modes of manual, control-stick steering (CSS), autopilot, or research. The flight-control portion of the V/STOLAND system uses a combination of a full-authority parallel servo and a limited authority (20% to 30%) series servo in each control linkage. In addition, disconnect devices exist in the left cyclic controls to allow for a fly-by-wire mode through this research cyclic stick. The right stick, or safety pilot side, retained the standard UH-1H cyclic and cockpit instruments. This experiment was conducted in the research mode, with the software providing a set of flight-control laws with variable gains and a set of flight-director laws with fixed gains.[11] Instrument flight was simulated with the use of an "IFR Hood."

Evaluation Tasks and Procedures

Although the evaluation tasks differed in detail among the six experiments, they were generically similar for all except the sixth. Each of the first five included a lateral guidance acquisition at constant altitude (about 1200 to 1600 ft AGL, depending on experiment), transition to a vertical descent at a constant speed of 60 knots (1000 ft/min for the VOR approaches of Experiments 1 and 2, acquisition of a 6° glide slope for Experiments 3 through 6), constant speed tracking during the descent (except Experiment 6), and transition to a constant-speed missed-approach maneuver consisting of a standard-rate turn at climb rates varying from 600 to 1000 ft/min, with the transition occurring at the missed-approach point in the first two experiments and at the decision height in Experiments 3 through 5. Experiment 6 included a deceleration while on instruments according to one of three deceleration profiles, and considered two approach geometries (Fig. 8), but a missed approach was not included. Table 3 summarizes the individual details of the evaluation tasks.

Cooper-Harper pilot ratings were assigned to each configuration on the basis of the evaluation task for each experiment, and comments made relative to comment card; task performance and control usage data were also obtained for each. Across all the experiments, the total number of participating pilots by affiliation was as follows: NASA, 3; U.S. Army, 4; Federal Aviation Administration, 4; NAE Canada, 2; and Civil Aviation Authority, UK, 1. Approximate total evaluations for Experiments 1 through 6 were, respectively, 60, 200, 150, 50, 200, 160; taken together, therefore, over 800 evaluations were obtained.

Discussion of Results

Influence of Longitudinal Control Gradient

In Figs. 9a and 9b the average Cooper-Harper pilot ratings from each experiment are plotted as functions of longitudinal static stability without turbulence and in turbulence, respectively. The data are for configurations with a rate-damping-input-decoupling SCAS and a dual-pilot crew-loading situation; they include both hingeless- and teetering-rotor systems in the results for Experiments 1 and 2. To emphasize the important aspects, the pilot ratings are shown versus the gradient level (in./15 knots) for the stable cases but versus the inverse of the time-to-double-amplitude of the divergent root for the unstable cases.

As can be seen, the correlation among all the experiments is quite good. The data show a consistent trend toward a degraded capability as the static stability is reduced to neutral and then unstable, with the trend being more obvious in turbulence. In terms of Cooper-Harper ratings, however, the aircraft systems were still rated as adequate for the tasks considered, irrespective of the static stability. Note that, with this type of SCAS, average ratings in the satisfactory category were not attained, even at the most stable level. In commenting about these configurations, the pilots noted increasing difficulties in maintaining trim and controlling speed precisely as the static stability was decreased, but also noted that the instrument tracking performance was still adequate at least down to neutral stability.

The IFR Appendix requires positive longitudinal control force stability at approach speeds for both transport and normal category helicopters, regardless of crew loading.[1] In these experiments, control force and control position stability were tied together through the use of electrohydraulic control loaders, and so the requirement would prohibit the neutral and unstable gradients that were considered. Considerations for airworthiness acceptance are likely to center on those configurations whose flying qualities are assessed to fall between satisfactory and adequate, but there is no clear correlation between acceptance and the Cooper-Harper pilot rating. All of the ratings fall within the adequate category, and the differences between stable and neutral gradients in individual experiments generally amount to about

one pilot rating or less.[8,11,12] Taken together, therefore, the results indicate that the achievement of a clearly adequate (e.g., CHPR < 5) capability probably justifies the requirement for a stable gradient, but a neutral gradient might be marginally acceptable for the dual-pilot situation.

Influence of Other Baseline Characteristics

As was discussed earlier, some modifications to some baseline teetering-rotor model characteristics were considered in the fifth experiment to ascertain any influence of these characteristics on the types of results discussed above. Figure 10 shows the data from this experiment for configurations with a high steady-state attitude-speed relationship (obtained through the introduction of high-drag damping X_u). As can be seen, little change in average rating is evident for the neutral or stable gradients, with a small improvement for the unstable gradient. The pilot comments for these configurations demonstrate mixed reactions and difficulties. One pilot consistently rated the high-drag configurations as better than the low-drag ones because small speed changes resulted in fairly significant rate of climb changes as a result of the increased negative $d\gamma/du$; hence rate of climb could be well controlled using pitch attitude. The other pilots, however, noted that the requirement for large power changes with speed was a detriment, particularly since power was still the primary controller for rate-of-descent; therefore the required changes for speed led to apparent speed-and-rate-of-descent coupling, thereby negating any advantages of more precise speed control. As a result, therefore, in general the average ratings for the equivalent high-drag and low-drag configurations were about the same, both in no turbulence and in light turbulence. As a result, it is unlikely that the low attitude-to-speed gradient of the baseline machine significantly influenced the ratings shown earlier.

Another modification to the baseline characteristics was the introduction of a large increment in angle-of-attack stability. The data for this modification are shown in Fig. 11. As can be seen, the influence on the pilot rating is high in turbulence, with the high angle-of-attack stability configurations being rated as inadequate for the task. As is discussed in Ref. 12, the addition of this stability did not significantly influence the longitudinal control position gradient, but did lead to an "insidious" coupling between rate-of-descent and speed control. Pilot comments indicated that for these configurations the angle-of-attack stability coupled through pitch attitude to large inadvertent speed changes when large changes in rate-of-descent were made with the collective. The important point brought out by these data is that coupling effects have a major influence, and yet the criteria of Ref. 1 do not consider such effects at all. For helicopters, other typical types of coupling are cross-axis inputs (eliminated for most of the configurations investigated in the program) and pitch-roll coupling, particularly for hingeless-rotor machines; such effects should probably be considered quantitatively for airworthiness acceptance.

Influence of the Stability and Control Augmentation System

It was noted in discussing the static gradient results that no ratings in the satisfactory category were achieved for the tasks considered using rate-damping stability augmentation. Figure 12 shows the ratings assigned to the three types of pitch and roll SCAS considered most consistently across all the experiments: rate damping with input decoupling, rate-command-attitude-hold, and attitude command. These cases are primarily for the SCAS incorporated on a machine with neutral basic longitudinal stability; note that a rate-damping SCAS does not alter the control position gradient, a rate-command-attitude-hold SCAS *results* in a neutral gradient, and an attitude SCAS stabilizes the gradient because of the M_θ term. As has been pointed out in the reference for each experiment, attitude augmentation in pitch and roll (implemented either as rate-command-attitude-hold or attitude command) is required to achieve ratings in the satisfactory category.[7,12] The advantages include a reduction in interaxis coupling, reduced turbulence excitation, and improved short-term and long-term dynamics. It is interesting to note that the failed longitudinal damper considered in Experiment 5 still had characteristics that met the criteria of Ref. 2 (with stable gradient) and yet was rated marginal at best in turbulence.[12] Because the criteria do not directly assess short-term dynamics, acceptance of a failed state for this configuration would rest entirely in the hands of the certification pilot and would likely not be granted, even though the criteria are met.

Influence of Flight Director Displays

Figure 13 illustrates some of the data obtained concerning the influence of three-cue flight directors compared with raw-data displays. The Experiment 5 configurations shown were selected because their stability and control characteristics are virtually identical to those of the Experiment 6 configurations; these Experiment 6 data were "calibration" evaluations obtained with no deceleration on instruments. As can be seen, some beneficial influence of the three-cue flight director displays is apparent in the Experiment 3 results, particularly with the higher level of SCAS (attitude augmentation). Considering all the experiments, in general the flight director assistance did improve ratings given to the rate-damping control system sufficiently to provide a clearly adequate capability, but did not improve this SCAS type sufficiently to move it into the satisfactory category. With the attitude-type SCAS, however, the assistance of the flight directors generally pushed the ratings clearly into the satisfactory category. This lack of substantial overall benefit of the flight directors for the rate-damping SCAS type was not expected at the outset of the experiments, and it should be cautioned that the results are likely to be quite sensitive to the design method used.[10,13] Based on these data, relaxed airframe airworthiness requirements, because of "credit" for advanced displays, may be warranted in some cases, and the absence of consideration for displays in the IFR Appendix[1] may require further attention.

Influence of Task

Because the Cooper-Harper pilot rating applies to an airframe-control-system display combination for a specific task, and because the evaluation tasks have varied somewhat across these experiments, it is useful as a final comparison to examine the influence of the task on the ratings. Ratings from several of the experiments are compared in Fig. 14 for similar stability and control characteristics and displays as a function of the task that was considered. It should be noted in particular that the difference between the dual-pilot and single-pilot tasks considered in Experiment 3 resulted in a change of almost one pilot rating, justifying in principle the division in criteria for normal-category helicopters in the IFR Appendix, but leaving in question the lack of distinction for transport-category helicopters.[1] It may also be seen that a decelerating instrument approach leads to worse ratings than even the single-pilot task with a constant-speed approach. Decelerating approaches are not explicitly considered by the IFR Appendix,[1] and these data intimate that more stringent criteria may be required for these more demanding tasks.

Concluding Remarks

A sequence of ground- and flight-simulation experiments concerning helicopter IFR airworthiness has been described in this paper. A total of over 800 piloted evaluations of several aspects of concern for helicopter instrument flight was obtained in these experiments. Although there are variations in detail among the experiments, the general results with respect to IFR airworthiness can be compared. On the basis of these results, as presented here and in previous documentation of the experiments, the following conclusions may be drawn, particularly concerning the proposed IFR Appendix:

1) The criterion requiring a stable longitudinal force gradient with speed is probably justifiable for rate-damping types of SCAS, although little significant degradation has been shown with neutral or slightly unstable gradients; hence the neutral gradient, at least, could be considered marginally acceptable. It should be emphasized that a rate-command-attitude-hold-type of SCAS, as considered in these experiments, results in a neutral longitudinal gradient; this type of configuration was generally rated in the satisfactory category. Hence, this type of criterion needs to be linked to the type of SCAS employed, which it currently is not.

2) Inherent characteristics of the helicopter lead to a variety of types of interaxis coupling. One type explicitly considered in these experiments led to a considerable degradation in pilot ratings. The current IFR Appendix does not address off-axis coupling; perhaps future versions should.

3) In all the experiments, attitude augmentation in pitch and roll has been required to achieve pilot ratings in the satisfactory category. Rate damping augmentation, even at a fairly high level and with input decoupling, generally has received ratings ranging from marginally adequate to just worse than satisfactory, depending on other factors. A failed rate damper was considered marginally inadequate, even though the aircraft characteristics were still within the IFR Appendix criteria.

4) The addition of three-cue flight directors did not improve the IFR capability for rate-damping control systems to the satisfactory category, if all the experiments are considered; some beneficial effect in achieving ratings in the satisfactory category with an attitude-augmented SCAS was apparent. Inadequate flying qualities could not be improved to satisfactory with the use of flight directors, but the improvement might take a marginal configuration into the clearly adequate category. This possible improvement is not considered in the current criteria.

5) Increasing the difficulty of the task (e.g., single-pilot or inclusion of an instrument deceleration) did result in degraded ratings for equivalent configurations. A difference in requirements for single- and dual-pilot operations was therefore shown to be warranted. Similarly, a difference in requirements of future versions which consider decelerating instrument operations may be projected.

References

1. "Rotorcraft Regulatory Review Program Notice No. 1; Proposed Rulemaking," Federal Register, Vol. 45, No. 245, 18 Dec. 1980.

2. "Federal Aviation Regulation Part 27 - Airworthiness Standards: Normal Category Rotorcraft," Federal Aviation Administration, Feb. 1965.

3. "Federal Aviation Regulation Part 29 - Airworthiness Standards: Transport Category Rotorcraft," Federal Aviation Administration, Feb. 1965.

4. "General Requirements for Helicopter Flying and Ground Handling Qualities," Military Standard MIL-H-8501A, Sept. 1961.

5. Lebacqz, J. V., "Survey of Helicopter Control/Display Investigations for Instrument Decelerating Approach," NASA TM-78656, 1979.

6. Traybar, J. J., Green, D. L., and DeLucien, A. G., "Review of Airworthiness Standards for Certification of Helicopters for Instrument Flight Rules (IFR) Operations," Federal Aviation Administration Report No. FAA-RD-78-157, Feb. 1979.

7. Forrest, R. D., Chen, R. T. N., Gerdes, R. M., Alderete, T. S., and Gee, D. R., "Piloted Simulator Investigation of Helicopter Control Systems Effects on Handling Qualities During Instrument Flight," Preprint No. 79-26, 35th Annual National Forum of the American Helicopter Society, Washington, D. C., May 1979.

8. Lebacqz, J. V., and Forrest, R. D., "A Piloted Simulator Investigation of Static Stability and Stability/Control Augmentation Effects on Helicopter Handling Qualities for Instrument Approaches," Preprint No. 80-30, 36th Annual National Forum of the American Helicopter Society, Washington, D. C., May 1980.

9. Lebacqz, J. V., Forrest, R. D., and Gerdes, R. M., "A Piloted Simulator Investigation of Static Stability and Stability/Control Augmentation Effects on Helicopter Handling Qualities for Instrument Approach," NASA TM-81188, Sept. 1980.

10. Lebacqz, J. V., Forrest, R. D., Gerdes, R. M., and Merrill, R. K., "Investigation of Control, Display, and Crew-Loading Requirements for Helicopter Instrument Approach," AIAA Paper 81-1820, Albuquerque, N. Mex., Aug. 1981.

11. Lebacqz, J. V., Weber, J. M., and Corliss, L. D., "A Flight Investigation of Static Stability, Control Augmentation, and Flight Director Influences on Helicopter IFR Handling Qualities," Preprint No. 81-25, 37th Annual National Forum of the American Helicopter Society, New Orleans, La., May 1981.

12. Lebacqz, J. V., Forrest, R. D., and Gerdes, R. M., "A Ground Simulator Investigation of Helicopter Longitudinal Flying Qualities for Instrument Approach," NASA TM-84225, 1982.

13. Lebacqz, J. V., "Summary Report - Fifth NASA/FAA Helicopter Instrument Certification and Operation Simulation Experiment," informal memorandum available from FAA, Ames Research Center, Moffett Field, Calif., Dec. 1981.

14. Chen, R. T. N., Talbot, P. D., Gerdes, R. M., and Dugan, D. C., "A Piloted Simulator Investigation of Augmentation Systems to Improve Helicopter Nap-of-the-Earth Handling Qualities," NASA TM-78541, 1979.

15. Chen, R. T. N., "A Simplified Rotor System Mathematical Model for Piloted Flight Dynamics Simulation," NASA TM-78575, 1979.

16. Aiken, E. W., "A Mathematical Representation of an Advanced Helicopter for Piloted Simulator Investigations of Control System and Display Variations," NASA TM-81203, 1980.

Table 1. Summary of longitudinal control position gradients.

Experiment	Rotor	Configuration	Gradient, in./15 knots	Time-to-double amplitude, sec
1	Teetering		+0.06	5.8
	Hingeless		-0.05	
2	Hingeless	Neutral	~0	
	Hingeless	Stable	-0.63	
	Teetering	Neutral	-0.02	
3	Teetering		-0.02	
4	Teetering	More stable	~-0.50	
		Base UH-1H	~-0.25	
		Neutral	~0	
5	Teetering	Most stable	-1.03	
		Stable	-0.53	
		Neutral	-0.03	
		Unstable	+0.03	11.0
		Most unstable	+0.125	6.3
6	Teetering		-0.41	

Table 2. Longitudinal derivatives of baseline teetering-rotor helicopter at 60 knots.

Derivative	Units	Value
M_u	rad/sec^2/ft/sec	-0.00022[a]
M_w	rad/sec^2/ft/sec	-0.00278
M_q	1/sec	-0.847[b]
M_p	1/sec	+0.143[b]
$M\delta_e$	rad/sec^2/in.	0.17[b]
$M\delta_c$	rad/sec^2/in.	0.0223[b]
X_u	1/sec	-0.005[a]
X_w	1/sec	0.026
Z_u	1/sec	-0.013[a]
Z_w	1/sec	-1.28
$Z\delta_e$	ft/sec^2/in.	-2.58[b]
$Z\delta_c$	ft/sec^2/in.	-10.00

[a]Baseline, unmodified for gradient changes.

[b]No SCAS.

Table 3. Task details.

Experiment	Guidance	Speed profile	Decision height, ft AGL	Missed approach
1	VOR	60 knots, constant	600	Yes
2	VOR	Decelerate 80-60 knots before let-down, 60 knots constant thereafter	600	Yes
3	6° MLS	Decelerate 80-60 knots before vertical intercept, 60 knots constant thereafter	300	Yes
4	6° MLS	Constant 60 knots	200	Yes
5	6° MLS	Decelerate 80-60 knots before vertical intercept, 60 knots constant thereafter	300	Yes
6	6° MLS	Constant 60 knots until ~0.5 n.mi. to go, decelerate to ~15 knots on instruments	130	No

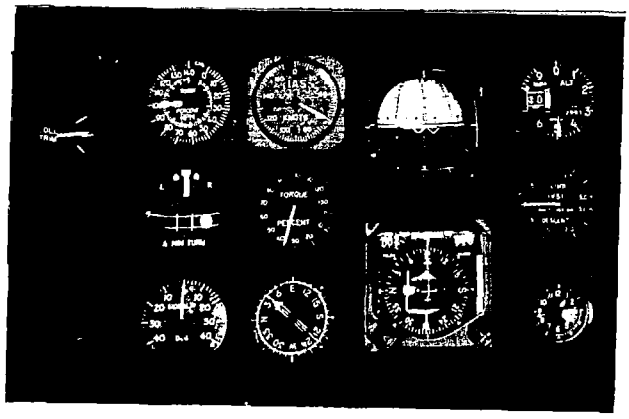

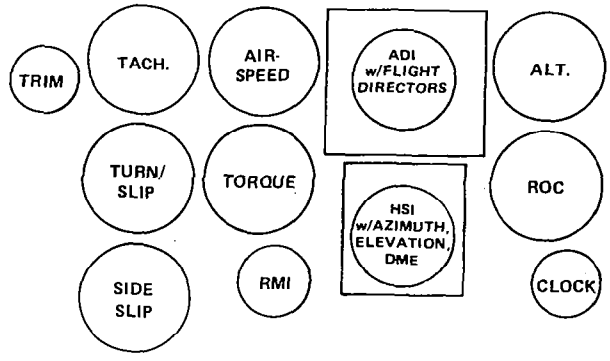

Fig. 1 Instrument panel layout.

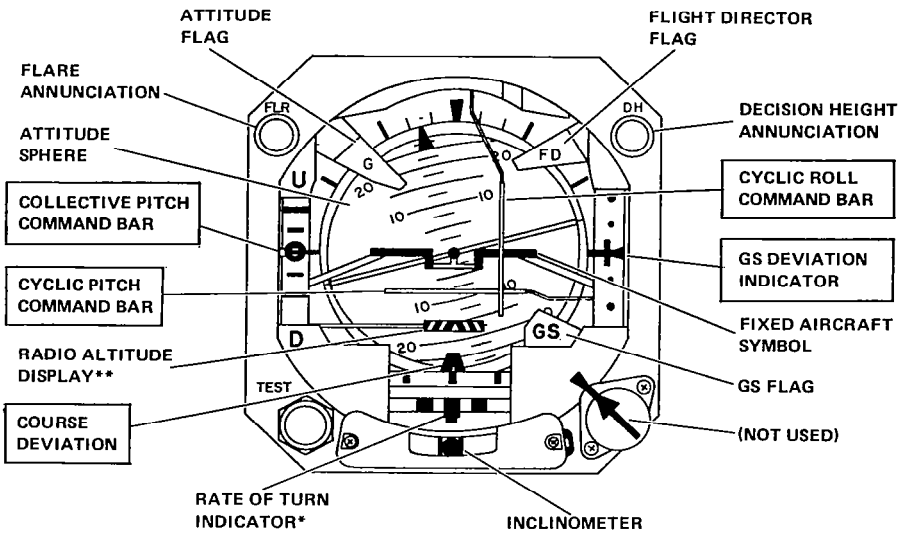

(a) Attitude director indicator.

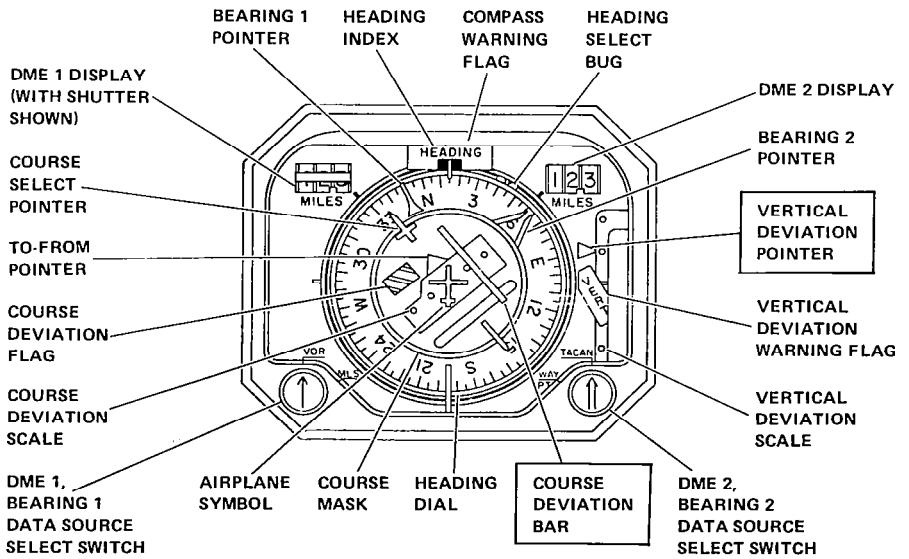

(b) Horizontal situation indicator.

Fig. 2 Flight director displays.

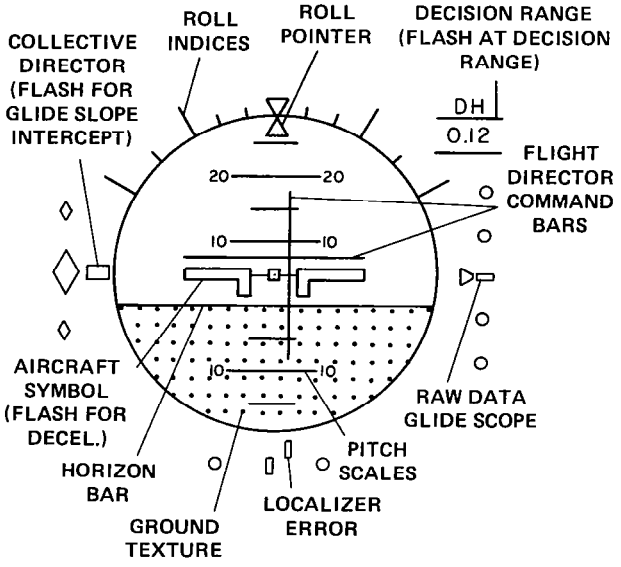

Fig. 3 C format for Experiment 6.

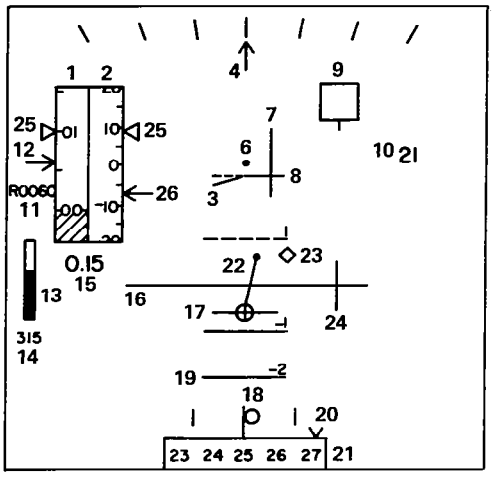

1. ALTITUDE TAPE
2. VERTICAL SPEED
3. THRUST MAGNITUDE CONTROL DIRECTOR
4. ROLL POINTER
6. PITCH & ROLL STICK DIRECTOR INDEX
7. LATERAL STICK CONTROL DIRECTOR
8. LONGITUDINAL STICK DIRECTOR
9. LANDING PAD (APPEARS AT DECISION RANGE)
10. AIRSPEED
11. RADAR ALTITUDE
12. ALTITUDE INDEX
13. TORQUE
14. ROTOR RPM
15. RANGE
16. HORIZON BAR
17. AIRCRAFT SYMBOL (FLASH FOR DECEL)
18. SIDESLIP
19. PITCH ATTITUDE
20. WIND DIRECTION
21. HEADING SCALE
22. GROUND VELOCITY STATUS VECTOR (APPEARS AT DECEL.)
23. GROUND VELOCITY VECTOR COMMAND (APPEARS AT DECEL.)
24. LATERAL COURSE OFFSET
25. GLIDE SLOPE (FLASHES AT INTERCEPT)
26. IVSI

Fig. 4 X format for Experiment 6.

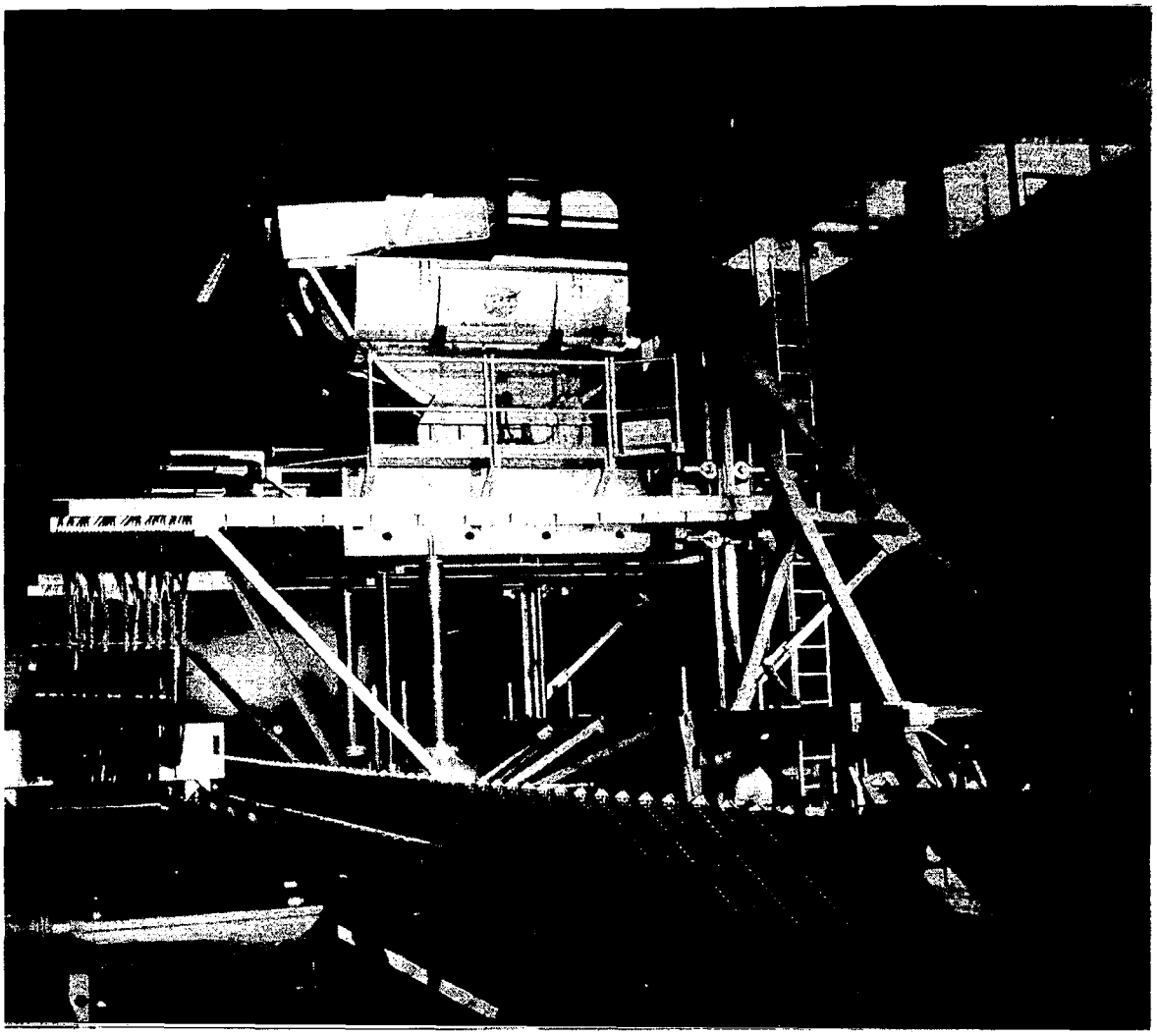

Fig. 5 Flight Simulator for Advanced Aircraft.

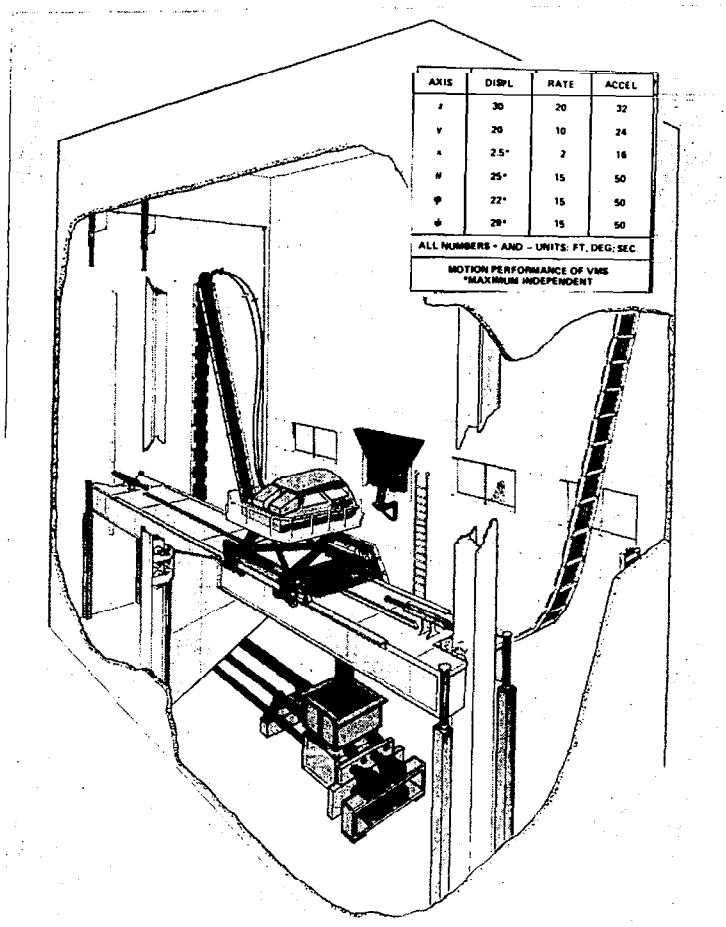

Fig. 6 Vertical Motion Simulator.

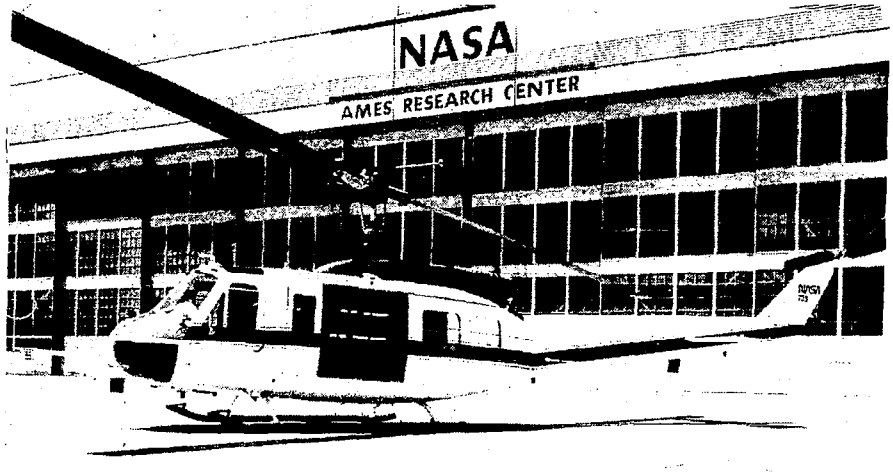

Fig. 7 UH-1H V/STOLAND helicopter.

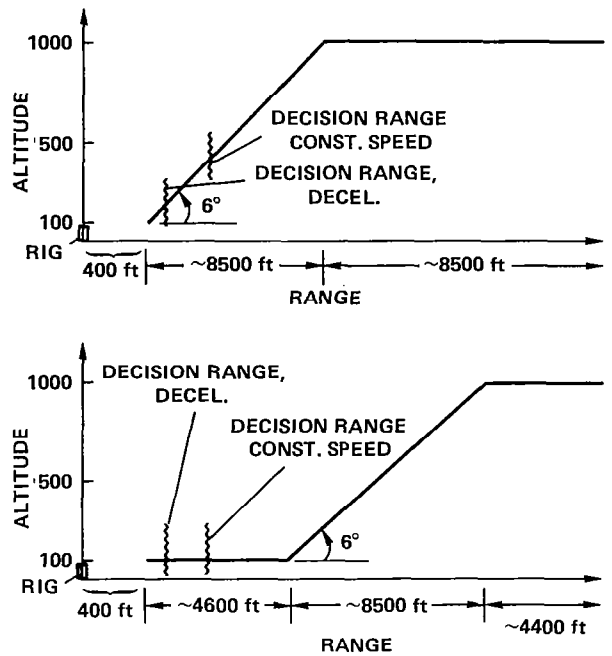

Fig. 8 Approach profile geometries.

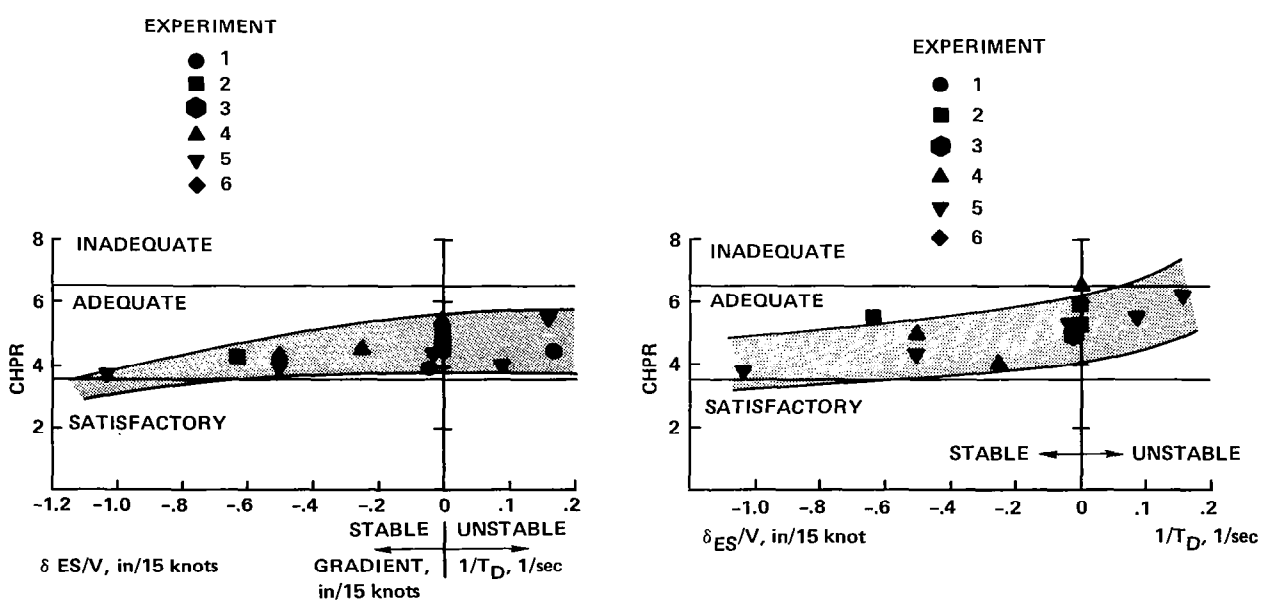

(a) No turbulence, no flight directors.

(b) In turbulence, no flight directors.

Fig. 9 Pilot rating data as function of longitudinal stick gradient.

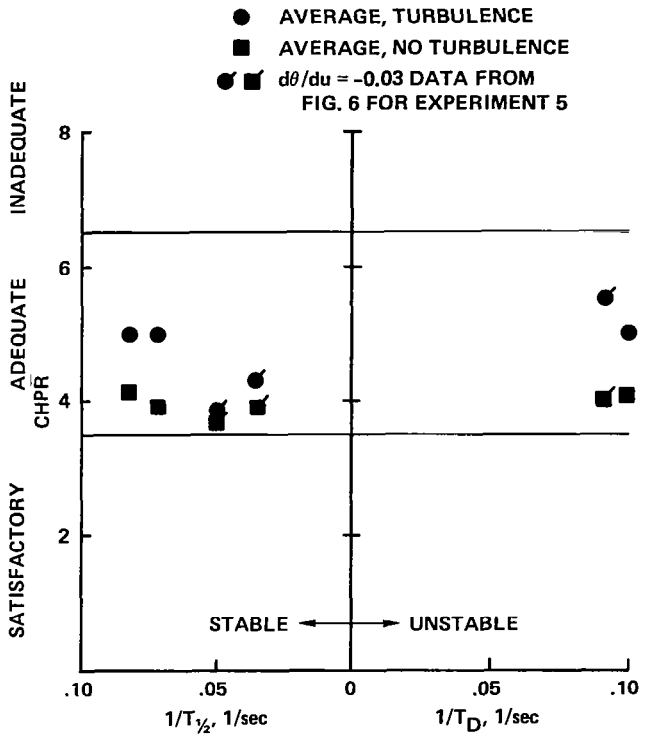

Fig. 10 Influence of $d\theta/du$ = -0.33°/knot (from Experiment 5).

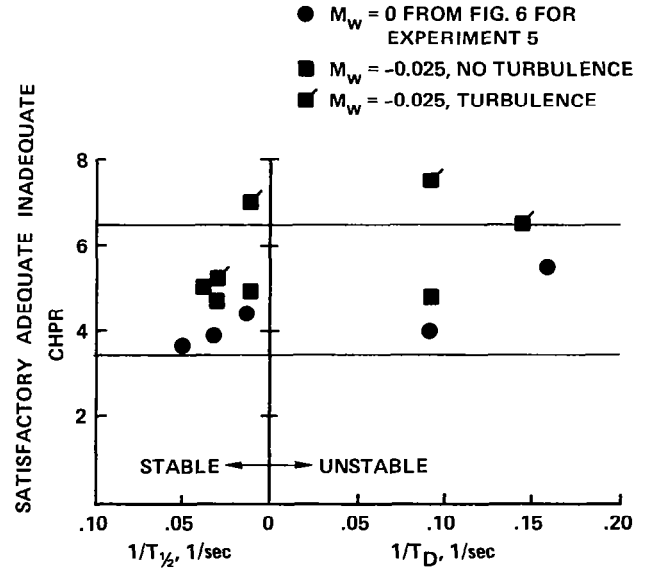

Fig. 11 Influence of M_w = -0.025 (from Experiment 5).

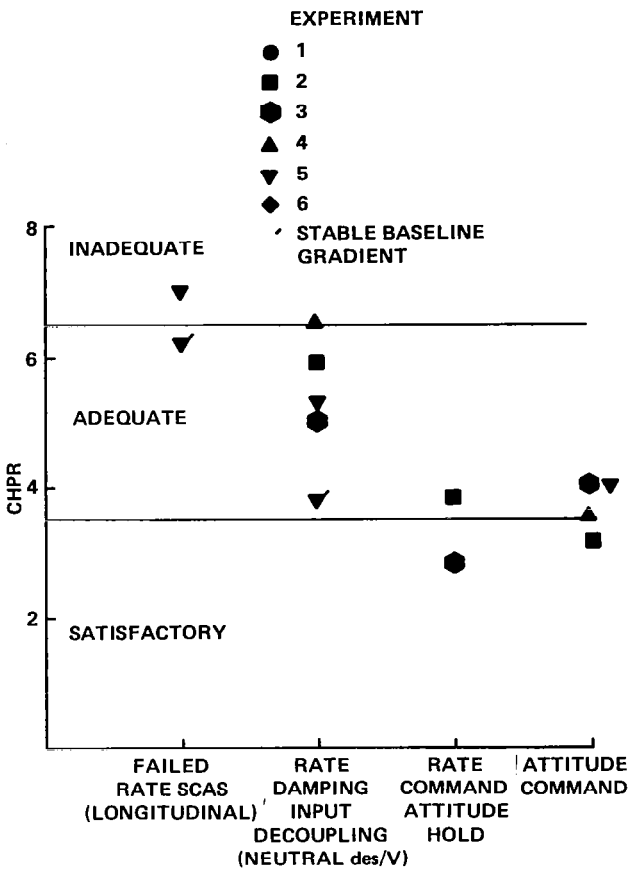

(a) No turbulence, no flight directors.

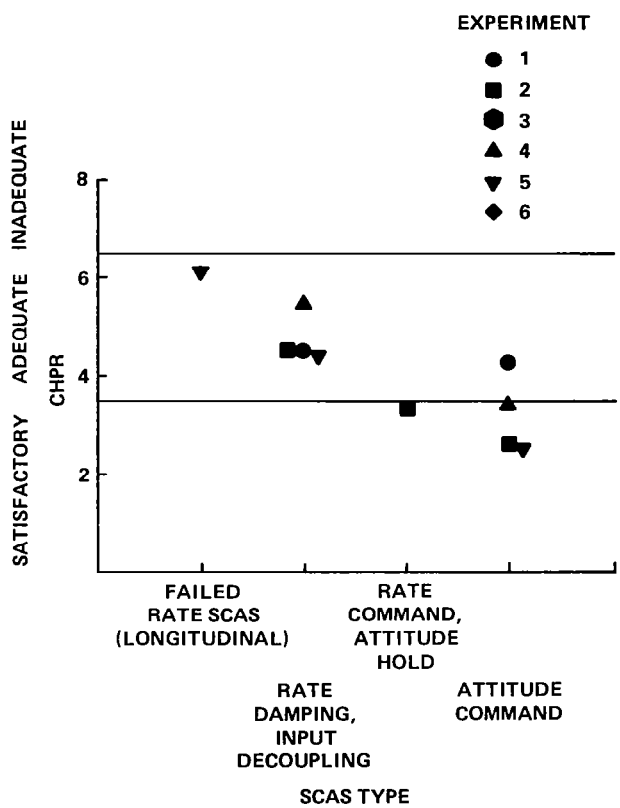

(b) In turbulence, no flight directors.

Fig. 12 Influence of SCAS.

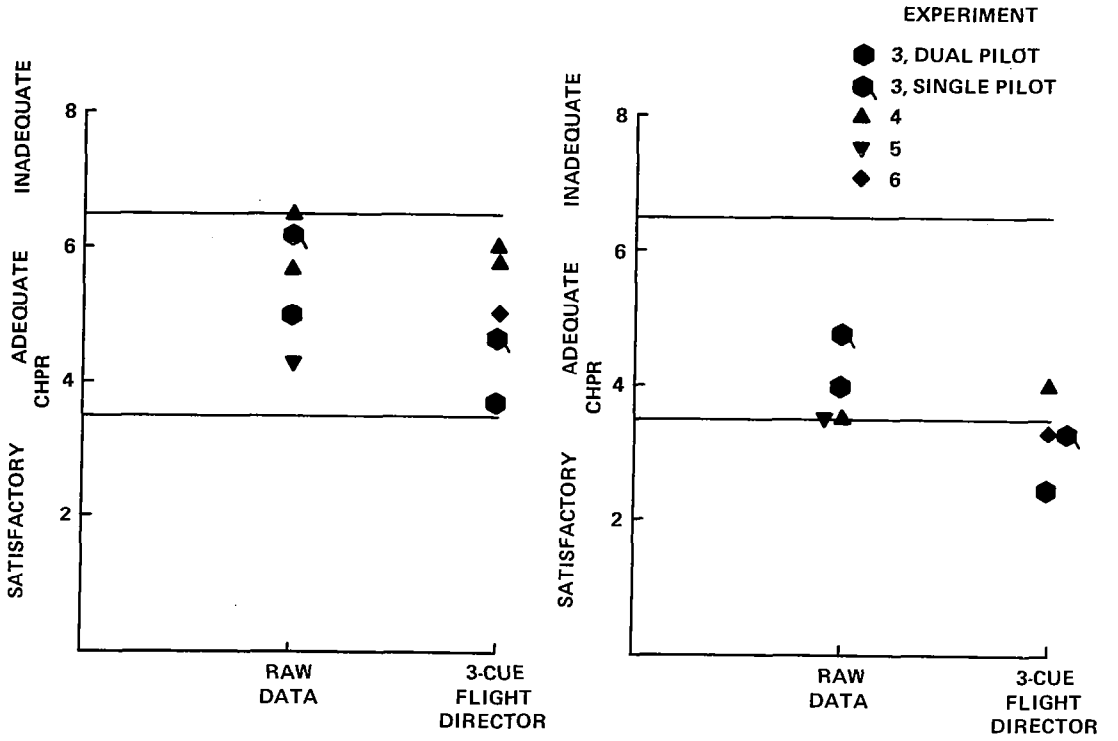

a) Rate-damping, input-decoupling SCAS.

b) Attitude-command SCAS.

Fig. 13 Influence of three-cue flight director: in turbulence, dual pilot.

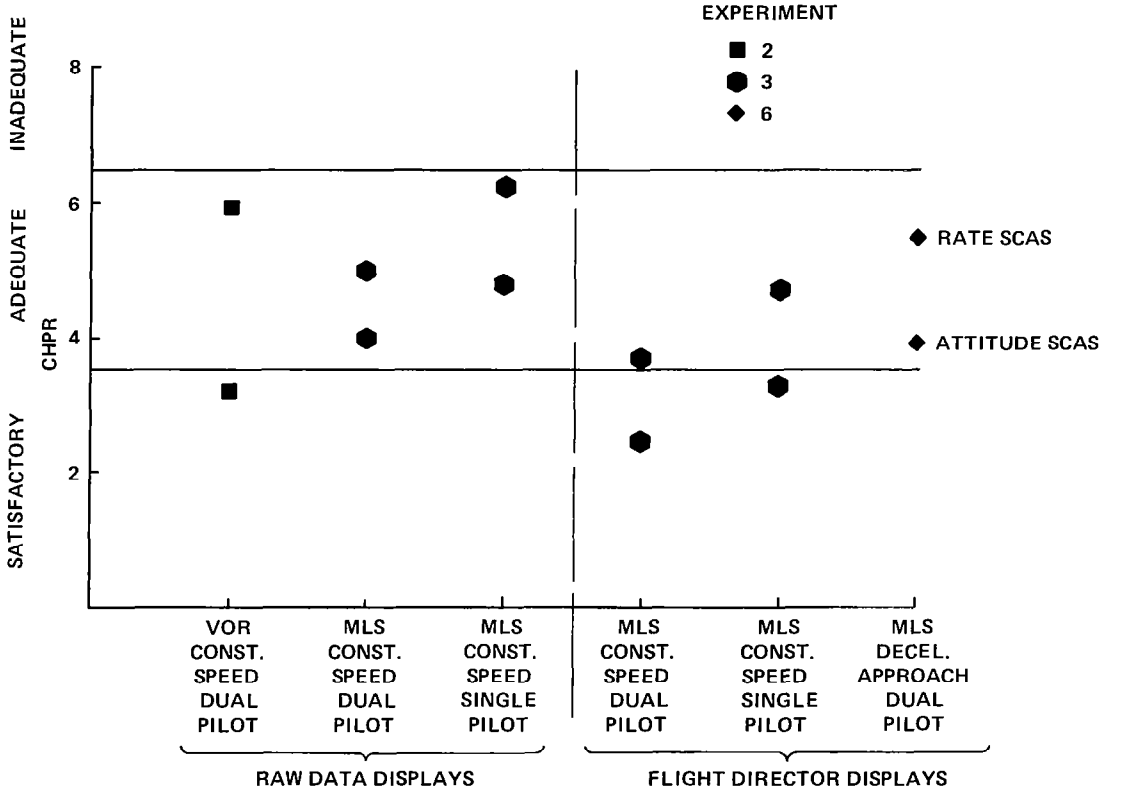

Fig. 14 Influence of task: in turbulence.

STATE-OF-THE-ART COCKPIT DESIGN FOR THE HH-65A HELICOPTER

Daniel E. Castleberry
HX Program Manager
and
Marsha Y. McElreath
Avionics Pilot Instructor
Collins Government Avionics Division of Rockwell International
Cedar Rapids, Iowa

Abstract

The design of the US Coast Guard HH-65A "Dolphin" cockpit employs advanced integrated electronics systems technology to achieve several important goals in this multimission aircraft:

1) Integrated systems operation with consistent, simplified cockpit procedures

2) Mission-task-related cockpit displays and controls

3) Reduced pilot instrument scan effort with excellent outside visibility

In order to meet these goals, Rockwell-Collins has implemented the integrated avionics system to depend heavily upon distributed but complementary processing, multiplex digital bus technology, and multifunction CRT controls and displays. This avionics system has been completely flight tested and will soon enter operational service with the Coast Guard.

Introduction

"On weekend duty, I always expected to be awakened in the middle of the night," recounts a veteran pilot of the USCG, "and when flying search and rescue (SAR) off San Francisco Bay in summer, I always expected fog." So it came as no surprise when an early morning call interrupted his sleep. Tasked with finding an overdue sailboat and two-man crew, the pilot and copilot strapped themselves in their HH-52 and lifted off. Passing over the harbor lights, they soon disappeared into the night. Searching amidst dense fog, the pilot contacted the harbor radar control and asked for position confirmation plus advisories of nearby objects or vessels. The controller quickly warned him of a ship at his twleve o'clock position and asked if he could see it. "I don't see anything," responded the pilot. Suddenly, the drone of a fog horn cut through the night fog. Max power! Positive climb! Forward airspeed! With reflex action, the pilot executed an instrument take off, a Coast Guard maneuver which transitioned the helicopter up into San Francisco's terminal control area—also, a less than desirable flight situation, but in the pilot's judgment, the better option.

Communication, navigation, flight control, and search sensor management are classical avionics functions which constitute every SAR operation. In theory, however, communication, navigation, and flight control are merely handmaids to the search effort—the sole reason for the mission. Yet, how much attention could the pilot in this account devote to finding the missing sailboat? Because routine cockpit duties often monopolize crew attention during SAR operations and thus impair crew effectiveness, the United States Coast Guard presented industry with a challenge: Build an avionics system that automates the routine tasks of communication, navigation, mission management, and flight control, and therefore, frees the crew to focus on the mission tasks which only they can perform—the visual search and FLIR or RADAR interpretation.*

On 14 June 1979, the USCG awarded Aerospatiale Helicopter Corporation (AHC) a contract for a Short Range Recovery (SRR) helicopter, the HH-65A. Teamed with AHC, Collins Government Avionics Division of Rockwell International designed the avionics system for the SRR helicopter.

Integrated Cockpit Design

The Rockwell solution to the Coast Guard design mandate exceeds mere automation. The HH-65A cockpit design achieves three additional goals: (1) integrated systems operation with consistent, simplified cockpit procedures, (2) mission-task-related cockpit displays and controls, and (3) reduced pilot instrument scan effort with excellent outside visibility.

To achieve these goals, Collins Division of Rockwell has designed the avionics system to rely heavily upon distributed but complementary processing, multiplex digital bus technology, and multifunction CRT controls and displays.

Distributed but complementary processing is an important integration concept used in the HH-65A. Its architecture does not hinge on one centralized computer for processing all navigation signals, displays, control inputs, etc. Instead, distributed processors perform specialized functions. The system coupler unit (SCU) manages communications between the boxes and controls radio tuning. The control display unit (CDU) provides pilot access to all flight management operations. The horizontal situation video display (HSVD) driver unit generates the navigation displays, and the mission computer (MCU) acts as both navigator and flight engineer. Without pilot action, the MCU calculates a "best estimate" of present position and velocity, automatically tunes the navigation sensors, enables flight planning, RNAV-style (including the generation of special USCG patterns), monitors fuel consumption, and records the engine and transmission condition (Fig. 1).

These specialized processors perform distinctive tasks; yet, they cooperate as a single integrated system to accomplish mission objectives. A high-speed multiplex digital data bus enables uninterrupted communication between the avionics. Using discrete addresses, any two boxes can communicate with each other on the bus. To fly to a point, for example, the pilot indicates his intent on the CDU, which in turn communicates that intent to the mission computer. The MCU computes and displays the aircraft's navigational situation on the HSVD and CDU, then, sends roll commands to the flight director (FD), which executes the commands through the automatic flight control system.

Although centralized versus distributed processing does not necessarily alter cockpit operation, system survivability argues for distributed processing. A mission computer failure, for instance, impacts only RNAV capability; automatic navigation via TACAN, VOR, or localizer is not impacted. LORAN, controlled through the system coupler unit, also remains valid; and since the HSVD display drivers process all VOR and TACAN signals plus generate the navigation displays, the crew retains display guidance.

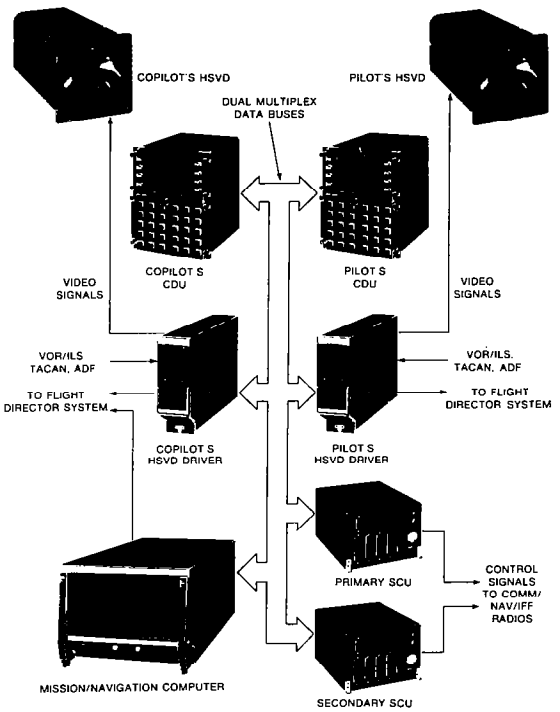

Fig. 1. Distributed but complementary processing.

Another important integration tool is using one device to do the work of many. Four multifunctional CRT devices, dual control display units (CDU's) and dual horizontal situation video displays (HSVD's), inhabit the HH-65A cockpit (Fig. 2).

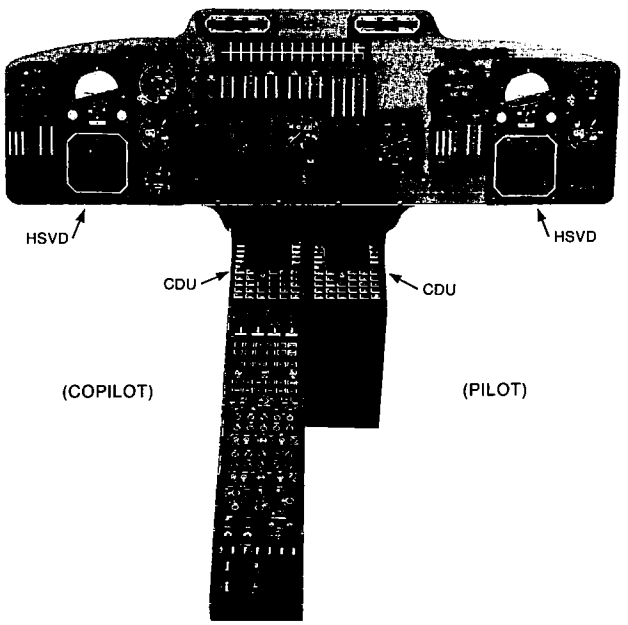

Fig. 2. HH-65A panel and console layout.

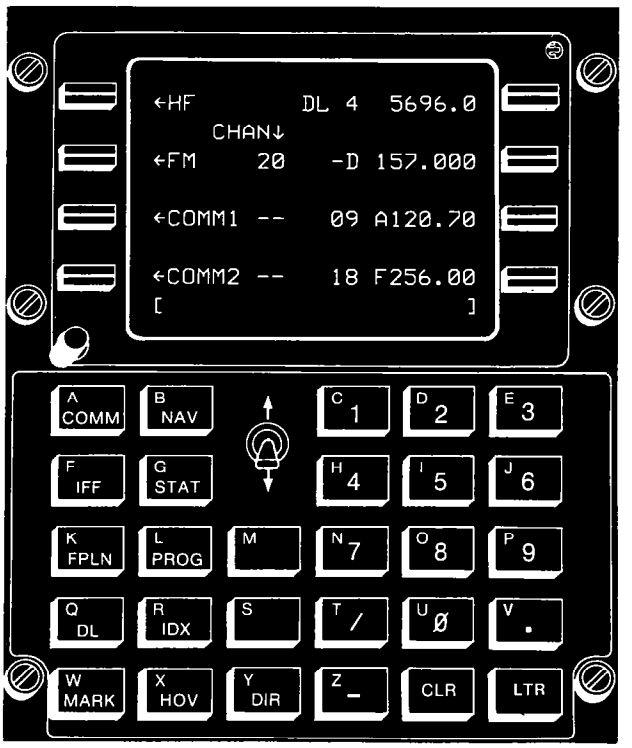

Fig. 3. Control display unit (COMM radio control display).

The CDU is a single-point control for all flight management operations. By incorporating "function keys," the CDU controls numerous mission tasks: For example, pushing the COMM or NAV button dedicates the CDU to COMM or NAV radio tuning. Selecting FPLN dedicates the CDU to flight planning. Likewise, pushing the PROG or STAT keys transforms the CDU into a flight progress or status reporting device. Having assigned the control display unit to a particular function, the crew uses the "line select keys" adjacent software labels to (1) tune individual radios, (2) set transponder codes and modes, (3) insert waypoints, plus a host of other functions (Fig. 3).

Because the CDU centralizes all operational inputs, it simplifies pilot procedures. He communicates, navigates, flight plans, etc, without having to manage dedicated controls scattered throughout the cockpit. Furthermore, CDU pilot procedures are uniform. Whether the pilot tunes a COMM/NAV radio, changes the transponder code, or enters a waypoint, he uses identical procedures.

As the CDU is a central point of avionics control, so the horizontal situation video display (HSVD) is a central point for flight situation displays. The HSVD supplants several dedicated instruments: the conventional HSI, projected map, RADAR and FLIR displays, as well as a hover indicator (Fig. 4).

Nonetheless, merely replacing conventional instruments is not the purpose of the HSVD. Rather, it organizes data into "task-related" modes which not only present the pilot information needed for specific mission phases but also eliminate extraneous information. Consider the low altitude hover over water at night. Because the pilot generally faces a centrally

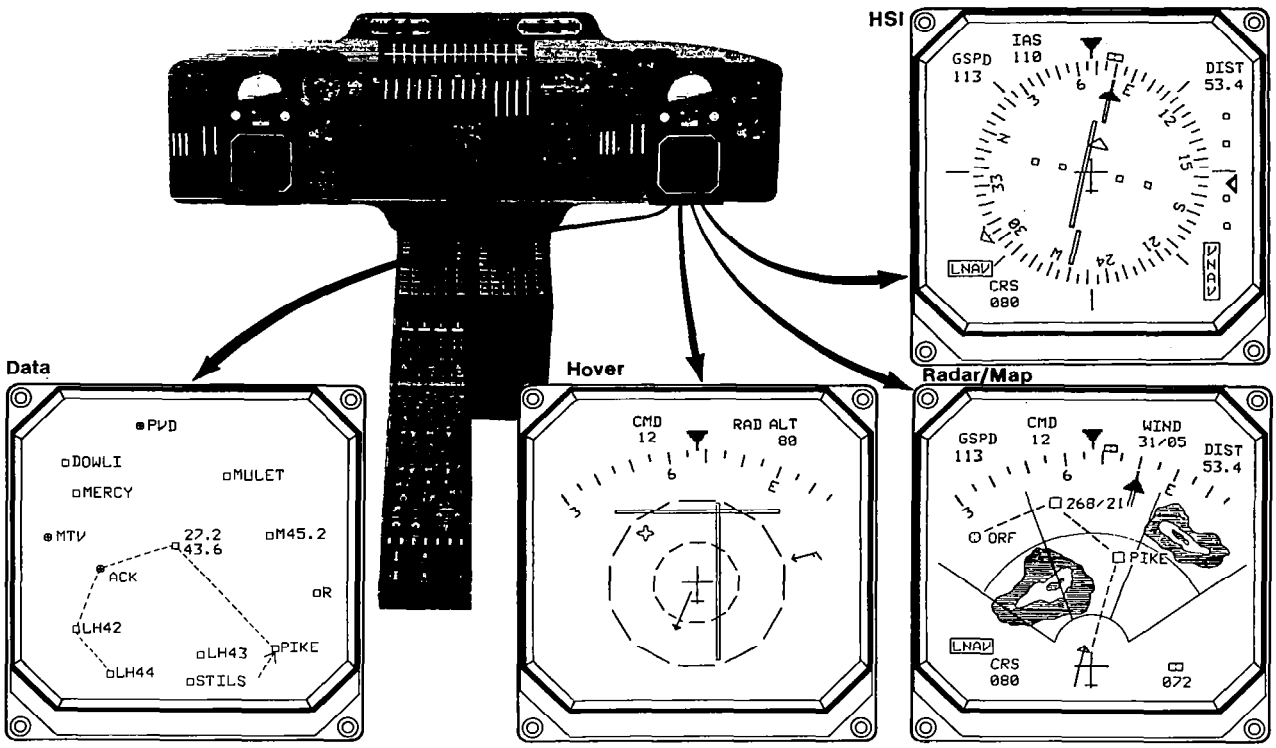

Fig. 4. Horizontal situation video display modes.

positioned HSI which provides virtually no hover information, he scans several other instruments to interpret his hover situation. The HSVD's hover mode integrates all hover data into one central display: omnidirectional airspeed, longitudinal/lateral drift, radar altitude, computed wind, plus target position.

Remaining HSVD modes, likewise, satisfy other flight phase requirements: The HSI mode is primarily an approach display. The MAP mode serves en route navigation, where the flight plan ahead may be viewed. The RADAR and FLIR modes display the video images from these sources for searching. The RADAR MAP mode relates radar returns (weather/ground) to the flight plan. And the DATA mode, a north-up chart presentation, facilitates impromptu flight planning.

Besides suiting information to flight phases, task-related displays denote "complementary formatting." For example, because a pilot navigating cross-country uses wind information to plan the flight, the MAP mode incorporates a digital wind readout. By contrast, the pilot in a hover does not need wind information for flight planning; he needs to visualize wind velocity relative to the helicopter. Consequently, the hover mode incorporates a modified Beaufort wind arrow, which instantly pictures the changing wind velocity. Each pilot needs computed wind information but in a complementary format—dictated by the flight situation.

Typical SAR Operation

Thus far, we have described technical features of the HH-65A avionics system. At this juncture, one might ask, "How does the integrated avionics system aid the pilot in the context of the SAR environment?" The following scenario intends to demonstrate integrated system operation, specifically, as it impacts cockpit procedures and workload in the SRR helicopter. Assume that a pilot were flying a routine patrol when the rescue coordinator calls and instructs him to proceed directly to the site of a ditched aircraft, initiate a search and rescue reported survivors.

To navigate to the downed aircraft, the pilot types in the LAT/LONG position on his CDU (the mission computer also recognizes LORAN TD's, place-bearing-distance, or identifiers) and selects DIRECT TO. The mission computer creates a direct course to the point. It also continuously plots present position using dual LORAN, dual VOR, TACAN, dual compass systems, and precision omnidirectional airspeed sensor inputs; manages the navigation sensors (ie, automatically selects navigation stations and tunes the LORAN, VOR and TACAN receivers); and flies the aircraft to the waypoint through the flight director. The HSVD MAP mode simultaneously displays the flight plan. This mode combines a tactical map presentation of flight plan waypoints and an abbreviated HSI, which the pilot uses with the progress and flight plan displays of the CDU to monitor en route progress.

Meanwhile, the mission computer has already assessed the fuel situation. Accounting for wind, the MCU calculates the fuel required to fly to the search point, proceed to the destination, and leave a 30-minute reserve. If on-board fuel is insufficient, the system warns the crew by announcing FUEL ALERT on the CDU. If sufficient fuel exists, the STATUS display translates the fuel reserve (ie, fuel in excess of what's needed to fly to the destination) into hours and minutes of flight time, labelled BINGO. MCU fuel management gives the pilot instant visibility of his fuel status, and thus, how long he can search.

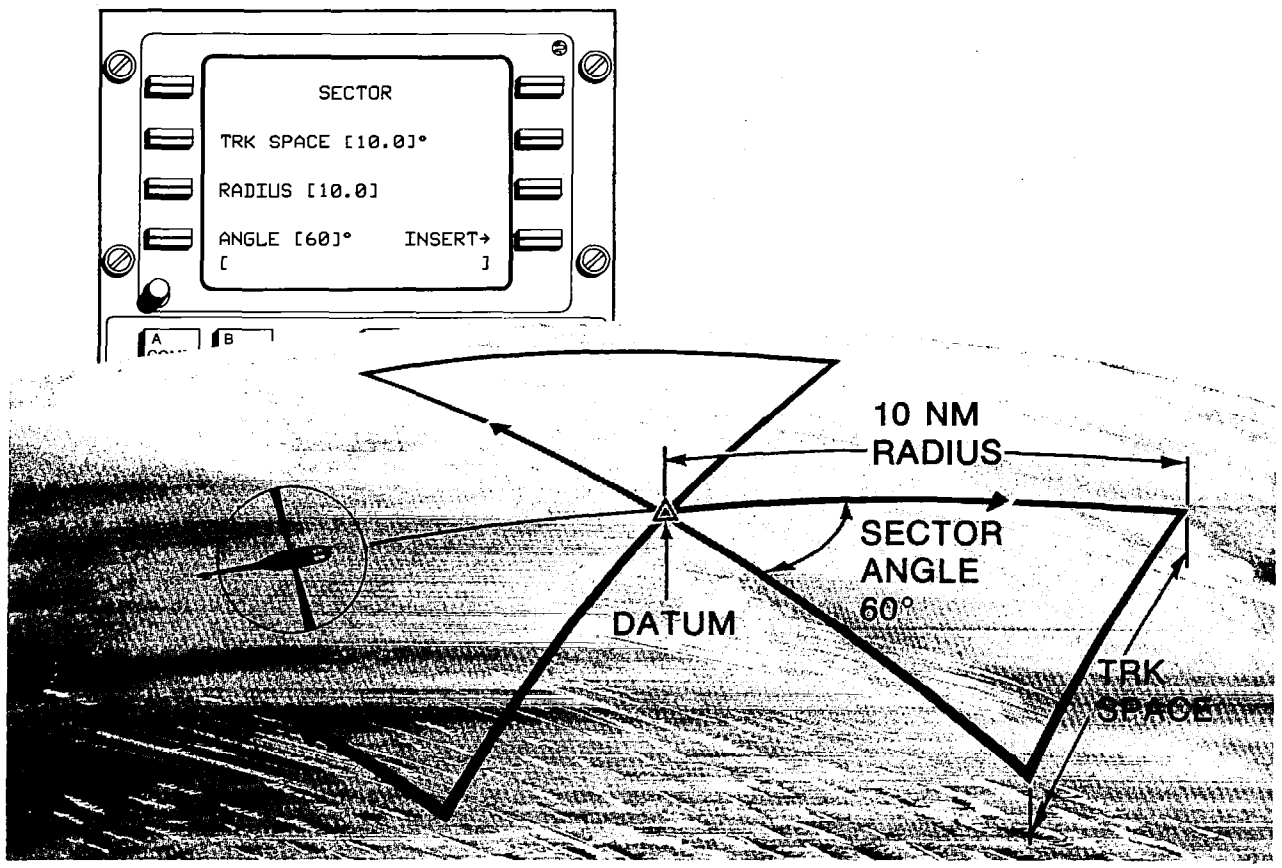

Fig. 5. Sector search entry into flight plan.

While the mission computer monitors fuel consumption, the data link system reports en route progress to the search coordinator, relieving the pilot of routine position reporting. He merely designates the communication radio and transmission interval on the CDU DATA LINK display. At the specified time, the integrated system automatically downlinks 9 pieces of information regarding aircraft position, status, and flight progress.

Eliminating routine flight management tasks frees the pilot to concentrate on system performance and flight progress. Pushing the PROG key on the CDU calls up the computed present position (LAT/LONG) and ground speed. Pushing the line key adjacent any flight plan waypoint provides instant access to "waypoint data" for that geographical point—time, distance and course to the waypoint via the flight plan or via direct.

As the aircraft nears the search area, the pilot plans his search. He selects one of three available patterns (sector, ladder, or expanding square) and then defines the pattern parameters. For example, if he selects a sector search, the computer asks what track spacing is desired (Fig. 5). (NOTE: The pilot may request search advisories by entering the sea state, visibility, cloud cover, and altitude; the MCU will compute the optimum track spacing.) Selecting "INSERT →" displays the flight plan, where inserting the pattern requires only pushing a line key at the desired datum point. The mission computer automatically plots the pattern waypoints and displays them on the HSVD.

Upon reaching the target area, the aircraft automatically initiates the search while the crew concentrates on the search RADAR, FLIR (forward-looking infrared), and DF radio homing, or they scan the white caps below. When the target is spotted, the integrated system, with minimal crew effort, abandons the search and expedites the rescue operation. Over-flying the target location, the pilot pushes two buttons: MARK — to mark the target's location, and HOVER — to call up the approach-to-hover pattern. He inserts the approach-to-hover pattern into the flight plan and selects APPR on the flight director panel — triggering a chain of operational events. The system turns the aircraft downwind to ensure a final approach into the wind, directs a minimum time procedure turn, and computes a five degree descent to the hover transition point. Using the FD speed beep, the pilot may vary the approach speed. At 100-feet radar altitude, the FD APPR mode drops; T-HOV mode captures and slows the helicopter to zero ground speed at 50 feet RA — just short of the target (Fig. 6). During the transition to hover, the HSVD automatically displays the HOVER mode. The computed wind, HOVER velocity commands, omnidirectional airspeed vector, and the marked target position enable the pilot to monitor the approach-to-hover maneuver as well as modify the hover conditions. If the pilot beeps either radar altitude or longitudinal/lateral airspeed, the indicators instantly verify his input.

While the survivors are hoisted to safety, the pilot decides his next course of action. Should a victim require immediate medical attention, he may choose to fly to a medical center

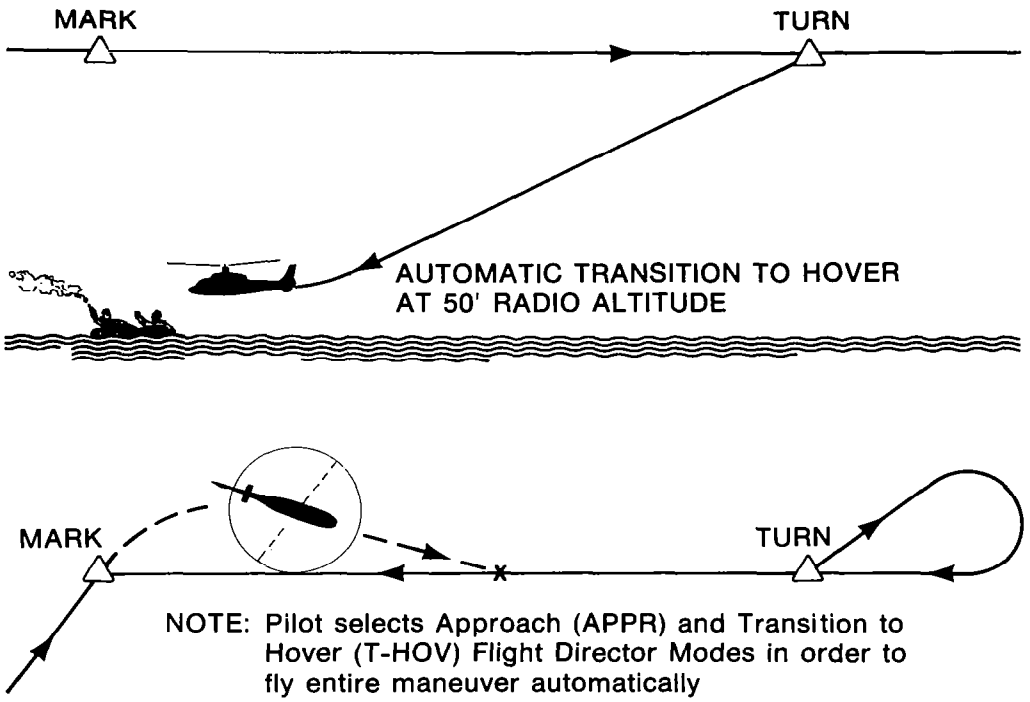

Fig. 6. Approach-to-hover maneuver.

rather than home base. With the push of the DATA mode button, the HSVD displays surrounding hospital locations in a north-up, chart presentation (Fig. 7). To examine direct distance, time or course to any viable alternate, the pilot simply calls up waypoint data for the respective hospital through his CDU. If desired, the MCU will also compute the maximum range on that course. Once again, minimal pilot action activates integrated system response, to enhance crew effectiveness.

The technological tools of digital data bus communication, distributed but complementary processing, and multifunction CRT controls and displays have effected integrated cockpit operation in the HH-65A. Although this system has been implemented for a SAR application, these techniques and this approach to operational cockpit integration will adapt to any helicopter mission. A system coupler unit and CDU which currently controls radios could as easily control weapons systems. A mission computer and HSVD might as easily display terminal area approach procedures or tactical combat command and control data. Meanwhile, the HH-65A with its integrated cockpit operation, will benefit Coast Guard line pilots who undertake SAR despite adverse conditions.

*Cdr. David A. Young, "Avionics System Design Requirements for the United States Coast Guard HH-65A Dolphin": Presented at the Sixth European Rotorcraft and Powered Lift Aircraft Forum, Bristol, United Kingdom, September 16-19, 1980.

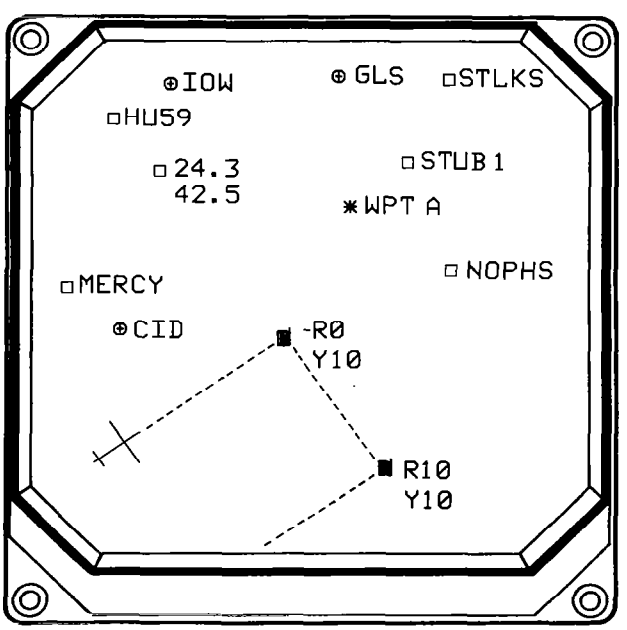

Fig. 7. HSVD data mode.

PERFORMANCE EVALUATION OF A KINESTHETIC-TACTUAL DISPLAY

Richard J. Jagacinski, John M. Flach, and Richard D. Gilson
Associate Professor, Graduate Student, and Professor
The Ohio State University
Columbus, Ohio

Richard S. Dunn
Engineering Psychologist
U. S. Army Research and Technology Laboratory
Moffett Field, California

Abstract

Simulator studies demonstrated the feasibility of using kinesthetic-tactual (KT) displays for providing collective and cyclic command information, and suggested that KT displays may increase pilot workload capability. A dual-axis laboratory tracking task suggested that beyond reduction in visual scanning, there may be additional sensory or cognitive benefits to the use of multiple sensory modalities. Single-axis laboratory tracking tasks revealed performance with a quickened KT display to be equivalent to performance with a quickened visual display for a low frequency sum-of-sinewaves input. The trackers approximated a lag in these tasks. In contrast, an unquickened KT display was inferior to an unquickened visual display. The trackers approximated a proportional element in these tasks. Full scale simulator studies and/or inflight testing are recommended to determine the generality of these results.

Introduction

The kinesthetic-tactual (KT) display has been under development and evaluation since 1966. It provides a useful display alternative for helicopter tasks which have high visual workload or which are incompatible with visual or auditory display devices. Examples include terrain flight with high demands for visual attention outside the cockpit and night flight with viewing aids which are not fully compatible with cockpit visual displays. Numerous laboratory and simulation studies have been conducted to develop prototype KT displays and to measure performance with these displays. These studies show the concept to be feasible for helicopter application and effective at visual workload relief. This report first summarizes some early studies oriented to workload and feasibility issues, and then discusses some data which provide more detailed quantification of KT display performance.

The KT display was invented by Dr. Robert Fenton of the Ohio State Department of Electrical Engineering. In a series of studies[1,2,3] he and his colleagues demonstrated the display's usefulness in improving the precision with which car drivers could control the distance between themselves and a vehicle in front of them.

An example of a single dimensional KT display as it might be used on a helicopter collective handgrip is shown in Fig. 1. An electromechanical slide protrudes from the surface of the handgrip to indicate the direction and magnitude of tracking error. If there is zero error, the slide is flush with the handgrip. If the slide protrudes downward, the pilot moves the collective in the downward direction until the slide returns to the flush position.

A two-dimensional KT display as might be used on a helicopter cyclic handgrip is shown in Fig. 2. The electromechanical slide is in the form of a ring that is flush with the control grip when there is zero tracking error. The protrusion of the ring from the control grip represents a vector composite of lateral and longitudinal errors. The appropriate response is to move the cyclic in the direction of the protrusion until the ring is again in the flush position. The vectoral nature of this display seems to be highly compatible with the two dimensional cyclic movement.

Fixed Wing Aircraft Study

One use of the KT display has been to provide pitch commands in fixed wing aircraft. Gilson and Fenton[4] measured the performance of novice pilots in a Cessna 172 with three different types of displays: (1) a visual display of airspeed; (2) a visual display of deviations from a desired angle of attack; (3) a KT display of deviations from a desired angle of attack. The KT display was mounted on the control yoke handle, and pilots minimized protrusion of the display from its zero error position with fore-aft movements of the yoke. For controlling angle of attack in an approach to landing maneuver, the visual and tactual displays of angle of attack were comparable to each other, and both were superior to the visual display of airspeed. In a tight turn about a point at constant speed and constant altitude, the KT display

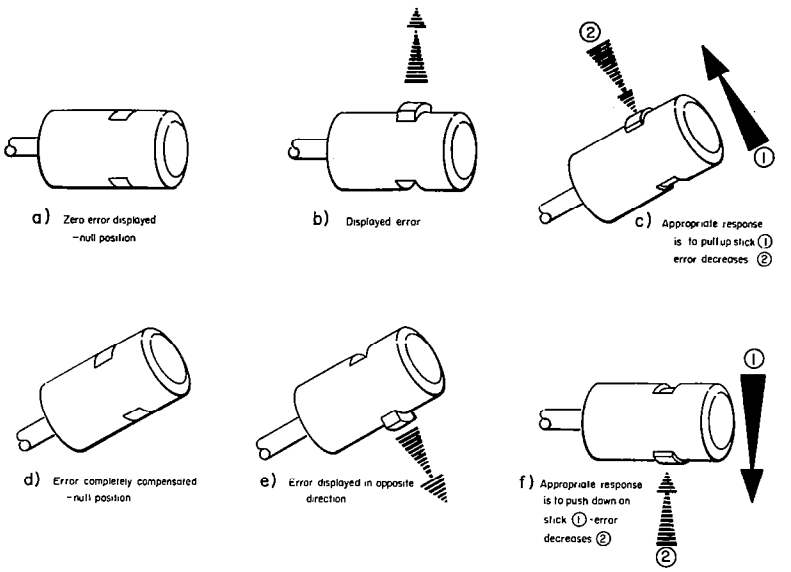

Fig. 1 Control-display relationship for a one-dimensional kinesthetic-tactual display suitable for a helicopter collective. (Copyright 1979, Human Factors, Vol. 21, p. 80)

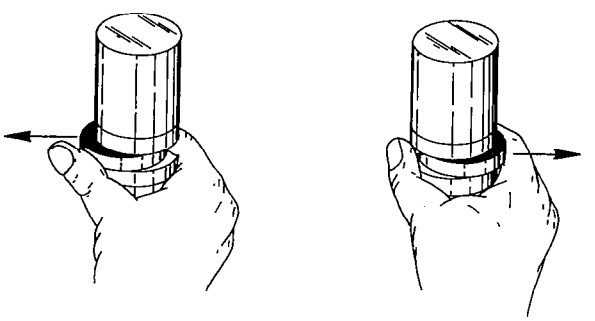

Fig. 2 Control-display relationship for a two-dimensional kinesthetic-tactual display suitable for a helicopter cyclic.

permitted superior performance to the two visual displays in controlling angle of attack, altitude, and airspeed. This latter maneuver requires considerable monitoring of visual cues outside the cockpit. The reduced need for visual scanning with the KT display may account for these results.

Helicopter Simulation Studies

Two helicopter simulation studies were conducted using the Tactical Avionics System Simulator (TASS) facilities at the U. S. Army's Avionics Laboratory, Fort Monmouth, New Jersey. The first study by Gilson, Dunn, and Sun[5] investigated performance of an instrument flight rules decelerated landing maneuver in a simulated UH-1 helicopter buffeted by wind gusts. Cyclic commands were indicated visually by horizontal and vertical crossbars; pedal commands were indicated visually by a rate of turn needle. Collective commands were presented either visually by a display similar to a glide slope pointer on the left-hand side of the flight director, or tactually by a single dimensional KT display mounted on the handgrip of the collective. Experimentally it was possible to make the overall task more difficult by adding a time delay to the cyclic roll dynamics. Adaptive circuitry adjusted this time delay so that the sum of absolute tracking errors of the four command signals reached a criterion value. The performance measure was the value of the time delay necessary to achieve this error criterion. For all five pilots in this study, the KT display permitted a longer time delay than the visual display. The superiority of the KT display may be due to reduced visual scanning or a more cognitive advantage regarding how the pilot processes information from multiple modalities. This issue was addressed in a later laboratory study.

A second helicopter simulation study by Sun[6] examined the feasibility of tactually providing both collective and cyclic commands while still providing other visual information, e.g.,

situational displays. The simulated helicopter was a UH-1. A single axis KT display was mounted on the collective handgrip as in the previous study. Additionally, a two dimensional KT display in the form of a ring was mounted on the cyclic handgrip. A nonlinear gain was used to magnify the protrusion of the ring for small tracking errors. Wearing flight gloves, pilots were able to use these KT displays to successfully perform an instrument flight rules decelerated landing maneuver. With pitch and roll rate signals used to quicken the cyclic display, pilots were also able to maintain a stable hover in the presence of simulated wind gusts, and concurrently perform a secondary light-cancelling task.

Recent Laboratory Studies

Single-Axis Tracking

In a recent laboratory study at The Ohio State University by Jagacinski, Flach, and Gilson,[7] student subjects were trained on a critical tracking task using one-dimensional visual or KT displays with or without quickening. A critical tracking task[8] requires subjects to stabilize the output of a first-order unstable system. Any unsteadiness in the subject's hand movements excites the instability and in turn requires corrective stabilization by the subject. The difficulty of this task is determined by the time constant of the unstable system. The shorter the time constant, the more rapidly the unstable system tends to exponentially amplify small deviations from the desired constant output. In a critical tracking task adaptive circuitry gradually shortens the time constant until the task becomes so difficult that the subject loses control. The inverse of this critical time constant at the instant control is lost is called the critical root, and is represented with the symbol λ_c.

In this experiment, the single dimensional KT display was mounted on a control stick similar to a helicopter collective. The visual display consisted of a vertically moving line on an oscilloscope screen. The quickened signals consisted of a simple addition of error and error velocity with the two equally weighted. The group means of the critical roots are shown in Fig. 3. These results replicate the basically additive effects of modality and quickening previously found by Jagacinski, Miller, and Gilson.[9] The visual modality was superior, and the quickened displays were superior. However, the quickened KT display was approximately equivalent to the unquickened visual display.

Following the critical tracking, subjects were transferred to a stationary compensatory tracking task in which they used the same displays. The input was a sum of nine sinewaves with the amplitudes of the three lowest frequency sinewaves (.35, .73, 1.08 r/s) five times greater than the amplitudes of the other sinewaves.

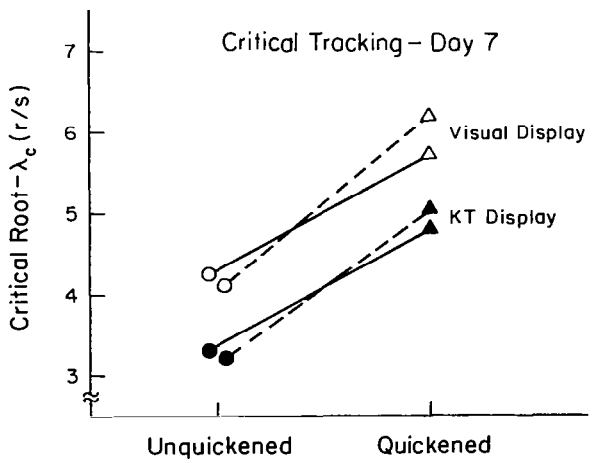

Fig. 3 Critical tracking scores for eight groups of four subjects. Groups connected by dashed and solid lines were respectively transferred to stationary tracking with system dynamics 1.5/s and 3.0/(s-1).

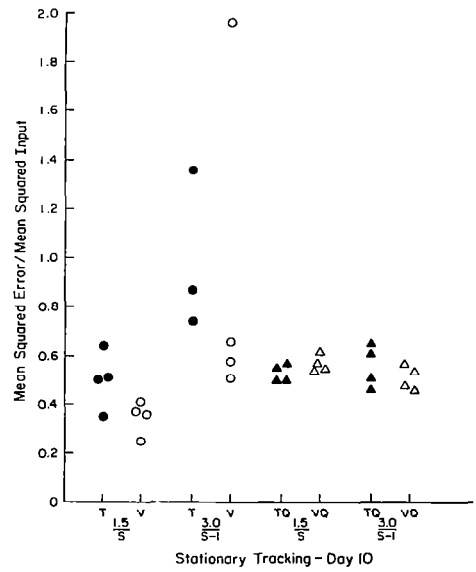

Fig. 4 Mean squared error normalized by mean squared input for thirty-one individual subjects. The symbols represent the same display conditions as in Fig. 3.

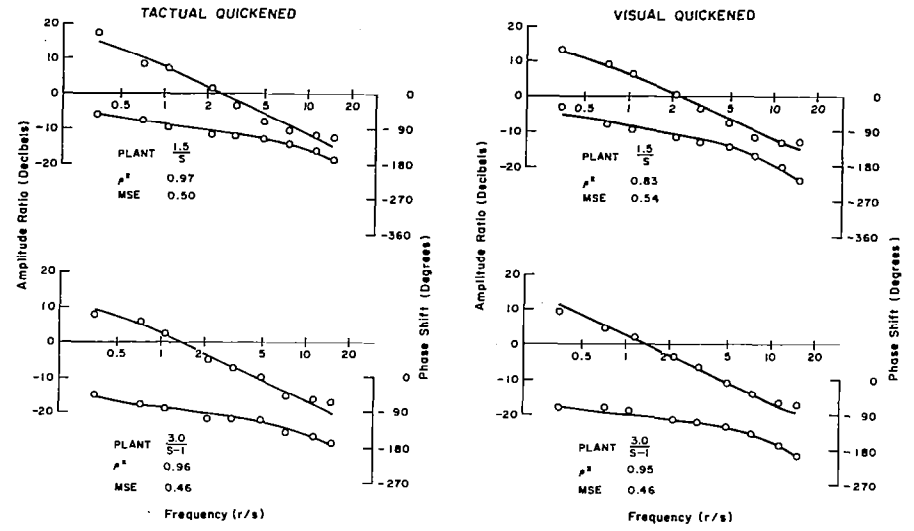

Fig. 5 Linear transfer functions for the subjects with the lowest mean squared error in each of four quickened display conditions. The circles indicate the data points, and the solid lines represent analytic approximations consisting of a low frequency lag, a high frequency lead, a gain, and a time delay.

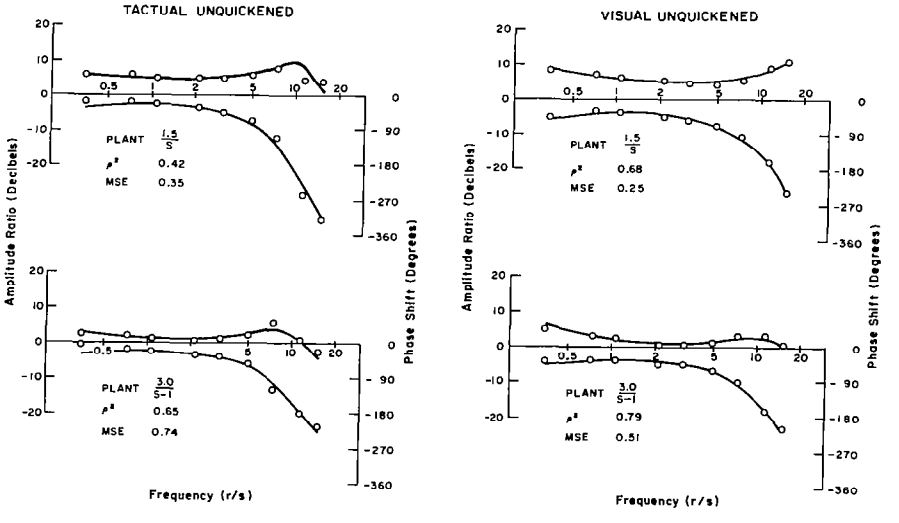

Fig 6 Linear transfer functions for the subjects with the lowest mean squared error in each of four unquickened display conditions. The circles indicate the data points, and the solid lines represent analytic approximations consisting of a low frequency lag and lead, a high frequency second-order lag, a gain, and a time delay.

Half the subjects controlled a single integrator system (1.5/s), and half controlled a first-order unstable system (3.0/(s-1)). Mean squared error scores are shown in Fig. 4. The unquickened visual displays were superior to the unquickened tactual displays. The quickened visual and tactual displays produced equivalent error scores.

Describing functions were calculated for each subject. For the quickened displays subjects were well approximated by a low frequency lag, a high frequency lead, a gain, and a time delay. As shown in Fig. 5, the describing functions were very similar for the tactual and visual displays and accounted for about 90% of the variance in the subjects' control movements (ρ^2).

For the unquickened displays, subjects were approximated by a low frequency lag and lead, a high frequency second-order lag, a gain, and a time delay (Fig. 6). Overall the linear transfer functions for the visual and KT displays were very similar. Subjects using the KT display did, however, exhibit less low frequency phase lag. About 60-70% of the variance in subjects' control was accounted for by the linear transfer functions for all but the tactual condition with the single integrator system. In this condition only about 40% of the variance was accounted for, and there were strong peaks in the spectra at non-input frequencies in the range of 3 to 7 rad/s. Apparently some strongly nonlinear behavior resulted in this condition.

Dual-Axis Tracking

A second laboratory study by Burke, Gilson, and Jagacinski[10] compared tracking with visual and KT displays when a secondary visual task was performed concurrently. The primary task required subjects to use their left hands to stabilize a subcritical first-order unstable system. Three different displays were used for this primary task: (1) a one-dimensional quickened KT display; (2) a one-dimensional unquickened visual display; (3) a one-dimensional quickened visual display for which the signal was additionally passed through an off-line KT display. This last visual display condition thus had the same benefit of quickening and the same detriment of the servomotor lag as the KT display condition.

The secondary task required subjects to use their right hands to stabilize a different first-order unstable system. Adaptive circuitry similar to that of Jex, Jewell, and Allen[11] adjusted the time constant of the secondary task, until subjects' time-averaged error on the primary task was 25% higher than when the primary task was performed without significant secondary task loading. The performance measures were the washout-filtered time-averaged error on the primary task and the inverse of the time constant for the secondary task, λ_s. In order to avoid the need for scanning in the visual-visual display conditions, the primary and secondary displays for these conditions were respectively the vertical and horizontal position of a single dot moving on an oscilloscope screen. For the KT display condition, a single dimensional visual display was used for the secondary task.

The results of this experiment for dual task performance are shown in Fig. 7. The quickened KT display permitted superior performance on both the primary and secondary tasks. In contrast to these results, the quickened KT display and the two primary visual displays yielded equivalent performance when subjects performed only a single-dimensional critical tracking task alone. Therefore, there seems to be some benefit of combining KT and visual displays in dual task performance beyond what one might expect from single task performance. This experimental result is not due to the elimination of visual scanning because the visual displays were integrated into a single moving dot. It may be that using two sensory modalities provides additional attentional resources, additional sensory buffers, and/or additional cue discriminability for processing the displayed signals. Further research is necessary to delimit these possibilities.

One cautionary note should be added concerning the generality of this experimental finding. Preliminary data on dual task tracking of sum-of-sinewaves inputs without crosscoupling of the two tasks has not so far revealed similar superiority of the combination of KT and visual displays. However, these data are still preliminary.

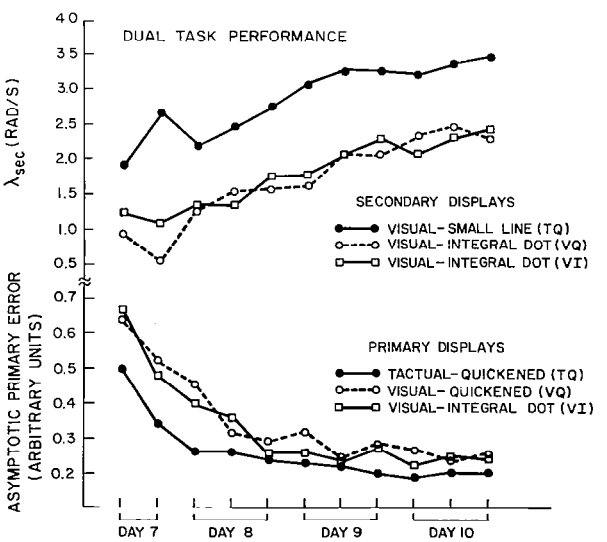

Fig. 7 Mean performance on a dual tracking task. (Copyright 1980, Ergonomics, Vol. 23, p. 970)

Recommendations

In summarizing the single axis tracking results with the KT display, it is helpful to consider separately the quickened and unquickened displays. The quickened displays may be considered analogous to command displays, whereas the unquickened displays are analogous to situation displays used in helicopters. With the quickened displays, the subjects approximated a lag, and tracking performance with the KT display was equivalent to that obtained with a visual display for a low frequency sum-of-sinewaves input. On the critical tracking task, the quickened visual display was superior to the quickened KT display. However, the results of Burke et al.[10] suggest that this difference is due to the servomotor lag in the implementation of the KT display.

In contrast to these results, the unquickened (situation-like) visual display was superior to the unquickened KT display for both sum-of-sinewaves tracking and critical tracking. With the unquickened displays subjects approximated a proportional element or gain. The present results therefore suggest that the KT display be used with command type displays that permit the tracker to behave in a lag-like manner. Under these conditions the KT servomotor lag must be carefully designed relative to the anticipated task requirements.

In dual task performance both the simulator and laboratory studies suggest that the combination of KT and visual displays may provide superior overall performance to the use of only visual displays. Part of the advantage of the KT display may be due to a reduction in visual scanning. Additionally, the use of a second sensory modality may provide some sensory and/or cognitive advantages over a single modality. However, these results need to be carefully tested for their generality beyond particular laboratory tasks. Full scale simulator studies and/or inflight testing appear to be warranted in light of the promising nature of the present findings.

Acknowledgement

Portions of this research were sponsored in part by the U. S. Army Research and Technology Laboratory, Moffett Field, California, and in part by the Avionics Laboratory, Electronics Command, Ft. Monmouth, New Jersey, through NASA-Ames Grant NSG-2179.

References

1. Fenton, R. E., "An improved Man-Machine Interface for the Driver-Vehicle System," IEEE Transactions on Human Factors in Electronics, HFE-7, (4), Dec. 1966.

2. Fenton, R. E., and Montano, W. B., "An Intervehicular Spacing Display for Improved Car-Following Performance," IEEE Transactions on Man-Machine Systems, MMS-9, (2), June 1968.

3. Rule, R. G., and Fenton, R. E., "On the Effects of State Information on Driver-Vehicle Performance in Car Following," IEEE Transactions on Systems, Man, and Cybernetics, SMC-2, (5), Nov. 1972.

4. Gilson, R. D., and Fenton, R. E., "Kinesthetic-Tactual Information Presentations--Inflight Studies," IEEE Transactions on Systems, Man, and Cybernetics, SMC-4, (6), Nov. 1974.

5. Gilson, R. D., Dunn, R. S., and Sun, P., "A Kinesthetic-Tactual Display Concept for Helicopter-Pilot Workload Reduction," Paper No. 77.33-22, American Helicopter Society 33rd Annual Forum, Washington, D.C., May 1977.

6. Sun, P., "Rotor Plane Control Device," FY-77 ILIR Final Report, U. S. Army Avionics Research and Development Activity, Fort Monmouth, New Jersey, 1977.

7. Jagacinski, R. J., Flach, J. M., and Gilson, R. D., "A Comparison of Tracking with Visual and Kinesthetic-Tactual Displays," Proceedings of the First Symposium on Aviation Psychology, APL-1-81, April 1981, pp. 74-83.

8. Jex, H. R., McDonnell, J. D., and Phatak, A. V., "A 'Critical' Tracking Task for Manual Control Research," IEEE Transactions on Human Factors in Electronics, HFE-7, (4), Dec. 1966.

9. Jagacinski, R. J., Miller, D. P., and Gilson, R. D., "A Comparison of Kinesthetic-Tactual and Visual Displays via a Critical Tracking Task," Human Factors, 21, (1), Feb. 1979.

10. Burke, M. W., Gilson, R. D., and Jagacinski, R. J., "Multi-modal Information Processing for Visual Workload Relief," Ergonomics, 23, (10), Oct. 1980.

11. Jex, H. R., Jewell, W. F., and Allen, R. W., "Development of the Dual-Axis and Cross-Coupled Critical Tasks," Proceedings of the Eighth Annual Conference on Manual Control, May 1972, pp. 529-552.

SYNTHESIS OF AN INTEGRATED COCKPIT MANAGEMENT SYSTEM

Joseph A. Dasaro

Charles T. Elliott

Avionics Laboratory

U.S. Army Avionics Research and Development Activity

Fort Monmouth, New Jersey

Abstract

This paper discusses the process used in the synthesis of an integrated cockpit management system. Areas covered include flight displays, subsystem management, checklists, and procedures (both normal and emergency). The process of evolving from the unintegrated conventional system to the integrated system is examined and a brief description of the results presented.

Introduction

One way to describe the process of designing an integrated cockpit management system is as the series of steps outlined below:

1) an analysis (functional and electrical) of all signals on-board the aircraft,

2) a feasibility analysis of each signal to determine if suitable for absorption into an integrated system based on safety of flight requirements and electronic considerations.

3) an analysis of the functions performed by the operator in a standard aircraft to determine which ones must be performed by the operator, which ones the operator must know the status of, and which can be performed automatically, and

4) following these analyses, the initial mapping of aircraft control and display functions from a conventional unintegrated cockpit to an integrated cockpit.

This last step is the first step in an iterative process in which the top down system design is continuously modified as a function of the specific detail uncovered as the process proceeds. This paper describes the application of this process in the synthesis of the integrated cockpit for the Army Digital Avionic System (ADAS). The objective of the ADAS effort is to apply in-so-far as possible, the latest advances in digital system technology to a current production conventionally designed rotary wing aircraft. The aircraft chosen to demonstrate the application of this technology is the Army UH-60A Black Hawk, a twin engined utility helicopter manufactured by Sikorsky Aircraft. The steps taken in the development of both the system hardware and system architecture are explained in detail in reference 1. At this point in the process, a system design has been established and hardware is being fabricated which integrates the following aircraft control and/or display subsystems:

a) flight instruments

b) engine instruments

c) caution/warning/advisory

d) communication/navigation/identification and security devices

e) aircraft survivability equipment (ASE)

f) electrical system circuit breakers (67)

g) secondary systems such as: cargo hook, lights (position, anti-collision), air source switching, environmental control unit, anti-ice (engine, windshield), pitot heaters, blade de-ice, attitude and heading reference system, gyros, radar altimeter, engine ignition, tail rotor servo, back-up hydraulic pump, and the hydraulic leak test subsystem.

In addition, it became apparent during the design effort that incorporation of the checklist and emergency procedures would be an important feature of this system.

The Hardware Baseline

A standard UH-60A Black Hawk cockpit is shown in figure 1. Figure 2 shows the instrument panel in detail, figure 3 shows the lower console, and figure 4 the upper console. In addition, circuit breaker panels are located above each operator. An initial top down design for a digital avionic cockpit for the Black Hawk was performed by Sperry Flight Systems and Bell Helicopter (reference 1) after performing the analysis described in steps 1, 2, and 3 in the introduction. As details in the areas of the flight displays, paging and fault tolerance schemes evolved a cockpit

design emerged (step 4) with an instrument panel as shown in figure 5, a lower console as shown in figure 6, and an upper console as shown in figure 7.

The primary display elements on the instrument panel consist of four identical 6.8 inch by 6.8 inch CRT's each with eight line select keys on a side. A momentary toggle switch is located below each display. The main reasons for driving all of the primary displays to be exactly alike stems from both fault tolerance requirements and also the need for line select keys on the flight displays for a modest interactive capability. A cluster of standby instruments is contained in the center of the instrument panel for safety of flight purposes.

The lower console contains a control display unit for each operator by which all communication, navigation, and identification equipments are controlled and their status displayed, an intercom control for each operator, and a keyboard terminal unit (KTU) for each operator. In the center of the lower console for use by both operators are the stabilator controls, the automatic flight controls, and a miscellaneous control panel.

The upper control contains a number of switch functions which were not integrated for various reasons and a small (10 lights) caution/advisory panel which will be used prior to onboard auxiliary power unit (APU) start. After the APU is started, the ADAS system provides these caution/advisories.

The four CRT's are configured such that either a full screen display or half screen display can be exhibited. In normal operation the outer CRT's are reserved for the full screen flight display or full screen waypoint map. These displays can be called up by either operator or depressing the FLT DIS or MAP buttons in the OUTER column of the KTU (see figure 8).

The inner CRT's can be used either for two half screen displays or a full screen display. For interactive paging routines the lower half of the inner CRT will be the primary display. The two columns of buttons on the top left of the KTU call up the functions which will appear in the lower half (viz CAU - caution, EMGY - emergency procedures, ASE - airborne survivability equipment, CHK LST - checklist, SEC SYS - secondary systems). The top half of the inner CRT will normally be devoted to the ENG MON (engine monitor) half page. The inner CRT can also be used to display a full screen engine page (FULL ENG) or the waypoint map (MAP).

The momentary toggle located below each CRT is used for slewing through pages displayed on the lower half of the CRT. A down motion causes slewing through a set of pages (e.g., 1 of 4, 2 of 4, etc.). An up motion returns the display to the branch page one level higher.

A system block diagram is illustrated in figure 9.

The Flight Displays

One of the major tasks of the ADAS design effort was to synthesize a flight display which would serve as a primary source of both vertical and horizontal information for the pilot. In addition the display had to have the ability to display a master caution, warnings, and advisories.

The display shown in figure 10 meets the flight display information requirements for the ADAS. The display is interactive in that by pushing certain line select keys and entering numerics from the KTU the high/low bugs on the radar altitude scale can be set, barometric pressure or field elevation can be set, VOR course selected, and the navigation mode chosen. Some other features worth noting are:

a) VOR radial information is continuously displayed (if VOR tuned to a station),

b) magnetic bearing to an ADF station is continuously displayed (if ADF tuned),

c) ground track angle is continuously displayed on the heading scale when the doppler is operating,

d) both magnetic bearing to destination from current position and course information (either doppler or VOR) are displayed.

In all cases information is presented only if the specific subsystem is operating and the functional mode selected.

A full page Waypoint Map (figure 11) can be selected for viewing by either operator on either CRT (see KTU dedicated buttons, figure 8). A single heading up display on a 1:1 M scale with doppler waypoints shown is depicted. Waypoint ordering can be selected by depressing the line select key (lower left). All line connections are erased and a new waypoint order can be entered via the KTU.

Engine Displays

A full page engine display (figure 12) will be used during the engine start mode and is available for call up at any time by either operator on the inner CRT. Analogous to the "yellow" and "red" indications used in the standard Black Hawk, reverse video and flashing reverse video are used. Allowable time remaining in an "out of limits" condition is displayed as shown in figure 13.

During normal flight operation an engine monitor half page (figure 14) will be displayed on the top half of the inner CRT. RPM and engine torque are displayed continuously in both analog and

digital form (see reference 2). Allowable time remaining in an "out of limits" condition is displayed as shown in figure 15.

The Paging Scheme

The primary areas for interactive functions are the lower half of the inner CRT and the integrated avionics control display unit on the lower console. This latter control display is used for all functions associated with the communication, navigation, identification, and security equipments. Five dedicated buttons (plus one spare) on the left side of the KTU are used to access the major branches of the interactive pages. The dedicated buttons are:

1) CAU - caution

2) CHK LST - check list

3) EMGY - emergency procedures

4) SEC SYS - secondary systems

5) ASE - aircraft survivability equipment

A total of 370 interactive pages were generated to map the functions associated with the above into the ADAS architecture. The process used in synthesizing the pages required a detailed knowledge of each of the subsystems, the current operator functions as described in the operator's manual, and the level of integration of the electrical/control function into ADAS.

Rules of operation and the hardware configuration were first postulated. Then as the detailed pages were synthesized, these rules and the hardware configuration were refined to provide for cases which were exceptions. Each significant change required a complete page analyses iteration. During this process the system input/output was modified several times (both by additions and deletions). Only after this process was completed could realistic flow charting for the functional portion of the operational software begin.

A brief description of some of the features of the ADAS paging scheme are:

1) Caution

When the word "CAUTION" appears in reverse video on the flight display (outer CRT), the actual caution message(s) appear on the bottom of the inner CRT (in priority order if more than one). If the operator then depresses the caution button on the KTU or a button on the cyclic (during flight), the reverse video master caution message on the flight display is extinguished and the inner CRT displays a complete half page caution message. This message will include the emergency procedure associated with the caution and, for those functions which are controlled through ADAS, interactive control provided. If a detailed procedure may be required, access to the detailed procedure is also provided. Figure 16 illustrates a caution message where both the operator procedure and access to a detailed procedure are provided. If more than one caution occurs at the same time, the messages are arranged in priority order and accessed through the paging switch. Depressing the caution button when the master caution is not exhibited will bring up in priority order all outstanding cautions (if any) or the message "NO CAUTIONS."

In addition to the master reverse video caution on the flight display, there are five reverse video warnings (ENG 1 OUT, ENG 2 OUT, LOW RTR, FIRE, HYD). In the case of a warning situation, a half page warning message is automatically displayed on the lower half of the inner CRT. There are twelve (12) warning pages to cover the various warnings and combinations of warnings. An example of a warning message with interactive capability and access to a detailed procedure is shown in figure 17.

2) Checklist

Checklist automation is accomplished in the ADAS by a series of messages which require yes (or OK) or no as operator response. The yes response (the looked for response) can always be given by depressing the left top line select (lower half inner CRT) or when on the ground a cyclic button. The ADAS checklist is divided into eight (8) branches as shown in figure 18. At system initiation (APU start), ADAS is automatically initialized to the first line of the Before Start sequence. As shown in figure 19, if the checklist requires an action normally accomplished through ADAS, the specific interactive page on which the action is accomplished is automatically displayed on the top half of the inner CRT. The checklist continues to sequence through to the end of the Before Takeoff sequence automatically. If the operator desires a detailed procedure (see figure 20), branching to the specific detailed procedure can be accomplished by depressing the line select opposite the > symbol.

3) Emergency procedures

Ninety-nine (99) pages of emergency procedures are contained in the ADAS. All can be accessed by depressing the emergency button and paging to the specific procedure. The primary purpose for this major branch is to allow the operators to gain familiarity with the ADAS version of the emergency procedures. In all cases, these procedures will appear either automatically in the case of warnings or with the caution message. In the case of a failure in the caution/warning sensors, this branch does provide a means for accessing the necessary emergency procedure if the operators ascertain the fault condition in another manner.

4) Secondary systems

Depressing the SEC SYS button on the KTU brings up a menu page which provides access to the control functions of eighteen (18) subsystems. An example of a secondary system page is shown in figure 21.

5) Aircraft survivability equipment

Depressing the ASE button, the KTU brings up a menu page which provides access to the survivability equipments on board the aircraft.

Future Plans

Functional verification of the ADAS cockpit is scheduled to take place during the first half of next year in the Tactical Avionics System Simulator (TASS) at Fort Monmouth. A complete dynamic system simulation will be performed by tying the ADAS 1553 data bus to a data bus port on a PDP 1145. Support software which simulates all the multiplex remote terminal units will be used.

After functional verification in the TASS, the system will be flight tested in the Avionics Laboratory System Test Bed for Avionics Research (STAR), a UH-60A.

Conclusions

Synthesis of an integrated cockpit management system requires an iterative multidisciplined process in which initial conceptual system design is continuously modified by the effects of the specifics of the system being addressed. This process does not end with fabrication of the system hardware but must be continued through carefully designed simulation and flight experiments. In addition, the system must possess the flexibility to incorporate changes in procedures (e.g., updated emergency procedures) which will occur during the system life cycle.

References

1. Dasaro, J. A., Elliott, C. T., *"Integration of Controls and Displays in U.S. Army Helicopter Cockpits,"* Proceedings of 32nd NATO Guidance and Control Panel Symposium on The Impact of New Guidance and Control Systems on Military Aircraft Cockpit Design, Stuttgart Bad-Cannstatt, Germany, May 1981.

2. *"Electronic Master Monitor and Display System, Human Engineering Summary Report,"* AVRADCOM Technical Report 79-0270-3, Aircraft Equipment Division, General Electric Company, Binghamton, New York, June 1981.

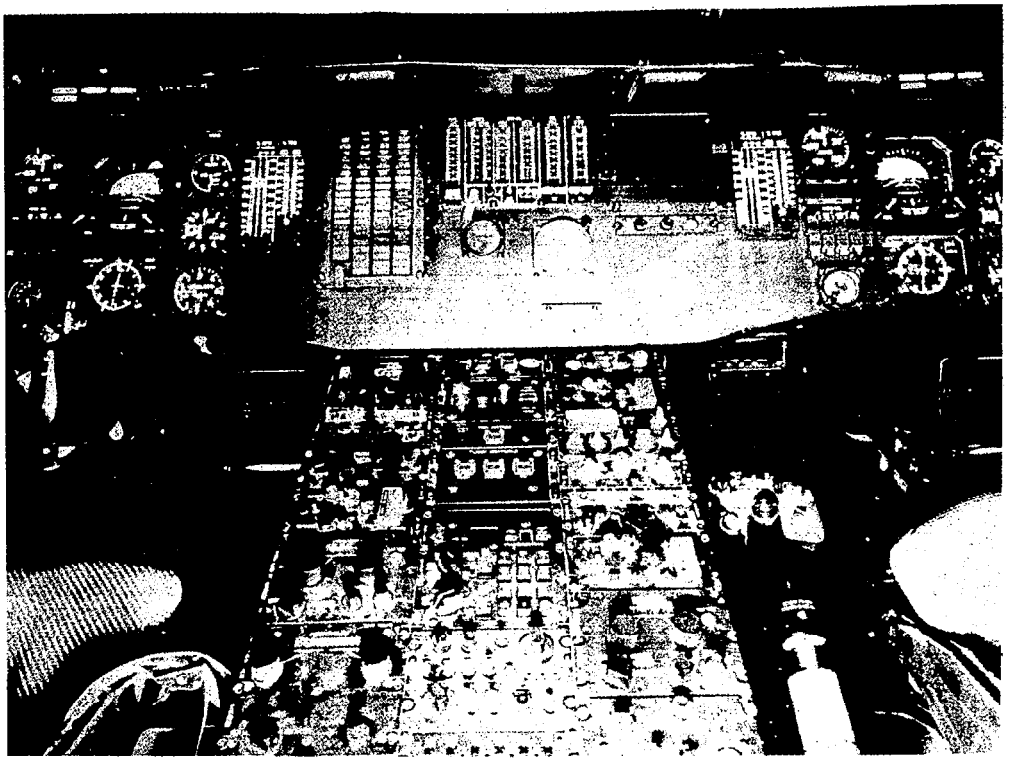

Fig. 1. UH-60A cockpit.

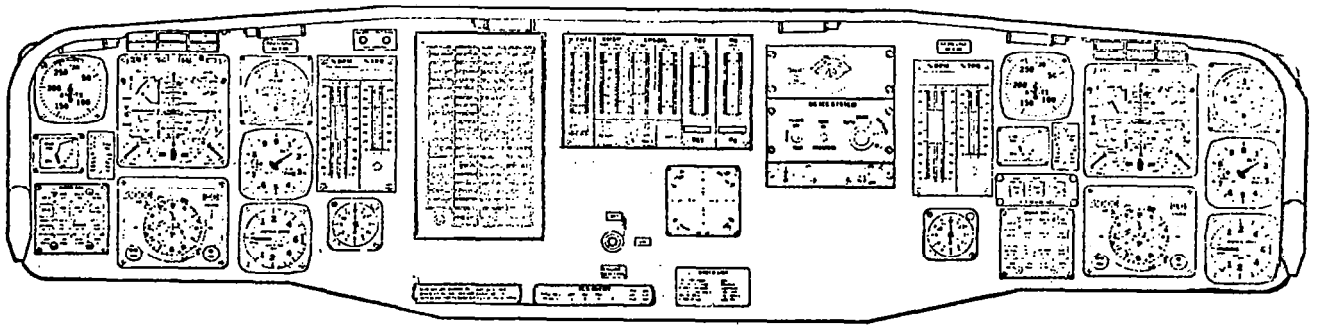

Fig. 2. UH-60A instrument panel.

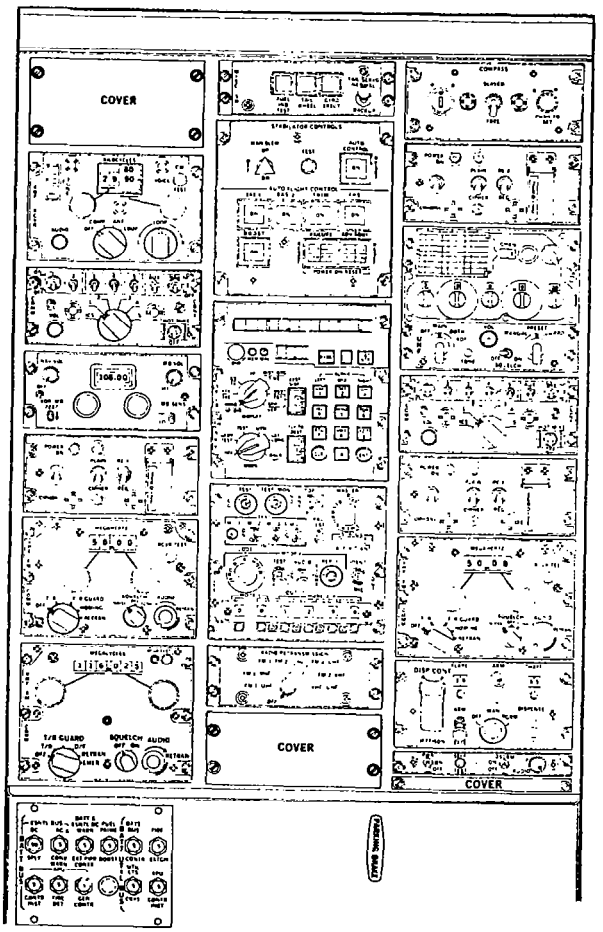

Fig. 3. UH-60A lower console.

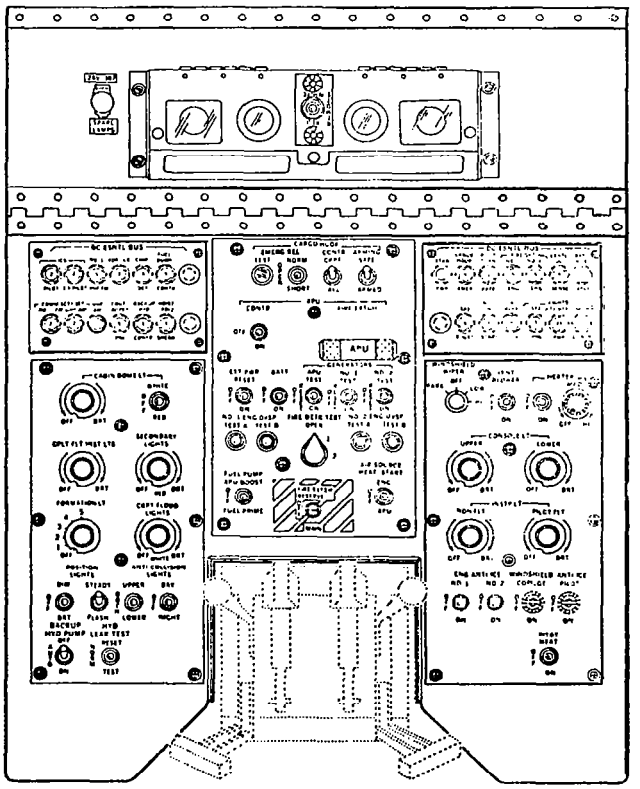

Fig. 4. UH-60A upper (overhead) console.

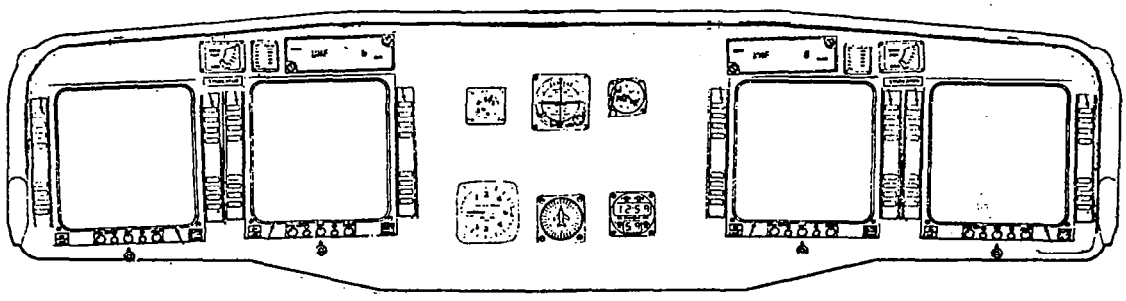

Fig. 5. ADAS instrument panel.

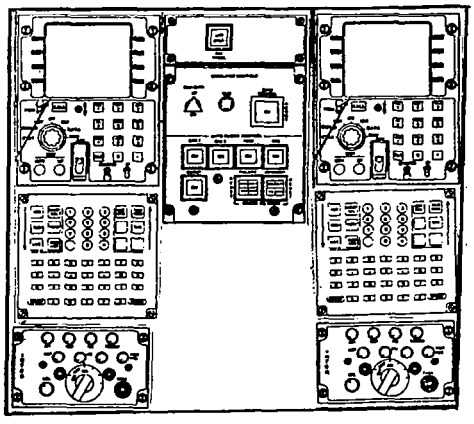

Fig. 6. ADAS lower console.

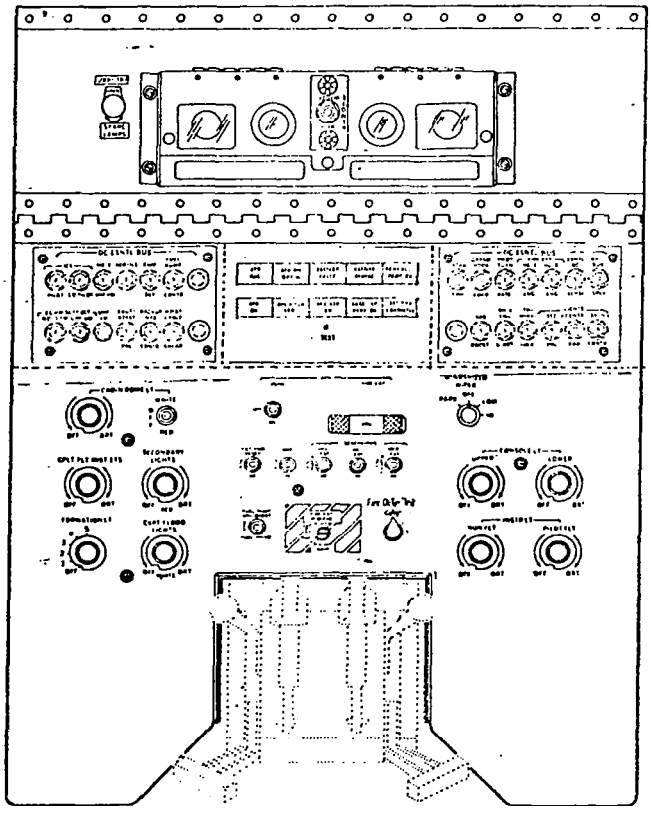

Fig. 7. ADAS upper (overhead) console.

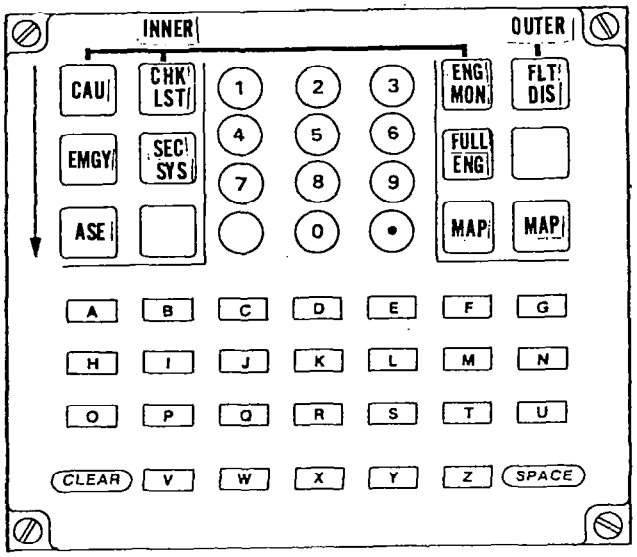

Fig. 8. Keyboard terminal unit (KTU).

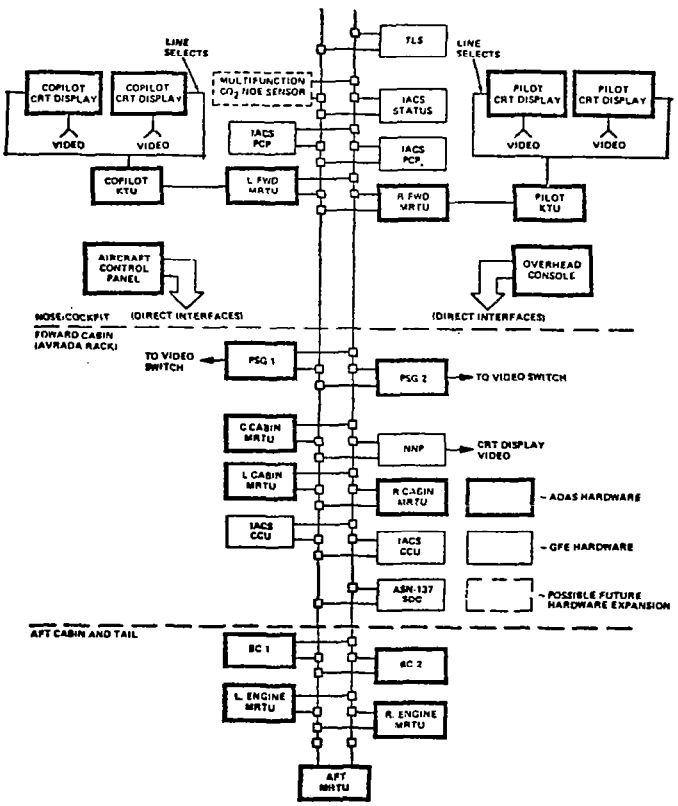

Fig. 9. ADAS system block diagram.

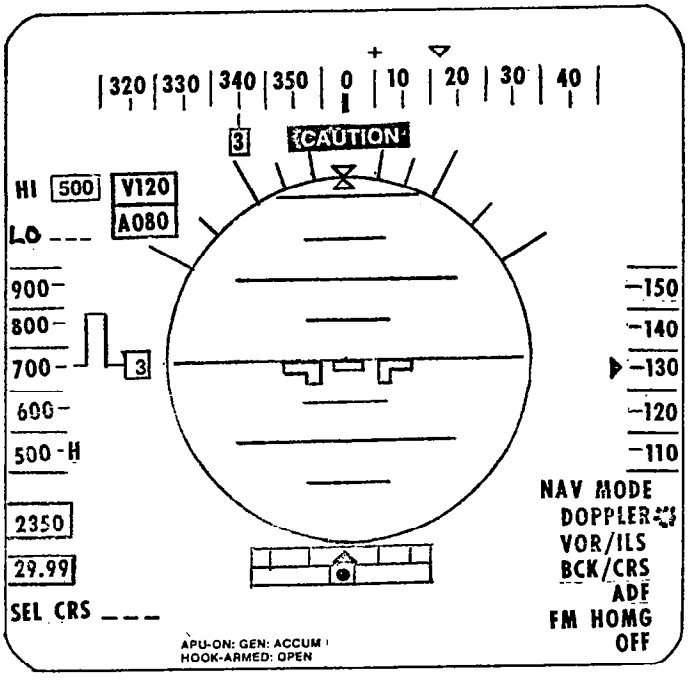

Fig. 10. ADAS flight display.

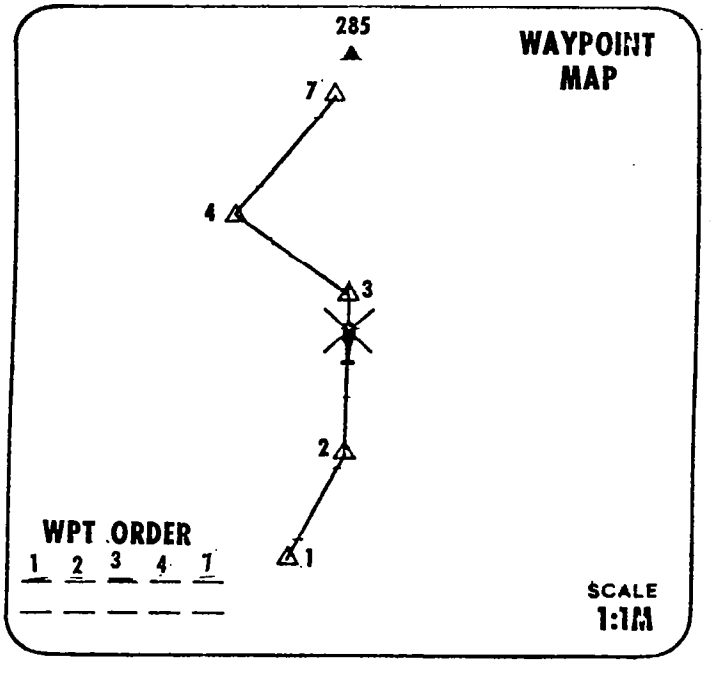

Fig. 11. ADAS waypoint map.

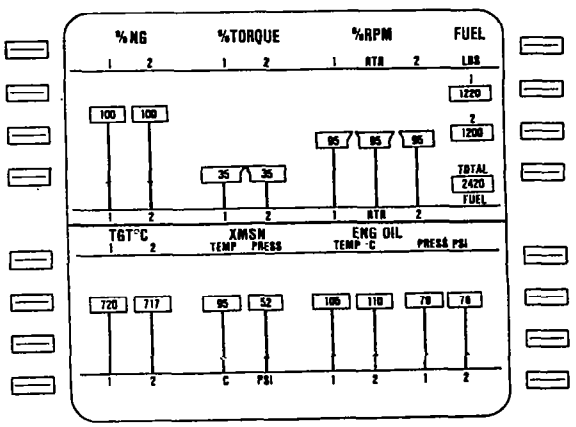

Fig. 12. Engine display (full page).

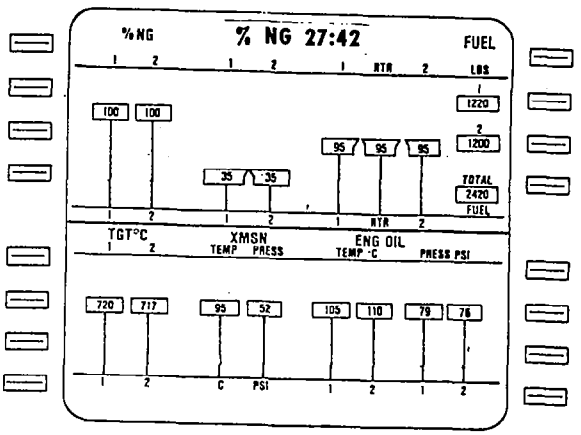

Fig. 13. Engine display without of limits condition.

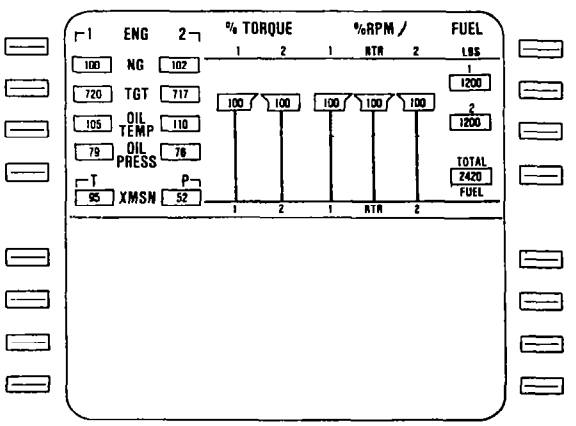

Fig. 14. Engine monitor (half page).

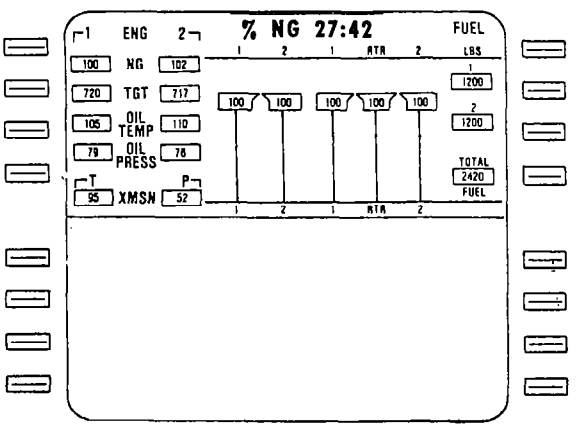

Fig. 15. Engine monitor without of limits condition.

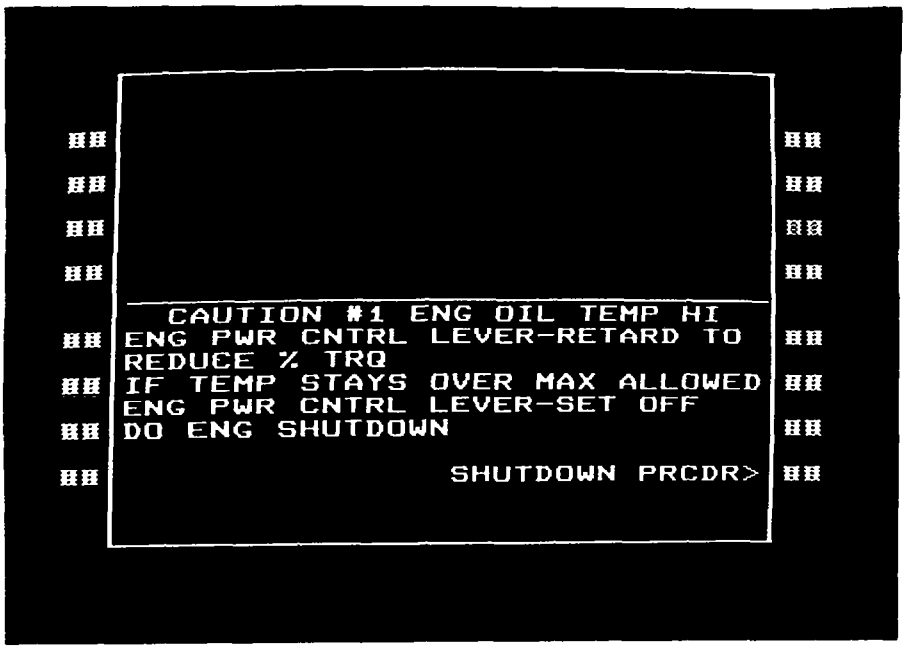

Figure 16. Caution page example.

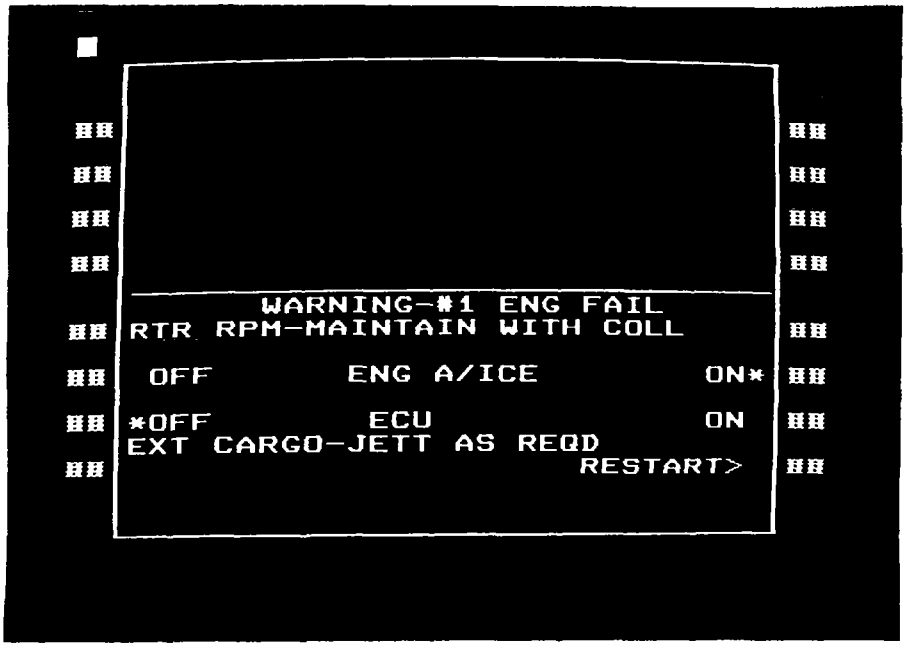

Figure 17. Warning page example.

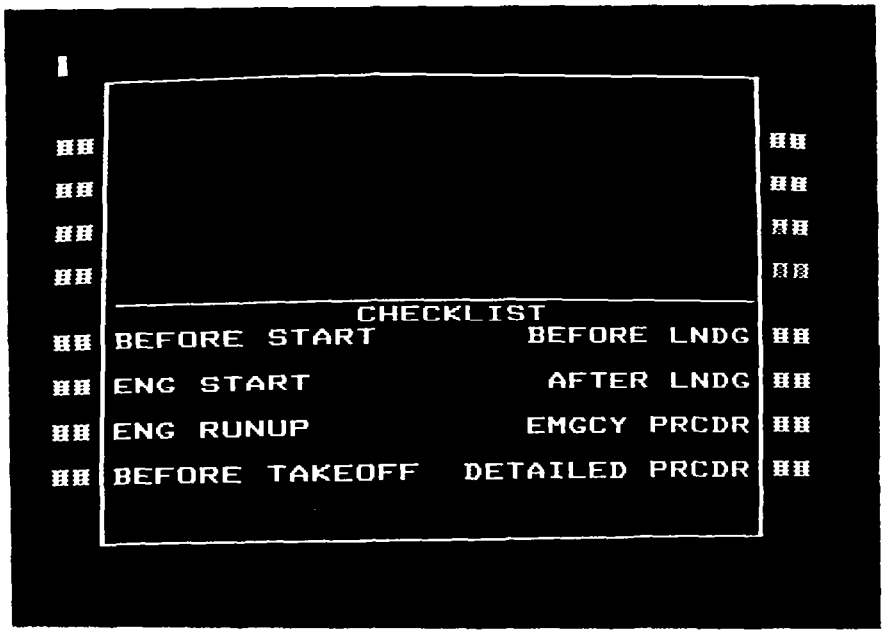

Fig. 18. Checklist (top page).

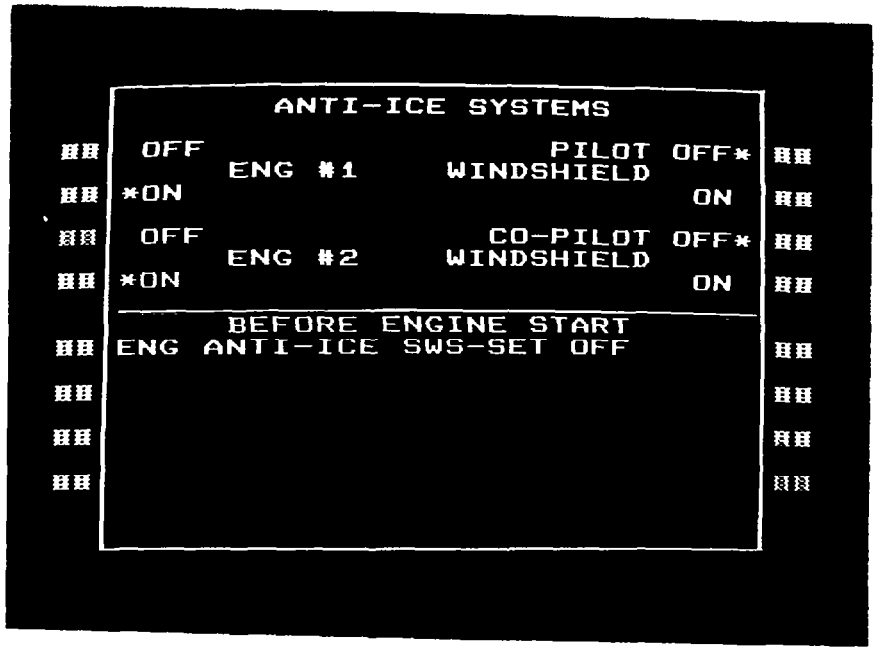

Fig. 19. Checklist example 1.

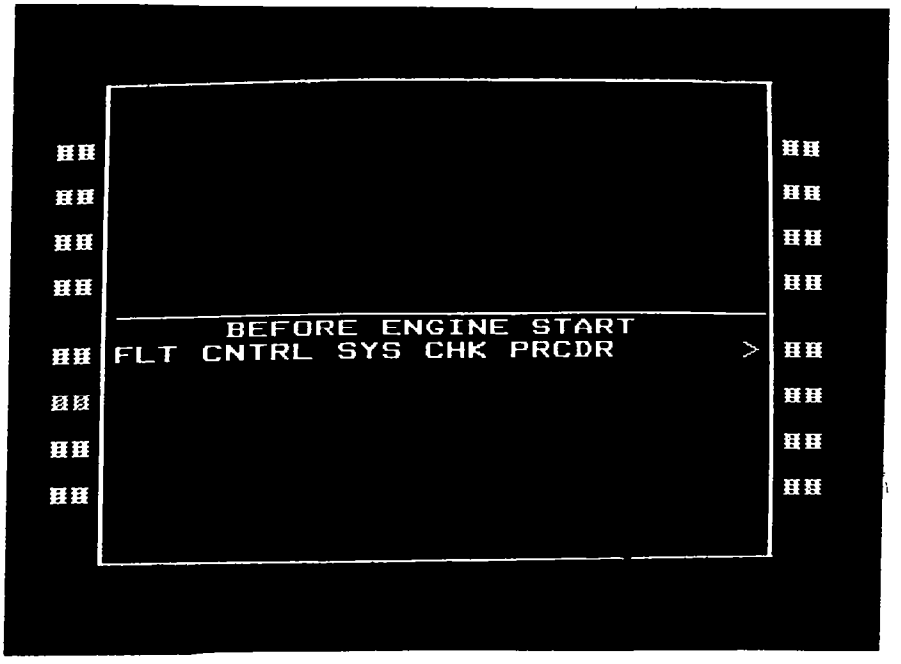

Fig. 20. Checklist example 2.

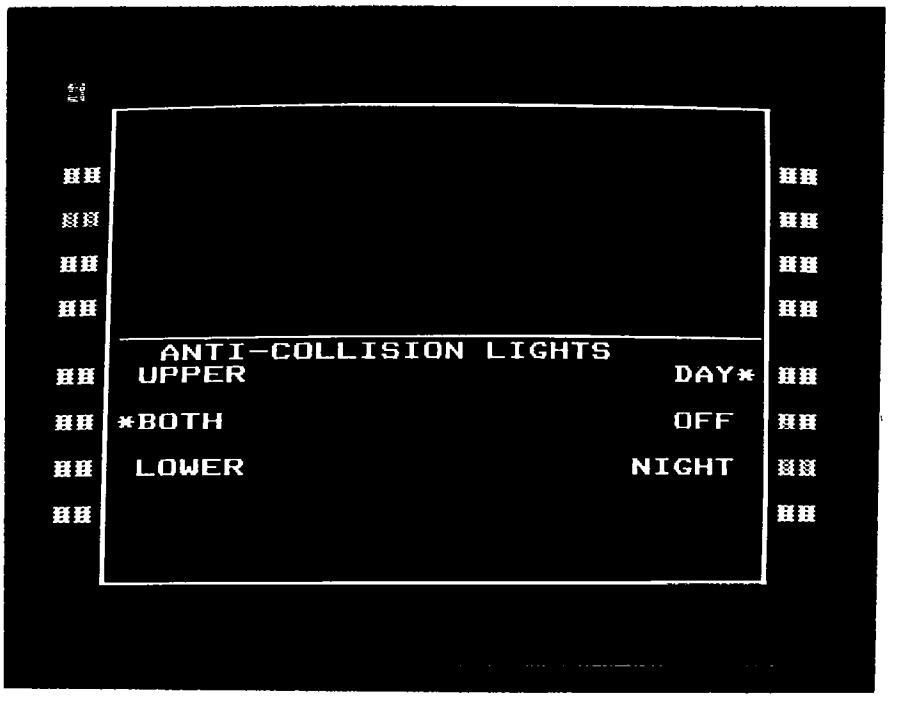

Fig. 21. Secondary system page example.

THE ROLE OF VOICE TECHNOLOGY IN ADVANCED HELICOPTER COCKPITS

Howard P. Harper
Senior Human Factors Engineer
Sikorsky Aircraft Division, United Technologies Corporation
Stratford, Connecticut

Abstract

This paper describes the status of voice output and voice recognition technology in relation to helicopter cockpit applications. The maturing of this technology provides many opportunities for new approaches to crew workload reduction. The paper covers the helicopter operating environment, potential application areas and the impact on advanced cockpit design.

Introduction

Utilizing increasingly more sophisticated and complex on-board systems, helicopter crews will be required during the conduct of missions to perform multiple tasks which include monitoring aircraft systems, monitoring and initiating communications, navigation, target detection, air-to-air attack/coordination, active/passive defense against radar, laser and infared air- and ground-based detectors and designators, obstacle detection and avoidance, and monitoring mission-specific subsystems.

In many cases the crews will be required to perform such tasks in an all-weather, night, nap-of-the-earth environment that demands out-of-the-cockpit visual attention and hands-on-stick control readiness. As a result of this increased task loading crew work load is approaching its maximum limit. In cockpit concepts where a single man crew is envisioned, this limit clearly will be exceeded unless a new technological approach is found. Computer voice interaction is one such approach. This paper reviews that technology and considers how it might be applied to solving some of the workload problems.

After reviewing the progress in this area it is apparent that now is an opportune time to seriously investigate cockpit applications. There are two aspects to voice technology: voice output and voice recognition. Both are currently being applied in aviation and elsewhere. In the voice output area applications range from toys and home appliances to sophisticated text-to-speech processors. The uses of voice recognition systems are not yet as wide spread but many applications are currently in full operational use. For example, they are in use for assembly line quality control and in post office mail sorting. Development of a voice input typewriter is the subject of major research efforts at several companies.

Voice Output

Techniques for producing voice output range from electro-mechanical recorders to digital sampling and storage to more sophisticated digital storage techniques such as linear predictive coding (LPC). Each of these methods has advantages and disadvantages which will be reviewed in the following paragraphs.

The best example of the use of a recorder based voice output system is the ASH-19 voice warning system used in a number of military aircraft including the CH-54 Flying Crane. Feedback from operational units has indicated that the system has functioned well over its twenty year life. It does, however, suffer from some of the reliability problems which one would expect from a complex electro-mechanical system designed in the 1950's. One drawback in an electro-mechanical system is the variation in access time to words due to positioning the playback head to the location of the next desired word.

The second technique for voice output is the use of digitally sampled and recorded voice signals. The method is simply analog to digital conversion of the speech signal and usually involves storage in read only memory (ROM). The resulting voice quality can be excellent, but depends largely on the sampling rate and encoding precision. A minimum of about 15,000 bits of storage is typically required per second of speech. The access time to words is extremely fast and as a result messages made up of strings of individually recorded words can be put together in a satisfactory manner.

Linear predictive coding was developed primarily to reduce the data storage requirements for voice output systems. This is the technique used by Texas Instruments in their "Speak 'N Spell" teaching system and in a series of chips designed to be incorporated into a variety of other applications. This technique allows storage of one second of speech with about 3,000 bits of digital memory. The result of the data compression is some loss in intelligibility when compared with a digitally sampled system. Standard vocabularies are available but special vocabularies must be processed by the manufacturer.

There are other systems available which are even more economical in terms of data storage

requirements. These may truly be called speech synthesizers because there is no recording and playback of a human voice. The speech is built up of phonemes which are the basic elements of speech sound. Using around 40 of these basic sounds along with the capability to vary pitch, intensity and timing, a synthesizer can produce understandable speech. The resulting speech has a robotic quality, but storage requirements are only about 80 bits per second of speech. While initially not as intelligible as the speech produced by other systems, it improves greatly with training and continued exposure.

The technology does exist now for the use of voice output in the cockpit environment. Considering this it would now be difficult to justify continuing the use of tone combinations as the primary auditory warning system. Defining a system will require a choice among the voice output technologies described above. Reliability considerations will probably rule out the electro-mechanical recorder. If voice quality is the primary criterion the pure digital sample and store system will likely be judged best. If, however, a large vocabulary is required one of the data compression techniques may be necessary. If a virtually unlimited vocabulary is required, as might be the case if the system were called on to output the emergency procedures now found in the flight manual, then a phoneme based system is the only practical choice.

Voice Recognition

Computer recognition of a speech input is a much more challenging problem than the production of a voice output. A variety of techniques have been used. The specific method depends on a number of variables: the size of the vocabulary, the necessary level of recognition accuracy, the number of users, the need for isolated word or continuous recognition, the time available for training of the system, and the environment in which the recognizer must be operated.

A typical isolated word recognizer works by having the user say all of the words in the vocabulary one or more times to train the system. During this process the voice signal is analyzed by a bank of filters which measure the amount of energy in a number of frequency bands. Each word is broken down into a number of equal temporal parts and the filter bank outputs for each are stored. This creates a template against which incoming words are tested. The computer finds the best match for the incoming word and carries out the appropriate action assigned to that word. There are at least ten recognizers on the commercial market today. Each claims 99% plus recognition accuracy and it probably is true that under some specific set of conditions that claim can be met. It is unlikely, however, that any of them will approach that accuracy in a military helicopter cockpit.

Current Research

Voice technology has generated a great deal of interest both commercially and in the government. Many companies are carrying out research and development activities directed toward military applications of both voice input and output tehnology. All branches of the military as well as NASA and the FAA have research programs in this area. There have been several conferences dealing with coordination of this work, the most recent sponsored by the Naval Air Development Center in Warminster, Pennsylvania.

The Navy has, perhaps, the longest history of military applications of this technology. They have demonstrated its usefulness in performing cockpit switching functions and in the more complex man-machine interactions of an airborne anti-submarine warfare system. NADC currently has a study under way to understand and define the problems of the Navy aircraft cockpit operating environment. This includes the effects of jet aircraft cockpit noise and the effects of G loading on the physiology of speech. This study relates primarily to the fixed-wing environment.

The Air Force is currently sponsoring a study directed toward flying a prototype voice interactive system in the F-16. This program is being conducted jointly by Lear Siegler Inc. and General Dynamics and is expected to fly this year. In the development program, progress has been made toward accommodating the unit to the jet aircraft cockpit environment. This has included dealing with problems such as the effects of the oxygen mask on speech recognition.

Helicopter Research

There are may differences in the mission and the operating environment of helicopters and fixed-wing aircraft that will have an important effect on the usefulness of voice interactive technology in the cockpit. First the missions are markedly different. The helicopter night, nap-of-the-earth, all-weather scenario imposes long duration, high workload conditions on the crew. Attention must be fixed outside the cockpit and for long periods hands cannot be taken off of primary flight controls. These conditions are often sustained for the major portion of the mission. On the other hand, fixed-wing aircraft have periods during the mission where workload is very high but these are generally of a much shorter duration.

Another factor differentiating the helicopter from the fixed-wing aircraft is the crew station environment. There are primarily two characteristics which contribute to this difference. The first is cockpit noise. Figure 1 shows typical spectra for the two aircraft types. This clearly shows the difference in frequency content. Much more energy occurs in the speech frequencies in the helicopter. The second aspect is the modulation of the voice due to cockpit vibration. This effect is shown in Figure 2 by noting the

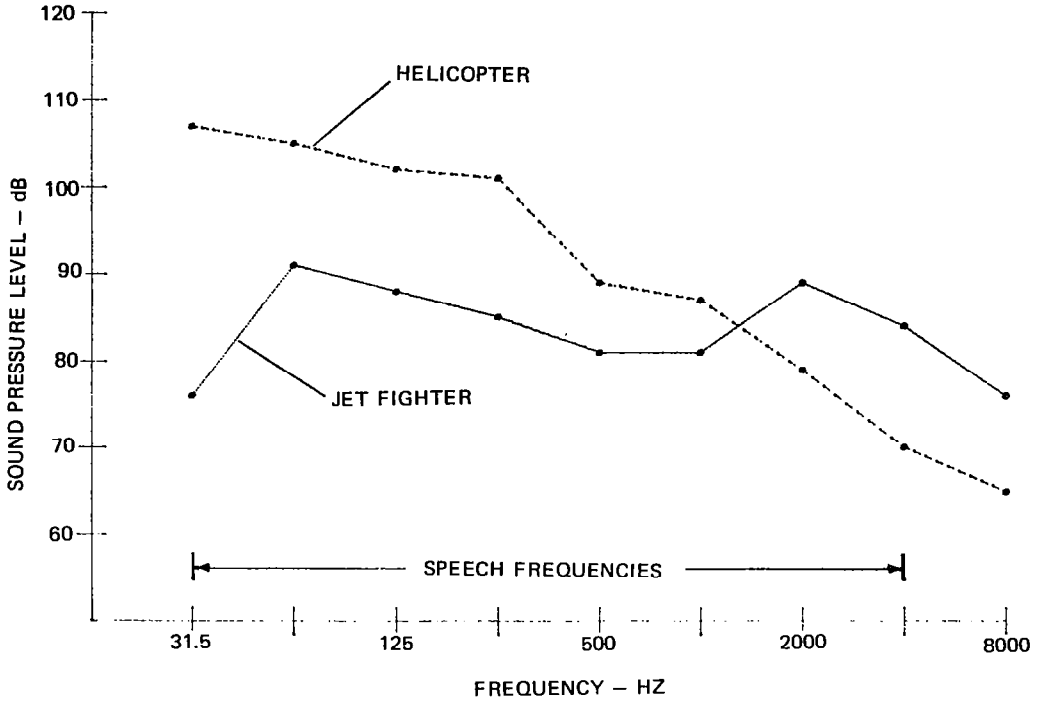

Figure 1. Cockpit Noise Spectral Differences for a Typical Military Helicopter, and a Jet Fighter

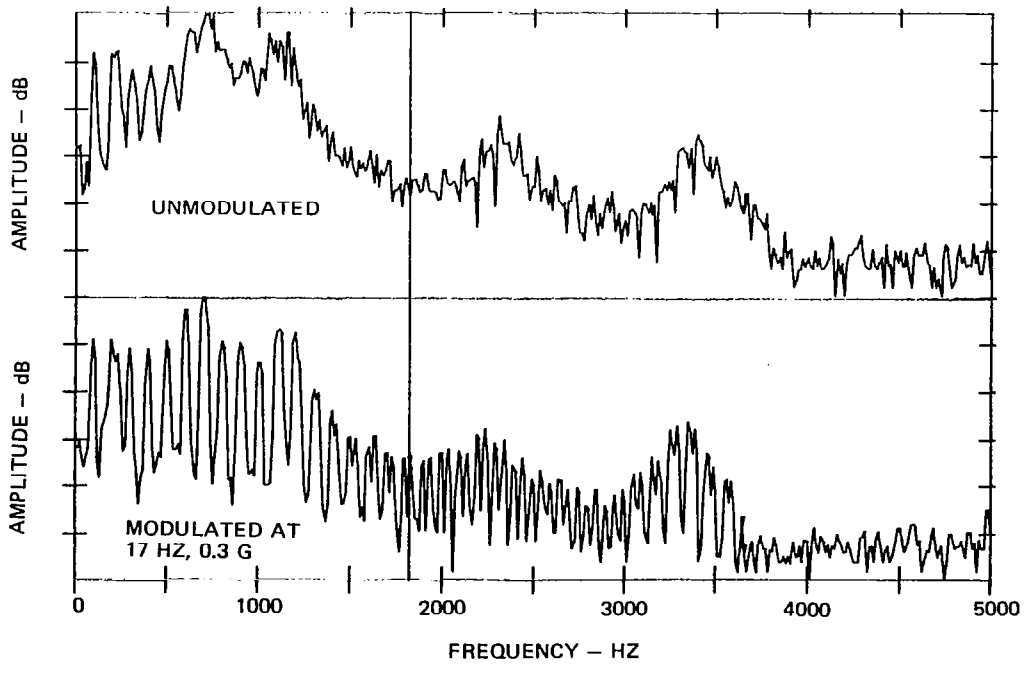

Figure 2. Modulation of a Speech Sound Due to Whole Body Vibration

difference between the voice spectra under conditions of vibration and no vibration. As might be expected, a system trained under one set of noise and vibration conditions and asked to recognize under other conditions may perform unreliably.

Helicopter cockpit-related voice technology research is currently going on at NASA Ames Research Center and at the U.S. Army Avionics Research Facility at Ft. Monmouth, N.J. The Ames facility has a long record of voice related research work. References 1 and 2 are Ames-sponsored studies relating to the cockpit use of synthetic voice warning concepts. More recent work has addressed problems of the voice recognizer in the helicopter's noise and vibration environment. The results are extremely encouraging. Even under the most adverse conditions, voice data entry compares favorably with keyboard entry. Accuracy differences never exceeded 2%. These results clearly establish the feasibility of using voice recognition in rotary-wing aircraft. In a second study currently underway, a commercial voice recognizer is being used to control an aircraft performance computer. This study is beginning to contribute information on the problems of using this equipment to perform a real function in a present day helicopter. The Army at Ft. Monmouth has taken the lead in military helicopter voice-related research. At present they are studying the noise environment of their inventory of helicopters to define the effects on the performance of currently available recognizers. Their plans call for implementation of a voice interactive system to become part of the advanced digital avionics system to be flown on a UH-60A.

Pragmatically we have to recognize that a military helicopter is far from the ideal location for a voice recognizer but, because of the work done at Ames and elsewhere, we can be reasonably certain that the problems can be solved. Therefore it should become our purpose to let the manufacturers of this equipment know that we are interested, that we can see many potential applications, and that there is a market in the helicopter industry. Furthermore we should define the operating environment so that they can do the necessary development to make equipment that will function adequately in our cockpits. Alternatively they may tell us what has to be done to our environment to make the equipment work. We will then have to address the problem of whether the value of a voice interactive system warrants the cost of an improved cockpit environment. This will provide parallel pathways for the solution of the operating environment problem and development of applications which make maximum use of the technology to reduce cockpit work.

Helicopter Applications

The following are some of the thoughts which must go into the preliminary design effort to specify the requirements for a voice interactive system for a rotary wing aircraft. This process is needed to determine whether the time and expense of doing a complete and detailed systems and human engineering analysis is warranted.

First it is necessary to list the assumptions on which the system design will be based: 1) the availability of a speech recognizer with 100 word vocabulary with the capability of training by two users and having a demonstrated accuracy of 95 to 99.9 percent under all flight conditions; 2) a voice output device with a demonstrated intelligibility at least as good as current inter-communications systems.

Ideally this preliminary design effort would take place after the completion of a detailed analytical study of all the man-machine interactions. The results would allow evaluation of the workload reduction quantitatively and allow the desginer to investigate the effects of design variables on the performance and usability of the system. The time to do such an analysis is before starting a design effort for a specific application. In the heat of a design effort the system designers cannot wait for the results of such an effort.

One of the design concepts planned is the use of the "intelligent copilot" model. All candidate voice interactive functions are evaluated in terms of whether they are consistent with the behavior of a hypothetical copilot who knows when to talk, when to listen and who prioritizes information in a logical way that is appropriate to the mission phase. A second design concept is that the system will provide feedback on all inputs and will require secondary verification of the more critical items. If, for example, the pilot were to say "Jettison Tank" the system might respond visually or orally: "Tank Jettison Requested" and the pilot would be required to confirm the request by giving an action command. Thirdly, all voice inputs are backed up with a manual entry mode which would be considered a secondary operational mode and, therefore, might require a deeper level of paging. The fourth concept is the use of a switch on the pilot and copilot cyclic grip which he will press to indicate that he is talking to the recognizer. Lastly the training of the recognizer will not be done on the aircraft, it will have been done earlier and stored on a cassette or in a ROM cartridge which can be plugged into the aircraft for a rapid data transfer.

The voice output must be unusual enough to be easily distinguished from other crewmen or air traffic controllers. This is not meant to imply that a robotic voice is required, however the voice must stand out clearly from the routine voice communication traffic. The major difficulty with robotic quality voice is that people have trouble taking it seriously and this effects its acceptability to pilots.

Next we will look at each of the various systems on the aircraft and try to understand where voice input and output technology might fit into operation of that system.

Communication

In the area of communications we will include radios for air-to-ground, air-to-air, and data links; and systems for communication within the aircraft. The functions which must be performed with this equipment include tuning, selection of the system, keying, and volume/squelch control. Tuning is a function which is particularly adaptable to a voice recognition system. The pilot might say "Tune VHF 122.7" or "Tune VHF Channel 5". Selection also fits in well with a recognizer system. The pilot would say "Select UHF" and subsequent transmissions would be made on the UHF radio. The use of voice to control volume, squelch, or keying does not seem to be practical because the voice command would interfere with the material being sent. On the voice output side, it seems possible that voice synthesis may be used to reconstruct messages encoded digitally and sent to the aircraft from the ground via a data link.

Navigation

Control and operation of navigation equipment offer opportunities where both voice input and voice output would be very effective in workload reduction. The systems which might be controlled are the doppler/inertial navigation system, Tacan, VOR/DME and ADF. The functions of this equipment are to provide: current position, steering information in X, Y, and Z coordinates, the map situation in terms of the relationship of current position to other geographical information, system updates and acceptance of flight planning inputs such as way point locations. These functions for the most part, are adaptable to voice interactive techniques. For example, current position might be called up with the voice input "Position". The system might respond in map coordinates or in terms of bearing and distance to a known point. Steering information could be requested and provided verbally. For example the pilot might ask for "Directions Waypoint 3" and the system would respond "325 Degrees, 2 Miles". Map situational information could be of the following types: request for nearest fuel or request for height and location of highest terrain in the area. Navigational system updates could easily be accomplished verbally; the pilot saying "Update Waypoint 3...Mark" when directly over the point. In addition the flight could be planned using a verbally prompted waypoint entry routine.

Flight Controls

The primary flight control system would not be directly interfaced with the voice recognizer, but system faults would trigger appropriate verbal messages. In the automatic flight control system (AFCS) there are a number of functions which can be considered for integration with a voice interactive system. These include system turn-on, function selection, monitoring of performance, response to problems, and system shut-down. The AFCS initiate and shut-down functions are best reserved for manual action since they generally occur before and after the crew workload is at its highest. The selection of AFCS functions is a good candidate for voice actuation. Here such functions as airspeed hold, altitude hold, heading hold, or approach to hover might be selected through inputs to the voice recognizer. This is one case where a very positive feedback system would be required. A secondary command would be required prior ro the initiation of any of these functions. The pilot would say "Hold Heading" and the system would respond "Heading Hold Requested". The pilot, after seeing that the system understood his input, would give an action command such as "Do It". Had the feedback been incorrect the pilot would cancel the input and try again verbally or, at his option, engage it manually. Voice output could be used effectively to provide the pilot with information on the status of the system.

Subsystems

The engine, fuel, APU, hydraulics, electrical, anti-ice and transmission subsystems might make use of voice. The possible crew functions would include system start, condition monitoring, system control, malfunction response and system shutdown. A specific engine parameter which is a very possible candidate for voice monitoring is power available. Information about power margin has a high priority at times when the pilot's attention is outside the aircraft and both hands are on the controls. The pilot might say "Power" and the system would respond with a voice message "10% Torque Remaining". Contingency power selection is a mode which allows pulling additional power from one engine when the other experiences a power loss. This selection must be set up quickly at a time when the pilot would be very reluctant to remove either hand from the controls. In the fuel system there are a number of possibilities. Voice requests could be made for fuel status with the system responding in pounds of fuel remaining or in terms of flight time remaining at the current flight condition. In addition to the low fuel warning normally provided, a programmable voice system could be used to provide a warning at any fuel state or time remaining selected by the pilot. The APU could be started and shut down by voice command but since this is generally a ground function where workload is not critical it would not be worth implementing in the voice system. Aircraft lighting is an area where a recognizer could be particularly effective. Lighting controls are numerous and frequently accessed. The voice system could select, actuate and control both interior and exterior lighting systems. In addition the voice recognizer could be used to select various sub-

system status monitor modes such as engine instruments, electrical or hydraulic parameters, or emergency procedures as suggested in Reference 3. Voice interaction with the remaining subsystems would be limited to voice messages related to malfunctions.

Caution, Warning, Advisory

The information provided to the crew by the caution, warning and advisory systems is potentially convertible to a voice output system. Those messages which are currently supplemented with an alerting tone pattern should be replaced with a voice message. With voice technology available pilots should not have to identify a failure by the pattern of tones in the alerting signal. It seems apparent that voice might become the primary alerting system for all of the warning messages and for the more critical of the caution messages. This would allow replacement of the current matrix of dedicated caution lights with a three or four line prioritized display. This type of alerting system will require some new thought because of the single dimensional quality of the auditory channel. Two messages cannot be presented simultaneously; all inputs are sequential rather than parallel. All possible messages must have a priority value which determines the order of their presentation. To complicate matters further these priorities may have to change with mission and phase within the mission.

Two recent studies (References 4 and 5) have presented conflicting data on the value of using voice warning to supplement the visual alerting system. Reference 4 found no important difference in the time required to respond various combinations of voice, tones and visual signals in a jet transport simulator. The author explains that this is because the pilots always checked the voice message against the visual caution panel before responding. The study reported in Reference 5 investigated the pilot reaction times from the presentation of a voice or light warning while flying nap-of-the-earth in a helicopter. In this case there was a dramatic improvement in response time with the voice system. It was found in this study that the pilots were willing to respond without confirming the malfunction on the caution panel because it took approximately 3 seconds to stabilize the flight path of the helicopter sufficiently to look inside. This is further indication that the helicopter and fixed-wing aircraft may require significantly different approaches to integration of cockpit voice technology.

There are several possible uses for voice input to the alerting system. One would be to acknowledge messages instead of pressing the master caution capsule to indicate recognition of the message. Another function might be to change caution priorities. If, for example, a particular system was operating marginally the pilot might want to raise its caution priority to the top of the list.

Cockpit Impact

Table I summarizes the possible voice system applications discussed in the last paragraphs. This is an exercise to identify what could be done. It is important to emphasize that the next logical step would be a thorough analysis of the functions reuqired by the mission to determine a reasonable design solution.

The single place cockpit is the application where the need for an "intelligent copilot" is greatest. The recognizer/synthesizer will be required to take over many of the functions normally assigned to the second cockpit crewman. A single place helicopter cockpit which includes a voice interactive system is shown in Figure 3. The physical impact of the voice system is not dramatic. The only special control is the switch on the cyclic to key the recognizer. In addition, the ROM cartridge with the pilot's voice characteristics is inserted in a slot. The remainder of the displays and controls will only differ slightly from a non-voice cockpit since manual and visual backups will probably be provided for the voice functions.

The major improvements will be in the pilot's ability to keep his hands on the controls during critical flight phases, and in his capability for being fully informed on aircraft system status without bringing his eyes inside the cockpit. The concept that the recognition system will respond to simple commands will eliminate the component workload associated with finding and actuating a manual control. The use of voice actuation facilitates the use of multifunction manual controls and thus reduces cockpit space requirements to some extent.

It should be further emphasized that voice cannot be successfully introfuced to cockpits on a piecemeal basis. We are beginning to see various individual systems such as ground proximity warning systems and altimeters with voice output capability. This is manageable now, but further poliferiation of voice systems could become chaotic. The full benefits will only be achieved by an integrated approach.

The design of a voice interactive cockpit system requires an appreciation of the single channel nature of the auditory system. With visual displays the designer can put up a great deal of information at one time in the hope that the pilot can pick out what he needs for a particular task. With a voice system, sequencing and prioritizing of inputs and outputs is necessary since only one thing can be going on at any time.

Conclusions

The following conclusions can be drawn from this investigation of helicopter cockpit voice interactive technology:

1) Voice output technology is available for use now.

2) Research results look very favorable for the development of an accurate, reliable voice recognition system for helicopters.

3) There are many possible voice interaction applications which will result in workload reduction.

4) A thorough systems and function analysis is required to maximize benefits and to be sure that the system is acceptable to crewmen.

References

1. Simpson, C. A. and Williams, D. H., "Human Factors Research Problems in Electronic Voice Warning System Design", NASA TM X 62,464, 1975.

2. Simpson, C. A., "Synthesized Approach Callouts for Air Transport Operations", NASA Contractor Report 3300, 1980.

3. McGee, J. and Harper, H. P., "Advanced Subsystem Status Monitor, Sikorsky Aircraft", USAAVRADCOM Technical Report 80-D-5, U.S. Army Applied Technology Laboratory, Ft. Eustis, Va., 1980.

4. Wheale, J., "The Speed of Response to Synthesized Voice Messages", AGARD-CP-311, 1981.

5. Reineck, M., "Voice Warning Systems: Some Experimental Evidence Concerning Applications", AGARD-CP-311, 1981.

TABLE I. POSSIBLE COCKPIT VOICE APPLICATIONS

SYSTEM	INPUT	OUTPUT
COMMUNICATION	TUNING RADIO SELECTION	DIGITAL MESSAGE RECONSTRUCTION
NAVIGATION	POSITION REQUEST STEERING REQUEST MAP INFORMATION REQUEST POSITION UPDATE	POSITION REPORT STEERING INFORMATION MAP INFORMATION
FLIGHT CONTROLS	FUNCTION SELECTION ACTION COMMAND	FEEDBACK
SUBSYSTEMS	POWER INFORMATION REQRS. SELECT CONTINGENCY POWER REQUEST FUEL STATUS LIGHTING CONTROL SELECT DISPLAY MODE	POWER INFORMATION FUEL STATUS
CAUTION, WARNING, ADVISORY	PRIORITY SELECTION	PRIMARY ALERTING SYSTEM

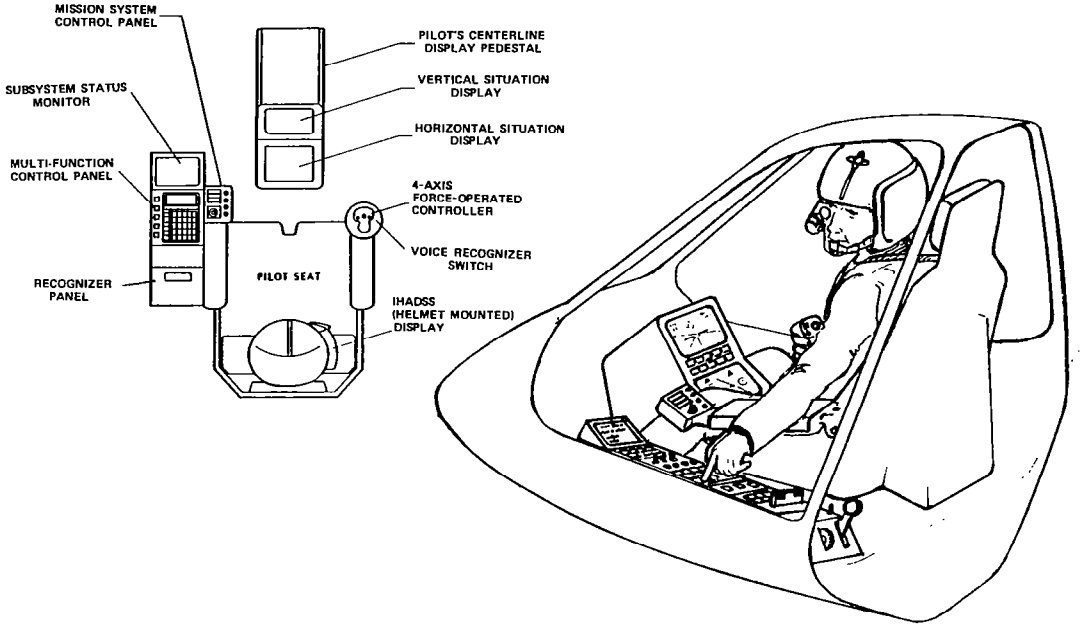

Figure 3. Single-Place Helicopter Cockpit Incorporating a Voice Interactive System

COCKPIT INTEGRATION FROM A PILOT'S POINT OF VIEW

David L. Green
Vice President

PACER Systems, Inc.
Arlington, Virginia

Abstract

Extensive experience in both operational and engineering test flight is used to suggest straightforward changes to helicopter cockpit and control system design that would improve pilot performance in marginal and instrument flight conditions. Basic differences from airplane fight characteristics justify distinct treatment of helicopter cockpit flight control configurations. Helicopter use of collective for direct lift control and collective to yaw coupling are emphasized in drawing these distinctions. Need for good downward peripheral visibility and truly horizontal glare shield profile are cited for natural visual cues during marginal VMC and approach transition. Needed control system improvements include: 1) separation of yaw from cyclic force trim; 2) pedal force proportional to displacement rate; and 3) integration of engine controls in collective stick. Needed display improvements include: 1) natural cuing of yaw rate in attitude indicator; 2) collective position indication and radar altimeter placed within primary scan; and 3) omnidirectional display of full range airspeed data.

Introduction

The helicopter has one very unique capability, the ability to hover efficiently and precisely for extended periods. And when compared to the airplane, it has the advantage of being able to fly into confined areas, hover, and land vertically without any concern for the stall-spin phenomena.

The trained pilot has no problem exploiting the capabilities of a helicopter during VMC, but when the task is proposed in the IMC environment, the pilot often appears to fall short. This same trend in performance also exists during marginal VMC and during transition from IMC to VMC for landing. That is, the pilot-machine combination is less capable when external visual cuing is marginal or non-existent.

Some of the reasons for this degraded capability are readily apparent when IMC operations are studied. Navigation must be conducted via reference to electronic aids and this means a new level of air traffic control is required, with a concomitant increase in the time consumed by radio communications. These procedural changes increase cockpit workload and reduce the time available for flight control. With less time available to allocate to flight control and dramatically degraded visual cues, the pilot flies with less vigor. Everything happens a bit slower, while the pilot tries to fly with greater precision.

One obvious solution to the IMC case is to incorporate sensor-display concepts which return the real world visual cues to the cockpit (FLIR). Under certain circumstances today's technology makes this type of visual augmentation possible, but even the best of these concepts still have serious shortcomings in truly bad weather. In any event, this type of visual augmentation is considered heroic for many military applications and all civil applications.

From a pilot's perspective, this inability to fully exploit the unique capabilities of the helicopter is a problem which is common to helicopters of all manufacturers. That is, there are a number of common man-machine interface characteristics, which as they stand, detract from the pilot's ability to accomplish the piloting task. And although pilots may desire change, they aren't always able to articulate a winning argument for the features they feel they need. They may not even understand the source problems they are experiencing. So without such convincing argument, many worthwhile improvements go unidentified or deferred.

What follows then are observations, explanations, and suggested requirements for change which do not require heroic efforts. These comments are principally based upon the author's personal experience and observations as an operational helicopter pilot, an engineering test pilot, a research pilot, an experimental test

pilot, and a flight test engineer. The intent is to provide insight into the factors which may be confusing to non-pilots and revisit a number of helicopter cockpit design features which have suffered at the hands of the "accepted convention".

The scope of this paper will not allow an in depth treatment of all applicable characteristics which are candidates for change. Nor is it possible to consider all phases of flight, or helicopter applications. Instead, this effort is generally focused on the high workload or high stress situations where pilots are routinely unable to accomplish the transition to hover, or to conduct other slow speed tasks safely. The purpose of the paper is to persuade the reader that there are many reasons to revisit cockpit design and question the conventional wisdom which has been handed down for generations. The premise is that given a bit more design consideration, a helicopter pilot can generally achieve more than is currently expected of him. He cannot only achieve more, he can do it more safely.

The Cockpit

But before we deal with the tough questions related to IMC flight, I would like to first conduct a walk through of the basic cockpit to pilot interfaces--the controls, external visibility, the seats, and some of the things that differentiate helicopter control from airplane control.

Seat Assignment

When a pilot gets into most helicopters (there is always an exception) he flies from the right side. This is true even though there is really no rational reason for such a choice. In fact, when you consider the need to work with airplanes in left-hand traffic patterns, it makes little sense at all. For when the helicopter is in a left bank, the pilot in the right seat generally can't see where he is going during the turn. The pilot's line of sight is blocked by the overhead of the cockpit cabin which normally supports circuit breakers, switches, and engine controls.

The real reason helicopter pilot's are in the right seat has nothing to do with any great engineering logic. It just happened to come out that way. Mr. Sikorsky meant for the pilot to be in the left seat, but because of early vehicle training problems, the first operational pilots learned to fly in the right seat. The point here is that there is nothing sacred about the pilot being in the right seat. But is there any reason to consider changes? There may be.

Approaching a hover spot the pilot must flare to stop. When he flares the view over the nose is often inadequate. When it is, or when there is an obstruction in the over-run, the pilot will often approach with a crab angle. A sideward flare will be used, or the helicopter will be stopped short and air-taxied so that the pilot can see the spot out the right side. When this type of approach is flown in U.S. helicopters, left pedal is required to sideslip to the right. More left pedal means that more tail rotor power is required. If the pilot were to sit on the left side he would hold right pedal and less power would be required to maintain hover altitude. Seems like the U.S. helicopter pilot is on the wrong side or the U.S. main rotor is turning the wrong way.

Collective

The importance of the collective and its control characteristics are substantially underappreciated by the helicopter community. This device should be recognized as a direct lift control, that permits precise and quick control of the vertical degree of freedom. The stored angular momentum permits small inputs to be accomplished without the need to trade airspeed for altitude and without concern for the engine(s') ability to accelerate or decelerate. Figure 1 further illustrates how the collective can be used to climb even while the nose is pushed over to accelerate and allow the pilot to keep the trees in visual contact.

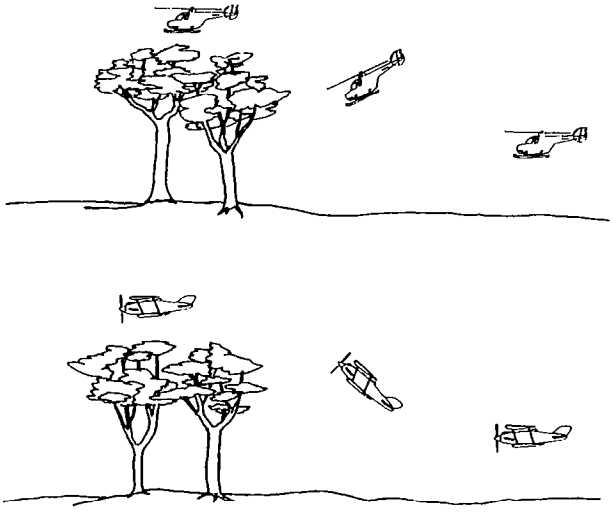

Figure 1. Comparison of Airplane and Helicopter Pitch Attitude Characteristics During Climb Over Obstruction.

When compared to the airplane task, the collective simplifies height control; but it makes horizontal speed control comparatively more difficult. For example, when an airplane pilot climbs back to glideslope, power is added and the nose is raised to increase angle-of-attack. In contrast, the helicopter pilot simply increases collective to climb. To change speed at constant altitude, the airplane pilot simply reduces thrust and the aircraft decelerates. Altitude is maintained via the elevator. The helicopter pilot pitches nose up and commands deceleration with attitude while maintaining height via the collective. This last technique requires more control coordination.

Some analysts tend to believe that airplanes and helicopters are controlled in the same basic way. Engineers with this viewpoint will read the two sets of descriptions above, and conclude that the airplane techniques and the helicopter techniques in forward flight are essentially the same. And this is where many of the helicopter pilot's problems begin.

On a more positive note, there has been one noteworthy innovation in physical design of the collective control. This new design was first installed on the Bell-222 and later on the Bell 214ST. The collective grip tends to move aft and upward as collective pitch is increased. I had no problem with this motion. The hand grip and arm motion were very comfortable. But more important, this design permits the installation of two engine controls on the collective. The left side of the split grip is for the No. 1 engine and the right side is for No. 2. With this design, one can readily advance or retard an engine in an emergency without releasing the collective. An admirable solution to a difficult problem (see Figure 2).

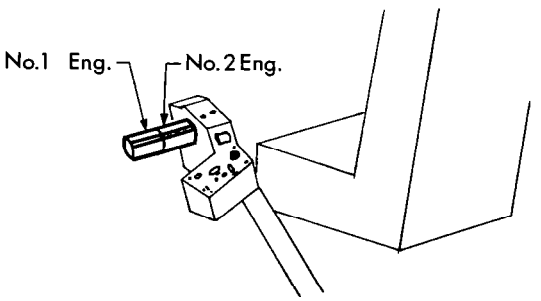

Figure 2. Characterization of the Collective Control Incorporated in the Bell-222 and Bell-214ST Helicopters.

Linear Force Cues

To further understand helicopter control techniques and the need for enhanced visual cues, it can be useful to consider the nature of the linear accelerations which are felt by the pilot (airplane vs helicopter) during a level deceleration. Consider the case where the throttle of an airplane is rapidly retarded. The linear force along the X axis causes the pilot to move forward, and is restrained by a seat belt and shoulder harness. In contrast, the pilot of a helicopter decelerates by lowering the collective as he pulls the nose up. If the pilot doesn't lean forward (so as to see out or keep his vertical orientation), the result can be no forces or an increase in the forces on the pilot's back as gravity pulls him against the seat.

Seats-Controls

Engineers underestimate the need for adjustable seats and pedals. The pilot must be able to comfortably locate himself around the controls. This includes the pedals which need to be adjustable as well. A pilot who is uncomfortable or must sit on an angle, is probably more susceptible to spatial disorientation.

Looking a little deeper, we find many pilots fly with their right forearm resting on their right leg, manipulating the cyclic control with their fingers. This is a method which is particularly appropriate for IMC flight. I fly this way and often feel like I have to adjust the seat too high relative to the pedals, just to obtain a satisfactory grip on the cyclic. I don't really see anything which one might do to improve pedal positioning but a cyclic which could be adjusted in height an inch or two might enhance many pilots' abilities to fit into their machine. Again it's important to be comfortable to avoid disorientation during high stress or high workload situations.

Force Trim Systems

There should be a cyclic force trim system in all IMC capable helicopters. This system should always incorporate an instantaneous Force Trim Release (FTR) switch, even if the system uses a Four Way Trim Switch (FWTS Coolie Hat) to trim fore and aft, and laterally (see Figure 3).

A simple force trim system is required to hold the cyclic control where the pilot puts it. And when such a spring system is added, the designer should not become confused as to its purpose. In a helicopter the Force Trim system holds the control at some pre-selected point. That is, the longitudinal and lateral-directional

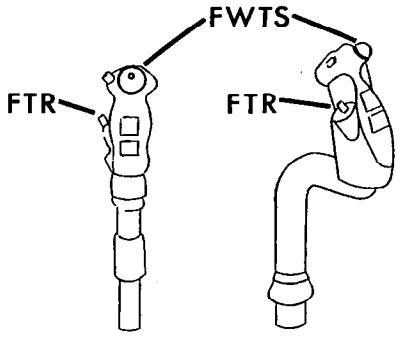

Figure 3. Typical Cyclic Control.

static stability of a helicopter are generally so weak that the force characteristics which can be developed (via a simple force feel system) do not substantially enhance helicopter handling qualities. But when augmentation is incorporated, it does become very important for the control to stay precisely where the pilot puts it.

In contrast, putting a force feel spring in the yaw control is totally counterproductive. Friction is more than adequate to hold the controls in place. And if you put a spring in yaw, the pilot is forever pushing the FTR switch so that the pedals can be repositioned. If the FTR releases cyclic trim at the same time the yaw control is released, you have defeated the reason for the cyclic force gradient. The best design, from a pilot's point of view, incorporates friction to hold the pedals in place, with the possible addition of a hysteresis damper that provides an opposing force, proportional to the rate of application. For VMC type maneuvers, the pedal rate damper is even more appropriate. That is, the pilot obtains the best feel for the maneuver he is conducting if he feels a control force which is proportional to the rate a given control is deflected.

This type of control rate damper can also be incorporated in the cyclic control with advantage. This is true because many pilots depress the FTR to release the stick centering forces during rapid maneuvering. If the rate feedback forces remain, even when the FTR is depressed, the pilot's reaction is very positive.

Visibility

There is a great deal of variation between designs when it comes to cockpit visibility. The importance of external visibility is hard to overstate. Yet, it is an aspect of design which seems to receive insufficient weight when cockpits are configured (see Figure 4).

For example, the need to see down through the feet seems to be one of the least appreciated needs for visibility. Yet the pilot receives much visual data through peripheral vision when he can see the ground down through or near the feet. In slow speed flight or hover, horizontal motion is best controlled via this cue source. It is even possible to receive a beneficial cue of pitch rate through this window when in a hover or even at altitude when operating without a horizon.

Some helicopters have little or no downward visibility, and experience has shown that they are clearly more difficult to land with equal precision. And flares from steep approaches are much more readily accomplished when the downward visual path is available. When forward visibility is poor, as it is during heavy haze, and at the bottom of an IMC approach, the pilot may actually acquire initial visual contact through the lower panel. This can happen even when he is heads up looking for the landing area. And when you depart vertically out of a confined area, there is no substitute for this downward visibility.

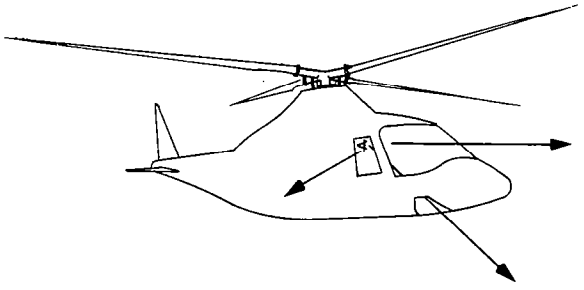

Figure 4. Typical Sources of Pilots Primary Visual Cues.

Another problem occurs during attempts to conduct steep approaches. This is illustrated in Figure 5. Here the pilot visually acquires the landing pad with his eye on a 20 degree approach angle. This is his limit of downward vision over the nose so that when he pitches up to decelerate, he loses visual contact with the pad. So he doesn't pitch up first. First he lowers the collective and flies down. As he descends he becomes able to pitch up for the deceleration while still keeping the target in sight. This may explain how tail rotors get involved in trees and fences on final approaches to confined areas.

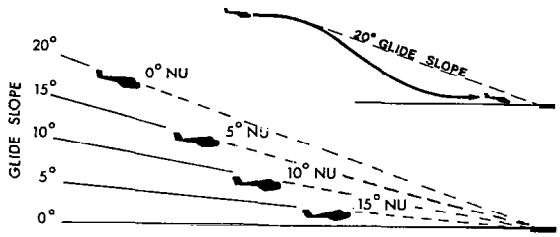

Figure 5. Flight Path Flown when Pilot Attempts to Keep Landing Site in View After Having Started a Steep Approach.

Horizon Reference

When the sun goes down, and the horizon reference weakens, the pilot trades the outside visual cues for the information available from the cockpit displays, aircraft sounds, cockpit control positions (and forces) and the force cues (vertical accelerations, etc.) impressed upon his person. In many cases there is a period of transition where the pilot is flying via primary reference to his instruments even through some of the outside cues are still there. During such periods the pilot can experience an unexplained uneasiness, and for some reason there is a problem keeping the ball centered on the inclinometer.

I believe this situation also develops during transitions from IMC to VMC on final approach and during certain other slow-speed hover tasks. This uneasiness is also related to the aircraft where a pilot has a much different feel when flying from right seat as compared to the left. A probable explanation is illustrated in Figure 6.

When the glass shield is curved, or it is sloped down to the outside, the pilot is presented a very strong erroneous attitude reference. And under certain circumstances, I believe there is an unconscious tendency to match the horizon and the glare shield line. This causes the ball to be out to the left when the pilot flies and out to the right when the co-pilot flies. This glare shield line needs to be truly level. When the aircraft visual reference is level, a weak horizon line, can be a powerful positive cue even when no conscious reference is made to it.

During night hover operation in the SH-3, it was not uncommon to work with no horizon. (Even if there is a horizon you still fly the machine on instruments). But there would be nights when just a faint hint of a horizon line was available. One never looks at it, but somehow you

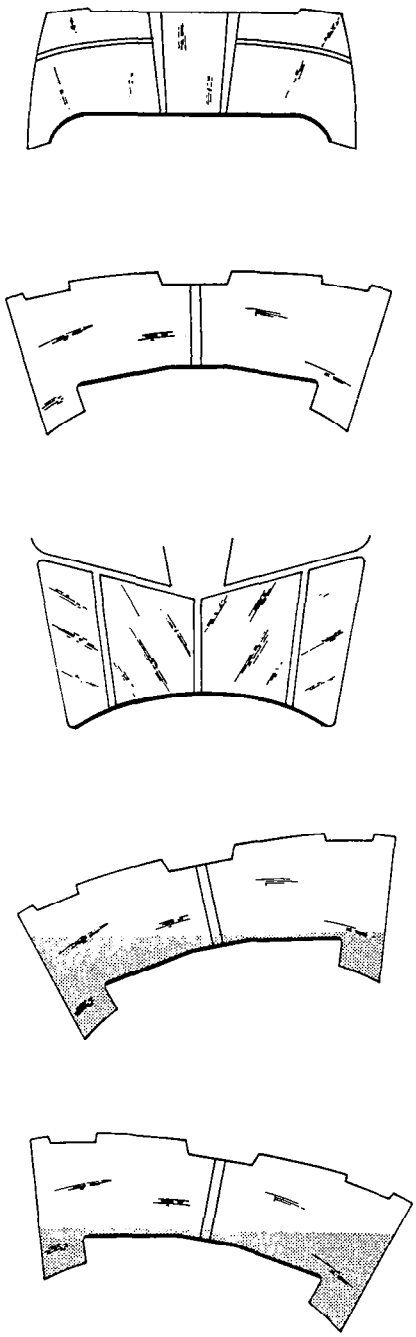

Figure 6. Impact of Glare Shield Design on Crew Visualization of the Wings Level Attitude.

would know it was there. But the running lights (navigation lights) would backscatter light into the cockpit from the mist over the ocean and this would often mask the faintest of horizons. When I was tired and I was uncomfortable, I would turn the running lights out (leaving the tail light on) while I hovered. I could then faintly make out the horizon reference and it made all the difference.

The IMC Problem

In a historical sense, the design of today's conventional IMC cockpit, was derived from a marriage of airplane instrumentation to the cockpits of helicopters which were originally designed for visual flight only. And when helicopter pilots were unable to accomplish an IMC hover, or an approach to hover on instruments, vehicle stability took a large share of the blame. Automatic Flight Control Systems (AFCS) were subsequently incorporated to solve the problem. The result was a dramatic improvement in man-machine performance, but the man had a new role. The pilot was now a manager, no longer in the direct control of the helicopter. The pilot became a safety pilot. He was able to fine tune the AFCS while it operated normally, while also being there to recognize failures so as to extract the aircraft from an approach or hover task if safe limits were exceeded.

Next came the Flight Director Indicator (FDI) which in many cases could double as an Auto Pilot Computer (APC). The FDI brought the pilot back into the direct control of the aircraft, but this time he was a servo. The pilot was instructed to follow commands on an ADI, matching pointers to their respective indices. Keeping all the pointers in their proper place would keep the aircraft on glide slope or in a hover. The two big advantages of this display format were that the pilot didn't have to think much, and all commands were centrally located on a single display. I might add that the basic flying qualities of the helicopter were improved so that Auto Pilots could control the outer loop. When this happened, it became possible for the pilot to fly almost as well with an FDI. But even when pilots are allowed to fly with reference to an FDI, they are typically required to operate above say 60 knots, unless features like heading hold are incorporated.

Collective to Yaw Couple

This last point is very important. The heading hold feature is required to accomplish an approach to hover (IMC) because the collective to yaw couple of the single rotor helicopter is so powerful and interactive that it dramatically increases pilot workload when it goes unchecked. Heading hold is not required to compensate for poor static directional stability; nor is control quality or control power of the directional control system at fault. The problem clearly stems from the fact that it is difficult to find the new directional control trim point when an input is required to compensate for the collective-to-yaw couple.

The desired yaw control position, which the pilot cannot easily locate, is the position which will yield a zero yaw rate. He does fine when visual cues are available, but during IMC he has trouble because the yaw rate cues available in the cockpit are totally inadequate. To understand why, lets review the fundamentals and actual experience.

When the collective of a U.S. helicopter is increased during hovering flight, the pilot must move the left pedal forward to compensate for an increase in main rotor torque. Right pedal is required under similar circumstances in a French helicopter where the main rotor turns in a direction which is opposite to that of the U.S. machine. One might expect a pilot to have trouble switching from the U.S. to the European convention. But generally there are no problems at all when the yaw rate cues are sufficiently strong. But some piloting errors do occur when the strength of the heading-rate cue decreases.

In reviewing my own experience, I can report that I have had no problem associated with takeoff or hovering flight; but at high altitude or while operating in heavy haze, I have found my left foot moving forward with up collective. That is, when the visual cues were powerful, I had no problem. But when the cues were weak, my learned response (which was nurtured for 22 years in U.S. helicopters) took over, even in the European machine.

This experience illustrates the importance of yaw rate cues. Although I had no problem adding right pedal with up collective during my first takeoff, I experienced confusion at altitude where the yaw rate cues were not lost, but distant and subdued. I didn't even have to enter IMC to start having trouble with directional control coordination.

Obviously static directional stability was not at fault. This parameter is obviously of greater aid during forward flight than in the hover where I had no problem at all. One can now conclude that the static directional stability and the yaw control system are adequate all the way to a hover. So what is missing?

For the answer, compare the function of the display which is provided for pitch and roll, to

the function of the display(s) provided for yaw control (or heading). The ADI is a fine analog of the real world. A nominal one-for-one match. But look what has been provided for yaw. The most obvious instrument is the RMI (or HSI). The cue is a dial that rotates in an indicator which is mounted below the ADI. You would have to look down through a hole in the floor of the helicopter to see real world motion which would relate to this display. The RMI and HSI are navigation and heading management indicators, not yaw rate displays.

Then there is the vertical needle of the turn-and-bank indicator. Today this indicator is so small and underdamped that it is virtually useless during IMC hover or approach flight.

Electronic HSI's generally provide an enhanced heading cue, but again, the cue is displaced from the primary cues of pitch and roll found on the ADI.

In the most modern military helicopters, we find the Electronic Vertical Situation Display (EVSD). A heading reference strip is normally presented across the top of the display. This is a step in the right direction, but it is clearly not conventional equipment. In any event, it is not currently offered for civil machines and generally beyond the scope of this paper.

Now revisit the piloting task for a moment. During hover and approach to hover, speed changes require collective adjustments. The collective couples to yaw, yaw produces a sideslip, and the helicopter subsequently rolls and pitches as a result. So in a conventional cockpit, when the pilot makes an adjustment to the collective to stay on glide slope, he excites a chain reaction, a chain of couples that impact the equilibrium of the aircrft as though they were gust upsets. So an unattended collective-to-yaw couple upsets yaw, roll and pitch, with an attendant deviation from the desired flight path.

Consider a helicopter in an ILS approach, on speed but below glide slope. If the pilot tries to control glide slope with collective (as we teach him to do) he exacerbates the pitch and roll attitude control task. And pitch attitude is the primary means of airspeed control. Years of observation leave no doubt that as the attitude control task becomes more difficult, the pilot becomes highly stressed. And when the pilot operates under a sufficiently high level of stress, the feet stop working.

The feet are relatively dumb control elements. They work well when the cues are strong, but when the workload goes up, and the visual cues are poor, this is the first control path which fails the pilot. Under the stress of maintaining altitude (or glideslope) and pitch attitude, the pilot's scan breaks down and the displays which are not directly in his compressed scan are ineffective.

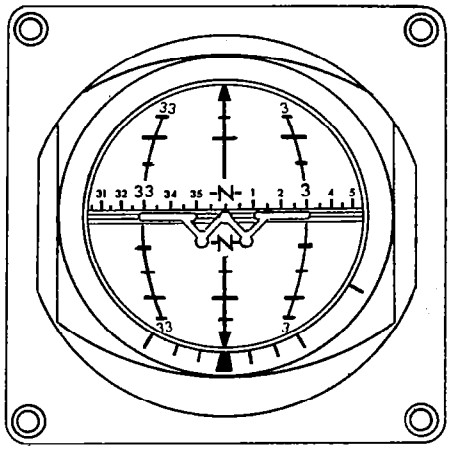

Figure 7. Pitch Roll Yaw Attitude Indicator (Characterized from ADI-811).

The yaw rate needle of the turn and bank indicator may still be in this compressed scan, but this indicator does not readily transfer the message. It does not exhibit any characteristics analogous to yaw rate and therefore it must be interpreted. Experience would suggest that control logic in the mind gives priority to control of the most life threatening parameter(s) and shuts down data inputs which either relate to low priority control or need interpretative processing. The turn needle fits both of these criteria for deferred priority. But if the cue is so strong that it works through peripheral viewing, the mind accepts and acts on the data. The explanation may not be entirely correct, but the observations of pilot response are absolutely accurate.

This brings us to consider one possible solution. Why not present heading on the attitude indicator? Rotate the attitude ball of the ADI when the aircraft turns. The cue will be so strong that it can be treated peripherally, as it is during VMC operations. The transfer is more real world. When you turn left the face of the indicator moves from left to right. This is not a new idea, it has been incorporated for years in combat aircraft (see Figure 7).

Height Control

Another problem control task in slow speed flight involves altitude control and maintenance of glide slope during IMC operation. As in the case of yaw control we find a quick, precise and powerful control in the collective. It is a direct lift device which has no lags to confuse its application. During VMC hover operations, one can hold hover height within inches of the desired value, even during turns and speed changes. But when the visual cues are gone, so is precision performance.

The pilot does feel vertical acceleration in the cockpit when a collective input is initiated. But during IMC maneuvers these forces are quite small and they often get masked by vibrations. Sometimes the vertical forces which are produced via (pitch) angular accelerations similarly mask collective inputs. So, as in the case of the yaw control, there are really no reliable natural cues which remain, once the external visuals are gone.

And as in the case of yaw control, we have another classic control trim problem. The pilot has a difficult time finding the control position for zero vertical rate. There are several reasons for this problem.

First, the trim point moves around anytime the horizontal speed changes. For example, starting from a stabilized constant altitude situation near hover, a small increase or decrease in horizontal airspeed will cause a change in the power required to maintain level flight. The aircraft then starts to climb or descend, requiring a collective adjustment to cancel this unwanted rate.

Reviewing the power required characteristic we find that the power for level flight decreases as speed decreases below V_{NE} in much the same way as it does for the airplane. It bottoms out in a typical bucket, then increases again to peak at zero airspeed. When speed is increased to the right, left, or rearward from zero, the power required by the rotor decreases in a way similar to forward flight (see Figure 8).

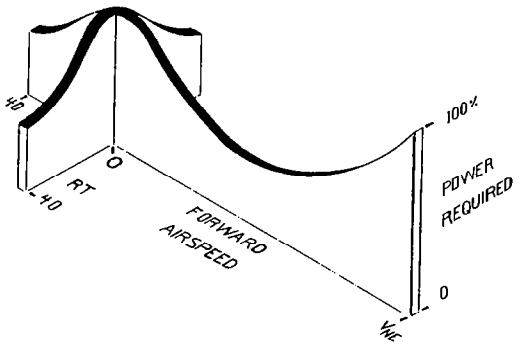

Figure 8. Helicopter Power Required for Level Flight.

The power curve is essentially flat or neutral in the bucket, stable on the front side and unstable on the back side. Finally, the gradient is typically much steeper in the slow speed regime than in high speed forward flight. The stability of the curve and the magnitude of the gradient all influence the pilot's ability to cope with the vertical degree of freedom. That is, all of these characteristics contribute to define the task. In summary, the task is least difficult on the front side and most difficult on the back side of the power curve. And it is easier to control the vertical degree of freedom with the collective when airspeed is held constant vs. control in conjunction with horizontal speed changes.

This doesn't mean to infer that the task is ever easy under IMC, slow-speed operations. Because the pilot must still observe the error and know how to precisely respond with the collective.

Take the easy case first. Flying an ILS approach, the glide slope signal is conventionally presented quite adequately. So visualizing "above" or "below" glide slope is not a problem. And in the real world we find pilots tend to lock down the collective with friction and use the cyclic control to fly up or down to achieve glide slope. This works during operation on the front side of the power curve which is where all civil IMC is flown.

Pilots probably use this technique for two reasons. They know they have trouble making accurate adjustments to the collective setting and that several adjustments will be required before they get it right. They also know that any collective change will require a directional control "pedal" input. We've already covered the last problem under the discussion of collective-to-yaw coupling. So why are there problems setting power (Collective)?

The pilot has no precise cue of collective position. When the pilot adjusts the collective he observes the results via a cockpit display of engine torque. But this indicated value of torque is subject to all sorts of masking. Changes in tail rotor thrust (pedal position), a nose up control input, a roll control input, a vertical gust, and a commanded change in rotor RPM will all cause the indicated torque to change more than the amount that the pilot typically needs to input to accomplish for a climb back to glide slope. So these miscellaneous inputs mask the pilot's collective input.

Another problem involves display location. Typically the torque indicator is displaced too far from the primary viewing area to be included in a high gain scan. This seems to be a very serious problem in the civil commmunity. In this

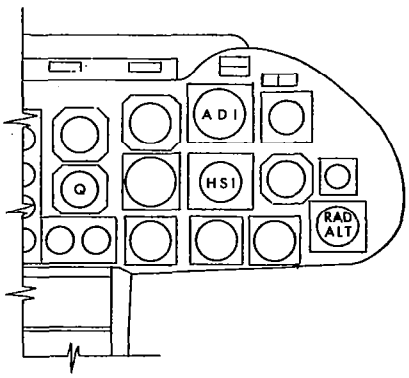

Figure 9. Typical Location of Radar Altitude Indicator and Engine Torque Meter (Q) Shown Relative to the Primary Attitude and Heading References.

group more priority is given to adding an additional attitude display than properly locating the torque indicator. (See "Q" in Figure 9).

Finally most torque indicators appear to be underdamped. I'm not sure why they are underdamped, but I believe this damping characteristic contributes to the problem of selecting the desired power setting. For in one case, a properly damped indication of main rotor torque (Bell-222) provided excellent results (as illustrated in Figure 10). Yet would anyone seriously consider asking an Auto Pilot to close the vertical control loop on torque information?

Designers of FDI's for helicopters were faced by the same problem, a problem which they solved by including a small edge mounted pointer to indicate collective control inputs. It is not the ultimate device but its presence lends credibility to the need. From personal experience I can say that a clear indication of collective position allows pilots to find trim very quickly with an absolute minimum of effort. So the solution is a full range collective position indicator.

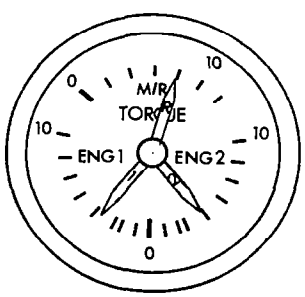

Figure 10. Characterization of Torque Meter Used in the Bell-222 Model Helicopter.

Radar Altitude

When we complete an IMC approach to a hover, and hold an IMC hover, another cue deficiency becomes evident. Arriving at the Decision Height (DH) altitude the pilot becomes more aware of his absolute altitude above the ground. And another instrument becomes important, the radar altimeter. And where is it located? In civil helicopters it is typically found in the lower right hand corner (see Figure 9).

This is a totally unsatisfactory location for such important data. The standard pressure altimeter is simply not adequate during transitions to, and operations in, the low-speed regime. Both altitude and altitude rate are unreliable to the degree generally required for controlling height during an IMC hover. Since radar altitude and visually derived "radar altitude rate" are the best cues available in the cockpit, these data need to be presented with higher priority in the cockpit. The display should be given higher priority, but I have another solution which seems to work very well. This solution is illustrated in Figure 11. Here the Decision Height (DH) and Radar Altitude are presented digitally on the lower edge of the ADI. This is an excellent format for the final phase of the ILS approach. The display I evaluated is by Sperry. It has an update rate which appears to be well suited to the task of interpreting radar altitude rate as well. If this is an accurate assessment, such a display clearly would enhance a pilot's ability to hover and maneuver in the slow speed regime. The Sperry ADI evaluated also has a rising runway indicator to display absolute height. I agree that this is a proper approach but not the total answer.

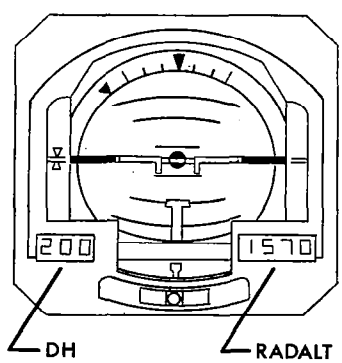

Figure 11. ADI Including Digital Presentation of Decision Height and Radar Altitude.

Back-Side Speed Control

Then there is the problem of speed control on the back side of the power curve. The power required curve typically has a steep gradient on the back side of the curve. And the slope represents an unstable situation when considered in the context of man-machine control. That is, if the aircraft slows down it will descend. This means that to climb back on glide slope the pilot cannot simply pull up (flare) and trade airspeed to regain the glide slope. Such an act causes the aircraft to lose speed, with a momentary positive response but then the aircraft settles further below glide slope.

So during a slow speed aproach, the collective is clearly the control which the pilot must use to modulate descent rate or angle. And to simplify the control activity, it is necessary to hold airspeed constant. But again there is a problem with the data available to the pilot.

Airspeed Display

When power is added, most pitot-static airspeed systems reflect an apparent change in airspeed. A change in slideslip angle or angle-of-attack will have a similar result. So even at airspeeds where the pitot-static airspeed system is still supposed to function (above 40 knots) the pilot can find himself chasing changes in "position error". Thus, he actually causes speed changes to occur in a needless attempt to hold speed constant. The real speed changes are therefore confused with the changes produced by changing values of position error, and the precision of the entire approach task deteriorates.

To avoid reliance on pitot-static airspeed, pilots are told to maintain a constant pitch attitude to hold airspeed. They are also told that more and more nose down trim attitude will produce a faster and faster trim airspeed, and vice a versa. The first concept is true only if the second is true. That is, the variation of pitch attitude must be stable or at least neutral before one can use pitch attitude to reliably attain and hold airspeed. In most cases the stable attitude characteristic required and desired does not exist.

Since pitot-static airspeed indicators become totally inoperative below about 40 knots anyway (depending on the aircraft and the flight profile), some sort of reliable speed cue is required so that a pilot can separate the speed control task from the vertical control task. Ground speed can be derived from many current equipments, so that is one possibility. But the aircraft is actually responding to the airmass, not ground speed. So it seems obvious that an airspeed system which operates down to zero airspeed is clearly required.

Again we are faced with a question of where to locate this additional data display. Collins in cooperation with PACER Systems, Inc. is developing such a display for the U.S. Navy (see Figure 12). This display is multi-mode, allowing both pitot-static and omnidirectional low range airspeed to be presented on a single indicator. Thus it can one-for-one replace the current airspeed indicator.

Experience has shown that this type of airspeed data is not subject to the problems that plague the pitot-static system. Now the pilot can use the longitudinal control to directly regulate airspeed. He no longer must try to hold a constant attitude to determine, after some several seconds, what might happen to airspeed. Thus, we have decreased the amount of time that the pilot must allocate to the ADI to accomplish the airspeed control task. This reduction in workload further releases the pilot's control logic to handle the heading and attitude control tasks discussed earlier.

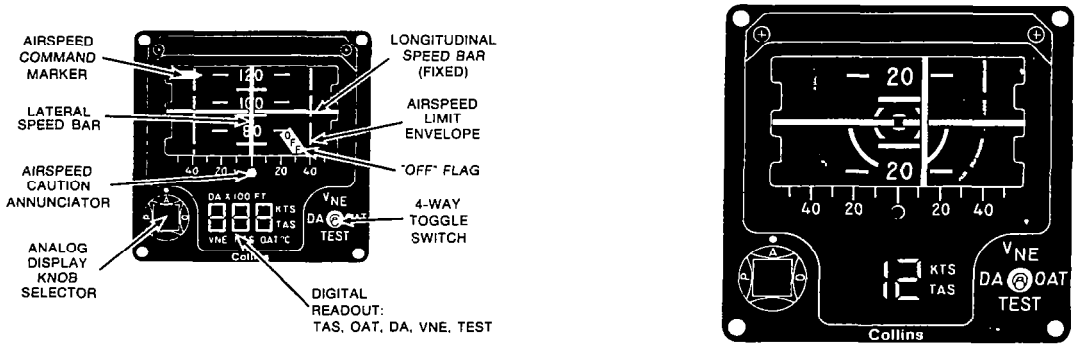

Figure 12. Collins ASI-800, Omnidirectional Airspeed Indicator (OAI).

Now the pilot is in a position to use airspeed and all the other new cues to get ahead of the aircraft. He no longer must put in control inputs and wait to see a response. In actual practice, the pilot can learn to anticipate the amount of collective change which is required to maintain level flight (or glide slope) as speed is gradually changed.

Since the Omnidirectional Airspeed Indicator (OAI) of Figure 12 is able to present airspeed for flight in all directions from zero, it is also now possible for pilots to observe the cross wind component as just that, a component of airspeed. They can learn what 5, 10, and 20 knot components will mean as he decelerates and achieves a hover. And when the component is too high for safe operations, the pilot will be able to anticipate the situation before an unmanageable hover is attempted near obstructions, etc.

The Landing

To land under IMC conditions, I would expect that for some long number of years into the future, pilots will be required to have visual contact with the ground. I really see no reason why there should ever be any reason for a CAT III type flight control system in a helicopter. What the industry needs is a system which the pilot can use to get into close proximity to the landing surface. I have hovered in some really dense fogs, but I can never remember a case where I couldn't see the ground at 20 feet. Here is where downward visibility re-enters the picture. Nothing is as accurate and reliable as the pilot when it comes to accomplishing a vertical landing. So mostly the problem is stopping the helicopter over the landing pad, at an altitude of 50 feet or less. With excellent downward visibility the pilot continues to fly the aircraft down to a touchdown.

Conclusions

In conclusion, let's review the highlights. Reducing the workload associated with horizontal speed control reduces the pilot's workload so that he is better able to use the other display-control enhancements such as:

- Pitch-Roll-Yaw Attitude Indicator
- Collective Position Indicator
- Radar Altitude Indicator
- Excellent downward visability

The net result is to bring the pilot's control task in line with what a human could be expected to achieve. The more the pilot can achieve with the basic helicopter the more viable the helicopter will become in civil and military applications.

INTEGRATED COCKPIT FOR A-129

Dott. Ing. Filippo Reina
Director, Helicopter Systems Engineering
Costruzioni Aeronautiche Giovanni Agusta S.p.A
Cascina Costa, Samarate, Italy

James A. Gracia
Systems Operations Engineer
and
Bryce W. Koth
Human Factors Engineer
Harris Government Information Systems Division
Melbourne, Florida

Abstract

The Agusta A-129 is a compact and lightweight tandem cockpit combat helicopter under development for multimission usage with a full complement of electronic aircraft control and ASE equipment. Weight, size, and mission requirements for the A-129 mandated an integrated system approach for the crew/cockpit interface design. Instead of the usual multitude of cockpit controls, indicators, gauges, and lights, the primary crew interface is a single multifunction keyboard and one or more multifunction CRT display units. This cockpit design approach imposed unusual constraints upon the system architecture to overcome the inherent information access limitations of a data input/output window that was restricted by the available space. This paper describes the conceptual approach and resulting design of the A-129 cockpit with the intent to enhance the development of cockpit standardization.

Introduction

The A-129 integrated cockpit is the crew's interface with a sophisticated weapon system. Its particularly small size and mission scenario flexibility make the A-129 man-machine interface a challenge to optimize. Its crew compartments must accommodate pilot and gunner comfortably, provide excellent forward quadrant visibility for the pilot to safely fly in the Nap-of-the-Earth (NOE) environment, and provide command and control capability for aircraft and mission equipment. A highly integrated helicopter system and a highly integrated cockpit are demanded to satisfy the A-129 requirements.

Integrated systems are presently emerging but the design technique has not. There are isolated examples of integrated cockpit design techniques, but a validated design practice that is fully accepted by the industry and the government-user community does not exist. The A-129 demanded a highly integrated cockpit, therefore a conceptual system design approach had to be evolved. This paper addresses the approach followed in the definition and development of this innovative highly integrated cockpit. However further refinements are planned during 1) the ground simulator test phase (October 1982 - August 1983), 2) the early flight test of the A-129 (late 1983), and 3) the prototype field trials. The ground simulator will validate the system for the most effective flyable configuration. The first flight will initiate fine tuning of this concept to the flight environment. Throughout the flight test of the four prototype helicopters, a large amount of experimental data will be amassed and used for the final definition of the operational cockpit system. The incorporation of these experimental test results will confirm the operational flexibility of the software intensive man-machine interface.

A-129 Definition*

The Agusta A-129 (Fig. 1) is a light, twin turboshaft powered, combat helicopter under development for the Italian Army to serve primarily in an anti-tank role. It has a single four-blade articulated main rotor and a two-blade semirigid tail rotor. The helicopter design, presently completed and frozen, reflects the results of extensive trade-offs down to the component level in order to satisfy the Italian Army's requirement for an agile, small size, limited cost aircraft, which retains the advantages of state-of-the-art technology.

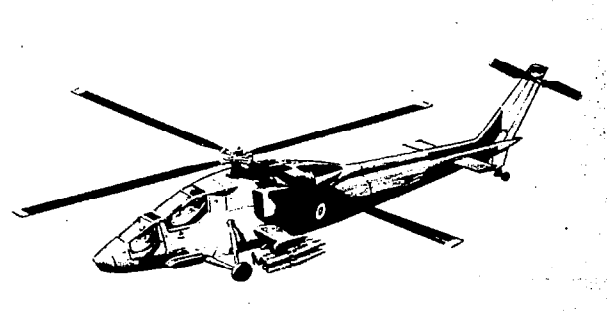

Fig. 1. A-129 Helicopter

* Lovera, Bruno, "The Agusta A-129", Vertiflite, 26 (6), November/December, 1980, pp 6-9.

The crew of two is seated in tandem with the aircraft commander/pilot located aft and above the copilot/gunner. Primary armament in the present plan is the TOW system with 8 missiles carried on 4 pylons mounted to the stub wings. Rockets, machine gun pods, and external fuel tanks can be interchanged in any combination with the TOW missiles.

The A-129 has some unique design features which give it unprecedented capability and flexibility as a combat air vehicle. The cockpit configuration provides both crew members with identical and unequaled flight visibility. The main transmission, main rotor shaft, rotor head, and primary flight controls are designed to provide protection against icing and ballistic and/or wire line damage as well as a stable mounting platform for a mast-mounted sight (MMS). Finally, the A-129 incorporates a modular, expandable, multiprocessor-based data bus system which is presently unequaled in comprehensiveness and flexibility in a rotary winged aircraft.

Extensive Italian Army and Agusta study and experimentation, including the use of full-scale cockpit mockups, were used to arrive at the A-129 cockpit configuration. The "camel" configuration, as shown in Fig. 2, was selected to maximize visibility for both crew members in NOE mission environments.

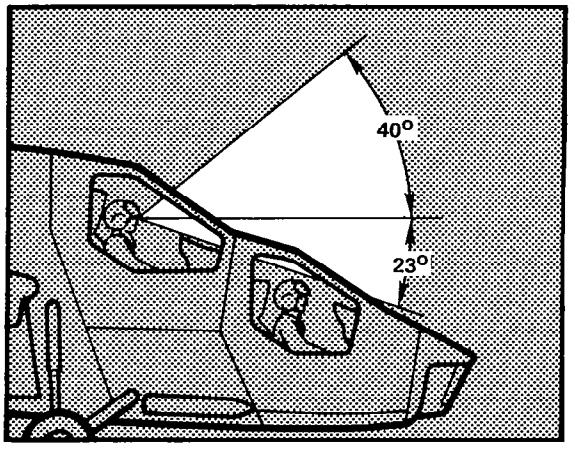

Fig. 2. A-129 Cockpit configuration

Baseline Configuration

The A-129 is equipped to fly and attack in day and night under instrument and visual flight conditions. In addition to full instrumentation, stability augmentation, and auto-pilot capability, the Integrated Multiplex System (IMS), the heart of the integrated system, incorporates a navigation computer capability. Inputs to this system come from the installed Doppler radar system, the radar altimeter, and standard navigational radios. For night visual flight, a Pilot's Night Vision System (PNVS) will be incorporated.

UHF-AM, VHF-AM, VHF-FM and HF communications radios with standard NATO encrypting devices are integrated and controlled though the A-129 IMS. Primary armament consists of the TOW M-65 missile system, but space, weight, and power provisions have been incorporated into the A-129 design for FLIR Augmented Cobra Tow System (FACTS), Laser Augmented Aerial Tow (LAAT), and second generation missile systems.

The A-129 will also be fully provisioned with a full suite of Aircraft Survivability Equipment (ASE). Candidates for inclusion are Radar and Laser Warning Receivers, Radar and Infrared Jammers, and Flare and Chaff Dispensers.

The A-129 baseline system capabilities are listed in Table 1.

Configuration Flexibility

Due to its size and performance, the A-129 is an attractive candidate for a variety of weapons options as well as other combat helicopter roles and missions. The possible armament options range from the heavier more potent HELLFIRE to the ultra-lightweight air-to-air Multi-Launch Missile System (MLMS). With respect to differing roles and missions, there is strong interest in several NATO countries in a capable, survivable, multi-role attack/scout helicopter. Consequently, the A-129 design had to be versatile and flexible. And the design of the integrated cockpit had to be sufficiently flexible to accommodate conversion to either HOT or HELLFIRE and for MLMS or other air-to-air missile systems.

In the visionics arena, the initial A-129 prototypes will incorporate the nose mounted, day only, M-65 TOW Sight Unit (TSU), with provisions for LAAT and FACTS. However, several other visionics options are either in production or R&D which will enhance the capabilities of the A-129 as a survivable attack or scout helicopter. In particular, provisions have been incorporated into the A-129 cockpit design for conversion to a Mast-Mounted Sight/Target Acquisition and Designation System (MMS/TADS). This equipment, presently under development, will retain commonality with the TADS developed by the U.S. Army. The visionics package will be completed with PNVS and IHADSS (Integrated Helmet and Display Sight System).

Integrated System

The Integrated Multiplex System (IMS) provides this small helicopter with unprecedented flexibility, and extends its basic capability via integration and automation. The heart of the IMS is a redundant MIL-STD-1553B data bus communication and centralized data processing system. The multitude of functions performed by the IMS fall into four major categories:

Mission Electronics - Optimized integration of all mission equipment, including radios and navigation equipment, which provides for change and growth as well as efficiency. Performs navigation,

weapons delivery, and provides performance monitor capabilities.

Basic Aircraft Systems - Handling of electrical power distribution, power plant monitoring, caution and warning presentations, and integration of other general airframe related electronics. Provides checklists and status of integrated equipment.

Flight Control and Stability - Including motion sensors, digital stability augmentation systems, and flight director functions, plus a complete redundant backup fly-by-wire control system which can be engaged and disengaged at will.

Cockpit Control and Display - Including integrated flight management, equipment control, instrumentation, and workload reducing automation.

The cockpit is where the benefits of the IMS are most apparent. The need for a multitude of controls, switches, indicators, displays, and lights is eliminated. In their places are a single multifunction keyboard (MFK) unit and one or more video-type multifunction display (MFD) units for each crew position.

Schedule and Cost Objective

Agusta's objective is to enter production in the mid-1980's with a modern, versatile combat helicopter which is (1) capable of performing effectively and surviving in a NATO threat environment; (2) capable of being adapted to a variety of attack, scouting/reconnaissance, and battlefield management roles; and (3) reliable, maintainable and affordable.

Requirements Summary

In essence the basic requirements for the A-129 integrated cockpit design can be distilled as follows:

1) Control a comprehensive complement of aircraft/mission equipment
2) Flexibility to modify mission requirements with ease of fleet retrofit
3) Commonality of tandem cockpits
4) Limited cockpit real estate
5) Acceptability of crew workload
6) Integrated system approach to meet mission/weight requirements
7) Program cost and schedule objectives

Table 1. A-129 Baseline system capability

EQUIPMENT	INTEGRATED FUNCTIONS
COMMUNICATION/IDENTIFICATION UHF/VHF TRANSCEIVERS HF TRANSCEIVER IFF TRANSPONDER	COMMUNICATIONS CONTROL AND DISPLAYS PRESET SELECTION
NAVIGATION AIR DATA SYSTEM DOPPLER RADAR DIRECTIONAL GYRO RADAR ALTIMETER AUTO DIRECTION FINDER	NAVIGATION/FLIGHT CONTROLS FLY-BY-WIRE DOPPLER/AIR DATA NAVIGATION STABILITY/CONTROL AUGMENTATION ATTITUDE HOLD HEADING HOLD ALTITUDE HOLD GROUND SPEED/AIR SPEED HOLD VERTICAL SPEED HOLD HOVER COURSE HOLD WAYPOINT ENTRY COUPLED FLIGHT PLAN
FLIGHT CONTROLS VERTICAL GYROS (THREE) ACCELEROMETER TRIAD STANDBY INSTRUMENTS AFCS ACTIVATORS	
SURVIVABILITY EQUIPMENT RADAR AND LASER WARNING RECEIVERS FLARE AND CHAFF DISPENSERS	WEAPONS STORES MANAGEMENT WEAPONS DELIVERY FLIGHT CONTROLS
WEAPONS M-65 TOW TOW SIGHT UNIT 2.75 ROCKETS	POWER TRAIN ENGINE MONITOR SYSTEM ROTOR TRANSMISSION MONITOR HYDRAULICS MONITOR AND CONTROL VIBRATION MONITOR FUEL CONTROL FUEL MONITOR
ENGINE ROLLS ROYCE GEM-2 ENGINES (TWO) ENGINE MONITOR SENSORS	
FUEL ROTOR TRANSMISSION HYDRAULICS ELECTRICAL POWER DISTRIBUTION INTEGRATED COMPUTER/MULTIPLEX BUS SYSTEM	COCKPIT INTERFACE ELECTRICAL POWER CONTROL SUBSYSTEM CONTROL PERFORMANCE MONITOR STATUS CHECKLISTS

Cockpit System Design

The A-129 cockpit system design was constrained by requirements for duplicate capability in each cockpit and the limited real estate in each cockpit. A perspective view of the pilot's cockpit is shown in Fig. 3. Since all A-129 subsystems are not incorporated within the integrated system, some space was allocated to conventional controls and displays for these subsystems. The remainder of the cockpit was dedicated to the integrated cockpit system which functions as the crew/IMS interface. Programmable displays and controls for the integrated cockpit system were located to optimize visibility and accessibility. The balance of the cockpit real estate was budgeted by priority — criticality of information and control and/or frequency of usage.

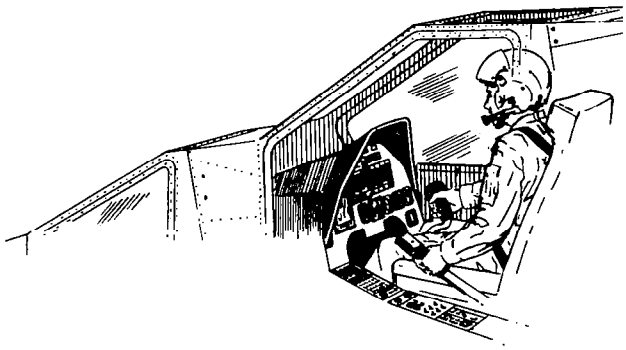

Fig. 3. Pilot cockpit perspective

The crew interface aspects of the A-129 IMS modular subsystems can be grouped into seven general categories:

1) Automatic Flight Control System (AFCS) is a high priority module that demands dedicated controls and displays.

2) Basic Equipment Controls and Displays are represented by callable display pages that have been translated from conventional control/display devices. Communications, Weapons Stores Management, Engine Monitor, Fuel, Rotor/Transmission, Hydraulics, Vibration, Electrical Power Control, and Utility (e.g., IMS test and configuration control) are subsystems that fall within this category.

3) Caution/Warning Subsystem consists primarily of dedicated programmable display space for instant presentation of alerts and a means of storing alerts for later retrieval.

4) Status Monitor Subsystem is a branching structure which collects and reports on-line BIT fault indications from throughout the IMS. Starting with a top level display, the crew can access lower level status summaries to isolate faults.

5) Performance Monitor Subsystem computes information required by the crew for mission planning.

6) Navigation Subsystem provides graphic and interrelated alphanumeric displays which allow the crew to use, control, or update the aircraft navigation.

7) Checklist Subsystem provides a semi-automated sequence for crew execution of procedures normally listed in flight manuals.

These seven subsystem categories are interfaced by the crew through a common basic dialogue design.

Basic Design

The cockpit system consists of two interface devices — a multifunction display unit (MFD), which is basically an interactive video display terminal, and a multifunction keyboard (MFK), which provides the control interface for the crew to select displays, create IMS entries, and manage the Automatic Flight Control System (AFCS). Cockpit panel space restricted the CRT for the MFD to a usable viewing area of only 4.80 inches square. Accounting for U.S. DOD and other recognized requirements on minimum character size, and the expected viewing distance, a maximum MFD data window (page size) of 15 lines and 28 characters per line was provided. A summary of character requirements and design parameters of the A-129 alphabet is shown in Table 2. The MFK was similarly constrained by the limited space in the upper left cockpit console area: the baseline A-129 allocation was 5.75 in. wide by 7.50 in. long, of which only about 50 percent could be utilized each for the AFCS controls and indicators area and the MFK keypad area. Despite the use of a maximum density U.S. DOD compliant keypad configuration, the requirement for full alphanumeric pilot entry capability limited the number of special function display call keys to 15. Access to all alphanumeric MFD data and controls representative of all subsystems integrated within the A-129 IMS therefore had to be prioritized under a 15 key hierarchy. The graphic displays are called by three dedicated MFD keys.

The A-129 control/display access hierarchy is shown in Fig. 4. At the far left are listed all dedicated control and display devices: these devices are available at all times for the A-129 crew usage. The second column lists all IMS subsystem displays and controls which are directly accessed by depressing one MFK or one MFD button. The third column lists all secondary subsystems and functions accessed through menus called by single button pressings, while the fourth column lists displays accessed only from the secondary menu displays or from other secondary display pages. The directly callable subsystem displays were selected with a sensitivity to pilot needs in the presently defined Agusta mission scenarios. Appropriate priority was given to basic aircraft

Table 2. A-129 Alphanumeric character font requirements and design (3)

PARAMETER	REQUIREMENT(1)	DESIGN
Vertical Height	20'(2)	0.192 in. (20' @ 33 in.)
Width to Height Ratio	60-100%	62.5%
Stroke Width to Character Height Ratio	12.5-14%	12.5%
Vertical Spacing (Between Characters)	≥1 Stroke Width	2 Stroke Widths
Horizontal Spacing (Between Lines, Relative to Character Height)	50%	62.5%

NOTES:

(1) Applicable requirements from "Human Engineering Design Criteria for Military Systems, Equipment, and Facilities, "MIL-STD-14728, Note 1, 10 May 1976; Woodson, W.E., Human Factors Design Handbook, 1981; and Shurtleff, D.A., How to Make Displays Legible, 1980.

(2) Symbol size must additionally be corrected for off-axis viewing angles per Reinwald (as published in Shurtleff, 1980).

(3) The font is 10x16 pixels with 2 pixel stroke width.

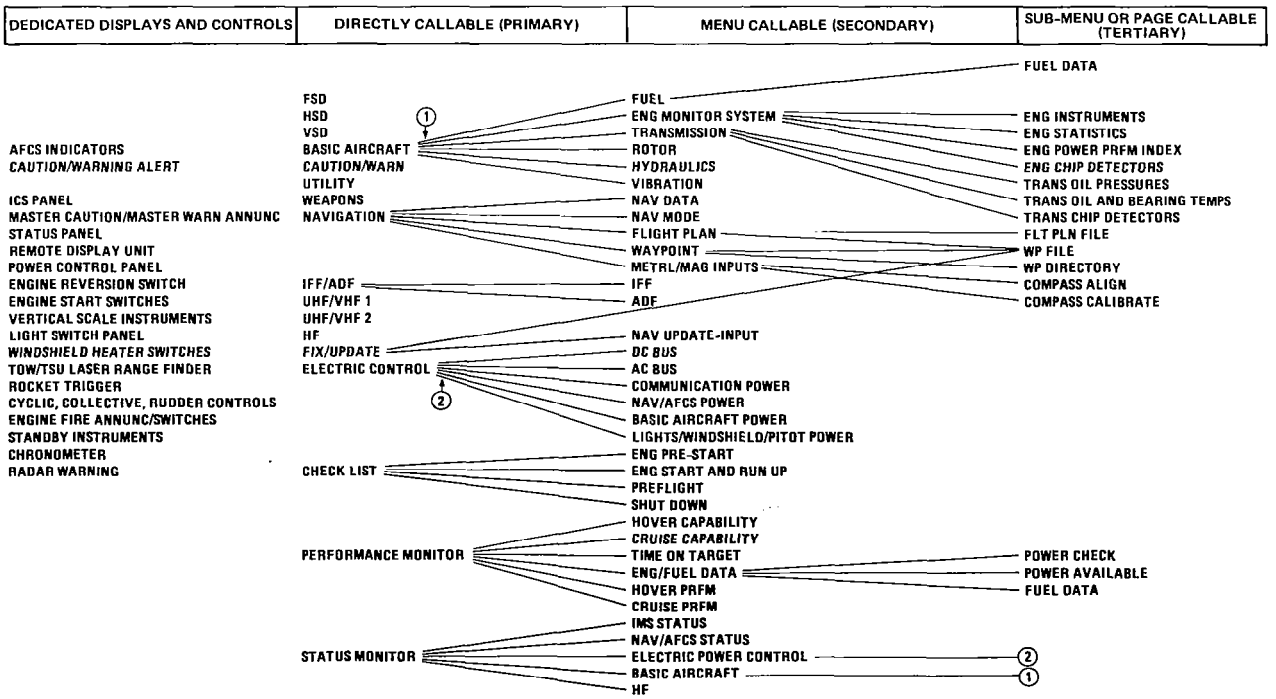

Fig. 4. Agusta A-129 control/display system hierarchy

subsystems (such as the Basic Aircraft subsystem, which accesses the Engine, Transmission, and Fuel subsystems, etc., as well as Electric Power Control that provides access to all remote control circuit breakers throughout the aircraft), the special graphics displays (which when coupled to the AFCS provide flight guidance cues), emergency and fault condition monitoring (Status, Caution/Warning), Navigation, and mission critical Weapons. Priority was also given to special requirements (such as the full complement of readily-accessed communications units) and automated pilot information aids (Performance Monitor and Checklists).

Enhancement of the pilot/IMS cockpit system interface was addressed through automation, systematic standardization of visual coding for control options and display types, and a friendly dialogue style requiring simple keyboard entries from the pilot and providing fixed visual prompts. Further automation is a subject for future growth. It has been implemented in the present IMS where tradeoffs with system complexity were acceptable. Automation is most apparent in the caution/warning alert generation and recording, in the collection of all on-line BIT type status information for easily accessed pilot viewing, in the coupled aircraft control and weapons delivery subsystem, in the aircraft performance monitor calculus, and in the manner in which sequences of displays were automated to follow a logical mission task orientation. A standardized method of information coding was implemented to help the pilot differentiate between data, control requests, and control status information displayed simultaneously on the same page. Some of these coding techniques included the use of character attributes: control status positions are designated by boxes, special timely or cautionary information is displayed in inverse video, and keypad entry control prompts are underlined. Coding conveys contextual information to the operator; standardization reduces training and learning requirements; and both simplify the task.

AFCS Design

The Automatic Flight Control System is managed by the pilot using the upper portion of the MFK. The AFCS interface includes IMS redundancy control, Fly-By-Wire (FBW) control, Stabilization functions (attitude hold, heading hold, vertical speed hold, altitude hold, airspeed and groundspeed hold, autotrim, and wings level) and Flight Director modes (hover, attack, course hold, and flight plan). The interface was implemented using 0.75 in square lighted legend pushbuttons for an integrated control/indicator design. Switches have visible legends (backlighted at night) and dead face indicators; legends are visible in full 10,000 footcandles ambient sunlight; indicators are color coded for daytime cue enhancement; legend lighting is compatible with present (second generation) Night Vision Goggle systems (NVGs).

IMS redundancy control switches allow the pilot to manually select one of two redundant processors or to engage the automated self-selection mode. Status indicators present operational status and passage of self-tests. The FBW switches control main rotor and tail rotor electronic control systems and arm the automatic sensing of control linkage severances. The Stabilization section of AFCS provides pilot control over A-129 augmentation systems in pitch, roll, yaw and collective, provides automatic hold in altitude, attitude, heading, and speed (vertical, ground, and air) and provides automatic trim and command to wing level attitude. All Stabilization modes have fly-through capability.

The Flight Director functions, in the display mode, provide flight cues to the pilot on the graphic situation displays. In the engage mode, the Flight Director operates as a full autopilot with fly-through capability. The Flight Director indicators, supplemented by aural alarms, are used for visual command cues while in the Flight Plan mode. The Flight Plan indicator flashes as waypoints are attained: this button must be depressed to commit to the next flight plan leg, otherwise the flight plan mode disengages.

Basic Equipment Control/Display Design

A generic example of pilot usage of the A-129 cockpit system for basic aircraft equipment control and monitoring is shown in Fig. 5. The hydraulics subsystem is first accessed by depressing the MFK "BSC ACFT" key. The MFD displays the basic aircraft menu list and the line address key adjacent to "HYD" is pressed to call the HYDRAULIC display page. This page contains switches for the three hydraulic power supplies and presents status information on the position of each switch, and present values from three pressure sensors and three temperature sensors. The HPS switches are controlled as shown. Pushing the line address keys shown operates the switches in rotating fashion with the present switch position always indicated by a box.

Pressure and temperature data is conveyed in digital format and in an analog gauge format. The gauge displays are analogous to dedicated cockpit instruments and provide dynamic range information as well as a "quick look" capability. Gauges may contain up to one "green", two "red", and two "yellow" zones as indicated by the steps shown. The boxed double arrow in the lower left hand corner of the display indicates paging options to the pilot. In this case, the pilot can slew the display "up" (allowing a return to the basic aircraft menu) or "down" (to the second page of hydraulics information). The box indicates that these options are enabled and available to the pilot via the MFD rocker switch.

Caution/Warning Subsystem Design

Caution and warning alerts to the pilot are critical to success of the mission and the safe operation of the A-129 aircraft. Accordingly, the caution/warning subsystem has a dedicated display: the 15th (bottom) line of all MFD graphic and alphanumeric displays. Other dedicated cockpit

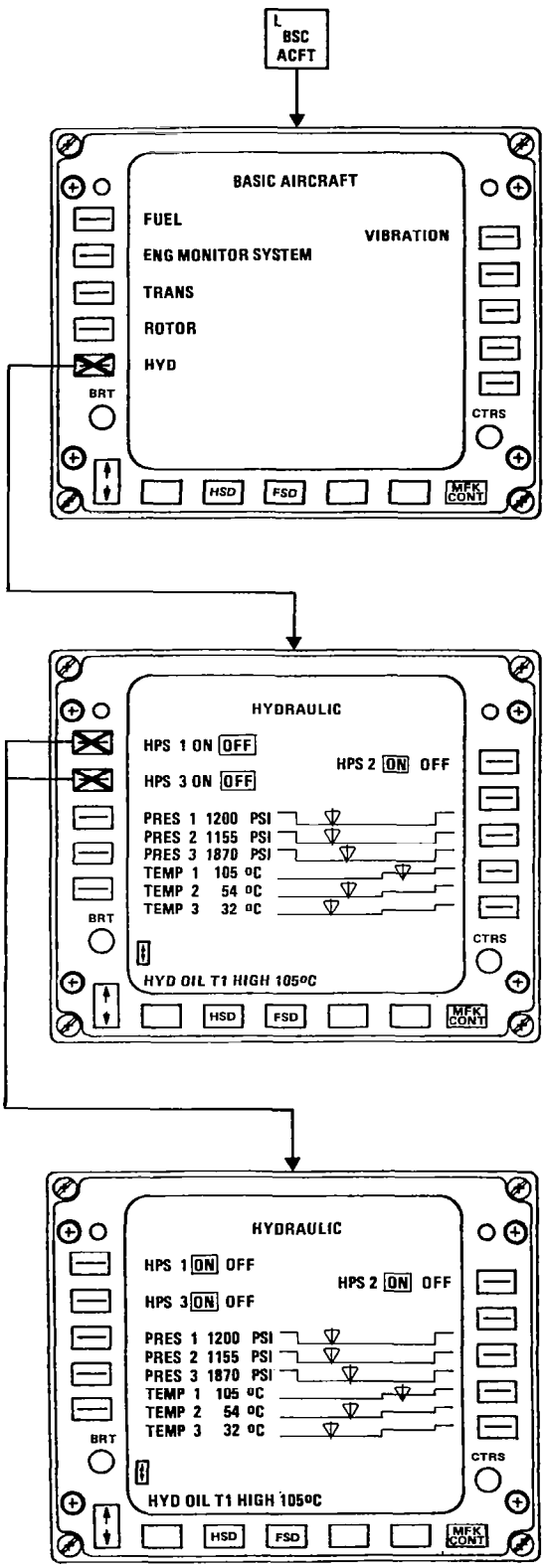

Fig. 5. Basic aircraft function

interface devices for this subsystem include the MASTER WARN and MASTER CAUTION annunciators and switches. Some critical warning alerts are accompanied by an audible alarm from the ICS.

The caution and warning subsystem for A-129 continuously compares data from various sensors and other subsystems to predetermined thresholds and failure criteria. When a caution or warning condition occurs, the alert name is presented on the MFD (in a priority queue with all warnings presented first) and the MASTER WARN or MASTER CAUTION annunciator is lighted. When the pilot acknowledges the alert by depressing the appropriate annunciator, the alert name and other information are entered into a quasi-LIFO list which is retained in nonvolatile memory for retrieval by the pilot or by ground support personnel. The list is accessed by depressing the MFK "CAUT" key and a sample display as shown in Fig. 6 is presented to the pilot. In addition to the alert name, information is also presented to indicate whether the alert was a caution or warning, whether it is a historical alert or is presently active, and whether the alert sensing device is inhibited or active. Line address keys adjacent to each caution/warning alert provide the capability of inhibiting (or re-activating) a sensor which may be faulty or to suppress repetitive presentations of the same alert. For switch type alerts, the number of occurrences is also reported. For analog sensor alerts, the value reported is always the highest value attained.

Status Monitor Subsystem Design

The status monitor subsystem continuously monitors and collates the status of on-line BIT results throughout the A-129 IMS system and presents this information to the pilot when the "STAT" key on the MFK is depressed. Two of the unique status monitor displays presently implemented on the A-129 IMS are shown in Fig. 7. Three information display conventions are used. A subsystem fault is indicated as a "NO GO" in inverse video. Absence of a fault indication for any subsystem is indicated simply by a blank field. Where it is possible to track down a fault condition from a subsystem to a lower equipment level, the inverse video NO GO is supplemented by a downward arrow symbol. Depressing the adjacent line address key calls up a lower-level display which may contain the fault. In the example shown, the IMS status is NO GO because of a failed Master Unit (MU 2) and a failed Data Bus (D/B) Test A. Lower level access to status information is available for the IMS equipment, the Navigation and AFCS equipment, the Electrical Power Control subsystem (e.g., remote circuit breaker trips), the Basic Aircraft subsystems, and the radios.

Performance Monitor Subsystem

The A-129 performance monitor subsystem provides information to the pilot for making preflight and inflight plans and decisions based on aircraft performance predictions. By viewing

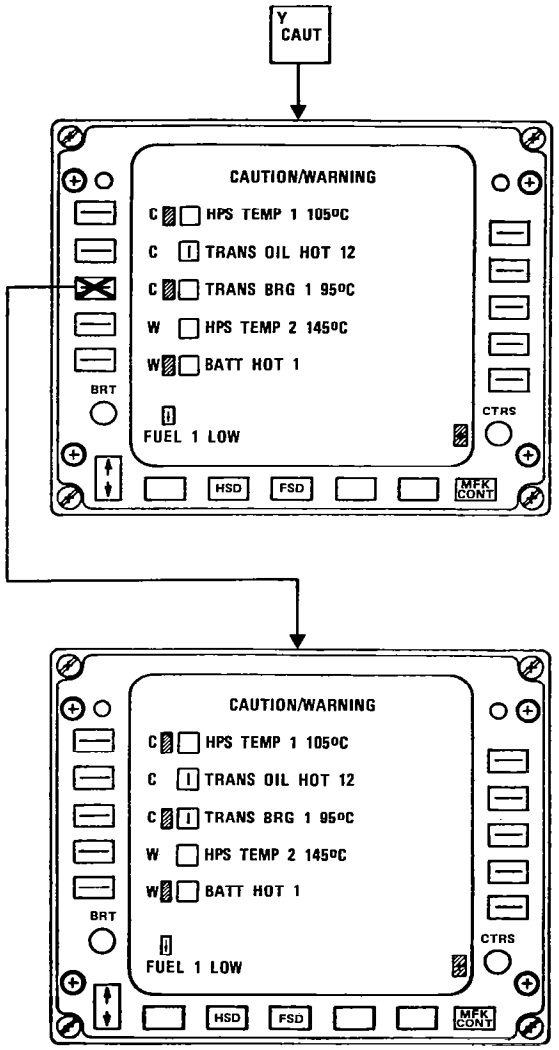

Fig. 6. Caution/Warning inhibit function

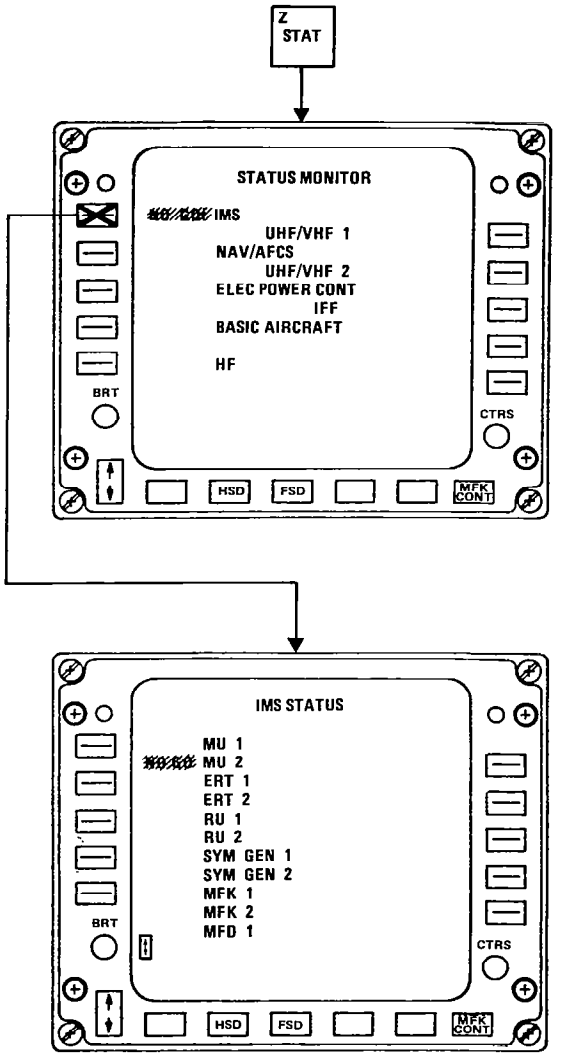

Fig. 7. Status function operation

the MFD, the pilot has available all information normally accessed in the typical pilot's flight manual. Data such as flight range, flight time, autorotation envelope, etc. are presented using either actual environmental conditions (e.g., OAT, ALT, etc.) from aircraft sensors or pilot input values for either preflight or inflight calculations. One of the most critical variables to these calculations, aircraft weight, is derived in real time by interaction with the weapons and fuel subsystems. Engine performance data calculated in the Engine Monitor Subsystem is utilized to provide actual aircraft performance characteristics. Predictions and calculations obtained through usage of the performance monitor subsystem are thus greatly improved over results formerly obtained through conventional pilot usage of manuals or nonintegrated standalone performance systems.

Navigation Subsystem

The navigation subsystem integrated within the A-129 IMS provides a highly complex, highly pilot-interactive, and highly automated capability that combines on-board sensors to calculate current aircraft position and progress against a prestored flight plan. When coupled with the AFCS in the flight director mode, a prestored flight plan can be executed automatically.

The principal sensors providing inputs to the A-129 navigation subsystem include three orthogonal accelerometers, Doppler velocity sensor, vertical gyros, TSU range and bearing data, magnetic heading, air data (air speed, barometric altitude, rate of climb), and radar altimeter. Interfaces with directional gyros and DF radios are also integrated within the navigation subsystem, allowing automatic tuning, compass/gyro synchronization, and compass calibration. Other

navigation subsystem functions include computation of track, cross track, and track angle errors; position update over a known waypoint, and target position acquisition by pilot input or TSU; computations of corrected heading considering magnetic heading variations and wind speed and direction.

The highly pilot interactive navigation subsystem accepts manual keyboard entry of up to 100 waypoints (specified by latitude/longitude or UTM coordinates, elevation and altitude, and a target/enemy/friendly designation) which may be arranged into as many as ten different flight plans. Full editing capability of flight plans and waypoints is provided. Flight plans can be created prior to flight or while in flight and allow a fly-to-waypoint capability. Other pilot interactive capabilities include the selection of navigation mode, input of meteorological and magnetic data, waypoint fix in offset or flyover modes, and navigation update in flyover or manual position input modes.

Besides an alphanumeric navigation data page, the primary display outputs of the navigation subsystem are the graphic situation displays — the Horizontal Situation Display (HSD), Forward Situation Display (FSD), and Vertical Situation Display (VSD). The A-129 HSD is shown in Fig. 8. The HSD is a graphic map display with compass rose, a variety of aircraft control and guidance cues, several aircraft performance indications, and flight plan related data. Aircraft control cues include aircraft heading, aircraft track, a track-offset based steering cue, a digital aircraft course readout, and a crosstrack error scale. Aircraft flight performance indicators present digital values for air speed, ground speed, and vertical speed and direction. Flight plan related data that are presented on the HSD include a connected waypoint sequence with leg distances, interest and avoidance area waypoints, waypoint type, number, and alpha identifiers, selected flight plan number, next waypoint, time and distance to next waypoint, and time remaining on target.

Other display related information included on the HSD are the display scale and map orientation, both of which are pilot-controllable using the MFD line address keys and rocker switch. As in all MFD display formats, the HSD has dedicated fields for a pilot entry scratch pad and for presentation of caution/warning alerts.

The FSD is a subset of the HSD with the aircraft in the lower center of the screen. A linear course prediction line is also provided. The VSD is similar in concept but it displays a perspective ground plan pictorial relative to aircraft position, aircraft to ground and aircraft to tree top distance cues, and aircraft velocity vectors in all dimensions.

Checklist Subsystem

The A-129 checklists subsystem provides a semi-automated mechanism for interactive control and prompting of pilot procedures normally performed with flight manuals. Engine Pre-Start, Engine Start and Run-Up, Preflight, and Shut Down procedures are implemented as sequences of alphanumeric checklist pages with quick access to other subsystem status pages where required (e.g., to monitor aircraft oil pressures and temperatures during run up).

Future Activities

The definition and design phases of the A-129 integrated cockpit system are complete. The implementation phase is currently under way. The next steps in the system evolution are the integration of the many IMS subsystems, checkout of the A-129 prototype, field trials, and eventually production.

Parallel with the cockpit system implementation phase a simulation is being constructed which mechanizes the display hierarchy. This computerized simulator will serve a dual function: 1) to familiarize the test pilots with the integrated system and gain their acceptance, and 2) to provide pilot feedback for system fine tuning.

The system integration and checkout phases of the A-129 IMS will provide the first real measure of pilot workload. The overall goal of the IMS cockpit design is obviously to enhance pilot mission performance through reduction of the workload associated with normal aircraft control and mission operations. The pilot acceptability of the workload reduction afforded by the IMS cockpit system is ultimately the final measure of success.

Integration and checkout phase activities will be followed by the A-129 operation and field trial phase. This will be the final test of the IMS cockpit design concept, and the outcome of this

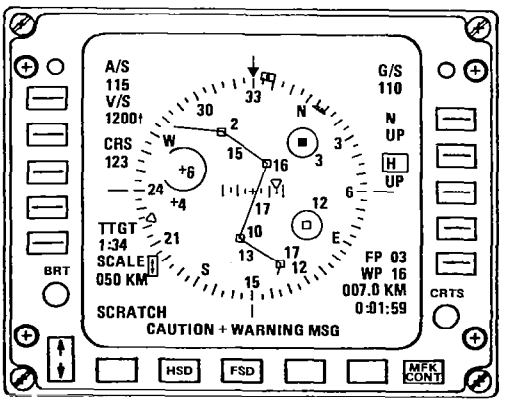

Fig. 8. Horizontal situation display

phase will be the production IMS system baseline. The test trials will provide an environment for further evaluation of the design in meeting multi-mission sortie requirements, another opportunity to evaluate the pilot acceptability of the workload. To improve system orientation to a particular mission, field trial results may indicate the need to retrofit the A-129 cockpit design. Any subsequent redesign activity will be easily accommodated by the overall flexibility and modularity of the cockpit system design.

During the production phase and remainder of the life cycle of the A-129 IMS, many opportunities to enhance the cockpit system design and aircraft mission capability will occur. The new emerging technologies in pilot interactive devices (e.g., visionics, supplemental helmet mounted displays, voice recognition command and synthesized voice alerts, color CRTs for additional information coding and workload reduction, digital moving maps and perspective terrain presentations, etc.) are all software-driven. At the center of the A-129 integrated cockpit system is a separate operator interface software subsystem. This system architecture isolates and thereby simplifies the process of updating the cockpit interface design to accommodate emerging technologies.

There are of course many different approaches to pilot interaction in an integrated cockpit design. The approach we have followed incorporates a set of concepts which represent a quantum advance to integrated cockpit technology. We anticipate that this design evolution will provide information to foster further development of standards for cockpit interface systems, thereby freeing future creative effort to concentrate on other technology aspects of the operator interface.

Concluding Remarks

The A-129 integrated cockpit design is driven by a stringent requirement for handling a sophisticated system within a small cockpit area. This has resulted in a highly integrated system.

Its conceptual design has been completed and it is in the implementation stage. In a short time the prototype models will be integrated with the A-129 helicopter systems and then they will be field tested. At this point the design will have matured to a state that it will be ready for production and deployment.

The modularity of the integrated system's software has separated the subsystems to permit easy retrofitting of new or other subsystems required to support new mission requirements. This modular design was carried into the integrated cockpit design so that the controls/displays of additional subsystems can be easily incorporated. This modular approach was also planned to permit the incorporation of new developments in the design of cockpit interface equipments. Hopefully this degree of technology independence will permit cost-effective optimization of the A-129 during its fielded life while maximizing operational capability.

Flight tests of the A-129 prototypes will provide data to verify the integrated cockpit design approach, which will then be useful in establishing pilot accepted standards that may become as popular as round dials have been in the past.

NEW DEVELOPMENTS IN FLYING QUALITIES CRITERIA WITH APPLICATION TO ROTARY WING AIRCRAFT

Roger H. Hoh
Principal Research Engineer
Systems Technology, Inc.
Hawthorne, California

Abstract

Some recent considerations and developments in handling quality criteria are reviewed with emphasis on using fixed wing experience gained in developing MIL-F-8785C and the more recent Mil Standard and Handbook. Particular emphasis is placed on the tasks and environmental conditions used to develop the criterion boundaries, SAS failures, and potential fixed wing criteria that are applicable to rotary wing aircraft.

Introduction

Historically, the handling qualities of rotary wing aircraft have been vastly inferior to their fixed wing counterparts. For example, the pitch attitude control of many operational helicopters will not even meet the Level 3 requirements of MIL-F-8785C. (Level 3 is defined as a Cooper-Harper rating of worse than 6-1/2 or "Flying qualities such that the airplane can be controlled safely but pilot workload is excessive or mission effectiveness is inadequate or both."). An example is illustrated in Fig. 1 where it is shown that the time to double amplitude for several operational helicopters is in the extreme Level 3 region. The major deficiencies of rotary wing aircraft are nearly always associated with: excessive cross-axis coupling; inadequate dynamic stability; and unacceptable stick force gradients. Interestingly, the Cooper-Harper pilot ratings from many helicopter handling quality studies (for example, Refs. 1 and 2) indicate that rotary wing pilots are willing to accept much less than their fixed wing counterparts. This is shown in Fig. 2 where pilot ratings of 2 to 3-1/2 are found well into the Level 2 region defined for pitch control in MIL-F-8785C. (Level 2 corresponds to pilot ratings of 3-1/2 to 6-1/2 in MIL-F-8785C.) This is felt to occur for two reasons: 1) helicopter pilots are trained to cope with, and expect as "normal," severe instabilities and cross-axis coupling; and 2) the tasks used in the evaluations were not sufficiently demanding.

Consideration of Handling Quality Evaluation Tasks

In recent years the task used in experiments to obtain handling quality pilot ratings has been found to have a profound effect on the results. For example, in the landing approach experiments of Ref. 4 the pilots were required to touch down at a precise point on the runway. In a paper presented to the AGARD Flight Mechanics Panel in 1981 the authors of Ref. 4 cited a case where a pilot gave a surprisingly good rating to what should have been a particularly poor configuration. However, the landings were not in the prescribed touchdown area and the author (who was also the safety pilot) insisted that the evaluation pilot improve his performance. On the very next run, in an attempt to achieve the required precision, a severe PIO was encountered near touchdown. Needless to say, the

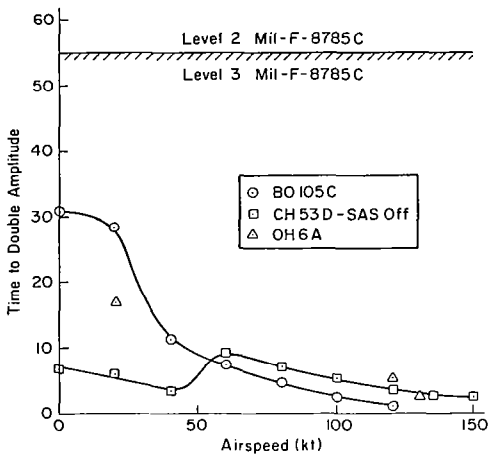

Fig. 1 Illustration that conventional unaugmented helicopters fall well below fixed wing standards even for a failed SAS (data from Ref. 3)

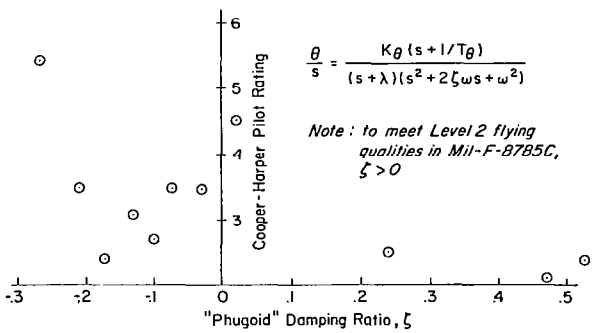

Fig. 2 Cooper-Harper pilot ratings vs. damping ratio in hover; $\omega < 0.5$ rad/sec (data from Ref. 1)

evaluation pilot revised his rating downward considerably. The point here is that only by insisting on a precision task was the experimenter able to expose deficient handling qualities that would have otherwise gone unnoticed. In using existing data to develop boundaries for the helicopter handling qualities specification, we must critically evaluate the task. Some suggested evaluation factors might be:

1) Does the task require the same precision as required by operational missions?

2) Does the task require the same degree of aggressive maneuvering as the proposed operational missions?

3) Are the tasks well defined, or does the task encompass a series of subtasks such as an entire approach, hover, and vertical descent? If the latter is true, can we identify what subtask has the most impact?

4) Are the data being used as a compromise because no better data are available?

5) Are the atmospheric disturbances of low enough frequency and large enough magnitude to displace the aircraft from its path?

6) Are the available outside visual cues consistent with the proposed mission?

Unfortunately, these factors may well eliminate most existing data. The last factor was found to be especially important for low speed and hover in Refs. 5 and 6 and is briefly reviewed in the following section.

Effect of Outside Visual Cues on Required Level of Augmentation and Display

Most of the available data for low-speed and hover handling criteria have been obtained with good visual outside references and with no requirement for unattended operation. The real-life existence of secondary tasks, and intermittent to total loss of visual references, places increased demands on the pilot -- an effect which is not discernible from such data. For example, pilot ratings for an unaugmented helicopter (Ref. 2) and a highly augmented translational rate command (TRC) system (Ref. 7) all fall within the acceptable region (pilot rating better than 3.5). This result is a consequence of experimental scenarios that tend to be tailored toward the systems being investigated. That is, with pure rate systems the scenario is usually benign, thereby usually allowing intense, full-time attention; whereas with a translational rate command system the task tends to be more demanding. The most critical contributor to the total pilot workload appears to be the quality of out-the-window cues for detecting aircraft attitudes, and, to a lesser extent, position and velocity. Currently, these cues are categorized in a very gross way by designating the environment as either VMC or IMC. A more discriminating approach is to classify visibility in terms of the detailed attitude and position cues available during the experiment (or proposed mission), and to associate handling qualities requirements with these finer-grained classifications.

The need for certain specific outside visual cues has been inferred from closed-loop considerations. These OVC levels have been logically quantified in terms of a scale as shown in Fig. 3a. Certain specific closed-loop considerations, which were considered in formulating the scale, are summarized below and by the generic closed-loop structure in Fig. 3b.

1) A requirement for closure of the attitude loop implies VMC conditions and must prevail for adequate control.

2) If the equivalent system dynamics require closure of position and position rate, but not attitude, a minimum set of operating conditions quantified as OVC = 3 is defined.

3) OVC = 4 quantifies the operating condition where velocity and attitude cues are not available; that is, only the outer loop in Fig. 3b can be closed by the pilot.

4) OVC = 5 indicates that no outside visual cues are available.

Pilot workload can also be reduced via improved displays. Recent work in the control/display tradeoff area includes the Calspan X-22 flight tests (Ref. 8) and the CH-46 variable-stability helicopter (Ref. 9).

Based on the above considerations, the required level of augmentation and cockpit displays can be related to the visibility levels associated with the missions defined for the helicopter. An initial attempt was made to establish a format for specifying the augmentation and displays required for various levels of outside visual cues in Refs. 1, 4, and 5 and is repeated in Table 1 for convenience.

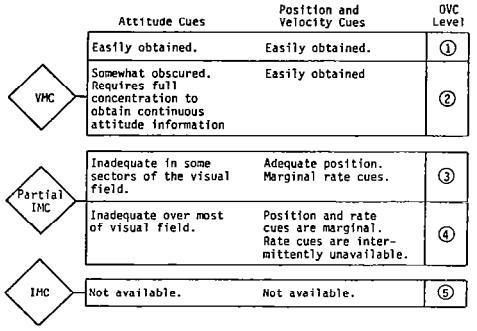

a) Quantification of Outside Visual Cues (OVC)

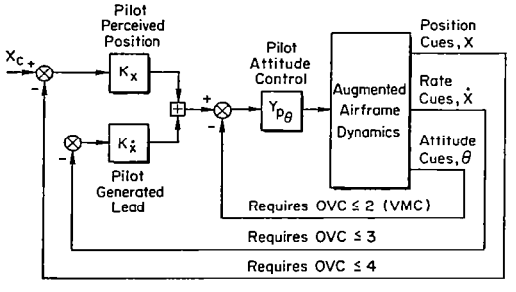

b) Required Outside Visual Cues for Control

Fig 3 Development of outside visual cue scale

Table 1. Augmentation and displays required for various levels of outside visual cues

Augmentation	MIL-F-8785C flying quality level	Pilot display: Raw data	Pilot display: Mechanical flight director	Pilot display: Integrated display-flight director plus aircraft velocity information
Rate	Level 1	1	2	3
	Level 2	2	4	5
Rate command/ attitude hold	Level 1	2	3	3
	Level 2	2	5	5
Attitude (response feedback)	Level 1	2	3	3
	Level 2	2	5	5
Attitude (model following)	Level 1	2	4	4
	Level 2	2	5	5
Translational rate with attitude	Level 1	3	5	5
	Level 2	3	5	5
Translational rate with direct force control	Level 1	3	5	5
	Level 2	3	5	5

SAS Failures

The concept of "Levels" is used in MIL-F-8785C to specify the allowable degradation in handling qualities in the presence of failures. The specification of Level 2 and 3 handling qualities will tend to be more critical in rotary wing aircraft in terms of driving the cost and complexity of the SAS. This is a result of the relatively poor handling qualities of the unaugmented helicopter and hence the large change in dynamics before and after a failure of the SAS. This is illustrated in Fig. 4, which shows a dramatic shift in the characteristic modes after a SAS failure in the CH-53D. Clearly, the specification of Level 2 handling qualities that are better than most unaugmented helicopters would have significant implications on complexity and cost.

Potential Fixed Wing Criteria Applicable to Rotary Wing Aircraft

The mission requirements for rotary wing aircraft have become increasingly severe to the point where marginal handling qualities can no longer be tolerated. In most cases satisfactory inherent stability and coupling cannot be obtained without some level of stability augmentation. Indeed, many modern helicopters employ a stability augmentation system. It is therefore not unreasonable to expect the same quality of response (to control inputs and turbulence) in helicopters that is currently enjoyed by fixed wing pilots. In fact, the rapid and precise maneuvering required in some NOE missions may make it necessary to impose more stringent requirements than are necessary for fixed wing aircraft.

The applicability of some requirements currently proposed for the fixed wing Mil-Standard to rotary wing aircraft are reviewed in the following paragraphs.

Lower-Order Equivalent Systems

The basic intent of lower-order equivalent systems is to define a very high-order system in terms of a few variables that describe the fundamental response characteristics important to the pilot (see Ref. 10). This can be done in the time domain or in the frequency domain, although all work done to date has been in the frequency domain. Equivalent systems are a viable concept for defining Level 1 flying qualities for helicopters.

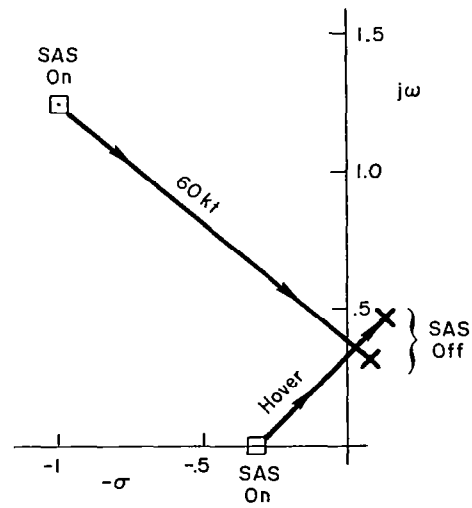

Fig 4 Effect of SAS failure on key response modes of CH-53D (Data from Ref. 3)

However, the complexity of the responses of unaugmented helicopters, due to inter-axis coupling, makes it unlikely that useful equivalent system forms of sufficient generality can be defined for the Level 2 and 3 boundaries.

Bandwidth Criterion

The bandwidth criterion was developed originally for fixed wing aircraft with direct force control. Because of the almost infinite variety of responses that can occur due to inter-axis coupling, it was difficult to define a lower-order equivalent system form for aircraft with direct force control. In looking for an alternative solution it was hypothesized that the coupling itself was incidental, and mattered only to the extent that it interfered with the pilot's ability to adequately perform tight closed-loop tracking. This of course is directly related to the bandwidth, which was defined in Ref. 11: "The bandwidth of the specified response to a particular control input is defined as the lowest frequency for which the (open-loop) phase margin is at least 45 deg and the gain margin is at least 6 dB." (See Fig. 5 for a graphical description.)

The Ref. 11 variable-stability in-flight simulation results indicated that the Bandwidth Hypothesis was indeed valid, i.e., the coupling itself mattered only to the extent that it affected bandwidth. These results were extended to pitch attitude control in Ref. 12.

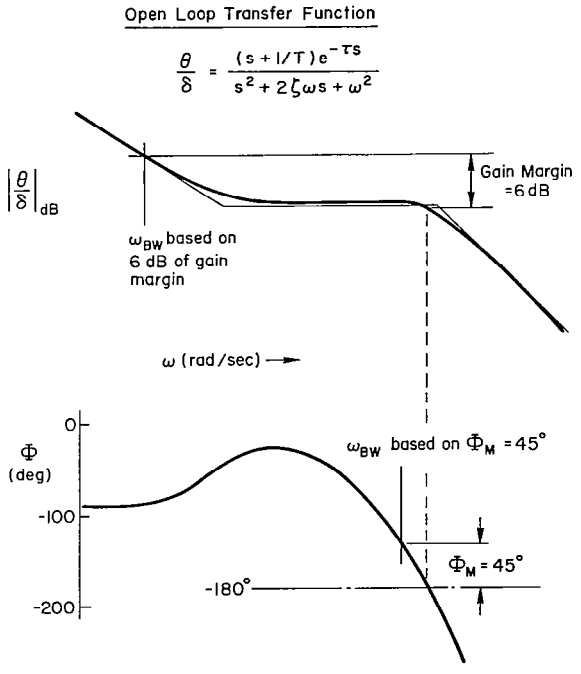

Fig. 5 Effect of using gain and phase margins to define bandwidth

From a pilot's point of view, a high-bandwidth response would be described as "crisp" or perhaps "rapid and well damped." Typical commentary for a low-bandwidth response might be "sluggish response to control input" or "tends to wallow." There is a long history of correlating such commentary with basic aircraft stability derivatives and/or parameters made up of such derivatives (e.g., $\omega_{sp} \doteq \sqrt{Z_w M_q - M_\alpha}$, etc.). The term bandwidth comes more naturally into play when feedbacks and crossfeeds are combined to produce aircraft responses that are unconventional in that the classical modes are no longer appropriate definitions.

The advantage of this approach is that it does not assume a particular form of response. Hence it may be suited for helicopters, where coupling tends to mask the classical response forms. The deficiency of the bandwidth criterion in its present form is that it does not directly account for the pilot's ability to supply crossfeeds to counteract coupling. It seems intuitively obvious that responses requiring only a simple crossfeed (such as pure gain) would be more acceptable than those requiring complex shaping. This concept was investigated in Refs. 13 and 14 for the turn coordination problem in fixed wing aircraft and is reviewed briefly in the following section.

Inter-Axis Coupling

Inter-axis coupling is well recognized as one of the most severe handling quality problems with unaugmented rotary wing aircraft. While fixed wing aircraft tend to be much less affected by such coupling, a significant amount of yaw response to roll control inputs is not uncommon at high angles of attack. In such cases the pilot must use rudder coordinated with aileron inputs to eliminate the undesirable heading excursions that occur. It was hypothesized in Ref. 14 that the pilot opinion of roll-yaw coupling would be directly related to the magnitude and shaping of the rudder control required. Such an approach is expected to be directly applicable to the inter-axis coupling characteristics of helicopters. Because of its possible direct application to helicopter coupling, the results of Ref. 13 are briefly described below.

While the use of "coordinated" aileron and rudder is accepted as common piloting technique, a quantitative measure of what exactly is acceptable or desirable is not known. The purpose of this study was to provide a quantitative measure of the aileron-rudder sequencing required to eliminate roll-yaw coupling and thereby achieve coordinated turns, and to correlate this with pilot opinion ratings from available data. To achieve this end Ref. 13 considered the aileron-to-rudder crossfeed necessary to exactly cancel the inter-axis coupling. This idealized crossfeed provides a measure of pilot acceptability of heading control because it is indicative of: the complexity of the rudder activity necessary to achieve perfectly coordinated turns; and the heading excursions that occur when the pilot does not use rudder. Note that these considerations apply equally well to the known coupling between pedal, power, cyclic and collective in an unaugmented helicopter.

Two parameters are defined in Ref. 13: μ, which defines the shaping of the rudder crossfeed; and $N'_{\delta_{ac}}/L'_{\delta_{ac}}$, which defines the magnitude. The frequency response characteristics of the aileron-to-rudder shaping as a function of the sign of μ are shown in Fig. 6 in terms of literal expressions for the Bode asymptotes. These asymptotes indicate that the magnitude of the rudder required to coordinate is a function of $N'_{\delta_{ac}}/N'_{\delta_{ac}}$ at all frequencies and that the shaping of the rudder response is determined by μ. These parameters are summarized in terms of their analytical and pilot-centered functions in Table 2.

The details of the criterion are presented in Refs. 13 and 14. The criterion boundaries and the data used to support these boundaries are given in Fig. 7. It is interesting to note that the ideal crossfeed was not a pure gain ($\mu = 0$). Actually, a little proverse yaw ($\mu = -1$) is seen to be desirable. Similar results could be expected with helicopters, i.e., the coupling can actually be favorable.

Conclusions

A great deal of the experience gained in developing handling quality criteria for fixed wing aircraft is directly applicable to rotary wing aircraft as well. In this paper we have reviewed a

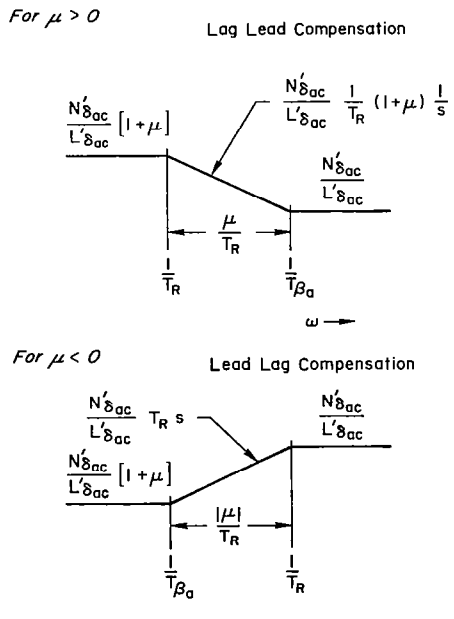

$\bar{\delta}_{rc}$ = normalized rudder control

$\bar{\delta}_{ac}$ = normalized aileron control

Fig. 6 Asymptotes of aileron-rudder crossfeed

Table 2. Parameters defining the aileron-rudder crossfeed

Parameter	Analytical function	Pilot-centered function
μ	Defines shape of Y_{CF}	Determines complexity of rudder activity necessary for ideally coordinated turns; also defines phasing of heading response when rudder is not used.
$N'_{\delta_{ac}}/L'_{\delta_{ac}}$	Defines magnitude of Y_{CF}	Determines magnitude of required and/or high-frequency yawing induced by aileron inputs.

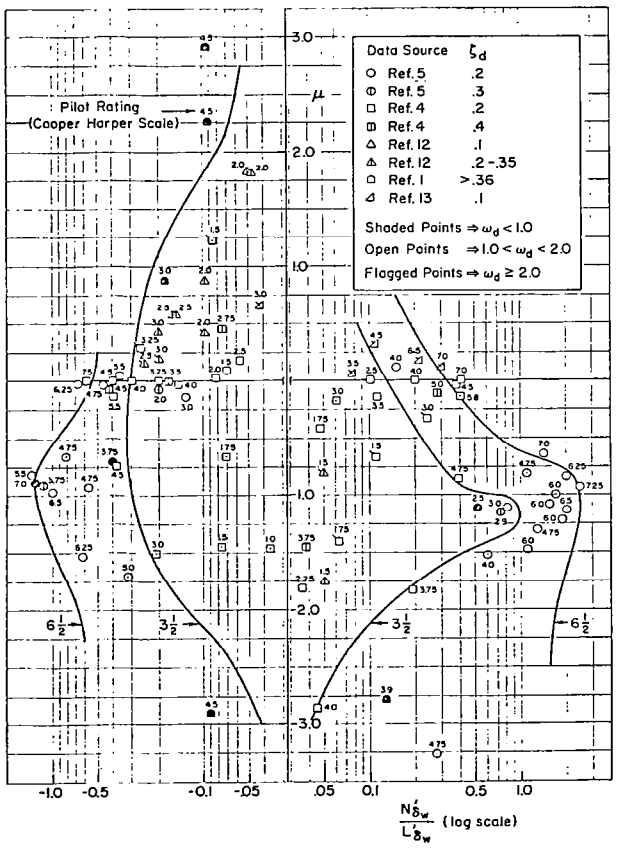

Fig. 7 Pilot rating correlation with crossfeed parameters

few areas that seem particularly salient. Summarizing, these are:

1) The piloting task and environment are overriding considerations in developing and using handling quality criterion boundaries.

2) Helicopter pilots have historically been willing to put up with considerably more degraded handling qualities than have fixed wing pilots. The increasing severity of helicopter missions is reversing this trend.

3) Outside visual cues and cockpit displays must be considered when structuring a helicopter handling quality specification.

4) The poor inherent handling qualities of rotary wing aircraft make SAS failures more critical than for fixed wing aircraft. Attempting to impose fixed wing requirements for Levels 2 and 3 is probably not practical in terms of cost and complexity.

5) Many handling qualities criteria developed for fixed wing aircraft should be directly applicable to helicopters with appropriate revisions in the numerical limits and boundaries.

References

1. Hoh, R. H., and Ashkenas, I. L., "Development of VTOL Flying Qualities for Low Speed and Hover," NADC-77052-30, Naval Air Development Center, Warminster, PA, Dec. 1979.

2. Seckel, E., Traybar, J. J., and Miller, G. E., "Longitudinal Handling Qualities for Hovering," Princeton University, Department of Aeronautical Engineering, Rept. 594, Dec. 1961.

3. Heffley, R. K., Jewell, W. F., Lehman, J. M., and Van Winkle, R. A., "A Compilation and Analysis of Helicopter Handling Qualities Data. Volume One: Data Compilation," NASA CR-3144, Aug. 1979.

4. Smith, R. E., "Effects of Control System Dynamics on Fighter Approach and Landing Longitudinal Flying Qualities (Volume I)," AFFDL-TR-78-122, Air Force Flight Dynamics Laboratory, Wright-Patterson AFB, OH, Mar. 1978.

5. Hoh, R. H., and Ashkenas, I. L., "Effect of Reduced Visibility on VTOL Handling Quality and Display Requirements," Journal of Guidance and Control, 4, (2), Mar.-Apr. 1981.

6. Hoh, R. H., and Ashkenas, I. L., "Handling Quality and Display Requirements for Low Speed and Hover in Reduced Flight Visibility," Journal of the American Helicopter Society, 26, (1), Jan. 1981.

7. Bryant, W. B., Cattel, J. C., et al., "VTOL Advanced Flight Control System Studies for All-Weather Flight. Vol. I: Task I Report," USAAMRDL-TR-75-13A, July 1975.

8. Lebacqz, J. V., and Aiken, E.W., "A Flight Investigation of Control, Display, and Guidance Requirements for Decelerating Descending VTOL Instrument Transitions Using the X-22A Variable Stability Aircraft. Vol. I: Technical Discussion and Results," Calspan Corp., Buffalo, NY, Rept. AK-5336-F-1, Sept. 1975.

9. Niessen, F. R., Kelly, J. R., Garren, J. F., et al., "The Effect of Variations in Controls and Displays on Helicopter Instrument Approach Capability," NASA TN D-8385, Feb. 1977.

10. Hodgkinson, J., and LaManna, W. J., "Equivalent System Approaches to Handling Qualities Analysis and Design Problems of Augmented Aircraft," AIAA Atmospheric Flight Mechanics Conf., Hollywood, FL, 8-10 Aug. 1977.

11. Hoh, R. H., Myers, T. T., Ashkenas, I. L. Ringland, R. F., and Craig, S. J., "Development of Handling Quality Criteria for Aircraft with Independent Control of Six Degrees of Freedom," AFWAL-TR-81-3027, Air Force Wright Aeronautical Laboratories, Wright-Patterson AFB, OH, Apr. 1981.

12. Hoh, R. H., Mitchell, D. G., and Hodgkinson, J., "Bandwidth -- A Criterion for Highly Augmented Airplanes," AIAA-81-1890, AIAA Atmospheric Flight Mechanics Conference, Albuquerque, NM, 19-21 Aug. 1981.

13. Ashkenas, I. L., Hoh, R. H., and Craig, S. J., "Recommended Revisions to Selected Portions of MIL-F-8785B(ASG) and Background Data," AFFDL-TR-73-76, Air Force Flight Dynamics Laboratory, Wright-Patterson AFB, OH, Aug. 1973.

14. Hoh, R. H., and Ashkenas, I. L., "Handling Quality Criterion for Heading Control," Journal of Aircraft, 14, (2), Feb. 1977.

HELICOPTER SIMULATION TECHNOLOGY: AN AMES RESEARCH CENTER PERSPECTIVE

Richard S. Bray
Ames Research Center, NASA, Moffett Field, California

Abstract

Helicopter handling qualities have been the subject of many simulator programs at Ames Research Center over the past decade. The earlier experiences, in fixed-cockpit simulators, demonstrated the basic difficulties of simulating the inherently complex control tasks of helicopter flight to the level of subjective fidelity required for confident evaluation. It became recognized that deprivations in visual and motion cueing were probably major factors in the problem. More recent simulations have utilized large-amplitude cockpit motion systems, and efforts have been made to optimize the effectiveness of the visual simulations. This paper reviews the total experience for evidence regarding the levels of motion- and visual-cueing fidelity required for handling-qualities research in ground-based simulators. Positive contributions of cockpit motion were identified, but much remains to be learned regarding the sensitivities of individual control modes to cueing attenuation. A firmer understanding of the pilot's utilization of visual and motion cues is the key to more efficient use of simulation in helicopter control-systems research.

Introduction

Flight-simulation technology is especially challenged by the helicopter. Mathematical modeling and verification procedures are difficult. Flight modes include those often characterized by low stability and cross-axis control coupling, conditions that tend to produce unrealistically high workloads in simulation. A sense of realism, better termed subjective fidelity, in the simulated flight task is essential for its use in research; and, depending on the research objective, some moderate to high level of objective, or engineering, similarity to the flight task is required to create that realism. There is no basic obstacle to the attainment of objective fidelity in the simulation of an aircraft except in the areas of cockpit motion and the outside visual scene. At best, simulation can provide only part of the cues available in the aircraft. The effects of these deprivations, their individual contributions to the diminution of subjective fidelity, is not clearly understood; they have not been subjected to adequate study. In the absence of better information, research simulations are configured and used in the manner that experience indicates to be probably effective.

It is the objective of this paper to review recent helicopter simulation experience at Ames Research Center for evidence relating fidelity of motion and visual cueing to subjective fidelity and confidence in research results. The scope of this experience in terms of objectives, facilities, and simulated flight tasks is briefly described. Approaches to optimization of the utilization of unique cockpit motion- and visual-simulation capabilities are discussed, and several experiences that offer hints regarding the role of vertical acceleration in hovering tasks are described. Concluding remarks address the need for a firmer understanding of the effects of cueing deprivations and suggest a program of directed research on the subject.

Scope of Research Activities

Objectives and Tasks

Several papers presented at this meeting discuss recent helicopter research conducted in Ames simulators. A series of handling-qualities studies, in the context of a "nap-of-the-Earth" flight task, is discussed in Ref. 1. That paper touches on the relationships of simulation facilities and procedures to the interpretation of results. The results of tests to guide the development of helicopter IMC flight certification criteria are presented in Ref. 2. Control systems and guidance displays were evaluated in an ILS-like approach that included deceleration to hover on instruments. The study of Ref. 3 closely examined variations in engine and control-system response in critical height-control maneuvers. This simulation required optimized visual cues and, like the study of Ref. 2, anticipated benefits from the utilization of a simulator with a large-amplitude cockpit motion system. Motion- and visual-cueing considerations in that study will be expanded upon in a later section of this paper.

Although these are typical of helicopter simulation studies being conducted at Ames, others must be mentioned to indicate the broad scope of objectives pursued. The XV-15 Tilt Rotor aircraft has been the subject of simulation exercises for the 9 years since concept proposals were evaluated. This program, conducted in support of the vehicle development and flight tests, used a variety of Ames facilities; it is documented in Ref. 4. Another example of support of a research aircraft is the recent simulator studies defining optimum operating procedures for the winged, or "compound" version of the Rotor Systems Research Aircraft (RSRA). A dedicated simulator cab is being constructed for continued support of the two flight vehicles.

Individual simulator exercises in these flight-support programs might have one or several specific objectives, but collectively they involve tasks covering the operational envelope of the aircraft. They represent a specific challenge and opportunity. The requirements for fidelity are severe, but since the aircraft exists in a flight-test configuration, the opportunities for verification are excellent. Reference 4 reports several illuminating exercises comparing simulation responses with those of the Tilt Rotor aircraft, and relating them to the pilot's subjective impressions.

Another helicopter research effort in its early stages is one that joins VTOL studies in addressing the special guidance and control problems of approaching and landing on a destroyer in very adverse weather, perhaps among the most difficult tasks to simulate adequately. This task will also be the subject of further discussion.

A number of helicopter simulations have been used in terminal-area traffic control studies, and a current program is assessing airborne radar concepts of guidance to offshore oil platforms. These are IMC flight tasks with very modest maneuvering requirements.

This overview has not touched on all of the Ames helicopter simulation activity, but perhaps it has described those efforts in which the quality of visual or motion cueing, or the effects of their absence, should have been a consideration.

Facilities

Cockpit and Motion Systems. This discussion of facilities is limited to those factors defining the pilot's immediate environment: displays, controls, and, most importantly, cockpit motion- and visual-cueing systems. The simulator cab illustrated on Fig. 1, designated Chair 6, is popular with experimenters who are in the preliminary phases of a research program, or who are studying navigation or display questions unrelated to the higher frequency dynamics of the helicopter. It is a box on wheels that can be located handily in the computer laboratory, but like most Ames simulations, it is equipped with a collimated TV monitor for displaying a scene generated by a model-board system. It also has provisions for a collimated head-up display. To avoid the complications of hydraulics, control loaders are simple electromechanical devices. Another fixed-cockpit simulator, which utilizes a salvaged UH-1 cab and control hardware, is used primarily in the development of software for a helicopter avionics flight program.

The Flight Simulator for Advanced Aircraft (FSAA), illustrated in Fig. 2, features a lateral motion envelope of 30 m, together with 3 m of vertical travel and 2.5 m of fore-and-aft movement. Three independent drives provide generous amplitudes of angular motion. All drives are electric. Linear acceleration capabilities are modest, less than ±0.5 g, but are generally satisfactory for helicopter simulation. The large transport-type cockpit has two pilot stations, and is equipped with hydraulic control loaders, visual simulation TV monitors, and head-up display equipment. As in all simulators (except the several "dedicated cockpit" simulators), this cab is reconfigured for each new simulation. Over the past decade, this facility has been used in simulation of a wide range of aircraft. Currently, helicopter simulations make up about 25% of its operation.

The newest facility, the Vertical Motion Simulator (VMS), is shown in Fig. 3. The present cab is of the same specifications as the FSAA, but is driven in angular motion by a small, six-actuator hydraulic system. This is mounted on a laterally driven carriage with 13 m of travel atop a beam which can be moved vertically in a 19 m envelope. These latter two drives are electric, and are capable of nearly 1-g accelerations. A second horizontal motion component is not provided; however, the cab can be rotated to substitute fore-and-aft motion for lateral motion. A later section of this paper will discuss the capabilities of those large motion systems to reproduce the motion cues of maneuvering flight.

Visual Simulation Systems. Ames operates two Redifon TV model-board visual scene generators. These systems can provide a 34° by 48° visual field on a 525-line color televison raster format. The model-boards have accumulated a variety of features modeled at scales from 1:300 to 1:1200. Half of one of the model-boards is devoted to hilly terrain appropriate for helicopter NOE flight tasks. A variety of aviation ship models, mechanized to provide deck motion, are provided. An oil drilling platform is also available. A recent acquisition at Ames is a Singer-Link computer-generated-image (CGI) visual simulation system. This device can produce four independent 34° by 48° visual fields on 1024-line raster formats. The scenes, which are in color, can present simulations of day, dusk, and night conditions. Scenes presently available include an airfield and surrounds, a destroyer with helicopter landing facilities, and a small carrier. A new simulator cab, shown in Fig. 4, is configured for a helicopter pilot's station and is equipped with four collimated CRT "windows" for display of the CGI scenes. It has operated as a fixed-cockpit simulator. Within the year, this cab, which is the first of a series of "interchangeable" cabs, will be installed on the VMS motion system to combine the increased viewing area with the large-motion capability.

Cueing Effectiveness

The preceding descriptions of the motion and visual systems fall short of defining the extent to which those systems can reproduce the cues sensed by the pilot in flight. This definition can be obtained only through examination of the specific simulated flight task -- the accelerations of flight compared with the limited spectrum available

in the simulator -- and the visual information vital to the task in flight compared with what is available in the simulator. The following paragraphs initiate this process by establishing generalized maneuver-cueing relationships for the VMS motion system and the visual simulation devices. The high-frequency dynamic response capabilities of these systems will not be addressed here. The general topic of allowable lags in motion and visual systems is well covered in the recent literature.

Motion-Cueing Capabilities

The motion commands to the VMS drives are composed of 1) the computed motions of the modeled aircraft subjected to second-order high-pass filtering and possibly attenuated; and 2) discrete limiting logic that arrests the motion at the excursion limits, if the primary mode of confinement is overpowered. The characteristic frequencies of these "washout" filters are directly related to the maximum amplitudes of the lower-frequency accelerations anticipated in the simulated maneuvers, the degree to which direct attenuation of the accelerations is acceptable or necessary, and the excursion envelope of the related motion-system mode. The roll and pitch modes are not usually constrained by their own angular excursion limits, but rather by the consequences of logic that attempts to minimize spurious longitudinal or lateral accelerations owing to cockpit tilting. Thus, roll excursions are limited by the capability of the lateral drive to retain the specific force vector in its proper orientation as the cab is rolled. Gains and washout frequencies typical of those used in the VMS in helicopter simulation are indicated in the Bode diagrams of Fig. 5. This diagram describes the "band-pass" of the system -- those portions of the maneuvering spectrum that can be reproduced accurately. It also illustrates that motions at frequencies near the washout frequency will be highly distorted in phase. The roll-off in dynamic response shown at the high frequencies is typical of the drive system, not the motion constraint logic.

Lateral Motion. The curves labeled "roll" in Fig. 5 represent the combined mode of cockpit roll and lateral motion mentioned earlier. The indicated gain of 0.5 and the washout frequency of 0.7 rad/sec are appropriate for the simulation of lateral maneuvers involving angles-of-bank seldom greater than 30°, which in this case would result in a lateral excursion of about 5 m. Accommodation of higher-amplitude lateral maneuvering would require more attenuation or an increase of the washout characteristic frequency. Experience has indicated that for active lateral maneuvering, the former is the preferred option. In simulated visual flight tasks, motion-vision phase disparities can be consciously disturbing, as washout frequencies are increased above 0.7 rad/sec. It is seen in this case that motions in the frequency range from 0.7 to 1.5 rad/sec are transmitted with large leading-phase distortions. Fortunately, many of the simulated helicopter tasks involve less lateral maneuvering than provided for in this case, although one series of experiments at Ames, conducted in a fixed-cockpit simulator, utilized a high-speed NOE task that included 60° to 60° roll reversals.

Body-axis lateral accelerations are produced essentially undistorted, the short-term components provided by the lateral drive system and the low-frequency components generated by easing a "tilt" component into the cockpit roll attitude.

Vertical Motion. Two response curves are shown for vertical motion. They describe the relative capabilities of the VMS and the FSAA to reproduce the vertical motions seen in a flight task involving maximum lower-frequency vertical accelerations of about ±0.3 g. Helicopter low-speed tasks and hovering tasks usually fall in this category. It can be seen that the VMS, with a washout frequency of 0.4 rad/sec, provides an unattenuated, effective (less than 30° phase error) band-pass between 1 and 6 rad/sec. The relatively limited excursion capability of the FSAA defines a washout frequency of 1.4 rad/sec and an effective band-pass between 3.0 and 6 rad/sec. Such increases in vertical washout frequency have not produced the strong conscious motion-visual disparity disturbance seen in roll.

Visual-Cueing Capabilities

The comparison of visual cues provided in simulation with those present in flight is not the straightforward process demonstrated for motion cues. A visual scene has many measures, and the significance of each to the pilot's perception of his position and velocity remains ill-defined. However, some of the obvious capabilities and limitations of the model-board and CGI systems can be noted.

Field-of-View. In Fig. 6, the extent of four visual fields, as might be generated by the CGI system, is compared with the pilot's outside visual field in a typical helicopter. The model-board systems are capable of supplying only the single forward scene. The fourfold increase in field offered by the CGI system still falls short of matching the flight condition, though it adds sideward and downward scenes that are assumed to be of prime importance for position and velocity cues in precision hovering. Also, the argument is made that the more generous lateral field improves the pilot's perception of rates-of-change of aircraft attitude.

Quality of the Scene. Visual systems are most severely tested in simulations of flight in proximity to the terrain or structures, exactly the tasks usually chosen for critical helicopter control-systems evaluations. There is no inherent limit to the extent that real-world textures and detail can be reproduced on the model-board; however, models are only seldom detailed to match the

limited resolution capability of the camera optics and video system. Even without the deliberate detail, objects on the model-board usually possess some level of resolvable texture. By comparison, the CGI system, because of the limited number of lines it can draw, is severely limited in presentation of detail. The CGI scene, with its comparatively high resolution, is excellent at medium to large distances but tends to lose its realism as the terrain is approached. The concentration of the system's image-producing capacity on a limited scene feature, as in a ship model, offers at least a partial solution to the difficulty. More will be said about simulated scene content in discussions of several specific simulation applications.

Observations and Discussion

Validity of Simulation

The foregoing has considered a variety of research objectives, and the varying limitations of the facilities used in the investigations. From this experience, observations can be made relating objective, cueing capabilities, and validity of the simulation. As defined here, validity is the effectiveness of the simulation as a means of achieving the research objective, and thus does not imply a specified level of subjective or objective fidelity in the vehicle simulation itself.

Fixed-Cockpit Simulations. In the earlier experience at Ames, handling-qualities issues were addressed in fixed-base simulation, with limited results. The simulations of light, agile vehicles drew strong adverse comment from the pilots who experienced exaggerated, unrealistic workloads in conventional helicopter maneuvers. Pilots required considerable practice to reach a stable level of performance, and performance differences between pilots tended to be large. Subjectively, the pilots considered the aircraft model suspect, and judged the limitations of the model-board visual system to be another prime source of their difficulties. The experimenters, recognizing that motion-cue deprivation might be a major part of the problem, began to seek the use of the FSAA and the VMS for their stability and control studies. However, lack of motion did not appear to present serious problems to all experimenters. Simulations of larger stabilized vehicles, used in studies of navigation and display systems, were generally accepted by the pilots. The summary observation is made that if the character and workload of the vehicle control task is not severely distorted, and if the pilot is not asked to pass critical judgment on the vehicle's dynamic responses, the fixed-cockpit simulation appears to be adequate.

Adequacy of the Visual System. The single forward window provided by the model-board visual system places a limit on the fidelity of helicopter simulation in visual tasks. In turning flight near the terrain, the inability to see what lies ahead in the predicted path is disconcerting and unrealistic. Quick stops are almost prohibited because of the loss of virtually all visual information at large nose-up pitch attitudes. Precision hover is made difficult because of the lack of translational velocity cues that normally are obtained from sideward and downward views. The extent to which these factors limit the validity of the simulation varies with the maneuvers of the simulated flight task. Validity also depends to some degree on the pilot's sense of subjective fidelity. In the fixed-cockpit simulations, visual-scene limitations were often assessed as a major cause of performance difficulty. In the more recent programs using cockpit motion, these criticisms have been less strident. The visual constraints on the task are recognized, but performance difficulties within that constrained task are not so often attributed to a lack of visual cues. This latter assessment more closely agrees with the results of flight tests[5,6] in which limitations of the pilot's field of view affected performance to a lesser degree than anticipated in view of early simulator experiences.

Cueing Optimization

The experimenter has the opportunity, and the obligation, to shape the simulated flight tasks to take best advantage of motion- and visual-cueing capabilities in the pursuit of his research objective. A standardized procedure is not offered here; instead, the simulation of Ref. 3, which is considered a particularly effective example of cueing optimization, is discussed in detail. The objective of those experiments was the evaluation of variations in height-control parameters. The critical maneuvers were determined to be climbs over obstacles at low forward speeds while minimizing exposure time above the obstacles, deceleration to hover under cover of obstacles, and a "bob-up" to a momentary surveillance position above the obstacles before a return to hover. A particular arrangement of simulated obstacles, identifying a course on the model-board, minimized the significance of visual limitations while defining flight maneuvers that optimized the cueing potential of the VMS.

Visual Simulation. The pilot's view of the experimental course, as seen at the instant of passing over one of the obstacles, is shown in Fig. 7. Obstacles are laid out between two rows of trees that define the straight-line course. This avenue is terminated in the distance by a crossing row of trees. The obstacles were arbitrary in form, and made no contribution to a sense of realism in the scene. Rows of trees might have been more aesthetically pleasing. Models of ground vehicles were included to help establish a sense of scale, and the level surface between obstacles included scattered shrubbery to aid in the sense of proximity to the ground. The avenue of high trees did more than identify a course; it served to optimize visual perception of height and height-rate from the limited forward field-of-view. This cueing augmentation was vitally important during the deceleration to hover. The pilot's view during

this maneuver is seen in Fig. 8. Even though the pitched-up attitude severely constrains the view of the surface, the trees offer an effective set of references for the perception of vehicle velocities. Some of this effectiveness is attributed to the fact that the trees did not completely obscure the more distant scene. It has been noted that in restricted viewing fields, in which close objects or surfaces completely predominate, the visual cues of angular and linear motions can become confused.

At several points in the task, field-of-view limitations were especially noted. It was difficult for the pilot to assess his clearance distance when passing over the obstacles; and during his bob-up maneuver, it was very important to retain sight of some tree tops over the nose in order to maintain position reference.

Cockpit Motion. Because no lateral maneuvers were required other than to maintain position between the rows of trees, the lateral motion constraints of the VMS were minimized. Altitudes in the task did not exceed 80 ft, a height that is only slightly greater than the vertical excursion capability of the VMS. Thus, vertical accelerations were reproduced with unusual fidelity for ground-based flight simulation. The vertical acceleration band-pass noted for the VMS in Fig. 5 was realized; and moreover, because the task was so limited in altitude, vertical accelerations to the limits of the machine could be utilized.

Another Optimization Opportunity. Recent limited experience with the four-window CGI display suggests that the radically increased field of view does not relieve the experimenter of the need to seek optimization of the visual information. If, for example, aircraft systems are to be evaluated for their adequacy in landing on a moving ship deck, the visual simulation must approach the real-world scene in the provision of attitude and position cues. As mentioned earlier, the four-window CGI system falls short of presenting the in-flight field-of-view. In Fig. 9 are shown the four scenes, as presently configured, representing the pilot's view near touchdown. His only significant view of the deck is in the lower right window, and this view is notably separated from the other visual information sources. What we see is a problem of limited (or perhaps non-optimally oriented) field of view compounded by the geometry of the deck and superstructure.

The argument is made that neither the window placement nor the simulated ship geometry should be constrained by real-world measures, if as a result of either constraint the task is made unrealistically difficult. Window placement should be optimized and the scene elements designed to provide attitude and position cues of maximum effectiveness. Unfortunately, there is little in the literature to guide the experimenter in this quest. Great effort is being expended on the development of more sophisticated computer-generated scenes, but little research is under way to address the question of how to use current capabilities most effectively.

Benefits of Improved Cueing

What benefits are seen as a result of such efforts to increase the cueing fidelity of simulation? Like the cues themselves, the benefits tend to be subtle, though, as will be seen shortly, startling effects can be demonstrated if the appropriate tests are made. Even with the motion cueing provided by the FSAA or the VMS, there remain many reminders to the pilot that he is operating a simulation. The motion system contributes its own reminders if the motion logic is improperly conditioned for the simulated flight task. The introduction of large-amplitude cockpit motion to helicopter simulations does lead to these general observations: 1) the pilot's initial assessment of subjective fidelity is somewhat improved; 2) his "transition time," or time to a performance plateau with an unfamiliar vehicle and task is shortened; 3) maneuver amplitudes and control "style" compare more favorably with those of flight; 4) less variation in performance and assessment is seen across a group of pilots; and 5) ratings and commentary regarding handling-qualities issues appear to be offered with greater ease and confidence.

Two peripheral observations are worth noting: there is noticeably less criticism of the visual system's limitations, and comments regarding motion are limited almost exclusively to those inspired by anomalies, such as limit encounters, or by audible noise from the motion drives. Again, the reader is reminded that even with excellent motion cues, the pilot is dealing with a simulated flight task; he will have reservations regarding the fidelity and validity of the simulation until he has accommodated to the remaining artificialities, especially those of the visual simulation.

Some effects of improving the visual cues are more obvious. In the example discussed earlier, a particular flight task was enabled by configuring model-board elements to optimize the information in the single forward field. The increased field of view offered by the CGI system enables a simulated landing on a ship or a drilling platform. These additions are consciously appreciated by the pilots; they see an increased validity of the simulated mission, but contributions to a sense of subjective vehicle fidelity are unclear.

Some Observations Regarding Vertical-Motion Cueing

The most unique aspect of the Ames simulation experience has been the availability of vertical motion in the VMS. Though this facility has been operational for nearly 2 years, no formalized investigation has been conducted in an attempt to identify the contribution of the vertical motion cues to the validity of simulation. Other than

helicopter studies such as those discussed earlier, the use of the facilities has been limited to Space Shuttle control-systems verification studies. The pilots recognized the Shuttle simulations to be of unique quality, particularly in their examinations of the pitch-control modes for PIO tendencies, but perhaps their most significant specific comment relative to motion cues was, "This is the first time we have experienced realistic turbulence in a simulator." The turbulence model was conventional, the same as they had experienced in FSAA Shuttle simulations. For the first time, they were physically sensing the lower frequency vertical gusts.

Another limited, but striking, item of evidence of vertical-motion effects was obtained during the experiments of Ref. 3. The objectives and the task of that study were described earlier in this paper. The pilots were asked to evaluate a number of collective-control and engine-response configurations in terms of a formalized handling-qualities rating scale and subjective commentary. As in many experiments of this kind, the evaluations were "blind"; that is, the pilot was not made aware of the specific variations as his evaluations progressed from one configuration to another. During the latter part of his participation in the tests, one pilot, in several instances, was subjected to a variation in vertical motion instead of a variation in the vehicle model. He was not informed of this change during the tests, nor did he consciously sense that the simulator motion had been changed. He assumed he was evaluating modifications to aircraft parameters. The change effected was an increase of the vertical-motion washout frequency from 0.4 to 1.4 rad/sec, constraining the cockpit motion to that experienced in the FSAA (see Fig. 5). The effects of this change on the pilot's subjective ratings of two helicopter configurations is shown in Fig. 10. Subsequently, the pilot was informed of the experiment and asked to repeat the evaluations in the absence of cockpit motion. His commentary accompanying the ratings of those cases with attenuated motion cited insufficient vertical rate damping in the vehicle.

The two helicopter configurations differed only in their values of vertical damping. With the full VMS vertical motion, they were given the same rating. The descriptor associated with the 4.5 rating is "minor to moderate annoying deficiencies requiring pilot compensation." With reduced cockpit motion, one configuration displayed "very objectionable but tolerable deficiencies, requiring extensive pilot compensation," and the other was assessed as having "major deficiencies requiring improvement." In the fixed-cockpit evaluations, the ratings were further degraded.

It might be inferred from these results that if the research program had been conducted in the FSAA, the degraded evaluations would have prevailed, leading to quite erroneous experimental conclusions. It is likely that such an inference is somewhat pessimistic. In the brief "back-to-back" tests in the VMS, the pilot had no opportunity to accommodate to the altered visual-motion relationship. It is probable that if the entire program had been conducted with reduced vertical motion, ratings would have been degraded less than demonstrated here; however, it remains for some directed studies to consider this question in the detail it deserves.

Another example of evaluations differing with variations in vertical motion cues was seen in a fixed-base simulator investigation of the use of a multiaxis, integrated side-stick controller (SSC) in lieu of conventional helicopter controllers for nap-of-the-Earth flight. It was discovered that with sufficient levels of stability and control augmentation, up to three axes of control (pitch, roll, and yaw) on the SSC provided handling-qualities equivalent to those achieved with the conventional controller. However, the addition of the fourth controlled axis (vertical) to the SSC yielded significant degradation in pilot rating. In contrast, in a follow-on moving-base simulation on the Vertical Motion Simulator, the same four-axis SSC configuration was given pilot ratings equivalent to those achieved with conventional controllers.

The sensitivity of this height-control problem to cockpit motion brings to mind the difficulty of achieving subjective fidelity and flight-like performance in the simulated airplane landing maneuver. The hypothesis is offered that the visual cues of linear motion are often very weak, especially in the case of vertical motion; thus, vertical acceleration cues are heavily relied upon in the conduct of precise control of height rate. This dependency might extend to the lower ranges of maneuvering frequency (near 1 rad/sec). Visual cues of angular motions are much stronger. Sensitivities to angular-motion-cue deficiencies are usually manifested at the higher frequencies typically seen with high-response control systems (3-6 rad/sec).

Concluding Remarks

A review of helicopter simulation experience at Ames Research Center indicates that experimenters seeking sound pilot evaluation of vehicle handling qualities have developed an appreciation for, if not an understanding of, cockpit motion. It is observed that low-order, well-damped, uncoupled control modes, in the presence of strong visual cues, are not sensitive to motion-cue deprivation. As these descriptions -- order, damping, coupling -- move toward the other end of their scales, or if visual cues are weakened, sensitivity to motion-cue deprivation is increased. There are indications that helicopter height control, with its collective and cyclic contributions, benefits strongly from large-amplitude simulator motion.

All significant experience at Ames with simulation of visual flight tasks has been obtained

with a limited forward field of view. The advantages of a fourfold increase of viewing area are anticipated, though they remain undefined. With optimization of scene elements, the single-window model-board view has demonstrated surprising adequacy in a number of simulator studies.

These are very generalized observations, and they do guide the utilization of simulation facilities at Ames; but still lacking are the well-documented demonstrations of effects of cue deprivation that are required in the development of an understanding of the motion- and visual-cueing processes. The experiences with the VMS vertical-motion capabilities suggest their use in carefully conditioned studies of the roles played by vertical acceleration in helicopter piloting tasks. To be "carefully conditioned," such experiments should employ the most promising human performance measurement and modeling techniques, and should be designed in recognition of the probably influences of learning and task complexity on the pilot's utilization of motion cues. The visual simulations used during these experiments, in combination with the piloting tasks, must be of the highest achievable fidelity to minimize contamination of the results as a result of visual deficiencies.

Another attractive objective is the further development and evaluation of substitute cueing mechanisms (variable geometry seats, torso/helmet pullers) in the context of helicopter flight tasks; the VMS offers the opportunity for direct comparison of the effectiveness of such devices with that of essentially unattenuated motion. Also, the VMS offers some opportunity to study visual fidelity factors in the presence of high-quality motion cues. The studies suggested here should produce results facilitating more graceful and intelligent accommodation to simulations with limited cueing capabilities, and providing a firmer basis than presently exists for further simulation technology development.

References

1. Chen, R. T. N., "Unified Results of Several Analytical and Experimental Studies on Helicopter Handling Qualities in Visual Terrain Flight," presented at AHS/NASA Specialists' Meeting on Helicopter Handling Qualities, Ames Research Center, NASA, Apr. 1982.

2. Lebacqz, J. V., Chen, R. T. N., Gerdes, R. M., Weber, J. M., and Forrest, R. D., "Results of NASA/FAA Ground and Flight Simulation Experiments Concerning Helicopter IFR Airworthiness Criteria," presented at AHS/NASA Specialists' Meeting on Helicopter Handling Qualities, Ames Research Center, NASA, Apr. 1982.

3. Corliss, L. D., "The Effects of Helicopter Engine Response Dynamics and Excess Power on NOE Handling Qualities," presented at AHS/NASA Specialists' Meeting on Helicopter Handling Qualities, Ames Research Center, NASA, Apr. 1982.

4. Churchill, G. B. and Dugan, D. C., "Simulation of the XV-15 Tilt Rotor Research Aircraft," presented at SES-SFTE Conference on Simulation -- Aircraft Test and Evaluation, Naval Air Test Center, Patuxent River, Md., Mar. 1982.

5. Milleli, R. J., Keane, W. A., and Keneally, W. U., "A Flight Program to Define V/STOL Visual Simulator Requirements," presented at the Second Flight Simulation Symposium, the Royal Aeronautical Society, May 1973.

6. Carico, G. D. and Corliss, L. D., "Effect of Field of View on Performing a Low Altitude Maneuvering Task," proceedings of the Third Interservice Industry Training Equipment Conference, Orlando, Fla., Nov. 1981.

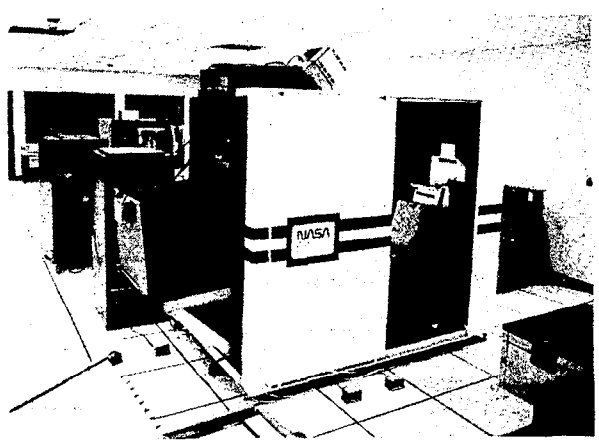

Fig. 1. Typical "fixed-base" simulation cab incorporating visual simulation and head-up display.

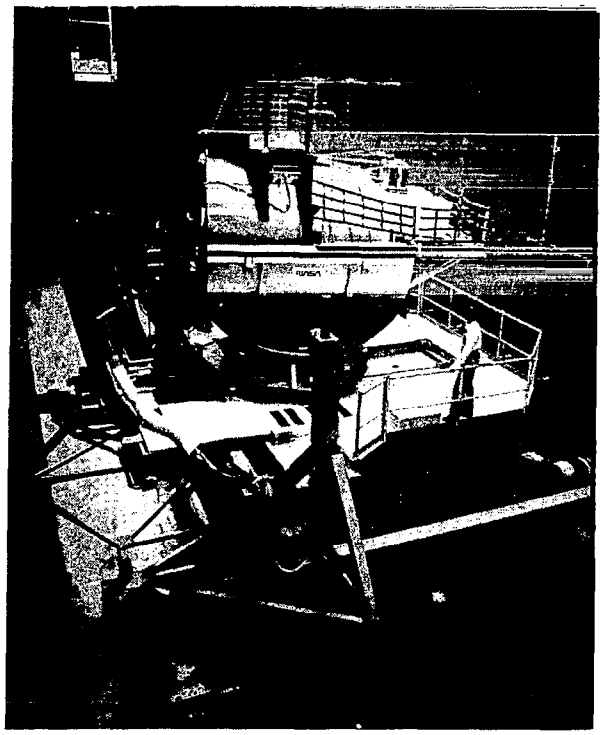

Fig. 2. The Ames Flight Simulator for Advanced Aircraft (FSAA).

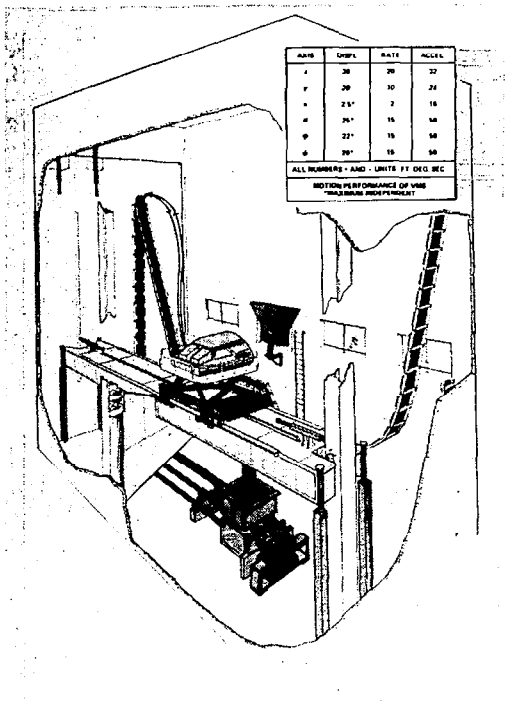

Fig. 3. The Ames Vertical Motion Simulator (VMS).

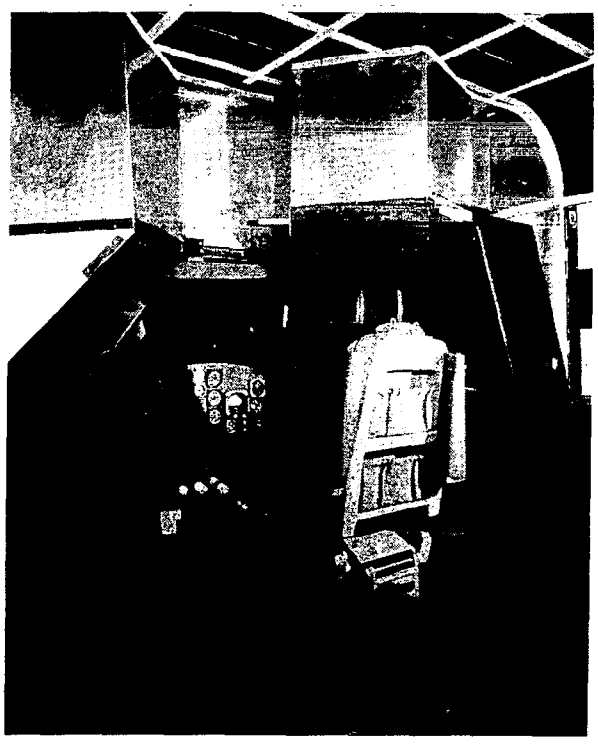

Fig. 4. "Interchangeable Cab," with four-window CGI visual simulation display.

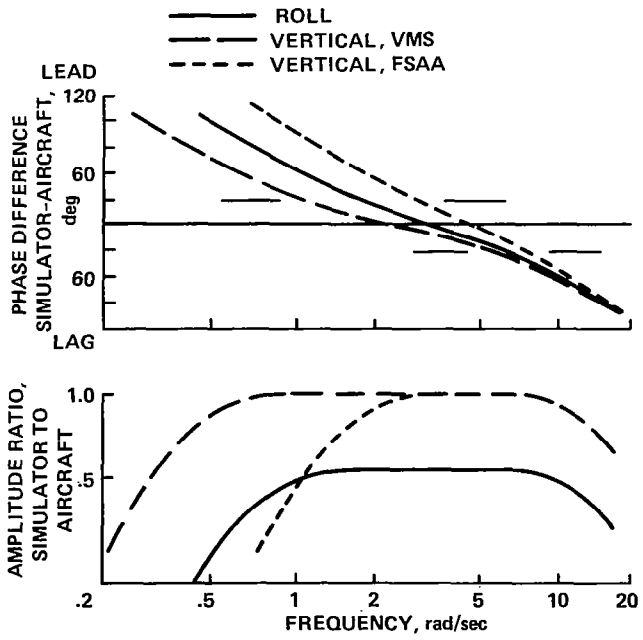

Fig. 5. Simulator motion response relative to that of the modeled aircraft.

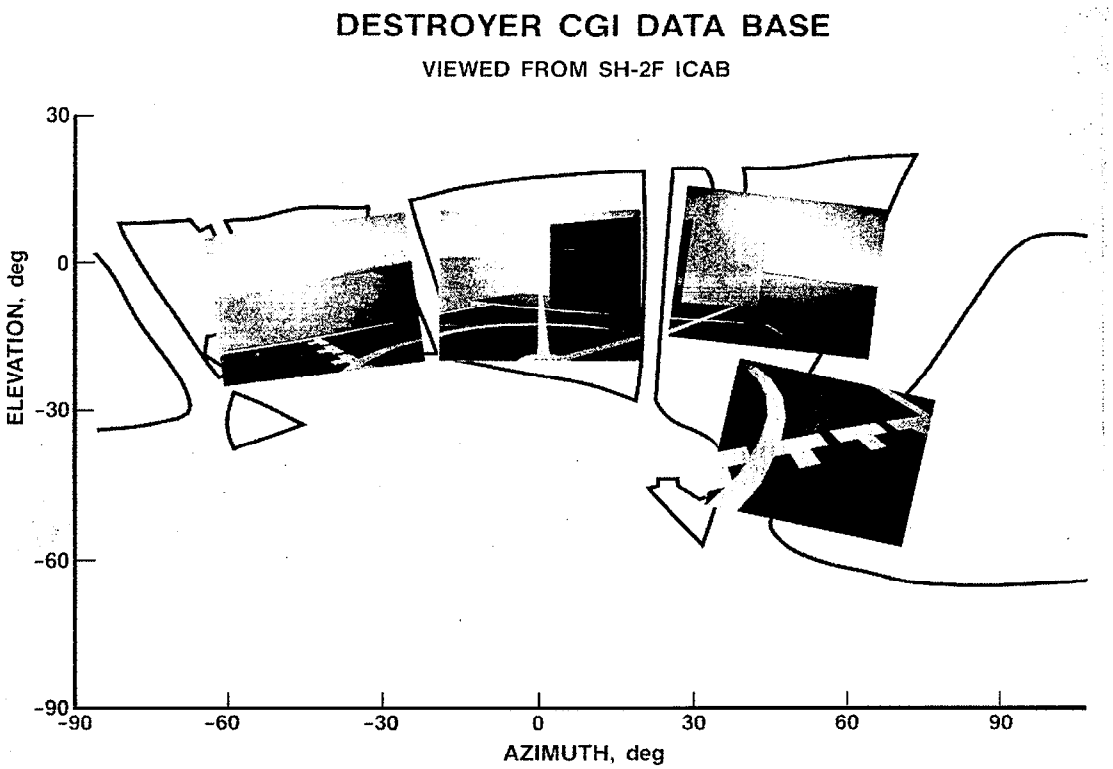

Fig. 6. Windows provided by visual simulation systems compared with typical helicopter fields of view.

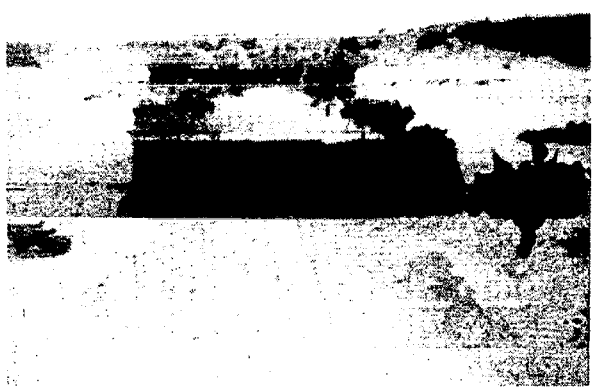

Fig. 7. View of helicopter longitudinal maneuvering course on visual simulation model-board.

Fig. 8. Pilot's view while decelerating to hover.

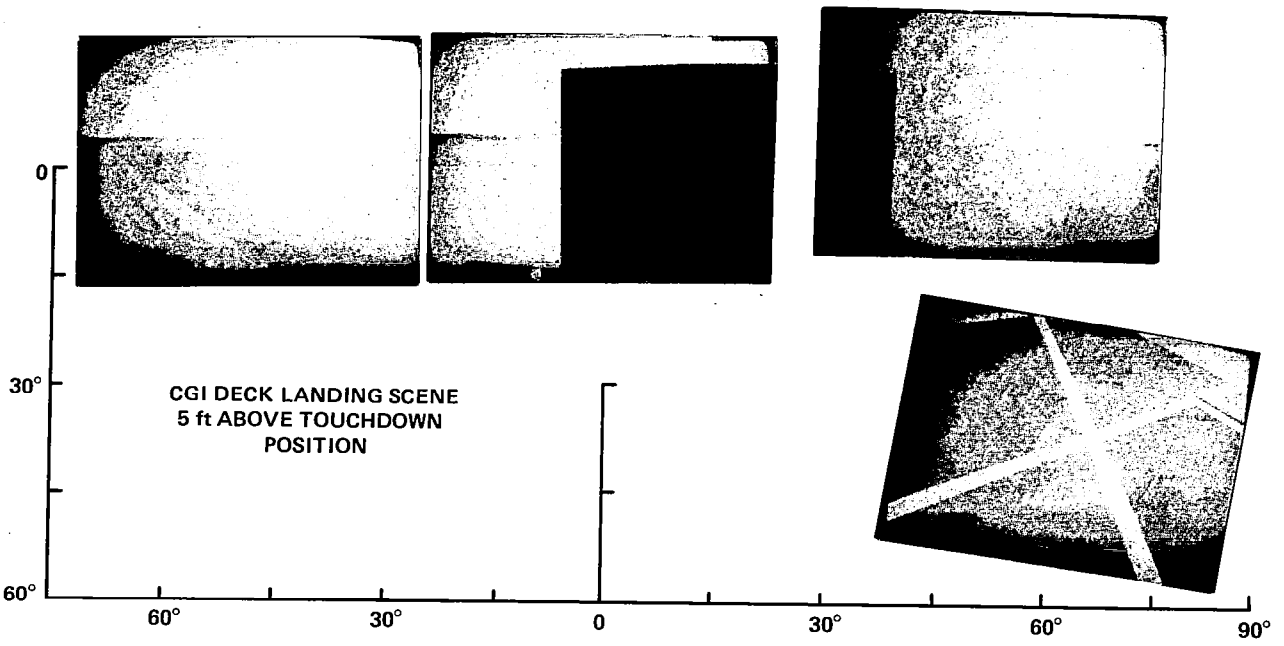

Fig. 9. Pilot's views just before touchdown on deck as provided by CGI visual system.

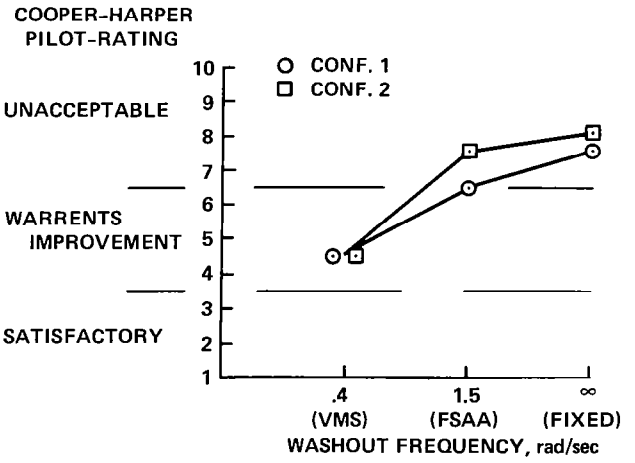

Fig. 10. The effects of changes in cockpit motion on pilot ratings of helicopter handling qualities.

PAST APPLICATIONS AND FUTURE POTENTIAL OF VARIABLE STABILITY RESEARCH HELICOPTERS

William S. Hindson

Senior Research Associate

Joint Institute of Aeronautics and Acoustics

Stanford University

Stanford, California

Summary

Variable-stability research helicopters began to be used more than 25 years ago to investigate flying qualities criteria for helicopters. However, their application was soon diverted to investigate mainly the problems of V/STOL aircraft. This emphasis prevailed until the past decade when the greatly increased use of helicopters for a wide variety of more demanding applications resulted in renewed use of these facilities for rotary-wing research. The historical development of variable-stability research helicopters and some of their previous applications are presented as a guide for assessing their future potential. The features of three general-purpose rotary-wing flight research aircraft that provide complementary capabilities are described briefly, and a number of future applications are proposed.

Introduction

In the past 25 years, variable-stability aircraft have made major contributions to the formulation of flying qualities criteria, guidance, control, and display systems requirements. They have also been used as development tools for particular designs, and as training vehicles to demonstrate a wide range of generic control characteristics or to provide pilot familiarization prior to flying a new aircraft. In the early days, use of these airborne simulation facilities was fairly extensive, since ground-based simulation equipment, if it existed, had extremely limited capabilities. Until recently, this was particularly true for helicopters and V/STOL aircraft, for which the motion and visual requirements in hover and in low-speed maneuvering flight placed severe demands on simulation fidelity. Today, however, major advances in the capabilities of ground-based simulators, exemplified by the Vertical Motion Simulator at NASA-Ames and by multi-window computer-generated imagery systems, have tended to cause much greater confidence to be placed in this means of aircraft and systems design, and criteria development. Nevertheless, variable-stability research aircraft have continued to be used throughout this period, during which their capabilities have improved and their applications have diversified.

It is the purpose of this presentation to review briefly the evolution of variable-stability research helicopters, with a view to emphasizing that these facilities are general-purpose in nature and represent major long-term investments similar to a large wind-tunnel or a sophisticated ground-based simulator installation. Some past and recent applications of several variable-stability research helicopters are reviewed as a means towards understanding the role that these facilities may have in the future. The features of three different variable-stability helicopters having complementary capabilities, and some of the considerations involved in airborne simulation technology are summarized to provide a basis for determining their future potential. To conclude, a number of applications to future rotorcraft research are noted.

The three variable-stability research helicopters which are given particular attention in this paper are the NASA/Army CH-47B and the NASA/Army UH-1H helicopters operated at the Ames Research Center, and the Bell model 205A-1 airborne simulator operated by the National Aeronautical Establishment (NAE) in Ottawa, Canada. A BO 105 rigid-rotor variable-stability helicopter operated in Germany (Reference 1), the NASA/Army Rotor Systems Research Aircraft (RSRA) described in Reference 2, and various other rotary-wing aircraft having a variable-stability capability, but which are in the class of technology demonstration or training vehicles, are not discussed.

Evolution and Past Applications

Historically, variable-stability research aircraft have usually evolved with the appearance of new classes of vehicles that have exhibited unsatisfactory or unusual flying qualities in their basic

design, or in their subsequent application to more demanding flight tasks. For helicopters, one of the first developments of a variable-stability research vehicle that involved an electromechanical control system and electrical response-feedback techniques was at the NACA Langley Aeronautical Laboratory in 1955 (Reference 3). With this helicopter, various levels of control power, control sensitivity, and rate damping augmentation were evaluated in an effort to provide a data base for handling qualities criteria during instrument approach. For this control task, the military helicopter flying qualities criteria, MIL H 8501A (Nov 52), developed for visual flight, were found to be inadequate (Reference 4). However, it seems that the profusion of V/STOL configurations that also began to appear at this time re-oriented the application of variable-stability helicopters largely toward this field of research, an emphasis that persisted until about 1970.

During the period 1955-1970, more than 25 different VTOL and V/STOL non-rotary-wing configurations were test-flown by NATO countries. Although this number of V/STOL concepts was probably significantly smaller than the number of new helicopters introduced in the same period, attention was focussed on them because of their novel operational capabilities and the diversity in the design of their propulsive-lift and flight control systems, not to mention their often notorious safety record. In response to the need for criteria which could more efficiently lead to a successful and capable V/STOL design, a succession of efforts was undertaken by NASA (Reference 5), AGARD (References 6-9), and the U.S. military (Reference 10). To create an additional source of data for these efforts, the U.S. Army provided helicopters to NASA Langley and to NAE for modification as V/STOL research vehicles. These flight research aircraft, described in References 11 and 12, were the first to use the model-controlled method of airborne simulation which was originally proposed in Reference 13. As shown in Fig. 1, this method is virtually identical to a ground-simulation implementation except, in this case, the moving "cab" can follow the model-generated motion commands without restriction, and with fidelity determined by the bandwidth of response and the degree of pure (uncoupled) control achievable in that axis. Because only four relatively uncoupled controls are normally available in a helicopter, the motion can be accurately controlled only in four degrees-of-freedom, hence creating some limitations for the simulation of V/STOL and STOL aircraft. Nevertheless, significant contributions to the V/STOL criteria were made by these helicopters, and by other variable-stability research vehicles such as the Ryan X-14A operated at NASA-Ames, the Bell X-22A operated by Calspan, and the Short SC-1 at RAE Bedford.

In addition to the use of these facilities for the development of general V/STOL criteria, some of them were also used as development tools for specific designs. The use of the NAE airborne simulator in separate development programs for the Canadair CL-84, the Hawker-Siddeley P-1127 (Kestrel), the Vereinigte Flugtechnische Werke VAK 191B, and the DeHavilland DHC-7 is summarized in Reference 14.

Although some of these research efforts were also applicable to helicopters, such as in the areas of lateral-directional flying qualities and steep low-speed instrument approaches, it was not until the early to mid-seventies that rotary-wing applications began to be emphasized by the NASA and NAE variable-stability helicopters. By then, these facilities consisted of second and third generation research vehicles equipped with much higher capacity hybrid computing equipment (References 15-17). In response to an emphasis on all-weather capability, and in recognition of the potential for trading-off vehicle control system complexity for sophistication in cockpit displays, these aircraft also began to acquire the capability for flight-systems research involving advanced navigation equipment and programmable CRT displays. This change in emphasis away from V/STOL applications was perhaps partly due to the failure of any V/STOL aircraft (with the notable exception of the Harrier) to achieve operational application, from which would have emerged the much needed experience with which to validate, revise, or extend the V/STOL criteria. However, it was precisely this stage of development that was taking place for the helicopter. New and more demanding mission requirements were creating the need for improved flying qualities beyond those which had been adequate in the past. The nature of these requirements, and some recent applications of variable-stability aircraft in addressing them, are discussed briefly in the following section.

Recent Applications

Perhaps the most significant factor influencing the recent use of variable-stability research helicopters has been the strong civil demand for dual or single pilot instrument flight capability to support natural resource operations, or to allow effective commercial use of helicopters in weather conditions at least equivalent to CTOL operations under Instrument Flight Rules (IFR). Although the first instrument flight certification of a civil helicopter occurred in 1960, the strong

demand of the seventies suddenly emerged at a time when the National Airspace System was ill-equipped to allow the unique capabilities of the helicopter to be used efficiently. This led the Federal Aviation Administration (FAA) to institute a broad program in cooperation with industry and NASA (Reference 18), parts of which were to better define the minimum requirements for helicopter IFR certification, and to investigate systems for improving the operational efficiency of rotary-wing aircraft in instrument flight conditions. Among research facilities that have been used in this program are the extensive ground-based simulation facilities at the Ames Research Center, and the UH-1H and B205A-1 variable-stability helicopters operated by Ames and NAE respectively. Three flight programs that were carried out in support of this requirement are described in References 19-21. As indicated, this requirement for flying qualities criteria arose differently than had been the earlier case for V/STOL aircraft, since in general, the helicopter manufacturers and the avionics companies were able to provide a satisfactory capability,without the need for detailed guidelines. Rather, the motivation for this effort was more to assess the validity and, where necessary, extend the scope of a set of "interim standards" which previously had been employed in the certification process.

Although there do not appear to be any major flying quality problems in current helicopters for the relatively conventional instrument approach task, there has been general agreement that their very low-speed capabilities have not yet been exploited for all-weather operations. As reviewed in Reference 22, a considerable amount of research in this area has already been carried out, much of it at the NASA Langley Research Center using the CH-46C and CH-47B variable-stability helicopters. Control and display requirements for carrying out decelerating approaches to hover in instrument conditions were investigated for both manual and automatic control as described, for example, in References 17 and 23. A more recent investigation in this area using the NASA/Army UH-1H helicopter, combined an automatic decelerating approach with a helical let-down trajectory designed to perhaps permit helicopter instrument approaches to a busy airport without impacting existing CTOL operations (Reference 24). The investigation of means to improve the operational efficiency of rotary-wing aircraft in the National Airspace System is well-suited to these variable-stability helicopters. Their broad sensor complement and programmable navigation, control and display systems allow for fairly rapid implementation of system conepts, followed by comprehensive evaluation in the real environment.

Unlike the need for helicopter all-weather capability that has persisted to varying degrees for the past 20 years, the military requirement for Nap-of-the-Earth (NOE) operations has more recently created genuinely new needs for flying qualities and agility criteria, and cockpit engineering advances to include both displays and controllers. This mission requirement is so severe that it can only be partially addressed in even the most advanced moving-base ground simulator, or in airborne simulators, where well-designed task elements perhaps could be separately developed towards a satisfactory solution. One research effort using the NASA/Army UH-1H variable-stability helicopter to evaluate different flying qualities during a simulated NOE mission is described in Reference 25. Another investigation, carried out in the NAE B205A-1, evaluated various multi-axis, isometric, side-arm controller configurations as alternatives to the conventional helicopter cyclic stick, pedals and collective controls (Reference 26).

Variable-stability helicopters have not been widely used by the rotorcraft industry as development tools for particular designs. However, some recent examples where specific flight programs have been conducted are described in Reference 27, pertaining to the RSRA, and in Reference 28, which describes the role of airborne simulation during part of the development program for the Sikorsky S-76.

The broad capabilities of these general-purpose research facilities have been characterized by referring to their past and recent applications. In the following sections, the principal features of three current variable-stability research helicopters having complementary capabilities are summarized, along with a short discussion of some of the considerations involved in implementing the technology of airborne simulation.

Principal Capabilities of Three Variable-Stability Research Helicopters

General Features

The NASA/Army CH-47B is a twin-engine tandem-rotor cargo helicopter capable of lifting an internal or external payload of approximately 10,000 pounds. The aircraft is specially equipped with high bandwidth parallel electrohydraulic actuators that are able to drive the basic helicopter control system over its full range through electrohydraulically-operated clutches. During variable-stability operation, the evaluation pilot's electrical control inputs drive these actuators through the flight computer and the engaged clutches, thereby

operating the basic CH-47B controls. The parallel control mechanization permits the safety pilot's controls to follow the basic helicopter controls at all times, although in general, the action of the safety pilot's controls will be quite different than that of the evaluation pilot's. Several mechanical safety features are incorporated to insure that the safety pilot can control the aircraft in the event that a clutch fails to disengage following a system disconnect. This helicopter had originally been used in the technology demonstration program described in Reference 29. After its completion, the aircraft was acquired by NASA-Langley where it was modified for use as their third-generation variable-stability research helicopter (Reference 17). The aircraft was transferred to the Ames Research Center in 1979.

The NASA/Army UH-1H is equipped with the V/STOLAND avionics systems described in Reference 30. Its variable-stability control system consists of high bandwidth limited authority electrohydraulic series servos as well as lower bandwidth limited rate but full authority parallel electromechanical servos. The parallel actuators are used to off-load or to assist the series servos during sustained or aggressive maneuvers commanded by the evaluation pilot, or for following the lower frequency components of automatic control laws implemented in the flight computer. Although the action of the parallel servos can be isolated from the evaluation pilot's longitudinal and lateral cyclic controls, any action of the parallel servos in the main or tail rotor collective channels is reflected to the collective and pedal controls of both pilots. (The evaluation pilot can momentarily disable these parallel servos if their action interferes with his own control inputs; however, the series actuators may saturate during this time.) Despite these limitations, this aircraft can be an extremely effective research tool since it is supported by a dedicated fixed-base simulation facility that permits efficient development of flight software. The aircraft has been in operation at the Ames Research Center since 1977.

The NAE B205A-1 (Reference 16), essentially the civilian equivalent of the UH-1H, has been extensively modified to maximize its capabilities as an airborne simulator. It is equipped with full authority dual-mode actuators that were specially designed to replace the boost actuators of the basic production helicopter. The actuator servo valves are mechanically signalled when the safety pilot has control; in the variable-stability mode they are commanded electrically from the evaluation pilot's control via the flight computers. Other modifications include removal of the stabilizer bar to improve rotor responsiveness to cyclic inputs, and installation of a separate electrohydraulic actuator to drive the horizontal stabilizer which was disconnected from the longitudinal cyclic. The latter feature is generally not used except to trim fuselage attitudes in forward flight. This airborne simulator is the third such general-purpose research facility that has been developed by NAE. It has been carrying out various research programs since 1974.

Simulation Envelopes

The capability of a variable-stability helicopter to simulate the flight regime and dynamic response characteristics of other aircraft is limited in part by its own flight envelope, the control power available in each axis, and the bandwidth and authority limits of the electromechanical or electrohydraulic actuators used in the variable-stability system. As mentioned in a previous section, when only the four conventional helicopter controls are available, then motion can be controlled accurately in only four degrees-of-freedom. This has greater implications than just precluding accurate simulation of V/STOL or compound helicopter designs with their special longitudinal force-generating features, since sideforce and turbulence responce characteristics are also compromised. Although several airborne simulators for conventional aircraft have been operating for several years now with additional control devices installed to provide control over all six degrees-of-freedom, only NAE has undertaken serious study of possible configurations that could provide this capability in a helicopter.

An important consideration that can also strongly influence the available simulation envelope is the method used to monitor the acceptability of maneuvers generated during the in-flight simulation. Automatic monitoring of control rate and position is usually incorporated, particularly in the case where series servos are used in the variable-stability system. If only parallel or dual-mode actuators, such as those in the NAE B205A-1, are employed, then the safety pilot can be relied upon to a much greater extent for monitoring the remaining control margins. This usually permits simulations of more aggressive maneuvers such as may be encountered following simulated engine or stability augmentation system (SAS) failures. Flight programs where these considerations influenced the simulated evaluation task in contrasting ways are described in References 25 and 31.

A summary of factors influencing the available simulation envelopes of the three aircraft described here is provided in Table 1.

Modeling Techniques

A central issue in the use of variable-stability aircraft, and one which also influences the simulation envelope, is the fidelity of motion response that can be achieved during the in-flight simulation. For some investigations, such as those involving only generic flying qualities, the importance of accurately representing specific dynamic response characteristics may not be of great concern. However, the accurate simulation of a specific design, the investigation of higher frequency modes of motion, or the representation of turbulence response characteristics may require a level of performance from the variable-stability control system that is very difficult to achieve.

In general, control of the dynamic response characteristics is accomplished either using response-feedback and control-feedforward techniques, effectively equivalent to most conventional stability and control augmentation system implementations, or with model-following systems such as that shown in Fig. 1. Some of the considerations involved with each method are summarized in Table 2, which identifies that there are major advantages, at least theoretically, in using model-following techniques. Although model-following autopilots with quite good performance (i.e. moderate bandwidth) were relatively easy to develop for some of the earlier light single-rotor variable-stability helicopters (Reference 12), the larger facilities presently in use have presented difficulties that tend to be associated with control crosscoupling and higher frequency structural modes, which are in addition to the usual difficult aerodynamic and vibrational environments. The use of modern multivariable control system design techniques (e.g. References 32,33), or methods involving the inverse solution of the equations of motion of the basic platform (Reference 34), are possible means for improving the motion fidelity of variable-stability helicopters which could benefit the three facilities described here.

Platform Instrumentation

The in-flight simulation objective imposes severe accuracy requirements on the motion measurements of the helicopter which, in the final analysis, are used to validate the dynamic response characteristics. Particular attention must usually be devoted to in-flight steady-state and dynamic calibrations, especially for airspeed measurements, to obtain the degree of precision required of a general-purpose research facility. For example, the inertial and air mass velocity measurements in the NAE airborne simulator were developed to sufficient accuracy to warrant its use for several atmospheric wind and turbulence measurement programs (Reference 35). Of additional benefit, the frequent availability of redundant measurements from a variety of sensors, combined with the recent remarkable advances in digital computing equipment, now make it possible to implement modern state estimation and filtering algorithms to achieve improved accuracy and noise suppression.

While navigation equipment usually plays a supporting role for pilot in-the-loop flying qualities investigations, it can assume a more central role for investigations of a systems nature, such as curved decelerating approaches. These may be carried out using either manual or automatic control.

The motion and navigation sensor complements of the NASA and NAE research helicopters are summarized in Table 3.

Evaluation Pilot Controls and Displays

An important requirement in any piloted simulation is the representation of control force characteristics. Similar to sophisticated ground-based research simulators, nearly all variable-stability aircraft today have the capability to model a wide range of force-deflection characteristics, including breakout, hysteresis, viscous and coulomb friction, and nonlinear spring gradients. These characteristics may also be influenced by the motion of the simulated aircraft being "flown" by the evaluation pilot. The flexibility that the three variable-stability research helicopters have for varying the evaluation pilot's control characteristics is summarized in Table 4.

Rapid advances have also taken place in cockpit display system hardware that now make it possible to consider more difficult control tasks such as curved or decelerating approaches. The programmable display equipment available in the NASA and NAE helicopters is also noted in Table 4.

Computational Capacity

It is usually not possible for variable-stability aircraft today to employ the full potential of current computer technology. To take advantage of increasingly

compact and more powerful computing equipment would compromise the availability of the aircraft for conducting research programs. As a notable exception to this statement, the NAE B205A-1 has recently been equipped with a locally-designed multi-microprocessor digital computing system that replaced the original minicomputer installation. This development has provided the ability to carry full laboratory operating-system software,and to implement on-line data handling programs in addition to the necessary flight programs.

While the NAE capability is exceptional, the computational capacity of the CH-47B and the UH-1H(V/STOLAND) research helicopters, listed in Table 5, is adequate to meet requirements at their current stages of development.

The objectives of presenting these brief descriptions have been to illustrate the differing yet complementary capabilities of these research helicopters, to identify areas where further development could be warranted, and to provide a basis for assessing the potential of these facilities to carry out future rotorcraft research. These considerations are discussed briefly in the following section.

Future Potential of Variable Stability Research Helicopters

There is little doubt that the application of variable-stability helicopters to various general or specific research and development problems would be broadened significantly if their capabilities were improved. Such indeed turned out to be the case when several of the conventional variable-stability aircraft developed five or six degree-of-freedom simulation capabilities in the past decade. Some of their applications to new classes of aircraft and to basic research in the field of human response studies, for example, are noted in Reference 36. However, achieving full six degree-of-freedom controlled motion capability in a helicopter is admittedly more complex. (The additional longitudinal and lateral force-generating capability in hover needs to be provided by an auxiliary reactive propulsion system.) Increased application to V/STOL vehicles is the usual justification given for proposing this capability, but may also be one reason why it has not yet been realized. A fairly large amount of longitudinal-force control power is usually considered necessary for this application; whereas, a considerably smaller amount could still permit investigation of important rotorcraft problems such as instrument flying qualities criteria with external loads (where oscillatory longitudinal motions can be a source of difficulty). In addition, simulations of large heavy-lift helicopters and airships might be possible.

Associated with an expanded simulation envelope is the continuous need for improved simulation fidelity. Greatly enhanced computational capacity combined with modern multivariable control system design methods should ultimately result in improved variable-stability system performance. If model-following methods are employed, an associated area to benefit is the simulation of wind and turbulence, including windshear. Also requiring improvement is the simulation of instrument flight conditions, particularly the transition to visual flight at instrument approach minimums. Technology to permit more realistic representation of this critial area would be of major benefit to all in-flight simulators, and possibly ground-based simulators as well.

The three variable-stability helicopters that are described briefly in this presentation could indeed benefit from these and other improvements. However. each has distinctly different and complementary capabilities that tend to focus its applications. The UH-1H (V/STOLAND) helicopter's navigation sensors make it ideally suited to investigations of a systems nature, such as terminal-area approach procedures, or the implementation and testing of new automatic guidance and control concepts. In this regard, a full-flight-envelope autopilot designed using the inverse model techniques described in Reference 34, is under development and is nearing flight test. Although the capability of this aircraft to simulate a wide range of flying qualities or to perform aggressive NOE-type maneuvers even with low levels of stability augmentation is severely limited by its variable-stability system actuators, the facility is considered adequate for representing the generic flying qualities of most current SAS-equipped helicopters during conventional instrument approach tasks.

Alternatively, the NAE B205A-1 is undoubtedly the superior vehicle for general flying qualities research, including the simulation of specific designs. Limited only by the inherent control power available from its teetering rotor, and its four controlled degrees-of-freedom, it is able, among other attributes, to accommodate aggressive maneuvers such as might arise from simulated systems failures, even when close to the ground. However, it has a limited cockpit display and navigation system capability with which to conduct advanced integrated systems investigations.

The CH-47B, also intended primarily for pilot in-the-loop flying qualities investigations, is distinctive for its ability to address problem areas associated with external load control. In addition, its greater amount of control power in pitch, which arises from the use of differential collective for this purpose, permits simulation of the response characteristics that may be associated with different rotor system designs. The aircraft is also equipped with a programmable symbol generator and associated electronic CRT cockpit displays, giving it the greatest capability in this area of the research helicopters discussed in this paper. However, the CH-47B is presently at a considerably lower level of development than the other facilities.

These aircraft are capable of making significant contributions to the development of flying qualities criteria and systems requirements for a variety of mission requirements applications, such as the FAA certification and military NOE programs mentioned earlier. In addition to the research programs that have already been undertaken, a number of other applications also within these general areas are as proposed:

1) The development of sensors and control laws for automatic hover control, including precision control of an external load and hover relative to a moving platform; and the development of stability augmentation systems and displays to support the manual execution of these tasks.

2) The investigation of stabilization systems for external loads in hover and in forward flight, along with associated flying qualities in instrument flight conditions.

3) The development of navigation, guidance, control and display system requirements necessary to exploit the very low-speed capabilities of the helicopter in instrument flight conditions in both remote and congested areas.

4) The evaluation of new man-machine interface technology, such as voice actuation, tactile controllers, and multi-axis side-arm controllers, that requires development to exploit new electronic flight control systems.

5) The investigation of energy management techniques and associated control and display requirements applied to engine-failure situations in single or twin-engine helicopters.

6) The evaluation of advanced theoretical control system concepts for which modeling errors and sensor noise and accuracy may represent major limitations.

An important aspect of these criteria and system development efforts that is sometimes overlooked is the determination of boundaries defining minimum acceptable standards for FAA criteria, or to meet Level II and Level III military flying qualities and performance specifications. This usually involves the systematic variation of configurations in realistic mission simulations for which general-purpose ground-based or airborne simulators are well-suited. Rarely, however, can a single facility provide all of the required data with the level of confidence necessary to establish criteria. Instead, a number of carefully planned investigations using facilities with complementary capabilities are usually conducted. The unique features of variable-stability research helicopters, such as those described in this presentation, offer important capabilities with which to address these issues.

Concluding Remarks

The application of variable-stability research helicopters to support new developments in the rotorcraft industry has increased significantly in the past several years. This has been associated mainly with developing criteria to support the recent widespread use of helicopters in more demanding missions, and to a lesser extent, with the development of new designs. Still, recognition of the potential of these facilities has been overshadowed by the confidence, much of it yet to be substantiated, that has been growing in the new capabilities of modern ground-simulation technology. This presentation has called attention to the historical development of these aircraft that places them in the class of long-term general-purpose flight research facilities. The review of their previous applications, and the summary of their current and potential capabilities that have been presented, suggest the nature of the applications that could emerge for these vehicles in the future. At a time when rotorcraft and flight control system technologies are making rapid advances, and the use of helicopters for a variety of new tasks is becoming more widespread, it is probable that variable-stability reseach helicopters will continue to serve an increasingly useful role.

References

(1) Attfellner, S., and Rade, M.,"BO 105 In-Flight Simulator for Flight Control and Guidance Systems," First European Rotorcraft and Powered-Lift Aircraft Forum, Southampton, September 1975.

(2) White, S., Jr., and Condon, G.W., "Flight Research Capabilities of the NASA/Army Rotor Systems Research Aircraft," Presented at the Fourth European Rotorcraft and Powered-Lift Aircraft Forum, Stresa, September 1978.

(3) Whitten, J.B., Reeder, J.P., and Crim, A.D., "Helicopter Instrument Flight and Precision Maneuvers as Affected by Changes in Damping in Roll, Pitch, and Yaw," NACA TN 3537, November 1955.
(4) Salmirs, S., and Tapscott, R.J., "The Effects of Various Combinations of Damping and Control Power on Helicopter Handling Qualities During Both Instrument and Visual Flight," NASA TN D-58, October 1959.
(5) Anderson, S.B., "An Examination of Handling Qualities Criteria for V/STOL Aircraft," NASA TN D-331, July 1960.
(6) Anon., "Recommendations for V/STOL Handling Qualities," NATO, AGARD Rep. 408, October 1962.
(7) Anon., "Recommendations for V/STOL Handling Qualities with an Addendum Containing Comment on the Recommendations," NATO, AGARD Rep. 408A, October 1964.
(8) Anon., "V/STOL Handling," NATO, AGARD Rep. 577, Part I-Criteria and Discussion, December 1970, Part II-Documentation, June 1973.
(9) Anon., "V/STOL Display for Approach and Landing," NATO, AGARD Rep. 594, July 1972.
(10) Anon., "Military Specification-Flying Qualities of Piloted V/STOL Aircraft," December 1970.
(11) Garren, J.F., Jr., and Kelly, J.R., "Description of an Analog Computer Approach to V/STOL Simulation Employing a Variable-Stability Helicopter," NASA TN D-1970, January 1964.
(12) Daw, D.F., and McGregor, D.M., "Development of a Model-Controlled V/STOL Airborne Simulator," National Aeronautical Establishment Rep. LR-352, August 1962.
(13) Gould, D.G., "The Model-Controlled Method for Development of Variable Stability Aircraft," National Aeronautical Establishment Rep. LR-345, June 1962.
(14) Hindson, W.S., "The NAE Airborne V/STOL Simulator as a Design and Development Tool for V/STOL Aircraft," Canadian Aeronautics and Space Journal, December 1970.
(15) Daw, D.F., Lum, K., and McGregor, D.M., "Description of a Four Degree of Freedom V/STOL Aircraft Airborne Simulator," National Aeronautical Establishment Rep. LR-499, February 1968.
(16) Sinclair, S.R.M., Roderick, W.E.B., and Lum, K., "The NAE Airborne V/STOL Simulator," Presented at AGARD Flight Mechanics Panel on Rotorcraft Design, May 1977.
(17) Kelly, J.R., et al., "Descrition of the VTOL Approach and Landing Technology (VALT) CH-47 Research System," NASA TP 1436, August 1979.
(18) Nelson, J.R., "The FAA Helicopter Operations Development Program," Presented at the Fifth European Rotorcraft and Powered-Lift Aircraft Forum, Amsterdam, September 1979.
(19) Lebacqz, J.V., Weber, J.M., and Corliss, L.D., "A Flight Investigation of Static Stability, Control Augmentation, and Flight Director Influences on Helicopter IFR Handling Qualities," Presented at the 37th AHS Forum, New Orleans, May 1981.
(20) Kereliuk, S., and Sinclair, M., "Evaluation of IFR Handling Qualities of Helicopters Using the NAE Airborne V/STOL Simulator," Atlantic Aeronautical Conference, Williamsburg, March 1979.
(21) Peach, L.L., Jr., et al., "NASA/FAA Flight-Test Investigation of Helicopter Microwave Landing System Approaches," Presented at the 36th Forum, Washington, May 1980.
(22) Lebacqz, J.V., "Survey of Helicopter Control/Display Investigations for Instrument Decelerating Approach," NASA TM 78565, March 1979.
(23) Niessen, F.R., et al., "The Effect of Variations in Controls and Displays on Helicopter Instrument Approach Capability," NASA TN D-8385, February 1977.
(24) McGee, L.A., et al., "Automatic Helical Rotorcraft Descent and Landing Using a Microwave Landing System," Presented at AIAA Atmospheric Flight Mechanics Conference, Albuquerque, August 1981.
(25) Corliss, L.D., and Carico, D.G., "A Preliminary Flight Investigation of Cross-Coupling and Lateral Damping for Nap-of-the-Earth Helicopter Operations," Presented at the 37th AHS Forum, New Orleans, May 1981.
(26) Sinclair, M., and Morgan, M., "An Investigation of Multi-axis Isometric Side-arm Controllers in a Variable Stability Helicopter," National Aeronautical Rep. LR-606, August 1981.
(27) Sinclair, S.R.M., Kereliuk, S., and Wood, A.D., "Simulation of Hovering Flight Characteristics of the Rotor Systems Research Aircraft Using the NAE Airborne V/STOL Simulator," National Aeronautical Establishment Rep. LTR-FR-53, July 1977.
(28) Wright, G.P., and Lappos, N., "Spirit Handling Qualities Design and Development," Presented at the 35th AHS Forum, Washington, May 1979.
(29) Anon., "Tactical Aircraft Guidance System Advanced Development Program Flight Test Phase Report Vols I and II," USAAMRDL TR 73-89A and B, April 1974.

(30) Baker, F.A., et al., "V/STOLAND Avionics System Flight-Test Data on a UH-1H Helicopter," NASA TM 78591/ AVRADCOM TR 79-23, February 1980.
(31) Sattler, D.E., et al., "An Investigation of the Recovery from an Engine Failure in a Twin Engine Augmentor Wing Aircraft Using the NAE Airborne Simulator," Canadian Aeronautics and Space Journal, First Quarter 1981.
(32) Rynoski, E.G., "Adaptive Multivariable Model-Following for Aircraft," Presented at the Joint Automatic Control Conference, San Francisco, August 1980.
(33) Stengel, R.F., et al., "The Design of Digital Adaptive Controllers for VTOL Aircraft," NASA CR 144912, March 1976.
(34) Meyer, G., "The Design of Exact Non-Linear Model Followers," Presented at the 1980 Joint Automatic Control Conference, San Francisco, 1980.
(35) Sinclair, M., and Hindson, W.S., "The Wind and Turbulence Measuring System of the NAE Airborne Simulator," DME/ NAE Quarterly Bulletin No. 1977(4), National Research Council, Canada.
(36) Anon., "V/STOL Flight Simulation," NASA TM 81156, November 1979.

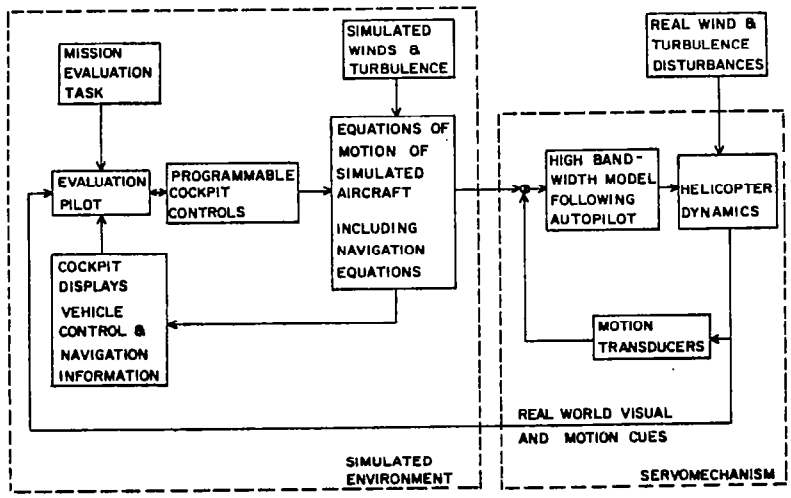

Figure 1. Model-Following Method for Airborne Simulation

Table 1. Comparison of Variable Stability Helicopter Simulation Envelopes

		NASA CH-47B	NASA UH-1H(V/STOLAND)	NAE B 205A-1
Flight envelope of basic production aircraft.		-30 to 160 kts longitudinally 35 kts in lateral flight. Maximum bank angle 40 deg below 145 kts, 20 deg at 160 kts.	-30 to 120 kts longitudinally 35 kts in lateral flight.	-30 to 120 kts longitudinally 35 kts in lateral flight.
Rotor system.		Fully articulated tandem counter-rotating rotors.	Single teetering rotor.	Single teetering rotor, stabilizer bar removed.
Basic controls available	. pitch . roll . yaw . heave . longitudinal pitch trim	Differential collective Lateral cyclic Differential lateral cyclic Main rotor collectives Independent longitudinal cyclic trim	Longitudinal cyclic Lateral cyclic Tail rotor collective Main rotor collective Mechanical elevator interconnect	Longitudinal cyclic Lateral cyclic Tail rotor collective Main rotor collective Independent elevator trim
Approximate control power in hover	. pitch . roll . yaw . heave[1]	1.9 r/sec^2 1.9 r/sec^2 0.9 r/sec^2 1.4 g	1.0 r/sec^2 2.5 r/sec^2 1.8 r/sec^2 1.15 g	1.0 r/sec^2 2.5 r/sec^2 1.8 r/sec^2 1.2 g
Variable stability system actuator characteristics. Notes 2 vicinity 50hz 3 vicinity 40hz		Parallel ectrohydraulic actuatorsin 4-axes with 100% authority high bandwidth[2]. Stop-to-stop travels achieved in approximately 1.5 sec.	Parallel electromechanical actuators in 4-axes with nearly 100% authority, lower bandwidth[3], and rate limits giving stop-to-stop control travels between 5.4 sec (collective) to 9.3 sec (tail rotor). Series electrohydraulic actuators in 4-axes with high bandwidth[2] and authority limited between 19% (collective) and 30% (tail rotor) of full travel. Rate limits 7 times faster than parallel servos.	Dual mode electrohydraulic actuators 4-axes 100% authority high bandwidth[2]. Stop-to-stop travels achieved within 0.75 sec.
Control system monitoring		Basic helicopter control rates monitored by hardware system with adjustable trip thresholds.	Hardware and software monitors with trip thresholds based on persisting servo command-response errors.	Safety pilot monitors control rate and position except for trips near max swash plate angles sensed by flapping angle transducers.
Remarks		Longitudinal cyclic trim gives very limited 5 degree-of-freedom control.		Extension to 5 or 6 degrees of freedom with auxiliary thrusting engines under investigation.

Note 1 T/W ≐ max wt for hover o.g.e. at s.l. with max cont. power/normal operating weight.

Table 2. Comparison of In-Flight Simulation Methods

Consideration	Response-Feedback	Model-Following
Implementation of simulated dynamics.	Desired dynamic response of each simulated configuration must be separately constructed from basic vehicle characteristics plus some combination of feedforwards/feedbacks.	Standard equations-of-motion model structure with aerodynamics of simulated vehicle incorporated directly for each program.
Requirement for precision on-line motion estimation.	Not necessarily required on-line.	Required for the degrees of freedom in which motion is controlled.
Requirement for in-flight dynamic calibrations for each simulated configuration.	Typically necessary to confirm characteristics.	Desirable but not generally required.
Knowledge required of basic vehicle response characteristics.	High precision.	Low precision except as needed for basic autopilot design.
Capability to control and simulate turbulence response.	Real turbulence effects not suppressed. Simulated turbulence response difficult to effect without influencing maneuver response.	Real turbulence effects suppressed. Simulated turbulence easily introduced, including windshears in the degrees of freedom that are controlled.

Table 3. Summary of Principal Instrumentation

	NASA CH-47B	NASA UH-1H(V/STOLand)	NAE B 205A-1
Motion Sensors in addition to 3-axis linear accelerometers 3-axis rate gyros Vertical and directional gyros	• INS linear velocities • INS gimbal angles • Laser doppler velocimeter low airspeed (3-axis) sensor planned • Instrumented boom with α,β vanes and static ports	• INS linear velocities • INS gimbal angles • 3-axis body-fixed Doppler radar • Loras and J-TEC low airspeed sensors • Laser doppler velocimeter low airspeed (3-axis) sensor planned (removable) • Instrumented boom with α,β vanes and static ports	• 3-axis body-fixed Doppler radar • Instrumented boom with α,β vanes and swivelling static port
Navigation and related sensors input to flight computers	• MLS • INS • Radar altimeter	• VOR/LOC, ILS • TACAN, DME • INS • MLS Cubic DME-based triangulation system • Radar altimeter	• MLS • Radar altimeter

Table 4. Summary of Evaluation Pilot Control and Display Hardware

	NASA CH-47B	NASA UH-1H(V/STOLAND)	NAE B 205A-1
Evaluation Pilot Controls	2-axis (pitch-roll) programmable force-feel system in procurement. Magnetic brake on collective lever and pedals. Adjustable spring cartridges on pedals.	Spring cartridge hungees with magnetic brake release and fixed gradients.	3-axis programmable force-feel system. Electric power lever or a collective can be installed. Side-arm controllers can be installed.
Cockpit Displays	Programmable electromechanical flight director (AD-350). Black and white CRT Displays-Electronic Attitude Director Indicator (EADI) and Multifunction Display with Programmable Symbol Generator.	Programmable electromechanical flight director (HZ-6F) and HSI. Programmable multifunction CRT display for situation and systems data.	Programmable electromechanical flight director (FD-109).

Table 5. Summary of Computational Capacity

	NASA CH-47B	NASA UH-1H(V/STOLAND)	NAE B 205A-1
Digital Computers	1 Sperry 1919A minicomputer 32K 18 bit words of RAM 50hz frame rate.	2 Sperry 1819B minicomputers each with 16K 18 bit words of RAM 50hz and 25hz frame rates.	3 PDP 11/23 microprocessors 48K RAM 64hz frame rate.
Analog Computers	EAI TR-48		120 operational amplifiers 60 integrators 120 manual pots 30 servo-set pots.

A PILOT-IN-THE-LOOP ANALYSIS OF SEVERAL KINDS OF HELICOPTER ACCELERATION/DECELERATION MANEUVERS

Robert K. Heffley
Principal Research Engineer
Systems Technology, Inc.
Mountain View, California 94043

Abstract

It is becoming increasingly convenient to measure and analyze directly the control strategy of pilots involved in performing authentic tasks — both in simulators and in flight. As a result, it is now possible to begin compiling a catalog of engineering descriptions of various flight tasks, the associated piloting technique, and the perceptual pathways involved. This paper describes how a certain class of helicopter flight tasks, namely acceleration/ deceleration maneuvers, can be quantified and put to use in the fields of handling qualities, flight training, and evaluation of simulator fidelity. The three specific cases include the normal speed change maneuver, the nap-of-the-earth dash/ quickstop, and the decelerating approach to hover. All of these maneuvers share common generic features in terms of pilot adaptation and mathematical description; yet each differs in terms of the essential feedback loop structure, implications for handling qualities requirements, and simulator fidelity criteria.

Notation

A	Gilinsky's perceived range constant
g	Gravity constant
h	Height
$\dot{h}$	Vertical velocity
$\dot{h}_{pk}$	Maximum sink rate during terminal landing maneuver
$\dot{h}_{td}$	Touchdown sink rate for landing maneuver
K_a	Pilot's effective gain in approach task
K_I	Pilot's integral gain in normal speed change maneuver
K_U	Pilot's speed loop gain
K_R	Pilot's position gain in dash/quickstop
$K_{\dot{R}}$	Pilot's closure rate gain in dash/ quickstop
R	Range (actual)
R_c	Position command
R_p	Perceived range
$\dot{R}$	Closure rate
$\dot{R}_{max}$	Maximum closure rate
$\ddot{R}$	Deceleration
u	Perturbation forward speed
U	Forward speed
U_c	Speed command
x	Fore-and-aft displacement
X_u	Speed damping stability derivative
$Y_{c_{()}}$	Controlled element transfer function
$Y_{p_{()}}$	Pilot control strategy transfer function
$\Delta\theta$	Perturbation pitch attitude
ζ	Damping ratio
$\zeta_{()}$	Closed-loop damping ratio of () task
r	Pitch attitude
θ_c	Pitch attitude command
θ_{pk}	Maximum pitch attitude during quickstop maneuver
ϕ_M	Phase margin
$\phi_{M_{()}}$	Phase margin of () task

ω	Natural frequency
$\omega_{()}$	Closed-loop natural frequency of () task
ω_c	Crossover frequency
$\omega_{c_{()}}$	Effective crossover frequency of () task

Subscripts

a	Approach to hover task
f	Landing flare task
r	Dash/quickstop task
u	Normal speed change task
x	Fore-and-aft position regulation task
θ	Pitch attitude regulation task

Introduction

The purpose of this paper is to describe, using a set of examples, certain elements of an approach to handling qualities which can quantitatively account for the pilot-vehicle response needs in performing specific flight tasks or maneuvers. This is accomplished by modeling the flight task or maneuver in a way which permits the inference of the pilot's loop structure and the relative dependence of task performance on various essential and supporting loops. This complements and is fully compatible with the equivalent systems approach to describing the vehicle dynamics[1,2] and, in fact, provides the needed context for applying bandwidth criteria[3].

If handling qualities are "those stability and dynamic response characteristics of an aircraft and its control system which impact the pilot's ability to complete some useful task or mission,"[4] then we must be prepared to quantify not only the vehicle but also the task. Task quantification is the real subject of this paper; and we illustrate the concept using examples of several kinds of helicopter acceleration/deceleration maneuvers.

Historically, handling qualities requirements have not been very closely tied to specific flight tasks. This holds for fixed-wing[5], V/STOL[6], and rotary-wing aircraft[7]. Perhaps the closest that existing specifications come to dealing with individual flight tasks is the fixed-wing handling qualities specification, MIL-F-8785C, and its three "flight phase categories;" however, we shall be dealing with at least one or two additional tiers of detail in the individual task or maneuver description (i.e., specific flight tasks and then individual axes of control for each task). With regard to the rotary-wing specification, MIL-H-8501A, there is the mention of specific flight tasks in connection with various power and speed conditions but, again, no quantitative definition. Hence, as specialized environments such as NOE have entered the scene, it has been necessary to consider significantly more stringent response standards such as those suggested by Edenborough and Wernicke[8]. An example of the level of task breakdown which should be considered is shown in Table 1[9]. This is based, in part, on careful tabulation of Army training objectives.

Table 1. Army Flight Tasks and Maneuvers (Rotary- and Fixed-Wing)

BASIC FLIGHT
- Straight and Level
- Climb/Descent
- Level Turns
- Climb/Descending Turns
- • Acceleration/Deceleration
- Traffic Pattern
- Slow Flight
- Stalls

HOVERING
- Takeoff to Hover
- Hover
- Hover Checks
- Hover Turns
- Forward Hover
- Land from Hover
- Hover Out of Ground Effect
- Confined Area
- Pinnacle/Ridgeline
- Slope

TAKEOFF
- Normal Takeoff
- Maximum Performance
- Short Field
- Obstacle Clearance
- Terrain Flight Takeoff

APPROACH/LANDING
- • Normal Approach/Landing
- Steep Approach
- Shallow Approach
- Go Around
- Short Field
- Obstacle Clearance
- Terrain Flight Approach
- VASI Approach

LOW ALTITUDE OPERATIONS
- Terrain Flight Navigation
- Low Level Flight
- Contour Flight
- NOE Flight
- Unmask/Remask
- • Dash/Quickstop
- Evasive Maneuvers

WEAPON DELIVERY
- Hover Fire
- Running Fire
- Diving Fire
- ACM

INSTRUMENT FLIGHT
- Takeoff
- Level Flight
- Turns
- Timed Turns
- Climbs/Descents
- Climb/Descending Turns
- Acceleration/Deceleration
- Autorotation
- VOR Navigation
- ADF Navigation
- Holding
- Unusual Attitude Recovery
- Navaid Approach
- GCA Approach
- Tactical Instrument Takeoff
- Tactical Instrument Approach

EMERGENCIES
- Hover Autorotation
- Standard Autorotation
- Standard Autorotation with Turn
- Low-Level Autorotation
- Hydraulic Malfunction
- Anti-Torque Malfunction
- Engine Failure at Altitude
- Engine Failure at Hover
- Flight at VMC (Single Engine)
- Single Engine Landing
- Single Engine Go Around
- Engine Failure at Takeoff
- Engine Failure During Approach

• Cases considered in this paper.

The aim of this paper, then, is to show how a more thorough treatment of individual flight tasks and maneuvers can result in better

understanding of the piloting technique, the perceptual pathways, crucial vehicle characteristics, and the role of supporting pilot loops. The hope is to arrive at a more rational and selective approach to handling qualities which looks after the key ingredients of any particular piloting task. This approach can also be useful in judging the validity of simulator investigations of handling qualities.

In order to illustrate the above concepts we shall consider one class of helicopter flight tasks, namely speed changes. Representing this class are three rather specific maneuvers:

1) Normal speed change maneuvers
2) NOE dash/quickstop
3) Decelerating approach to hover.

As we shall see, each involves a unique combination of abruptness, pilot compensation, essential loop structure, and crucial vehicle features. In effect, each maneuver represents a particular context for judging handling qualities.

Technical Approach

The approach to analyzing the speed change maneuvers listed above is adapted from a particularly successful and insightful analysis of the landing flare for a DC-10 jet transport[10]. Based on a direct estimation of closed-loop flight path response for the flare maneuver, pilot control strategy was quantified in considerable detail. This resulted, in turn, in identifying differences between landings performed in flight and in a simulator, the effects of training pilots in flight as opposed to on a simulator, and the key features in the pilot or aircraft responsible for any landing difficulties.

The analysis procedure applied to the DC-10 landing flare consisted of identifying the effective second-order closed-loop response parameters (e.g., frequency and damping) and subtracting the open-loop aircraft response in order to infer the pilot's control strategy. Each of these components, of course, has value, i.e.,

1) **Closed-loop pilot-vehicle response:** abruptness or urgency of the task and specific context for supporting loops or pilot actions.

2) **Open-loop aircraft response:** specific roles or influences of vehicle stability, control, and performance characteristics.

3) **Pilot control strategy:** availability of cues, ease of compensation, and level of skill.

One important tool in the DC-10 analysis was the use of a phase plane plot of the "command loop" (extreme outer loop) — in that case height versus height rate-of-change. Based on the phase plane trajectory, it was observed that the landing flare was equivalent to an unforced second-order response beginning with a set of state initial conditions and a set of state commands appropriate to touchdown. This is shown in the sketch in Fig. 1.

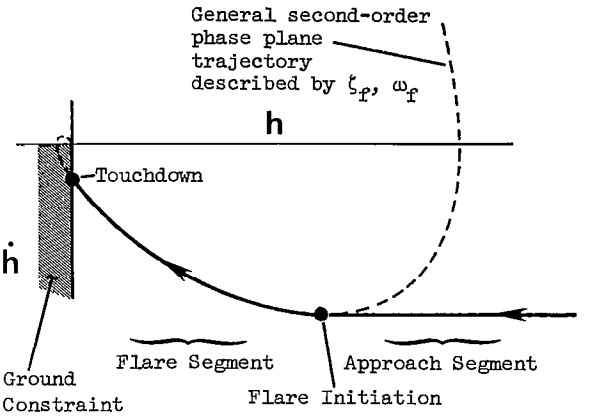

Figure 1. Phase Plane Depiction of Landing Flare

The closed-loop damping and natural frequency parameters, ζ_f and ω_f, can be found using rigorous parameter identification procedures, although even simple phase plane estimation methods work well. The sketch in Fig. 2 outlines all that we shall need in order to address the speed change maneuvers of interest here.

For the landing flare, it was found that a fairly large sample of pilots preferred a closed-loop damping ratio of about 0.7 ± 0.1 and a closed-loop natural frequency of about 0.4 ± 0.1 rad/sec. In terms of an effective bandwidth (crossover frequency) and phase margin, the DC-10 flare was found to have:

$$\text{Crossover Frequency, } \omega_{c_f} \approx 0.2 \text{ to } 0.33 \text{ rad/sec}$$

$$\text{Phase Margin, } \phi_{M_f} \approx 70 \text{ to } 90 \text{ deg}$$

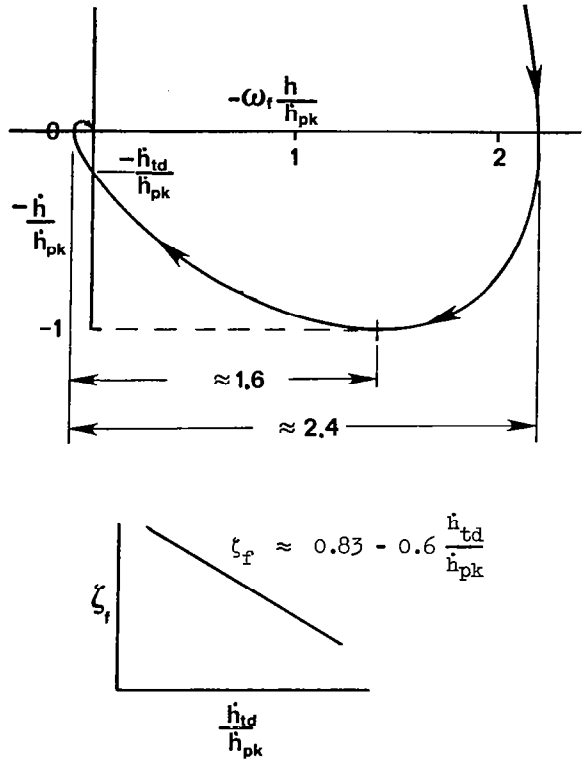

Figure 2. Normalized Phase Plane and Relationships for Extracting Closed-Loop Damping and Natural Frequency

These values therefore establish a highly quantitative context by which to judge basic airplane response characteristics and the degree of precision and control of pitch attitude required for support of the landing maneuver. As an example we might apply a factor-of-five rule of thumb for setting the necessary inner-loop pitch response bandwidth. Hence the equivalent-system pitch attitude bandwidth requirement for landing in the DC-10 should be at least 1 to 1.7 rad/sec —— a reasonable range of values.

Normal Speed Change Maneuver

The normal speed change maneuver in a helicopter might include takeoff as well as up-and-away flight. It is not unlike the corresponding maneuver in a fixed-wing aircraft. Cyclic pitch (or elevator) and collective (or throttle) are coordinated so as to effect an x-axis acceleration with minimal disturbance to flight path. In a helicopter the normal technique for slowing down is to simultaneously pitch up and lower the collective. The relative amount of collective control change tends to be in direct proportion to the airspeed; but collective control is a separate issue which can be handled apart from the pitch attitude control, per se.

The main determinant of a helicopter speed change is the use of pitch attitude since it can be shown that to a good first-order approximation[11]:

$$\Delta\dot{u} \approx X_u \Delta u - g\Delta\theta \qquad (1)$$

To this we can add the pilot's closed-loop control of attitude in terms of a first-order lag approximation involving pitch crossover frequency, ω_{c_θ}, i.e.,

$$\frac{\dot{\Delta\theta}}{\omega_{c_\theta}} \approx -\Delta\theta + \Delta\theta_c \qquad (2)$$

Thus a pilot control law can be expressed in terms of a pitch attitude command rather than a cyclic pitch control command, per se.

The basic control strategy for either regulating or changing speed will involve a speed feedback in the "command loop," i.e., as shown in Fig. 3. The job of the pilot is to adopt a speed

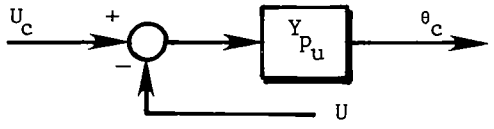

Figure 3. Control Strategy for the Normal Speed Change Maneuver

control strategy, Y_{P_u}, which will result in an effective management of speed, and we can obtain strong clues of the pilot's control strategy by observing a phase plane plot of speed versus acceleration. In several available flight cases, it can be observed that the phase plane trajectory of a speed change is essentially second order. Figure 4 shows some examples.

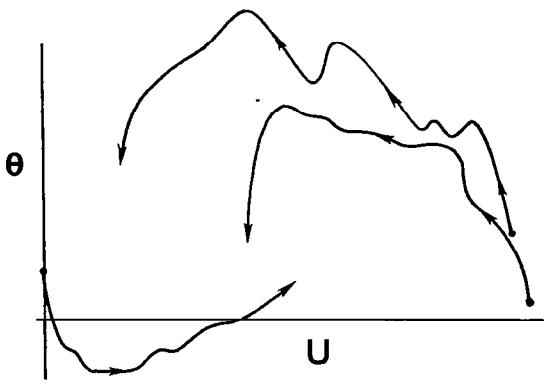

Figure 4. Typical Flight Examples of Normal Speed Changes

The kind of data shown in Fig. 4 can be replotted in conventional phase plane terms as shown in Fig. 5, even though good definition of the terminal condition is lacking. Where it is so ill-defined, we must estimate or assume a closed-loop damping ratio, ζ_u. A value of 0.7 to 0.9 is probably reasonable in view of the desire to avoid significant overshoot in any discrete maneuver. (Recall that for the landing flare a damping ratio of 0.7 was measured.) The ratio of peak pitch attitude change (or x-acceleration) to total speed change is directly related to the closed-loop natural frequency. According to the relationships shown in Fig. 2.

$$\omega_u \approx 2.4\, g\, \frac{\Delta\theta_{pk}}{\Delta U} \qquad (3)$$

Using the predominant closed-loop response and the essential helicopter dynamics, it is thus possible to solve directly for the pilot's control law, Y_{p_u}.

$$\text{i.e.,}\quad 0 = 1 + Y_{p_u} \cdot Y_{c_u} \approx s^2 + 2\zeta_u\omega_u s + \omega_u^2 \qquad (4)$$

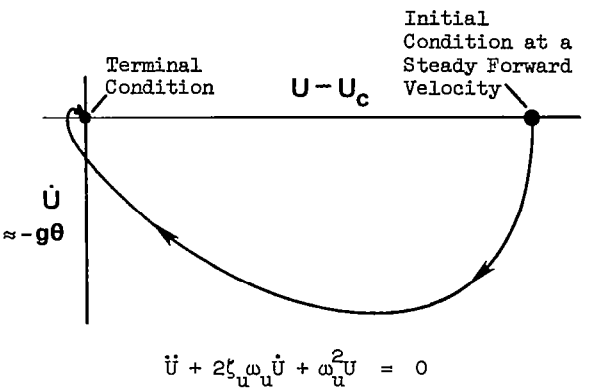

Figure 5. Typical Phase Plane of a Normal Speed Change

where $$Y_{c_u} \approx \underbrace{\frac{g}{s - X_u}}_{\text{Airframe Speed Response}} \cdot \underbrace{\frac{1}{\left(1 + \frac{s}{\omega_{c_\theta}}\right)}}_{\text{Closed-loop Pitch Response}} \qquad (5)$$

and, assuming an integral-plus-proportional speed control,

$$Y_{p_u} \approx K_U \left(1 + \frac{K_I}{s}\right) \qquad (6)$$

then

$$\frac{s^3}{\omega_{c_\theta}} + \left(1 + \frac{X_u}{\omega_{c_\theta}}\right) s^2 + \left(gK_U - X_u\right) s + gK_UK_I = 0 \qquad (7)$$

It can be shown that for $\omega_{c_\theta} \gg \omega_u$, the s^3 term is negligible and the s^2 coefficient is nearly unity. (Also X_u is often negligible.)

Thus

$$K_U \approx \frac{2\zeta_u\omega_u + X_u}{g} \quad \text{and} \quad K_I \approx \frac{\omega_u^2}{2\zeta_u\omega_u + X_u} \qquad (8),(9)$$

Typical flight data may show a 10 deg pitch change for an 80 kt speed change which therefore corresponds to an ω_u of 0.1 rad/sec according to Eqn. (3). For a ζ_u of 0.7, this would yield a crossover frequency of 0.07 rad/sec and a phase margin of about 85 deg. It should also be noted that only a pitch attitude cue and a speed cue (i.e., indicated airspeed) are needed to accomplish this task. The integral term implies a trimming function in parallel with the basic pitch attitude command. Thus the basic pilot gains (assuming a typically negligible X_u for helicopters) would be

$$K_U \approx 0.4\,\frac{\text{deg}}{\text{kt}} \quad \text{and} \quad K_I \approx 0.07/\text{sec} \qquad (10),(11)$$

In retrospect it can be seen that the usual closed-loop pitch attitude bandwidth (ω_{c_θ}) of about 1 rad/sec is not critical to the performance of a the normal speed change maneuver; in fact, it could be as low as 0.35 rad/sec and still provide adequate support to the task. Takeoff time histories for a UH-60[12] seem to substantiate these estimates well in that an airspeed inverse time constant of about 0.1/sec and an attitude inverse time constant of about 0.33/sec can be observed.

NOE Dash/Quickstop Maneuver

This is a far more aggressive variety of speed change maneuver than that considered above. The NOE speed change — really a position change — also involves use of collective pitch to offset height changes and prevent ground contact. As before, though, we shall treat only the x-axis, i.e., the pilot's control law for effecting a speed change through use of pitch attitude control, and set aside the important collective control aspects. (At the same time, we are establishing the context of the collective control task.)

The basic control strategy for the NOE maneuver involves a range command-loop (Fig. 6) since position is of ultimate importance. A phase plane portrait of the dash/quickstop is therefore correctly depicted in the $\dot{R}$ - R plane of Fig. 7. Note that we can handle either the dash-quickstop combination or the quickstop alone depending upon how we pick initial conditions, but the family of phase plane trajectories would be the same.

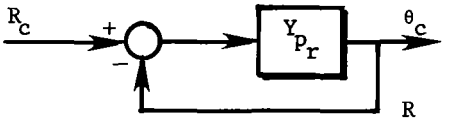

Figure 6. Command Loop for the NOE Speed (Position) Change

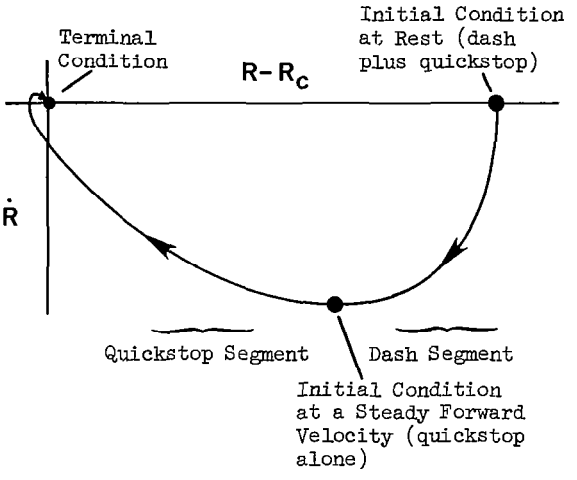

$$\ddot{R} + 2\zeta_r\omega_r\dot{R} + \omega_r^2 R = 0$$

Figure 7. Range Phase Plane Assuming Second-Order Closed-Loop Behavior

If the NOE speed change is assumed to involve both a range and a velocity feedback, then

$$Y_{p_r} = K_R + K_{\dot{R}}s \qquad (12)$$

The controlled element is the same as before except for an additional integration, i.e.,

$$Y_{c_r} \approx -\frac{g}{s(s - X_u)} \cdot \frac{1}{\left(1 + \frac{s}{\omega_{c_\theta}}\right)} \qquad (13)$$

Airframe x-Position Response | Closed-Loop Pitch Response

$$\text{thus } 0 = Y_{p_r} Y_{c_r} + 1 \approx s^2 + 2\zeta_r \omega_r s + \omega_r{}^2 \qquad (14)$$

and

$$\frac{s^3}{\omega_{c_\theta}} + \left(1 - \frac{X_u}{\omega_{c_\theta}}\right)s^2 + (gK_R^{\bullet} - X_u)s + gK_R = 0 \qquad (15)$$

and with the same simplifying conditions as before for the s^3 and s^2 terms,

$$K_R^{\bullet} \approx \frac{2\zeta_r \omega_r}{g} \quad \text{and} \quad K_R \approx \frac{\omega_r^2}{g} \qquad (16), (17)$$

Observations made for a UH-1H performing quickstops in flight[9] were that

$$\frac{\theta_{pk}}{\dot{R}_{max}} \approx 1 \frac{\text{deg}}{\text{kt}} \qquad (18)$$

e.g., starting from 40 kt, the peak pitch-up during the deceleration was about 40 deg. Based on these observations,

$$K_R^{\bullet} \approx 4 \frac{\text{deg}}{\text{kt}} \quad \text{and} \quad K_R \approx 1 \frac{\text{deg}}{\text{ft}} \qquad (19)$$

This corresponds to $\omega_r \approx 0.8$ rad/sec and, for $\zeta_r \approx 0.7$, the effective crossover frequency is 0.5 rad/sec and the phase margin is 85 deg. This is an extraordinarily high bandwidth for an x-axis task! Again applying a factor-of-five bandwidth requirement for pitch attitude, an NOE dash/quickstop should require about 2.5 rad/sec ω_{c_θ} —— nearly an order of magnitude higher than the normal speed change task. Also, this value agrees well with the pitch damping (essentially pitch attitude bandwidth) suggested by Edenborough and Wernicke[8] for the NOE regime. This bandwidth requirement, of course, is at great variance with the pitch damping specified in MIL-H-8501A (see Ref. 11).

Decelerating Approach to Hover

This is a flight task for which the estimation of a simple pilot control strategy is obscured by the effects of visual perception of range. Moen, et al.,[13] collected numerous approach profiles, such as those shown in Fig. 8; but it is not possible to fit simple linear, constant-coefficient models as in the previous two cases.

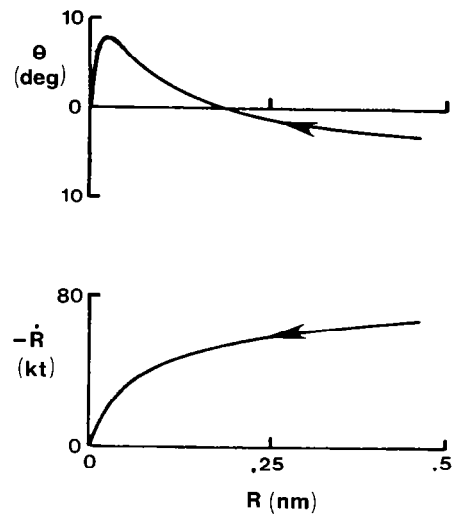

Figure 8. Typical Approach Profiles Measured by Moen, et al.[13]

It was found, however, that if the "perceived range" function of Gilinsky[14] was assumed to be operating, i.e.,

$$\text{Perceived Range, } R_p = \frac{R}{1 + R/A}, \qquad (20)$$

where A is an empirically obtained perceived range constant and R is the actual range, then the pilot control strategy for the entire

approach followed by hover is a simple, stationary form such as shown in Fig. 9.

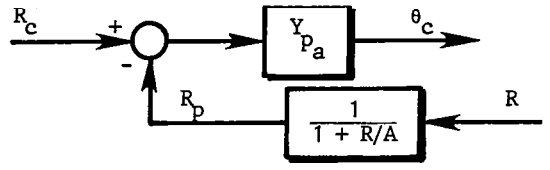

Figure 9. Decelerating Approach-to-Hover Control Strategy

A closed-form solution of the approach profile can be derived[15] in terms of deceleration or pitch attitude versus range:

$$g\Delta\theta \approx \ddot{R} \approx \frac{K_a^2 R}{(1 + R/A)^3} \qquad (21)$$

where K_a is an effective pilot control strategy gain and the effective crossover frequency can be expressed as a function of range by

$$\omega_{c_a} \approx K_a \cdot \frac{1}{1 + R/A} \qquad (22)$$

The goodness of this model is shown in Fig. 10 along with two fittings to a set of flight data — one slightly better at long range and the other at short range.

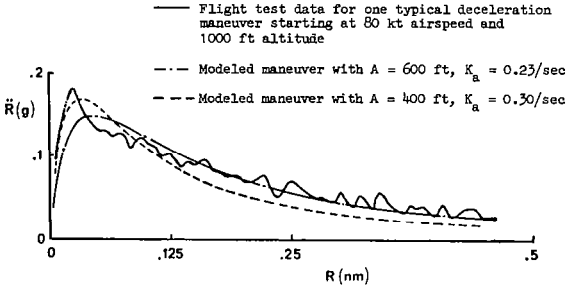

Figure 10. Comparison of Deceleration Profiles Between Analytical Model and Flight Test Data

Note that a value of 0.25 for K_a and 500 ft for A would give a crossover equal to about 0.035 rad/sec at 0.5 nm, 0.065 rad/sec at 0.25 nm, and 0.25 rad/sec at hover, i.e., a steadily increasing bandwidth. It is particularly interesting that the model applies to a steady hover as well as to the entire speed transition. Furthermore, the above estimated value of ω_{c_a} at hover agrees well with the simulator measurements made by Ringland, et al.,[16] using an open cockpit on the NASA Ames Research Center S.01 six-degrees-of-freedom simulator. Those data showed hover position bandwidth $\omega_{c_x} \approx 0.2$ rad/sec for three pilots.

One last observation for this case is that the supporting pitch attitude bandwidth requirement would be about 1.3 rad/sec, and crucial only during the very last portion of the maneuver. This agrees with the Ringland data[16] (the measured ω_{c_θ} was about 1.4 rad/sec) and other multiloop analytical approaches as exemplified by Craig, et al.,[17].

Handling Qualities Implications

As a result of the above analysis, we have defined the x-axis control for three basic helicopter speed change maneuvers. In each case there were variations in cues used and in the abruptness and, therefore, the quickness required in the attitude response. This is summarized in Table 2.

Table 2. Summary of Helicopter Speed Change Characteristics

Maneuver	Loop Structure, Pilot Cues	Effective Crossover in Outer Loop	Implied Bandwidth Requirement for Pitch Attitude
Normal Speed Change	$\dot{U} \rightarrow \theta_c$ (integral-plus-proportional compensation)	≈0.07 rad/sec	≈0.35 rad/sec
Decelerating Approach to Hover	$R_p \rightarrow \theta_c$ (Pure gain using "perceived range")	Increasing to ≈0.25 rad/sec	Increasing to ≈1.3 rad/sec
NOE Dash/Quickstop	$R, \dot{R} \rightarrow \theta_c$	≈0.5 rad/sec	≈2.5 rad/sec

It should be noted that certain handling qualities requirements having fair agreement with present standards have been derived from a direct, simple analysis of basic discrete-maneuver flight tasks. Furthermore, the parameters used to characterize the outer-loop discrete maneuvers are identical in form to the inner-loop regulatory or tracking functions such as attitude control. For example we can deal with pilot control strategy gains, pilot compensation, crossover frequencies, phase margins, etc.

The very limited depth of the foregoing analysis must be recognized, however. The amount and quality of flight data supporting the numerical results presented is grossly inadequate for setting design standards. Data for individual flight tasks must be gathered systematically for reasonably large populations of skilled pilots and various vehicle types. As shown, analysis methods do not require large arrays of vehicle state records, therefore extensive flight test instrumentation is not really needed. To an extent, existing flight and simulator data could be reanalyzed. Useful data can also be obtained nonintrusively from flight and simulator investigations having other primary objectives.

A thorough quantitative definition of helicopter flight tasks and maneuvers should include those listed in Table 1 with special emphasis on the critical mission segments such as NOE or air-to-air combat or difficult operating environments such as nighttime, instrument meteorological conditions, or extreme atmospheric disturbances.

Handling qualities are not solely tied to "stability and control" but can also impact "performance" aspects, especially in extreme maneuvers. For example, in normal speed change maneuvers (including takeoff) or in an approach to hover, large torque transients due to the pilot's use of collective pitch are not likely. Performance of a very abrupt quickstop, on the other hand, requires collective pitch applied with commensurate quickness to avoid ground-tail contact or excessive increase in altitude. The specific amount of maneuver abruptness (in terms of ω_r or ω_{c_r}) implied by the quickstop analysis presented here is likely to lead to the rotor drive-system/fuel-control coupling discussed in Ref. 18. The result may be significant rotor underspeed/overspeed transients which, in effect, limit just how aggressively the pilot performs in a critical situation. It should be further noted that the pilot model arising from the flight task analysis can also be used as a tool for unmanned computer simulation in very early design stages. Thus realistic closed-loop investigations can be conducted into "stability and control" and "performance" interactions.

The main handling-qualities-related objective of the analysis approach presented has been to emphasize the rational, direct relationship between a task and its supporting handling qualities features.

Simulator Fidelity

Simulator fidelity is a basic issue in the field of handling qualities when flight simulation is the main source of pilot and performance data. Normally simulator fidelity is established by focusing on the correctness of dynamic response of the simulator motion and visual systems and the vehicle mathematical model. The result is frequently great simulator system sophistication and model complexity.

One criterion for simulator fidelity is the extent to which the simulator induces the same piloting technique or control strategy for a given task as does the actual aircraft[9]. Thus we might measure pilot control strategy in the simulator in the manner suggested here and compare it to flight. This was done in the case of the DC-10 landing maneuver[10] and found to reveal significant differences accounting for landing performance problems. In addition, certain adverse training effects were spotted in terms of pilot control strategy.

A simulator fidelity effect which relates to the speed change maneuvers analyzed here was found in a recent set of unpublished data obtained from an Army UH-60 training simulator. These data, shown in Fig. 11, describe a quickstop maneuver as performed by an instructor flying at low altitude over a runway.

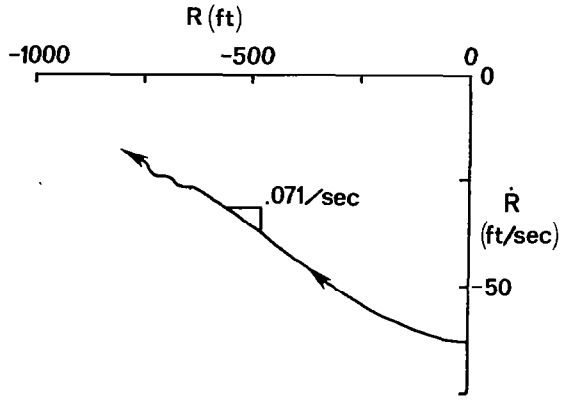

Figure 11. Quickstop Phase Plane Data From UH-60 Training Simulator

Direct inspection of the phase plane of $\dot{R}$ versus R reveals a constant slope of 0.071 ft/sec/ft with no apparent preference for range. The approximate closed-loop roots are therefore $(s + \omega_{c_\theta})(s + 0.065)s$. Equation (15) can thus be used to estimate $K_{\dot{R}}^{\bullet}$ and K_R, i.e.,

$$0 = \frac{s^3}{\omega_{c_\theta}} + s^2 + g K_{\dot{R}}^{\bullet} s + g K_R$$

$$\approx \frac{s^3}{\omega_{c_\theta}} + \left(1 + \frac{0.071}{\omega_{c_\theta}}\right) s^2 + 0.065s \qquad (22)$$

Hence

$$K_{\dot{R}}^{\bullet} \approx 0.2 \frac{\text{deg}}{\text{kt}} \quad \text{and} \quad K_R \approx 0 \qquad (23), (24)$$

Comparing these values to the 4 deg/kt and 1 deg/ft, respectively, estimated from flight, we see that in the simulator the closure-rate feedback was more than an order of magnitude smaller and that the range feedback was essentially nonexistent. Having such a disparity should, of course, discourage any use of the simulator for that particular maneuver, but it also can help to diagnose the source of simulator fidelity problems. In the case cited above, it is likely that the main limiting feature was the downward field of view over the nose. According to the simulator specification[19] this was 18 deg, and the maximum pitch attitude recorded during the maneuver was 13 deg.

Conclusions

Using, as an example, three specific kinds of helicopter speed change maneuvers, we have demonstrated how each of the maneuvers can be modeled and interpreted in terms of its own individual pilot control strategy. The normal speed change maneuver relies only on a speed feedback loop with some proportional-plus-integral compensation. The maneuver is mild and requires minimal response bandwidth in the supporting pitch attitude regulation.

The NOE dash/quickstop contrasts greatly with the normal speed change maneuver in terms of abruptness and requires both range and closure-rate feedbacks. The pilot's aggressiveness in the maneuver calls for a very large pitch attitude bandwidth in order to adequately control the vehicle. In addition, the collective pitch control response required to support the maneuver in terms of height regulation may precipitate engine/fuel-control deficiencies in adequately controlling rotor rpm.

The third maneuver, the decelerating approach to hover, is intermediate to the other two in terms of abruptness but involves pilot perception in a special way. It is shown that the pilot control strategy can remain relatively invariant throughout the approach and ensuing hover and that the main source of closed-loop variation arises from the nonlinear effect of range perception.

Handling qualities implications can be drawn in each case by inspecting the role of vehicle dynamics either in the direct response (in these cases, speed response) or in the response of supporting axes or controls (e.g., pitch attitude due to cyclic pitch change). This was demonstrated for the simple cases considered here by applying a "factor-of-five" inner-loop/outer-loop bandwidth criterion. A more thorough, systematic treatment would, of course, be required to set firm handling qualities requirements.

Simulator fidelity was also addressed in terms of the analysis approach illustrated here. The main fidelity criterion used was the direct, quantitative comparison of the pilot control strategy induced in a particular simulator versus that induced by an actual aircraft counterpart. Discrepancies in control strategy

can then be used to aid in searching for specific sources of deficiencies in the simulator motion or visual systems or in the computer mathematical models of the vehicle and environment.

It is suggested that the general approach illustrated here be applied in a broader, more thorough manner to the field of handling qualities. The approach provides a rational way to account for the handling-qualities needs in supporting a given flight task. It also offers a means for evaluating the validity and effectiveness of flight simulation tools which must be used in establishing handling qualities requirements.

References

1. Stapleford, R. L.; McRuer, D. T.; Hoh, R. H.; Johnston, D. E.; and Heffley, R. K., "Outsmarting MIL-F-8785B(ASG), the Military Flying Qualities Specification," Systems Technology, Inc., Technical Report No. 190-1, August 1971.

2. Hodgkinson, J., "Equivalent Systems Approach for Flying Qualities Specification," SAE Control and Guidance Systems Committee Meeting, Denver, CO, March 1979, (MCAIR Paper 79-017).

3. Hoh, R. H.; Mitchell, D. G.; and Hodgkinson, M., "Bandwidth - A Criterion for Highly Augmented Airplanes," AIAA Paper No. 81-1890, AIAA Atmospheric Flight Mechanics Conference, Albuquerque, NM, August 19-21, 1981.

4. George, Frank L.; and Moorhouse, David J., "Relationship of the Flying Qualities Specification to Task Performance," AIAA Workshop on Flight Testing to Identify Pilot Workload and Pilot Dynamics, AFFTC, Edwards AFB, CA, January 19-21, 1982.

5. Anon., "Military Specification -- Flying Qualities of Piloted Airplanes," MIL-F-8785C, November 5, 1980.

6. Chalk, Charles R.; Key, David L.; Kroll, John, Jr.; Wasserman, Richard; and Radford, Robert C., "Background Information and User Guide for MIL-F-83300-Military Specification -- Flying Qualities of Piloted V/STOL Aircraft," AFFDL-TR-70-88, March 1971.

7. Anon., "Military Specification -- Helicopter Flying and Ground Handling Qualities; General Requirements For," MIL-H-8501A, Amendment 1, April 3, 1962.

8. Edenborough, H. K.; and Wernicke, K. G., "Control and Maneuver Requirements for Armed Helicopters," AHS Twentieth Annual National Forum, Washington, D. C., May 13-15, 1964.

9. Heffley, Robert K.; Clement, Warren F.; Ringland, Robert F.; Jewell, Wayne F.; Jex, Henry R.; McRuer, Duane T.; and Carter, Vernon E., "Determination of Motion and Visual System Requirements for Flight Training Simulators," Systems Technology, Inc., Technical Report No. 1162-1, August 1981 (forthcoming ARI report).

10. Heffley, Robert K.; Schulman, Ted M.; Randle, Robert J., Jr.; and Clement, Warren F., "An Analysis of Airline Landing Flare Data Based on Flight and Training Simulator Measurements," Systems Technology, Inc., Technical Report No. 1172-1R, March 1982 (forthcoming NASA TM).

11. Heffley, Robert K., "A Compilation and Analysis of Helicopter Handling Qualities Data. Volume Two: Data Analysis," NASA CR-3145, August 1979.

12. Nagata, John I.; Skinner, Gary L.; Buckanin, Robert M.; Robbins, Robert D.; and Williams, Robert A., "Airworthiness and Flight Characteristics Evaluation, UH-60A (Black Hawk) Helicopter," Final Report on USAAEFA Project No. 77-17, September 1981.

13. Moen, Gene C.; DiCarlo, Daniel J.; and Yenni, Kenneth R., "A Parametric Analysis of Visual Approaches for Helicopters," NASA TN D-8275, December 1976.

14. Gilinsky, Alberta S., "Perceived Size and Distance in Visual Space," Psychological Review, Vol. 58, 1951, pp. 460-482.

15. Heffley, Robert K., "A Model for Manual Decelerating Approaches to Hover," Proceedings of the Fifteenth Annual Conference on Manual Control, AFFDL-TR-79-3134, November 1979, pp. 545-554.

16. Ringland, R. F.; Stapleford, R. L.; and Magdaleno, R. E., "Motion Effects on an IFR Hovering Task -- Analytical Predictions and Experimental Results," NASA CR-1933, November 1971.

17. Craig, Samuel J.; and Campbell, Anthony, "Analysis of VTOL Handling Qualities Requirements. Part I: Longitudinal Hover and Transition," AFFDL-TR-67-179, Part I, October 1968.

18. Kuczynski, W. A.; Cooper, D. E.; Twomey, W. J.; and Howlett, J. J., "The Influence of Engine/Fuel Control Design on Helicopter Dynamics and Handling Qualities," Journal of the American Helicopter Society, Vol. 25, No. 2, April 1980, pp. 26-34.

19. Schalow, P. S., "Specification for the UTTAS Helicopter Synthetic Flight Training System, Device 2B38," NTEC 2222-1152, October 30, 1975.

Applications of System Identification Methods to the Prediction of Helicopter Stability, Control and Handling Characteristics

G. D. Padfield
RAE Bedford, UK

R. W. DuVal
NASA - Ames Research Center

Abstract

The paper describes a set of results from the first phase of an RAE/NASA collaborative programme on rotorcraft system identification that has the main objective of improving prediction methods. Flight measurements collected at RAE Bedford on an experimental Puma helicopter are reviewed and some notable characteristics highlighted. Following a brief review of previous work in rotorcraft system identification, the results of state estimation and model structure estimation processes applied to the Puma data are presented. The results, which were obtained using NASA developed software, are compared with theoretical predictions of roll, yaw and pitching moment derivatives for a 6 degree of freedom model structure. Anomalies reported in other investigations have reappeared in this study. The theoretical methods used are described in the Appendix where a framework for reduced order modelling is outlined.

Notation

A	-state matrix (equation (7))
B	-control matrix (equation (7))
C_{Qi}	-rotor induced torque coefficient (equation (10))
C_T	-rotor thrust coefficient (equation (3))
C_{YFN}	-fin sideforce coefficient (Fig 5)
$\underset{\sim}{F}$	-force and moment vector (equation (7))
g	-gravitational acceleration
h_R	-height of aircraft cg below rotor (ft,m) (equation (7))
I_{xx}, I_{yy}, I_{zz}	-moments of inertia of aircraft in roll, pitch and yaw (slugs ft^2, kg m^2)
L_v, L_p etc	-rolling moment concise derivatives (normalised by I_{xx})
M_u, M_w etc	-pitching moment derivatives (normalised by I_{yy})
$M_{\beta_{1c}}$	-pitching moment derivative wrt flapping (normalised by I_{yy})
N_v, N_r etc	-yawing moment derivatives (normalised by I_{zz})
N_{Ri}	-yawing moment from main rotor (normalised by I_{zz})
p, q, r	-roll, pitch and yaw rates (rad/s)
R	-rotor radius (ft,m)
R^2	-(multiple correlation coefficient)^2
s	-solidity
$T_{\frac{1}{2}}$	-time to half amplitude (s)
U_e, W_e	-trim values of aircraft forward and normal velocity components (ft/s, m/s)
u, v, w	-velocity perturbations along body x,y and z axes (ft/s, m/s)
v_o, w_o	-sideways and vertical velocity components (ft/s, m/s)
$\underset{\sim}{u}$	-control vector (equation (7))
$\underset{\sim}{x}$	-state vector (equation (7))
β	-sideslip angle (rad)
β_{1c}, β_{1s}	-rotor longitudinal and lateral disc tilts respectively (equation (1))
γ	-Lock number (equation (1))
ζ	-relative damping
η_{1s}, η_{1c}	-longitudinal and lateral stick position (% aft, std)
η_p	-pedal position (% left)
θ_{1s}, θ_{1c}	-longitudinal and lateral cyclic pitch angles (equation (1))
θ	-aircraft pitch angle
λ	-system eigenvalue
λ_o	-rotor downwash (normalised) velocity (equation (10))
λ_β	-flap frequency ratio
μ_z	-normal velocity component at rotor disc (equation (10))
ρ	-air density
σ	-relative air density
ϕ	-aircraft roll angle
Ω	-rotorspeed
ω_o	-dutch rollfrequency (equation (9))

Introduction

A collaborative programme between the Royal Aircraft Establishment and the NASA - Ames Research Center to develop and exchange information on rotorcraft system identification is now underway with the main objective of improving prediction methods. In the first exercise of this kind at RAE, flight tests have been made on a Puma helicopter and the results have been analysed at NASA - Ames, using software developed in support of the Rotor Systems Research Aircraft programme. This paper reports on the first phase of this activity. The paper begins by describing the aircraft and data processing system at RAE Bedford and attempts a preliminary interpretation of selected flight data based on comparison with theory. Aspects of rotorcraft system identification are then reviewed and the techniques currently in use are described.

Derivatives, estimated by these techniques for the Puma at a nominal 100 kn trim condition, are presented and compared with results predicted by a linear, 6 degree of freedom theoretical model developed at RAE[1]. Some of the major anomalies are discussed. Finally the use of reduced order linear models for handling studies is reviewed, and approximations to the natural modes discussed in some detail.

Flight Mechanics Investigations with Puma XW 241 at RAE Bedford

The Aircraft and Data Processing System

Puma XW 241 (Fig 1) is a multi-purpose experimental aircraft operated and managed by the Helicopter Section of the Flight Research Division at RAE Bedford. Since its procurement in 1974, the Puma has been used in a variety of research programmes and has recently been fitted with a digital Pulse Code Modulated (PCM) recording system; the results described in this paper were obtained with this equipment. A block diagram highlighting the features of the current data acquisition and processing system is shown in Fig 2.

The instrumentation system includes three packs of linear accelerometers of both ac pickoff and force feedback type, two packs of rate and attitude gyros and a heading gyro. Air data sensors give airspeed measurement from a conventional pitot static and incidence and sideslip angles from vanes located on a nose boom. All four control displacements, the three swash plate jacks and the tail rotor pitch jack are sensed by potentiometers. In addition, one of the four blades is currently instrumented to measure flap, lag and feather angles at the bearings. Sampling rates vary from 32 to 256 per second, the lower rate restricted to slowly varying quantities, *eg* airspeed. The current overall rate for the multiplexed system is 8024 words (12 bit) per second but the pattern of signals in each data field is flexible.

During the Spring of 1981 a trial was conducted with the object of data gathering for a system identification exercise. Trims and responses to pilot shaped control inputs over a range of flight conditions were recorded. Data tapes from one of these flights, designated 325, were sent to the Ames Research Centre for analysis using NASA software during the first round of the RAE/NASA collaborative programme in Rotorcraft Flight Mechanics. Results described in this paper are drawn from this exercise and used in subsequent interpretation, analysis and comparison with theory.

Data pertaining to the trim conditions for flight 325 are given in Table 1. The nominal trim IAS was 100 kn from which a series of shaped control inputs were made and the ensuing response measured and recorded. The inputs included steps, doublets and "3211" multisteps and generally produced repeatable response patterns; atmospheric conditions at the test points were very smooth.

Time to recovery varied with input type and size but typically step inputs gave about 10 s of data and 'return-to-trim' multisteps gave about 20-30 s duration.

Typical results from cyclic and pedal inputs are reproduced in Figs 3 and 4. Before introducing the system identification process a preliminary interpretation will be attempted on these results together with a limited comparison with theoretical predictions.

Preliminary Interpretation of Flight Results and Comparison with Theory

An initial assessment of the flight results and comparison with theory provides a suitable background to judge the effectiveness of both the theory itself and the system identification method, described later. The theoretical results presented in this paper are based on a 6 degree of freedom linearisation of the nonlinear simulation model described in Ref 1. During the development of this nonlinear model, a degree of validation was achieved through flight/theory comparisons of Puma data; these results are reported in Refs 1 and 2.

The short term pitch and roll rate response to longitudinal and lateral cyclic steps inputs respectively are shown in Fig 3. The comparisons with theory are encouraging and indicate that the principal damping, control sensitivity and 'static stability' parameters ought to be predicted with reasonable accuracy by theory. There is some evidence that the 'initial' angular acceleration is sharper in theory but this is to be expected with a quasi-steady rotor model. This phenomenon and the difficulties it can present to a derivative estimation process are discussed in more detail in the next section.

Turning now to the flight results shown in Fig 4, we see the coupled response to a doublet input applied to the pedal. This set of data reveals the presence of a lightly damped lateral/directional oscillation that was very apparent to the pilot and observer performing these tests. This oscillatory 'dutch roll' mode is also predicted by theory and a comparison of the measured and predicted characteristics is

shown in Table 2. It can be seen that the lateral/directional characteristics are roughly in agreement whereas the longitudinal couplings, particularly the phase relationships, are significantly different. Having established possible basic ingredients of this mode it is useful to examine the theory to determine the origins. The derivative matrix used in the analysis is given in Table 3 and the system eigenvalues in Table 4. Included in Table 4 are the longitudinal and lateral subsystem eigenvalues derived with coupling terms set to zero. Conventional fixed-wing aircraft terminology is used to describe the different modes. The frequency of the dutch roll oscillation is determined primarily by the directional stability, *ie*

$$\omega_{\text{dutch roll}} \sim \sqrt{U_e N_v} = 1.011 \text{ rad/s.}$$

An important effect displayed in Table 4 is the considerable reduction in damping of this mode when the coupling terms are included. The damping is rather low even for the lateral subsystem and this can largely be attributed to the low value of the yawing moment derivative N_v. This derivative contributes to the mode damping when the effective centre of the oscillation is a condition of non-zero sideslip. Wind tunnel data[3] for the Puma fin in sideslip, as used in the theoretical model, is shown in Fig 5. The sideforce is strongly nonlinear with sideslip, but over the range $-5^o < \beta < +8^o$, practically no lift is produced by the fin. It is believed that this effect is due to the suction on the rear of the 'lower surface' at small angles of attack; a characteristic of thick aerofoil sections with large trailing edge angles[4]. This aspect is discussed further in Ref 5, in relation to the Puma and how design improvements obviate the effect on the AS 332 Super Puma.

Returning to the coupled system, a sensitivity analysis reveals that the main coupling derivatives affecting the dutch roll damping are M_p and N_w. For a perfectly governed rotorspeed the derivative N_w reflects the torque changes produced by the powerplant, following rotorspeed variations due to incidence perturbations. The effect of this derivative on the dutch roll and longitudinal short period eigenvalues is illustrated in Fig 6. N_w is destabilising for the dutch roll mode and the roots are close to the longitudinal and lateral subset approximations when N_w is zero. Fig 7 illustrates how the phase relationship between w and r (incidence and yaw rate) perturbations vary with N_w for the dutch roll mode. They are seen to converge as N_w increases and clearly when they are in phase, torque reductions impose a positive yawing moment on the fuselage when the yaw rate is a maximum, giving a negative damping contribution. This effect is discussed in more quantitative terms in the Appendix. The above description of the increased instability of the lateral oscillation is dependent on the correct phase relationship between longitudinal and lateral variables. As highlighted earlier this is the area of most serious discrepancy between flight and theory. It should perhaps be emphasised that engine/rotor dynamics are not included in the theoretical model but that there is evidence[6] that including this degree of freedom can reduce the effective yaw damping. Included in Fig 4 is the main rotor torque variation (via shaft strain gauge measurement) during the oscillation. Although fairly noisy, the fluctuations are seen to be phased relative to yaw rate, so that as the aircraft is yawing to starboard, the engine is applying a clockwise torque (minimum) to the fuselage. This is in the same sense as predicted by theory and it may be surmised that the phase shift relative to pitch rate and vane oscillations is accounted for in the engine dynamics.

As a final note in this exploratory section some measurements were made on the Puma following a pedal doublet input with the pitch axis stability augmentation switched on, to give some indication of the effect of reducing the longitudinal coupling. A comparison of yaw and pitch vane responses with and without augmentation is shown in Fig 8. Clearly the damping of the oscillation has increased with the reduced longitudinal coupling. In fact, the time to half amplitude has now reduced to about one cycle, *ie* approximately the same as predicted by the lateral subset calculation. The frequency is practically unchanged. Longitudinal coupling obviously does play an important role in the damping of this oscillation.

Rotorcraft System Identification

The state of the art in the field of system identification has largely been developed in the fixed wing community, the most recent comprehensive review of which can be found in Ref 7. There have been several attempts to apply the various techniques to helicopters, a review of which also appears in Ref 7. Before describing the methods used in the RAE/NASA collaboration it is perhaps worth making a few observations on these past efforts and highlighting some of the lessons learned.

Observations on Previous Work

The ground rules for helicopter system identification were laid down in the pioneering work by Molusis in the early

seventies[8-10]. In his papers, Molusis emphasised the need for long data records and combined manoeuvres in order to provide sufficient information for reliable estimation. He also stressed the importance of providing satisfactory initial estimates of derivatives in maximum likelihood algorithms by using an optimal filter/smoother in conjunction with a least squares estimator. Of particular relevance to the helicopter problem were Molusis's observations on the effects of rotor/fuselage coupling on derivative estimation. These were clearly demonstrated by attempting an identification of a 6 degree of freedom (dof) model from simulation data that included rotor flapping modes[10]. The identified derivatives were substantially different from quasi-steady predictions even though time histories showed reasonable correlation. Including the three principal multi-blade coordinates in the assumed model and performing the reduction to a 6 dof model after the identification, resulted in very good agreement with quasi-steady values. The conclusion was not that 6 dof quasi-steady theoretical models were necessarily inadequate but that profound difficulties could be expected in trying to estimate these from flight measurements of fuselage motion alone. Molusis suggested an empirical correction based on computed theoretical data but his own results showed that this was not very satisfactory[10]. A perusal of the simulation results in Ref 10 reveals that perhaps the most serious discrepancy is the underestimation of the primary rate damping derivatives by the 6 dof identification. These usually produce dominant effects about all axes and relatively simple theory should be fairly reliable. A gross underestimation of this effect will obviously lead to a further corruption of secondary effects in each equation when the time histories are forced to agree. A possible cause of this anomaly can be demonstrated by a fairly simple example.

Consider a hovering rotor with zero flapping hinge offset and centre of gravity (cg) on the rotor shaft. The first order flapping equations in multi blade coordinates β_{1c} and β_{1s}, that represent longitudinal and lateral disc tilt respectively, can be written as

$$\begin{bmatrix} 1 & \frac{16}{\gamma} \\ -\frac{16}{\gamma} & 1 \end{bmatrix} \begin{bmatrix} \beta_{1c} \\ \beta_{1s} \end{bmatrix} - \begin{bmatrix} 0 & -\Omega \\ \Omega & 0 \end{bmatrix} \begin{bmatrix} \beta_{1c} \\ \beta_{1s} \end{bmatrix} = \begin{bmatrix} \frac{16}{\gamma} p + \Omega\theta_{1c} + q \\ -\frac{16}{\gamma} q + \Omega\theta_{1s} + p \end{bmatrix} \quad \ldots\ldots(1)$$

where γ is the rotor Lock number, Ω the rotor speed, p and q the body roll and pitch rates and θ_{1s}, θ_{1c} the longitudinal and lateral cyclic pitch respectively. Non-uniform inflow effects have been neglected for this example. Constraining the body to rotate only in pitch and neglecting forward speed effects, the above equations can be augmented by the body pitching moment equation

$$\dot{q} = \frac{1}{I_{yy}} M_{\beta_{1c}} \beta_{1c} \qquad (2)$$

I_{yy} is the pitching moment of inertia and the pitching moment derivative $M_{\beta_{1c}}$ can be written in terms of the rotor thrust coefficient C_T,

$$M_{\beta_{1c}} = - h_R \rho (\Omega R)^2 \pi R^2 C_T \quad . \qquad (3)$$

Here h_R is the cg distance below the rotor, ρ the air density and R the rotor radius. For present purposes we have assumed in equation (3) that the rotor thrust remains normal to the disc during pitching motions. The quasi-steady form of equation (2) can be written in the form

$$\dot{q} = M_q q + M_{\theta_{1s}} \theta_{1s} \qquad (4)$$

where $M_q = \frac{M_{\beta_{1c}}}{I_{yy}} \frac{\partial \beta_{1c}}{\partial q}$, $M_{\theta_{1s}} = \frac{M_{\beta_{1c}}}{I_{yy}} \frac{\partial \beta_{1c}}{\partial \theta_{1s}}$ . .....(5)

From equation (1) the quasi-steady flapping derivatives can be written as

$$\frac{\partial \beta_{1c}}{\partial q} = 16/\gamma\Omega \quad , \qquad \frac{\partial \beta_{1c}}{\partial \theta_{1s}} = -1. \qquad (6)$$

To demonstrate the phenomenon in question we now attempt to estimate the derivatives M_q and $M_{\theta_{1s}}$ in a model structure given by equation (4) from data generated by equations (1) and (2), following a step input in θ_{1s}. Configuration data used for the numerical study are $\gamma = 8.0$, $\Omega = 27.8$ rad/s and $M_{\beta_{1c}}/I_{yy} = -6.36$. Using a least squares estimator, the effect of data length on the estimated derivatives is shown in Fig 9. A sampling interval of 0.04 s was used for this case. The effect is dramatic, particularly on the estimated damping M_q. Using only a short data length a positive M_q is predicted and even after 2 s the estimation is still only 70% of the quasi-steady value. For a 2 s data run, the effect of sampling interval on the estimation is shown in Fig 10. Increasing the sampling interval to 0.2 s results in an accurate estimation of the quasi-steady derivatives. Obviously the model structure given by equation (4) is inadequate for portraying the short term

dynamic effects of the flapping equation (1), which in this case produces a mode with frequency 5.5 rad/s and time to half amplitude of about 0.1 s. A comparison of pitch rate response using the full equations and the quasi-steady representation is illustrated in Fig 11. Clearly the angular acceleration in the former case is zero at the origin and builds up to the quasi-steady value after about 0.2 s. Using data in this interval for estimating quasi-steady derivatives tends, therefore, to underestimate the damping in the motion to the extent that for, very short data lengths, an unstable system is predicted as shown in Fig 9.

When analysing flight data one would, of course, use a much longer data record than used in the previous example and the step input is rather limited in its excitation spectrum. However, a multi-step input would typically extend over about 30% of the data record and the contamination effects described above might persist well into the record.

Several other attempts to identify 6 dof helicopter models have resulted in underestimation of primary damping derivatives relative to the quasi-steady values (Refs 11-13). All these references report using advanced statistical methods for estimating derivatives but the phenomenon is still present in the results. The obvious solution to the problems highlighted by Molusis is to measure individual blade motions and to use higher order model structures in the estimation process. There will obviously be flight cases when such a solution is mandatory to the identification of certain phenomena, particularly when 6 dof theoretical models are known or suspected to be inadequate. For a wide range of conditions within the normal flight envelope, however, it is hoped that 6 dof models can be used to predict handling characteristics adequately and it is worthwhile exploring other potential solutions to the data processing problems before resorting to the measurement of blade motions. One approach is to use an input signal with a frequency content that excludes the rotor modes. A possible shortcoming of this method is that the data could be starved of information necessary to predict some of the derivatives, particularly for hingeless rotor helicopters where the lower frequency rotor modes are not far removed from some of the body modes. Nevertheless, the use of smooth inputs rather than sharp steps or ramps has an obvious appeal in this context. A similar and perhaps complementary solution involves filtering the data to exclude the 'higher' frequency content but again this could mean coming down to frequencies as low as $\frac{1}{2}$ Hz. Some exploratory work was done on this theme by one of the present authors in Ref 14, where the estimation process was transferred to the frequency domain. The data can then be filtered by excluding data beyond the frequency range of interest. This idea will now be exploited for the analysis of the Puma data.

Current Methods

The techniques used in this paper are based on the system identification approach described in Ref 15, where the data analysis is divided into three main stages; state estimation, model structure estimation and parameter identification. The state estimation stage involves the reconstruction of all states and controls from the available sensor measurements using a Kalman filter/smoother[16]. This process also eliminates the biases and scale factor errors from the measured data and reduces the level of measurement noise. The second stage utilises a stepwise least squares regression technique[17] to derive an adequate model structure from a range of possible candidates. The method uses certain statistical criteria to determine which states should be included in the model and estimates the corresponding coefficients. The third stage adopts these estimates as starting values for a maximum likelihood estimation process that generates unbiased, efficient, parameter estimates.

The analysis of results described in the next section will be confined to the first two stages described above. The equations used in the state estimation process are essentially kinematic relationships. For the present data set the reconstructed states include the three velocity components and the translational and rotational accelerations of the aircraft centre of gravity. The external forces and moments are then directly related to the acceleration estimates and for the model structure estimation we choose the 6 dof formulation of the form

$$\underset{\sim}{F} = A\underset{\sim}{x} + B\underset{\sim}{u} \qquad (7)$$

$\underset{\sim}{F}$, $\underset{\sim}{x}$ and $\underset{\sim}{u}$ are the external force and moment vectors, vehicle state vector and control vector respectively. The regression process currently used treats each equation separately, but rather than find the coefficients of this limited model that are valid for the entire frequency range of the data, it is more appropriate to determine the best set for the frequency range of interest. This is readily accomplished by transforming the data to the frequency domain using a Fast Fourier Transformation (FFT) and then truncating the data beyond the bandwidth of interest. If it is

assumed that the coefficients do not vary with frequency then the regression can be performed in the frequency domain with the vectors in equation (7) interpreted as the corresponding Fourier transforms. An additional advantage of estimation in the frequency domain is that the resolution can be improved by padding the data with zeros. This effectively forces the spectral lines to be more closely spaced without affecting the frequency content of the data. The higher resolution should result in more accurate estimation of the low frequency modes, which are difficult to identify from a limited duration data record[14].

Model Structure Estimation with Puma Data

The results presented in this section were produced at the Ames Research Center and forwarded to RAE Bedford for interpretation. The inherent communication difficulties in this process limited the scope of this first phase of the collaboration. The analysis software is currently being implemented on a VAX computer at Bedford when these difficulties should be largely overcome.

From the assortment of data collected during Puma flight 325, three manoeuvres were selected for analysis, namely doublet inputs in lateral cyclic, pedal and longitudinal cyclic. The data used consisted of measurements from one of the packs of inertial instruments (accelerometers, rate gyros, attitude gyros), the airspeed sensor and the pitch and yaw vanes. The instrument pack referred to included a 2-pole Butterworth filter ($\omega_n \sim 10.6$ Hz , $\zeta = 0.73$) that effectively removed the dominant 4/rev noise in the measurements. The results of the model structure estimation process reveal a marked variation in estimated coefficients, particularly the contributions from coupling effects. The reasons for this are not yet understood and we therefore choose to concentrate on a synthesis of the primary moments for each input, *ie* rolling moment for lateral cyclic doublet, yawing moment for pedal doublet and pitching moment for the longitudinal cyclic doublet. The sample rate for all channels was 64/s, a rate that limited the record lengths to about 15 s. This limitation will be removed in future analysis. The results from each manoeuvre will be discussed in turn.

Lateral Cyclic Doublet/Rolling Moment Synthesis

Results from the filter/smoother process are shown in Fig 12, where it can be seen that only two cycles of the lateral oscillation are available. Two further points are worth noting; a bias has been detected and corrected for in the pitch rate gyro and the initial slope of the normal velocity component (w) indicates an initial climbing and decelerating flight condition. The effect of this unsteady initial condition has not been explored. In discussing the results of the model structure estimation we will refer to the multiple correlation coefficient (R) for the fit. In essence, the closer R^2 is to unity, the better the overall fit of the data in the frequency domain. Table 5 summarises the estimated rolling moment coefficients (derivatives) for the cases studied, along with the current quasi-steady theoretical predictions. Derivative estimates with a structure containing only lateral variables are compared for three frequency ranges, 0 to 0.5 Hz, 0 to 1 Hz, 0 to 4 Hz. In all cases the high R^2 values indicate a reasonably good fit with this limited model. The roll damping L_p is seen to increase by about 50% as the bandwidth is reduced but is still markedly lower than the theoretical prediction. The Fourier transform of the rolling moment is compared with the estimated fit in Fig 13, for the two lower frequency ranges. Most of the data is contained in the range 0 to 0.5 Hz, and the dominant peak at 0.25 Hz corresponds to the lightly damped lateral oscillation. The fairly close fit at and above this frequency appears to be achieved at the expense of the fit at lower frequencies. Referring again to Table 5, it can be seen that R^2 rises to 0.96 when the longitudinal variables w and q are added, with some associated modification to the lateral variable coefficients. Comparing the estimated and theoretically predicted derivatives in Table 5 we can see that the major anomalies are for the rate derivatives L_p and L_r . The magnitude of these effects seems to have been reversed for the flight results but it is difficult to rationalise the physical significance of this; indeed the result seems rather dubious. Further exploration into the details of the regression analysis is clearly required.

Pedal Doublet/Yawing Moment Synthesis

The smoothed state estimates for this manoeuvre are illustrated in Fig 14 and the yawing moment derivatives derived from the lower frequency bandwidth of data are compared with theoretical predictions in Table 6. Results from two different model structures are included, one with lateral variables only and the other with the addition of the longitudinal variables w and q . The multiple correlation coefficient is hardly affected by these additions.

It can be seen that the directional stiffness (N_v) and damping (N_r) compare very well with theory but the control power (N_{η_p}) is somewhat larger according to theory. The most striking differences are in the coupled rate derivatives N_p and N_q. The small value of N_p predicted by theory is the result of the cancellation of two larger effects from the main (negative N_p) and tail-rotor (positive N_p). It is interesting to note that the value of R^2 was raised to 0.91 by the first two variables drawn into the regression, v and η_p, the remaining variables then being added to account essentially for the out of phase component of the response. For the lightly damped yawing mode the sum of these contributions should obviously be small. Once again, a detailed breakdown of the in-phase and quadrature components of these 'damping' terms is required to aid further interpretation of the results.

Longitudinal Cyclic Doublet/Pitching Moment Synthesis

The state estimates derived for this manoeuvre are shown in Fig 15, where the bias error in the pitch rate gyro is again apparent; also the normal and longitudinal velocity estimates again indicate an initial decelerating climb. The least squares estimates in the frequency domain are compared, in Table 7, with the quasi-steady theoretical predictions for the derivatives. Results are presented for the longitudinal model structure for the three frequency ranges. Both the pitch damping (M_q) and control power ($M_{\eta_{1s}}$) are seen to increase as the bandwidth is reduced and both rise to nearly 80% of the theoretical predictions. The remarkable agreement for the speed stability derivative (M_u) is somewhat overshadowed by the incidence stability derivative (M_w) comparison. The variable w actually just managed to become part of the fit, accounting for only the last few per cent in the value of R^2. It is possible that the estimation of an unstable M_w is related to the unsteady initial conditions for this manoeuvre, as the effects of the initial deceleration persist for the duration of the record as shown in Fig 15. It is intended to explore this topic further.

The results from the three manoeuvres discussed above are both encouraging and perplexing. Unfortunately, time was not available to explore further the uncovered anomalies, for this paper. The underestimation of roll damping, relative to theory, a feature common to several earlier attempts at rotorcraft parameter estimation, is perhaps of greatest concern. The reduction effect of the lower frequency flapping modes, described in an earlier section, should be minimized by truncation in the frequency domain. The least squares regression analysis does of course have its shortcomings, particularly when noise is present in the data[18], but also when there is strong correlation between states. However the technique is appealing in that it offers a simple and systematic approach to model structure estimation, and investigations of the type described above will be pursued in the continuing collaborative programme. When fully exploited and understood, the results of the model structure estimation stage will then be used to initiate the more complex maximum likelihood process.

The model structure estimation stage serves another useful purpose in the validation of reduced order approximate models of helicopter flight mechanics. Simplified models, which still indicate trends accurately, have obvious advantages and various schemes are suggested in the Appendix for the 6 degree of freedom helicopter as a framework for analytic model reduction. The results described are based on the theoretical predictions of Puma characteristics discussed earlier in the paper. Clearly, however, we have failed to validate the theoretical arguments put forward to explain the low damping of the lateral oscillation. In particular, the yawing moment derivatives N_w and N_q in Table 6 bear little resemblance to their theoretical counterparts, and, unfortunately for this study no estimate was obtained for the derivative M_p (another important effect in the theory). There is no reason to believe that any major physical effect has been neglected in the theoretical quasi-steady derivatives, but it is possible that the omission of the rotorspeed degree of freedom has distorted the model structure estimation. With this possibility in mind, future estimations will include this additional state.

Concluding Remarks

Results from the first phase of an RAE/NASA collaborative programme in rotorcraft system identification have been described. Flight data from three manoeuvres with an RAE Puma helicopter have been processed by the state estimation and model structure estimation processes of a NASA system identification software package. A comparison of moment derivative estimates with theoretical predictions has been used as a guide to the likely accuracy involved. No firm conclusions can be drawn from this first exploration but a number of features are worth highlighting.

(1) Encouraging results have been obtained by performing the regression analysis in the frequency domain. Reducing the bandwidth of data used resulted in an increase in roll and pitch damping and control power, as expected from time domain considerations,

but, in some cases, the results still fall well short of expected quasi-steady values.

(2) Primary yawing moment derivatives estimated from a pedal doublet manoeuvre show good agreement with theory but the adverse yaw (N_p) and coupling from longitudinal motion (N_w,N_q) show significant differences. The contribution of these coupling terms to the 'dutch roll' mode damping, so elegantly expressed by simple theory, cannot, therefore, be substantiated.

(3) Roll damping (L_p) and control power ($L_{\eta_{1c}}$) estimated from a lateral cyclic doublet manoeuvre are considerably lower than theory predicts - a result in keeping with previous reports. This anomaly in the rolling moment is accompanied by a very high estimate for the derivative L_r and the temptation at this stage is to question the structure estimation, rather than theory, for these effects.

(4) The closest agreement with quasi-steady predictions were obtained for pitching moment derivatives from a longitudinal cyclic doublet manoeuvre, except for the static stability derivative M_w which is estimated to be very small and positive by the least squares regression.

(5) A theoretical framework for exploring reduced order model structures has been outlined in an Appendix to the paper. A coupled longitudinal/lateral fourth order system is required to describe the current theoretical predictions of the Puma 'dutch roll' oscillation.

The collaborative programme is still at an early stage and more detailed investigations using the model structure estimation process are planned for different manoeuvres of longer duration and possibly improved model structures.

Appendix

The Use of Reduced Order Theoretical Models

The complex nature of helicopter flight mechanics make it a prime candidate for treatment as a sum of interacting subsystems, with the attraction that phenomena may be described by considering a series of lower order problems and their interactions. Conditions under which this type of approximation is valid are often based on intuitive reasoning but they can be formulated more precisely using notions of subsystem dynamic separation (eg widely separated characteristic times) and interaction strength. For aircraft flight dynamics such opportunities often arise for describing rigid body/aeroelastic interaction or in the description of the individual modes using familiar arrangements of motion variables, eg longitudinal short period mode made up of incidence and pitch rate excursions. Once again, the attractions of performing such a 'partitioning' analysis can often stem from the enhanced physical appreciation it inspires. In this Appendix we concentrate on the theoretical results discussed earlier and outline a framework for reduced order analysis. One can clearly imagine the 6 dof model as already being a reduced order approximation of a higher order system containing rotor as well as engine/fuel control system degrees of freedom.

The method of analysis is described in Ref 19 where the concept of weak coupling is introduced and conditions of application are quantified. The technique has been applied to strongly controlled aircraft motions[20] and more recently to describe the range of application of the longitudinal short period approximation for helicopters[21]. In the present paper, a form of approximation for lateral/directional motion is sought. For the Puma results described the strong coupling from longitudinal motion renders the search in vain. In the following, aspects of open loop stability characteristics only will be addressed.

The reduction process is based on a partitioning of the system matrix into lower order subsystems that are weakly coupled. Details of the method can be found in any of the references cited above and will not be elaborated upon here. In order to achieve the correct partitioning for rigid body modes of motion we need to introduce the vertical velocity w_0 and sideways velocity v_0 as new variables, replacing pitch attitude and yaw rate in the equations of motion. The system matrices, in partitioned form, for decoupled longitudinal and lateral motions are shown in Table 8, along with the approximating characteristic polynomials. One would not expect these formulae to give very accurate results in general but they do serve as a yardstick against which the effects of coupling terms can be measured. For the Puma derivative data given in Table 3 the weakly coupled approximate results are shown in Table 9.

A comparison with the decoupled longitudinal/lateral results given in Table 4 indicates again that the dutch roll damping is badly overpredicted. This poor comparison will result when the oscillatory sideslip motion has a significant component of sideways motion superimposed on the sideslip due to yawing motion. The overprediction of the phugoid damping can be attributed to a similar effect in the longitudinal plane. For the other three modes the approximations are clearly satisfactory. The importance of the directional stiffness N_v on the dutch roll damping is not, of course, predicted at all by this type of approximation. The root loci in Fig 16 illustrates this effect; the two curves

shown are for the coupled longitudinal/lateral system and for the lateral system alone. Both loci are approaching the asymptotic value given in Table 9 as N_v increases, ie dutch roll damping $\simeq (N_r + Y_v)$. The point being made is that as directional stability increases the formulae given in Table 8 are not only becoming better approximations to the lateral subset damping but that both are improving relative to the fully coupled result. In these conditions the other modes are also approximated fairly accurately, eg spiral mode marginal stability is well predicted, although these results are not shown here.

The results discussed above indicate that the degree of coupling between longitudinal and lateral motion can be strongly influenced by the directional stiffness or, in other words, by the frequency of the lateral oscillation. This result is somewhat intuitive and for the present coupled system the coincidental similarity between the longitudinal short period and dutch roll frequencies is bound to result in strong longitudinal/lateral interactions. As discussed in an earlier section these interactions are brought about mainly through the derivatives M_p and N_w ; the main rotor contribution to these derivatives being negative and positive respectively for 'clockwise' rotating rotors. The strong coupling present leads to a further reduction in dutch roll damping through the mechanism discussed earlier. This effect can be quantified by considering a reduced order system made up of both the longitudinal and lateral 'fast' oscillatory modes.

Assuming on the one hand that translational velocity excursions (u, v_0, w_0) are much slower and weakly coupled, and, on the other, that the roll subsidence approximation interacts in a quasi-steady manner, the 4th order approximate system takes the form,

$$\frac{d}{dt}\begin{bmatrix} w \\ q \\ v \\ \dot{v} \end{bmatrix} - \begin{bmatrix} Z_w & Z_q + U_e & 0 & 0 \\ M_w & M_q & -M_p L_v/L_p & M_p L_r/U_e L_p \\ 0 & 0 & 0 & 1 \\ -N_w U_e & 0 & -\left(U_e N_v + (L_v/L_p)(g - N_p U_e)\right) & N_r + Y_v + (L_r/L_p)(g - N_p U_e) \end{bmatrix} \begin{bmatrix} w \\ q \\ v \\ \dot{v} \end{bmatrix} = Q. \qquad \ldots\ldots(8)$$

Here we have neglected all coupling terms except M_p and N_w , but with the strong coupling remaining, no further reduction would be reliable. Examination of the Routhian for this 4th order system indicates that the oscillatory stability boundary is crossed when $N_w \sim 0.02$, which is in accordance with the results presented earlier in Fig 6. The eigenvalues for the above system are,

$$\lambda_{\text{short period}} = -1.0 \pm 1.079i$$

$$\lambda_{\text{dutch roll}} = -0.114 \pm 1.115i$$

giving the right order of damping reduction for the dutch roll mode. If we assume a neutrally stable oscillation exists for the above system then a good approximation to this damping decrement can be obtained by deriving the steady state frequency response of equation (8). For this case w is approximately 180^0 out of phase with $\dot{v}$ (hence in phase with yaw rate) and the effective damping becomes,

$$\text{damping}_{(\text{dutch roll})} \simeq -\left(N_r + Y_v + \frac{L_r}{L_p}(g - N_p U_e) + \frac{N_w M_p}{L_p \omega_0}\frac{U_e^2 L_v}{(Z_w + M_q)}\right) \qquad \ldots\ldots(9)$$

$$\simeq 0.234 ,$$

hence

$$R_e(\lambda) \simeq -0.117$$

(where ω_0 is the dutch roll frequency)

which agrees with the result given by equation (8) above.

The derivative N_w , as stated earlier, represents the quasi-steady torque variation produced by the engine, in response to rotorspeed variations. The validity of this implicit weak coupling assumption can only be assessed when an engine/rotorspeed control system model structure, representative of Puma, is incorporated. The derivative N_w itself is produced mainly by the 'induced torque', written in coefficient form,

$$C_{Q_i} = -C_T(\mu_z - \lambda_0) . \qquad (10)$$

C_T is the rotor thrust coefficient and $(\mu_z - \lambda_0)$ is the upwash, normal to the disc. The variation in the semi-normalised yawing moment (yaw acceleration), from this source, with normal velocity w is shown in Fig 17. The variation is seen to be moderately non-linear particularly in the normal helicopter working state ($w < 0$). The derivative N_w is seen to increase as autorotation is

approached ($\mu_z - \lambda_0 \sim 0$) but the effect will, of course, disappear once the engine disengages. It is known that the directional stiffness can also reduce in this region due to fin shielding effects; the loss of 'dutch roll' damping for these flight conditions should, therefore, be fairly severe if the current predictions are correct.

Acknowledgements

Grateful thanks are extended to colleagues by both authors for the help given in the preparation of material for this paper; in particular to Mustafa Demiroz and Susan Chu at NASA Ames and to Tony James and Jane Whitbread at RAE Bedford.

References

1. Padfield, G.D. "A Theoretical Model of Helicopter Flight Mechanics for Application to Piloted Simulation." RAE Technical Report 81048, Apr. 1981.

2. Padfield, G.D., Tomlinson, B.N., Wells, P.M. "Simulation Studies of Helicopter Agility and other topics." RAE Technical Memorandum

3. Sarconi, G. "Simulation Hélicoptere caracteristique du SA 330." Aerospatiale Note Technique, 330.05.0080, 1975.

4. Hoerner, S.F., Borst, H.V. Fluid Dynamic Lift, Hoerner Fluid Dynamics, N.J., 1975.

5. Roesh, P., Vuillet, A. "New Designs for Improved Aerodynamic Stability in Recent Aerospatiale Helicopters." Proceedings of the 37th AHS Annual Forum, New Orleans, May 1981.

6. Kuczynski, W.A., et al. "The Influence of Engine/Fuel Control Design on Helicopter Dynamics and Handling Qualities." Proceedings of the 35th AHS Annual Forum, Washington, May 1979.

7. Parameter Identification, AGARD Lecture Series 104, Nov. 1979.

8. Molusis, J.A. "Helicopter Stability Derivative Extraction and Data Processing Using Kalman Filtering Techniques." 28th AHS National Forum, Washington, May 1972.

9. Molusis, J.A. "Helicopter Stability Derivative Extraction from Flight Data Using the Bayesian Approach to Estimation." Journal of the American Helicopter Society, Jul. 1973

10 Molusis, J.A. "Rotorcraft Derivative Identification from Analytical Models and Flight Test Data." AGARD CP 172 (Methods for Aircraft State and Parameter Identification)." Nov. 1974.

11 Kaletka, J., Rix, O. "Aspects of System Identification of Helicopters." Proceedings of the 3rd European Rotorcraft and Powered Lift Aircraft Forum, Aix-En-Provence, France, Sept. 1977.

12 Kloster, M., Kaletka, J., Schaufele, H. "Parameter Identification of a Hingeless Rotor Helicopter in Flight Conditions With Increased Instability." Proceedings of the 6th European Rotorcraft and Powered Lift Aircraft Forum, Bristol, UK, Sept. 1980.

13 Hodge, Ward, "Comparison of Analytical and Flight Test Identified Aerodynamic Derivatives for a Tandam Rotor Transport Helicopter." NASA TP-1581, Feb. 1980.

14 DuVal, R.W. "The Use of Frequency Methods in Rotorcraft System Identification." First AIAA Flight Testing Conference, Paper 81-2386, Las Vegas, Nov. 1981.

15 Hall, W. Earl, Jr., Gupta, Narendra K., Hansen, Raymond S., "Rotorcraft System Identification Techniques for Handling Qualities and Stability and Control Evaluation." Proceedings of the 34th AHS National Forum, Washington, May 1978.

16 Bryson, A.E., Jr., Ho, Y.C. "Applied Optimal Control, Blaisdell Publishing Co. Waltham, Mass, 1969.

17 Jennrith, R.I. "Stepwise Regression." Statistical Methods for Digital Computers, Wiley, NY, 1966.

18 Fiske, Philip H., Price, Charles F. "A new Approach to Model Structure Identification." AIAA Paper 77-1171, 1977.

19 Milne, R.D. "The Analysis of Weakly Coupled Dynamical Systems." Int. J. Control, 2, No.2, 1965.

20 Milne, R.D., Padfield, G.D. "The Strongly Controlled Aircraft." Aeronautical Quarterly, May 1971.

21 Padfield, G.D. "On the Use of Approximate Models in Helicopter Flight Mechanics." Vertica, Vol 5, pp. 243-259, 1981.

Nominal* IAS	100 kn
Relative density, σ	0.818-0.837
Rotorspeed, Ω	26.6-27.2 rad/s
Rotor torque ~	11500 ft lb (564 hp, 421 kW)
AUW	13018-12169 lb (5904-5519 kg)
I^{**}_{xx}	6380 slug ft^2 (8650 kg m^2)
I^{**}_{yy}	25483 slug ft^2 (34550 kg m^2)
I^{**}_{zz}	20283 slug ft^2 (27500 kg m^2)
Cg location below rotor hub	7.05 ft (2.157 m)
Cg location forward of rotor hub	0.086 ft (0.026 m)
Rotor Lock number	7.86
λ^2_β	1.0516
Solidity, s	0.0917

* Actual IAS varied from 95-100 kn giving an EAS ~ 105-110 kn.
** Manufacturer's estimates (Ref 3).

Table 1. Puma flight 325 — nominal trim conditions

Parameter	Flight (approx)	Theory
Period (s)	4.5	6.0
$T_{\frac{1}{2}}$ (s)	14.0	15.36
$\lvert p/v \rvert$	0.02	0.019
$\angle p/v$	135°	158°
$\lvert r/v \rvert$	0.012	0.0096
$\angle r/v$	-95°	-85°
$\lvert q/v \rvert$	0.006	0.0027
$\angle q/v$	98°	-48°
$\lvert w/v \rvert$	0.336	0.354
$\angle w/v$	30°	-107°

Table 2. Comparison of measured and predicted 'dutch roll' oscillation characteristics

	u	w	q	v	p	r
X	-0.2650E-01	-0.9340E-03	0.3970E 01	0.1890E-02	0.1010E 01	0.0000E 00
Z	-0.3190E-01	-0.7050E 00	0.1680E 03	0.1450E-01	0.2100E 01	0.0000E 00
M	0.2460E-02	-0.5570E-02	-0.8310E 00	-0.4000E-03	-0.2070E 00	0.0000E 00
Y	-0.8120E-02	0.2930E-02	0.1040E 01	-0.1360E 00	-0.3980E 01	-0.1680E 03
L	-0.5620E-02	-0.2730E-03	0.8390E-00	-0.2200E-01	-0.2050E 01	0.2940E 00
N	0.2880E-02	0.1270E-01	-0.3280E 00	0.6050E-02	-0.9290E-03	-0.5280E 00

Table 3. Theoretical estimates of Puma derivatives

Mode	Coupled system	Decoupled long/lat subsystems
Roll subsidence	-2.242	-2.209
'Dutch roll'	-0.0451 ±1.047i	-0.193 ±1.079i
Spiral	-0.1166	-0.1194
'Short period'	-0.9054 ±1.186i	-0.7645 ±0.9354i
'Phugoid'	-0.00833 ±0.1764i	-0.0168 ±0.2038i

Table 4. Comparison of coupled and uncoupled longitudinal/lateral system eigenvalues — Puma, 100 kn

	Flight estimates lateral variables only			+ w and q	Theory
	0-0.5 Hz	0-1 Hz	0-4 Hz	0-0.5 Hz	
R^2	0.92	0.91	0.9	0.96	
L_v	-0.013	-0.013	-0.013	-0.0123	-0.022
L_p	-0.4	-0.32	-0.28	-0.35	-2.05
L_r	1.7	1.82	1.9	3.03	0.294
$L_{\eta_{1c}}$	0.022	0.021	0.02	0.019	0.044
L_w				0.0054	-0.00027
L_q				1.39	0.839

Table 5. Rolling moment derivatives — estimates from flight and theory

	Flight estimates (0-0.5 Hz)		Theory
	Lateral variables only	+ w and q	
R^2	0.97	0.98	
N_v	0.0053	0.0071	0.00605
N_p	-0.6	-0.53	-0.0009
N_r	-0.636	-0.572	-0.528
N_{η_p}	-0.027	-0.028	-0.043
N_w		-0.003	0.0127
N_q		0.322	-0.328

Table 6. Yawing moment derivatives — estimates from flight and theory

	Flight estimates			Theory
	0–0.5 Hz	0–1 Hz	0–4 Hz	
R^2	0.802	0.76	0.73	
M_u	0.00243	0.00243	0.00245	0.00246
M_w	0.00092	0.00085	0.00074	−0.0056
M_q	−0.683	−0.667	−0.648	−0.831
$M_{\eta_{1s}}$	0.0316	0.0302	0.029	0.038

Table 7. Pitching moment derivatives — estimates from flight and theory

(Note $\overleftrightarrow{M_w(Z_q + U_e)} = M_w(Z_q + U_e) - M_q Z_w$)

Longitudinal subset $\underset{\sim}{X} = \{u, w_o, w, q\}$; $w_o = w - U_e\theta$

$$\left[\begin{array}{cc|cc} X_u & g/U_e & X_w - g/U_e & X_q - W_e \\ Z_u & 0 & Z_w & Z_q \\ \hline Z_{\dot{u}} & 0 & Z_w & Z_q + U_e \\ M_u & 0 & M_w & M_q \end{array}\right]$$

$\lambda_{1,2}$ (phugoid);

$$\lambda^2 + \left\{ -X_u + \frac{\left(X_w - \frac{g}{U_e}\right)\left(\overleftrightarrow{M_u(Z_q + U_e)} + (X_q - W_e)\overleftrightarrow{Z_u M_w}\right)}{\overleftrightarrow{M_w(Z_q + U_e)}} \right\}\lambda - \frac{g}{U_e}\left(Z_u - \frac{\overleftrightarrow{Z_w M_u(Z_q + U_e)}}{\overleftrightarrow{M_w(Z_q + U_e)}}\right) = 0$$

$\lambda_{3,4}$ (short period); $\lambda^2 - (Z_w + M_q)\lambda - \overleftrightarrow{M_w(Z_q + U_e)} = 0$.

Lateral subset $\underset{\sim}{X} = \{\dot{v}_o, v, \dot{v}, p\}$; $\dot{v}_o = \dot{v} + U_e r$

$$\left[\begin{array}{c|cc|c} 0 & 0 & Y_v & g \\ \hline 0 & 0 & 1 & 0 \\ -N_{\dot{r}} & -U_e N_v & N_r + Y_v & g - N_p U_e \\ \hline L_{\dot{r}}/U_e & L_v & -L_{\dot{r}}/U_e & L_p \end{array}\right] \quad (Y_p = Y_{\dot{r}} = 0)$$

λ_5 (spiral) ; $\lambda = \dfrac{g}{U_e}\dfrac{\overleftrightarrow{L_v N_{\dot{r}}}}{\left(\overleftrightarrow{L_p N_v} + \frac{g}{U_e} L_v\right)}$

$\lambda_{6,7}$ (dutch roll); $\lambda^2 - \left(Y_v + N_r + \frac{L_{\dot{r}}}{L_p}\left(\frac{g}{U_e} - N_p\right)\right)\lambda + \left(N_v + \frac{L_v}{L_p}\left(\frac{g}{U_e} - N_p\right)\right)U_e = 0$

λ_8 (roll subsidence) ; $\lambda = L_p$

Table 8. Approximate formulae for longitudinal and lateral eigenvalues

Roll subsidence	−2.05
'Dutch roll'	−0.346 ±1.116i
Spiral	−0.1124
'Short period'	−0.768 ±0.968i
'Phugoid'	−0.0349 ±0.1969i

Table 9. Approximate eigenvalues for longitudinal and lateral subsystems

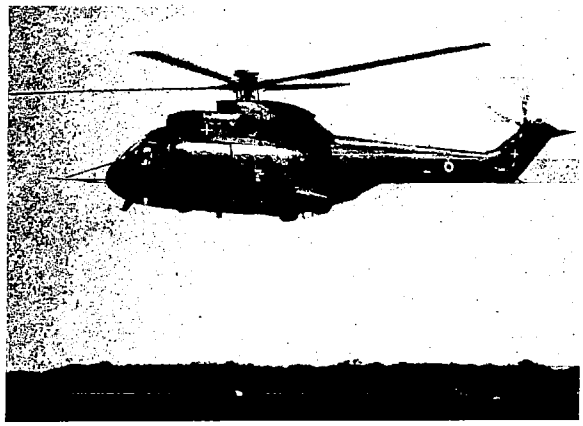

Fig 1 Puma XW241

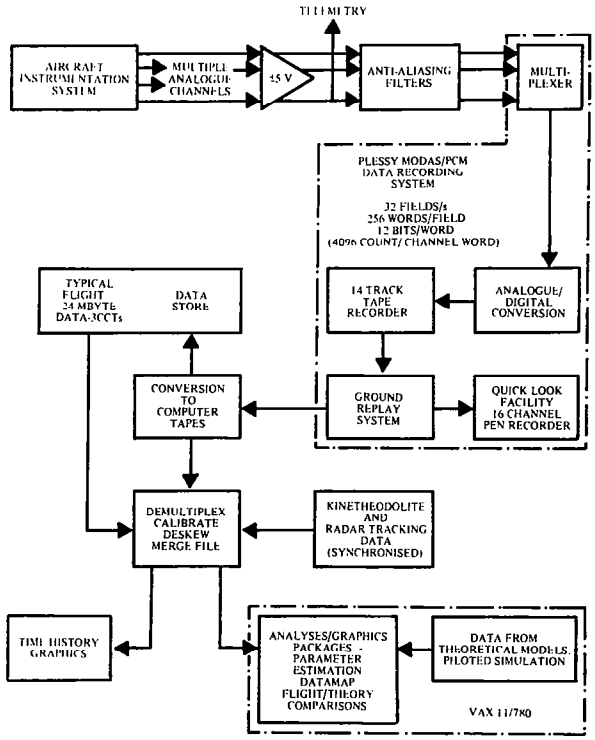

Fig 2 Puma flight mechanics data acquisition and processing at RAE Bedford

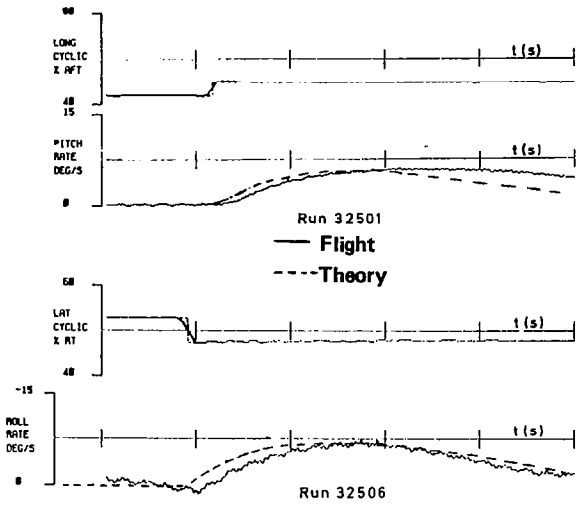

Fig 3 Flight/theory comparison of rate response to cyclic inputs

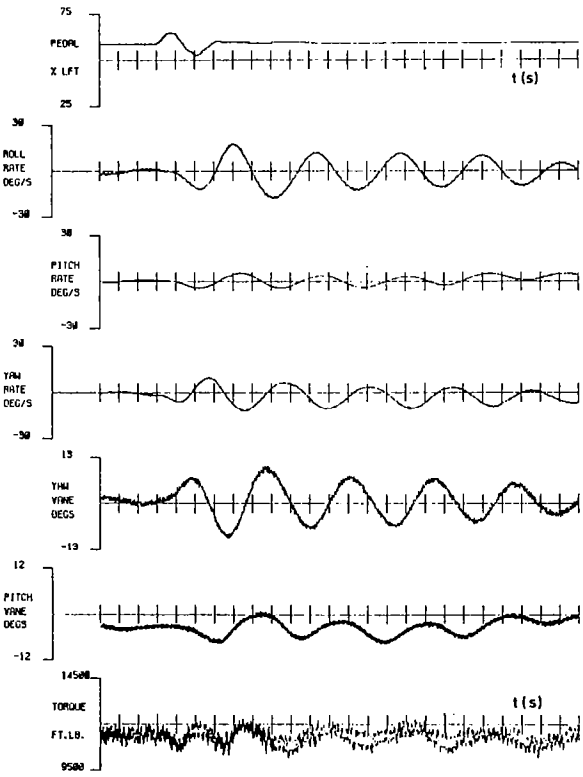

Fig 4 Puma flight 325, Run 12 — response to pedal doublet

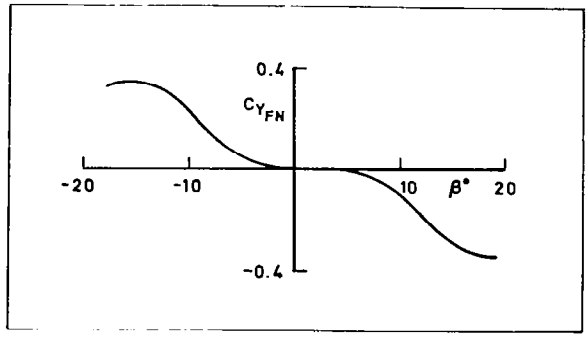

Fig 5 Puma fin sideforce coefficient vs sideslip angle

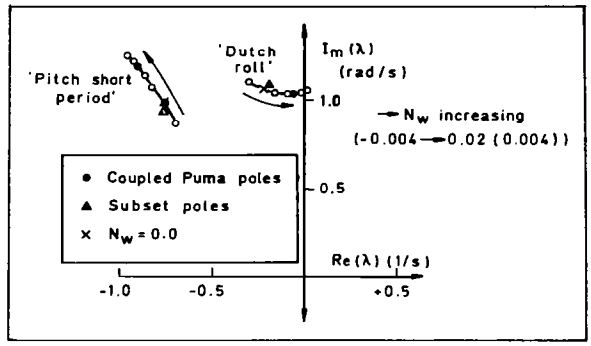

Fig 6 Root loci for fast oscillatory modes with varying yawing moment due to incidence (N_w)

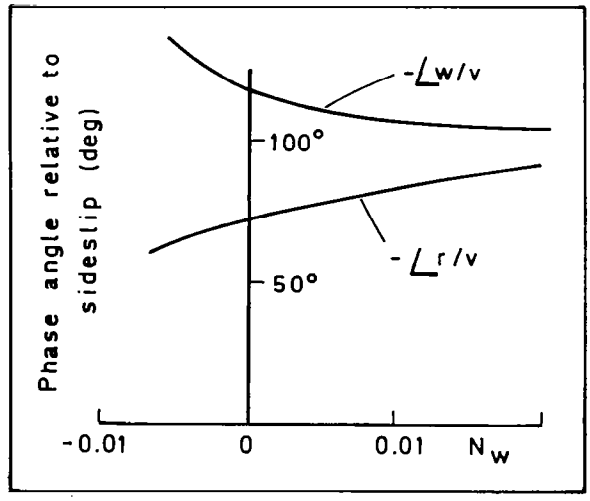

Fig 7 Variation of the phase angle in incidence and yaw rate excursions during 'dutch roll' oscillation with N_w — theoretical predictions

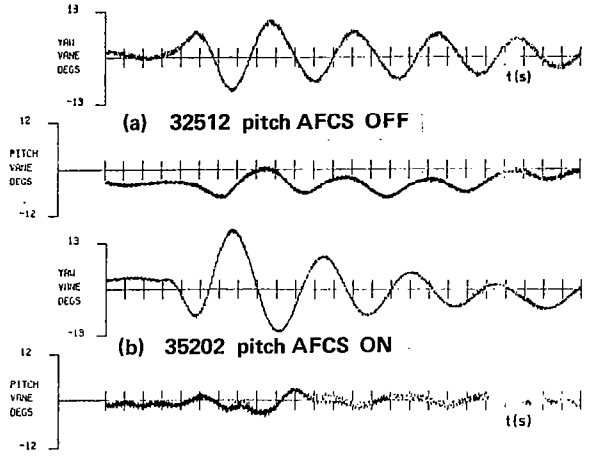

Fig 8 Puma — yaw and pitch vane response to pedal doublet

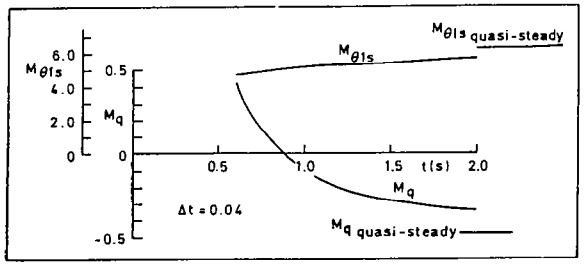

Fig 9 Variation of derivative estimates with record length

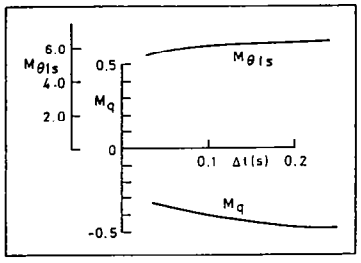

Fig 10 Variation of derivative estimates with sampling interval

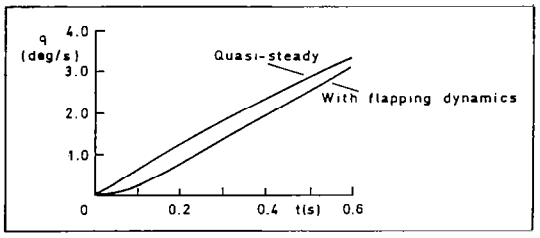

Fig 11 Comparison of pitch rate response with and without flapping dynamics

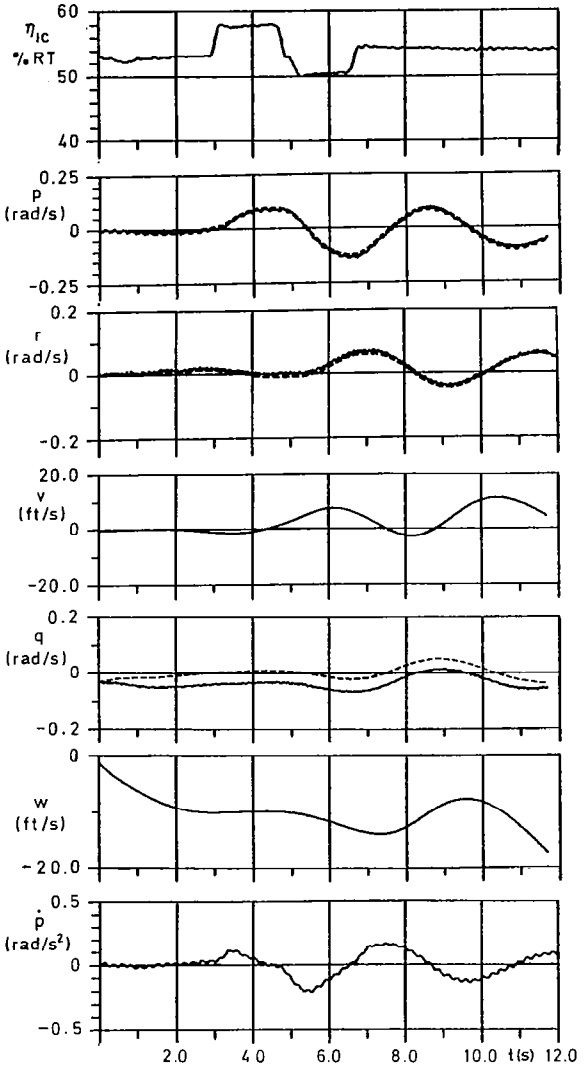

Fig 12 Comparison of measured (—) and estimated (- - -) states (Kalman filter/smoother) for lateral cyclic doublet manoeuvre

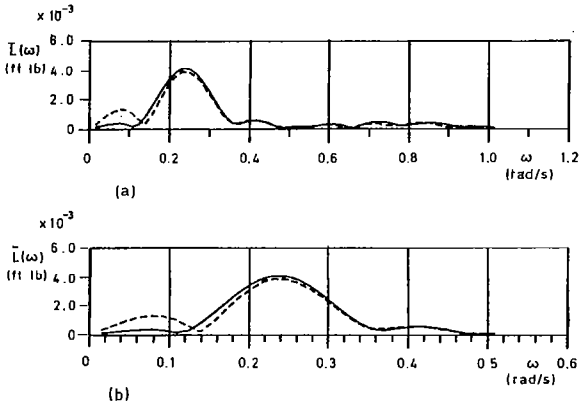

Fig 13 Fourier transform of measured (—) and estimated (- - -) rolling moment — lateral cyclic input

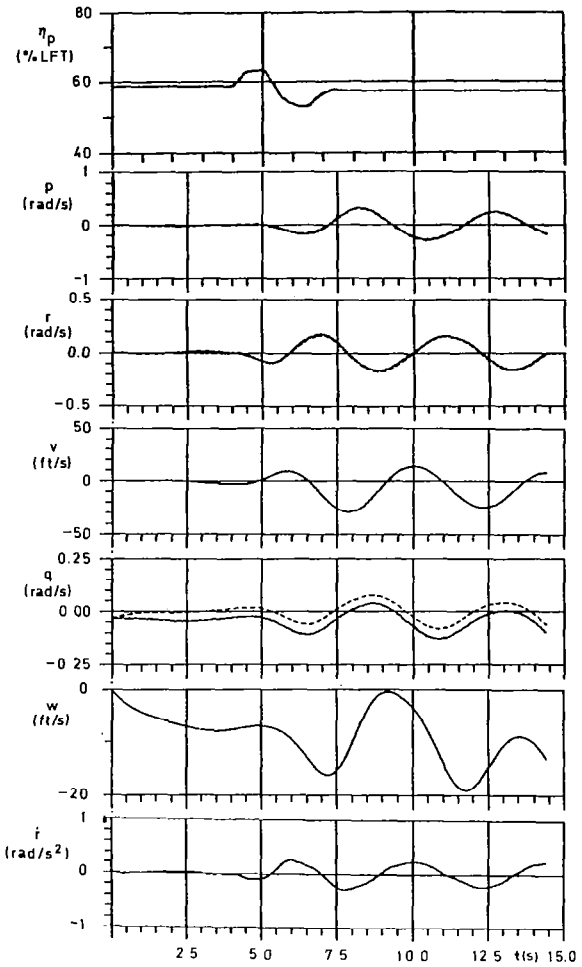

Fig 14 Comparison of measured (—) and estimated (- - -) states (Kalman filter/smoother) for pedal doublet manoeuvre

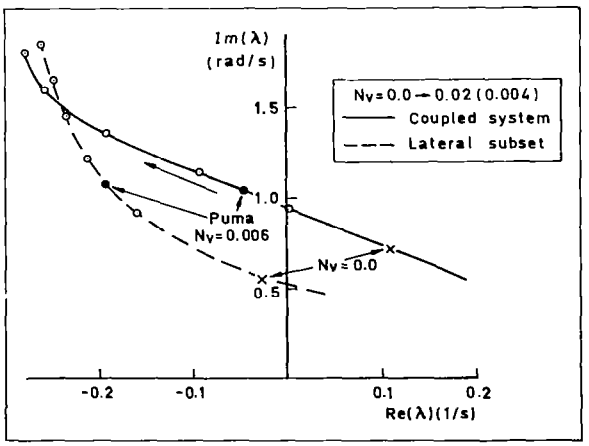

Fig 16 Root loci for 'dutch roll' mode with varying N_v — comparison of coupled and lateral/directional subset modes

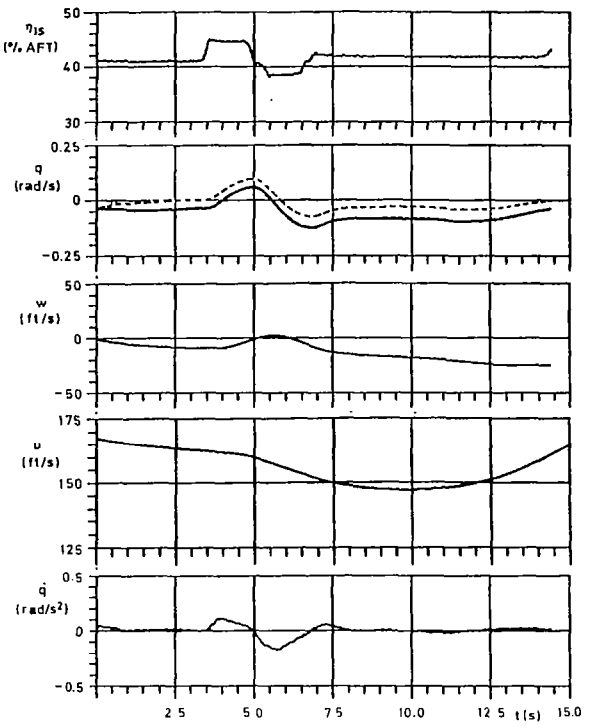

Fig 15 Comparison of measured (—) and estimated (- - -) states (Kalman filter/smoother) for longitudinal cyclic doublet manoeuvre

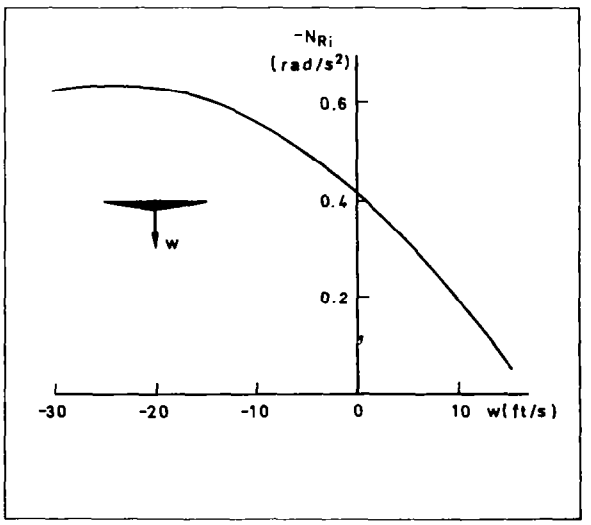

Fig 17 Variation of 'induced' rotor torque reaction with normal velocity perturbations

1. Report No.	2. Government Accession No.	3. Recipient's Catalog No.
NASA CP-2219		

4. Title and Subtitle	5. Report Date
HELICOPTER HANDLING QUALITIES	April 1982
	6. Performing Organization Code
7. Author(s)	8. Performing Organization Report No. A-8891
	10. Work Unit No. T-4007Y
9. Performing Organization Name and Address San Francisco Bay Area Chapter of the American Helicopter Society, Washington, D.C. 20546 and NASA Ames Research Center, Moffett Field, CA 94035	11. Contract or Grant No.
	13. Type of Report and Period Covered Conference Publication
12. Sponsoring Agency Name and Address National Aeronautics and Space Administration Washington, D.C. 20546 and the American Helicopter Society, Washington, D.C. 20036	14. Sponsoring Agency Code

15. Supplementary Notes

Chairman and Organizer: David L. Key, Aeromechanics Laboratory (AVRADCOM), Ames Research Center, Moffett Field, CA 94035
Phone: (415) 965-5839, FTS: 448-5839, Autovon: 359-5839

16. Abstract

This conference publication contains the formal papers of a specialists' meeting on helicopter handling qualities. The conference was co-sponsored by the American Helicopter Society and the NASA Ames Research Center, and was held in April 1982.

Helicopters are being called upon by the military and civilian communities to perform more and more tasks, and extend operations into poor weather and at night. Accompanying this increased use is a significant increase in pilot workload and a need for better handling qualities. The ability to define handling qualities required to perform such missions has not kept pace with the actual uses. The objective of this specialists' meeting was therefore to develop an overview of the status and problems in the development and specification of helicopter handling-qualities criteria, and highlight topics for future research efforts by government and industry.

17. Key Words (Suggested by Author(s))	18. Distribution Statement
Helicopter handling qualities Pilot workload Integrated cockpits All-weather and night operations Agility and maneuverability	Unclassified - Unlimited Subject Category 03

19. Security Classif. (of this report)	20. Security Classif. (of this page)	21. No. of Pages	22. Price*
Unclassified	Unclassified	254	A12

*For sale by the National Technical Information Service, Springfield, Virginia 22161

NASA-Langley, 1982

National Aeronautics and Space Administration

Washington, D.C.
20546

Official Business
Penalty for Private Use, $300

SPECIAL FOURTH CLASS MAIL
BOOK

Postage and Fees Paid
National Aeronautics and
Space Administration
NASA-451

U.S.MAIL

NASA

POSTMASTER: If Undeliverable (Section 158 Postal Manual) Do Not Return